Hawaii Ocean Time-series
Data Report 4
1992

Luis Tupas
Fernando Santiago-Mandujano
Dale Hebel
Roger Lukas
David Karl
Eric Firing

University of Hawaii
School of Ocean and Earth Science and Technology
1000 Pope Road
Honolulu, Hawaii 96822
U. S.A.

SOEST TECHNICAL REPORT 93-14

Preface

Scientists working within the Hawaii Ocean Time-series (HOT) project have been making repeated observations of the hydrography, chemistry and biology at a station north of Hawaii since October 1988. The objective of this research is to provide a comprehensive description of the ocean at a site representative of the central North Pacific Ocean. Cruises are made approximately once a month to Station ALOHA, the HOT deep-water station (22□ 45' N, 158□W) located about 100 km north of Oahu, Hawaii. Measurements of the thermohaline structure, water column chemistry, currents, primary production and particle sedimentation rates are made over a 72-hour period on each cruise.

This document reports the data collected during 1992. However, we have included some data from 1988 - 1991 in order to place the 1992 measurements within the context of our time-series observations. The data reported here are a screened subset of the complete data set. Summary plots are given for CTD, biogeochemical, optical, meteorological and ADCP observations.

In order to conserve paper and to provide easy computer access to our data, CTD data at National Oceanographic Data Center (NODC) standard pressures for temperature, potential temperature, salinity, oxygen and potential density are provided in ASCII files on the enclosed diskette. Chemical measurements are also summarized in a set of Lotus 1-2-3™ files on the enclosed diskette. A more complete data set resides on a Sun workstation at the University of Hawaii. These data are in ASCII format, and can easily be accessed using anonymous ftp via Internet. Instructions for using the Lotus files and for obtaining the data from the network are presented in Section 8. The entire data set will also be submitted to the NODC and will eventually be available through that service.

Acknowledgments

Many people have participated in cruises sponsored by the HOT program. They are listed in Table 1.4. We gratefully acknowledge their contributions and support.

Special thanks are due to Christopher Carrillo, James Christian, John Dore, Terrence Houlihan, Sean Kennan, Elaine Kotler, Ricardo Letelier, Richard Muller, Daniel Sadler, Jefrey Snyder and Christopher Winn for participating in many of the CY 1992 cruises and for the tremendous amount of time and effort they have put into the program. In addition, we would like to acknowledge the contributions made by Sharon DeCarlo and Joanne Houng for programming and data management, Julie Ranada and Xiaomei Zhou for ADCP processing and Lance Fujieki for programming and data processing. Toshiaki Shinoda and Fred Bingham helped with the quality controlling of the WOCE bottle data. Carl Chun and Nava Zvaig provided additional computer support. Ursula Magaard performed many of the routine chemical analyses. Ted Walsh performed the nutrient analyses, Sean Kennan, Sophia Asghar, and Reka Domokos conducted the salinity measurements, and Jason Killam provided additional technical support. We also would like to thank the captains and crew members of the R/V MOANA WAVE, R/V KILA, and R/V WECOMA for their efforts and to thank Nancy Koike for producing this document. Without the assistance of these people, the data presented in this report could not have been collected, processed, analyzed and reported.

This data set was acquired with funding from the National Science Foundation (NSF) and the National Ocean and Atmospheric Administration (NOAA). The specific grants which have supported this work are NSF grants OCE-8717195 (WOCE), OCE-8800329 (JGOFS), and OCE-9016090 (JGOFS) and NOAA grant NA-90-RAH-00074.

1. Introduction

In 1987, the National Science Foundation established a special-focus research initiative termed 'The Global Geosciences Program." This program is intended to support studies of the earth as a system of interrelated physical, chemical and biological processes that act together to regulate the habitability of our planet. The stated goals of this program are two-fold. The first goal is to understand the earth-ocean-atmosphere system and how it functions. The second goal is to describe, and eventually predict, major cause-and-effect relationships. Two components of the Global Geosciences Program are the World Ocean Circulation Experiment (WOCE) and the Joint Global Ocean Flux Study (JGOFS). The former is focused on physical oceanographic processes and the latter on biogeochemical processes.

The Hawaii Ocean Time-series (HOT) project has been initially funded under the sponsorship of both the WOCE and JGOFS programs to make repeated observations of the physics, chemistry and biology for five years at a station north of Hawaii. The objectives of HOT are to describe and understand the physical oceanography, and to identify and quantify the processes controlling biogeochemical cycling in the ocean at a site representative of the oligotrophic North Pacific Ocean.

Time-series cruises are made on approximately monthly intervals with two stations routinely occupied each month. The HOT deep-water station, also known as Station ALOHA (A Long-term Oligotrophic Habitat Assessment), is approximately 100 km north of Kahuku Point, Oahu, Hawaii (Figure 1.1). Station ALOHA is defined as a circle with a 6 nautical mile radius centered at 22°45' N, 158° 00 W. All sampling at Station ALOHA is conducted within this circle (Figure 1.1). The maximum depth at Station ALOHA is about 4750 m. Along the transit route to Station ALOHA another station is also occupied at 21° 20.6' N, 158° 16.4' W, off Kahe Point, Oahu. Station Kahe is used primarily to test the CTD and other equipment, but it also provides additional time-series data at a near-shore site. Station Kahe is located in approximately 1500 m of water about 16 km from shore (Figure 1.1). Approximately 3 to 4 hours are spent at the Station Kahe, and about 72 hours are spent at Station ALOHA during each cruise. The cruise length is dictated by the minimum time necessary to obtain enough sample material for reliable estimates of particle flux using the free-drifting sediment traps deployed at Station ALOHA. On several cruises in 1992, extra stations were occupied along longitude 158°W at 22° 25' N (Stn. 3), 21° 57.8' N (Stn. 4) and 21° 46.6' N (Stn. 5).

The JGOFS and WOCE components of the program measure a variety of parameters during the regular monthly sampling work at Station ALOHA (Table 1.1). JGOFS sampling includes primary production, particle flux, a variety of chemical determinations at discrete depths

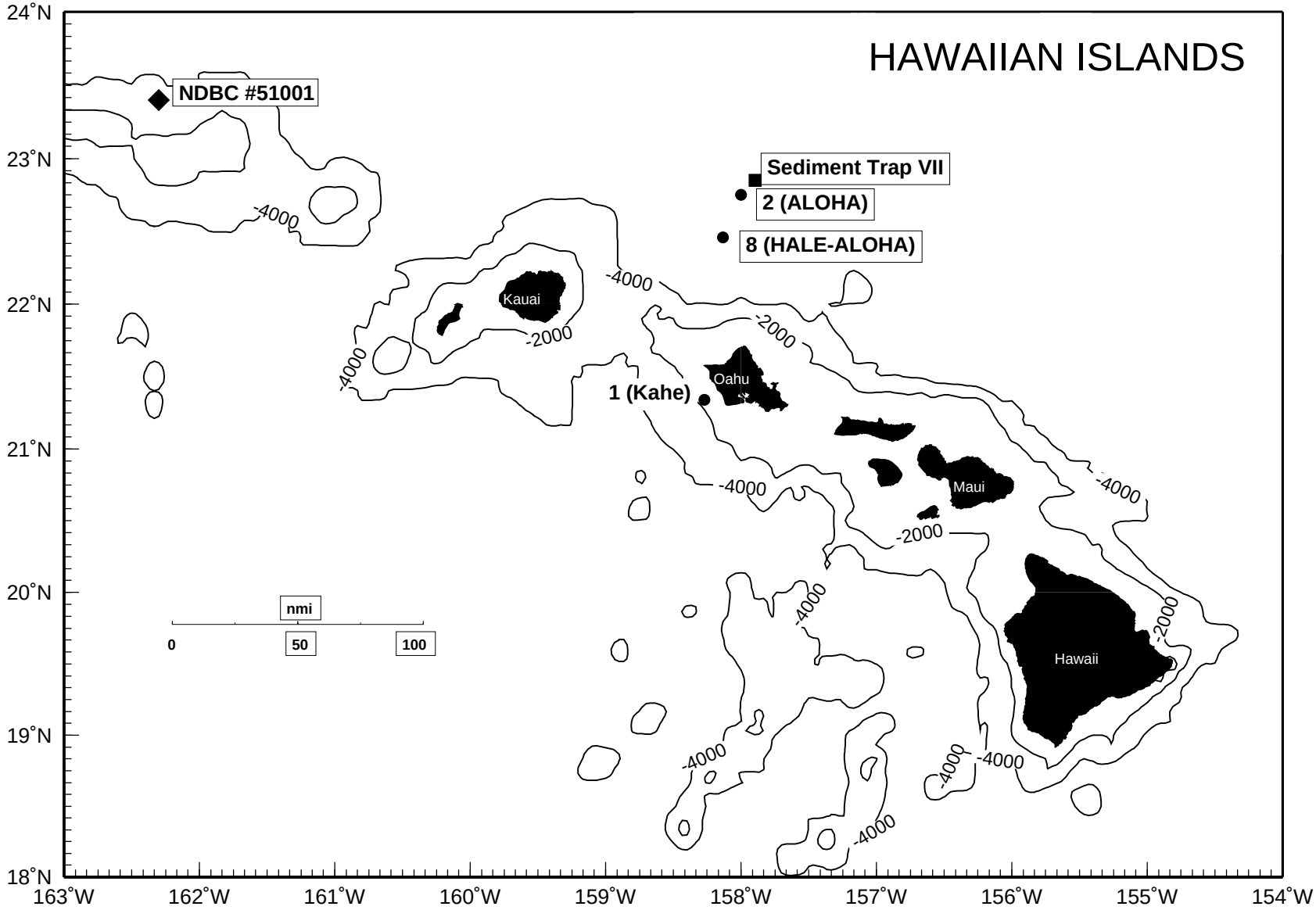

Figure 1.1: Map of the Hawaiian Islands showing the locations of the open ocean hydrostation (ALOHA), coastal hydrostation (KAHE) and the NDBC weather buoy. Also shown are two additional stations (Stations 3 and 4) that have been occupied since HOT-31. Lower panel: Expanded view of the geographically-defined Station ALOHA region (a 6 nautical mile radius circle centered at 22° 45'N, 158°W) also showing the locations of the four inverted

Table 1.1: Time-Series Parameters Measured at Station ALOHA

Parameter	Depth Range (m)	Analytical Procedure
1. CTD Measurements		
Temperature	0-4750	Thermistor on Sea-Bird CTD package with frequent calibration
Salinity	0-4750	Conductivity sensor on Sea-Bird CTD package, standardization with Guildline AutoSal #8400 against Wormley standard seawater
Oxygen	0-4750	Polarographic sensor on Sea-Bird CTD package with Winkler standardization
Fluorescence	0-1000	Sea-Tech Flash Fluorometer on Sea-Bird CTD package
Beam Transmission	0-1000	Sea-Tech 25 cm path length beam transmissometer on Sea-Bird CTD package
II. Optical Measurements		
Solar Irradiance (PAR)	Surface	Licor Cosine Collector and Biospherical 2 pi Collector
Underwater Irradiance (PAR)	0-150	Biospherical Profiling Natural Fluorometer 4 pi Collector
Solar Stimulated Fluorescence (683nm)	0-150	Biospherical Profiling Natural Fluorometer
III. Water Column Chemical Measurements		
Oxygen	0-4750	Winkler Titration
Total Dissolved Inorganic Carbon	0-4750	Coulometry
Titration Alkalinity	0-4750	Automated Titration
PH	0-4750	Potentiometry
Dissolved Inorganic Nitrate Plus Nitrite	0-4750	Autoanalyzer
Dissolved Inorganic Phosphorus	0-4750	Autoanalyzer
Dissolved Silica	0-4750	Autoanalyzer
Low Level Nitrate Plus Nitrite	0-200	Chemiluminescence
Low Level Phosphorus	0-200	Magnesium-induced Coprecipitation
Dissolved Organic Carbon	0-1000	High Temperature Catalytic Oxidation
Total Dissolved Nitrogen	0-1000	U.V. oxidation
Total Dissolved Phosphorus	0-1000	U.V. oxidation
Particulate Carbon	0-1000	High Temperature Combustion
Particulate Nitrogen	0-1000	High Temperature Combustion
Particulate Phosphorus	0-1000	High Temperature Combustion
IV. Water Column Biomass Measurements		
Chlorophyll *a* and Phaeopigments	0-200	Fluorometric Analysis
Chlorophyll *a, b, c* and Accessory Pigments	0-200	High Pressure Liquid Chromatography
Adenosine 5′-Triphosphate	0-1000	Firefly Bioluminescence
V. Carbon Assimilation and Particle Flux		
Primary Production	0-200	"Clean" ^{14}C Incubations
Carbon, Nitrogen, Phosphorus and Mass Flux	150, 300, 500	Free-Floating Particle Interceptor Traps
VI. Currents		
Acoustic Doppler Current Profiler	0-300	Hull Mounted, RDI #VM-150
Acoustic Doppler Current Profiler	0-4750	Lowered

and continuous profiles of optical parameters. WOCE sampling includes a 36-hour burst of CTD casts at roughly 3-hour intervals to obtain temperature, salinity and oxygen profiles from 0 to 1010 dbar. WOCE sampling also includes a deep CTD cast as close to the bottom as possible. Current measurements are made on HOT cruises using a shipboard Acoustic Doppler Current Profiler (ADCP) when a ship with the necessary equipment is available for monthly cruises. In addition, lowered ADCP measurements have been made on several HOT cruises. HOT cruises have continued to provide logistical support to a growing number of ancillary projects (Table 1.2).

Table 1.2: Ancillary Projects Supported by HOT

Principal Investigator	Institution
Charles Keeling	Scripps Inst. of Oceanography
Steve Emerson	University of Washington
Paul Quay	University of Washington
Lisa Campbell	University of Hawaii
Brian Popp	University of Hawaii
Christopher Measures	University of Hawaii
Marlin Atkinson	University of Hawaii
James Cowen	University of Hawaii

This report presents selected core data collected during the fourth year of the HOT Program (January-December 1992). During this period, 11 cruises were conducted using three research vessels (Table 1.3) and a total field scientific crew of 50 (Table 1.4). The R/V MOANA WAVE and R/V WECOMA are UNOLS vessels operated by the University of Hawaii and Oregon State University, respectively. The R/V KILA is a state of Hawaii owned and operated research vessel.

Table 1.3: Summary of HOT Cruises, 1991

HOT	Ship	Depart	Return
33	R/V WECOMA	3 January 1992	8 January 1992
34	R/V WECOMA	12 February 1992	17 February 1992
35	R/V WECOMA	3 March 1992	8 March 1992
36	R/V WECOMA	15 April 1992	20 April 1992
37	R/V MOANA WAVE	5 June 1992	11 June 1992
38	R/V MOANA WAVE	3 July 1992	7 July 1992
39	R/V MOANA WAVE	3 August 1992	8 August 1992
40	R/V MOANA WAVE	20 September 1992	25 September 1992
41	R/V MOANA WAVE	17 October 1992	22 October 1992
42	R/V KILA	23 November 1992	25 November 1992
43	R/V KILA	15 December 1992	17 December 1992

Table 1.4: University of Hawaii Cruise Personnel

	33	34	35	36	37a	37b	38	39	40	41	42	43
S. Chiswell, P. I.												
E. Firing, P. I.												
D. Karl, P. I.												
C. Winn, P. I.												
F. Bingham, Scientist												
P. Hacker, Scientist												
D. Hebel, Scientist												
C. Measures, Scientist												
F. Thomas, Scientist												
L. Tupas, Scientist												
M. Bushnell, Visiting Scientist												
S. Emerson, Visiting Scientist												
I. Hamann, Visiting Scientist												
S. Manganini, Visiting Scientist												
M. Mulroney, Visiting Scientist												
R. Shudlich, Visiting Scientist												
C. Stump, Visiting Scientist												
D. Wilbur, Visiting Scientist												
D. Wilson, Visiting Scientist												
C. Carrillo, Technician												
K. Constantine, Technician												
C. Crockett, Technician												
T. Houlihan, Technician												
U. Magaard, Technician												
R. Muller, Technician												

Table 1.4: (continued)

	33	34	35	36	37a	37b	38	39	40	41	42	43
H. Nolla, Technician									■			
M. Rosen, Technician	■	■	■									
J. Snyder, Technician	■		■			■	■					
A. Anbar, Graduate Student	■						■					
S. Asghar, Graduate Student				■		■	■	■				
S. Barker, Graduate Student		■										
J. Bower, Graduate Student			■		■							■
J. Christian, Graduate Student	■	■			■	■		■		■		■
R. Domokos, Graduate Student	■	■					■	■				
J. Dore, Graduate Student		■		■					■	■	■	
A. Ferrara, REU Student							■					
J. Girton, REU Student							■					
S. Kennan, Graduate Student	■					■		■	■	■		
N. Kerr, Graduate Student						■						
E. Kotler, Graduate Student	■	■	■	■		■	■	■				
K. Leckrone, Graduate Student	■											
R. Letelier, Graduate Student			■	■			■	■	■	■		
H. Liu, Graduate Student				■		■	■	■				
J. Pietraszek, Graduate Student		■	■									
J. Reichelderfer, Graduate Student							■					
D. Sadler, Graduate Student			■	■		■	■	■	■	■		■
F. Santiago-Mandujano, Graduate Student				■								
P. Troy, Graduate Student										■		
J. Wilcox, Graduate Student								■				
J. Yuan, Graduate Student			■			■				■		
X. Zhou, Graduate Student			■									
Y. Zhou, Graduate Student								■				

Shaded area = cruise participant Solid area = Chief Scientist

2. Sampling Procedures and Analytical Methods

2.1. CTD Profiling

CTD data were collected with a Sea-Bird SBE-09 CTD, which had an internal Digiquartz pressure sensor and external temperature, conductivity and oxygen sensors. The Sea-Bird temperature-conductivity duct, which was used to circulate seawater through both the temperature and conductivity sensors, was used on all cruises during 1992. A Sea Tech flash fluorometer was also incorporated into the CTD sampling on the majority of the casts. In 1991 a Sea Tech beam transmissometer was added to the CTD system and was used throughout 1992. The CTD was mounted in a rosette sampler and the package was deployed on a conducting cable, which allowed for real-time data acquisition and data display. Water samples were taken on the

upcasts for chemical analyses and for calibration of the conductivity and oxygen sensors.

A CTD cast to approximately 1010 dbar (equivalent to 1000 m depth) was made at Station Kahe on each cruise. At Station ALOHA, a burst of consecutive CTD casts to 1010 dbar was made over 36 hours to span the local inertial period (~31 hours) and three semi-diurnal tidal cycles. This sampling was designed so that energetic tidal and near-inertial period variability during each cruise could be averaged to prevent these components from aliasing the longer time-scale signals. In order to satisfy WOCE requirements, one deep cast to the near bottom was made on each cruise. When cruises were made on a ship equipped with a 12-kHz echo sounder, a Benthos acoustic pinger attached to the rosette was used to position the rosette to within 50 m of the sea floor (approximately 4750 m). When the research platform was not equipped with an echo sounder, this cast was made to 4500 dbar (unless cable length was shorter). On HOT-42 and 43 cruises a Seacat SB19 CTD on a Kevlar line was used to approximately 260 dbar, instead of the usual Seabird CTD. This was due to the lack of a conducting cable on the R/V KILA.

2.1.1. CTD Data Acquisition and Processing

CTD data were acquired at the instrument's highest sampling rate of 24 samples per second. Digital data were stored on a PC-compatible computer and, for redundancy, the analog CTD signal was recorded on VHS video tapes.

The raw CTD data were quality controlled and screened for spikes and missing data as described by Winn *et al.* (1991). The data were aligned as previously described, averaged to half-second values and the calibrations were applied. Salinity and oxygen were then computed in units of psu and μmol kg^{-1}, respectively. Details of these corrections are described in the following sections. A flowchart of the CTD processing is shown in Figure 2.1.

Eddy shed wakes, caused when the rosette entrains water, introduced salinity spikes in the CTD profile data. These contaminated data were handled using an algorithm which eliminated data collected when the CTD's speed was less than 0.25 m s^{-1} or its acceleration was greater than 0.25 m s^{-2}. The data were subsequently averaged into 2 dbar pressure bins. Temperature was reported in the ITS-90 scale. Salinity and all derived units were calculated using the UNESCO (1981) routines.

2.1.2. CTD Sensor Corrections and Calibration

2.1.2.1. Pressure

The pressure sensor calibration strategy was described in Winn *et al.* (1991). Briefly, this strategy used a high-quality quartz pressure transducer as the laboratory transfer standard and a

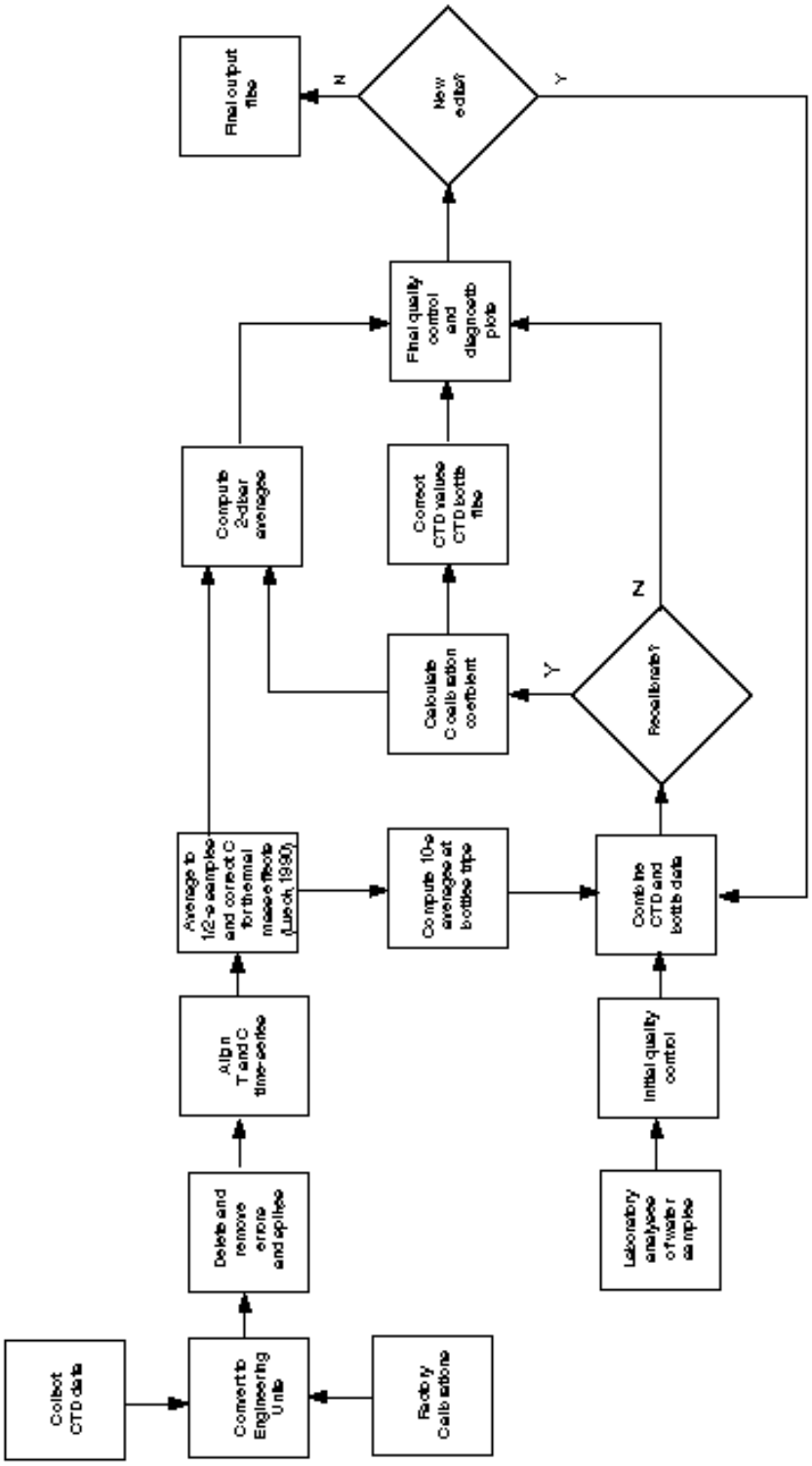

Figure 2.1: Flowchart of CTD data processing

Russka precision dead-weight pressure tester as a primary standard. The primary standard met National Institute of Standards and Technology specifications and was operated under controlled conditions. The transfer standard was a Paroscientific Model 760 pressure gauge equipped with a 10,000 PSI transducer. The transfer standard was calibrated at the Oceanographic Data Facility at Scripps Institution of Oceanography in May of 1991.

Laboratory calibrations of the CTD pressure sensor were done using a dead weight pressure tester and a manifold to apply pressure simultaneously to the CTD pressure transducer and the transfer standard. Calibrations were done over a pressure range of 0-5000 dbar with points collected as pressure was increased and as decreased.

Pressure transducer #26448 was used on all cruises in 1992. Subsequent calibrations against the transfer standard using its original calibration (Winn *et al.*, 1991) are given in Table 2.1. The drift in this sensor appeared to be relatively linear with time through 1992 (Table 2.1). An offset of 5.13 dbar was obtained after correction for the shift in the primary standard and was used for all cruises in 1992 (Note that this offset was only used for real-time data acquisition, as a more accurate offset was determined at the time that the CTD first enters the water on each cast). This shift was within the normal operating specifications of this sensor. The drift in the bias as

Table 2.1: CTD Pressure Calibrations
(all units are in decibars)

Sea-Bird SBE-09 #91361 / Pressure Transducer #26448

Calibration date	Offset @ 0 dbar	slope offset @ max pressure	hysteresis
10 May 1989	-1.1	-0.6 @ 4500	N/A
10 July 1990	-1.65	-0.8 @ 5000	0.2
20 February 1991	-2.15	-0.9 @ 4800	0.25
27 June 1991	-2.7	-0.3 @ 4600	0.2
27 August 1992	-4.83	-0.1 @ 4500	0.075
27 August 1992	-4.9	-0.2 @ 4500	0.05
Final correction for 1992	-5.13[a]	-0.75[a]	0.075

[a]Adjusted for shift in lab pressure standard calibrated 16 May 1991 at SIO/ODF.

estimated from the 27 June 1991 and 27 August 1992 calibrations is 1.6 dbar y^{-1}, which is within the expected 2 dbar y^{-1} for this sensor (N. Larson, Personal Communication, 1992).

2.1.2.2.Temperature

Our strategy for CTD temperature calibration also relied upon the use of a transfer standard periodically recalibrated at a primary calibration center using techniques traceable to the National Institute of Standards and Technology. As in 1991, three Sea-Bird SBE-3-02/F temperature transducers, serial numbers 741, 886 and 961 were available in 1992. These transducers were returned to Sea-Bird approximately once per year before 1992, and twice per year starting in 1992 for calibration by the Northwest Regional Calibration Center (NWRCC). The frequency of recalibration is a trade-off between confidence in the behavior of the sensor with time versus the risk of damage or loss during shipping to and from the calibration center. During 1992 sensor #741 was used only as a transfer standard during intercomparison runs with the other two sensors. Only sensor #886 was used at sea in 1992. Intercomparisons between #741 and #886 were done between cruises to provide a check on the nature of the drift of sensor #886 relative to the transfer standard.

Primary calibrations

The calibrations at NWRCC typically have a RMS residual of 0.25-1.0 m□C (Table 2.2). Consistent with previous experience (Chiswell *et al.*, 1990; Winn *et al.*, 1991, 1993) our sensors have exhibited a tendency towards higher temperature readings with time. After their electronics were reworked, sensors 961 and 886 gave lower temperature readings with time. Table 2.2 gives the calibration coefficients which were determined by NWRCC measurements. These coefficients were used in the following formula that gave the temperature (in □C) as a function of the frequency signal (f)

$$\text{Temperature} = 1/\{a+b[\ln(f_O/f)] + c[\ln^2(f_O/f)] + d[\ln^3(f_O/f)]\} - 273.15$$

Sensor #961

Sensor #961 electronics were reworked on 17 January 1992 at Sea-Bird to slow down the drift. The calibrations after this date were used to start a new drift history for this sensor. The sensor was calibrated on 29 January 1992 and on 31 July 1992. Relative to the 29 January 1992 calibration, the 0-30°C average offset was -0.87 m°C on July 31 1992. We modeled the drift of sensor #961 as a linear function of time as per the experience of Sea-Bird over many years of working with these sensors. A linear fit to these offsets gave an intercept of -0.4 m°C with a slope of 0.205 x 10^{-5}°C d^{-1}. The RMS deviation of the offsets from this fit was 0.48 m°C. We compare this drift to the 2.101 x 10^{-5}°C d^{-1} estimated drift for the cruises in 1991 (Winn, *et al.* 1993) which confirms the noticeable reduction in the sensor drift after the sensor's electronics were reworked.

Sensor #886

As was the case of sensor #961, sensor #886 electronics was reworked on 17 January 1992 to reduce the drift. The calibrations after this date were used to start a new drift history of the sensor. The sensor was calibrated on the dates given in Table 2.2. Relative to the 29 January 1992 calibration, the 0-30°C average offset was 0.97 m°C on 20 August 1992 and 3.26 m°C on 18 December 1992. A linear fit to these offsets gave an intercept of -0.26 m°C, with a slope of 0.95 x 10^{-5}°C d^{-1}. The RMS deviation of the offsets from this fit was 0.5 m°C. A comparison of this drift with the 1.871 x 10^{-5}°C d^{-1} obtained for the 1991 cruises (Winn *et al.*, 1993) shows the reduction in the sensor drift during 1992.

The 18 December 1992 calibration was used to calculate temperature from the sensor frequency data obtained after 17 January, this included all 1992 cruises except cruise 33, which took place from 3 to 8 January 1992. When corrected for linear drift to 15 May 1992, this calibration gave the smallest deviation in the 0-5°C temperature range from the ensemble of all the 1992 calibrations available for this sensor (also corrected for linear drift to 15 May 1992). In the 0-5°C temperature range, the mean deviation of this calibration was approximately 0.1 m°C with about 0.5 m°C variation. The 29 January 1992 calibration had a mean deviation of 0.55 m°C, while the 20 August 1992 calibration had a mean deviation of -0.46. Thus, for the HOT cruises conducted after 17 January 1992, we placed an error bound of 0.5 m°C. Cruise 33 was calibrated using the 21 June 1991 calibration and the drift rate calculated for the 1991 cruises (Winn *et al.*, 1993), as this cruise took place before the sensor was modified. The corrections applied to sensor #886 used during the 1992 HOT cruises are given in Table 2.3.

Sensor #741

The calibration procedure used for sensor #886 was also applied to sensor #741. Unlike the other sensors, this sensor has not been modified to reduce the drift. The offsets over the range 0-30°C from the original calibration of this sensor in March 1987 were 1.6 m°C (21 August 1987), 11.8 m°C (3 November 1989), 16.8 m°C (14 June 1991), 18.2 m°C (16 October 1991), 21 m°C (26 June 1992) and 21.7 m°C (18 December 1992). Computing a linear fit to this drift yielded an intercept of .62 m°C, a drift of 1.003 x 10^{-5}°C d^{-1}, with an RMS residual of 1.03 m°C. The calibrations after 26 June 1992 indicated a change in the sensor drift compared with the drift from previous calibrations. Using the 26 June 1992, 18 December 1992 and 13 May 1993 calibrations we estimated a sensor drift of 0.10 x 10^{-5}°C d^{-1}.

Table 2.2: Calibration Coefficients for Sea-Bird Temperature Transducers Determined at Northwest Regional Calibration Center. RMS Residuals from Calibration Give an Indication of Quality of the Calibration.

SN	YYMMDD	f_0	a	b	c	d	RMS (m°C)
961	930506	6719.05	3.68096927E-3	6.00707448E-4	1.56310803E-5	2.57218188E-6	0.06
961	930114	6791.28	3.67456115E-3	6.00413807E-4	1.56851516E-5	2.78999142E-6	0.43
961	920731	6782.47	3.67533262E-3	6.00279865E-4	1.51877355E-5	2.26314932E-6	0.05
961	920129	6789.88	3.67467693E-3	6.00392638E-4	1.56716646E-5	2.72527915E-6	0.09
961	920117	6609.38	3.67323279E-3	6.00527259E-4	1.64422903E-5	3.44995275E-6	0.10
961	901221	6596.33	3.67426509E-3	6.00296402E-4	1.50788252E-5	1.90331606E-6	0.28
961	901212	6555.62	3.67799766E-3	6.00589512E-4	1.54924845E-5	2.33356321E-6	0.27
961	891110	6593.31	3.67447767E-3	6.00431308E-4	1.54701351E-5	2.26236217E-6	1.42
961	891103	6570.80	3.67651910E-3	6.00440343E-4	1.54578885E-5	2.39329073E-6	0.48
961	891020	6584.74	3.67527037E-3	6.00529885E-4	1.60084763E-5	2.99271892E-6	0.80
961	891013	6569.50	3.67662353E-3	6.00261297E-4	1.45636785E-5	1.50324489E-6	0.26
961	890728	6585.62	3.67515137E-3	6.00521977E-4	1.58721052E-5	2.82022768E-6	0.81
886	921218	5967.82	3.67476787E-3	5.95715773E-4	1.48206068E-5	2.52835250E-6	0.39
886	920820	5935.78	3.67798061E-3	5.95648169E-4	1.41980725E-5	1.94572339E-6	0.60
886	920129	5969.00	3.67467842E-3	5.95638784E-4	1.45242521E-5	2.12848528E-6	0.20
886	920117	5753.52	3.67323321E-3	5.96294680E-4	1.60552655E-5	3.39478196E-6	0.12
886	910621	5734.40	3.67513498E-3	5.95897382E-4	1.39469939E-5	1.18908186E-6	0.71
886	901108	5736.72	3.67481987E-3	5.95946149E-4	1.44577231E-5	1.86030765E-6	0.72
886	891103	5720.16	3.67651936E-3	5.96264789E-4	1.52176908E-5	2.50122950E-6	0.57
886	891013	5719.06	3.67662109E-3	5.96299484E-4	1.50920606E-5	2.19842950E-6	0.30
886	881007	5738.95	3.67442955E-3	5.96116868E-4	1.52142776E-5	2.58643736E-6	0.42
741	930513	6170.47	3.68098624E-3	6.02116588E-4	1.52577583E-5	2.38750692E-6	0.26
741	921218	6234.70	3.67477118E-3	6.01755208E-4	1.48365899E-5	2.06062301E-6	0.38
741	920626	6246.37	3.67361468E-3	6.01608285E-4	1.48891820E-5	2.32038514E-6	0.61
741	911016	6233.18	3.67485170E-3	6.01645255E-4	1.46381280E-5	1.87675853E-6	0.17
741	910614	6242.89	3.67391737E-3	6.01617260E-4	1.44529212E-5	1.67976234E-6	0.96
741	891103	6215.18	3.67651726E-3	6.01684546E-4	1.44771486E-5	1.74730364E-6	0.26
741	870821	6233.01	3.67465365E-3	6.01497545E-4	1.43226522E-5	1.70524526E-6	0.37
741	870305	6227.60	3.67516234E-3	6.01775431E-4	1.52877814E-5	2.58640979E-6	0.48

Laboratory calibrations

Our laboratory temperature sensor intercomparisons were done in an insulated water bath, using the CTD for data acquisition and sensor power. The water bath had a circulation system which drew water from the bottom of the tank and spread it across the top of the water column. It was unlikely that there were persistent temperature variations within the bath greater than 1 m°C, though we have not made exhaustive tests of this assertion. Short-term variations in temperature differences between sensors were less than ± 0.5 m°C. The bath was initially chilled to near 0°C, the CTD and sensors were inserted, the bath was closed, and over a period of 2 days the system slowly warmed to the lab temperature of 23-25°C. An initial period when the temperature of the CTD was coming into equilibrium with the bath (and was acting as a heat source) was readily identified. Averaging temperature transducer output over several minutes gave exceptionally stable temperature differences at a variety of bath temperatures.

During 1992 we were not able to perform temperature intercomparisons among our three sensors after every cruise, the main reason being that sensors #741 and #961 were being used in other cruises for extended periods of time. From the available intercomparisons, the only ones that we could use in the 10-20°C range were between sensors #741 and #886 performed on 3 September 1992, 28 September 1992 and 2 November 1992. The results from these intercomparisons are consistent with the observed drift change of sensor #741 described above.

Using sensor #741 as a reference, with the linear drift correction as described earlier, sensor #886 showed a drift of 1.08×10^{-5} °C d^{-1}, with an RMS residual of 1.1 m°C for the 3 laboratory intercomparisons. This is compared to the 0.95×10^{-5} °C d^{-1} linear drift estimated from the NWRCC calibrations.

2.1.2.3 Conductivity

The conductivity cell was calibrated periodically at the NWRCC by varying the temperature of a saltwater bath as described by Winn *et al.* (1991). These nominal calibrations were used for data acquisition and final calibration was determined empirically by comparison with the salinities of discrete water samples acquired during each cast. Conductivity cell #679 was used during 1992 and was calibrated at NWRCC on 13 October 1989 and 12 October 1990.

Prior to the empirical calibration of conductivity data with water bottle salinities, conductivity was corrected for the thermal inertia of the glass conductivity cell as described by Chiswell *et al*. (1990). Table 2.3 lists the value of α used for each cruise. No drift corrections were necessary during 1992.

Table 2.3: Temperature and Conductivity Sensor Corrections

HOT	Temp #	T Correction °C	Cond #	α
33	886	-0.0036	679	0.037
34	886	-0.0029	679	0.037
35	886	-0.0027	679	0.028
36	886	-0.0023	679	0.028
37	886	-0.0018	679	0.028
38	886	-0.0016	679	0.020
39	886	-0.0013	679	0.028
40	886	-0.0008	679	0.020
41	886	-0.0006	679	0.028

Screening of bottle samples

Preliminary screening of the water sample salinities was done by comparing against all previous data deemed reliable that had been collected at the particular site (Stations Kahe or ALOHA). The nominally calibrated CTD salinity trace was also used to identify questionable discrete samples. Potential rosette mistrip problems were resolved, where possible, before data were excluded from use in the calibration of the conductivity cell.

After an initial calibration of the conductivity cell using all casts within a cruise, the deviations between CTD salinity and bottle salinity were tested against limits within 4 pressure ranges (3 standard deviations of the ensemble of 'good' data). Bottles were marked as 'suspicious' when the difference exceeded 3 standard deviations, and 'bad' when greater than 4. These bottles were not used in further iterations of the calibration. For HOT-33 to -41 the standard deviations were: 0.0034 psu (0-150 dbar), 0.0045 psu (150-500 dbar), 0.0021 psu (500-1050 dbar) and 0.0011 psu (1050-5000 dbar).

Empirical calibration

Salinity was determined on every discrete water sample as described in Section 2.2.1. Preliminary screening of the water sample salinities was done as described by Winn *et al.* (1991). Calibration of the conductivity cell was performed empirically by comparing its nominally calibrated output against the calculated conductivity values obtained from water sample salinities using the calibrated pressure and temperature of the CTD at the time of bottle closure. An initial

estimate of bias and slope corrections to the nominal calibration were determined from a linear least squares fit to the ensemble of bottle-CTD conductivity differences as a function of conductivity, from all stations and casts during a particular cruise. This calibration was then used to identify suspect water samples.

The second iteration allowed for the possible addition of a quadratic term in the correction to conductivity, as well as a revised estimate of slope and bias. The final conductivity calibration coefficients are given in Table 2.4.

Table 2.4: Table of Conductivity Calibration Coefficients

Cruise	b0	b1
HOT-33	0.002344227	-0.000971932
HOT-34	0.001441051	-0.000759007
HOT-35	0.001780625	-0.000925374
HOT-36	0.001426122	-0.000986657
HOT-37	0.001777003	-0.000856545
HOT-38	0.001815362	-0.000888495
HOT-39	0.001642849	-0.000850141
HOT-40	0.001967794	-0.001004826
HOT-41	0.001677812	-0.000975102

The quality of the CTD calibration is illustrated by Figure 2.2, which shows the differences between the corrected CTD salinities and the bottle salinities as a function of pressure for each cruise. Typically, the calibrations were best below 500 dbar, because the weaker vertical salinity gradients at depth lead to less error if the bottle and CTD pressures are slightly mismatched. Conductivity calibration coefficients for HOT-42 and -43 are inaccurate since the bottle depths are uncertain and are therefore excluded from this table.

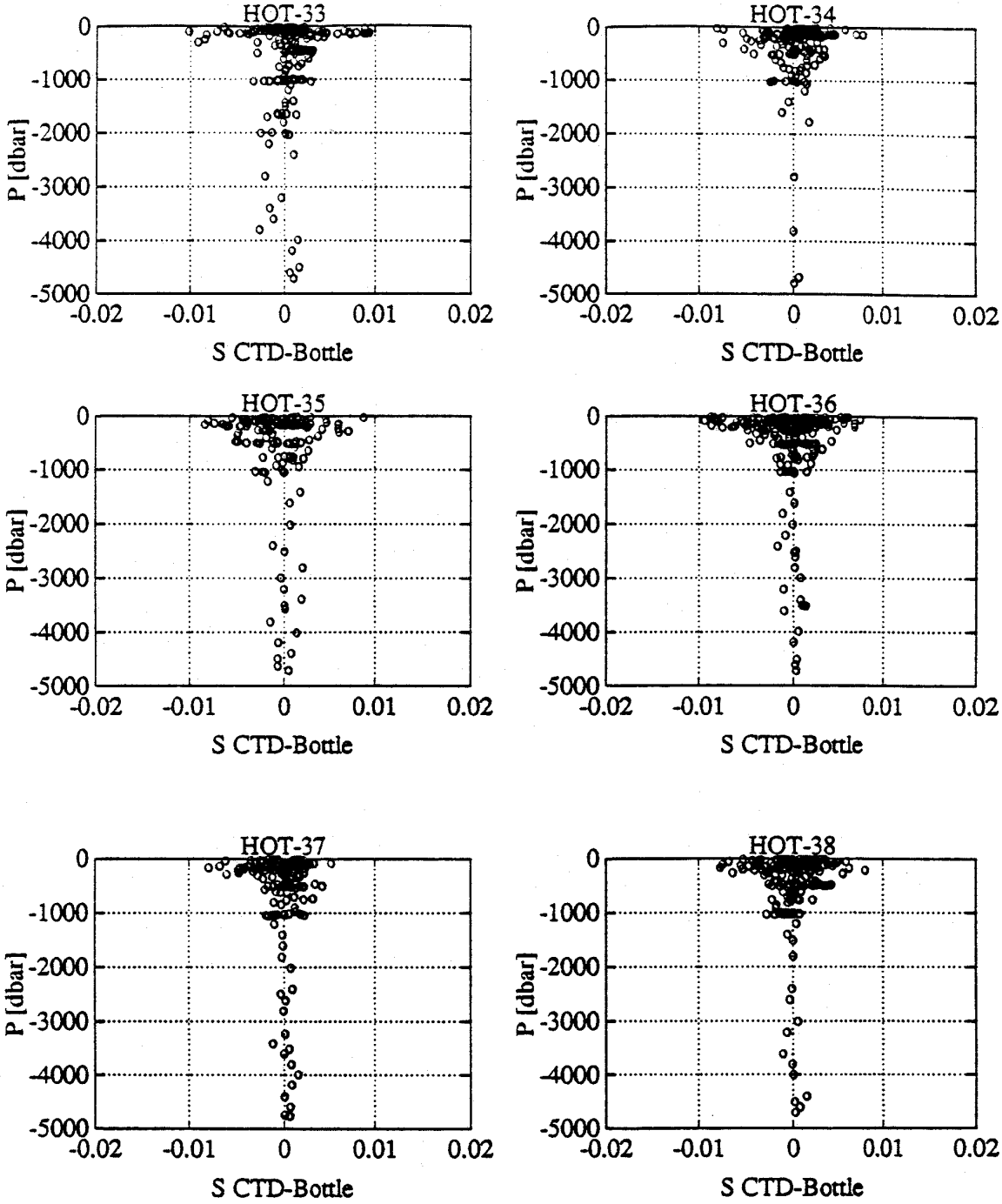

Figure 2.2: Differences between calibrated CTD salinities and bottle salinities for Station ALOHA, HOT-33 to 38.

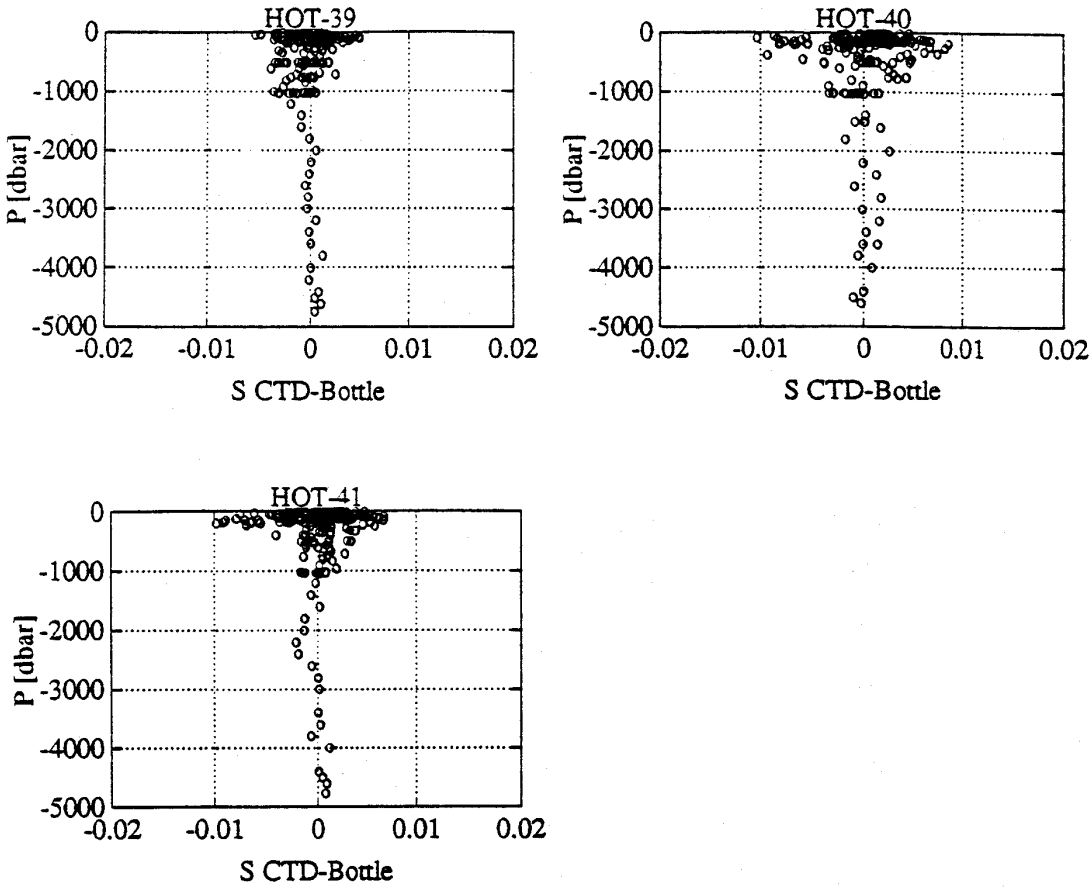

Figure 2.2: (continued): HOT-39 to 41.

The final step of the calibration was to perform a profile-dependent bias correction, to allow for drift during each cruise, or for sudden offsets due to fouling. This offset was determined by taking the median value of CTD-bottle salinity differences for each profile at temperatures below 5°C (Table 2.5.). Note that a change of 1 x 10^{-4} s m^{-1} in conductivity was approximately equivalent to 0.001 psu in salinity. The conductivity cell seemed to drift during HOT-36 for unknown reason. For this cruise, all the casts required correction for their individual drifts. The cell functioned normally in succeeding cruises. Table 2.6 gives the means and standard deviations for the final calibrated CTD values minus the water sample values.

Table 2.5: Individual Cast Conductivity Offsets. Units are Siemens $m^{-1} \times 10^{-4}$

Cruise	Station	Cast	Offset
HOT-33	2	1	-0.82
	2	2	0.33
	2	16	0.69
	2	17	0.22
	2	18	-0.47
	2	19	-0.95
	2	20	-0.45
	2	21	-0.45
	3	1	0.03
HOT-34	2	14	1.09
	2	17	2.18
	3	1	-1.30
	4	1	-0.67
HOT-35	2	1	-0.31
	2	5	-0.15
	2	6	-0.41
	2	7	-0.44
	2	12	1.53
	3	1	1.40
	3	2	-0.27
HOT-36	1	1	-2.13
	2	1	-4.01
	2	2	-5.51
	2	3	0.18
	2	4	-0.16
	2	5	1.19
	2	6	1.37
	2	7	0.50
	2	8	-2.18
	2	9	3.66
	2	10	1.50
	2	11	1.04
	2	12	0.28
	2	13	4.17
	2	14	2.65
	2	15	6.84
	2	16	6.41
	2	17	5.20
	2	18	4.66
	2	19	4.66
	3	1	5.91
	4	1	5.53
HOT-37	2	1	0.05
	2	4	1.97
	2	9	-1.06

HOT-38	1	1	-1.64
	2	1	-0.06
	2	3	0.99
	2	4	-3.29
	3	1	0.78
HOT-39	2	9	0.64
	3	1	0.95
HOT-40	1	2	-0.29
	2	2	-0.45
	2	12	-3.36
	2	16	-0.43
	3	1	1.77
HOT-41	2	1	0.93
	3	1	-1.23

Table 2.6: CTD-Bottle Salinity (psu) Comparison for Each Cruise

	0 < P < 4700 db		500 < P < 4700 db	
Cruise	**Mean**	**St. Dev.**	**Mean**	**St. Dev.**
HOT-33	0.0000	0.0030	0.0000	0.0013
HOT-34	0.0000	0.0023	0.0002	0.0014
HOT-35	0.0000	0.0029	0.0000	0.0013
HOT-36	-0.0002	0.0028	0.0000	0.0011
HOT-37	-0.0001	0.0021	0.0001	0.0012
HOT-38	0.0001	0.0023	-0.0002	0.0012
HOT-39	-0.0002	0.0018	-0.0006	0.0013
HOT-40	0.0001	0.0033	-0.0000	0.0018
HOT-41	0.0000	0.0029	0.0000	0.0011

2.1.2.4 Oxygen

As described in Winn *et al.* (1993) the YSI Inc. oxygen probe was used as the main oxygen probe on HOT cruises beginning with HOT-31. In previous years (Winn *et al.*, 1991), extra weight was generally given to oxygen values below 1000 m for the purpose of calibrating the O_2 sensor. It was not necessary to apply this procedure for data collected in CY 1992. Very low oxygen values were observed, however, in the upper 15 to 25 m of several casts, specifically, HOT-35 Station 2, casts 4 and 7; HOT-37, Station 2, casts 1 - 14; HOT-38, Station 2, cast 1, 2, 6, 7, 11-14 and 16; HOT-39, Station 1, cast 1, Station 2, casts 1 and 3 - 18. These oxygen values were flagged as suspect. Furthermore, the deep cast of HOT-38 had spikes in the oxygen signal

and the deep casts of HOT 33-35 showed abrupt offsets below 2200 db. These data were also flagged as suspect. The cause of these errors may have been related to deterioration of the sensor membrane. The membrane was replaced on 5 September 1992, just before HOT-40. Surface oxygen values appeared normal for this cruise but spikes were still observed in deep water. The sensor was sent back to Sea-Bird and was replaced by a new YSI sensor before HOT-41. The new sensor performed well on this cruise. Water bottle oxygen data were screened and the sensor was calibrated on all cruises during 1992 as described previously (Winn *et al.*, 1991).

Water sample analysis

Water samples were analyzed for oxygen as described in Section 2.2.2.

Screening of bottle samples

Bottle O_2 data were screened against the large historical data base generated for Stations Kahe and ALOHA by overplotting on the ensemble of all good data collected from each site. Both O_2 vs. pressure and O_2 vs. θ were inspected for suspicious values. Apparent rosette problems were investigated by looking at other water properties and resolved if possible.

The continuous O_2 profile from the CTD was also used for screening the bottle data. It was our experience that there was considerable finestructure in O_2, not always correlated with T-S finestructure. This was partly due to the biological processes which make O_2 a nonconservative tracer. Without the continuous profile to reveal this structure one might reject bottle oxygen values that were accurate. Thus, even though the sensor had some undesirable characteristics, it still provides useful information on the variability of O_2 on small scales.

Empirical calibration

CTD O_2 calibration was performed following Owens and Millard (1985). Six parameters (B_{oc}, S_{oc}, tcor, pcor, τ, w_T) were fit to the CTD oxygen current (O_c), oxygen temperature (O_T), and O_c time variation $\left(\frac{d\,O_c}{d\,t} \right)$ by the equation:

$$OX = \left[S_{oc} \cdot \left(O_c + \tau \frac{dO_c}{dt} \right) + B_{oc} \right] \cdot OXSAT\,(T, S) \cdot \exp\,[tcor\,[T + w_T \cdot (T_o - T)] + pcor \cdot p]$$

where the OXSAT (oxygen saturation) was calculated from the CTD temperature and bottle salinity, calibrated CTD salinities were used if the bottle salinity is absent or of suspect quality. The bottle O_2 values and the downcast CTD observations at the potential density of each bottle trip were grouped together for each cruise and used to find the best set of parameters using a nonlinear least squares algorithm based on the Levenberg-Marquardt method (Press *et al.*, 1988). Two sets of parameters were obtained per cruise, corresponding to the casts at Station 1 (Kahe)

and Station 2 (ALOHA). At Station 2, only WOCE casts were used for the fit. The set of parameters obtained was used to calculate oxygen (OX) for all the CTD casts of this station. The quality of the O_2 sensor calibration was assessed from Table 2.7.

Table 2.7: CTD-Bottle O_2 (µmol kg^{-1}) Comparison for Each Cruise

	Station 1, Kahe Point		Station 2, ALOHA			
	0 < P < 1500		0 < P < 4700		500 < P < 4700	
Cruise	Mean	St. Dev.	Mean	St. Dev.	Mean	St. Dev.
HOT-33	0.03	2.06	0.18	1.34	0.30	1.50
HOT-34	0.00	1.37	0.02	2.72	0.32	2.78
HOT-35	0.01	1.50	-0.12	2.46	0.20	2.45
HOT 36	0.01	1.65	0.06	3.31	0.29	3.23
HOT-37	0.11	2.98	0.28	2.88	0.44	3.15
HOT-38	0.00	1.75	0.45	2.45	0.97	2.25
HOT-39	0.15	2.56	0.04	2.06	0.00	1.76
HOT-40	0.01	1.19	0.17	1.70	0.27	1.54
HOT-41	0.00	2.25	0.02	1.63	0.00	1.47

2.1.2.5. Flash Fluorescence and Beam Transmission

In situ flash fluorescence was measured during all four years of the time-series program with a flash fluorometer manufactured by Sea Tech Inc. (model ST0250). Fluorescence data were collected with the Sea-Bird CTD system described previously. As described in section 2.1.1 data were collected at 24 hz and averaged to 2 hz. The data were then processed to remove spikes and averaged in 2 dbar bins. The binned data were then quality controlled and quality flags were assigned to each 2 dbar bin. The quality controlled 2 dbar bin data set was too extensive to be included in this report. These data files are available via Internet (see Section 8).

Flash fluorescence traces were collected on as many of the 1000 m casts as possible at both Station Kahe and Station ALOHA during 1992. Equipment problems prevented the collection of data on HOT-37 and 41. Unfortunately, an absolute radiometric standard is not available for flash fluorometers. In order to correct for instrument drift over the past four years we have checked the relative response of the instrument between each HOT cruise using fluorescent plastic sheeting. The sheeting was placed at a fixed distance (approximately 2 cm) from the instrument lamp in the

dark. This procedure determined if the instrument was performing consistently. As part of our maintenance program, the sensor was returned to the manufacturer for routine servicing on a regular basis. The instrument response changed slightly each time it was returned from servicing. Therefore, we normalized the instrument response each month using the voltage derived at two depth intervals (400-450 dbar and 900 to 1000 dbar). These depths were used because the *in situ* fluorescence at these pressure horizons remained remarkably constant with time. A linear relationship of the form Vn = b Vo + a was used to convert all fluorescence data to a common voltage scale, where Vn is the corrected voltage, Vo is the output voltage and a and b are constants derived from the two deep water intervals. The constants used to correct the fluorescence data for all three years of the time-series program are given in Table 2.8.

In situ beam transmission was collected beginning on HOT-28, using a Sea Tech 25 cm path length instrument. No transmission data were collected on HOT 33 because of equipment problems. Transmission data were collected using the Sea-Bird CTD in a fashion analogous to that described for flash fluorescence. The transmissometer was carefully calibrated as described by the manufacturer before each cruise to correct for instrument drift. The quality controlled 2 dbar binned data are also available via Internet (see Section 8).

Table 2.8: Fluorescence Calibration Factors

Cruise #	Station #	Cast #	a	b	Transmis-someter
33	0	0	0	.5	1
34	0	0	2.9318	0.3112	1
35	0	0	2.9318	0.3112	1
36	0	0	2.9318	0.3112	1
37	0	0	2.9318	0.1556	1
38	0	0	2.9318	0.3112	1
39	0	0	2.9318	0.3112	1
40	0	0	2.9318	0.3112	1
41	2	6	2.9318	0.3112	.9898
42	0	0	0	1	.9947
43	0	0	0	1	.9973

2.2. Water Column Chemical Measurements

Samples for water column chemical analyses were collected at both Station Kahe and Station ALOHA. Most of the samples were collected in the upper 1000 m. As much as possible,

depth profiles of specific chemical constituents were collected on consecutive casts in order to minimize the effects of time-dependent variation within the water column. In addition, samples were collected near the same density or pressure horizons each month in order to facilitate comparisons between monthly profiles. Our strategy was to sample at density horizons within the main thermocline and at pressure horizons above and below this region (i.e., < 150 dbar and > 2000 dbar).

A detailed description of our sampling procedures and analytical methods was given in a separate report (Karl *et al.*, 1990). Abbreviated descriptions of these procedures were given in Chiswell *et al*. (1990). Beyond a general description of our analytical methods, only changes in the procedures described by Winn *et al*. (1991, 1993) are given in this report.

During 1992, water samples were collected using a 24-place aluminum rosette manufactured by Scripps Institution of Oceanography's Oceanographic Data Facility (ODF). Twelve-liter polyvinylchloride sampling bottles, also made by ODF, were used on this rosette. These sample
bottles were equipped with Buna-N rubber O-rings, teflon-coated steel springs and standard General Oceanics sampling valves.

The primary objective of the HOT program is to assess variability in the central Pacific Ocean on annual and interannual time scales. One of our most important concerns, therefore, is to ensure that the highest possible precision and accuracy is consistently maintained for all water column chemical measurements. In order to achieve the highest possible data quality, we have instituted a quality-assurance/quality-control program (see Karl *et al.*, 1990), and have attempted to collect all ancillary information necessary to ensure that our data are not biased by sampling artifacts.

Although approximately 20% of our chemical analyses are replicated (see Karl *et al*., 1990), only mean values are reported in the data sets provided with the report. To assist in the interpretation of these data and to save users the time needed to estimate the precision of individual chemical analyses, we have summarized precision estimates from replicate determinations for each constituent on each HOT cruise during 1992. Whenever possible, we have also monitored the consistency of our analytical results between cruises by maintaining reference materials and by monitoring the concentration of the chemical of interest in the deep sea where month-to-month variability is believed to be small.

2.2.1. Salinity

Salinity samples were collected in 250 ml glass bottles and stored at room temperature in the dark for analysis in our shore-based laboratories. The time between sample collection and

analysis was about one week.

Salinity determinations reported for HOT cruises 33 to 41 were run on a Guildline Autosal #8400. Table 2.9 shows the results of the analysis of laboratory standards run with each set of monthly samples. Typical precision (one standard deviation of triplicate samples from the same Niskin bottle) during 1992 was about 0.001 psu.

Table 2.9: Results for Lab-substandards by Cruise

HOT	Mean Salinity (psu) & # of samples		
	Mean salinity ± standard deviation	# samples	batch #
33	34.46873 ± 0.0040	15	4
34	34.46917 ± 0.0012	16	4
35	34.46973 ± 0.0050	19	3
36	34.50000 ± 0.0024	21	7
37	34.49862 ± 0.0044	41	2
38	34.49970 ± 0.00050	17	5
39	34.49744 ± 0.0169	31	3
40	34.49531 ± 0.0056	18	4
41	34.49848 ± 0.0035	10	4

2.2.2. Oxygen

Oxygen samples were drawn as soon as possible after the rosette arrived on deck and before any other samples were taken. These samples were collected in gravimetrically calibrated (without air buoyancy correction) 125-ml iodine flasks, and immediately fixed for subsequent analysis. Oxygen concentrations were determined using the Carpenter modification (Carpenter, 1965) of the Winkler titration method as described by Winn *et al.* (1991). Starting on HOT 31 we initiated an at-sea computer controlled potentiometric end point titration procedure. This has the primary advantages of analysis at sea while maintaining high precision without operator subjectivity that is inherent in the visual starch end point method.

Oxygen concentrations are reported in units of μmol kg^{-1}. These concentrations were computed assuming that the samples come to the surface adiabatically (i.e., they were drawn into the 125 ml flasks at their *in situ* potential temperature). As was previously described (Winn *et al.*, 1991), this procedure can introduce a systematic error due to the water sample warming enroute to the surface.

As in previous years, we measured the temperature of the seawater sample within individual Niskin bottles at the time that the iodine flask was filled to evaluate the magnitude of this error (i.e., oxygen sample temperature). Oxygen sample temperatures were measured on all HOT cruises during 1992 using a digital thermistor.

Figure 2.3 (top panel) shows a plot of the difference between oxygen sample (on deck) temperature and potential temperature computed from *in situ* temperature at the time of bottle trip versus pressure. The bottom panel of this figure shows a plot of the difference between oxygen concentrations computed using on deck and potential temperatures for all samples collected from HOT 33-43. The scatter observed in delta temperature below 500 m is due primarily to the speed with which the CTD is raised through the thermocline. The depth dependent variability in delta oxygen is a result of the absolute magnitude of the oxygen concentration and the time-series sampling strategy as described by Winn *et al.* (1991). For work of the highest accuracy this systematic error should be considered and at its highest values is similar to the air buoyancy correction of ~0.1 μmol kg^{-1}.

It is interesting to note that although the delta temperature is positive below 100 m (i.e., increasing temperature), it is negative (i.e., decreasing temperature) above this depth to as much as 1.4° C. This can be due to a variety of processes which may include a thermal mass transfer (i.e., water bottle to sample), radiant cooling, evaporative cooling, convective cooling from surrounding water bottles. Periodically, the digital thermometer is compared to a certified NBS thermometer and is generally accurate to within < 0.2° C over the temperature range encountered. Therefore, inaccurate temperatures are unlikely. Since most casts are conducted to 1000 m where the water temperature is approximately 4° C, the PVC walls of the water bottles could be cooled to the point where they would act as a heat sink especially in the warm pool of the euphotic zone. In addition, the sample could lose heat when the air temperature is less than the sample temperature. Approximately half the casts where oxygen samples are collected and sample temperatures recorded are done at night. In the same sense it could gain heat when the ambient temperature is higher. It appears that the heat sink process may be dominant since the deep cast (~4700 m), produces a larger delta temperature than the 1000 m casts and because sample temperatures are

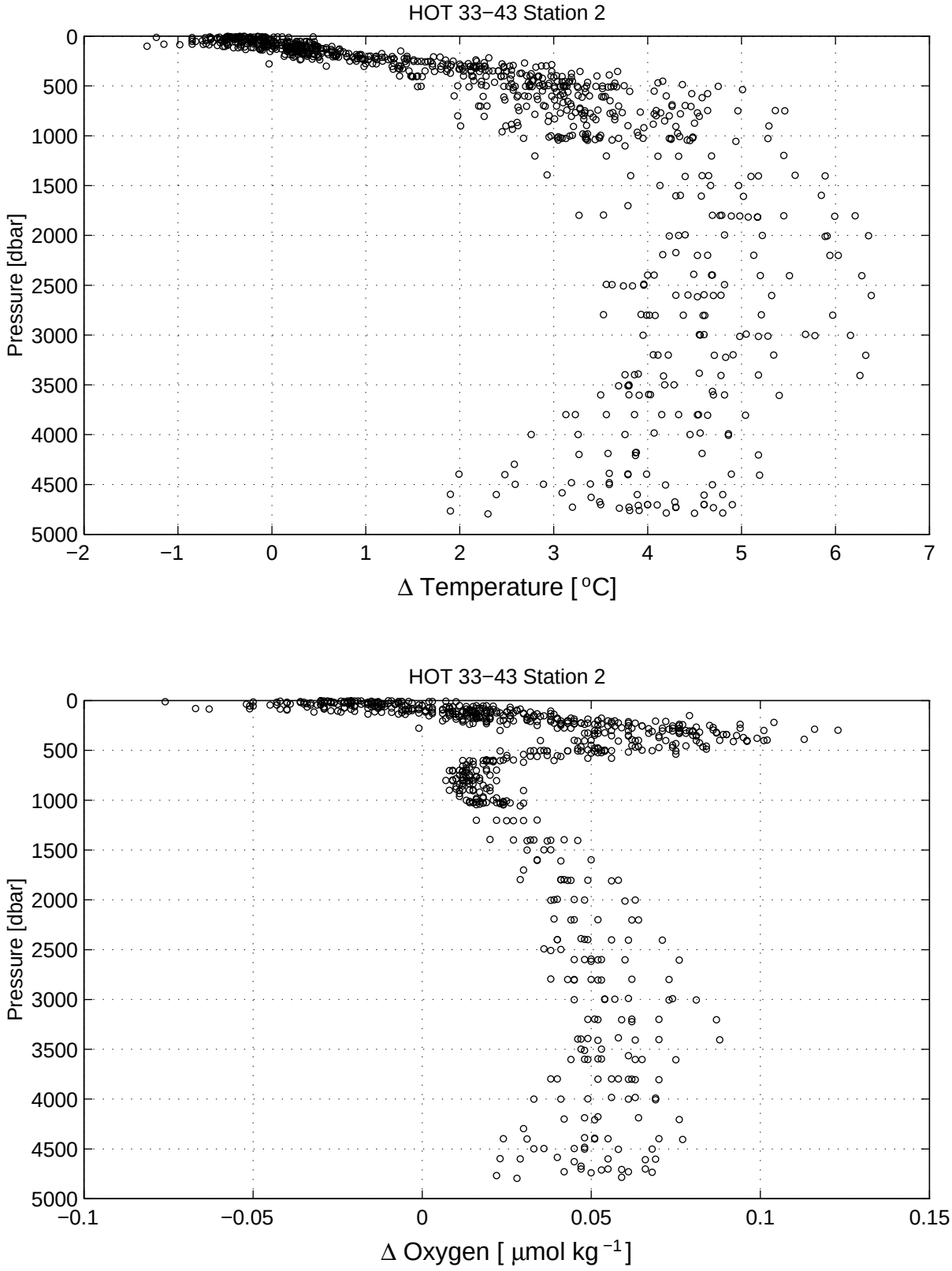

Figure 2.3: Upper Panel: Difference between sample temperature at the time of sample collection and potential temperature calculated from *in situ* temperature at the time of bottle trip. Lower Pannel: Difference in oxygen concentration in units of μmol kg-^{1} using temperatures measured at the time of sample collection and potential temperature computed from *in situ* temperature.

always below *in situ* temperatures even when collected during the heat of the day. It also appears that radiative cooling may play a contributing role since a greater delta temperature is observed at night versus during the day.

The precision of our oxygen analyses was assessed from both an analytical and field perspective. The precision data in Table 2.10 for analytical replicates reflects the pooled mean precision of the primary standards and certified reference standards (i.e., each replicate is the mean of 3 or more determinations). In actuality this is not a true analytical replicate in that there is an added variance component due to the pipetting of the primary standard. However, it does add useful interpretive information and also allows a first order assessment of accuracy from the variance component.

The mean analytical and field precision of our oxygen analysis during 1992 was 0.15% and 0.12% with a mean standard deviation of 0.20 and 0.23 µmol kg^{-1} respectively (Table 2.10). Oxygen concentrations measured over the first four years of the program are plotted at constant density horizons in the deep ocean along with their mean and 95% confidence intervals (Fig. 2.4). The delta values ranged from 3.2 µmol kg^{-1} at 27.675 kg m^{-3} to 6.3 µmol kg^{-1} at 27.758 kg m^{-3} similar to previous years indicating that analytical consistency was maintained throughout the first four years of the program.

2.2.3. Dissolved Inorganic Carbon

Samples for dissolved inorganic carbon (DIC) were measured using a commercial coulometer modified for high-precision measurements as described by Chiswell *et al.* (1990). During 1992 we were provided with primary DIC standards by Dr. Andrew Dickson to help ensure the accuracy of coulometric analyses. The results of these analyses indicated that the precision of replicate samples is approximately 1 µmol kg^{-1} and that our analyses are accurate to within 1 µmol kg^{-1} (Table 2.11).

Table 2.10: Precision of Winkler Titration

	Analytical			Field		
HOT	Mean CV(%) [a]	Mean SD (µM)	n [b]	Mean CV(%)	Mean SD (µM)	n [c]
33	0.37	0.43	4	0.10	0.19	9
34	0.15	0.17	5	0.30	0.63	19
35	0.10	0.15	5	0.09	0.17	17
36	0.13	0.15	3	0.12	0.24	29
37	0.08	0.17	8	0.05	0.09	9
38	0.06	0.10	6	0.16	0.24	10
39	0.95[d]	0.65[d]	1	0.11	0.17	8
40	0.12	0.21	7	0.10	0.17	12
41	0.11	0.18	4	0.12	0.22	19
42	0.17	0.24	9	0.03	0.07	3
43	0.24	0.18	2	0.14	0.29	4

[a]Coefficient of variation expressed as the difference between replicates as a percentage of the mean when duplicate samples were collected, and expressed as the standard deviation as a percentage of the mean for samples collected in triplicate.

[b]Number of mean replicates.

[c]Number of depths from which replicates were collected. Only replicates from depths where oxygen concentrations exceed 100 µmol kg^{-1} were included in the analysis.

[d]Not used in descriptive statistics calculations.

Figure 2.4: Oxygen versus time at three density horizons at Station ALOHA. Oxygen concentration at potential densities of 27.782, 27.758 and 27.675.

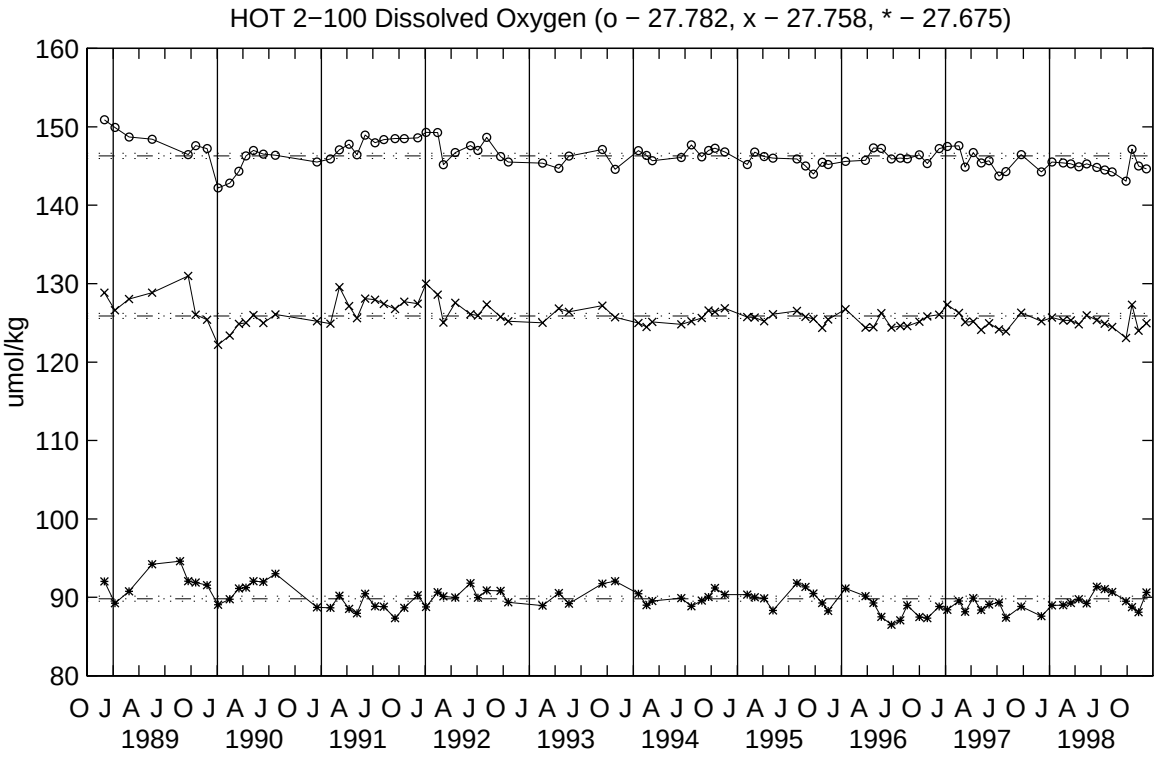

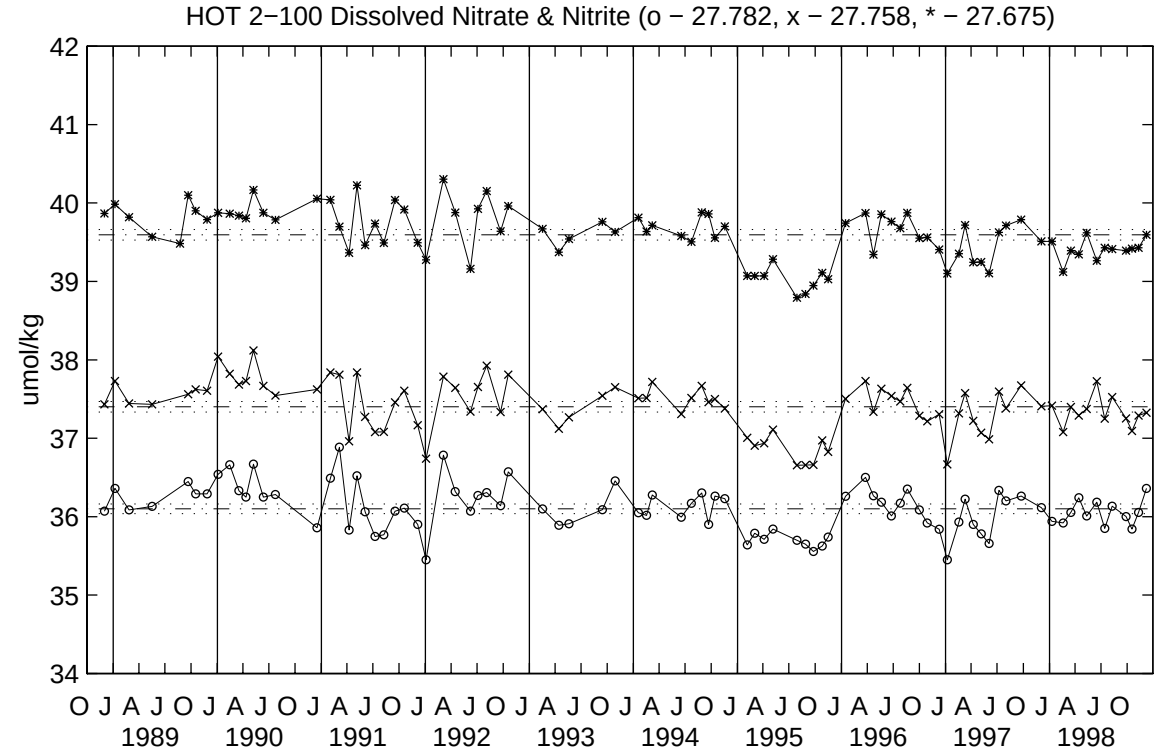

Figure 2.5: As in Figure 2.4, except for concentrations of dissolved [nitrate+nitrite].

Table 2.11: Analysis of Dissolved Inorganic Carbon Standards
(A. Dickson; Batch #10, 1960.7 ± 0.4 µmol kg^{-1})

Cruise	µmol kg^{-1}
33	1961.4
33	1961.0
34	1962.4
35	1962.1
35	1962.6
36	1960.7
37	1961.9
38	1962.2
39	1959.1
40	1960.6
41	1960.1
mean	1961.3
std	±1.1
accuracy	±0.03%

2.2.4. Titration Alkalinity

Titration alkalinity was determined using the Gran titration method of Edmond (1970) as modified by Bradshaw and Brewer (1988), except that an open titration cell was used. Samples were titrated with approximately 0.1 N HCl using a Dosimat 665 digital burette, a Corning semi-micro combination pH electrode and Orion model 940 pH meter. The titration system was computer controlled to automate the procedure. The second end point (V2) was determined with a modified Gran plot, which was corrected for the influence of sulfate and fluoride. The electrode was calibrated with seawater (Tris) buffer (Hansson, 1973; Dickson, 1993). The electrode slope and ε° were determined by an iterative procedure which minimized the residuals of the Gran function over the pH range of 3.5 to 3.0.

The precision of our titration procedure was approximately 5 µequiv/kg. Unfortunately, an absolute alkalinity standard was not available, and the accuracy was established primarily by the value determined for the normality of the titrant. We have intercalibrated the determination between our acid normality with that of Dickson's laboratory at Scripps Institution of Oceanography, where high-accuracy coulometric methods are used for this purpose.

2.2.5. pH

During 1992, pH was measured using recently developed spectrophotometric techniques (Byrne and Breland, 1989; Clayton and Byrne, 1993). We have used m-cresol purple for these measurements. This dye was chosen because it was most appropriate for the full-depth profile work that we are doing at Station ALOHA.

Samples are collected directly into cylindrical 10 cm spectrophotometer cells using tygon tubing attached to one of the two ports and allowing the overflow to pass out of second port. Samples were collected as soon as possible after the rosette sampling bottles arrived on deck. The spectrophotometer cells were flushed with at least three volumes of water and care was taken to ensure that air bubbles were excluded. The cells were then sealed without air spaces and transferred to a 25° C constant temperature bath.

Absorbance measurements were obtained using a dual beam model 3 Perkin-Elmer spectrophotometer. In order to maintain constant temperature during analysis the spectrophotometer cells were placed in a brass cell holder which was maintained at near 25° C with water circulated from a constant temperature bath. Under some circumstances, it was not possible to maintain the cell temperature at precisely 25° C. We therefore routinely measured the temperature of the solution in the spectrophotometer cell during analysis and corrected for slight offsets due to changes in temperature as described below.

Absorbance measurements were made using 0.2 M m-cresol purple in distilled water adjusted to pH 8 with approximately 0.1 N NaOH. After recording baseline absorbances, 50 microliters of 0.2 M m-cresol purple was added to the spectrophotometer cell and absorbance measurements made as described by Clayton and Byrne (1993). The pH on the "total scale" (Dickson, 1984) was calculated as described by Clayton and Byrne (1993). This pH was then converted to the "seawater scale" (Hansson, 1973), as described by DOE (1991). Finally, when pH measurements were made at temperatures slightly different than 25° C, the pH at the measured temperature was converted to the equivalent pH at 25° C using an interative procedure and the equations of Millero (1979).

2.2.6. Inorganic and Organic Nutrients

Samples for the determination of nutrient concentrations were collected in acid-washed 125-ml polyethylene bottles, and immediately frozen for transport to the laboratory. Analyses were conducted at room temperature on a four-channel Technicon Autoanalyzer II continuous flow system, using slight modifications of the Technicon procedures for the analysis of seawater samples (Winn *et al.*, 1991; Karl *et al.*, 1990). A summary of the precision of our dissolved inorganic nutrient analyses from HOT-33 through HOT-43 is shown in Table 2.12. In Figures

2.5-2.7, nutrient concentrations measured at three density horizons are presented along with the current year and all four years mean and 95% confidence intervals. Of the three inorganic nutrients, silicic acid exhibited the greatest variability and phosphate the least. Overall, phosphate ranged from 2.2%

Table 2.12: Precision of Dissolved Nutrient Analyses

	Phosphate				Nitrate + Nitrite				Silicic Acid			
	Analytical[a]		Field[b,c]		Analytical[a]		Field[b]		Analytical[a]		Field[b]	
HOT	mean cv[d]	mean sd[e]	mean cv[d]	mean sd[e]	mean cv[d]	Mean Sd[e]	mean cv[d]	mean sd[e]	mean cv[d]	mean sd[e]	mean cv[d]	mean sd[e]
33	0.7	0.007	0.1	0.003	0.2	0.04	0.1	0.05	1.3	0.25	1.3	1.09
34	0.3	0.012	0.3	0.010	0.4	0.21	0.3	0.10	0.5	1.02	0.4	0.24
35	0.4	0.014	0.1	0.003	0.4	0.24	0.6	0.16	0.2	0.23	0.7	0.78
36	0.2	0.005	0.3	0.010	0.2	0.05	0.2	0.04	0.3	0.24	0.7	0.33
37	0.3	0.012	0.4	0.009	0.2	0.11	0.2	0.08	0.2	0.26	0.4	0.58
38	0.1	0.002	0.1	0.003	0.2	0.06	0.2	0.05	0.1	0.11	4.2	0.66
39	0.3	0.010	0.5	0.011	0.1	0.09	0.2	0.04	0.3	0.50	1.6	0.31
40	1.0	0.008	0.4	0.016	0.5	0.04	0.2	0.08	0.8	0.24	0.8	1.46
41	0.5	0.009	0.8	0.013	0.3	0.07	0.3	0.11	0.4	0.29	0.3	0.20
42	1.0	0.012	2.1	0.005	0.8	0.02	1.1	0.02	0.4	0.02	5.7	0.20
43	1.1	0.009	7.5	0.013	0.5	0.04	1.9	0.02	0.4	0.03	0.4	0.02
Mean	**0.5**	**0.009**	**1.1**	**0.009**	**0.3**	**0.09**	**0.5**	**0.07**	**0.4**	**0.29**	**1.5**	**0.53**
sd	±0.4	±0.004	±2.2	±0.005	±0.2	±0.07	±0.6	±0.04	±0.3	±0.28	±1.8	±0.44
cv	66%	39%	191%	53%	58%	82%	114%	60%	76%	95%	119%	82%

[a]Average coefficient of variation (i.e., standard deviation as a percentage of the mean) for analytical replicates (i.e., replicate analysis of a single sample) for phosphate concentrations ≥ 0.4 µM, [nitrate+nitrite] concentrations ≥ 0.2 µM, and silicic acid concentrations ≥ 0.2 µM.

[b]Average coefficient of variation for field replicates (i.e., analysis of replicate samples from the same Niskin) for the above concentration ranges. HOT 42 and 43 on the R/V Kila used a different set of water bottles which, in retrospect, may have been contaminated.

[c]H42 and 43 phosphate field reps all <0.4µM.

[d]In %

[e]In µmol kg^{-1}

Figure 2.6: As in Figure 2.4, except for concentrations of dissolved phosphate.

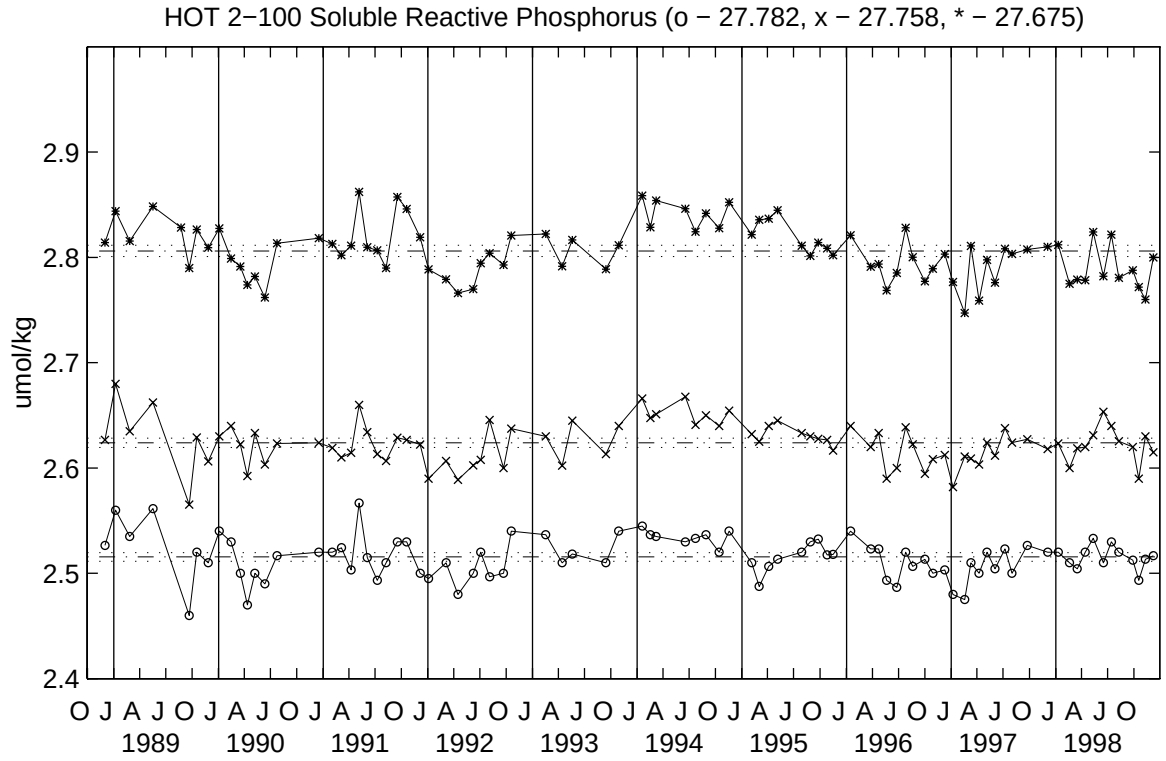

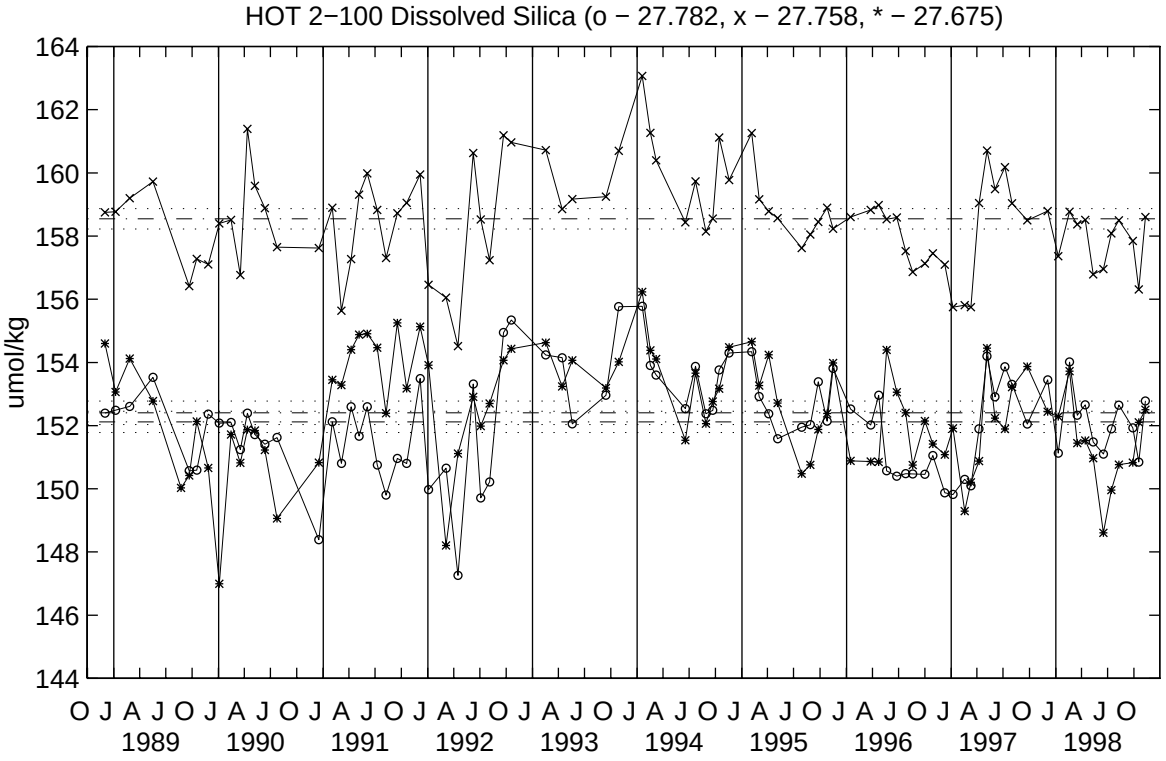

Figure 2.7: As in Figure 2.4, except for concentrations of dissolved silica.

of its deep water mean values while silicic acid ranged up to 4.4%. In addition to standard automated nutrient analysis, specialized chemical techniques were used to determine concentrations of nutrients that are normally on the detection limits of autoanalyzer methods, i.e., [nitrate+nitrite] (Section 2.2.6.5) and soluble reactive phosphorus (Section 2.2.6.6).

2.2.6.1. Nitrate plus Nitrite, Total Dissolved Nitrogen

The sum of [nitrate+nitrite] was measured after reduction of nitrate to nitrite in a copperized cadmium reduction column on the autoanalyzer as described by Chiswell *et al.* (1990) and Karl *et al.* (1990). Total dissolved nitrogen (TDN) was determined following ultraviolet (UV) photo-oxidation (Armstrong *et al.*, 1966; Walsh, 1989) and determinations of the ammonium and nitrate-nitrite mixture formed.

Attempts to measure ammonium by concentration and extraction methods showed that ammonium in these waters is at most 50 nmol kg^{-1}. Ammonium is therefore a very minor portion of total dissolved nitrogen at Station ALOHA. An estimate of dissolved organic nitrogen (DON) is thus determined from the difference between TDN and the sum of [nitrate+nitrite]. A summary of the precision with DON analysis is given in Table 2.13.

2.2.6.2. Soluble Reactive and Total Dissolved Phosphorus

Soluble reactive phosphorus (SRP) was measured by reaction with acidified molybdate reagent and potassium antimonyl tartrate, followed by the subsequent reduction with ascorbic acid. Total dissolved phosphorus (TDP) was measured by UV photo-oxidation, followed by analysis of the oxidation products (Chiswell *et al.*, 1990). Dissolved organic phosphorus (DOP) is measured as the difference between TDP and SRP as described by Chiswell *et al.* (1990). A summary of the precision of DOP analysis is given in Table 2.13.

2.2.6.3. Silica

Soluble reactive silica was measured by reaction with ammonium molybdate at low pH, followed by reduction with ascorbic acid as described by Chiswell *et al.* (1990).

2.2.6.4. Dissolved Organic Carbon

Dissolved organic carbon was determined by high temperature catalytic oxidation using a pure platinum catalyst and infrared detection of the produced carbon dioxide. We are presently participating in an intercalibration exercise to determine standard protocols for analyzing and reporting these data.

Table 2.13: Precision of Dissolved Organic Nutrient Analyses

HOT	DON		DOP	
	FIELD		FIELD	
	mean cv (%)	mean sd (µmol kg^{-1})	mean cv (%)	mean sd (µmol kg^{-1})
33	6.0	0.32	15.4	0.027
34	5.6	0.34	35.7	0.037
35	9.8	0.52	10.1	0.017
36	10.1	0.55	17.1	0.043
37	15.3	0.68	11.4	0.030
38	6.9	0.42	10.1	0.030
39	14.8	0.76	2.0	0.005
40	5.4	0.33	10.3	0.017
41	3.4	0.22	22.6	0.050
42	5.8	0.43	5.9	0.013
43	10.7	0.82	28.6	0.063
mean	**8.5**	**0.49**	**15.4**	**0.030**
sd	±3.9	±0.19	±10.0	±0.017
cv	46%	40%	65%	57%

2.2.6.5. Low Level Nitrate Plus Nitrite

Surface water samples (<100 m) have [nitrate+nitrite] concentrations below the approximately 0.03 µM detection limit of the Technicon Autoanalyzer. To achieve high-precision high-accuracy measurements at these low levels, we employed the chemiluminescent method of Cox (1980) and Garside (1982). In this method, nitrite and nitrate were chemically reduced to gaseous nitric oxide by an acidic solution of concentrated sulfuric acid, ferrous ammonium sulfate and ammonium molybdate. The reduced nitric oxide was carried by an inert carrier gas (argon) through a series of traps to remove acid and water vapors and then into an Antek model 720 chemiluminescent nitrogen analyzer. The nitrogen analyzer combined nitric oxide with ozone to produce a metastable nitrogen dioxide. The nitrogen dioxide subsequently emitted a photon as it returned to ground state, and the emitted light was detected by a photomultiplier tube. The integrated electrical signal produced by the photomultiplier is

proportional to the content of [nitrate+nitrite] in the sample. The calibration of the low level nitrate/nitrite analysis was performed using a stock solution of KNO_3 (1 µM) in deionized distilled water (DDW). Working standards were prepared fresh by volumetric dilutions of the stock using acid-washed glass pipettes and flasks. In order to maintain the accuracy of the analysis, serial dilutions of a certified reference standard (CSK) are included in every sample run, in case stock solutions become contaminated or microbially altered during storage. The limit of quantification for [nitrate+nitrite] was approximately 1-2 nM, while precision and accuracy of the analysis were approximately 1 nM.

2.2.6.6. Low Level Soluble Reactive Phosphorus

Phosphate concentrations in the euphotic zone were also below the approximately 0.02 µM detection limit of the Technicon autoanalyzer. In order to resolve variability in phosphate concentrations in the euphotic zone we employed the "MAGIC" procedure of Karl and Tien (1992). With this method, soluble reactive phosphate was concentrated by co-precipitation with $Mg(OH)_2$ and the standard molybdenum blue color reaction was used to quantify the orthophosphate in the concentrated samples. Samples were collected in acid washed 500 ml polyethylene containers and frozen immediately for transport to the laboratory.

2.2.7. Particulate Carbon and Nitrogen

Samples for particulate carbon (PC) and particulate nitrogen (PN) were prefiltered through a 202-µm Nitex mesh, collected onto a combusted GFF filter and analyzed using a commercial CHN analyzer (Chiswell *et al.*, 1990).

2.2.8. Particulate Phosphorus

Samples for particulate phosphorus (PP) were prefiltered through a 202-µm Nitex mesh, collected onto a combusted GFF filter and oxidized by high temperature ashing. The resultant orthophosphate was measured spectrophotometrically (Chiswell *et al.*, 1990).

2.2.9. Pigments

Chlorophyll a (chl *a*) and phaeopigments were measured fluorometrically using standard techniques (Strickland and Parsons, 1972). Analytical precision for fluorometric chl *a* on replicate field sample determinations in 1992 are summarized in Table 2.14. Data for 1991 determinations are also presented here because they were omitted in the previous data report (Winn *et al.*, 1993). Integrated values for pigment concentrations were calculated using the trapezoid rule. In addition to the fluorometric determination of pigments, we also measured chl *a* and accessory photosynthetic pigments (Table 2.15) by high-performance liquid chromatography (HPLC)

Table 2.14: Precision of Fluorometric Analyses of Chlorophyll *a* and Phaeopigment

Cruise	Chl *a* CV(%)	Std. (µg l^{-1})	Phaeo CV(%)	Std. (µg l^{-1})
23	3.3	0.003	4.3	0.003
24	3.5	0.005	5.7	0.011
25	3.0	0.004	3.2	0.007
26	6.1	0.010	9.6	0.014
27	3.5	0.007	3.6	0.008
28	4.6	0.005	4.3	0.008
29	4.8	0.006	5.5	0.010
30	4.1	0.007	3.3	0.009
31	4.2	0.005	3.5	0.006
32	4.6	0.007	5.4	0.014
mean	4.2	0.006	4.9	0.009
sd	±0.9	±0.002	±2.0	±0.004
cv	22%	33%	40%	39%
n	10	10	10	10

Cruise	Chl *a* CV(%)	Std. (µg l^{-1})	Phaeo CV(%)	Std. (µg $^{-1}$)
33	4.8	0.007	5.7	0.014
34	3.4	0.005	6.0	0.009
35	2.8	0.004	4.9	0.008
36	10.2	0.013	13.0	0.034
37	4.9	0.007	7.3	0.011
38	5.3	0.005	5.5	0.009
39	6.9	0.008	5.6	0.011
40	5.1	0.006	5.6	0.011
41	4.3	0.006	7.7	0.018
42	4.0	0.007	3.2	0.008
43	4.0	0.006	4.7	0.011
mean	5.1	0.006	6.3	0.013
sd	±2.0	±0.002	±2.5	±0.007
cv	40%	36%	40%	56%
n	11	11	11	11

Table 2.15: HPLC Pigment Analysis

Pigment	RF[a]	RT[b]
Chlorophyll c_3	0.000455	
Chlorophyll (c_1 + c_2) & Mg 3,8 DVP4A5	0.000455	
Peridinin	0.000587	.316
19'-Butanoyloxyfucoxanthin	0.000421	.380
Fucoxanthin	0.000454	.415
19'-Hexanoyloxyfucoxanthin	0.000401	.450
Prasinoxanthin	0.000434	.487
Diadinoxanthin	0.000261	.635
Zeaxanthin	0.000305	.766
Chlorophyll *b*	0.001423	.888
Chlorophyll *a*	0.000729	1.000
Chlorophyll c_4	0.000455	
Carotens	0.000264	1.612

[a]RF - Response Factor (mg pigment per unit absorbance peak area at 436 nm).
[b]RT - Retention Time (relative to chlorophyll *a*)

according to the procedure described by Bidigare *et al.* (1990). A known amount of canthaxanthin was added to each sample as an internal standard and all pigments were quantified using external standards provided during the JGOFS pigment intercalibration exercises.

2.2.10. Adenosine 5'-Triphosphate

Water column adenosine 5'-triphosphate (ATP) concentrations were determined as described by Winn *et al.* (1991). The precision of ATP determinations in 1992 are given in Table 2.16.

Table 2.16: Precision of ATP Analyses

Cruise	CV[a] (%)	Std (µg m^{-3})
33	9	1.8
34	16	1.4
35	12	1.5
36	10	2.4
37	13	1.4
38	19	2.3
39	11	1.6
40	13	1.7
41	10	1.4
Mean	13	1.7
Sd	±3	0.4
Cv	24%	22%
N	9	9

[a]Coefficient of variation as the percent of mean of all triplicate determinations for each cruise.

2.3. Biogeochemical Rate Measurements

2.3.1. Primary Productivity

Photosynthetic production of organic matter was measured by the ^{14}C method. Incubations were conducted *in situ* using a free-drifting array equipped with a VHF transmitter and a strobe light as described by Winn *et al.* (1991). Twelve-hour *in situ* incubations were conducted during 1992 on all cruises on which it was possible to do primary production experiments. Integrated carbon assimilation rates were calculated using the trapezoid rule. In all cases, the shallowest values (generally 5 m) were extended to 0 m. The deepest primary production measurements (generally 175 m) were extrapolated to a value of zero at 200 m.

2.3.2. Particle Flux

Particle flux was measured using sediment traps deployed on a free-floating array for approximately 72 hours each month. Sediment trap design and sample collection methods, as well as sample analysis, were performed as previously described in Winn *et al.* (1991).

2.4. ADCP Measurements

Shipboard ADCPs were available and used on the R/V WECOMA cruises (HOT-33 to -36) and on the R/V MOANA WAVE cruises (HOT-37 to -41). RDI model VM-150 instruments were used on both ships. The performance of the R/V WECOMA installation was superior to that on the R/V MOANA WAVE; the R/V WECOMA appears to generate much less acoustic noise when underway.

ADCP and navigation data were recorded successfully throughout most of the cruises. Major ADCP recording gaps occurred on the northbound section on HOT-34, on-station and southbound on the second leg of HOT-37, and on-station on HOT-41. Instrument malfunctions caused the many brief gaps in ADCP recording on HOT-38.

Navigation on all cruises was almost entirely from GPS. The raw reference layer velocity estimates were especially noisy on HOT-34, primarily caused by less accurate position information: position fixes were recorded at fixed 1-minute intervals, independent from the ADCP data, whereas a fix was recorded at the end of each ADCP data record for all the other cruises. The raw reference layer velocity estimates were moderately noisy on HOT-33 because of the shorter ensemble interval used, ranging from one to three minutes, compared to the 5-minute interval used throughout most of the other HOT cruises. The first day of HOT-40 exhibits extraordinarily clean and smooth reference layer velocity estimates, demonstrating the accuracy of GPS in the absence of Selective Availability (SA), the deliberate degradation of GPS signals by the Defense Department. The noisier reference layer velocities during the remainder of the cruise showed the effects of SA being turned on.

2.5. Optical Measurements

Incident irradiance at the sea surface was measured on each HOT cruise with a Licor LI-200 data logger and cosine collector. Irradiance levels were averaged over 10-minute intervals and integrated over the daylight period during the primary production experiment. Vertical profiles of Photosynthetically Available Radiation (PAR) were also obtained on most cruises during 1992 with a Biospherical Instruments model PNF-300 optical profiler. These data sets were too large to be included in this report. The entire data set is available via Internet as described Section 8.

2.6. Meteorology

Meteorological data were collected at four-hour intervals while on station. Wind speed and direction, atmospheric pressure, wet- and dry- bulb air temperature, sea surface temperature, cloud cover and sea state were recorded as described in Chiswell *et al.* (1990). In this report we

compared these data to those collected at the nearest NDBC (National Data Buoy Center) buoy. The buoy data were obtained from the National Oceanic Data Center.

2.7. XBT

On cruises where Stations 3, 4, and 5 were occupied, XBT casts were generally made spaced seven minutes of latitude apart during the transit to or from Station ALOHA. Sippican T-7 probes having a maximum depth of 750 m were used. The files were screened for bad and missing data, and no corrections were applied.

3. Cruise Summaries

3.1. HOT-33; January 3-8, 1992; R/V WECOMA;
C. Winn, Chief Scientist

HOT Science Party departed Snug Harbor at 1000, January 3 with 13 scientists on-board and returned at 0700, January 8. Weather was generally calm for the duration of the cruise. Station Kahe was occupied enroute to Station ALOHA. After core work at Station ALOHA was accomplished, CTD stations were occupied at 158°W at 23°25'N (Station 3) 21°57.8'N (Station 4) and 21°46.6'N (Station 5). Each of these stations was conducted with the 24-place rosette and with sampling like that at Station Kahe. The 100-mile section to Kahuku on 158°W was filled with XBTs. Shipboard ADCP was run throughout the cruise.

CTD operations

Two CTD casts were conducted at Station Kahe and 21 at Station ALOHA with no major problems. After the burst sampling period, the 24 place rosette was replaced with a 12 place rosette for lowered ADCP (LADCP) profiling. Five LADCP casts were made at Station ALOHA. Additionally, 4 expendable current profilers (XCP) were deployed. Single CTD casts were made at Stations 3, 4 and 5. Expendable bathythermographs (XBT) were deployed at regular intervals between Stations 3 and 5.

Water sampling

All water samples for WOCE and JGOFS measurements were obtained. A Go-Flo cast was conducted to collect water at eight depths for the primary production experiment.

Primary production and Particle flux

Sediment trap and primary production arrays were deployed and recovered without incident. All traps and incubation bottles were recovered.

Ancillary projects

A. Anbar (Caltech) collected water samples for rhenium analysis. L. Tupas (UH) and K. Leckrone (IU) tested a DOC analyzer and collected water samples for dissolved organic carbon measurements. Water samples were collected for D. Keeling (SIO-UCSD) and P. Quay (UW) for inorganic carbon measurements. Water samples were collected for L. Campbell (UH) for flow cytometric analysis of microorganisms.

3.2. HOT-34; February 12-17, 1992; R/V WECOMA; F. Bingham, Chief Scientist

HOT Science Party departed Snug Harbor at 1015, February 12 with 14 scientists on-board and returned at 0945, February 17. Weather was calm the first day but deteriorated as the cruise progressed. There was heavy rain on the 13th and 14th. A tarp was set up to cover the CTD-rosette package while on deck. The weather improved considerably after that. Station Kahe was occupied enroute to Station ALOHA. After core work at Station ALOHA was accomplished, Stations 3, 4 and 5 were occupied. Shipboard ADCP was run throughout the cruise.

CTD operations

One CTD cast was made at Station Kahe and 19 at Station ALOHA. The ALOHA casts included two deep casts for oxygen sensor calibration (M. Atkinson, P.I.). Yo-yo casts were then conducted between 400 and 700 meters for S. Kennan. Single CTD casts were made at Stations 3, 4 and 5. Expendable bathythermographs (XBT) were deployed at regular intervals between Stations 3 and 5.

Water sampling

All water samples for WOCE and JGOFS measurements were obtained. A Go-Flo cast was conducted to collect water at eight depths for the primary production experiment.

Primary production and Particle flux

Sediment trap and primary production arrays were deployed and recovered without incident. Additional sediment traps were deployed for L. Sautter (Lamont), J. Dore (UH) and J. Christian (UH). All traps and incubation bottles were recovered.

Ancillary projects

C. Stump (UW) collected water samples for oxygen analysis and respiration experiments. Water samples were collected for D. Keeling (SIO-UCSD) and P. Quay (UW) for inorganic carbon measurements. Water samples were collected for L. Campbell (UH) for flow cytometric analysis of microorganisms.

3.3. HOT-35; March 3-8, 1992; R/V WECOMA; S. Chiswell, Chief Scientist

HOT Science Party departed Snug Harbor at 1000, March 3 with 13 scientists on-board and returned at 0800, March 8. Weather was generally calm for the duration of the cruise. Station Kahe was occupied enroute to Station ALOHA. After core work at Station ALOHA was accomplished, Stations 3, 4 and 5 were occupied. At different times during the cruise, 5 inverted echo sounders (IES) were recovered at various locations. Shipboard ADCP was run throughout the cruise. Surface net tows at Station ALOHA collected two or three morphological forms of *Trichodesmium*.

CTD operations

One CTD cast was conducted at Station Kahe and 12 at Station ALOHA. Two CTD casts were made at Station 3 and one each at Stations 4 and 5. Expendable bathythermographs were deployed at regular intervals between Stations 3 and 5. A deep cast for oxygen sensor calibration (M. Atkinson, P.I.) was conducted at Station ALOHA and Station 3.

Water sampling

All water samples for WOCE and JGOFS measurements were obtained. A Go-Flo cast was conducted to collect water at eight depths for the primary production experiment.

Primary production and Particle flux

Sediment trap and primary production arrays were deployed and recovered without incident. All traps and incubation bottles were recovered.

Ancillary projects

Water samples were collected for D. Keeling (SIO-UCSD) and P. Quay (UW) for inorganic carbon measurements. Water samples were collected for L. Campbell (UH) for flow cytometric analysis of microorganisms. J. Bower (UH) collected net samples of *Trichodesmium*

and planktonic squid as well as adult squid by jigging. J. Yuan (UH) collected water samples for trace metal analysis.

3.4. HOT-36; April 15-20, 1992; R/V WECOMA; C. Winn, Chief Scientist

HOT Science Party departed Snug Harbor at 0900, April 15 with 13 scientists on-board and returned at 0700, April 20. Weather was generally calm with occasional rain showers during the cruise. Station Kahe was occupied enroute to Station ALOHA. After core work at Station ALOHA was accomplished, Stations 3, 4 and 5 were occupied. Shipboard ADCP was run throughout the cruise. There was some evidence of *Trichodesmium* in the surface waters at ALOHA on April 17th, but quickly disappeared thereafter.

CTD operations

One cast was made at Station Kahe and 19 at Station ALOHA. Single casts were made at Stations 3, 4 and 5. Expendable bathythermographs were deployed at regular intervals between Stations 3 and 5.

Water sampling

All water samples for WOCE and JGOFS measurements were obtained. A Go-Flo cast was conducted to collect water at eight depths for the primary production experiment. One Go-Flo bottle did not close properly during the operation resulting in the loss of one depth for the experiment.

Primary production and Particle flux

Sediment trap and primary production arrays were deployed and recovered without incident. One depth was eliminated from the primary production array due to lack of water sample. All traps and incubation bottles were recovered.

Ancillary projects

C. Stump (UW) collected water samples for oxygen analysis and respiration experiments. Water samples were collected for D. Keeling (SIO-UCSD) and P. Quay (UW) for inorganic carbon measurements. Water samples were collected for L. Campbell (UH) for flow cytometric analysis of microorganisms.

3.5. HOT-37; June 5-11, 1992; R/V MOANA WAVE;
D. Karl, Chief Scientist, Leg 1
D. Hebel, Chief Scientist, Leg 2

Leg 1 of HOT-37 departed Snug Harbor on June 5. During leg 1, 4 inverted echo sounders were successfully deployed at locations near Station ALOHA. Additionally, 4 Parflux-type (MK-21) sequencing sediment traps were deployed. The floating sediment traps were also deployed on this leg before the science party returned to Snug Harbor on June 7. HOT Science Party for leg 2 boarded on June 7 returned on June 11. Weather was generally calm for the duration of the whole cruise. Station Kahe was occupied enroute to Station ALOHA. Shipboard ADCP was run throughout the cruise.

Shortly after departing Station Kahe the R/V MOANA WAVE lost its starboard main engine. Only the core work was completed on this cruise. Stations 3, 4 and 5 were not occupied.

CTD operations

Two CTD casts were made at Station Kahe and 14 at Station ALOHA. After all work at Station ALOHA was accomplished, a spatial CTD survey by S. Kennan (UH) was conducted enroute to the recovery of the sediment traps.

Water sampling

All water samples for WOCE and JGOFS measurements were obtained. A Go-Flo cast was conducted to collect water at eight depths for the primary production experiment.

Primary production and Particle flux

Sediment trap and primary production arrays were deployed and recovered without incident. All traps and incubation bottles were recovered.

Ancillary projects

S. Emerson (UW) and R. Schudlich (UW) collected water samples for oxygen analysis and respiration experiments. Water samples were collected for D. Keeling (SIO-UCSD) and P. Quay (UW) for inorganic carbon measurements. Water samples were collected for L. Campbell (UH) for flow cytometric analysis of microorganisms.

3.6. HOT-38; July 3-7, 1992; R/V MOANA WAVE;
E. Firing, Chief Scientist

HOT Science Party departed Snug Harbor at 0800, July 3 with 18 scientists on-board and returned at 1445, July 7. Weather was moderate with a few showers for the duration of the cruise.

Station Kahe was occupied enroute to Station ALOHA. After core work at Station ALOHA was accomplished, Station 3 was occupied. Shipboard ADCP was run throughout the cruise.

CTD operations

One CTD cast was made at Station Kahe and 16 at Station ALOHA. Lowered ADCP casts were conducted from the stern in between the regular CTD casts. One CTD cast was made at Station 3.

Water sampling

All water samples for WOCE and JGOFS measurements were obtained. A Go-Flo cast was conducted to collect water at eight depths for the primary production experiment.

Primary production and Particle flux

Sediment trap and primary production arrays were deployed and recovered without incident. A. Ferrara (UH-REU) attached his experimental set-up for carbonate dissolution on the sediment trap line. All traps and incubation bottles were recovered.

Ancillary projects

A. Anbar (Caltech) collected water samples for rhenium analysis. C. Stump (UW) collected water samples for oxygen measurements and respiration experiments. D. Wilson, M. Bushnell (AOML) and E. Firing (UH) conducted the LADCP testing. REU students J. Girton and T. Ferrara conducted experiments. L. Tupas (UH) and J. Reichelderfer (UH) tested a DOC analyzer and collected water samples for DOC analysis. Water samples were collected for D. Keeling (SIO-UCSD) and P. Quay (UW) for inorganic carbon measurements. Water samples were collected for L. Campbell (UH) for flow cytometric analysis of microorganisms.

3.7. HOT-39; August 3-8, 1992; R/V MOANA WAVE; C. Winn, Chief Scientist

HOT Science Party departed Snug Harbor at 1700, August 3 with 14 scientists on-board and returned at 0730, August 8. Weather was generally calm for the duration of the cruise. Station Kahe was occupied enroute to Station ALOHA. After core work at Station ALOHA was accomplished, Station 3 was occupied. Shipboard ADCP was run throughout the cruise.

CTD operations

One CTD cast was made at Station Kahe and 18 at Station ALOHA. A single deep cast for oxygen sensor calibration (M. Atkinson, P.I.) was made at Station 3. The CTD transect was

canceled due to a defective block and XBT's were not working properly.

Water sampling

All water samples for WOCE and JGOFS measurements were obtained. A Go-Flo cast was conducted to collect water at eight depths for the primary production experiment.

Primary production and Particle flux

Sediment trap and primary production arrays were deployed and recovered without incident. All traps and incubation bottles were recovered.

Ancillary projects

D. Wilbur (UW) collected water samples for oxygen measurements and respiration experiments. Water samples were collected for D. Keeling (SIO-UCSD) and P. Quay (UW) for inorganic carbon measurements. Water samples were collected for L. Campbell (UH) for flow cytometric analysis of microorganisms.

3.8. HOT-40; September 20-25, 1992; R/V MOANA WAVE; D. Hebel, Chief Scientist

HOT Science Party departed Snug Harbor at 0900, September 20 with 11 scientists on-board and returned at 0700, September 25. Calm seas, sunny skies and light winds prevailed for the duration of the cruise. Station Kahe was occupied enroute to Station ALOHA. After core work at Station ALOHA was accomplished, Station 3 was occupied. Shipboard ADCP was run throughout the cruise.

CTD operations

Two CTD casts were conducted at Station Kahe and 16 at Station ALOHA. One CTD cast was made at Station 3. S. Kennan (UH) conducted a CTD tow-yo transect towards the sediment traps and continued the transect towards Kahuku Point after the trap pickup.

Water sampling

All water samples for WOCE and JGOFS measurements were obtained. A Go-Flo cast was conducted to collect water at eight depths for the primary production experiment.

Primary production and Particle flux

Sediment trap and primary production arrays were deployed and recovered without

incident. All traps and incubation bottles were recovered.

Ancillary projects

C. Stump (UW) collected water samples for oxygen measurements and respiration experiments. Water samples were collected for D. Keeling (SIO-UCSD) and P. Quay (UW) for inorganic carbon measurements. Water samples were collected for L. Campbell (UH) for flow cytometric analysis of microorganisms. Water samples were collected for T. Takahashi (Lamont) for pCO_2 measurements.

3.9. HOT-41; October 17-22, 1992; R/V MOANA WAVE; C. Winn, Chief Scientist

HOT Science Party departed Snug Harbor at 0900, October 17 with 14 scientists on-board and returned at 0900, October 22. Good weather prevailed for the duration of the cruise. Station Kahe was occupied enroute to Station ALOHA. After core work at Station ALOHA was accomplished, a spatial CTD survey was conducted. Shipboard ADCP was run throughout the cruise.

CTD operations

Two CTD casts were conducted at Station Kahe and 17 at Station ALOHA. After CTD operations at ALOHA were completed, S. Kennan (UH) conducted a CTD spatial survey along 158°W heading first towards the sediments traps, then towards Oahu.

Water sampling

All water samples for WOCE and JGOFS measurements were obtained. A Go-Flo cast was conducted to collect water at eight depths for the primary production experiment.

Primary production and Particle flux

Sediment trap and primary production arrays were deployed and recovered without incident. All traps and incubation bottles were recovered.

Ancillary projects

D. Wilbur (UW) collected water samples for oxygen measurements and respiration experiments. C. Measures (UH) and J. Yuan (UH) collected water samples for trace metal analysis. Water samples were collected for D. Keeling (SIO-UCSD) and P. Quay (UW) for inorganic carbon measurements. Water samples were collected for L. Campbell (UH) for flow cytometric analysis of microorganisms.

3.10. HOT-42, November 23-25, 1992: R/V KILA;
D. Hebel, Chief Scientist

Science party of 4 personnel departed Snug Harbor at 0830, November 23 and returned at 0730, November 25. Station Kahe was occupied prior to Station ALOHA. Weather was relatively good with calm seas.

CTD operations

Standard CTD casts were not possible for this cruise. Instead, a Seacat internal recording CTD with external transmissometer was attached to a Kevlar line and deployed with several Niskin bottles attached at different depths up to 250 meters. A total of seven casts were conducted within an 18 hour period.

Water sampling

Water samples for JGOFS measurements were collected.

Primary production and Particle flux

These experiments were not conducted on this cruise.

Ancillary projects

C. Stump (UW) collected water samples for oxygen measurements and respiration experiments. Water samples were collected for D. Keeling (SIO-UCSD) for inorganic carbon measurements. Water samples were collected for L. Campbell (UH) for flow cytometric analysis of microorganisms. Water samples were collected for T. Takahashi (Lamont) for pCO_2 measurements.

3.11. HOT-43, December 15-17, 1992: R/V KILA,
D. Hebel, Chief Scientist

Science party of 7 personnel departed Snug Harbor at 0830, December 15 and returned at 0730, December 17. The ship proceeded directly to Station ALOHA and operations were confined to the primary study site. Weather was overcast with some swell.

CTD operations

Standard CTD casts were not possible for this cruise. Instead, a Seacat internal recording CTD with external transmissometer was attached to a Kevlar line and deployed with several Niskin bottles attached at different depths up to 250 meters. A total of nine casts were conducted within an 21 hour period.

Water sampling

Water samples for JGOFS measurements were collected.

Primary production and Particle flux

These experiments were not conducted on this cruise.

Ancillary projects

C. Stump (UW) collected water samples for oxygen measurements and respiration experiments. Water samples were collected for D. Keeling (SIO-UCSD) and P. Quay (UW) for inorganic carbon measurements. Water samples were collected for L. Campbell (UH) for flow cytometric analysis. J. Bower (UH) collected squid samples by jigging.

4. Results

4.1. Hydrography

4.1.1. 1992 CTD Profiling Data

Continuous profiles of temperature, salinity, oxygen and potential density (σ_θ) were collected at both Station Kahe and Station ALOHA. The data collected for Station ALOHA during 1992 are presented in Figures 6.1.1a-11a. The results of bottle determinations of oxygen, salinity and inorganic nutrients are also shown. In addition, stack plots of CTD temperature and salinity profiles for all 1000 m casts conducted at Station ALOHA are presented (Fig. 6.1.1b-11b). The data collected for Station Kahe during 1992 are presented in Figures 6.1.1c-11c. The temperature, salinity and oxygen profiles obtained from the deep casts at Station ALOHA during 1992 are presented in Figures 6.1.12-14. Stack plots of CTD temperature and salinity profiles for stations other than Kahe or ALOHA are presented in Figures 6.1.15-17.

4.1.2. Time-series Hydrography, 1988-1992

The hydrographic data collected during the first four years of HOT are presented in a series of contour plots (Figures 6.2.1-14). These figures show the data collected in 1992 within the context of the longer time-series database. The CTD data used in these plots are obtained by averaging the data collected by a 36-hour period of burst sampling. Therefore, much of the variability which would otherwise be introduced by tidal and near inertial oscillations in the upper ocean has been removed. Figures 6.2.1 and 6.2.2 show the contoured time-series record for potential temperature and density in the upper 1000 dbar for all HOT cruises through 1992. Seasonal variation in temperature for the upper ocean is apparent in the maximum of near-surface temperature of about 26°C and the minimum of approximately 23°C. Oscillations in the depth of the 5°C isotherm below 500 m appear to be relatively large with displacements up to 75 m. The main pycnocline is observed between 100 and 600 dbar, with a seasonal pycnocline developing between June and December in the 50-100 dbar range (Figure 6.2.2). The cruise-to-cruise changes between February and July 1989 in the upper pycnocline illustrate that variability in density is not always resolved by our quasi-monthly sampling.

Figures 6.2.3-6 show the contoured time-series record for salinity in the upper 1000 dbar for all HOT cruises through 1992. The plots show both the CTD and bottle results plotted against pressure and potential density. Most of the differences between the contoured sections of bottle salinity and CTD salinity are due to the coarse distribution of bottle data in the vertical as compared to the CTD observations. Some of the bottles in Figure 6.2.6 are plotted at density values lower than the indicated sea surface density. This is due to surface density changing from cast to cast within each cruise, and even between the downcast and upcast during a single cast.

Surface salinity is variable from cruise-to-cruise, with no obvious seasonal cycle. The salinity maximum is generally found between 50 and 150 dbar, and within the potential density range 24-25 kg m^{-3}. A salinity maximum region extends to the sea surface in the latter part of 1988 and 1990, as indicated by the 35.2 psu contour reaching the surface. This contour nearly reaches the surface late in 1989. The maximum value of salinity in this feature is subject to short-term variations of about 0.1 psu, which are probably due to the proximity of the HOT site to the region where this water is formed at the sea surface (cf. Tsuchiya, 1968). The salinity minimum is found between 400 and 600 dbar (26.35-26.85 kg m^{-3}). There is no obvious seasonal variation of this feature, but there are distinct periods of higher than normal minimum salinity in early 1989, in the fall of 1990 and early 1992. These variations are related to the episodic appearance at the HOT site of energetic finestructure and submesoscale water mass anomalies (Lukas and Chiswell, 1991).

Figures 6.2.7 and 6.2.8 show contoured time-series for oxygen in the upper 1000 dbar at the HOT site. The oxygen data show a strong oxycline between 400 and 625 dbar (26.25-27.0 kg m^{-3}), and an oxygen minimum centered near 800 dbar (27.2 kg m^{-3}). During 1988-89 and 1991, there was a persistent oxygen maximum near 300 dbar (25.75 kg m^{-3}), which appeared only weakly and intermittently during 1990 and 1992. The oxygen minimum exhibited some interannual variability as well, with values less than 30 µmol kg^{-1} appearing in the last half of 1989 and the first half of 1990 and then reappearing, less intensely, in 1991 and 1992. The surface layer shows a seasonality in oxygen concentrations, with highest values in the winter. This roughly corresponds to the minimum in surface layer temperature (Figure 6.2.1). An oxygen maximum at about 100 m appears in the latter half of 1991 and persists through 1992.

Figures 6.2.9-14 show [nitrate+nitrite], phosphate and silicic acid at the HOT site plotted against both pressure and potential density. The nitricline is located between about 200 and 600 dbar (25.75-27 kg m^{-3}; Figures 6.2.9-10). Most of the variations seen in these data are associated with vertical displacements of the density structure, and when [nitrate+nitrite] is plotted versus potential density, most of the contours are level. The upper reaches of the water column show considerable variability in density space. There is some indication of an annual cycle with a depression in both [nitrate+nitrite] and in phosphate at the top of the nutricline in the spring of 1990 and 1991. This variability is probably due to a combination of biological and physical processes at the base of the euphotic zone. A third exception is found during March-April 1990 when elevated levels of [nitrate+nitrite] are seen between 25.5 and 26.25 kg m-3. The phosphate (Figures 6.2.11 and 6.2.12) and silicic acid (Figures 6.2.13-14) contour plots are, in general, similar to the [nitrate+nitrite] plot.

4.2. Flash Fluorescence and Beam Transmission

Stack plots of the flash fluorescence and beam transmission results from each HOT cruise in 1992 are presented in Figures 6.3.1-11. Transmission data were collected on all cruises except HOT-33 because of equipment problems. *In situ* flash fluorescence profiles show the fluorescence maximum at the base of the euphotic zone, characteristic of the central North Pacific Ocean. Percent transmission profiles consistently show increased attenuation due to increased particle load at depths shallower than 100 dbar. Both fluorescence and beam transmission profiles show the influence of internal waves when plotted against pressure, but remain relatively constant within a cruise when plotted in density space. However, both data sets show substantial cruise-to-cruise variability in these properties.

Representative fluorescence profiles for a period of three years are shown in Figures 6.3.12 and 13. In order to facilitate comparison, only night-time profiles are presented after normalization to the average density profile obtained from the CTD burst sampling for each cruise. Month-to-month variability in the average depth of the fluorescence maximum is apparent. This is particularly evident in year 3 where the depth of the fluorescence maximum appears to increase in mid to late summer and in year 4 from summer to winter (Figure 6.3.12). Beam transmission profiles for cruises in 1992 are shown in Figure 6.3.14. These profiles were collected at approximately midnight and were normalized to the average density profile obtained for each cruise. Beam transmission profiles also show considerable variability on monthly time scales.

4.3. Biogeochemistry

Biogeochemical data collected during 1992 are summarized in Figures 6.4.. In some cases the results from the first three years of the program have been combined to produce these figures.

4.3.1. Dissolved Inorganic Carbon and Titration Alkalinity

Dissolved inorganic carbon (DIC) and titration alkalinity measured in the upper 1000 dbar of the water column over the 4 years of the time-series program are presented in Figures 6.4.1 and 2. Time-series of titration alkalinity and DIC in the mixed layer are presented in Figure 6.4.3. Titration alkalinity normalized to 35 ppt salinity averages approximately 2305 μ equivalents kg^{-1} and, within the precision of the analysis, appears to remain relatively constant at Station ALOHA. This observation is consistent with the results of Weiss *et al.* (1982) who conclude that titration alkalinity normalized to salinity remains constant in both the North and South Pacific Subtropical Gyres. In contrast to titration alkalinity, the concentration of DIC varies annually. DIC in the mixed layer is highest in winter and lowest in summer. This

oscillation is consistent with an exchange of carbon dioxide across the air-sea interface driven by temperature dependent changes in mixed layer pCO_2.

Titration alkalinity shows considerable time dependent variability around the shallow salinity maximum, centered at about 125 dbar, and the salinity minimum, centered at about 400 dbar. These variations are largely associated with variability in salinity at these depths and disappear when alkalinity is normalized to 35 ppt. Titration alkalinity normalized to 35 ppt salinity is elevated in surface waters in spring of 1990. This corresponds to the appearance of mesoscale eddies at Station ALOHA at this time (Winn *et al.*, 1991).

4.3.2. Low Level Nutrient Profiles

Euphotic zone nutrient concentrations at Station ALOHA are at or well below the detection limits of the autoanalyzer methods. Other analytical techniques and instrumentation are used to measure the nanamolar levels of [nitrate+nitrite] and phosphorus (Sections 2.2.6.5 and 2.2.6.6) in these waters. Figures 6.4.4 and 6.4.5 show the profiles obtained from our low level nutrient analyses in 1992. At depths shallower than 100 dbar, phosphate is typically less than 150 nmol kg^{-1} and on occasion, as low as 15 nmol kg^{-1}. Phosphate concentrations appear to vary by at least 3-fold in this region (Figure 6.4.4). Concentrations of [nitrate+nitrite] between 0-100 dbar at less than 100 dbar are always less than 20 nmol kg^{-1} and are often less the 5 nmol kg^{-1} (Figure 6.4.5).

4.3.3. Pigments

A contour plot of chl *a* concentrations measured by using standard fluorometric techniques from 0 to 200 dbar over the first four years of the program is shown in Figure 6.4.6. As expected a chlorophyll maximum with concentrations up to 300 µg kg^{-3} is observed at approximately 100 dbar. No strong seasonal cycle is observed in the chlorophyll maximum layer. The chl *a* concentrations at depths shallower than 50 dbar appear to have steadily decreased from January 1989 to mid 1990. There is some indication that the chl *a* concentrations in the surface waters are increasing again toward the end of 1991 then appear to decrease towards the summer of 1992.

4.3.4. Particulate Carbon, Nitrogen and Phosphorus

Particulate carbon (PC), nitrogen (PN) and phosphorus (PP) in the surface ocean over the first four years of the program are shown in Figures 6.4.7 to 9. PC varies between 1.6 - 3.0 µmol kg^{-1}, PN between 0.15 -0.45 µmol kg^{-1} and PP between 12 - 30 nmol kg^{-1} in the upper 50 dbar of the water column. PC and PN show a clear annual cycle with peaks in particulate concentrations in summer of 1989, and 1990-1992.

4.4. Primary Production and Particle Flux

4.4.1. Primary Productivity

The results of the ^{14}C incubations and pigment determinations for samples collected from Go-Flo casts in 1992 are presented in Tables 4.4.1 and 4.4.2. Table 4.4.1 presents the primary production and pigment measurements made at individual depths on all 1992 cruises. Table 4.4.2 presents integrated values for irradiance, pigment concentration and primary production rates. The pigment concentrations and ^{14}C incorporation rates reported are the average of triplicate determinations. Integrated primary production rates measured over all four years of the program are shown in Figure 6.5.1 in order to place the 1992 results within the context of the time-series data set.

Variability in rates of primary production, integrated over the euphotic zone during the first four years of the time-series program, appear to be stochastic with no evidence of a seasonal cycle. Measured rates ranged between approximately 250 and 1100 mgC m^{-2} day^{-1} with the highest rate being observed in August 1989. This high rate of primary production coincided with a cyanobacterial bloom observed in surface waters near Station ALOHA on HOT cruise #9 (Karl *et al.*, 1992). This variability, with a range of almost a factor of 7, is surprisingly large. However, the majority of the primary production estimates were between 250 and 600 mg C m^{-2} day^{-1}, and the average rate of primary production was approximately 450 mg C m^{-2} day^{-1}. Although this value is higher than historical measurements for the central ocean basins (Ryther, 1969), it is consistent with more recent measurements using modern methodology (Martin *et al.*, 1987; Laws *et al.*, 1989; Knauer *et al.*, 1990).

4.4.2. Particle Flux

Particulate carbon (PC), nitrogen (PN), phosphorus (PP) and mass fluxes (150, 300 and 500 m) are presented in Table 4.4.3 and Figures 6.5.2 to 9 for the first 4 years of the program. Carbon flux displays a clear annual cycle with peaks in both the early spring and in the late summer months. The magnitude of particle flux varies by a factor of approximately 3. With the exception of anomalous PP fluxes measured on the first two HOT cruises, temporal variability in PN, PP and mass flux show similar temporal trends, and also vary between cruises by about a factor of three. Elemental ratios of carbon-to-nitrogen (by atoms) at 150 m are typically between 6 - 10 and show no obvious temporal pattern. These particle flux measurements and elemental ratios are consistent with those measured in the central North Pacific Ocean by the VERTEX program (Martin *et al.*, 1987). Nitrogen flux at 150 m, as a percent of photosynthetic nitrogen assimilation (calculated from ^{14}C primary production values assuming a C:N ratio [by atoms] of 6.6) ranges between 2 - 10%. The average value (approximately 6.5%) is consistent with the estimate of new production for the oligotrophic central gyres made by Eppley and Peterson

(1979) and with field data from the VERTEX program (Knauer *et al.*, 1990). Average fluxes of PC, PN, PP and mass at 150 m from the first four years of the time-series observations are shown in Figures 6.5.3-5. Contour plots of flux are shown in Figures 6.5.6-9. For carbon, nitrogen, phosphorus and total mass, the flux declines rapidly with depth, presumably due to the rapid dissolution and remineralization of organic particles sinking through the water column. The flux of carbon at 500 m is less than 50% of the flux at 150 m.

4.5. ADCP Measurements

An overview of the shipboard ADCP data is given by the plots of reference layer velocity versus time (Figures 6.6.1-9), the velocity as a function of time and depth (Figures 6.6.10a-18a) and the velocity as a function of position and depth (Figures 6.6.10b-18b). As during the previous three years, currents were highly variable from cruise to cruise and within each cruise.

4.6. Meteorology

The meteorological data collected by the HOT program include atmospheric pressure, sea-surface temperature and wet and dry bulb air temperature. These data are presented in Figures 6.7.1-3. As described by Winn *et al.* (1991), parameters show evidence of annual cycles, although the daily and weekly ranges are nearly as high as the annual range for some variables. Wind speed and direction are also collected on HOT cruises. These data are presented in Figures 6.7.4-12.

4.7. Light Measurements

Integrated irradiance measurements made with the on-deck cosine collector on days that primary production experiments were conducted are presented in Table 4.4.2.

Table 4.4.1: Primary Production and Pigment Summary

Cruise[a]	Depth (m)	Mean Chl *a* [b] mg m^{-3}	Std. Dev. Chl *a* [c] mg m^{-3}	Mean Phaeo[b] mg m^{-3}	Std. Dev. Phaeo[c] mg m^{-3}	Light[d] mg C m^{-3} Rep #1	Light[d] Mg C m^{-3} Rep #2	Light[d] mg C m^{-3} Rep #3	Dark[d] mg C m^{-3} Rep #1	Dark[d] mg C m^{-3} Rep #2	Dark[d] mg C m^{-3} Rep #3
33	5	0.140		0.124		7.88	8.07	7.50	0.12	0.14	0.13
33	25	0.136		0.141		4.65	6.85	6.55	0.11	0.14	0.14
33	45	0.181		0.153		5.12	5.31	4.47	0.08	0.09	0.07
33	75	0.153		0.198		1.78	1.46	1.59	0.09	0.07	0.07
33	100	0.209		0.370			0.55	0.48	0.11	0.08	0.07
33	125	0.053	0.009	0.144	0.002	0.09	0.10	0.09	0.06	0.07	0.07
33	150	0.024		0.063		0.03	nd[e]	0.04	0.04	0.06	0.05
33	175	0.010		0.031		0.03	0.02	0.03	0.03	0.05	0.05
34	5	0.151		0.144		nd		12.36	0.07	0.07	0.08
34	25	0.154	0.007	0.146	0.007	nd	1.087	10.89	0.07	0.07	0.08
34	45	0.155		0.137		7.85		8.32	0.08	0.07	0.08
34	75	0.142		0.127		3.66	3.29	1.65	0.07	0.08	0.07
34	100	0.164	0.005	0.149	0.010	1.15	1.13	1.19	0.06	0.07	0.08
34	125	0.115	0.005	0.342	0.006	nd	0.60	0.58	0.06	0.07	0.08
34	150	0.056		0.183		0.13	0.15	0.16	0.05	0.06	0.05
34	175	0.031		0.062		0.05	0.05	0.04	0.06	0.05	0.05
35	5	0.081	0.003	0.056	0.006	6.16	5.66	7.83	0.06	0.07	0.07
35	25	0.078	0.002	0.066	0.004	8.05	8.32	6.41	0.10	0.10	0.09
35	45	0.098	0.001	0.094	0.004	6.42	5.70	nd	0.14	0.16	0.14
35	75	0.130	0.002	0.125	0.003	4.21	3.80	3.68	0.13	0.13	0.11
35	100	0.119	0.003	0.155	0.010	0.50	0.48	0.60	0.06	0.05	0.06
35	125	0.194	0.000	0.405	0.021	0.75	0.82	0.77	0.06	0.06	0.06
35	150	0.109	0.000	0.302	0.017	0.17	0.17	0.17	0.03	0.03	0.03
35	175	0.034	0.002	0.100	0.005	0.04	0.04	nd	0.03	0.03	0.03
36	5	0.066	0.002	0.059	0.017	4.23	6.65	8.97	0.10	0.09	0.10
36	25	0.072	0.010	0.067	0.024	5.81	5.62	5.78	0.09	0.09	0.10
36	45	0.085	0.008	0.067	0.008	4.34	nd	4.30	0.12	0.11	0.02
36	75	0.165	0.004	0.185	0.006	3.17	3.97	3.55	0.10	0.11	0.10
36	100	0.160	0.009	0.276	0.008	1.78	1.92	1.88	0.08	0.09	0.10
36	125	0.206	0.011	0.588	0.021	0.87	0.52	0.83	0.04	0.05	0.04
36	150	0.061	0.003	0.209	0.002	0.14	0.11	0.12	0.03	0.03	0.03

Table 4.4.1: (continued)

Cruise[a]	Depth (m)	Mean Chl *a* [b] mg m^{-3}	Std. Dev. Chl *a* [c] mg m^{-3}	Mean Phaeo[b] mg m^{-3}	Std. Dev. Phaeo[c] mg m^{-3}	Light[d] mg C m^{-3} Rep #1	Light[d] mg C m^{-3} Rep #2	Light[d] mg C m^{-3} Rep #3	Dark[d] mg C m^{-3} Rep #1	Dark[d] mg C m^{-3} Rep #2	Dark[d] mg C m^{-3} Rep #3
37	5	0.054	0.003	0.049	0.005	nd	8.01	8.83	0.11	0.11	0.10
37	25	0.064	0.002	0.063	0.002	6.11	6.40	6.70	0.12	0.13	0.13
37	45	0.066	0.001	0.052	0.003	6.97	nd	7.04	0.14	0.13	
37	75	0.077	0.003	0.062	0.004	3.81	3.70	4.07	0.13	0.15	0.14
37	100	0.121	0.004	0.122	0.007	2.18	2.14	2.14	0.11	0.15	0.13
37	125	0.255	0.012	0.467	0.026	1.79	1.43	1.57	0.09	0.10	0.09
37	150	0.070	0.005	0.237	0.007	0.25	0.25	0.23	0.08	0.05	0.05
38	5	0.049	0.004	0.036	0.003	3.66	4.26	4.38	0.10	0.10	0.10
38	25	0.070	0.003	0.070	0.010	6.96	6.61	7.30	0.12	0.20	0.12
38	45	0.053	0.005	0.039	0.004	2.34	nd	3.13	0.09		0.08
38	75	0.186	0.000	0.183	0.004	3.93	3.78	4.44	0.11	0.08	0.07
38	100	0.178	0.000	0.373	0.007	2.11	2.62	2.25	0.04	0.04	0.05
38	125	0.166	0.001	0.481	0.021	0.97	0.98	0.95	0.04	0.04	0.5
38	150	0.064	0.006	0.252	0.016	0.17	0.17	0.15	0.03	0.03	0.03
38	175	0.004	0.000	0.152	0.007	0.06	0.06	0.05	0.03	0.03	0.03
39	5	0.067	0.002	0.052	0.006	4.70	6.60	6.59	0.13	0.13	0.14
39	25	0.073	0.004	0.053	0.002	6.63	6.40	6.47	0.12	0.13	0.13
39	45	0.085	0.002	0.063	0.002	5.37	nd	4.97	0.13	0.22	0.14
39	75	0.132	0.003	0.171	0.004	2.62	2.62	2.79	0.13	0.14	0.18
39	100	0.246	0.006	0.510	0.022	2.00	2.04	2.36	0.07	0.05	0.07
39	125	0.087	0.007	0.283	0.008	0.30	0.29	0.29	0.05	0.04	0.04
39	150	0.031	0.006	0.133	0.013	0.06	0.06	0.06	0.04	0.04	0.04
39	175	0.013	0.002	0.051	0.003	0.03	0.02	0.03	0.04	0.05	0.04
40	5	0.090	0.007	0.094	0.009	3.86	6.45	7.10	0.17	0.15	0.17
40	25	0.083	0.005	0.105	0.003	6.22	6.47	6.23	0.15	0.15	0.16
40	45	0.103	0.010	0.110	0.006	5.96	nd	4.72	0.16	0.26	0.17
40	75	0.183	0.007	0.233	0.017	2.67	2.77	2.67	0.15	0.16	0.22
40	100	0.195	0.009	0.572	0.012	2.07	2.21	2.60	0.08	0.06	0.08
40	125	0.055	0.000	0.210	0.006	0.63	0.31	0.31	0.06	0.05	0.05
40	150	0.037	0.001	0.120	0.009	0.06	0.06	0.06	0.04	0.05	0.05
40	175	0.039	0.000	0.139	0.014	0.03	0.02	0.03	0.04	0.06	0.05

Table 4.4.1: (continued)

Cruise[a]	Depth (m)	Mean Chl *a* [b] Mg m^{-3}	Std. Dev. Chl *a* [c] mg m^{-3}	Mean Phaeo[b] mg m^{-3}	Std. Dev. Phaeo[c] mg m^{-3}	Light[d] mg C m^{-3} Rep #1	Light[d] mg C m^{-3} Rep #2	Light[d] mg C m^{-3} Rep #3	Dark[d] mg C m^{-3} Rep #1	Dark[d] mg C m^{-3} Rep #2	Dark[d] mg C m^{-3} Rep #3
41	5	0.086	0.003	0.082	0.003	5.68	6.35	11.20	0.42	0.12	0.12
41	25	0.093	0.008	0.077	0.006	9.08	2.96	8.95	0.47	0.40	0.37
41	45	0.125	0.003	0.128	0.003	4.89	6.85	6.62	0.19	0.19	0.03
41	75	0.321	0.011	0.887	0.033	3.48	3.45	3.99	0.06	0.06	0.04
41	100	0.313	0.006	0.807	0.067	0.78	0.77	0.82	0.03	0.05	0.06
41	125	0.078	0.004	0.221	0.004	nd	nd	nd	nd	nd	nd
41	150	0.025	0.000	0.074	0.008	0.05	0.04	0.08	0.02	0.05	0.04
41	175	0.011	0.001	0.032	0.003	0.03	0.03	0.03	0.03	0.02	0.02

[a]IS = *in situ* incubations

[b]Generally average of 2 or more replicates

[c]SD (standard deviation) computed only at depths with three replicate subsamples

[d]Incubation times are approximations only (i.e., half day or full day). Actual incubation time for each measurement is given in Table 4.4.2.

[e]Not determined

Table 4.4.2: *In Situ* Primary Production and Pigment Summary
Integrated Values 0-200 m

Cruise	Incident Irradiance (E m^{-2} d^{-1}) cosine[a]	hemi[b]	Pigments (mg m^{-2}) Chl *a*	Phaeo	Incubation Duration (hrs)	Carbon Assimilation Rates (mgC m^{-2} d^{-1}) light	dark[c]
33	37[d]	66.7	20.9	29.2	12.9	439	27
34	39	68.6	22.4	33.9	12.5	732	24
35	55	93.9	22.4	33.7	13.2	546	26
36	57	98.5	20.5	38.5	11.7	490	26
37	51	88.3	19.2	29.4	13.1	674	35
38	56	96.2	20.3	39.9	14.8	451	20
39	ND[e]	ND	19.3	33.9	11.8	485	36
40	50.6	88	21.2	41.1	12.7	491	39
41	46.4	81	28.3	61.2	12.1	542	40
42	36.3	71	ND	ND	ND	ND	ND
43	ND	ND	ND	ND	ND	ND	ND

[a]cosine collector

[b]hemispherical collector

[c]extrapolated to daily rates

[d]Shaded cells are derived values using the regression y=1.58x + 7.7 with the cosine collector as the independent variable using all paired data points.

[e]ND = not determined

Table 4.4.3: Station ALOHA Sediment Trap Flux Data

Cruise	Depth (m)	Carbon mg m^{-2} day^{-1}	Carbon SD[a]	Carbon n	Nitrogen mg m^{-2} day^{-1}	Nitrogen SD[a]	Nitrogen n	Phosphorus mg m^{-2} day^{-1}	Phosphorus SD[a]	Phosphorus n	Mass Flux mg m^{-2} day^{-1}	Mass Flux SD[a]	Mass Flux n
33	150	26.0	4.4	6	3.2	0.17	6	0.38	0.01	3	61.7	6.7	3
33	300	27.8	5.7	5	1.8	0.017	5	0.24	0.02	3	65.7	11.1	3
33	500	12.6	3.9	6	0.8	0.03	6	0.08	0.00	2	30.4	5.7	3
34	150	18.2	3.2	4	3.1	0.39	4	0.29	0.05	3	52.4	9.8	3
34	300	11.7	1.2	6	1.7	0.04	6	0.10	0.05	3	44.4	ND[b]	2
34	500	4.3	1.7	6	0.9	0.16	6	0.02	0.00	3	15.3	2.7	3
35	150	29.0	4.3	6	4.4	0.37	6	0.46	0.08	3	47.8	11.7	3
35	300	12.2	2.1	6	1.7	0.32	6	0.16	0.03	3	21.1	9.0	3
35	500	9.5	0.8	6	1.2	0.22	6	0.18	0.11	3	29.2	17.3	3
36	150	17.3	3.8	6	2.7	0.44	6	0.26	0.03	3	84.2	5.3	3
36	300	13.5	3.1	6	2.4	0.47	6	0.11	0.02	3	41.8	4.8	3
36	500	9.5	2.1	6	1.5	0.26	6	0.02	0.03	3	35.2	9.4	3
37	150	22.3	6.8	6	2.7	0.33	6	0.21	0.02	3	43.2	6.6	3
37	300	8.7	2.2	6	1.1	0.18	6	0.08	0.03	3	34.8	11.1	3
37	500	6.7	1.4	6	0.5	0.08	6	0.09	0.01	3	20.5	5.3	3
38	150	28.4	5.7	6	4.2	0.46	6	0.38	0.06	3	77.6	17.9	3
38	300	13.4	1.7	6	1.7	0.14	6	0.09	0.00	3	41.3	4.8	3
38	500	11.5	1.1	5	1.4	0.09	5	0.09	0.03	3	40.2	8.4	3
39	150	25.8	7.5	6	3.2	0.85	6	0.22	0.03	3	65.5	4.6	3
39	300	7.4	3.8	5	1.3	0.61	5	0.17	0.07	3	49.7	14.3	3
39	500	11.8	4.7	5	1.3	0.38	5	0.18	ND[b]	2	41.3	5.6	3
40	150	19.3	7.2	6	2.6	1.10	6	0.26	0.03	3	58.6	16.3	3
40	300	9.7	2.9	6	1.3	0.50	6	0.12	0.03	3	30.5	2.8	3
40	500	9.1	4.1	5	0.8	0.10	5	0.12	0.03	3	30.3	3.3	2
41	150	10.7	3.8	6	2.1	0.24	6	0.17	0.02	3	27.0	3.7	3
41	300	8.1	4.9	6	0.8	0.27	6	0.10	0.01	3	22.2	12.0	3
41	500	3.6	3.3	6	0.3	0.36	6	0.10	0.03	3	18.6	7.0	3

[a]When n ≥ 3, the variability is expressed as standard deviation (SD).

[b]Not determined.

4.8. NDBC Buoy and Shipboard Observations

A NDBC meteorological buoy is located about 400 km west of Station ALOHA at 23°24'N, 162°18'W. This buoy collects hourly observations of air temperature, sea surface temperature, atmospheric pressure, wind velocity and significant wave height. Because continuous observations of atmospheric and surface ocean conditions may be valuable in the interpretation of our time-series observations, we have examined the coherence in the data sets collected at hourly intervals at the buoy and at approximately monthly intervals on the time-series cruises. In order to examine the coherence in these sets of observations, meteorological data collected on HOT cruises 14-39 were compared to buoy data collected over the same time interval. Both air temperature time-series records show an annual cycle, and a high correlation is observed between the buoy and cruise data (Figure 6.7.13). The root mean square (RMS) of the residuals is approximately 0.7°C. A close relationship is displayed between sea-surface temperatures (Figure 6.7.14), with a residual RMS of only 0.41°C. Atmospheric pressure also shows a good correlation between buoy and cruise data (Figure 6.7.15). Cruise data obtained on the R/V KAIMALINO in 1990 showed an offset of about 7 mb with respect to the buoy data (see Winn *et al.*, 1993), these data were corrected by this offset and are included in the plots. Wind speed measured by the buoy and on the HOT cruises show a relatively weak correlation with a correlation coefficient of 0.53 and a residual RMS of more than 2 m/sec (Figure 6.7.16). Wind direction is much better, with a correlation coefficient of nearly 0.9 and an RMS of about 37 degrees (Figure 6.7.17). Cross correlations between buoy data and ship-based measurements of air temperatures, sea-surface temperatures and atmospheric pressure were used to check for existence of a time delay between these datasets. No lagged correlations between these parameters were observed. We conclude from these analyses, that buoy data can be used to get useful estimates of air temperature, sea-surface temperature and atmospheric pressure at Station ALOHA.

5. References

Armstrong, F.A.J., P.M. Williams and J.D.H. Strickland, 1966: Photo-oxidation of organic matter in sea water by ultraviolet radiation, analytical and other applications. *Nature*, **211**, 481-483.

Bidigare, R.R., J. Marra, T.J. Dickey, R. Iturriaga, K.S. Baker, R.C. Smith and H. Pak, 1990: Evidence for phytoplankton succession and chromatic adaptation in the Sargasso Sea during Spring 1985. *Marine Ecology Progress Series*, **60**, 113-122.

Bradshaw, A.L. and P.G. Brewer, 1988: High precision measurements of alkalinity and total carbon dioxide in seawater by potentiometric titration: Presence of unknown protolytes? *Marine Chemistry,* **23**, 69-86.

Byrne, R.H. and J.A. Breland, 1989: High precision multiwavelength pH determinations in seawater using cresol red. *Deep-Sea Research*, **36**, 803-810.

Carpenter, J.H., 1965: The accuracy of the Winkler method for dissolved oxygen analysis. *Limnology and Oceanography*, **10**, 135-140.

Chiswell, S.M., E. Firing, D. Karl, R. Lukas, C. Winn, 1990: Hawaii Ocean Time-series Program Data Report 1, 1988-1989. School of Ocean and Earth Science and Technology, University of Hawaii, 269 pp.

Clayton, T.D. and R.H. Byrne, 1993: Spectrophotometric seawater pH measurements: total hydrogen ion concentration scale calibration of m-cresol purple and at-sea results. *Deep-Sea Research*, **40**, 2115-2129.

Cox, R.D., 1980: Determination of nitrate at the parts per billion level by chemiluminescence. *Analytical Chemistry*, **52**, 332-335.

Dickson, A., 1993: pH buffers for sea water media based on the total hydrogen ion concentration scale. *Deep-Sea Research*, **40**, 107-118.

Dickson, A.G., 1984: pH scales and proton-transfer reactions in saline media such as seawater. *Geochimica et Cosmochimica Acta*, **48**, 2299-2308.

DOE, 1991: Handbook of Methods for the Analysis of the Various Parameters of the Carbon Dioxide System in Sea Water. Version 1, Dickson, A.G., and C. Goyet (eds).

Edmond, J.M., 1970: High precision determination of titration alkalinity and total carbon dioxide content of seawater by potentiometric titration. *Deep-Sea Research*, **17**, 737-750.

Eppley, R.W. and B.J. Peterson, 1979: Particulate organic matter flux and planktonic new production in the deep ocean. *Nature*, **282**, 677-680.

Garside, C., 1982: A chemiluminescent technique for the determination of nanomolar concentrations of nitrate and nitrite in seawater. *Marine Chemistry*, **11**, 159-167.

Hansson, I., 1973: A new set of pH scales and standard buffers for seawater. *Deep-Sea Research*, **20**, 479-491.

Karl, D. M., R. Letelier, D. V. Hebel, D. F. Bird and C. D. Winn, 1992: *Trichodesmium* blooms and new nitrogen in the North Pacific gyre. In: E. J. Carpenter et al. (eds.), *Marine Pelagic*

Cyanobacteria: Trichodesmium and Other Diazotrophs, pp. 219-237. Kluwer Academic Publishers, Netherlands.

Karl, D.M. and G. Tien, 1992: MAGIC: A sensitive and precise method for measuring dissolved phosphorus in aquatic environments. *Limnology and Oceanography*, **37**, 105-116.

Karl, D.M., C.D. Winn, D.V.W. Hebel and R. Letelier, 1990: Hawaii Ocean Time-series Program Field and Laboratory Protocols, September 1990.

Knauer, G.A., D.G. Redalje, W.G. Harrison and D.M. Karl, 1990: New production at the VERTEX time-series site. *Deep-Sea Research*, **37**, 1121-1134.

Laws, E.A., G.R. DiTullio, P.R. Betzer, D.M. Karl and R.L. Carder, 1989: Autotrophic production and elemental fluxes at 26°N, 155°W in the North Pacific subtropical gyre. *Deep-Sea Research*, **36**, 103-120.

Lukas, R. and S. Chiswell, 1991: Submesoscale water mass variations in the salinity minimum of the north Pacific near Hawaii. *WOCE Notes*, **3(1)**, 1,6-8.

Martin, J.H., G.A. Knauer, D.M. Karl and W.W. Broenkow, 1987: VERTEX: Carbon cycling in the northeast Pacific. *Deep-Sea Research*, **34**, 267-285.

Millero, F.J., 1979: The thermodynamics of the carbonate system in seawater. *Geochimica et Cosmochimica Acta*, **43**, 1651-1661.

Owens, W.B. and Millard, R.C., 1985: A new algorithm for CTD oxygen calibration. *Journal of Physical Oceanography*, **15**, 621-631.

Press, W., B. Flannery, S. Teokolsky, W. Vetterling, 1988: Numerical recipes in C. Cambridge U. Press, 735 pp.

Ryther J. H., 1969: Photosynthesis and fish production in the sea: The production of organic matter and its conversion to higher forms of life vary through the world ocean. *Science*, **166**, 72-76.

Strickland, J.D.H. and T.R. Parsons, 1972: A practical handbook of seawater analysis. Fisheries Research Board of Canada, 167 pp.

Tsuchiya, M., 1968: Upper waters of the intertropical Pacific Ocean. *Johns Hopkins Oceanographic Studies*, **4**, 49 pp.

UNESCO, 1981: Tenth report of the joint panel on oceanographic tables and standards. *UNESCO Technical Papers in Marine Science*, No. 36, UNESCO, Paris.

Walsh, T.W., 1989: Total dissolved nitrogen in seawater: a new high-temperature combustion method and a comparison with photo-oxidation. *Marine Chemistry*, **26**, 295-311.

Weiss, R.F., R.A. Jahnke and C.D. Keeling, 1982: Seasonal effects of temperature and salinity on the partial pressure of CO_2 in seawater. *Nature*, **300**, 511-513

Winn, C., S.M. Chiswell, E. Firing, D. Karl, R. Lukas, 1991: Hawaii Ocean Time-series Program Data Report 2, 1990. School of Ocean and Earth Science and Technology, University of

Hawaii, 175 pp.

Winn, C., R. Lukas, D. Karl, E. Firing, 1993: Hawaii Ocean Time-series Program Data Report 3, 1991. School of Ocean and Earth Science and Technology, University of Hawaii, 228 pp

6. Figures

6.1. CTD Profiles

Figures 6.1.1a-11a: CTD and nutrient data collected at Station ALOHA. Upper left panel: Temperature, salinity, oxygen and density ($\sigma\theta$) as a function of pressure for WOCE deep cast. Salinity and oxygen water bottle data are also plotted. Upper right panel: Nutrients ([NO_3 + NO_2], PO_4 and silicic acid) and oxygen as a function of potential temperature for all water samples. Lower left panel: CTD temperature and salinity profiles plotted as a function of pressure. Lower right panel: Salinity and oxygen from CTD and water samples plotted as a function of potential temperature.

Figures 6.1.1b-11b: Stack plots of temperature and salinity against pressure to 1000 dbar for all CTD casts. Upper panel: Potential temperature versus pressure to 1000 dbar. Lower panel: Salinity versus pressure to 1000 dbar.

Figures 6.1.1c-10c: As in 6.1.1a-10a but for Station Kahe.

Figure 6.1.12: 1992 potential temperature profiles. Upper panel: Potential temperature versus pressure for all deep casts in 1992. Lower panel: Potential temperature for all deep casts in 1991 plotted from 2500 dbar.

Figure 6.1.13: 1992 temperature-salinity plots. Upper panel: Potential temperature versus salinity for all deep casts collected during 1992. Lower panel: Potential temperature versus salinity on same casts in the 1-5°C range.

Figure 6.1.14: 1992 oxygen profiles. Upper panel: Oxygen values derived from calibrated CTD sensor data versus potential temperature for all deep casts collected during 1991. Lower panel: Oxygen versus potential temperature for 1992 deep casts within the 1-5°C range.

Figure 6.1.15: Stack plots of temperature and salinity against pressure to 1000 dbars for all CTD casts at Station 3 (upper panels) and Station 4 (lower panels). HOT cruise numbers are shown at the top of each panel.

Figure 6.1.16: Upper panels: Same as 6.1.15 except for Station 5. Lower panels: Same as 6.1.15 except for CTD casts other than Station ALOHA or Station Kahe on HOT-37. Station numbers are shown at the top of each panel.

Figure 6.1.17: Same as lower panels of 6.1.16 except for HOT-40 and HOT-41.

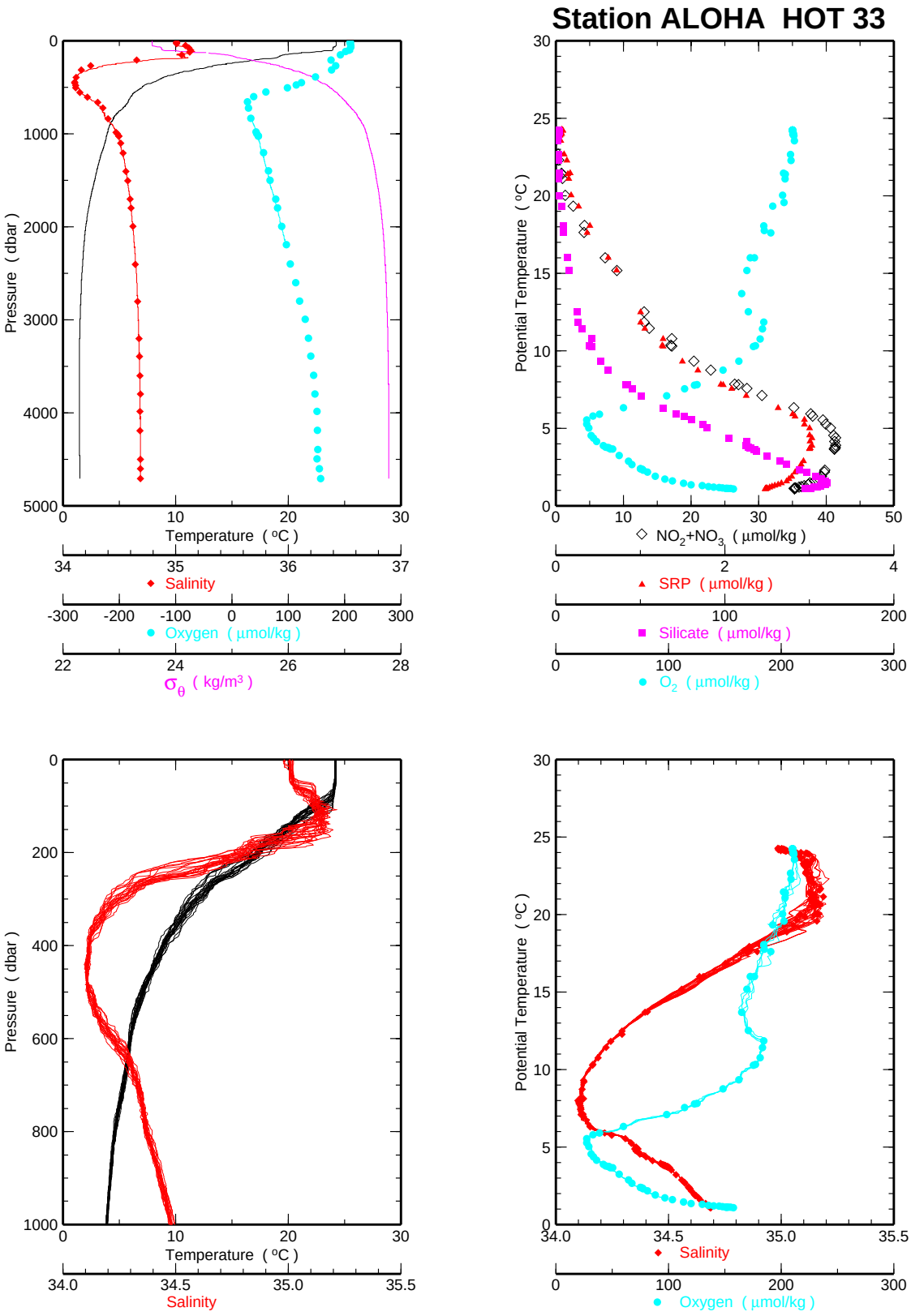
Station ALOHA HOT 33
Pressure (dbar)
Temperature (°C)
Salinity
Oxygen (µmol/kg)
σθ (kg/m³)
Potential Temperature (°C)
NO2+NO3 (µmol/kg)
SRP (µmol/kg)
Silicate (µmol/kg)
O2 (µmol/kg)

Figure 6.1.1a

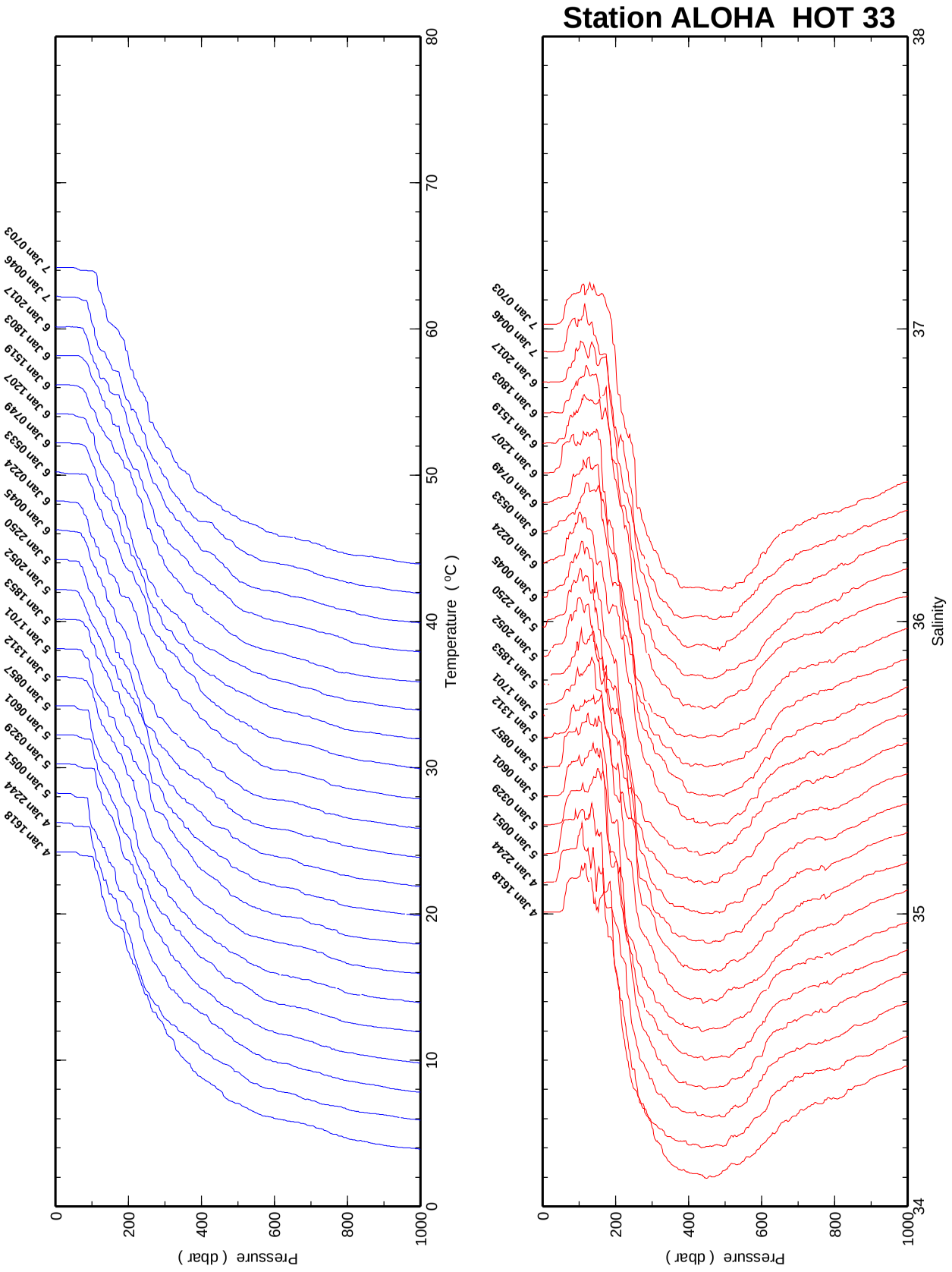
Station ALOHA HOT 33
Temperature (°C)
Salinity
Pressure (dbar)
Pressure (dbar)
4 Jan 1618
4 Jan 2244
5 Jan 0051
5 Jan 0329
5 Jan 0601
5 Jan 0857
5 Jan 1312
5 Jan 1701
5 Jan 1853
5 Jan 2052
5 Jan 2250
6 Jan 0045
6 Jan 0224
6 Jan 0533
6 Jan 0749
6 Jan 1207
6 Jan 1519
6 Jan 1803
6 Jan 2017
7 Jan 0046
7 Jan 0703

Figure 6.1.1b

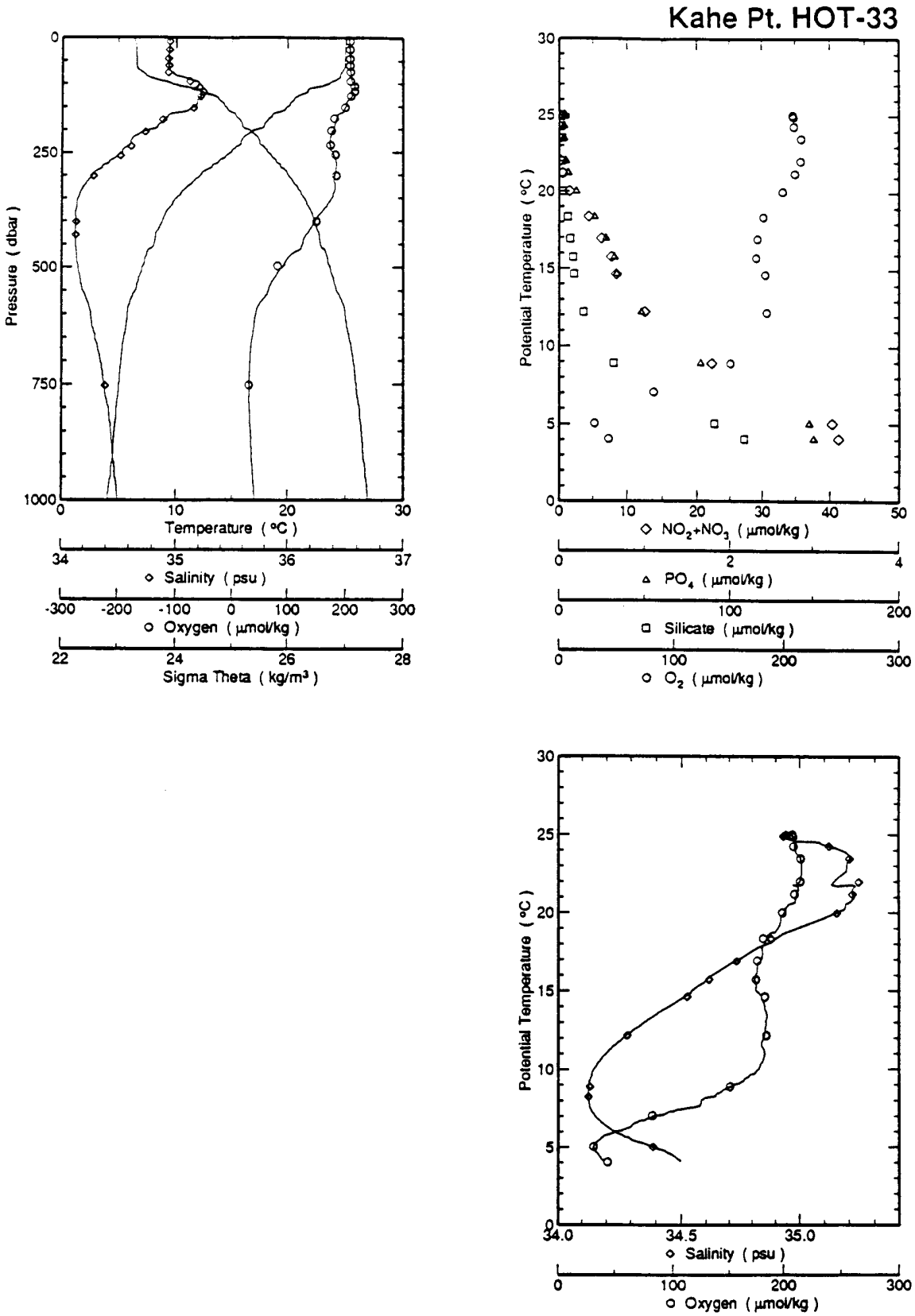
Kahe Pt. HOT-33
Pressure (dbar)
Temperature (°C)
Salinity (psu)
Oxygen (µmol/kg)
Sigma Theta (kg/m³)
Potential Temperature (°C)
NO2+NO3 (µmol/kg)
PO4 (µmol/kg)
Silicate (µmol/kg)
O2 (µmol/kg)
Potential Temperature (°C)
Salinity (psu)
Oxygen (µmol/kg)

Figure 6.1.1c

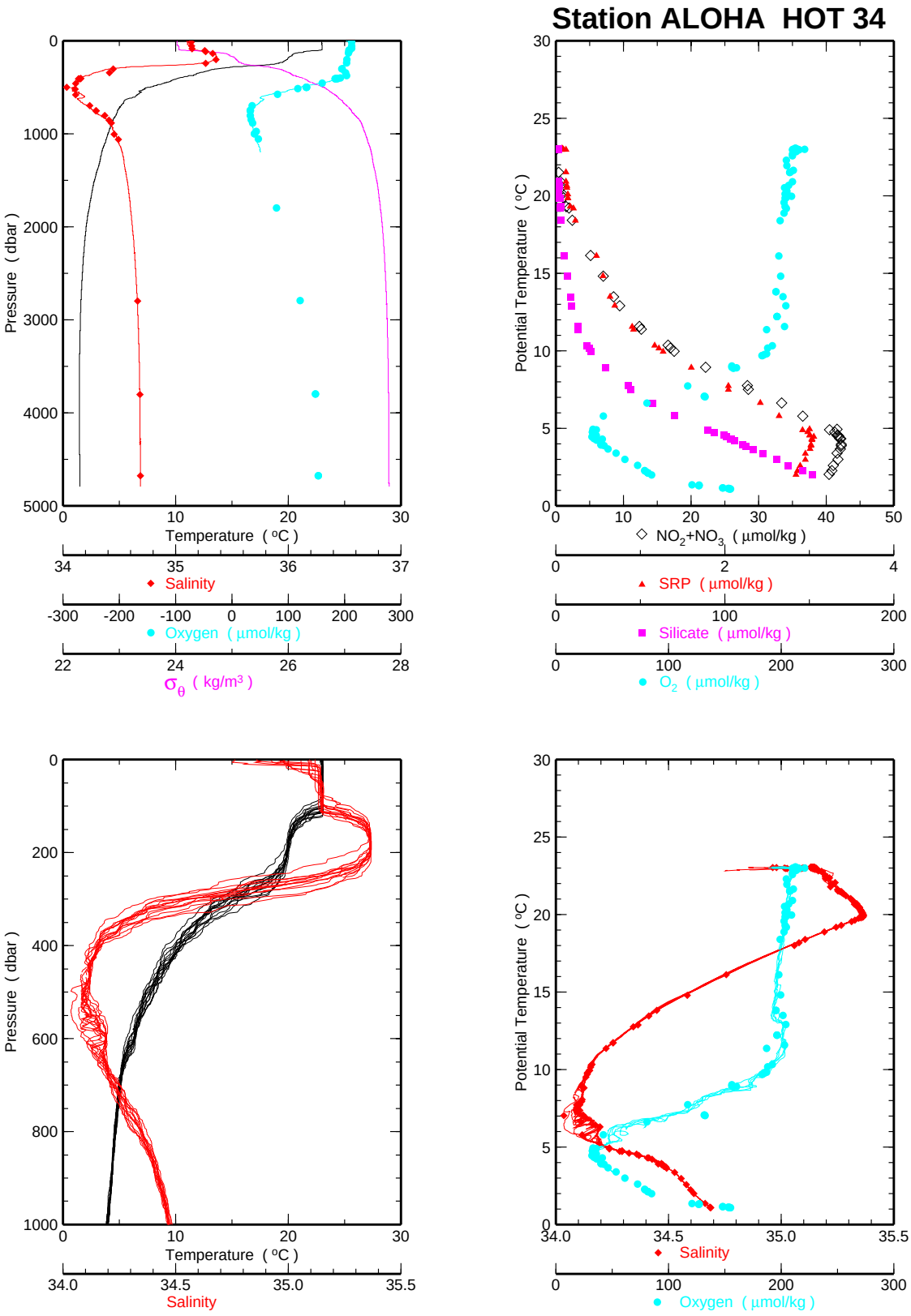
Station ALOHA HOT 34
Pressure (dbar)
Temperature (°C)
Salinity
Oxygen (µmol/kg)
σθ (kg/m³)
Potential Temperature (°C)
NO2+NO3 (µmol/kg)
SRP (µmol/kg)
Silicate (µmol/kg)
O2 (µmol/kg)

Figure 6.1.2a

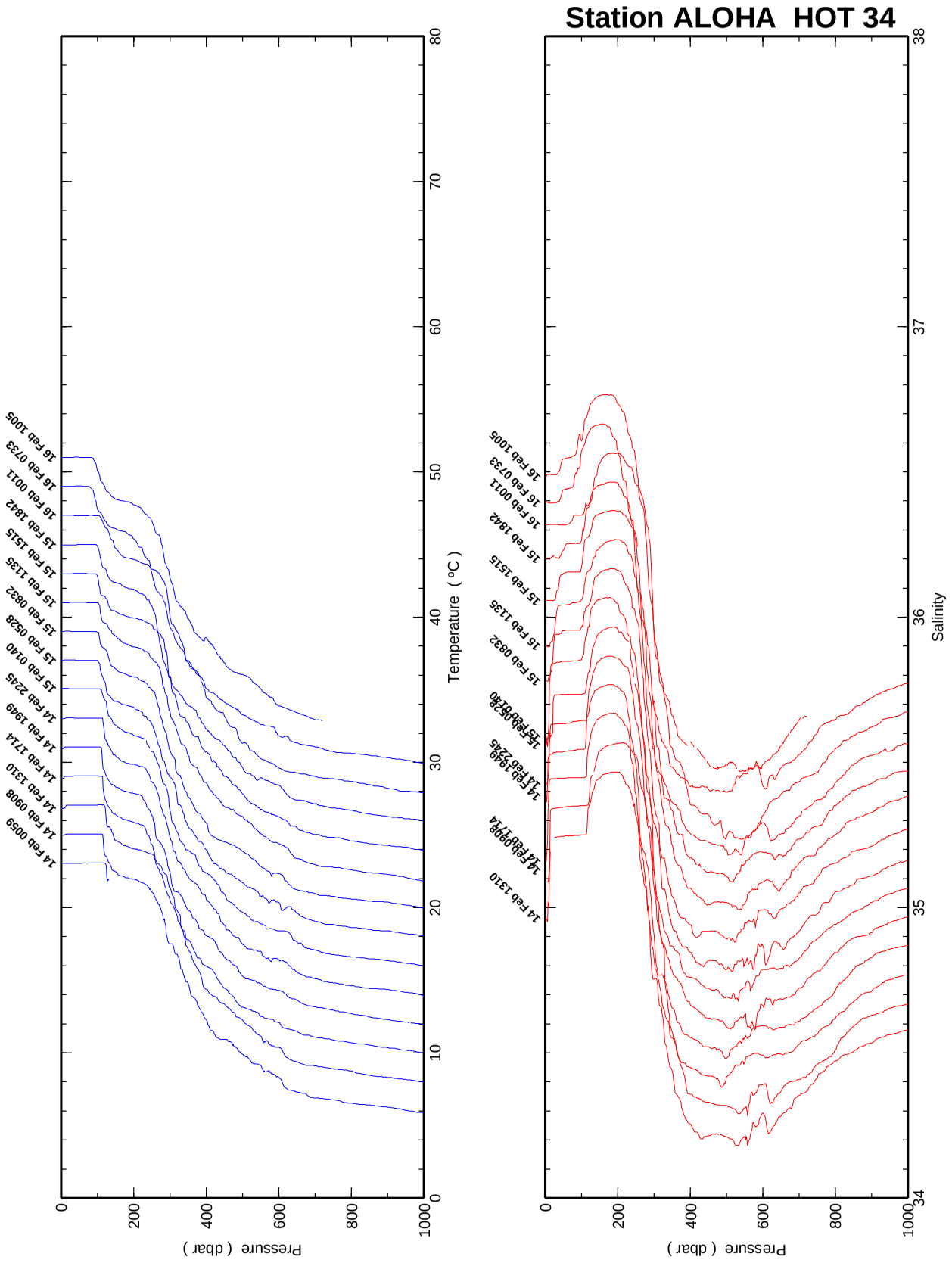
Station ALOHA HOT 34
Temperature (°C)
Salinity
Pressure (dbar)
Pressure (dbar)
16 Feb 1005
16 Feb 0733
16 Feb 0011
15 Feb 1842
15 Feb 1515
15 Feb 1135
15 Feb 0832
15 Feb 0528
15 Feb 0140
14 Feb 2245
14 Feb 1949
14 Feb 1714
14 Feb 1310
14 Feb 0908
14 Feb 0059

Figure 6.1.2b

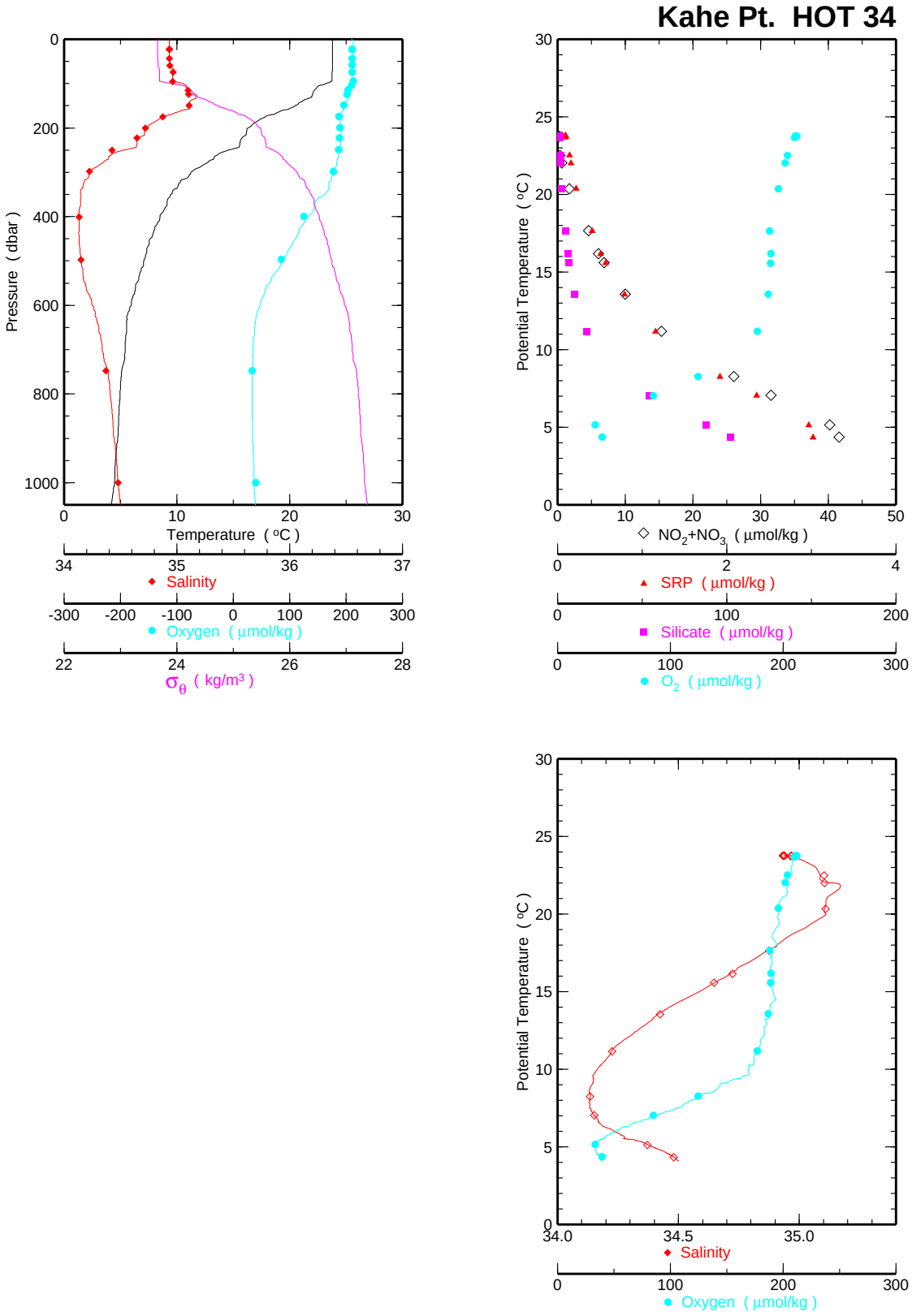
Kahe Pt. HOT 34
Pressure (dbar)
Temperature (°C)
Salinity
Oxygen (µmol/kg)
σθ (kg/m³)
Potential Temperature (°C)
NO2+NO3 (µmol/kg)
SRP (µmol/kg)
Silicate (µmol/kg)
O2 (µmol/kg)
Potential Temperature (°C)
Salinity
Oxygen (µmol/kg)

Figure 6.1.2c

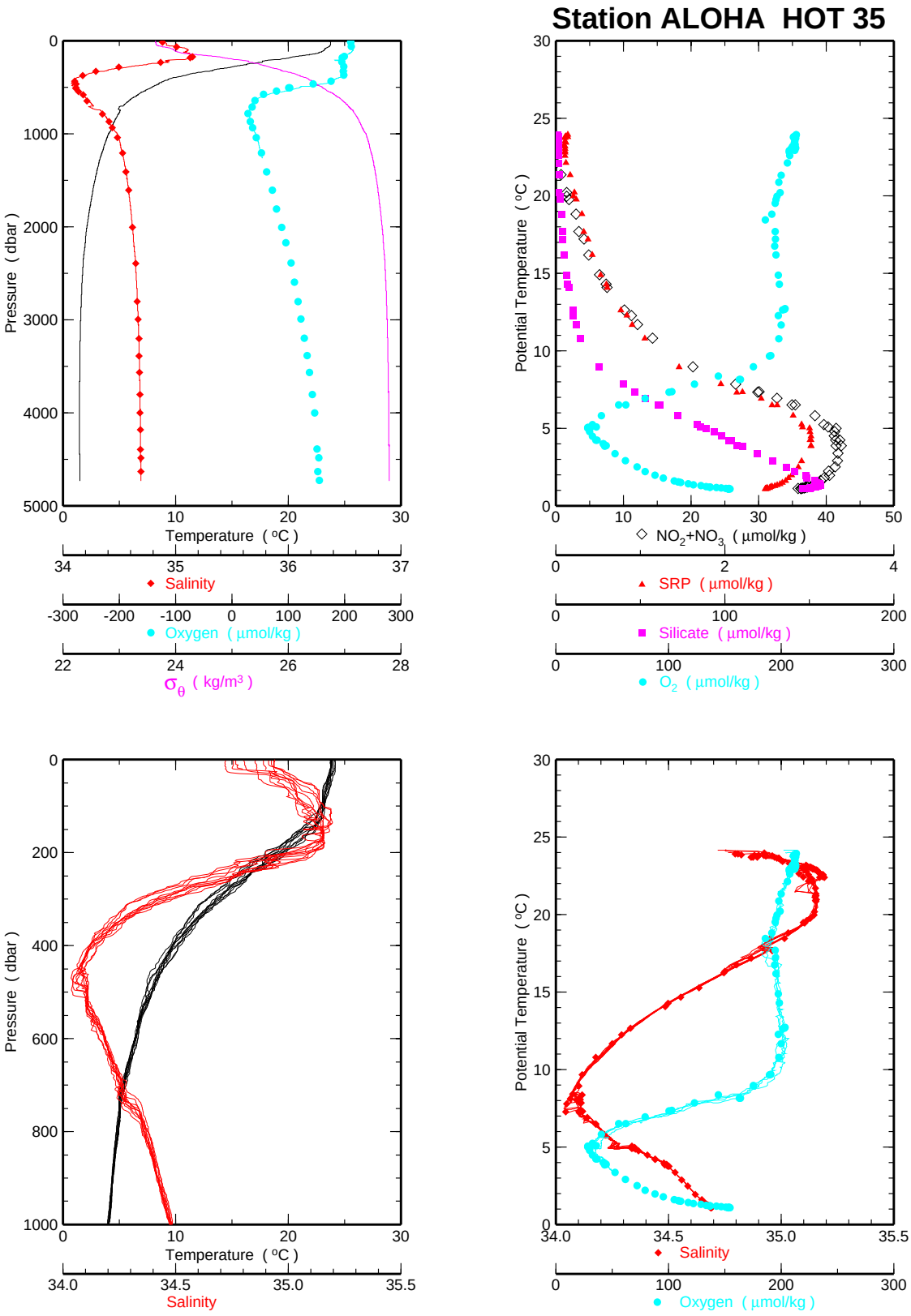
Station ALOHA HOT 35
Pressure (dbar)
Temperature (°C)
Salinity
Oxygen (µmol/kg)
σθ (kg/m³)
Potential Temperature (°C)
NO2+NO3 (µmol/kg)
SRP (µmol/kg)
Silicate (µmol/kg)
O2 (µmol/kg)

Figure 6.1.3a

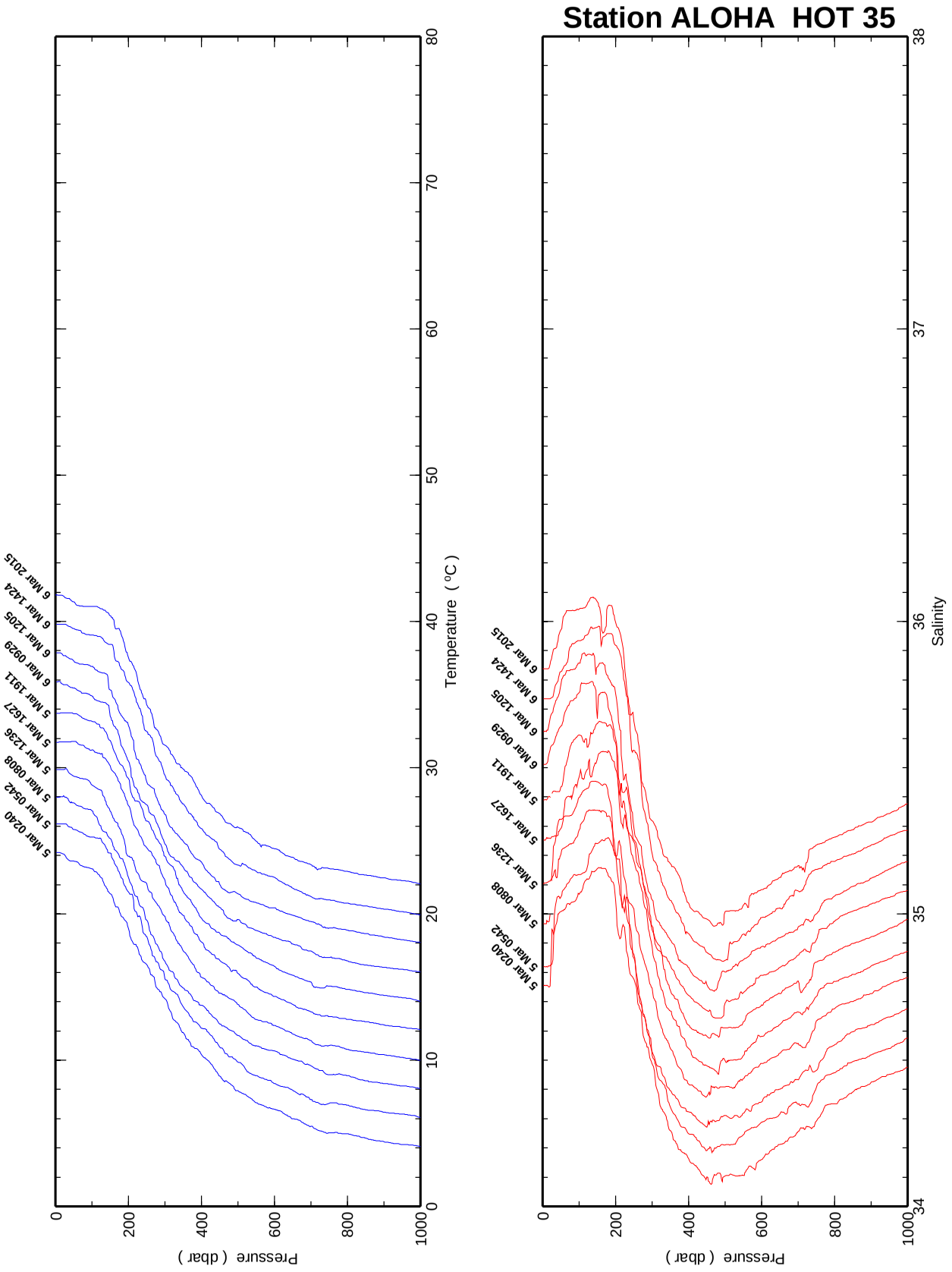
Station ALOHA HOT 35
Temperature (°C)
Salinity
Pressure (dbar)
0
200
400
600
800
1000
0
10
20
30
40
50
60
70
80
34
35
36
37
38
5 Mar 0240
5 Mar 0542
5 Mar 0808
5 Mar 1236
5 Mar 1627
5 Mar 1911
6 Mar 0929
6 Mar 1205
6 Mar 1424
6 Mar 2015

Figure 6.1.3b

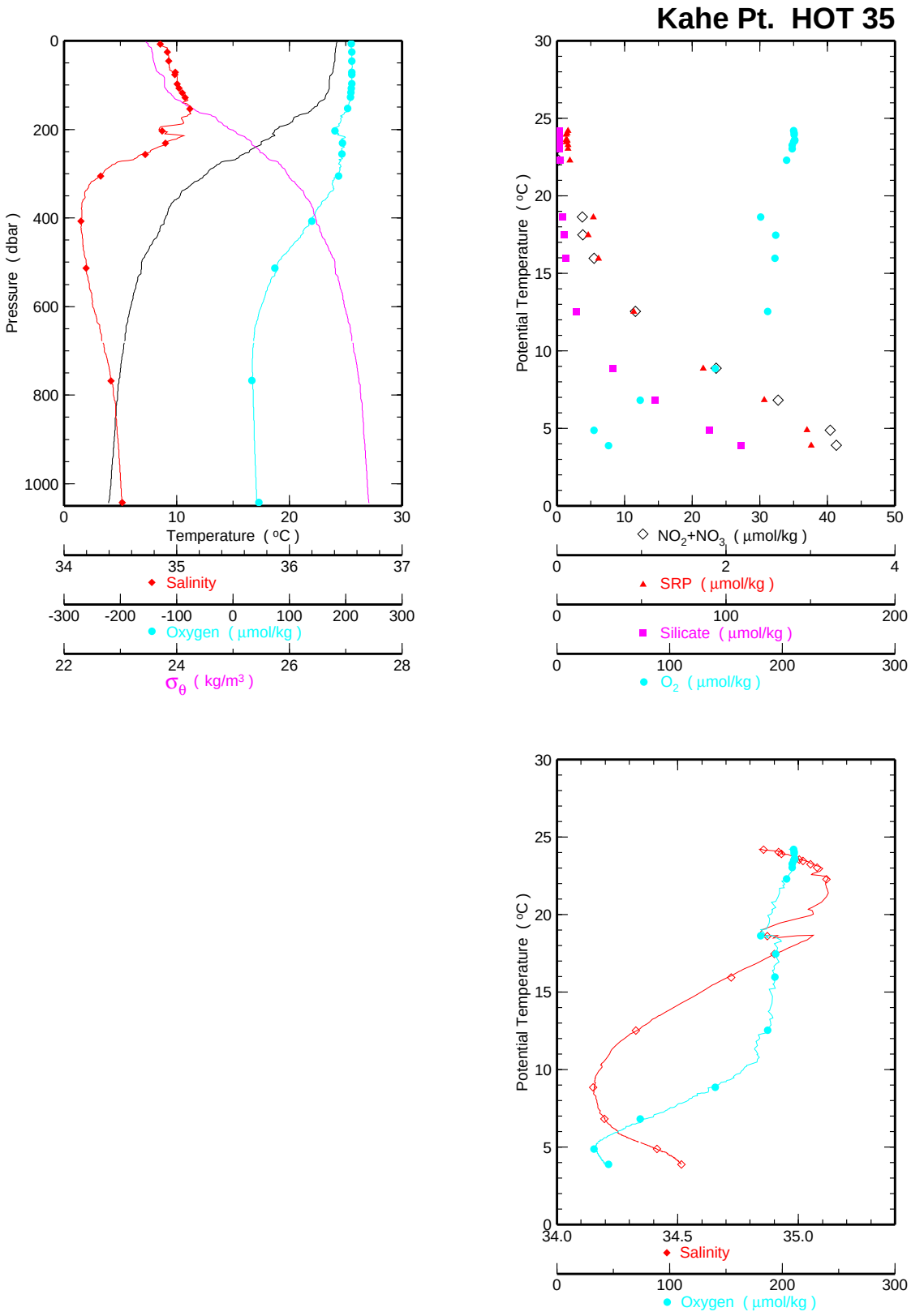
Kahe Pt. HOT 35
Pressure (dbar)
Temperature (ºC)
Salinity
Oxygen (µmol/kg)
σθ (kg/m³)
Potential Temperature (ºC)
NO2+NO3 (µmol/kg)
SRP (µmol/kg)
Silicate (µmol/kg)
O2 (µmol/kg)
Potential Temperature (ºC)
Salinity
Oxygen (µmol/kg)

Figure 6.1.3c

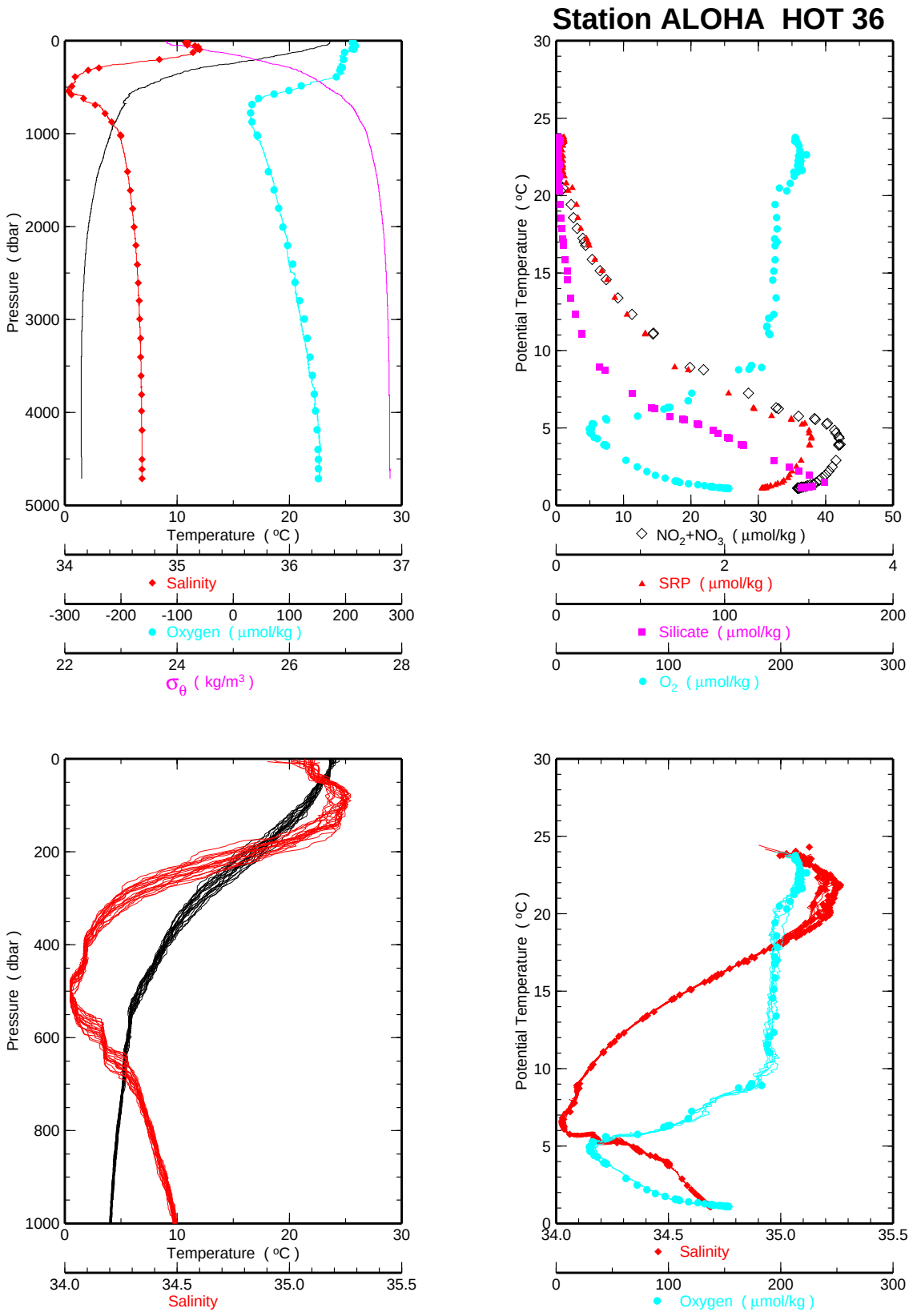
Station ALOHA HOT 36
Pressure (dbar)
Temperature (ºC)
Salinity
Oxygen (µmol/kg)
σθ (kg/m3)
Potential Temperature (ºC)
NO2+NO3 (µmol/kg)
SRP (µmol/kg)
Silicate (µmol/kg)
O2 (µmol/kg)

Figure 6.1.4a

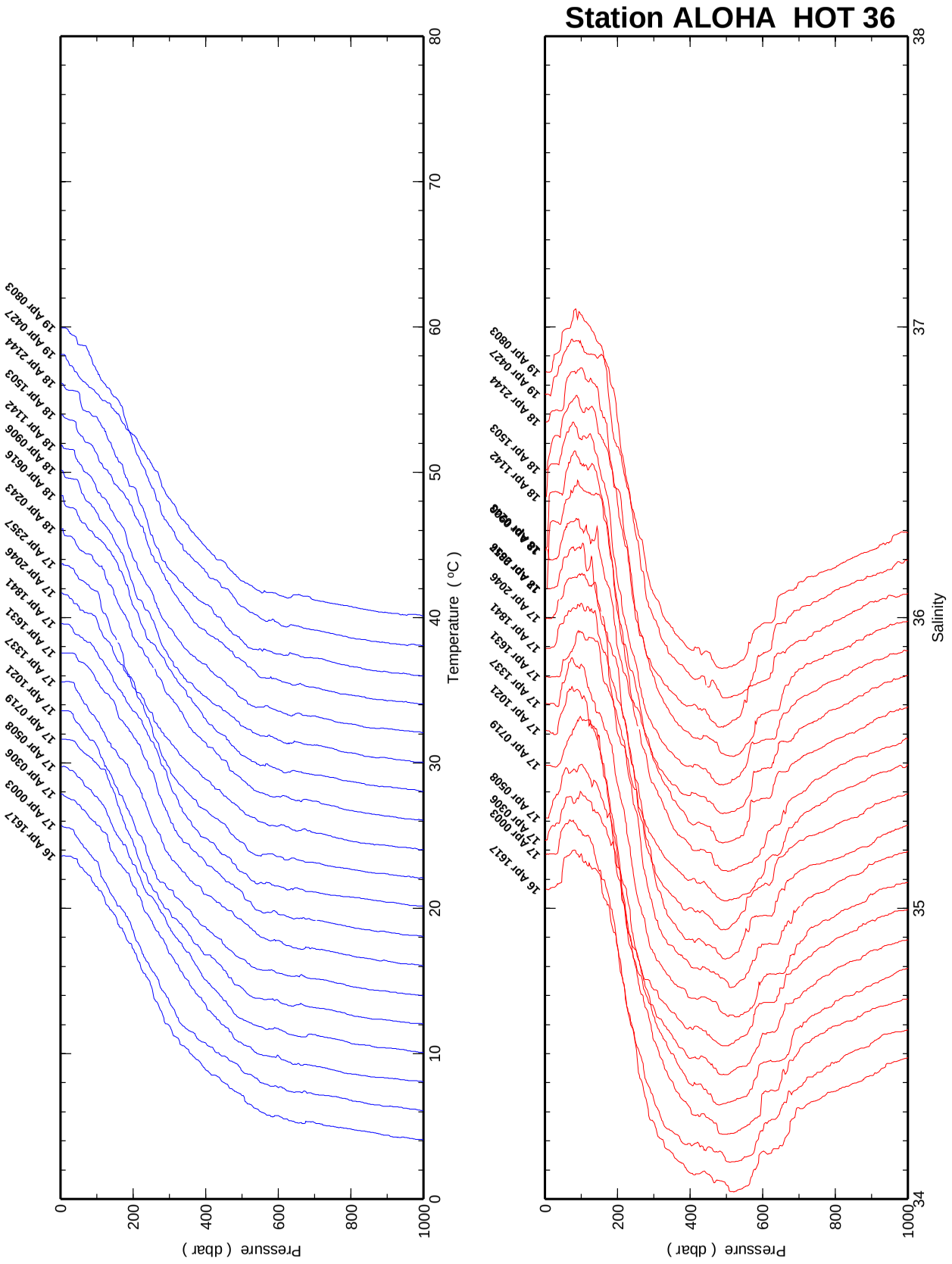
Station ALOHA HOT 36
Temperature (°C)
Salinity
Pressure (dbar)
Pressure (dbar)
0
200
400
600
800
1000
0
10
20
30
40
50
60
70
80
34
35
36
37
38
16 Apr 1617
17 Apr 0003
17 Apr 0306
17 Apr 0508
17 Apr 0719
17 Apr 1021
17 Apr 1337
17 Apr 1631
17 Apr 1841
17 Apr 2046
17 Apr 2357
18 Apr 0243
18 Apr 0516
18 Apr 0906
18 Apr 1142
18 Apr 1503
18 Apr 2144
19 Apr 0427
19 Apr 0803

Figure 6.1.4b

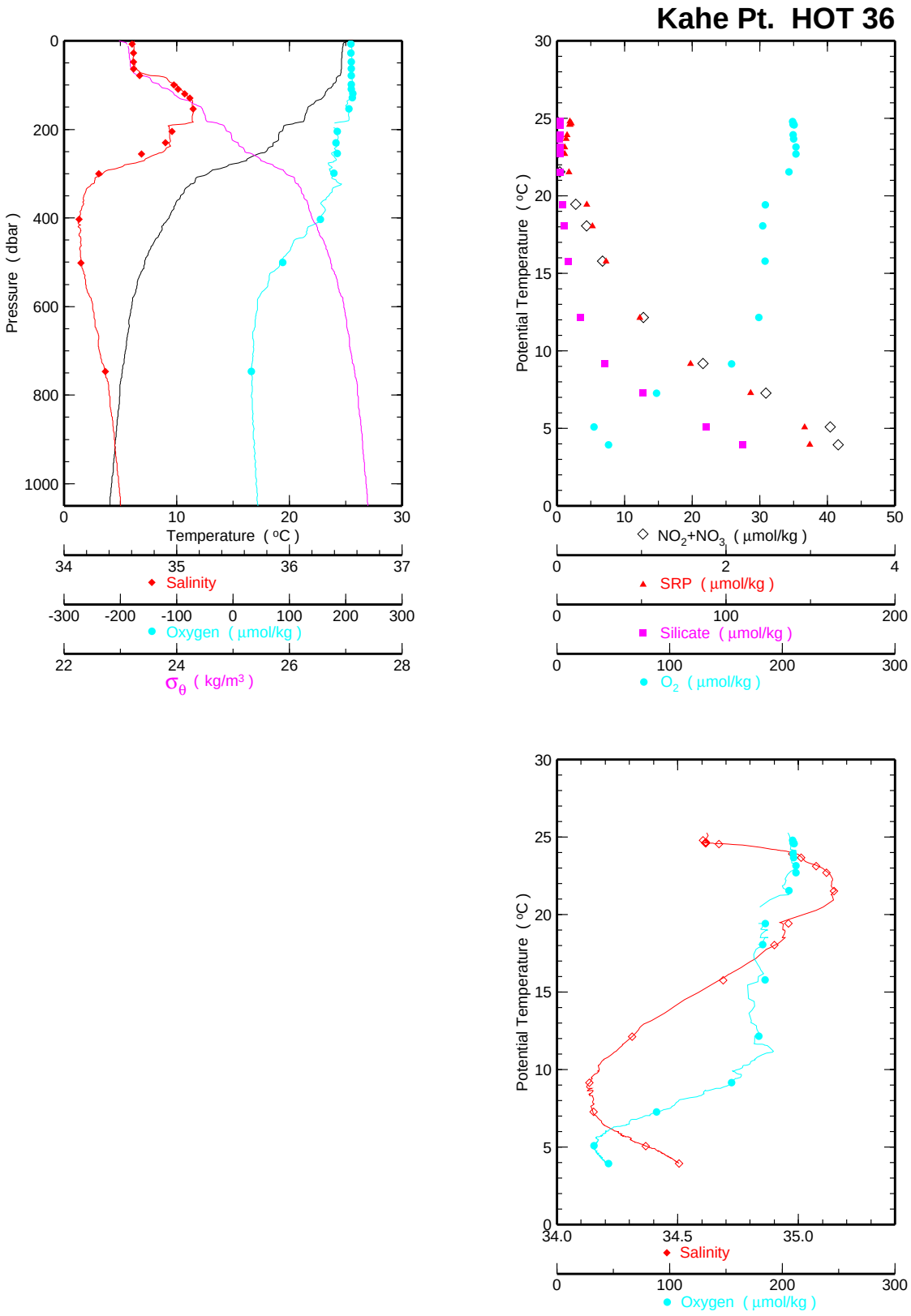
Kahe Pt. HOT 36
Pressure (dbar)
Temperature (ºC)
Salinity
Oxygen (µmol/kg)
σθ (kg/m³)
Potential Temperature (ºC)
NO2+NO3 (µmol/kg)
SRP (µmol/kg)
Silicate (µmol/kg)
O2 (µmol/kg)
Potential Temperature (ºC)
Salinity
Oxygen (µmol/kg)

Figure 6.1.4c

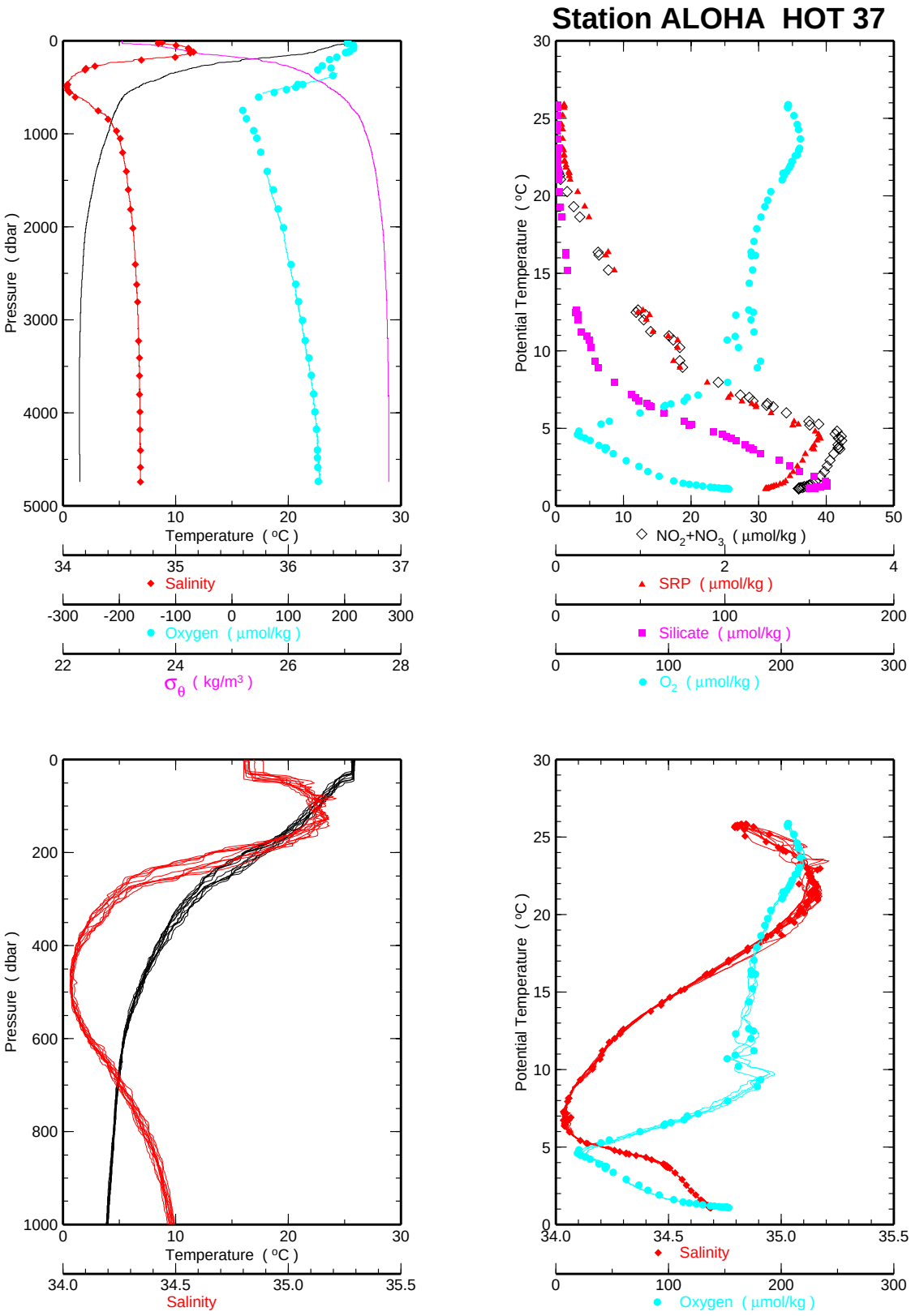
Station ALOHA HOT 37
Pressure (dbar)
Temperature (°C)
Salinity
Oxygen (µmol/kg)
σθ (kg/m³)
Potential Temperature (°C)
NO2+NO3 (µmol/kg)
SRP (µmol/kg)
Silicate (µmol/kg)
O2 (µmol/kg)

Figure 6.1.5a

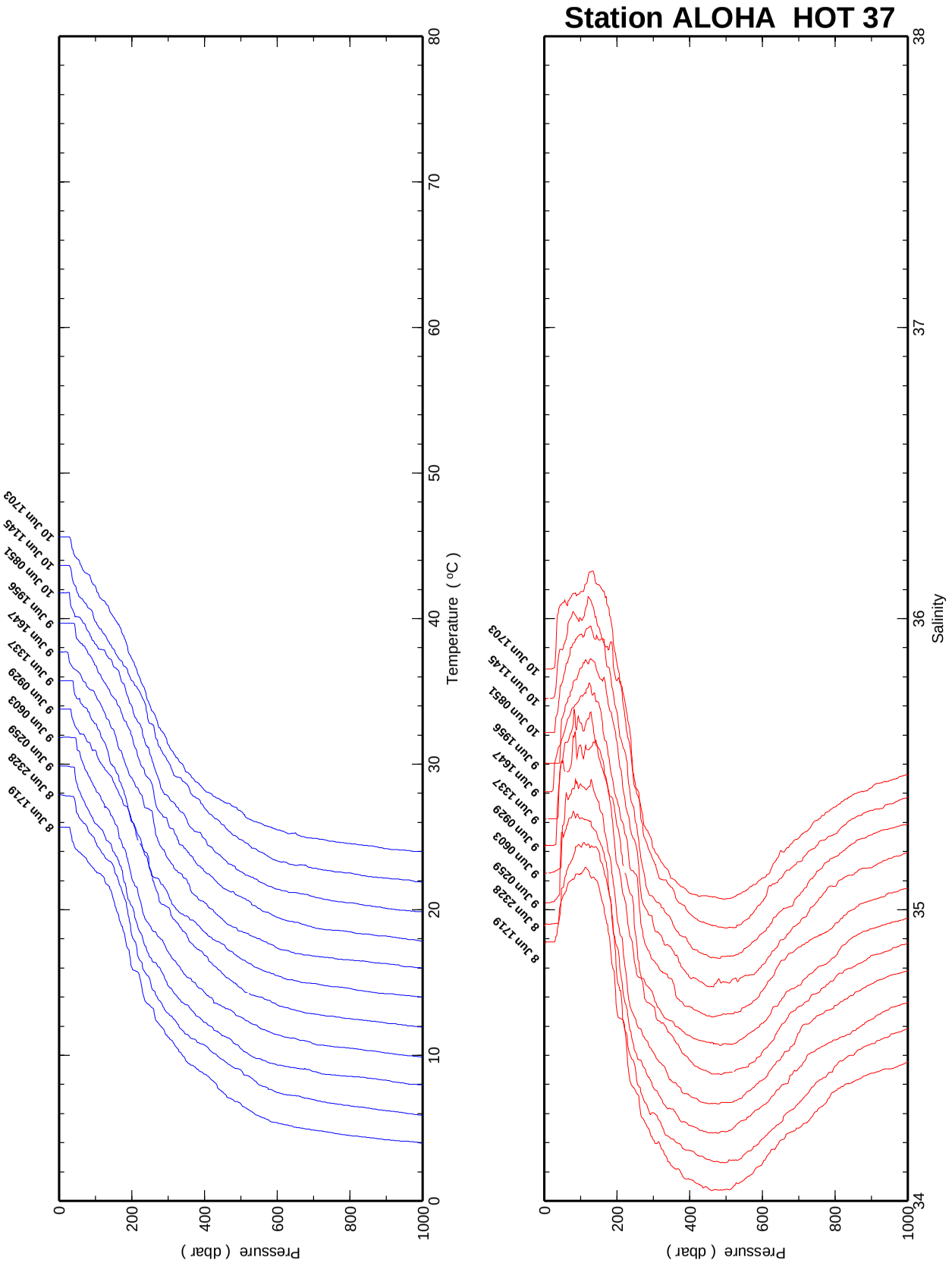
Station ALOHA HOT 37
Temperature (°C)
Salinity
Pressure (dbar)
Pressure (dbar)
0
200
400
600
800
1000
0
10
20
30
40
50
60
70
80
34
35
36
37
38
8 Jun 1719
8 Jun 2328
9 Jun 0259
9 Jun 0603
9 Jun 0929
9 Jun 1337
9 Jun 1647
9 Jun 1956
10 Jun 0851
10 Jun 1145
10 Jun 1703

Figure 6.1.5b

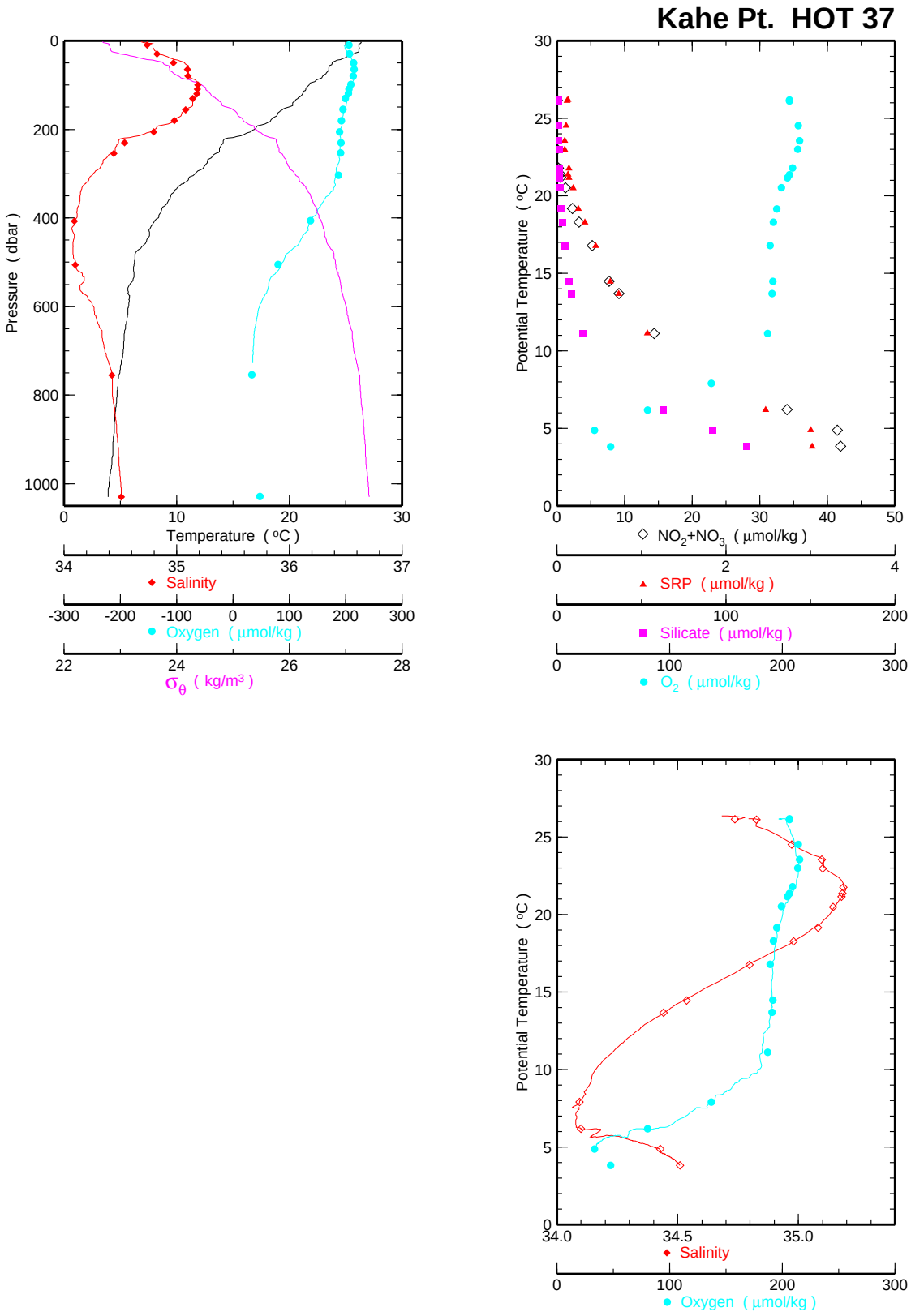
Kahe Pt. HOT 37
Pressure (dbar)
Temperature (ºC)
Salinity
Oxygen (µmol/kg)
σθ (kg/m³)
Potential Temperature (ºC)
NO2+NO3 (µmol/kg)
SRP (µmol/kg)
Silicate (µmol/kg)
O2 (µmol/kg)
Potential Temperature (ºC)
Salinity
Oxygen (µmol/kg)

Figure 6.1.5c

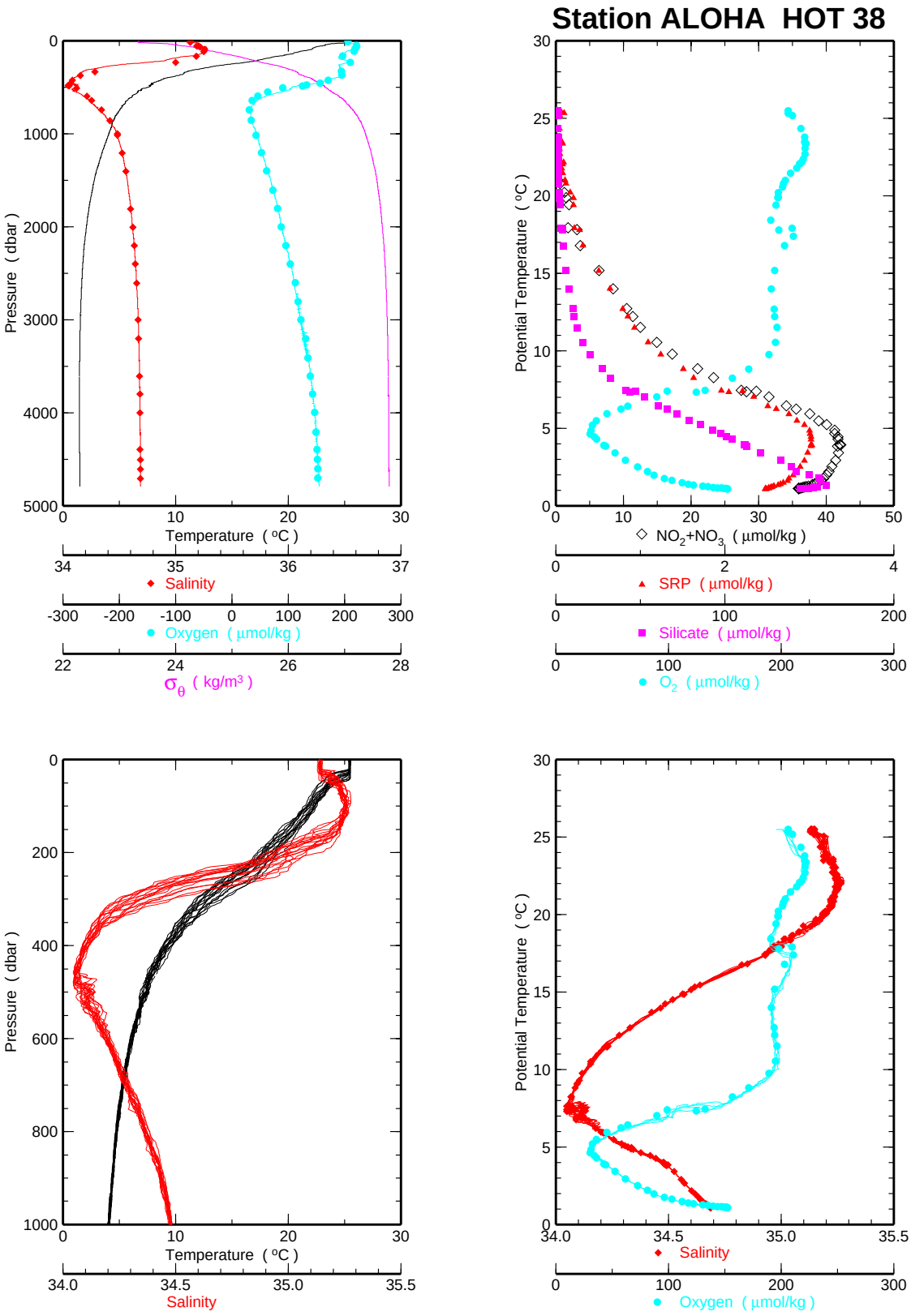
Station ALOHA HOT 38
Pressure (dbar)
Temperature (°C)
Salinity
Oxygen (µmol/kg)
σθ (kg/m³)
Potential Temperature (°C)
NO2+NO3 (µmol/kg)
SRP (µmol/kg)
Silicate (µmol/kg)
O2 (µmol/kg)

Figure 6.1.6a

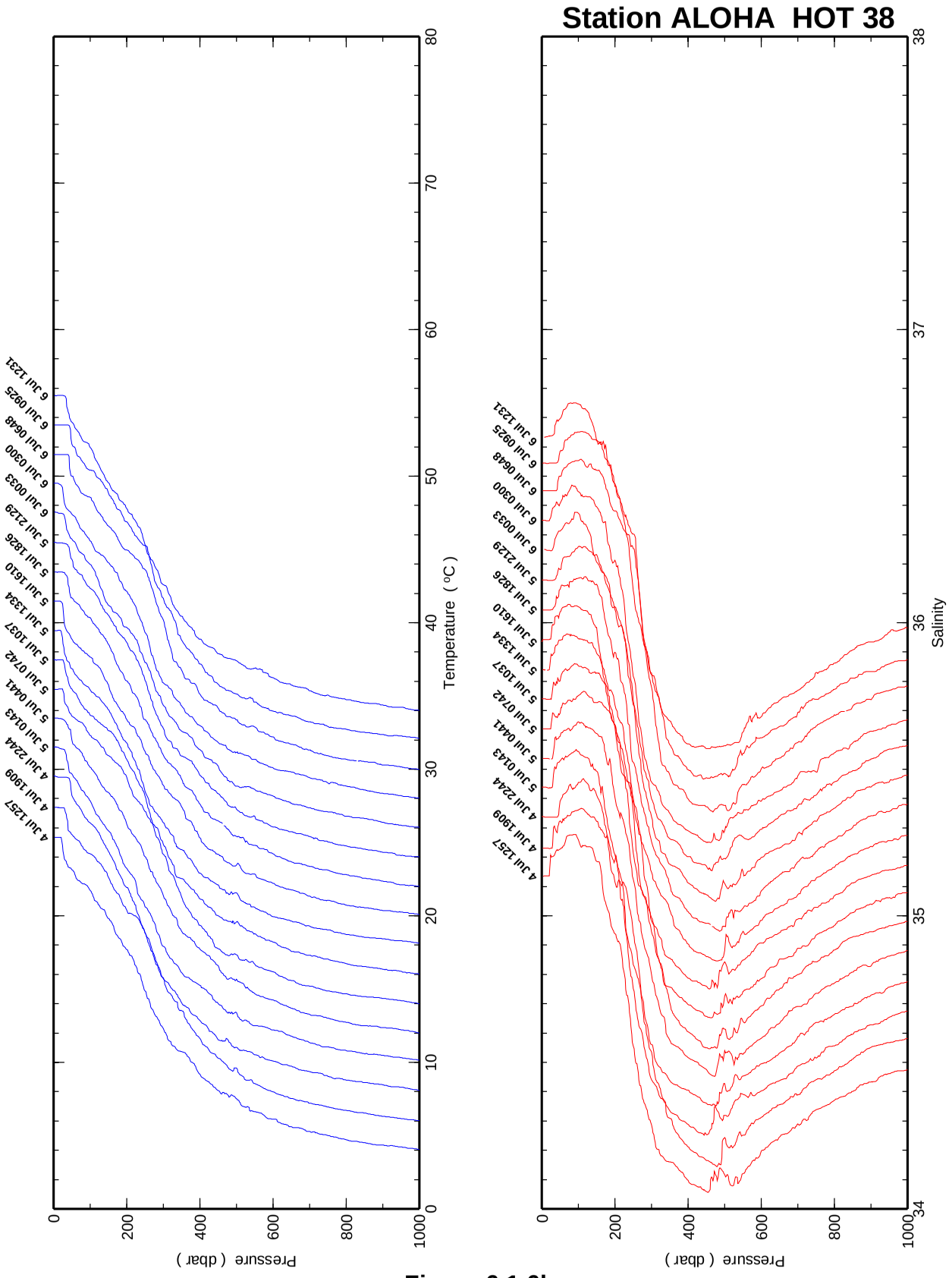
Station ALOHA HOT 38
Temperature (°C)
Salinity
Pressure (dbar)
Pressure (dbar)
0
200
400
600
800
1000
10
20
30
40
50
60
70
80
34
35
36
37
38
6 Jul 1231
6 Jul 0925
6 Jul 0648
6 Jul 0300
6 Jul 0033
5 Jul 2129
5 Jul 1826
5 Jul 1610
5 Jul 1334
5 Jul 1037
5 Jul 0742
5 Jul 0441
5 Jul 0143
4 Jul 2244
4 Jul 1909
4 Jul 1257

Figure 6.1.6b

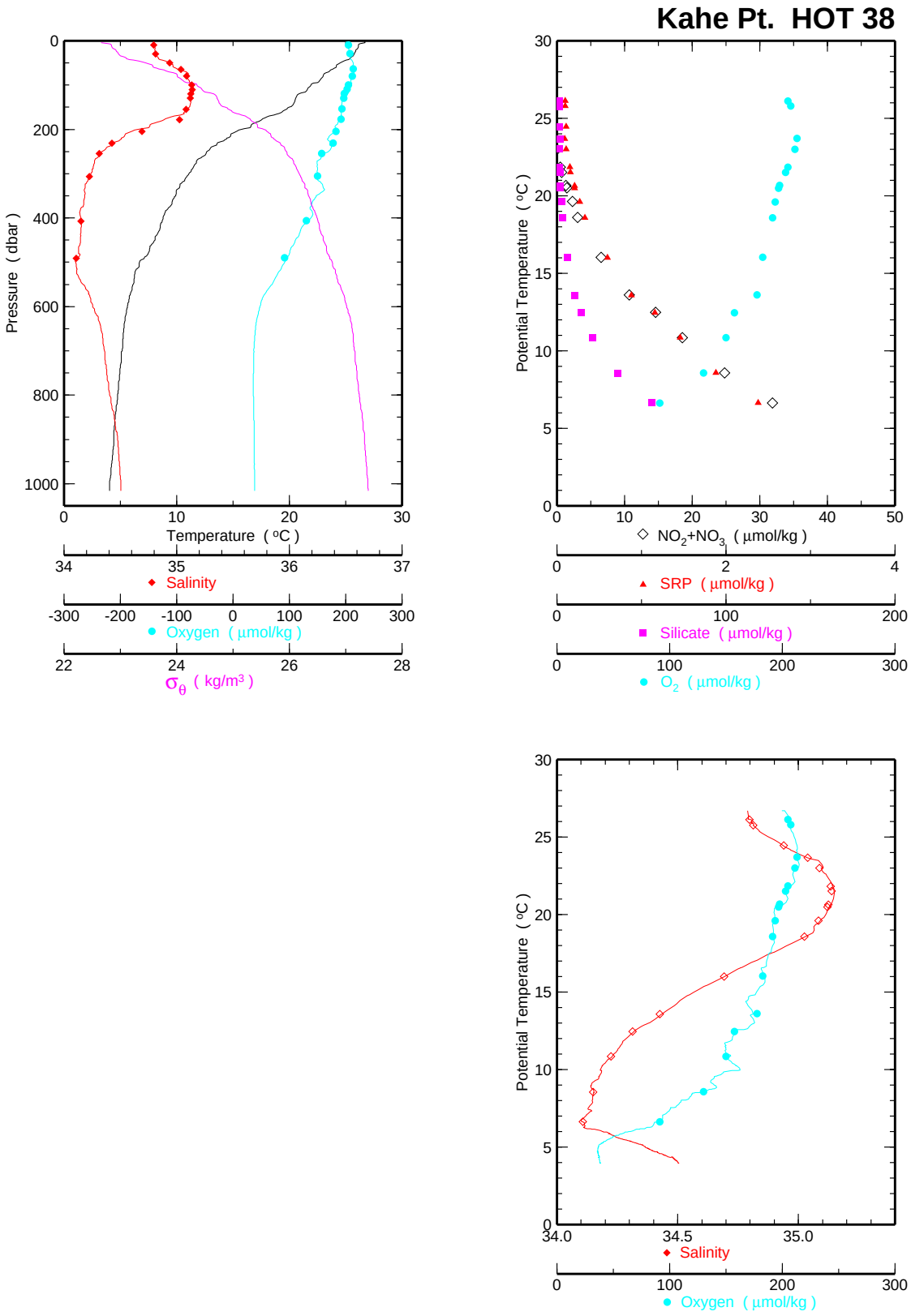
Kahe Pt. HOT 38
Pressure (dbar)
Temperature (ºC)
Salinity
Oxygen (µmol/kg)
σθ (kg/m³)
Potential Temperature (ºC)
NO2+NO3 (µmol/kg)
SRP (µmol/kg)
Silicate (µmol/kg)
O2 (µmol/kg)
Potential Temperature (ºC)
Salinity
Oxygen (µmol/kg)

Figure 6.1.6c

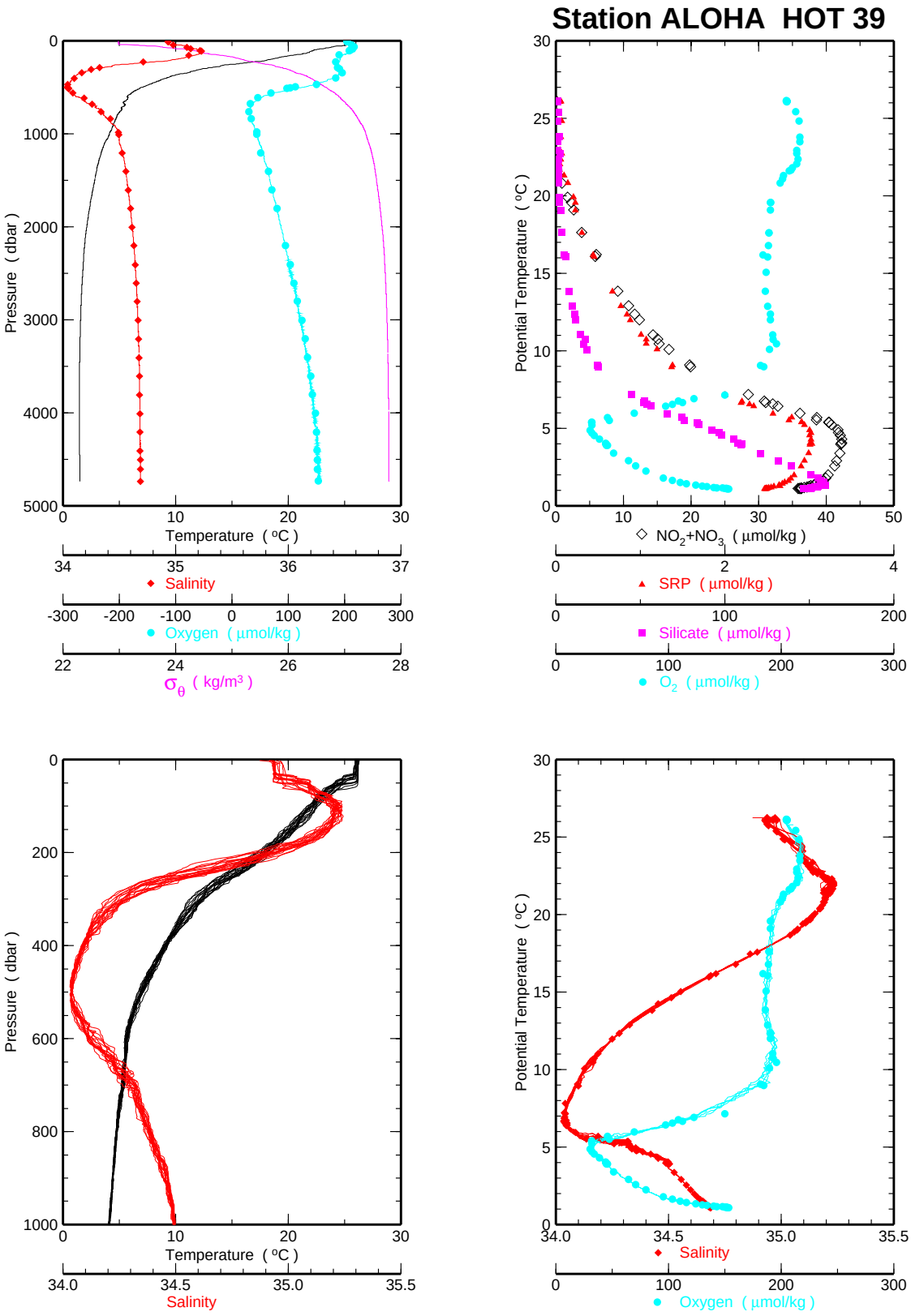
Station ALOHA HOT 39
Pressure (dbar)
Temperature (°C)
Salinity
Oxygen (µmol/kg)
σθ (kg/m³)
Potential Temperature (°C)
NO2+NO3 (µmol/kg)
SRP (µmol/kg)
Silicate (µmol/kg)
O2 (µmol/kg)

Figure 6.1.7a

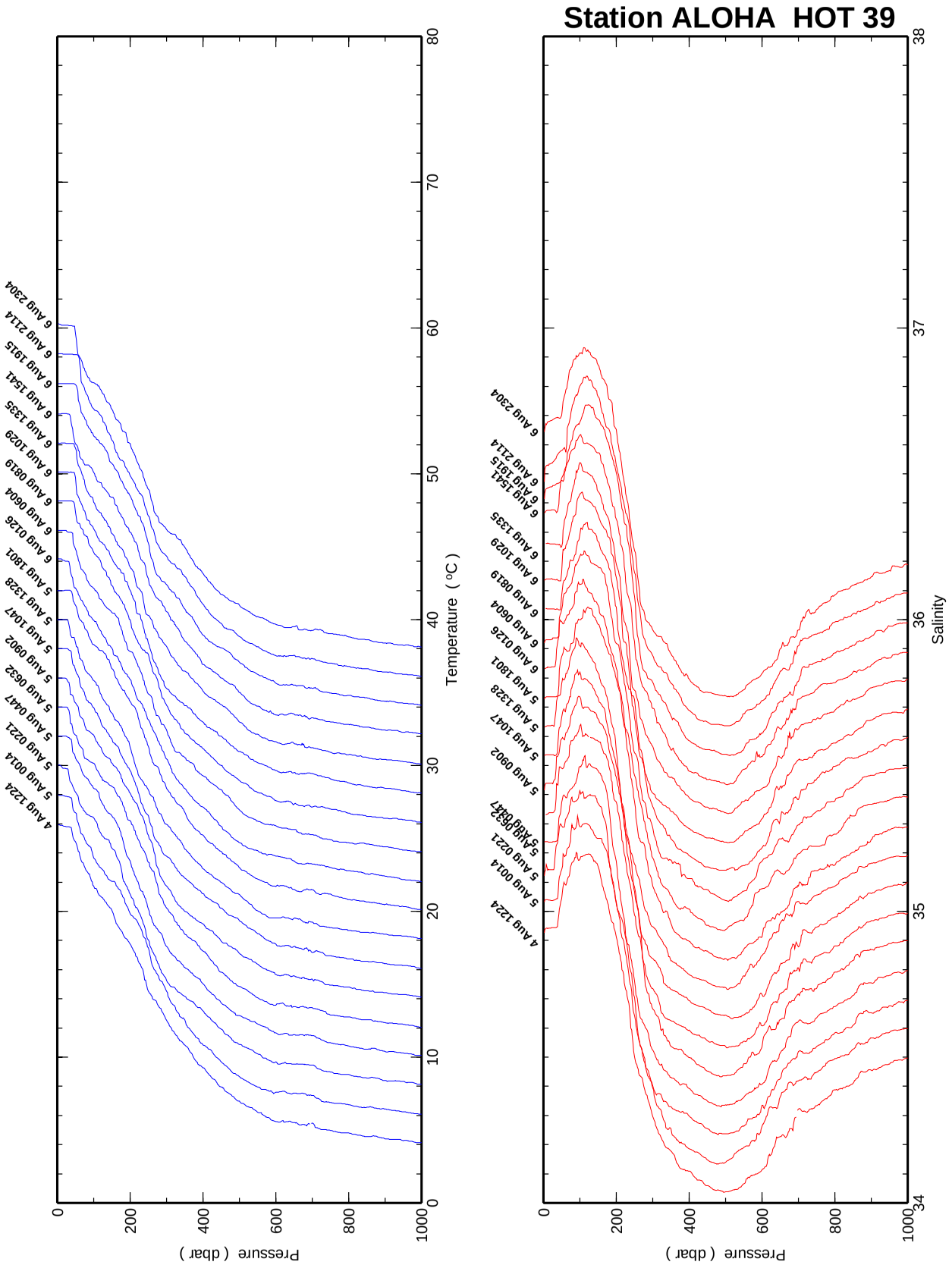
Station ALOHA HOT 39
Temperature (°C)
Salinity
Pressure (dbar)
Pressure (dbar)
0
200
400
600
800
1000
0
10
20
30
40
50
60
70
80
34
35
36
37
38
6 Aug 2304
6 Aug 2114
6 Aug 1915
6 Aug 1541
6 Aug 1335
6 Aug 1029
6 Aug 0819
6 Aug 0604
6 Aug 0126
5 Aug 1801
5 Aug 1328
5 Aug 1047
5 Aug 0902
5 Aug 0632
5 Aug 0447
5 Aug 0221
5 Aug 0014
4 Aug 1224

Figure 6.1.7b

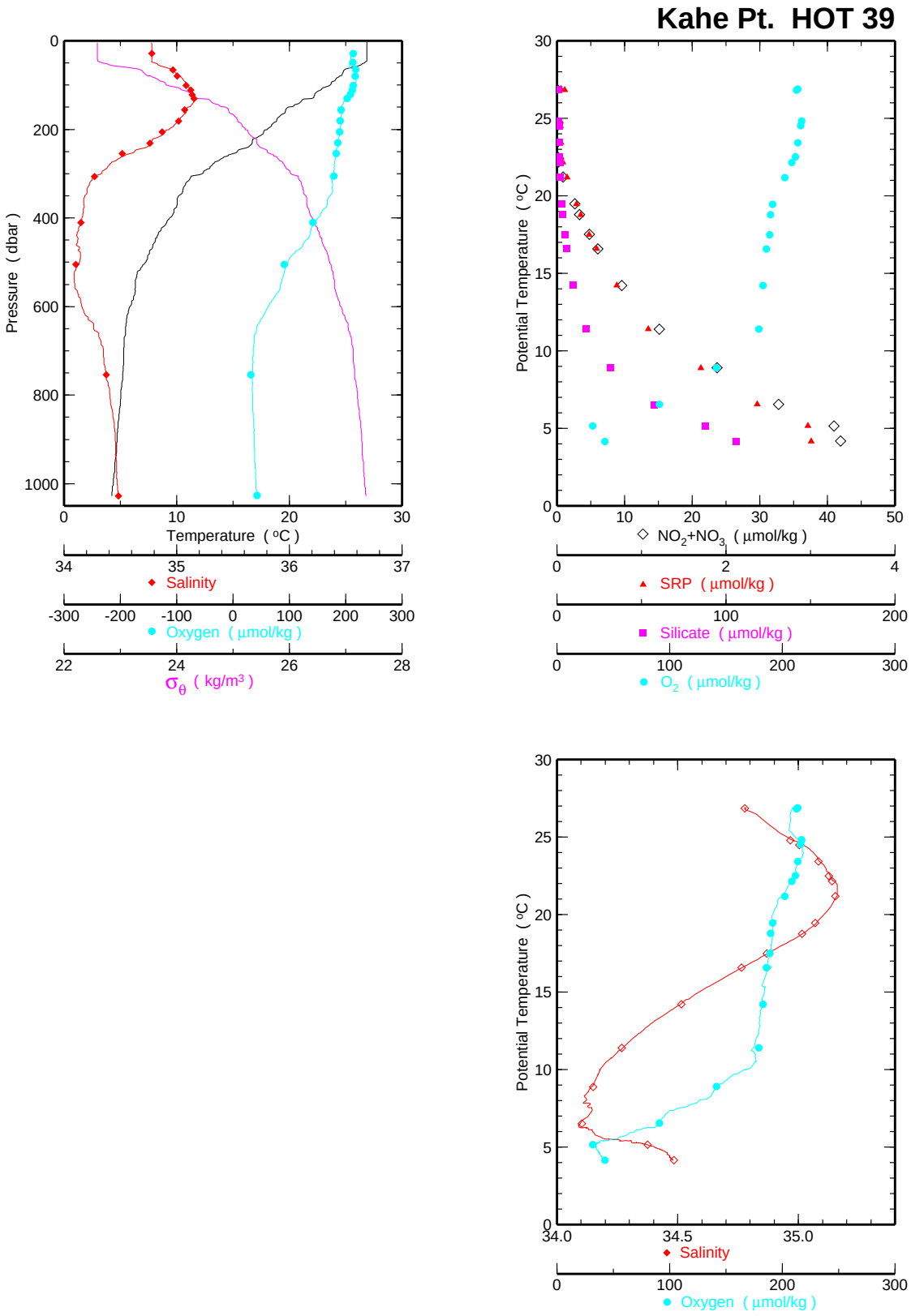
Kahe Pt. HOT 39
Pressure (dbar)
Temperature (ºC)
Salinity
Oxygen (µmol/kg)
σθ (kg/m³)
Potential Temperature (ºC)
NO2+NO3 (µmol/kg)
SRP (µmol/kg)
Silicate (µmol/kg)
O2 (µmol/kg)
Potential Temperature (ºC)
Salinity
Oxygen (µmol/kg)

Figure 6.1.7c

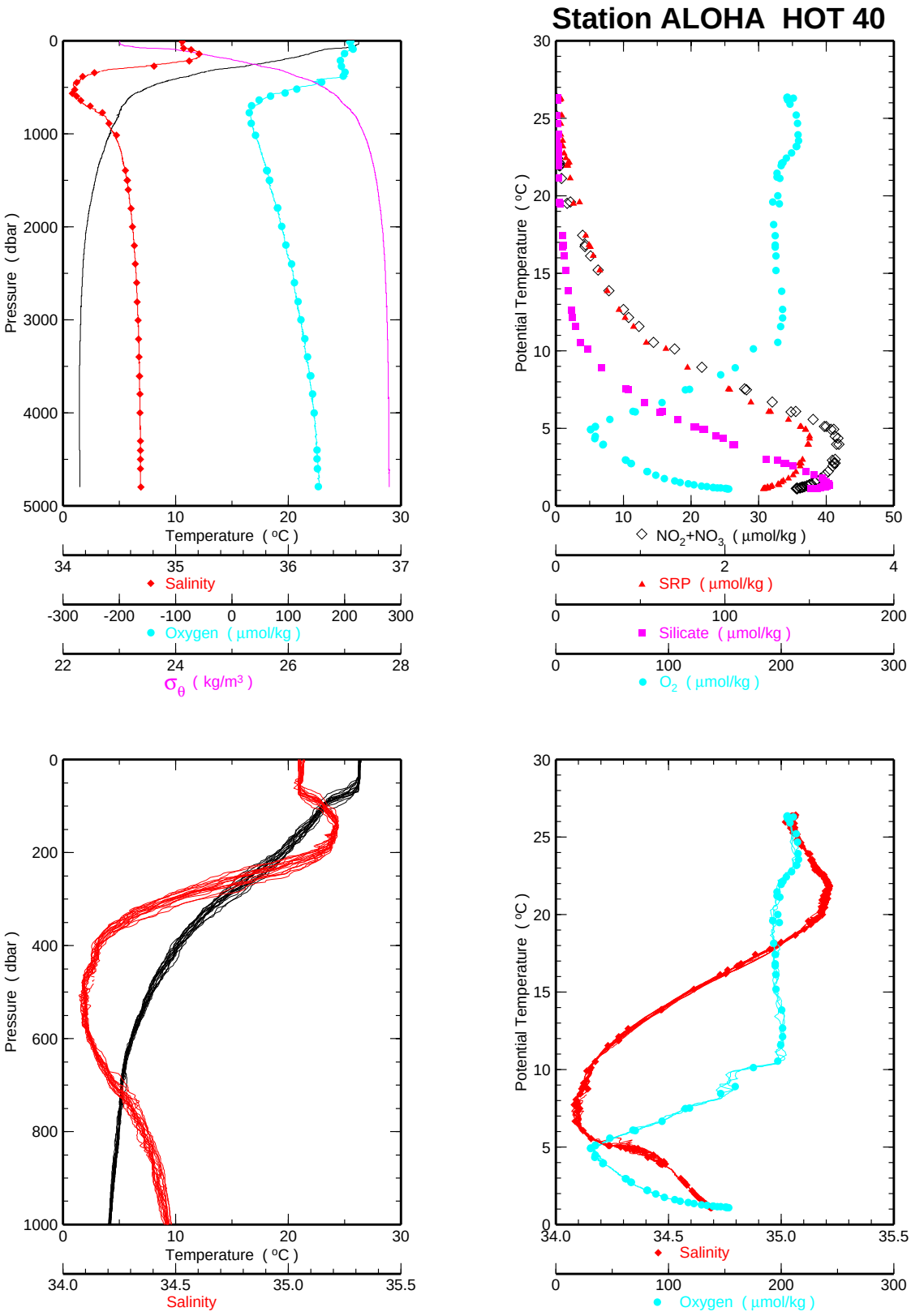
Station ALOHA HOT 40
Pressure (dbar)
Temperature (°C)
Salinity
Oxygen (µmol/kg)
σθ (kg/m³)
Potential Temperature (°C)
NO2+NO3 (µmol/kg)
SRP (µmol/kg)
Silicate (µmol/kg)
O2 (µmol/kg)

Figure 6.1.8a

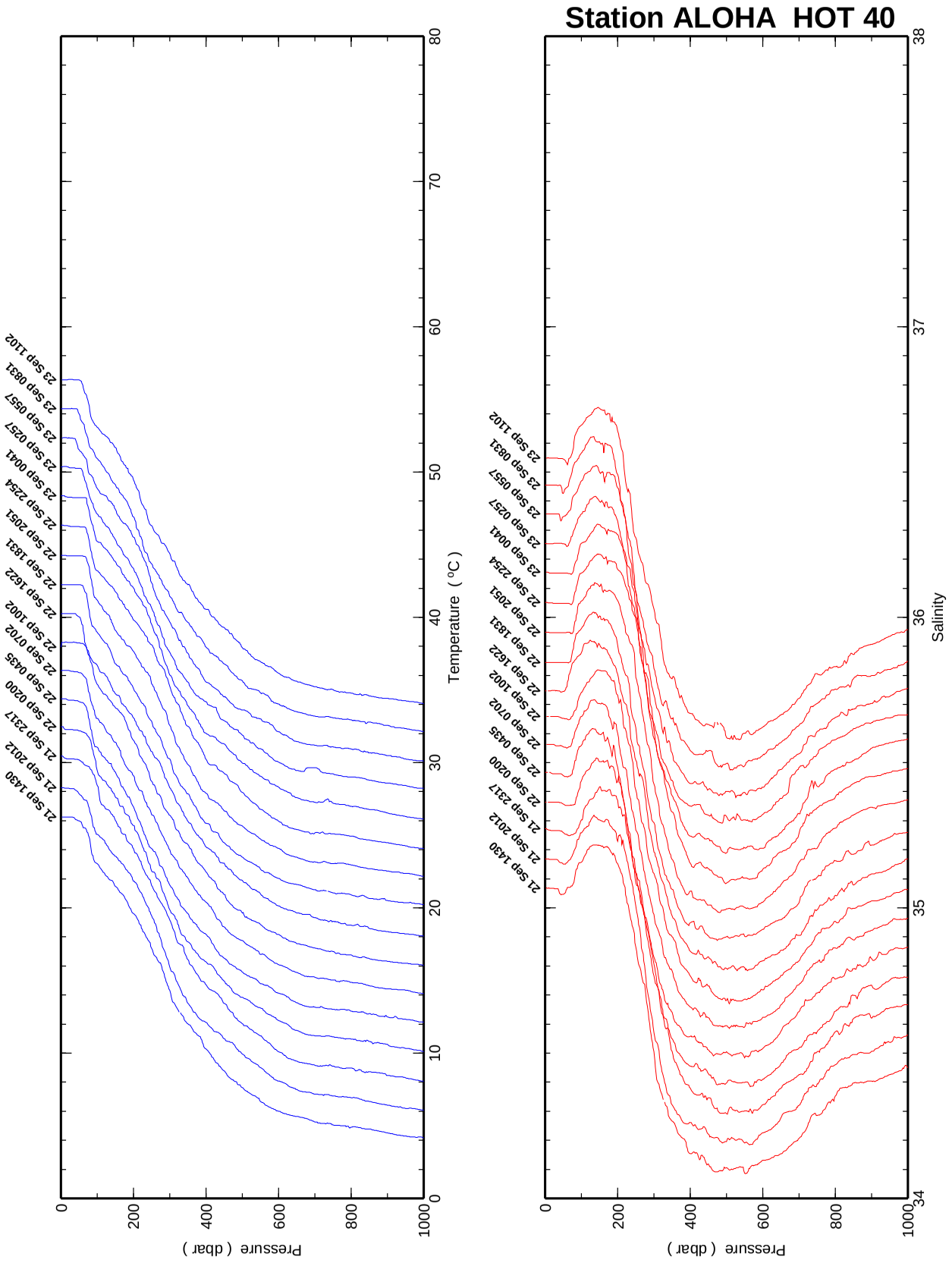
Station ALOHA HOT 40
Temperature (°C)
Salinity
Pressure (dbar)
Pressure (dbar)
23 Sep 1102
23 Sep 0831
23 Sep 0557
23 Sep 0257
23 Sep 0041
22 Sep 2254
22 Sep 2051
22 Sep 1831
22 Sep 1622
22 Sep 1002
22 Sep 0702
22 Sep 0435
22 Sep 0200
21 Sep 2317
21 Sep 2012
21 Sep 1430

Figure 6.1.8b

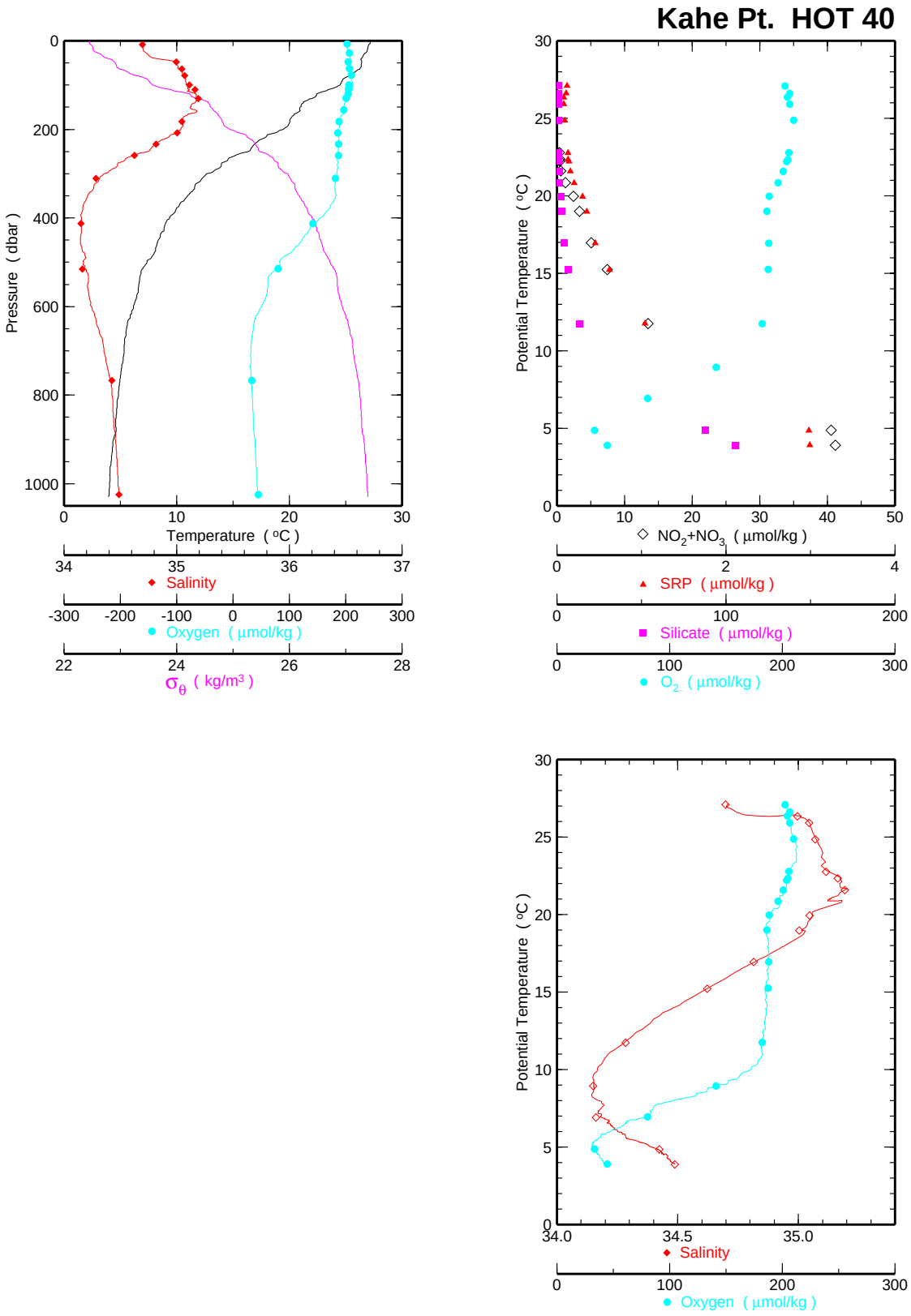
Kahe Pt. HOT 40
Pressure (dbar)
Temperature (ºC)
Salinity
Oxygen (µmol/kg)
σθ (kg/m³)
Potential Temperature (ºC)
NO2+NO3 (µmol/kg)
SRP (µmol/kg)
Silicate (µmol/kg)
O2 (µmol/kg)
Potential Temperature (ºC)
Salinity
Oxygen (µmol/kg)

Figure 6.1.8c

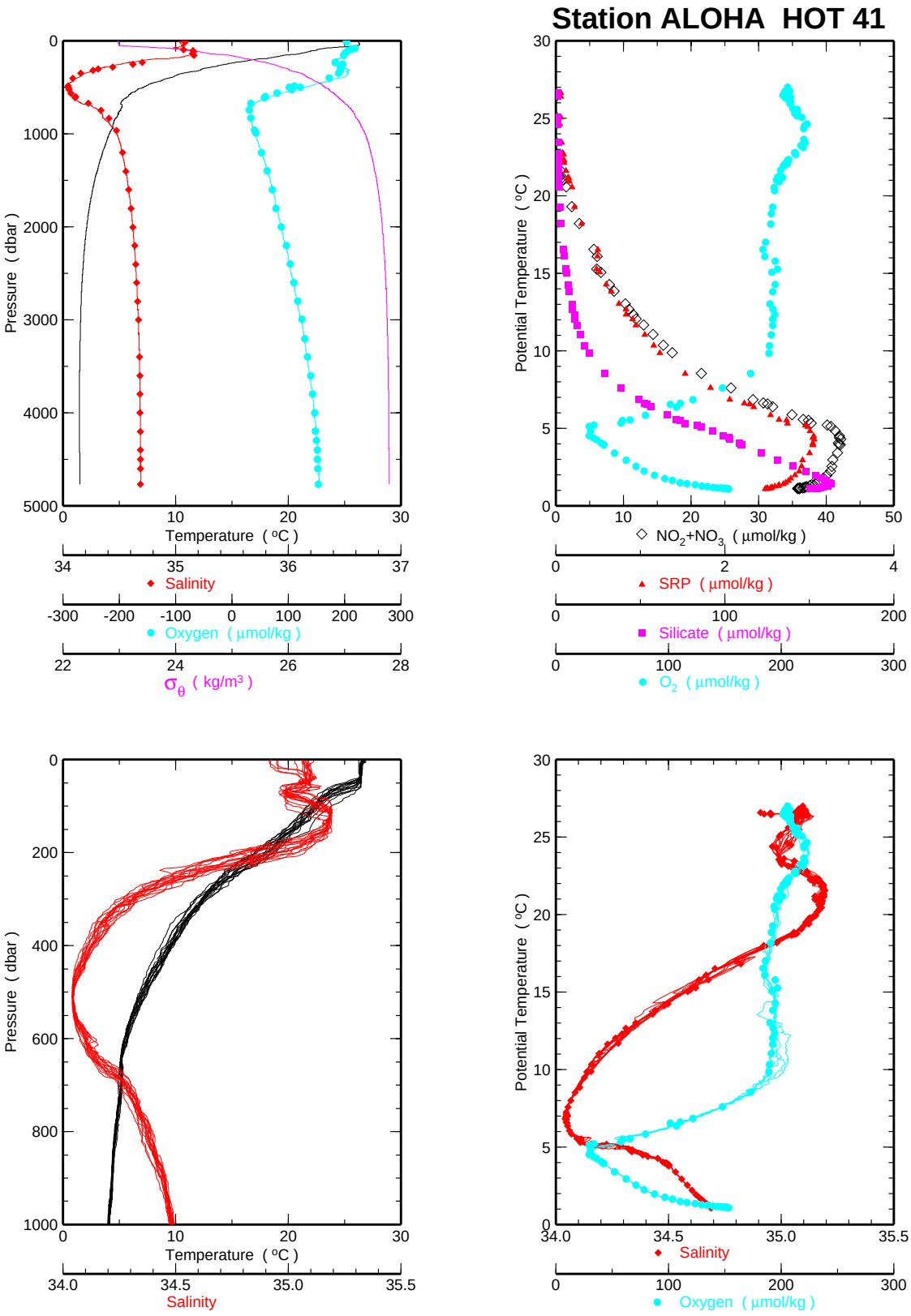
Station ALOHA HOT 41
Pressure (dbar)
Temperature (°C)
Salinity
Oxygen (µmol/kg)
σθ (kg/m³)
Potential Temperature (°C)
NO2+NO3 (µmol/kg)
SRP (µmol/kg)
Silicate (µmol/kg)
O2 (µmol/kg)

Figure 6.1.9a

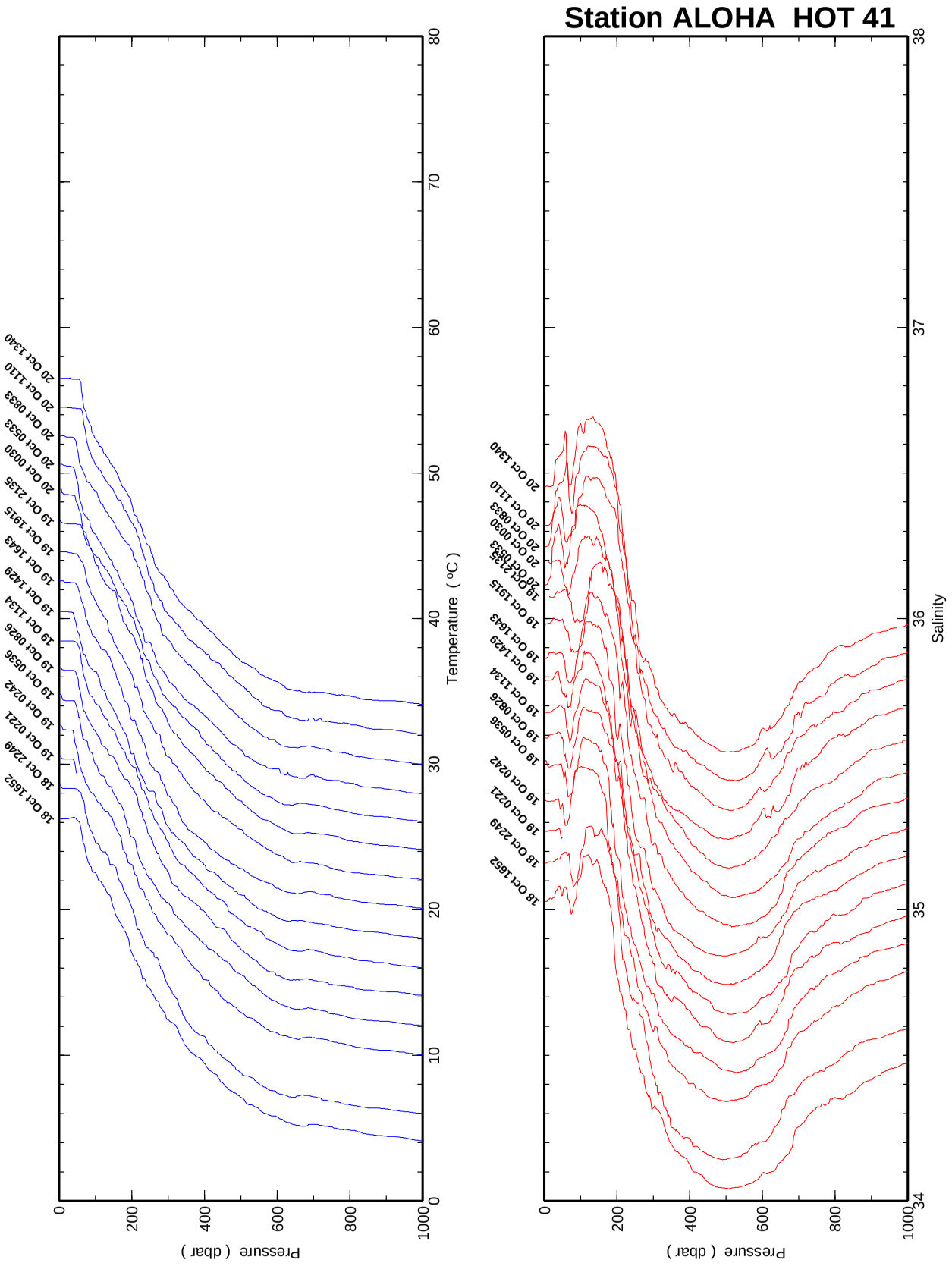
Station ALOHA HOT 41
Temperature (°C)
Salinity
Pressure (dbar)
Pressure (dbar)
0
200
400
600
800
1000
0
10
20
30
40
50
60
70
80
34
35
36
37
38
18 Oct 1652
18 Oct 2249
19 Oct 0221
19 Oct 0242
19 Oct 0536
19 Oct 0826
19 Oct 1134
19 Oct 1429
19 Oct 1643
19 Oct 1915
19 Oct 2135
20 Oct 0030
20 Oct 0533
20 Oct 0833
20 Oct 1110
20 Oct 1340

Figure 6.1.9b

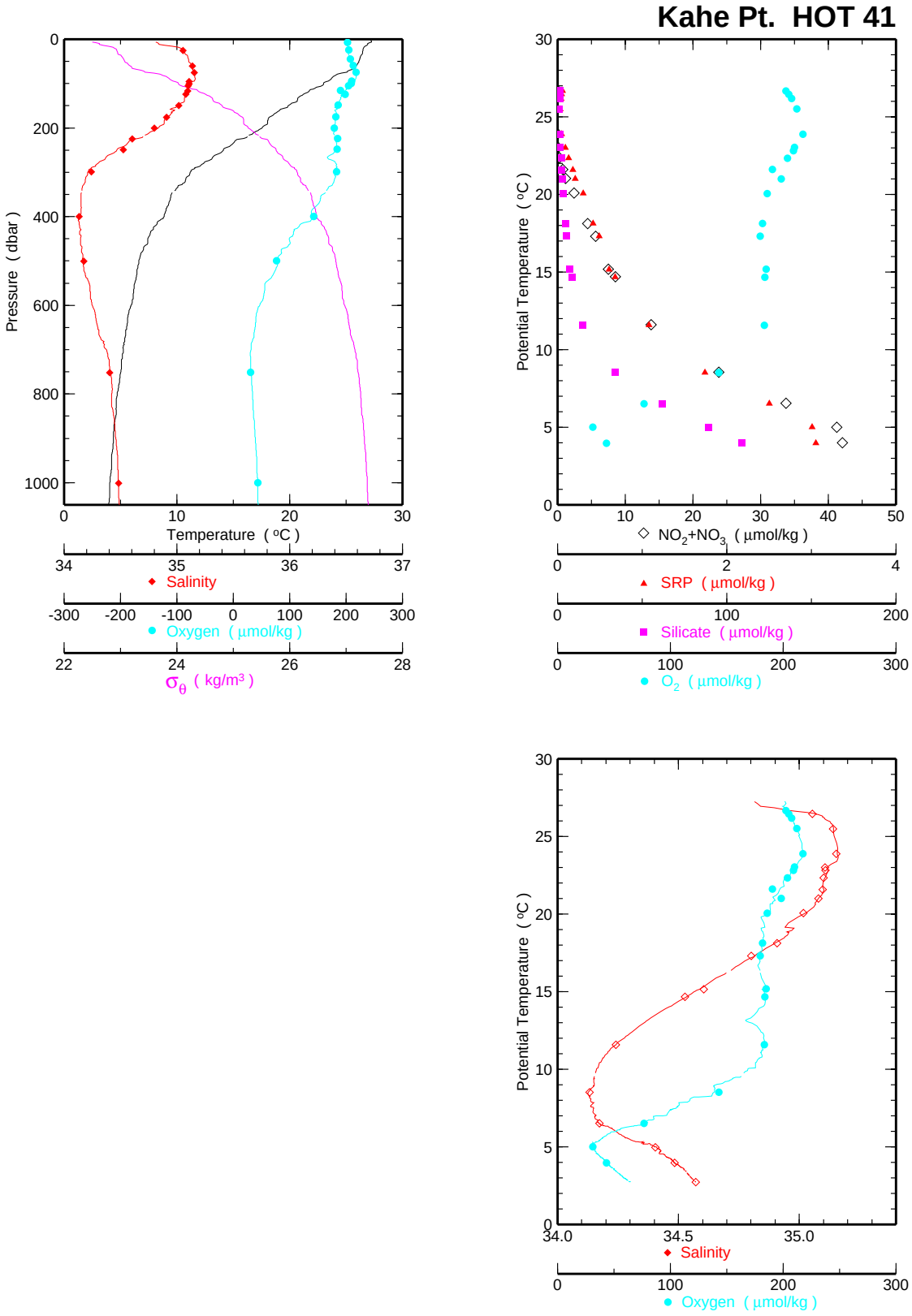
Kahe Pt. HOT 41
Pressure (dbar)
Temperature (°C)
Salinity
Oxygen (µmol/kg)
σθ (kg/m³)
Potential Temperature (°C)
NO2+NO3 (µmol/kg)
SRP (µmol/kg)
Silicate (µmol/kg)
O2 (µmol/kg)
Potential Temperature (°C)
Salinity
Oxygen (µmol/kg)

Figure 6.1.9c

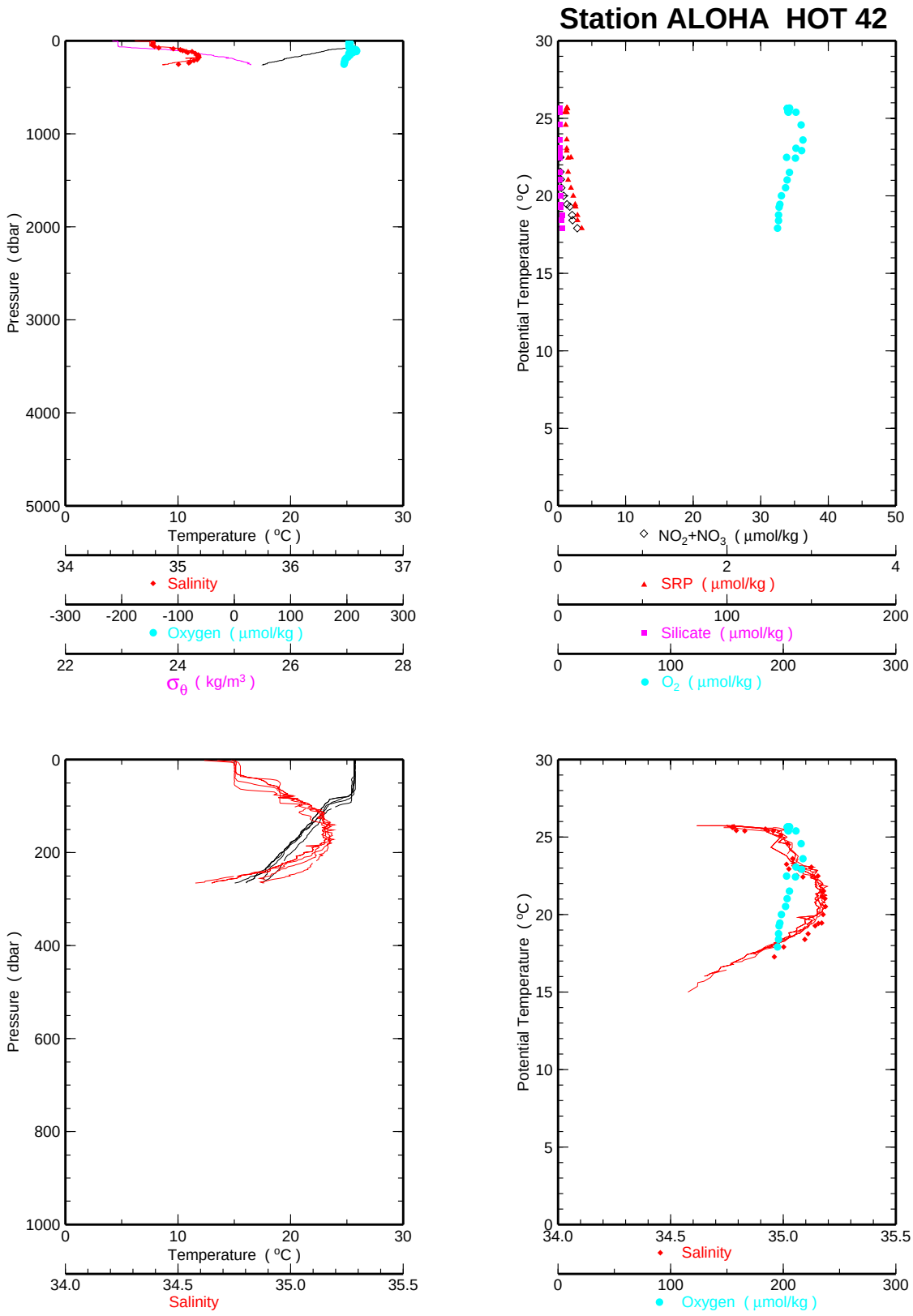

Figure 6.1.10a

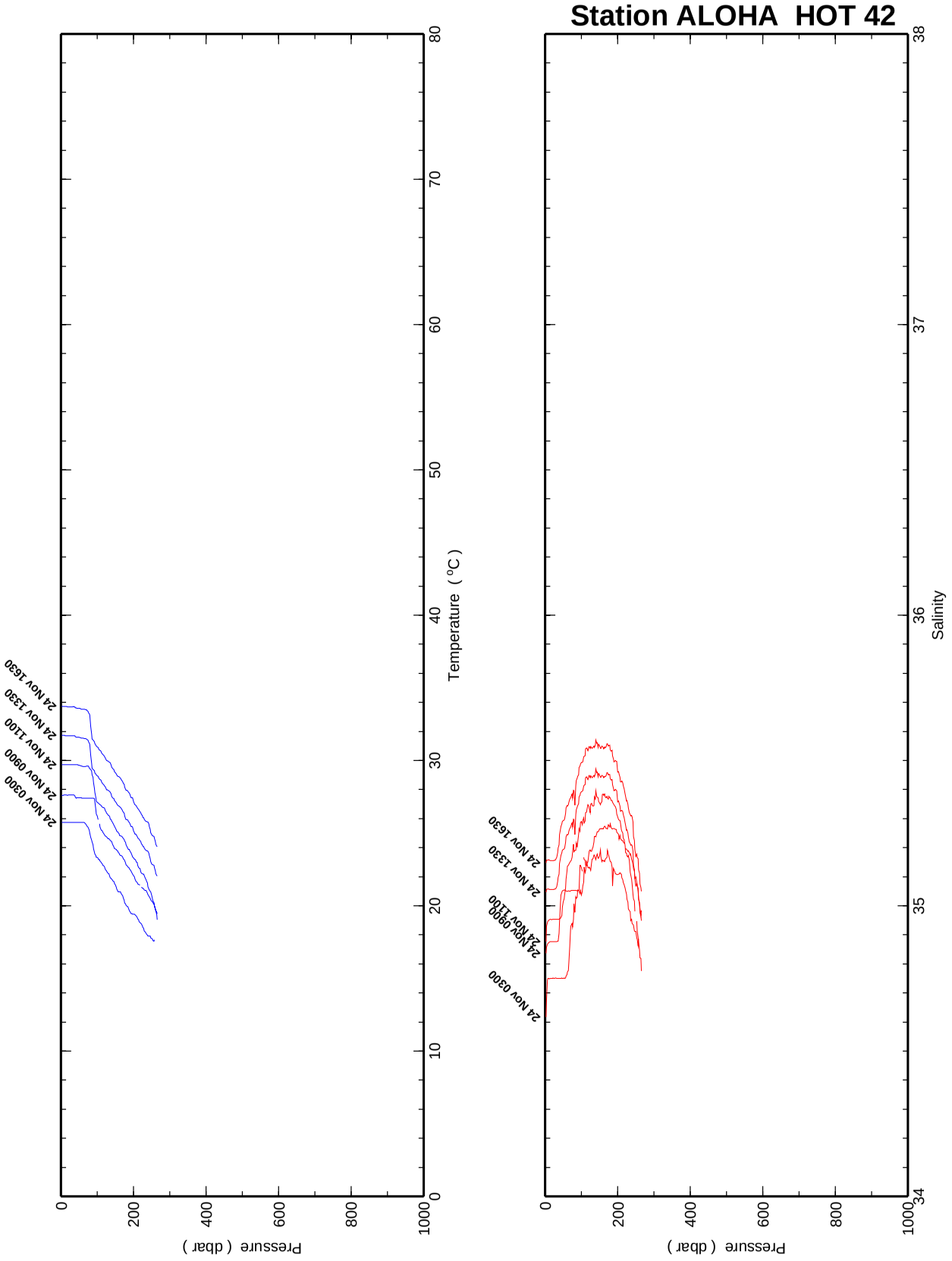

Figure 6.1.10b

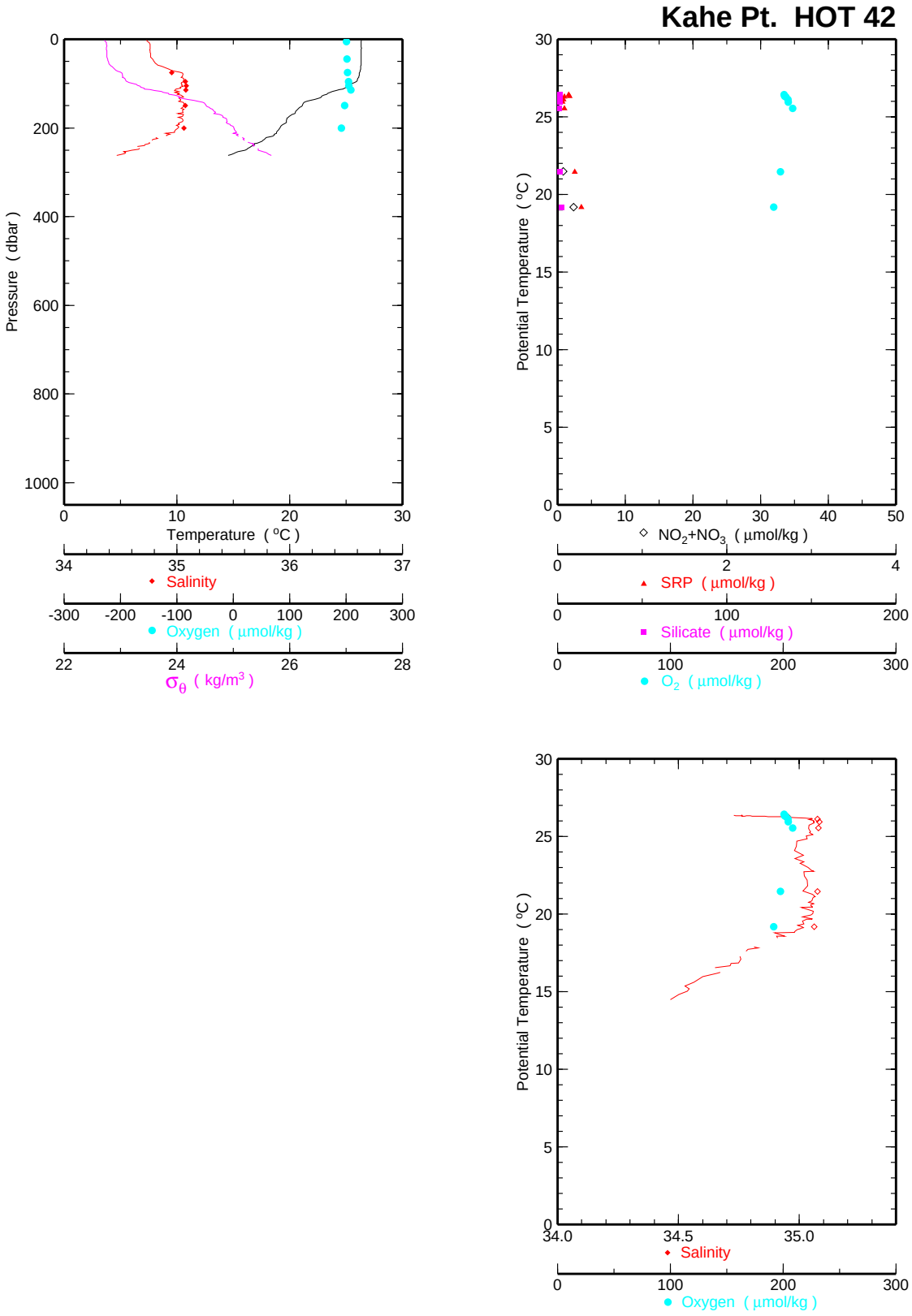

Figure 6.1.10c

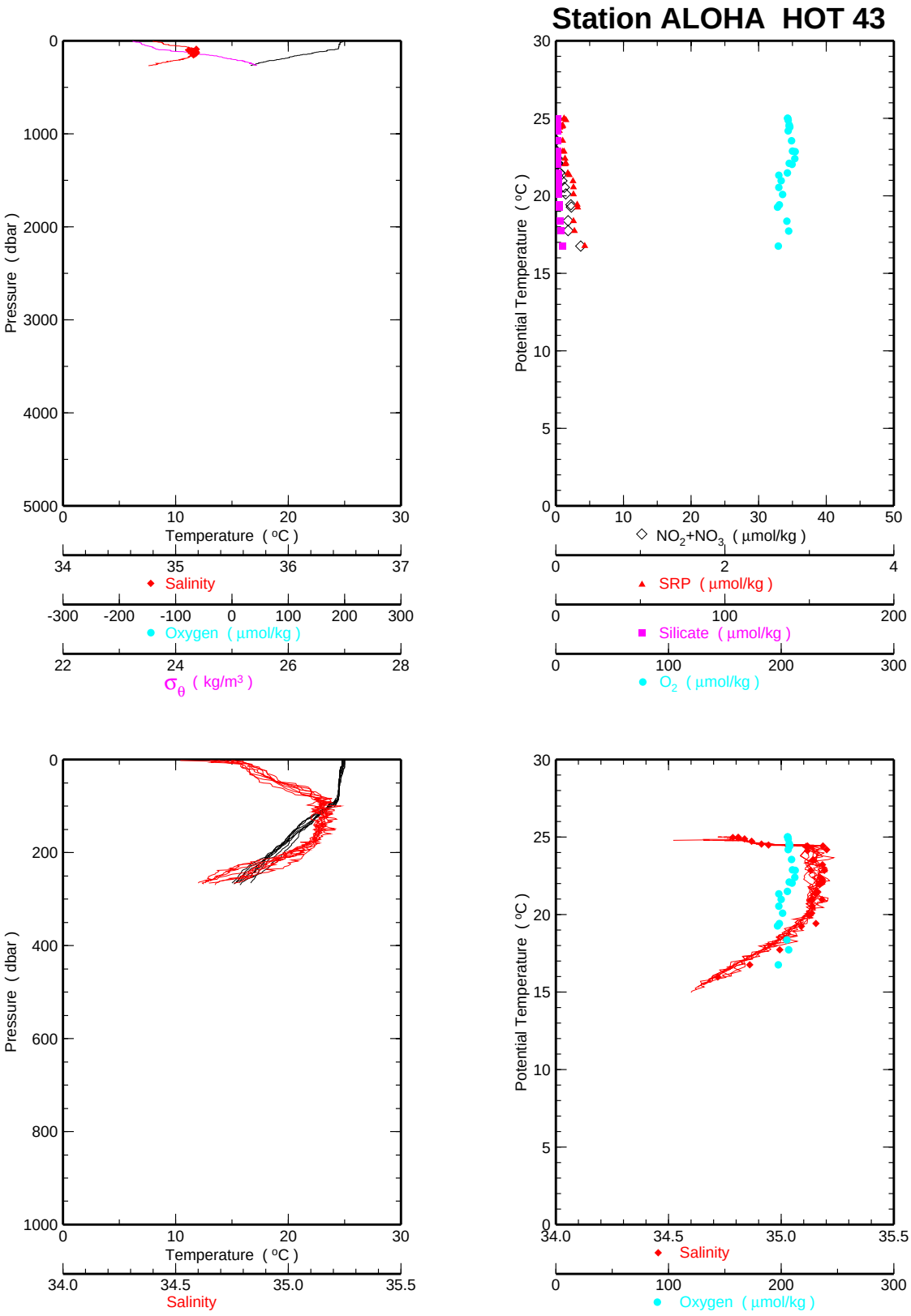

Figure 6.1.11a

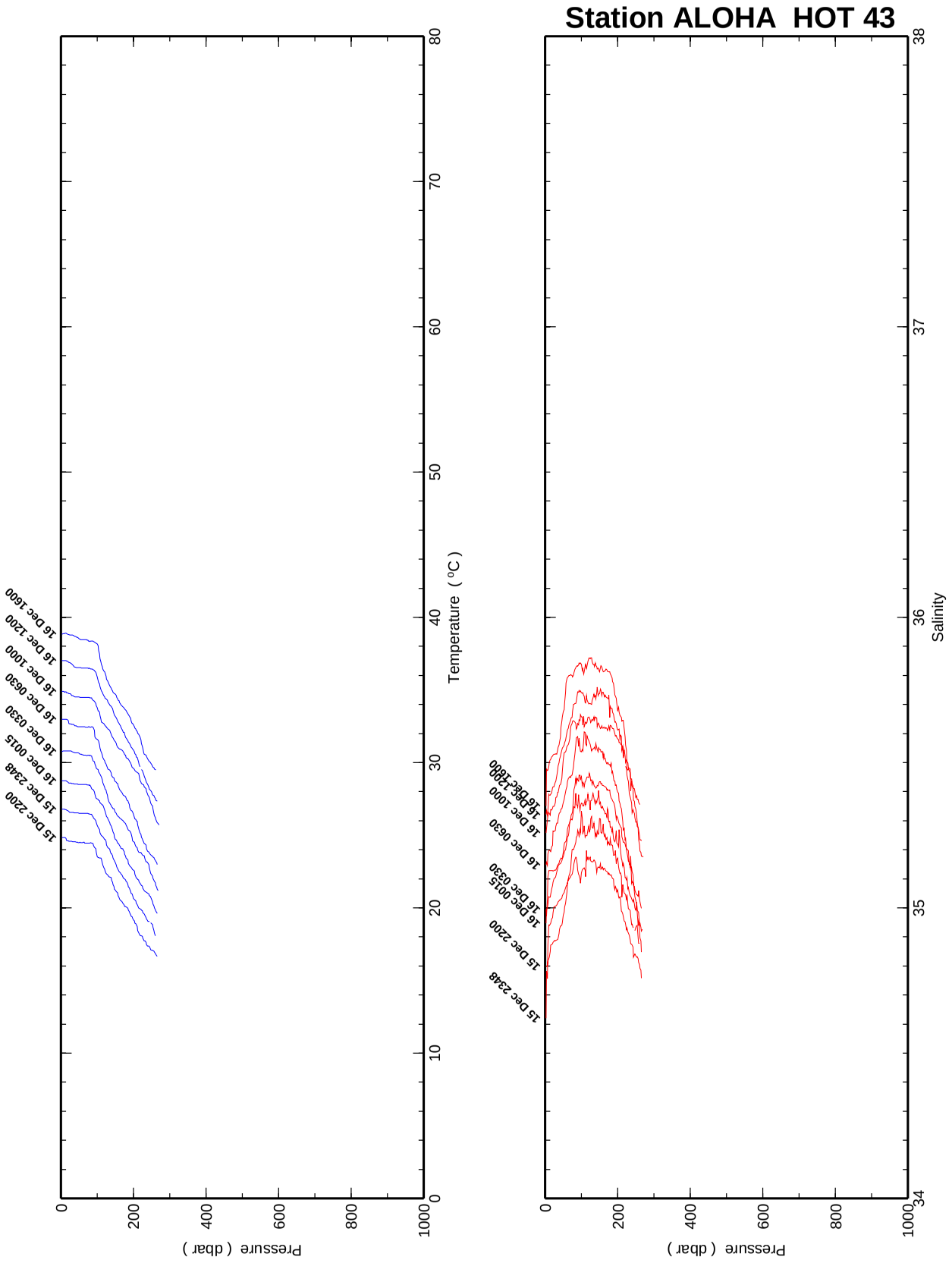

Figure 6.1.11b

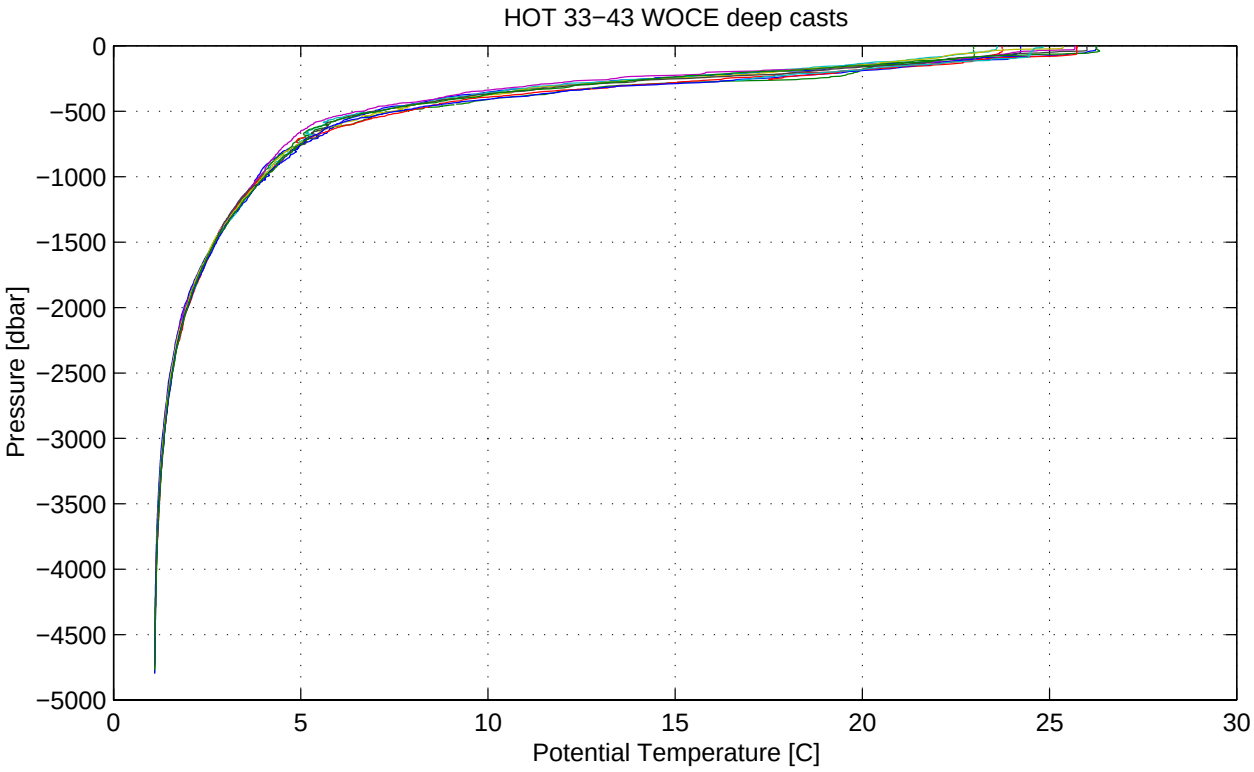
HOT 33−43 WOCE deep casts
Pressure [dbar]
Potential Temperature [C]
0
−500
−1000
−1500
−2000
−2500
−3000
−3500
−4000
−4500
−5000
0
5
10
15
20
25
30

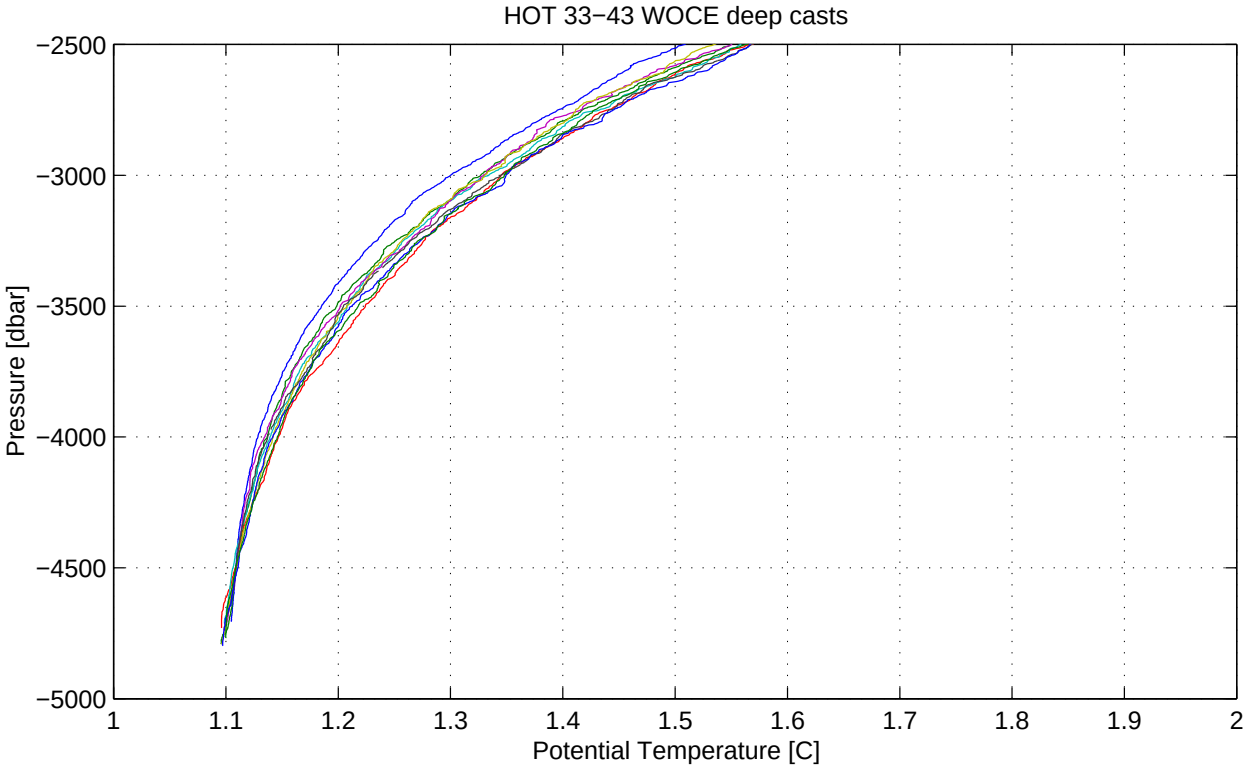
HOT 33−43 WOCE deep casts
Pressure [dbar]
Potential Temperature [C]
−2500
−3000
−3500
−4000
−4500
−5000
1
1.1
1.2
1.3
1.4
1.5
1.6
1.7
1.8
1.9
2

Figure 6.1.12

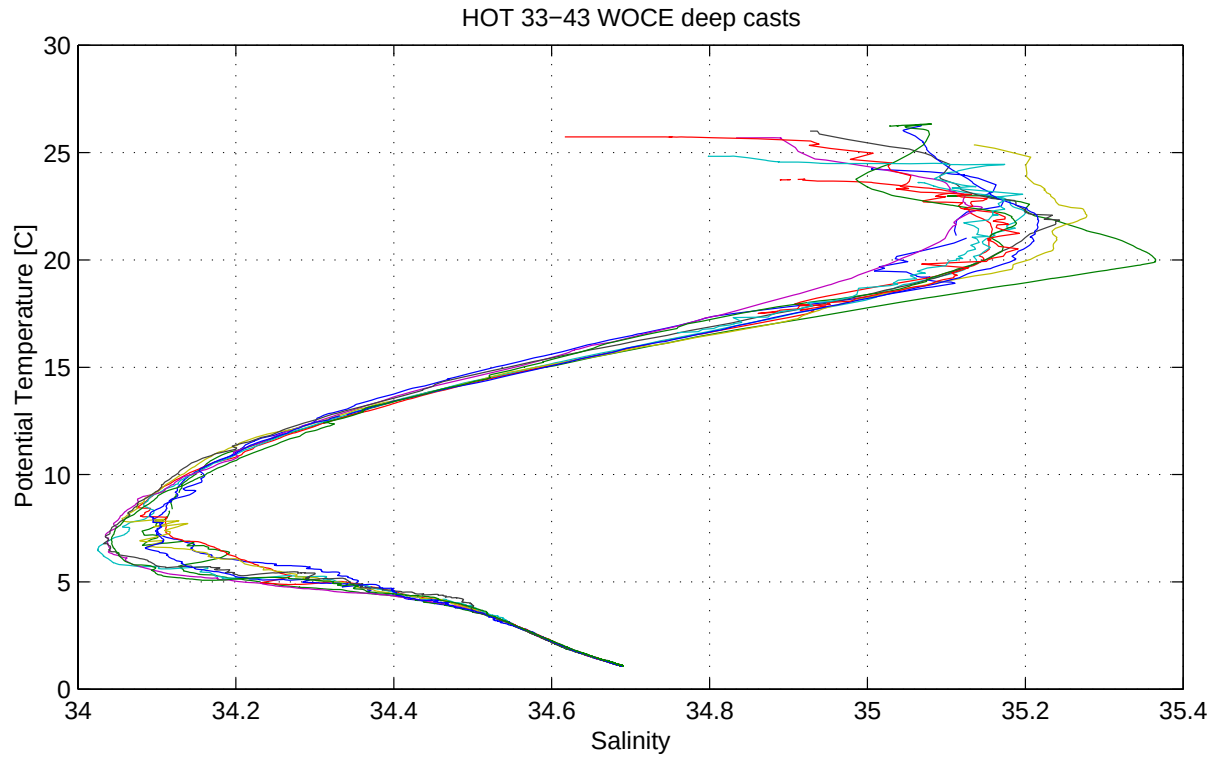
HOT 33−43 WOCE deep casts
Potential Temperature [C]
Salinity
30
25
20
15
10
5
0
34
34.2
34.4
34.6
34.8
35
35.2
35.4

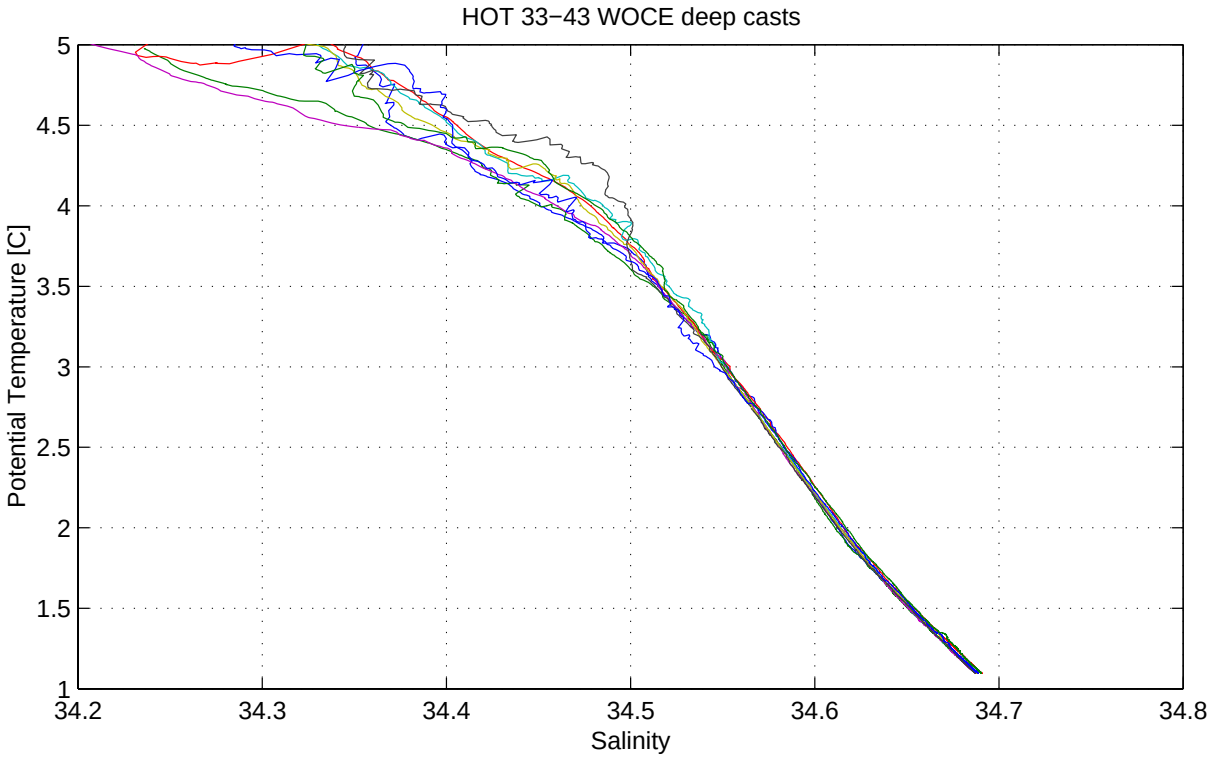
HOT 33−43 WOCE deep casts
Potential Temperature [C]
Salinity
5
4.5
4
3.5
3
2.5
2
1.5
1
34.2
34.3
34.4
34.5
34.6
34.7
34.8

Figure 6.1.13

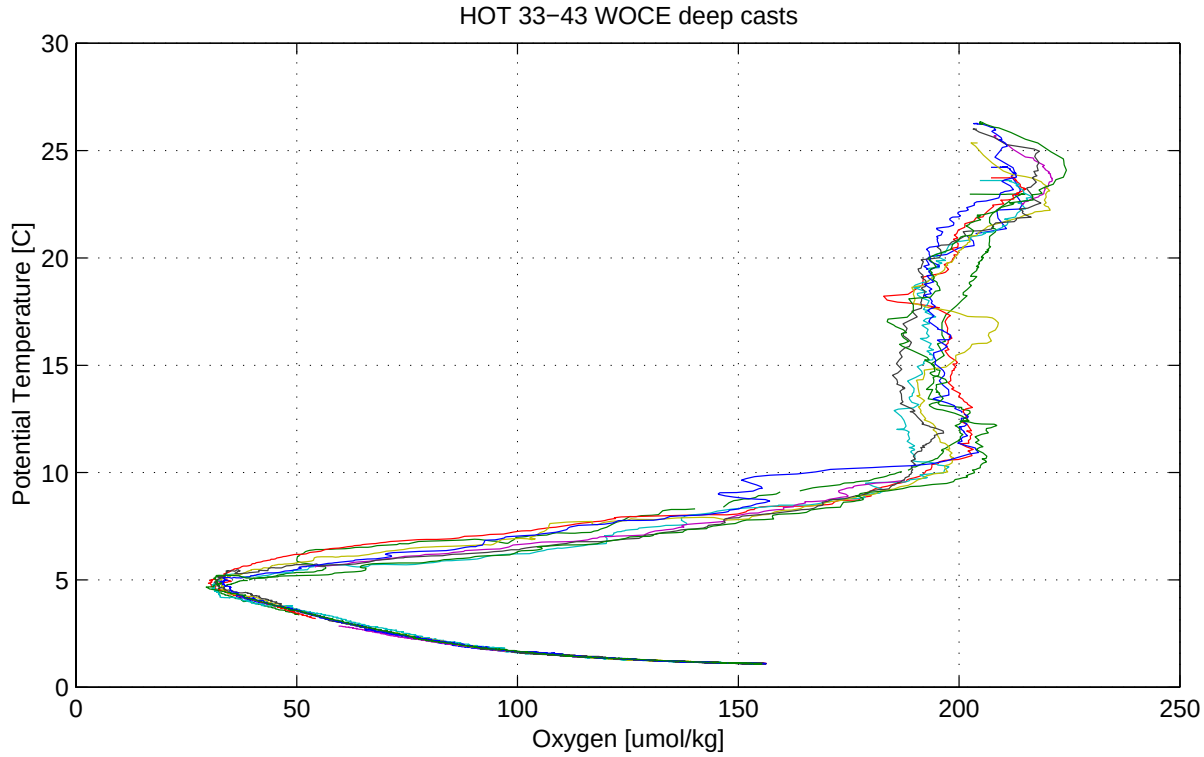
HOT 33−43 WOCE deep casts
Potential Temperature [C]
Oxygen [umol/kg]
0
5
10
15
20
25
30
0
50
100
150
200
250

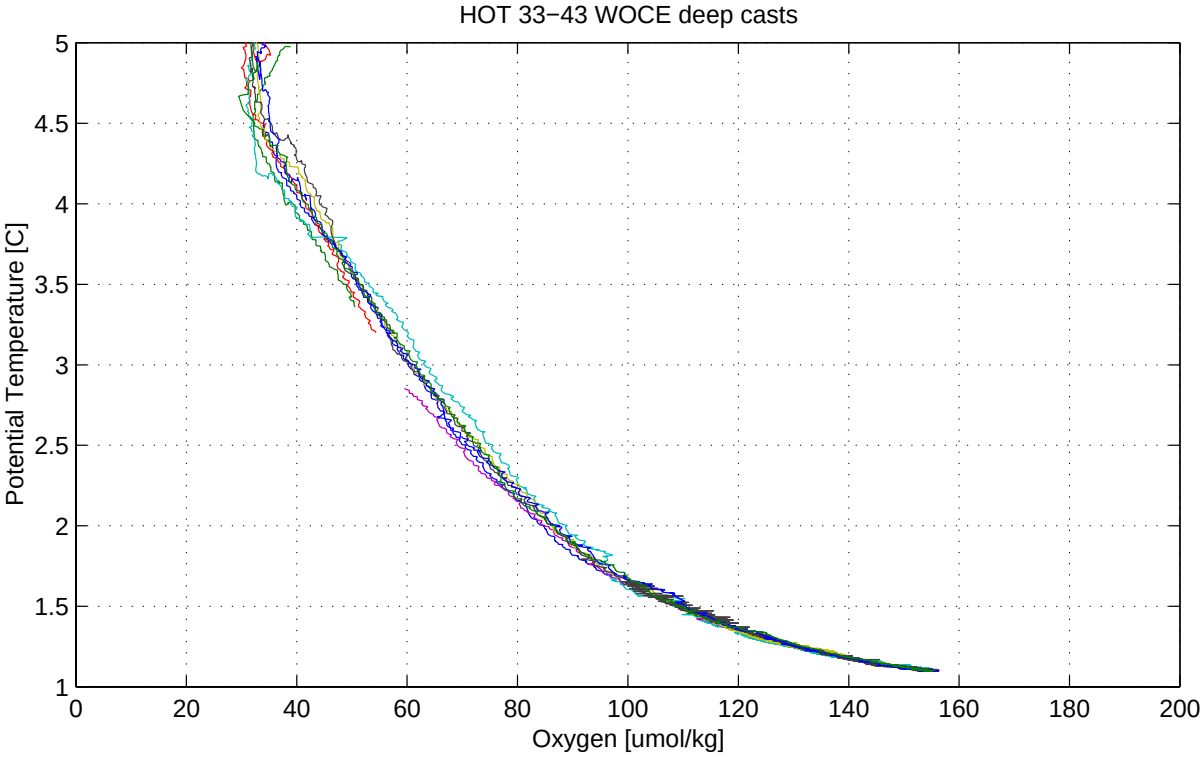
HOT 33−43 WOCE deep casts
Potential Temperature [C]
Oxygen [umol/kg]
1
1.5
2
2.5
3
3.5
4
4.5
5
0
20
40
60
80
100
120
140
160
180
200

Figure 6.1.14

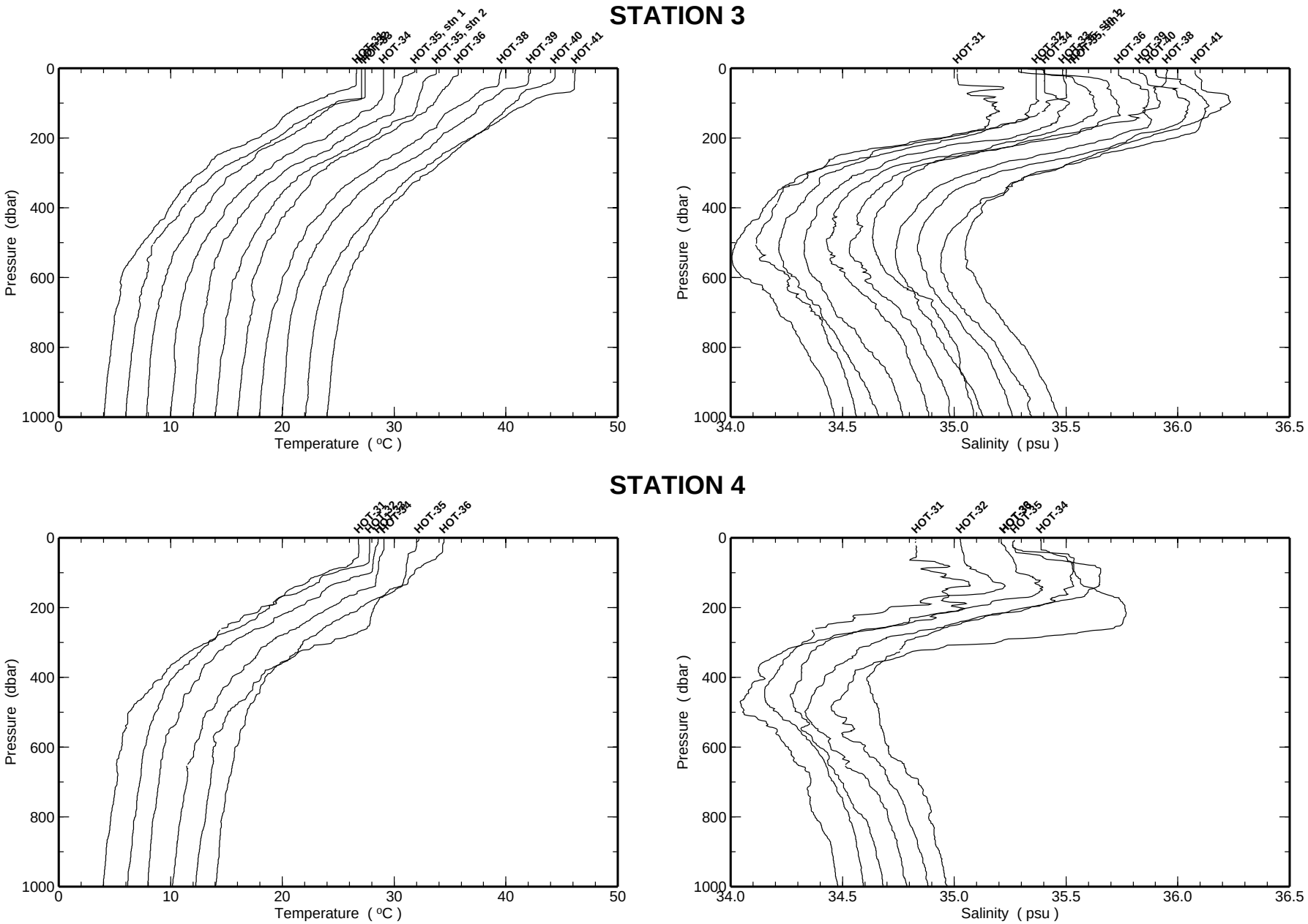
STATION 3
HOT-34
HOT-35, stn 1
HOT-35, stn 2
HOT-36
HOT-38
HOT-39
HOT-40
HOT-41
Pressure (dbar)
Temperature (ºC)
HOT-31
HOT-32
HOT-36
HOT-39
HOT-40
HOT-38
HOT-41
Pressure (dbar)
Salinity (psu)
STATION 4
HOT-31
HOT-32
HOT-35
HOT-36
HOT-34
Pressure (dbar)
Temperature (ºC)
HOT-31
HOT-32
HOT-35
HOT-34
Pressure (dbar)
Salinity (psu)

Figure 6.1.15

STATION 5

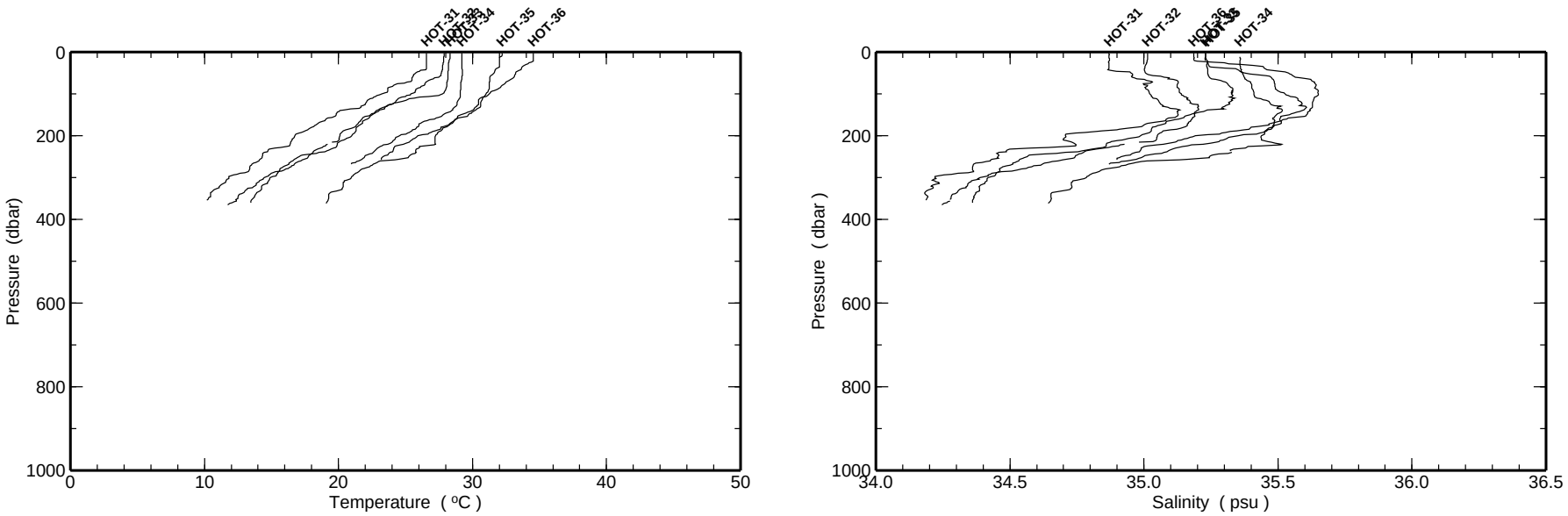

HOT 37

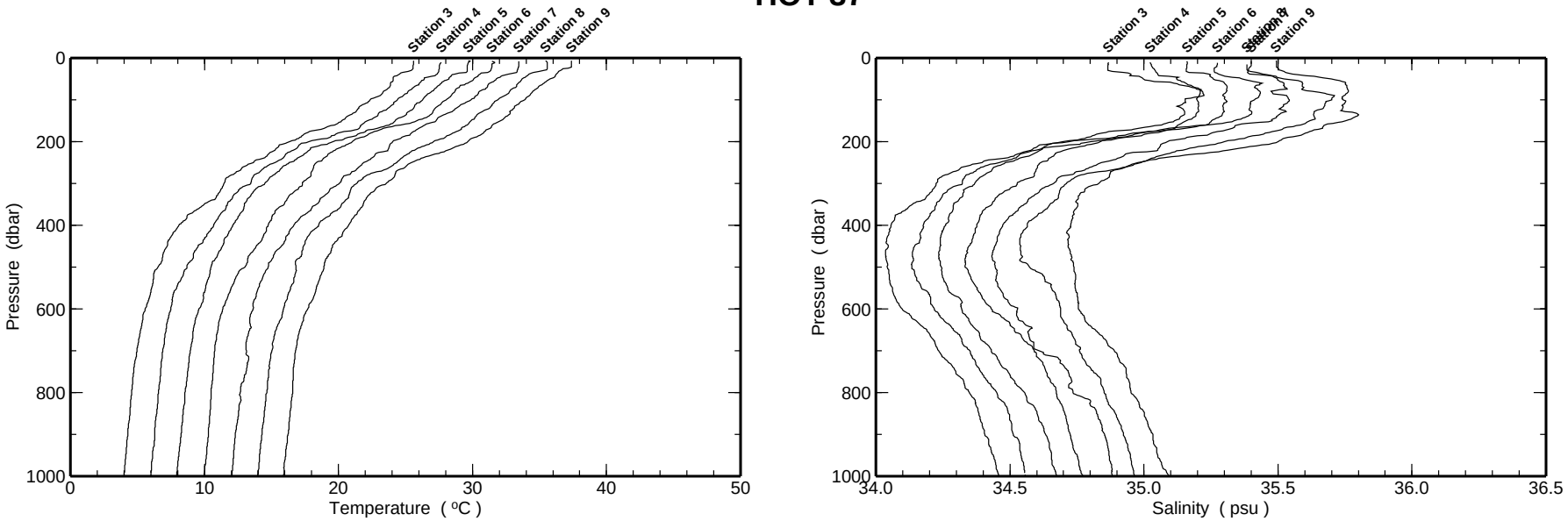

Figure 6.1.16

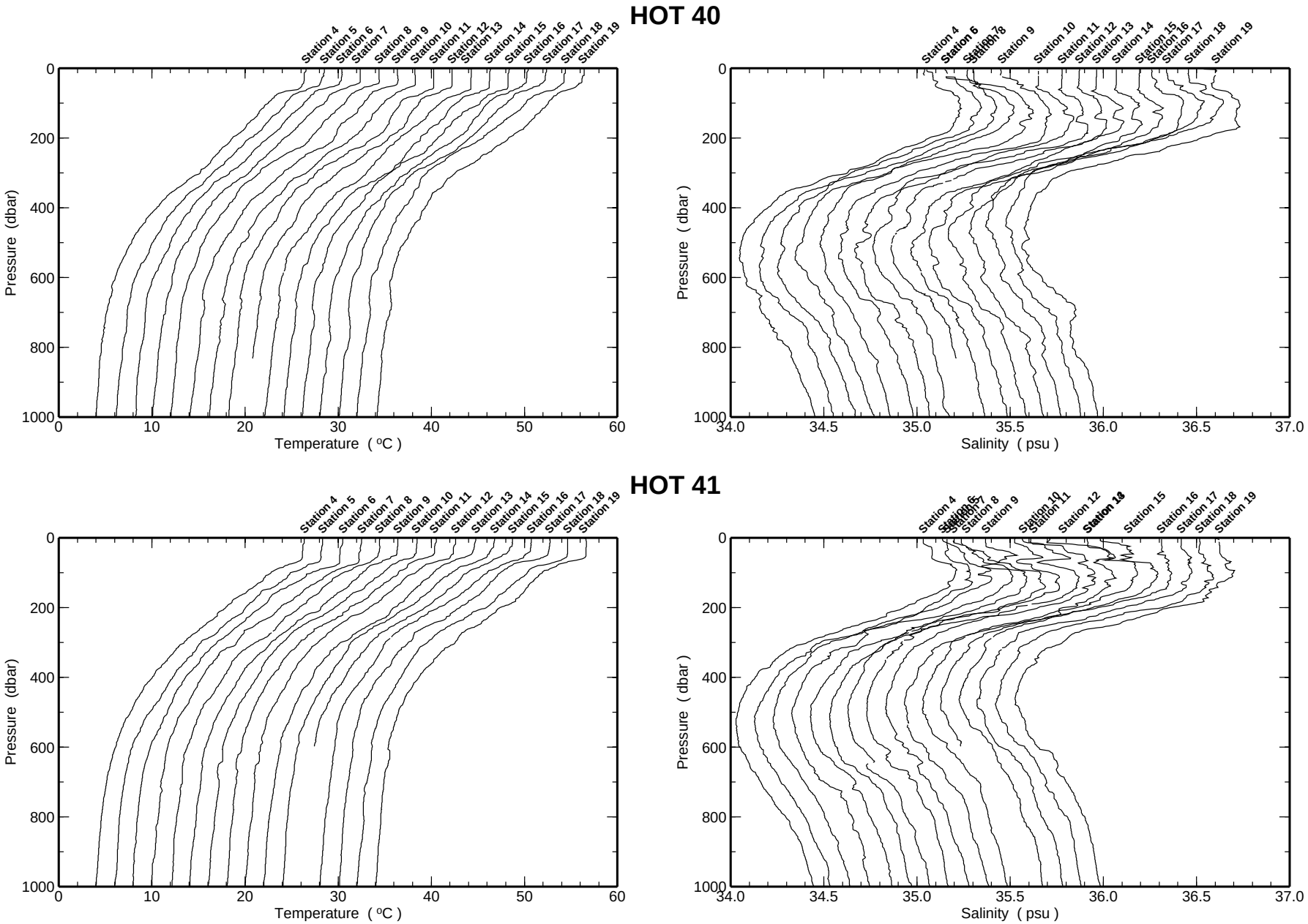
HOT 40
Station 4
Station 5
Station 6
Station 7
Station 8
Station 9
Station 10
Station 11
Station 12
Station 13
Station 14
Station 15
Station 16
Station 17
Station 18
Station 19
Pressure (dbar)
Temperature (ºC)
Pressure (dbar)
Salinity (psu)
HOT 41

Figure 6.1.17

6.2. Contour Plots

Figures 6.2.1-14 show data from HOT 1-43. Time of each cruise is indicated by a symbol along the time axis.

Figure 6.2.1: Potential temperature measured by CTD plotted versus pressure. All casts at the HOT site are averaged for each cruise.

Figure 6.2.2: Potential density, calculated from CTD measurements of pressure, temperature and salinity, plotted versus pressure. All casts at the HOT site are averaged for each cruise.

Figure 6.2.3: Salinity measured by CTD plotted versus pressure. All casts at the HOT site are averaged for each cruise.

Figure 6.2.4: Salinity measured by CTD plotted versus potential density. All casts at the HOT site are averaged for each cruise. The average density of the sea surface for each cruise is connected by a heavy line.

Figure 6.2.5: Salinity from discrete water samples plotted versus pressure. Locations of bottle closures are indicated by circles.

Figure 6.2.6: Salinity from discrete water samples plotted versus potential density. The average density of the sea surface for each cruise is connected by a heavy line. Locations of bottle closures are indicated by circles.

Figure 6.2.7: Oxygen from discrete water samples plotted versus pressure. Locations of bottle closures are indicated by circles.

Figure 6.2.8: Oxygen from discrete water samples plotted versus potential density. The average density of the sea surface for each cruise is connected by a heavy line. Locations of bottle closures are indicated by circles.

Figure 6.2.9: Nitrate plus nitrite from discrete water samples plotted versus pressure. Locations of bottle closures are indicated by circles.

Figure 6.2.10: Nitrate plus nitrite from discrete water samples plotted versus potential density. The average density of the sea surface for each cruise is connected by a heavy line. Locations of bottle closures are indicated by circles.

Figure 6.2.11: Phosphate from discrete water samples plotted versus pressure. Locations of bottle closures are indicated by circles.

Figure 6.2.12: Phosphate from discrete water samples plotted versus potential density. The

average density of the sea surface for each cruise is connected by a heavy line. Locations of bottle closures are indicated by circles.

Figure 6.2.13: Silicate from discrete water samples plotted versus pressure. Locations of bottle closures are indicated by circles.

Figure 6.2.14: Silicate from discrete water samples plotted versus potential density. The average density of the sea surface for each cruise is connected by a heavy line. Locations of bottle closures are indicated by circles.

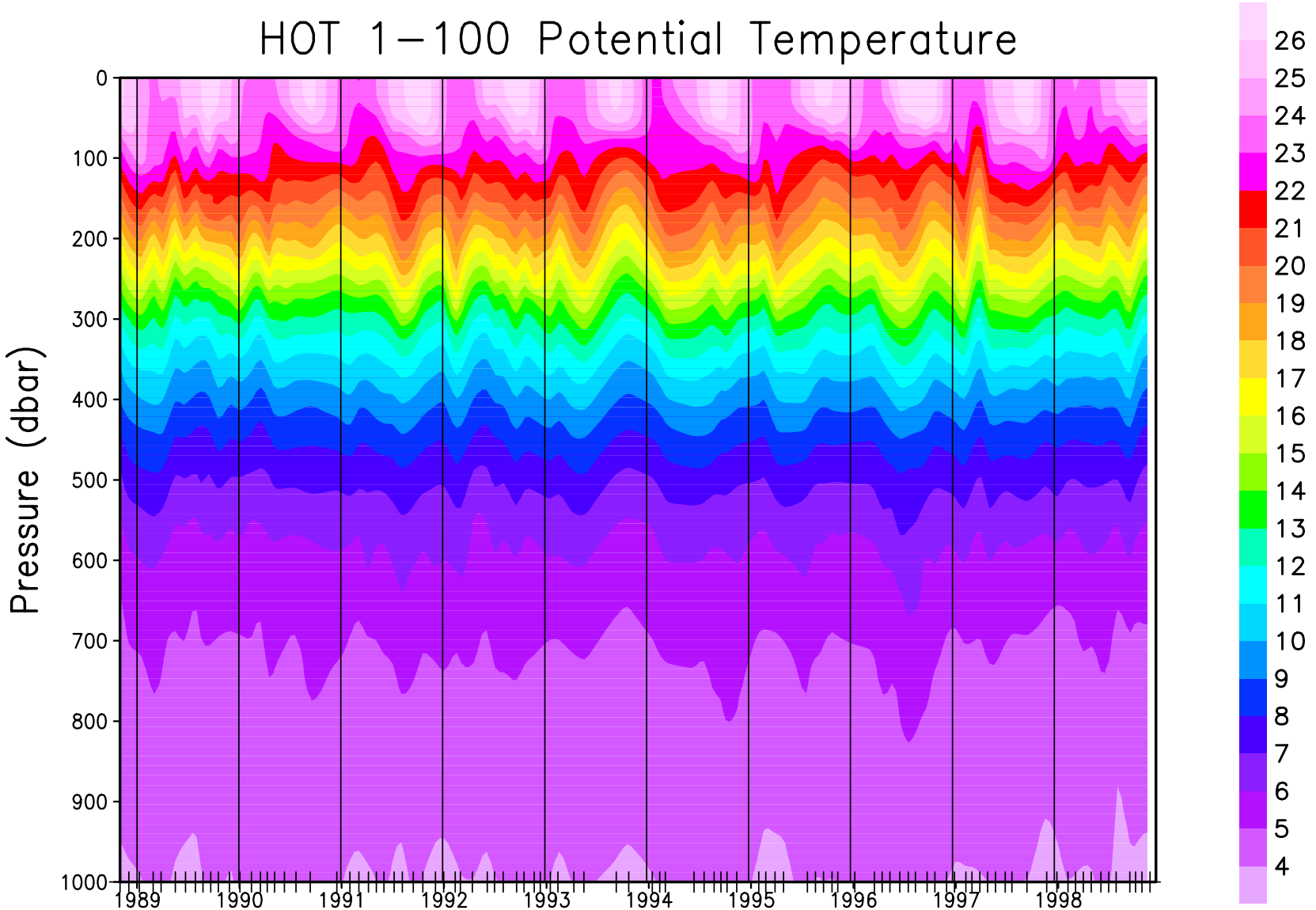

Figure 6.2.1: Contour plot of CTD potential temperature versus pressure for HOT cruises 1-100.

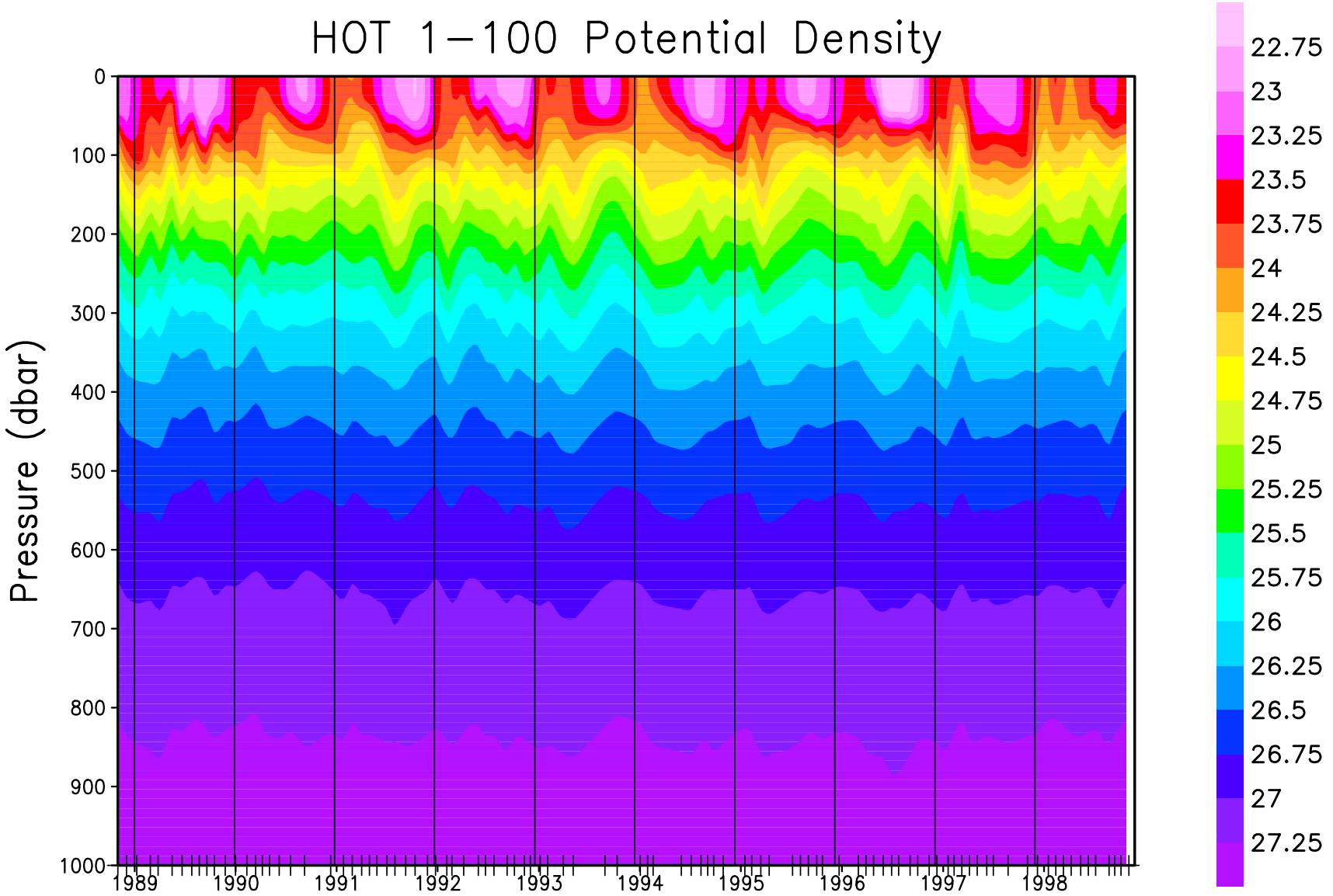

Figure 6.2.2: Contour plot of potential density (σ_θ), calculated from CTD pressure, temperature and salinity, versus pressure for HOT cruises 1-100.

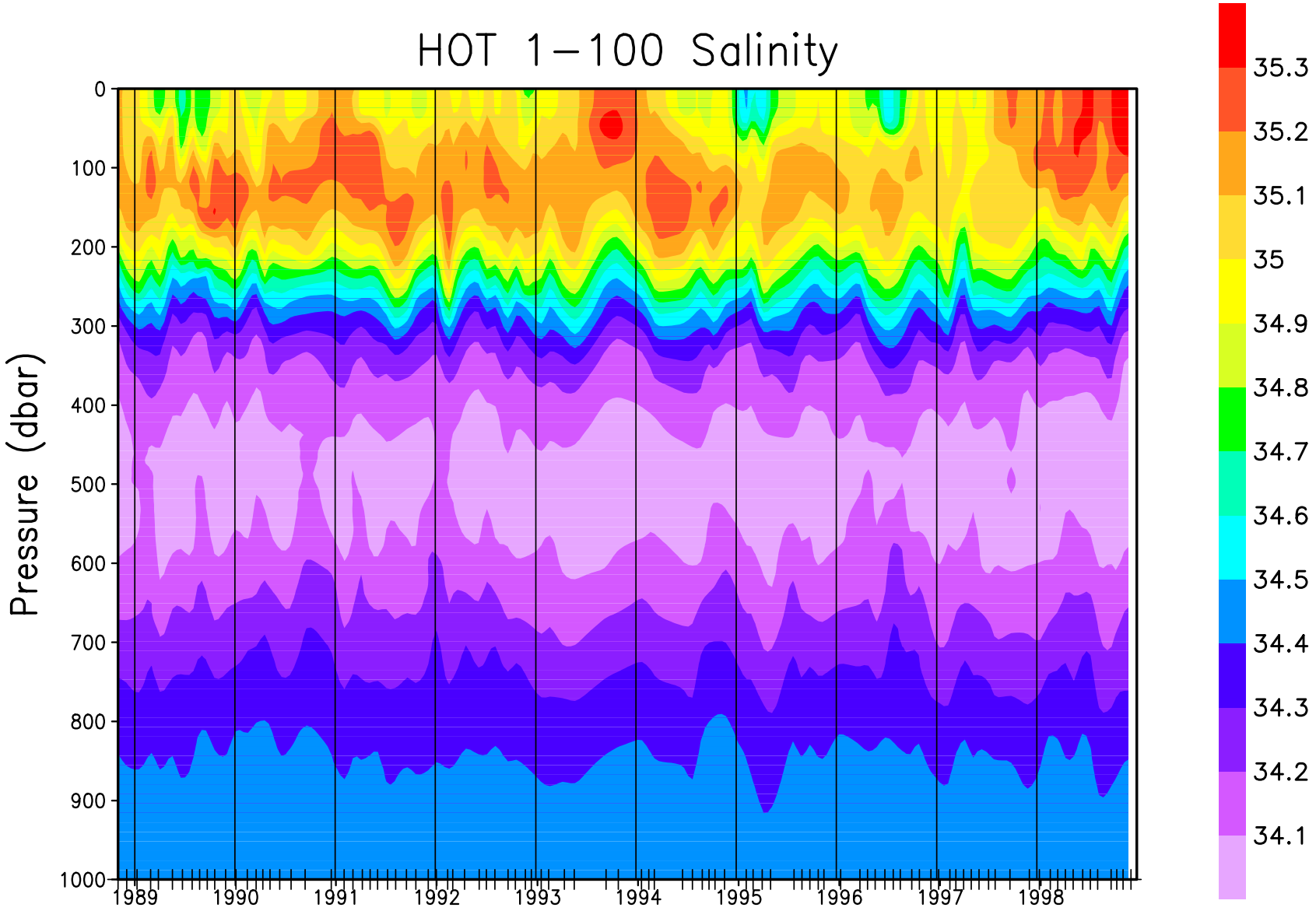

Figure 6.2.3: Contour plot of CTD salinity versus pressure for HOT cruises 1-

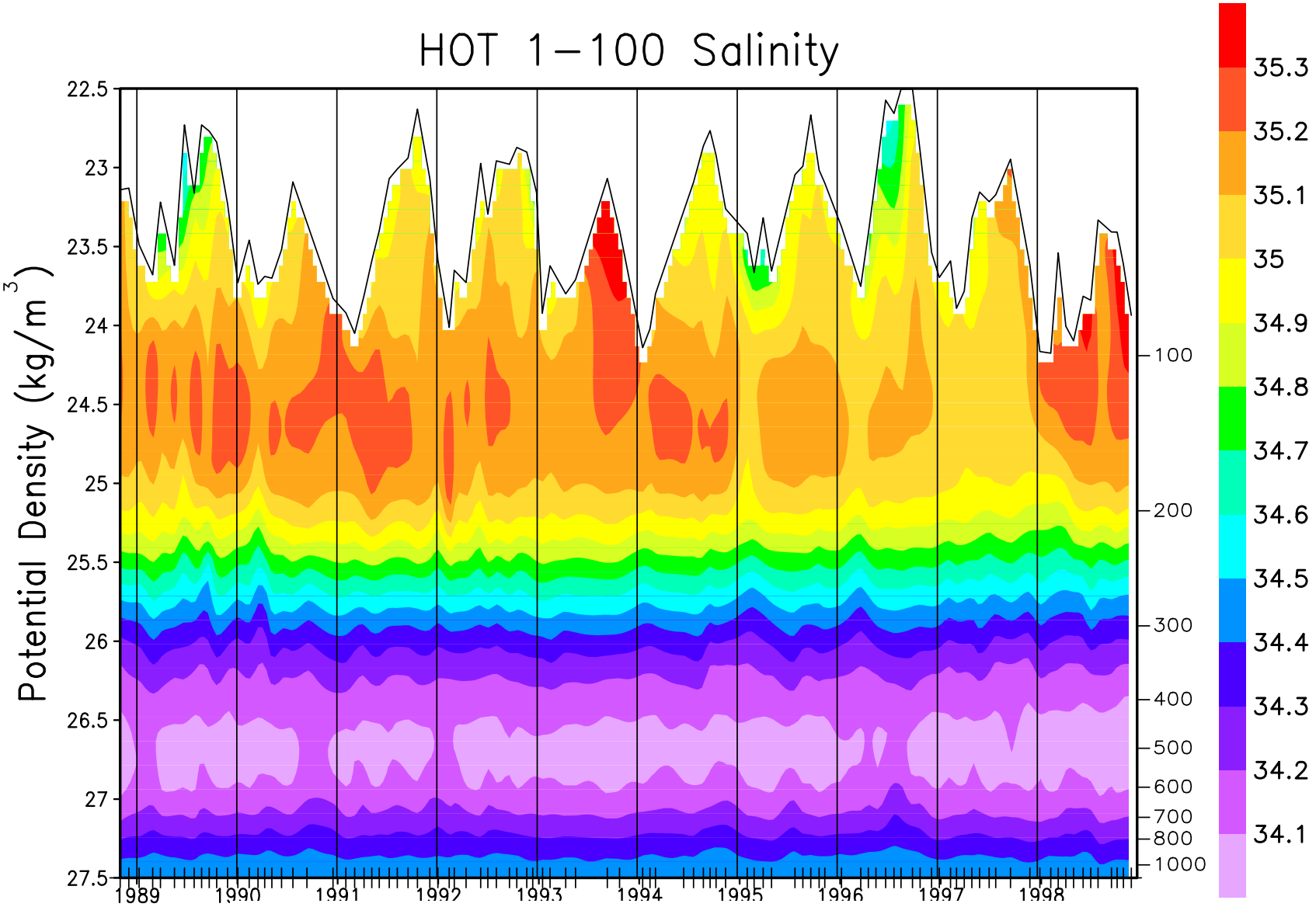

Figure 6.2.4: Contour plot of CTD salinity versus potential density (σ_θ) to 27.5 kg m^{-3} for HOT cruises 1-100. The average density of the sea surface is connected by the heavy line.

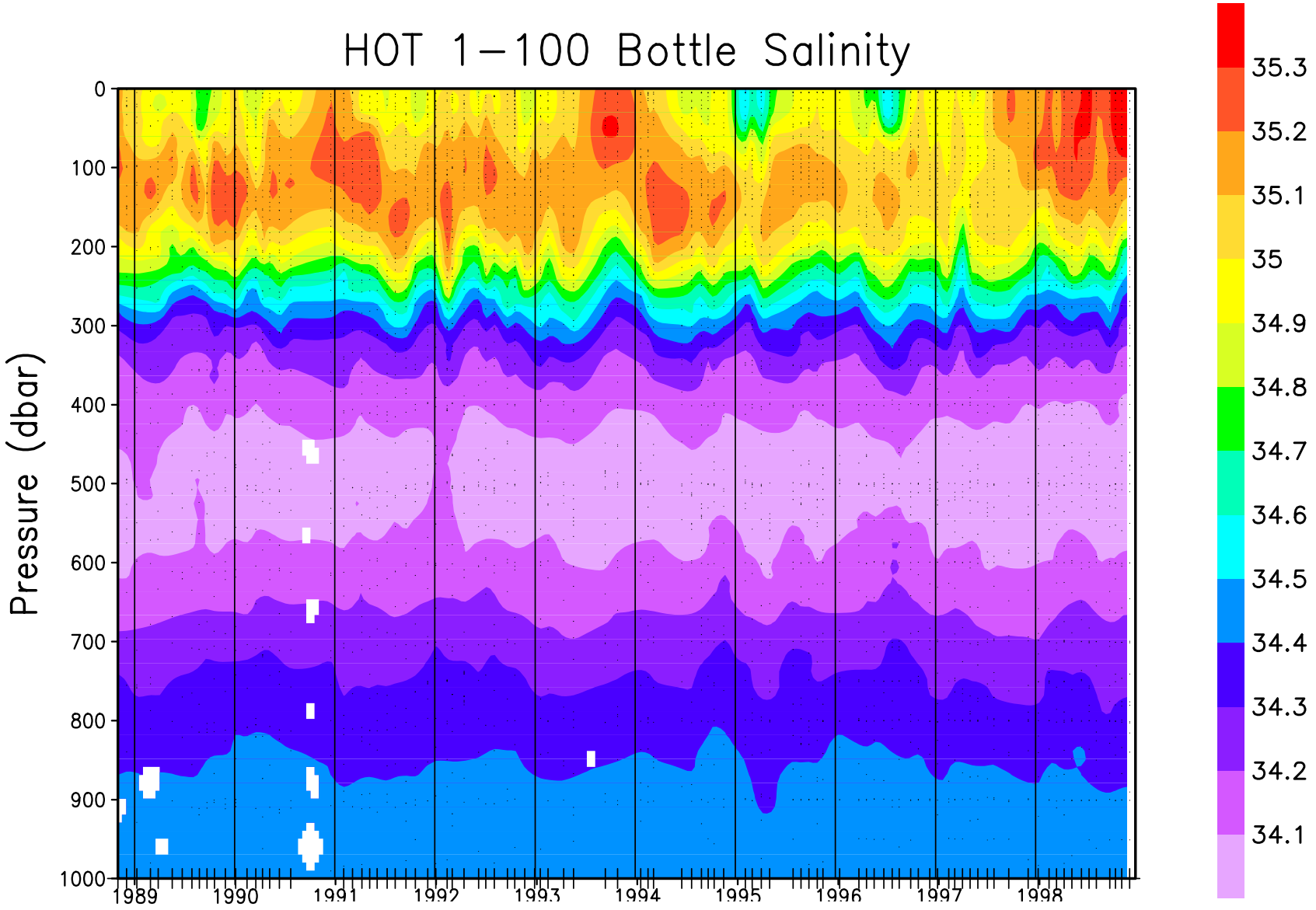

Figure 6.2.5: Contour plot of bottle salinity versus pressure for HOT cruises 1-100. Location of samples in the water column are indicated by the solid circles.

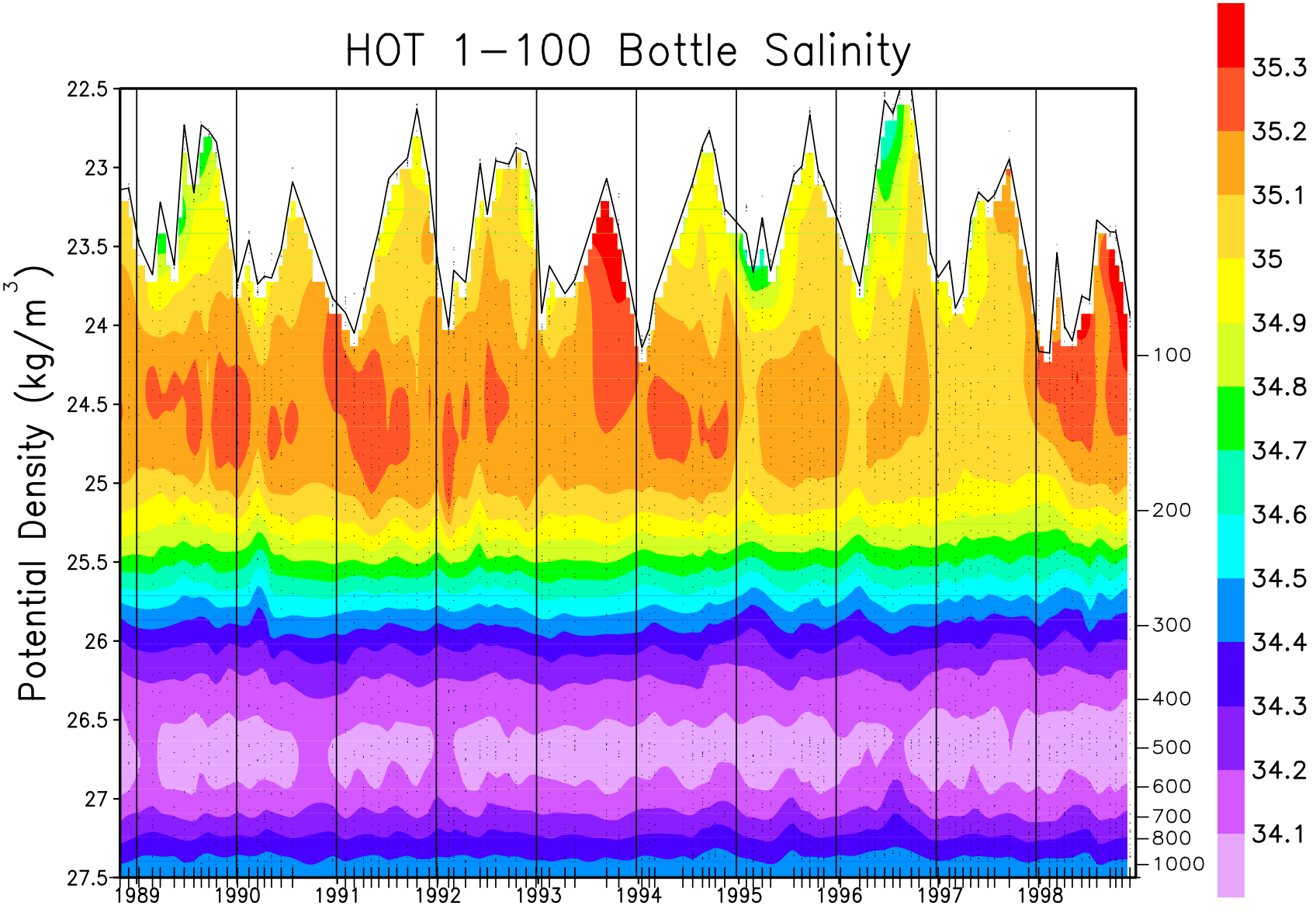

Figure 6.2.6: Contour plot of bottle salinity versus potential density (σ_θ)to 27.5 kg m^{-3} for HOT cruises 1-100. The average density of the sea surface is connected by the heavy line.

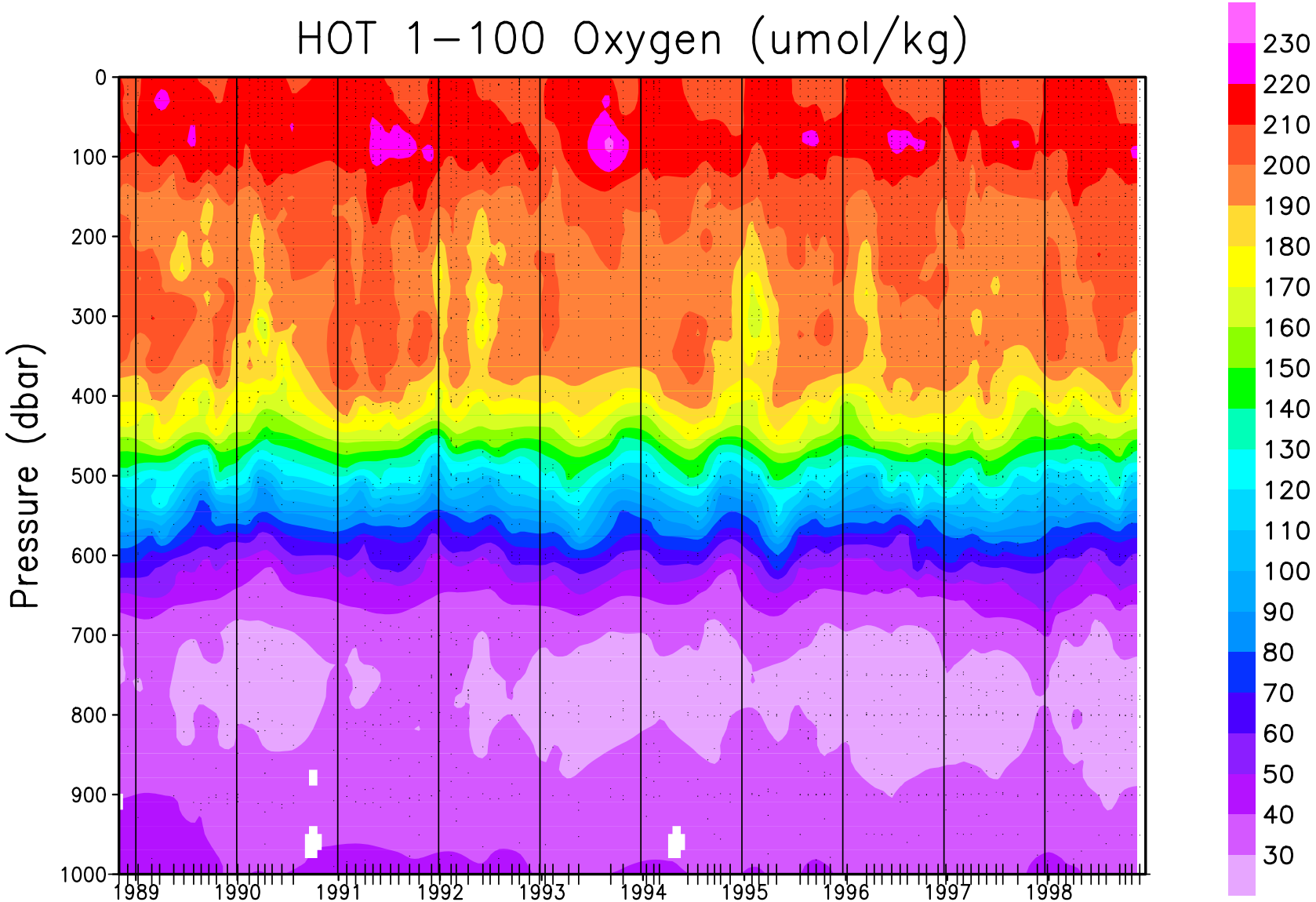

Figure 6.2.7: Contour plot of bottle oxygen versus pressure for HOT cruises 1-100. Location of samples in the water column are indicated by the solid circles.

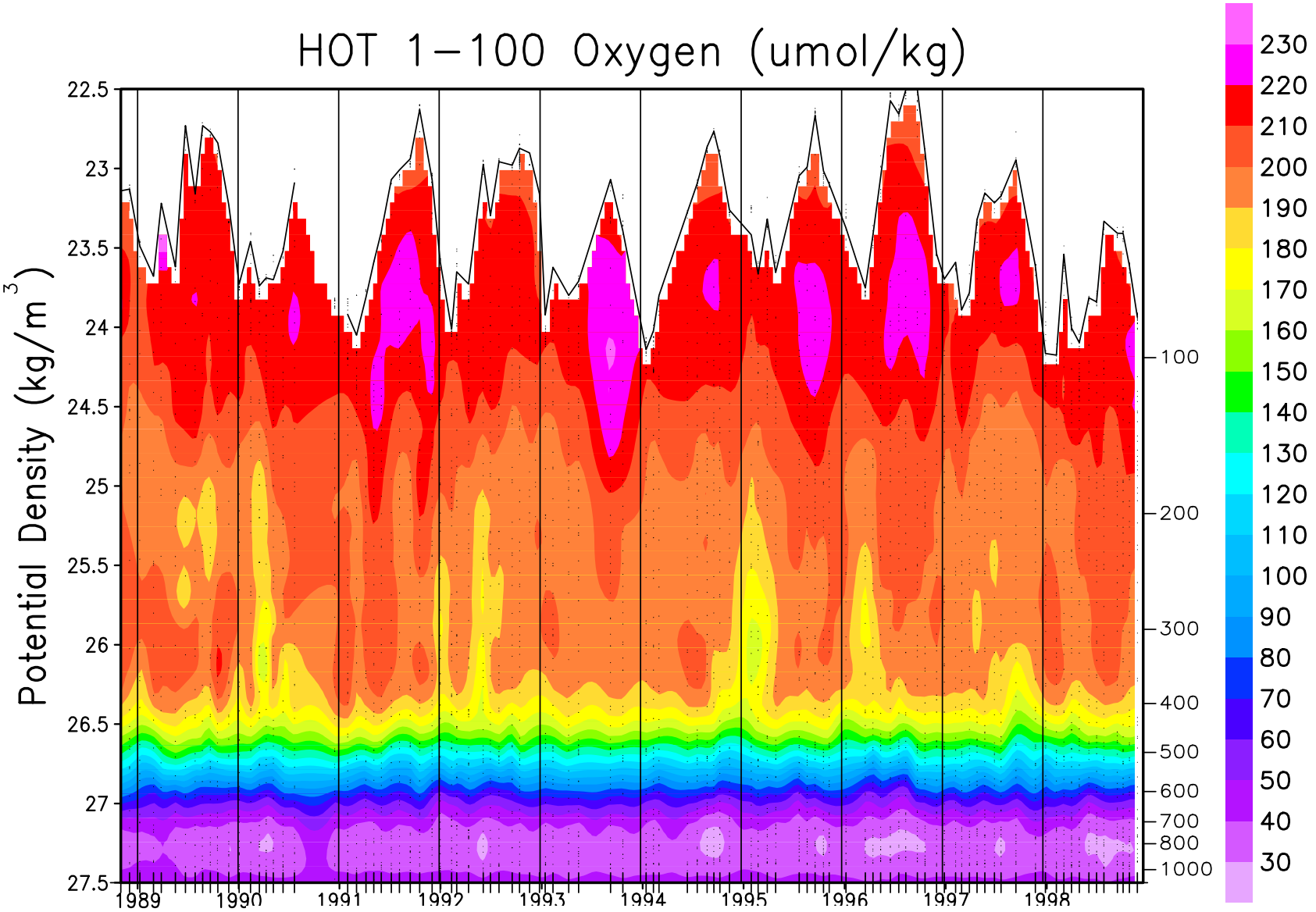

Figure 6.2.8: Contour plot of bottle oxygen versus potential density (σ_θ) to 27.5 kg m^{-3} for HOT cruises 1-100. The average density of the sea surface is connected by the heavy line.

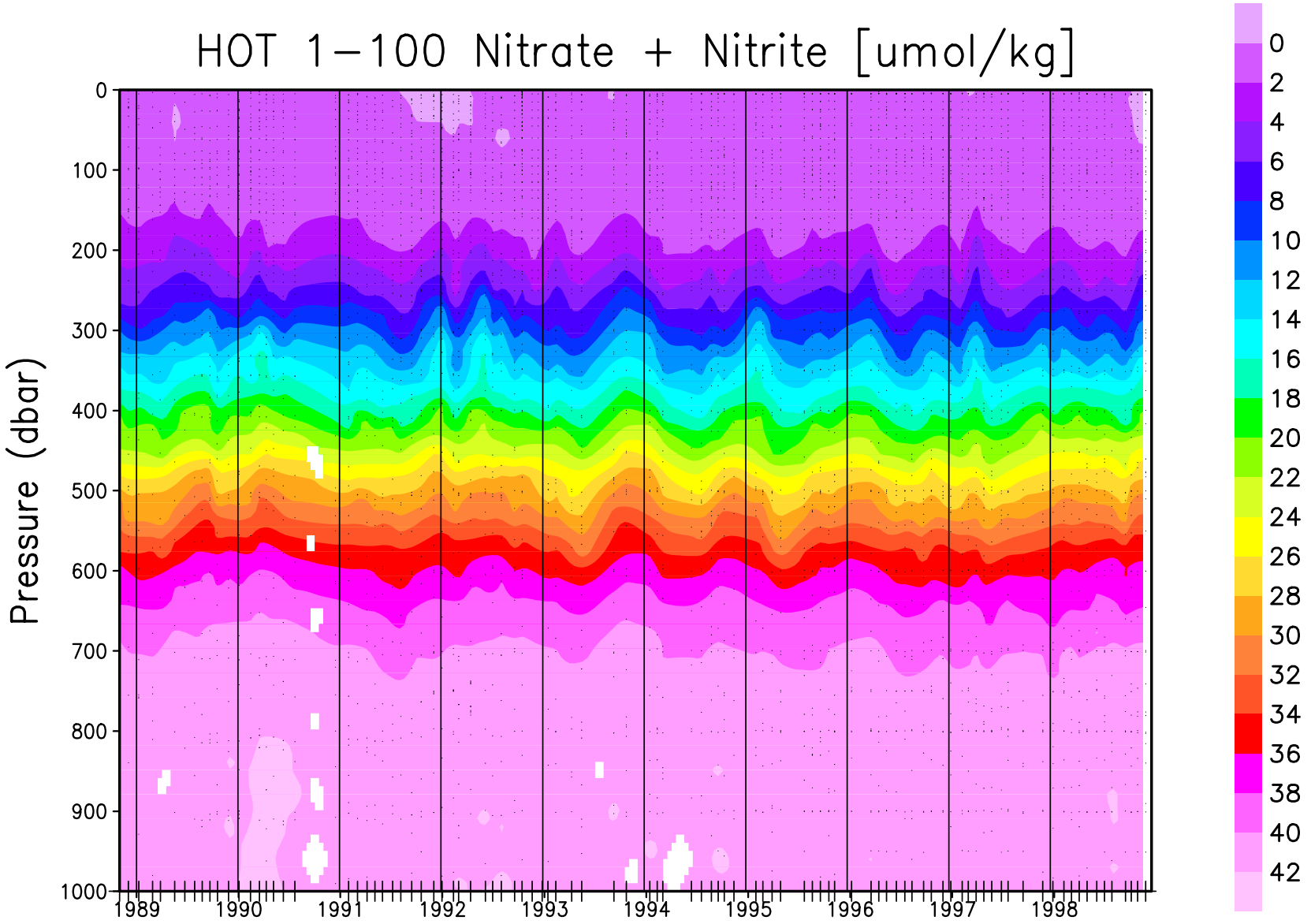

Figure 6.2.9: Contour plot of [nitrate + nitrite] versus pressure for HOT cruises 1-100. Location of samples in the water column are indicated by the solid circles.

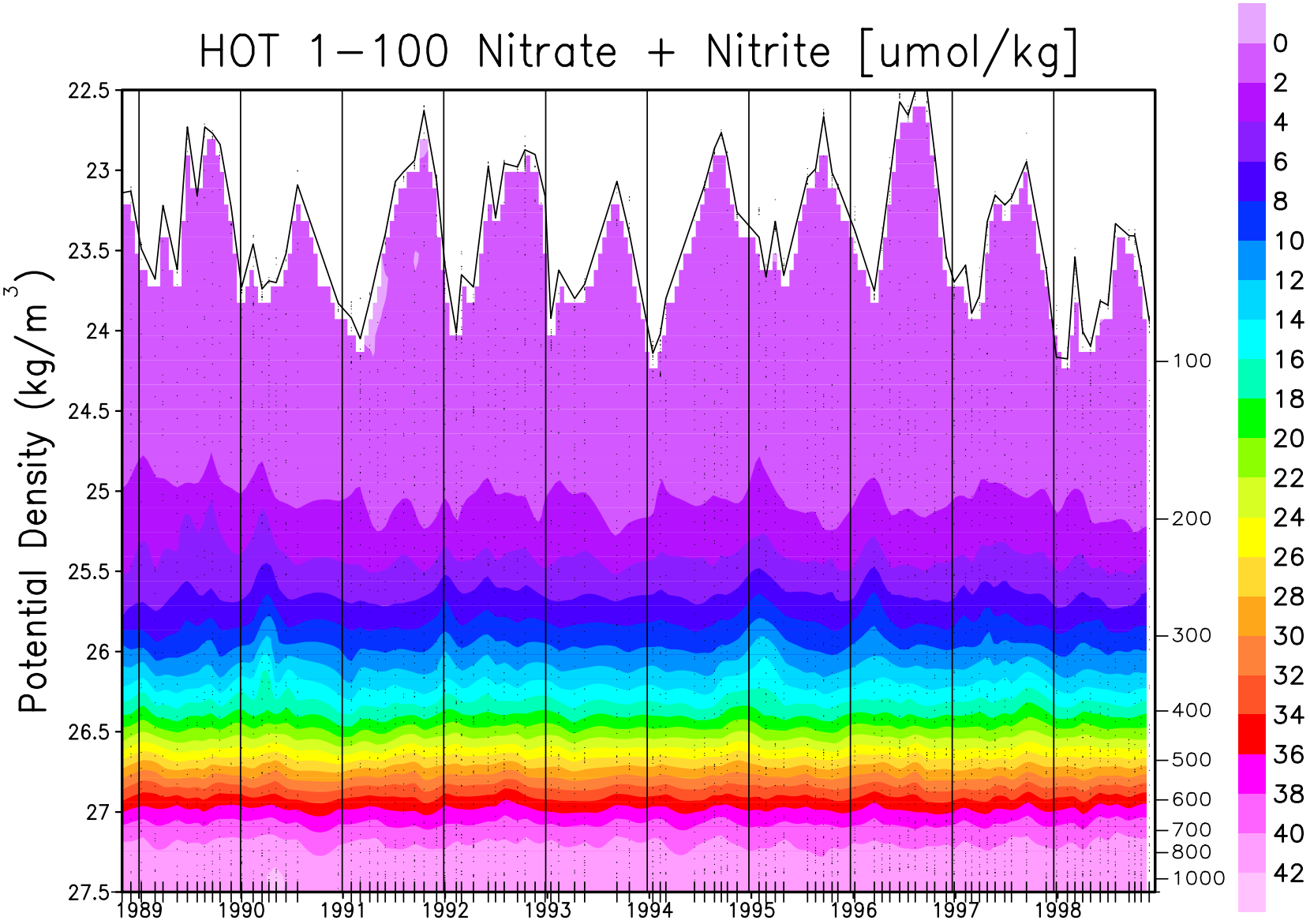

Figure 6.2.10: Contour plot of [nitrate + nitrite] versus potential density (σ_θ) to 27.5 kg m^{-3} for HOT cruises 1-100. The average density of the sea surface is connected by the heavy line.

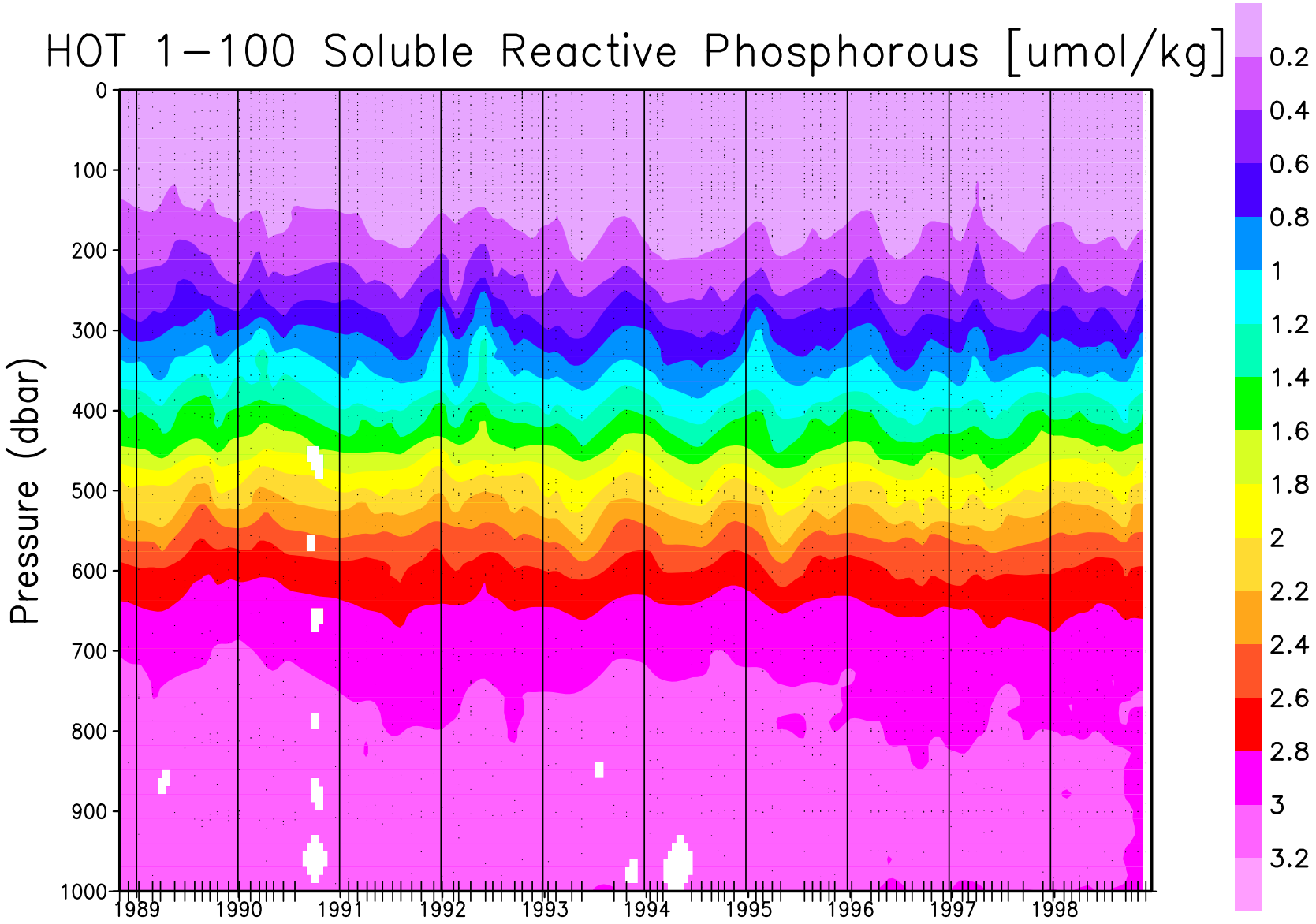

Figure 6.2.11: Contour plot of soluble reactive phosphate versus pressure for HOT cruises 1-100. Location of samples in the water column are indicated by the solid circles.

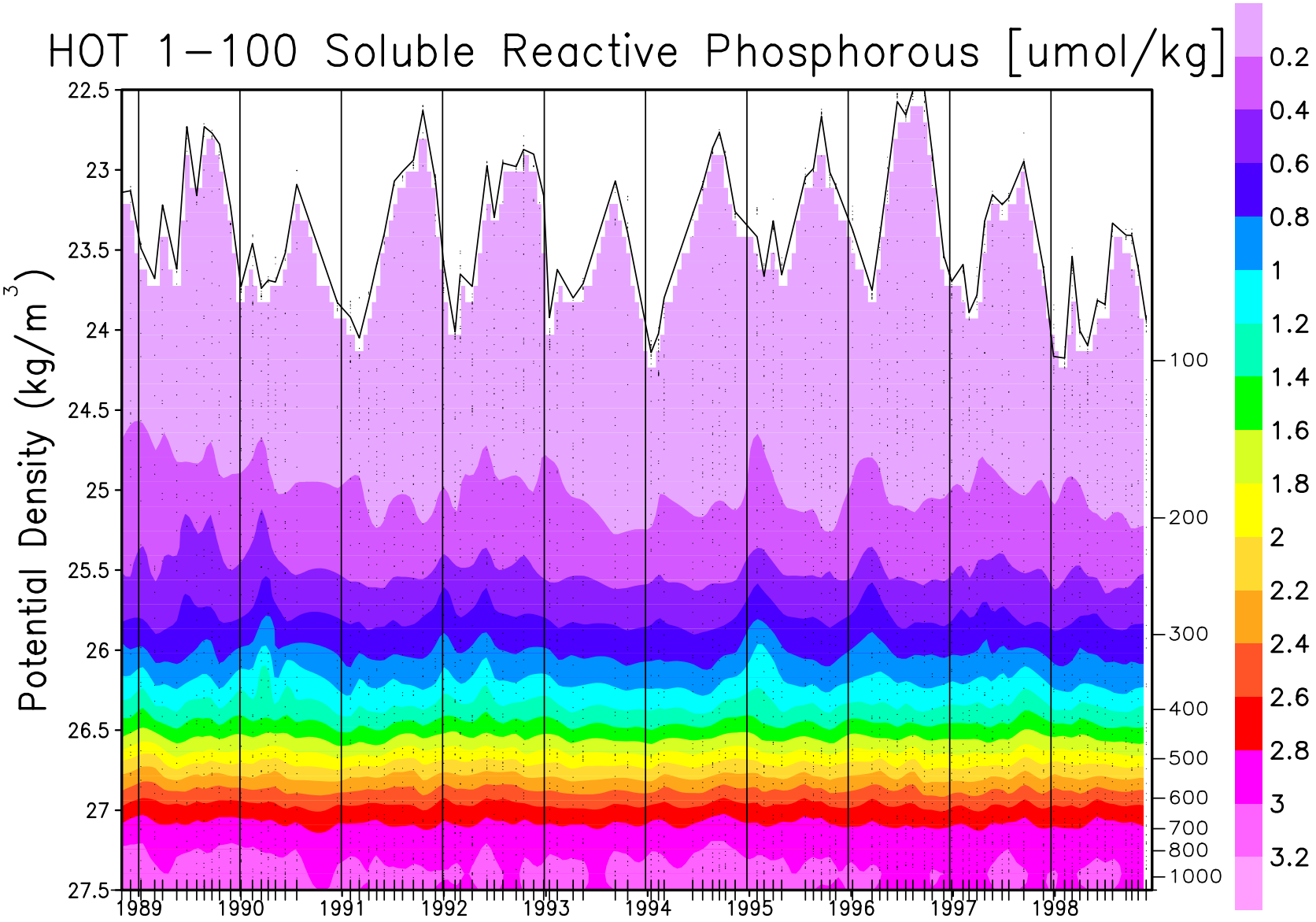

Figure 6.2.12: Contour plot of soluble reactive phosphate versus potential density (σ_θ) to 27.5 kg m^{-3} for HOT cruises 1-100. The average density of the sea surface is connected by the heavy line.

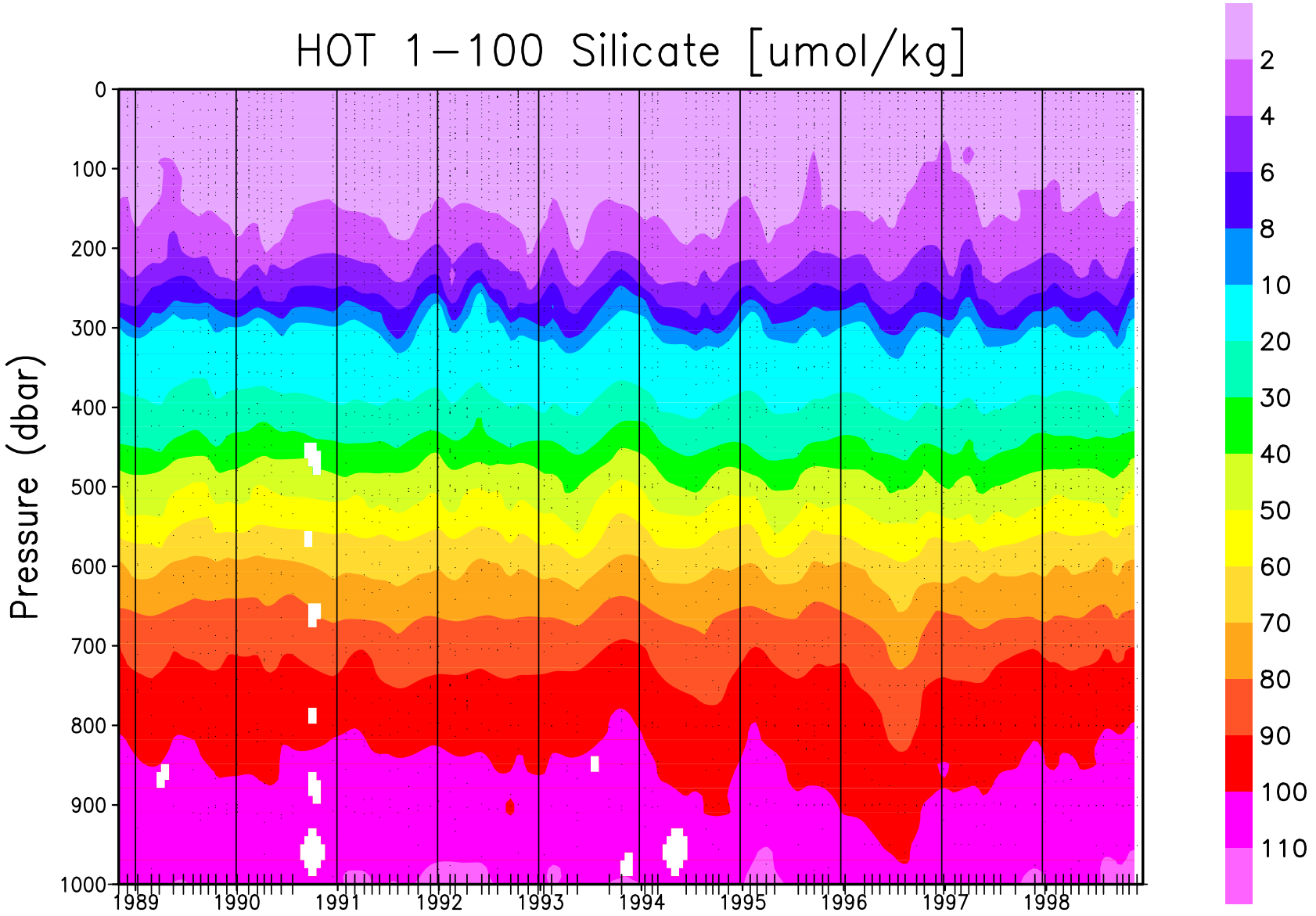

Figure 6.2.13: Contour plot of silicate versus pressure for HOT cruises 1-100. Location of samples in the water column are indicated by the solid circles.

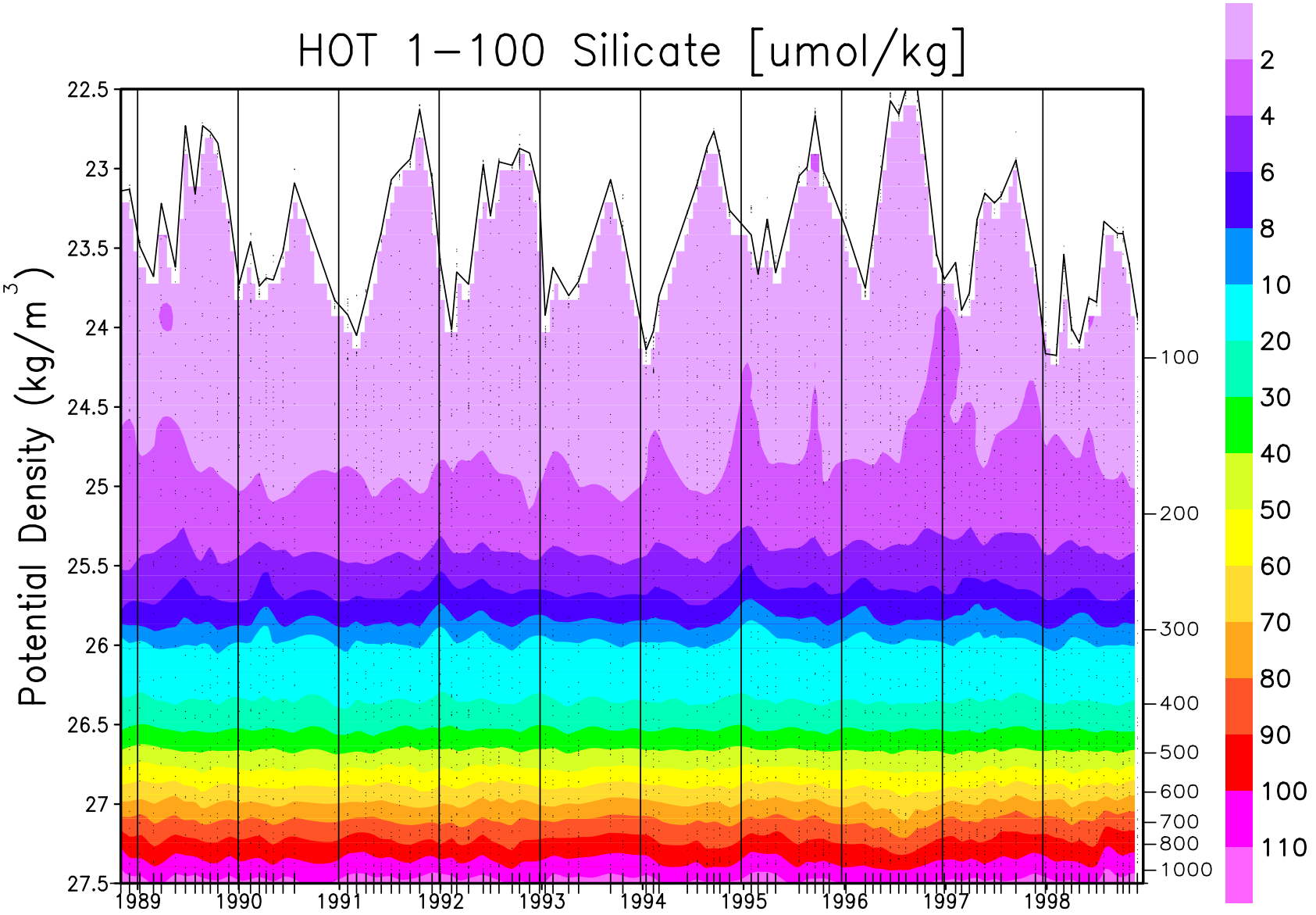

Figure 6.2.14: Contour plot of silicate versus potential density (σ_θ) to 27.5 kg m^{-3} for HOT cruises 1-100. The average density of the sea surface is connected by the heavy line.

6.3. Flash Fluorescence and Beam Transmission

Figures 6.3.1-11: Stack plots of flash fluorescence and beam transmission (when available) collected at Station ALOHA on HOT 33-43. Upper two panels show flash fluorescence data collected on each cruise plotted versus pressure to 250 dbar and potential density to 26 $\sigma\theta$.

Figure 6.3.12: Stack plots of averaged night-time fluorescence profiles plotted versus pressure to 250 dbar collected on each HOT cruise from 1988 through 1992. The HOT cruise number is shown at the top of each panel.

Figure 6.3.13: As in 6.3.11, except profiles are plotted versus potential density to 26 $\sigma\theta$.

Figure 6.3.14: Stack plots of averaged beam transmission profiles collected in 1991-1992. Upper panel shows profiles plotted versus pressure to 250 dbar. Lower panel shows profiles plotted versus potential density to 26 $\sigma\theta$. The HOT cruise number is shown at the top of each panel.

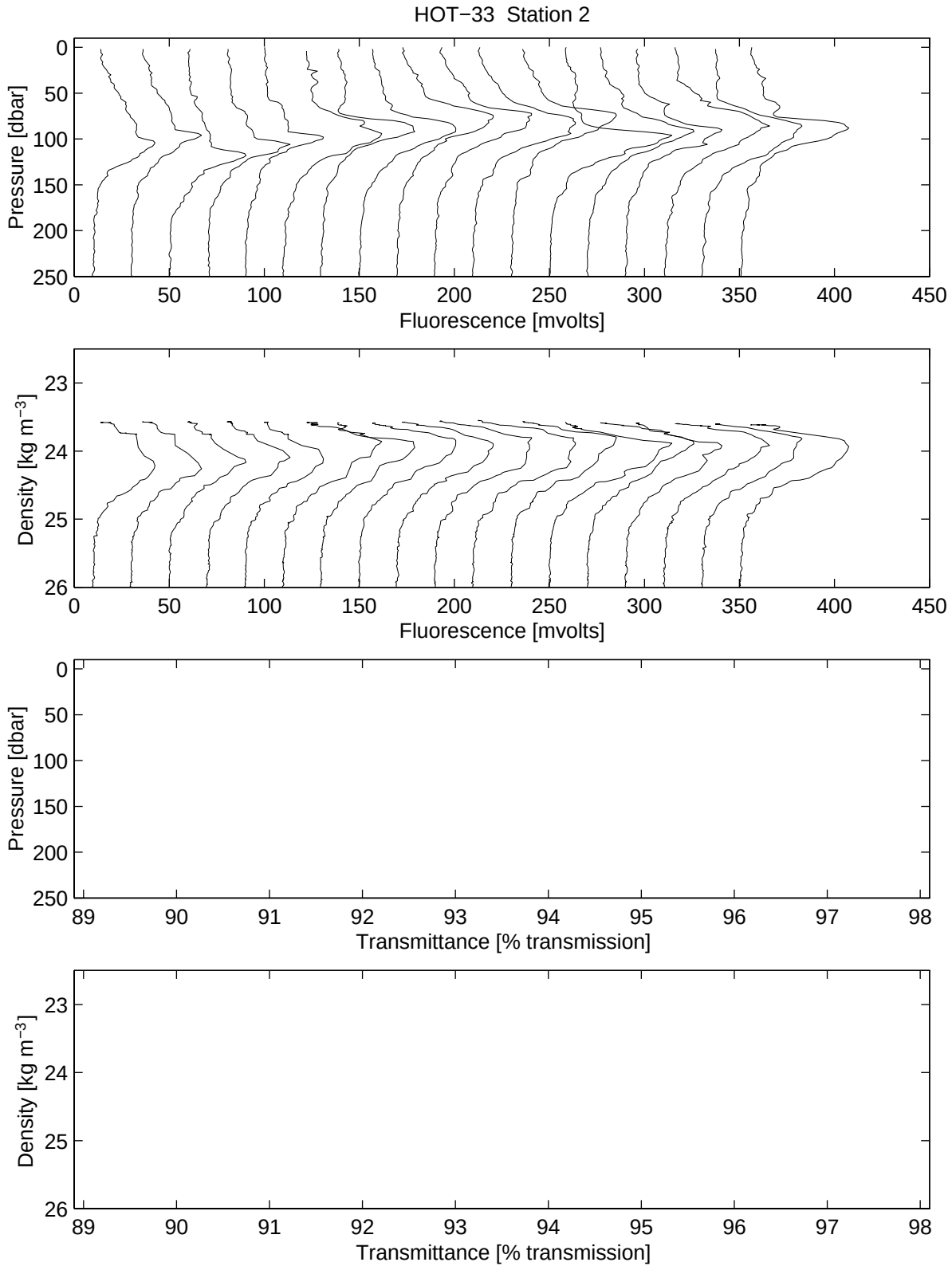
HOT−33 Station 2
Pressure [dbar]
Fluorescence [mvolts]
Density [kg m−3]
Fluorescence [mvolts]
Pressure [dbar]
Transmittance [% transmission]
Density [kg m−3]
Transmittance [% transmission]

Figure 6.3.1

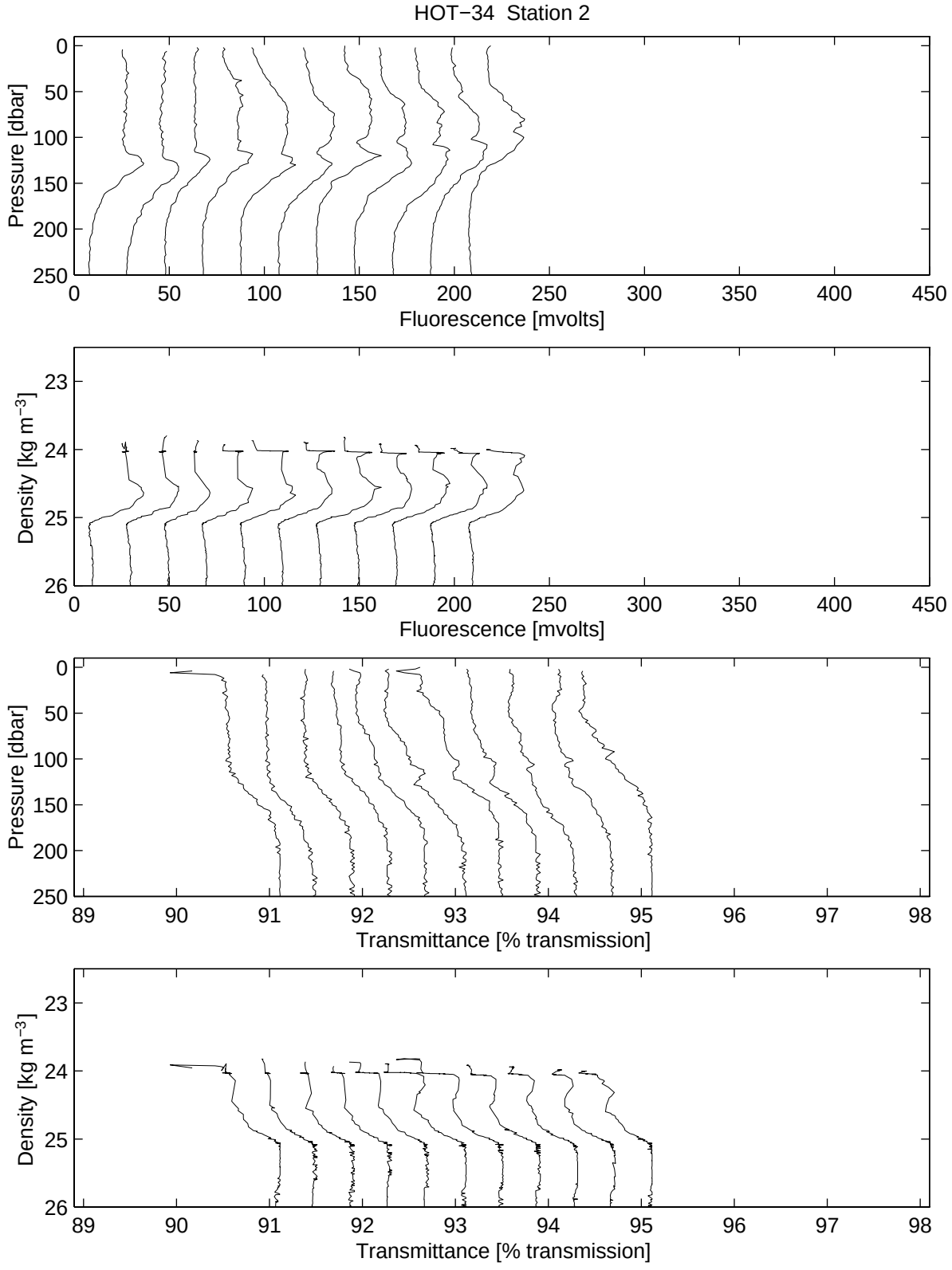
HOT−34 Station 2
Pressure [dbar]
Fluorescence [mvolts]
Density [kg m−3]
Fluorescence [mvolts]
Pressure [dbar]
Transmittance [% transmission]
Density [kg m−3]
Transmittance [% transmission]

Figure 6.3.2

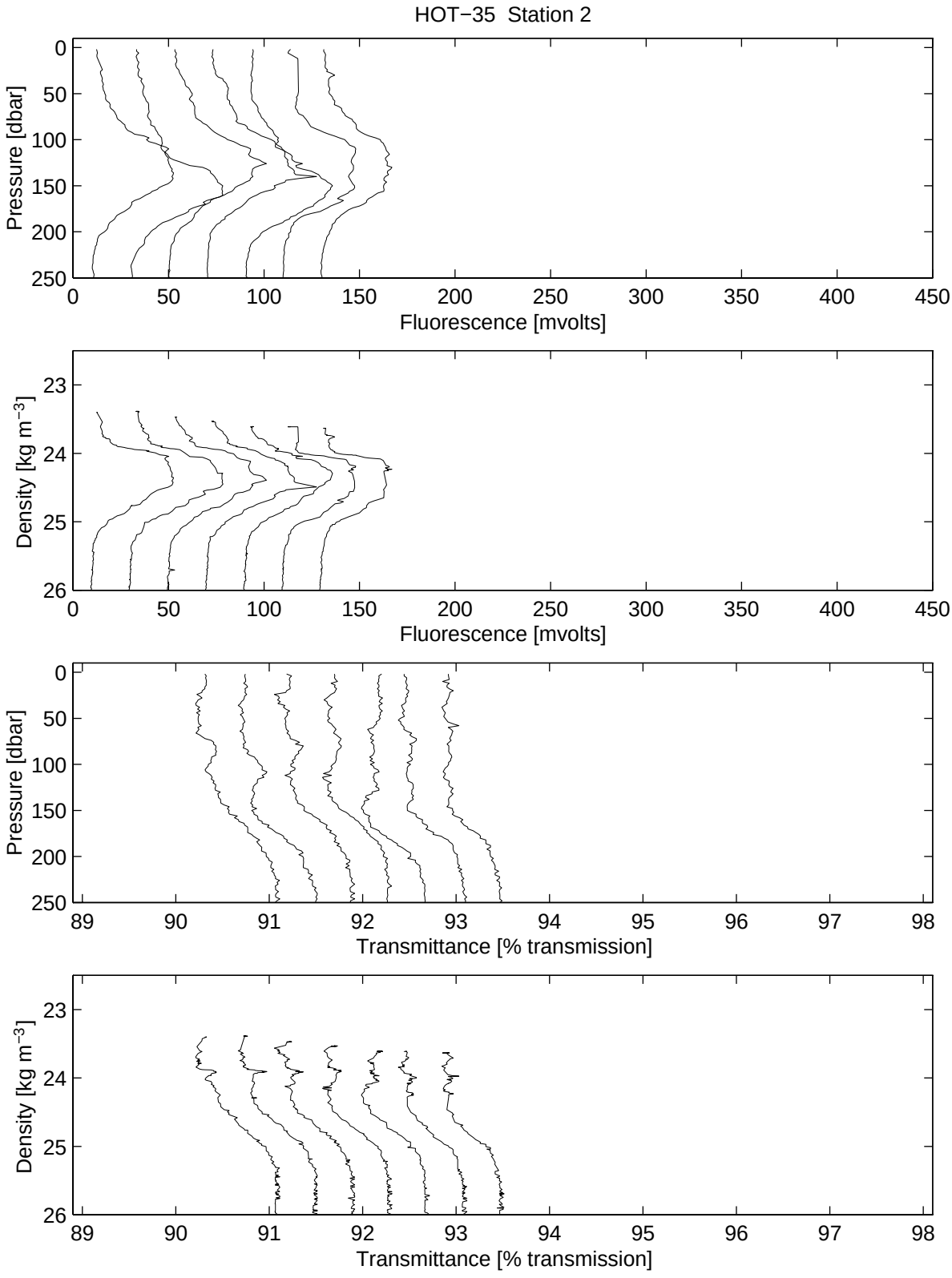
HOT−35 Station 2
Pressure [dbar]
Fluorescence [mvolts]
Density [kg m−3]
Fluorescence [mvolts]
Pressure [dbar]
Transmittance [% transmission]
Density [kg m−3]
Transmittance [% transmission]

Figure 6.3.3

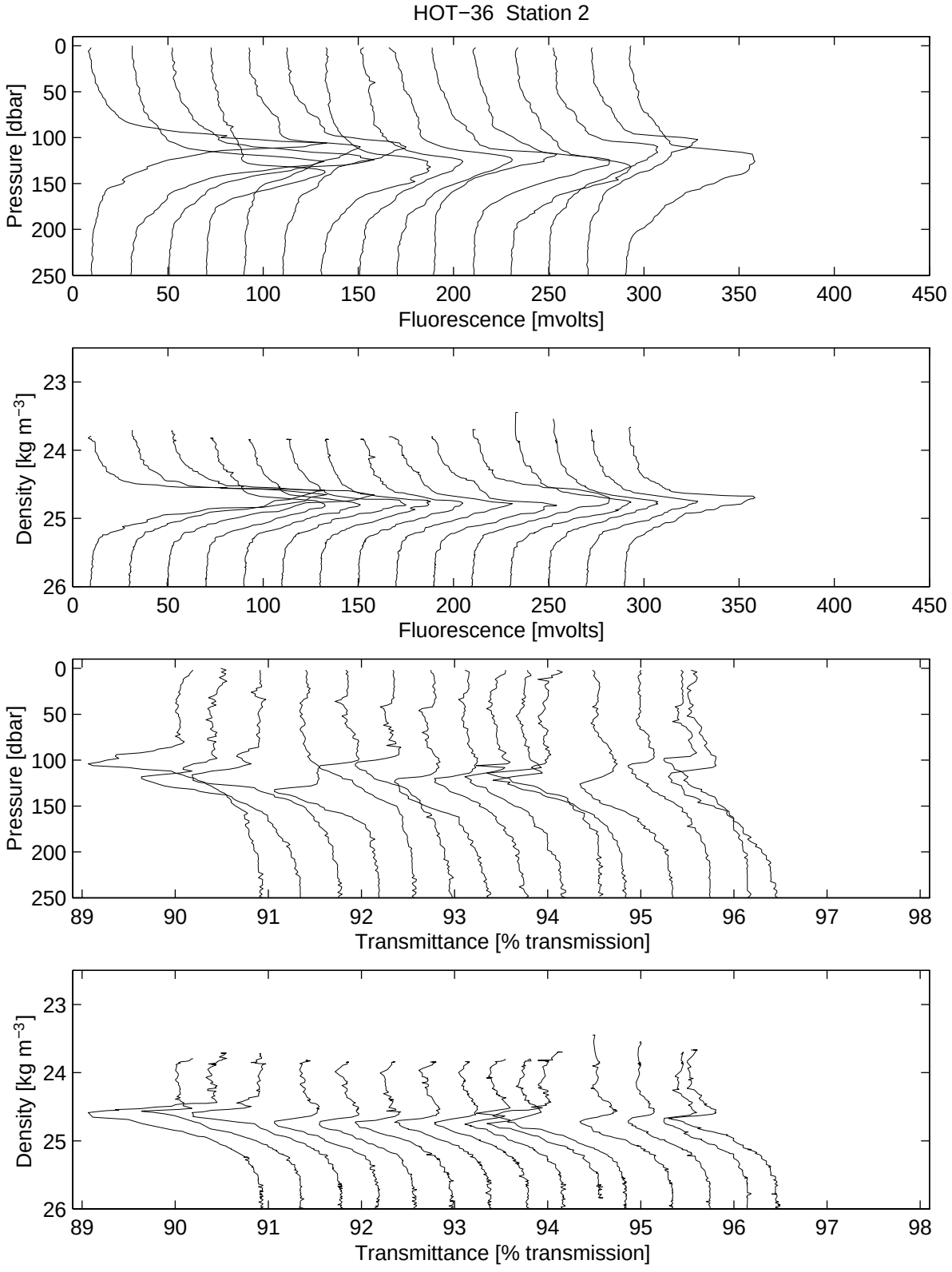
HOT−36 Station 2
Pressure [dbar]
Fluorescence [mvolts]
Density [kg m−3]
Fluorescence [mvolts]
Pressure [dbar]
Transmittance [% transmission]
Density [kg m−3]
Transmittance [% transmission]

Figure 6.3.4

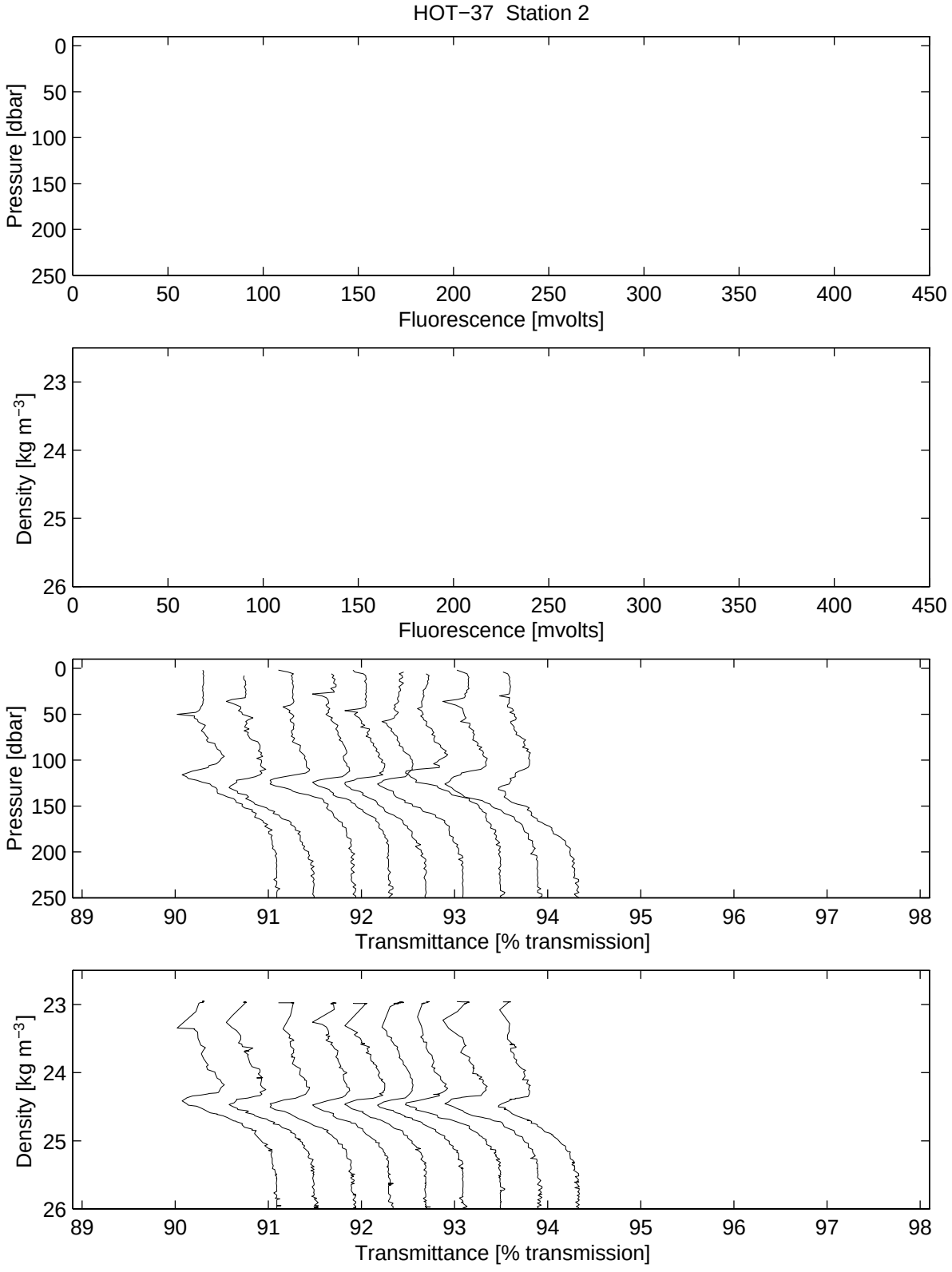
HOT−37 Station 2
Pressure [dbar]
Fluorescence [mvolts]
Density [kg m−3]
Fluorescence [mvolts]
Pressure [dbar]
Transmittance [% transmission]
Density [kg m−3]
Transmittance [% transmission]

Figure 6.3.5

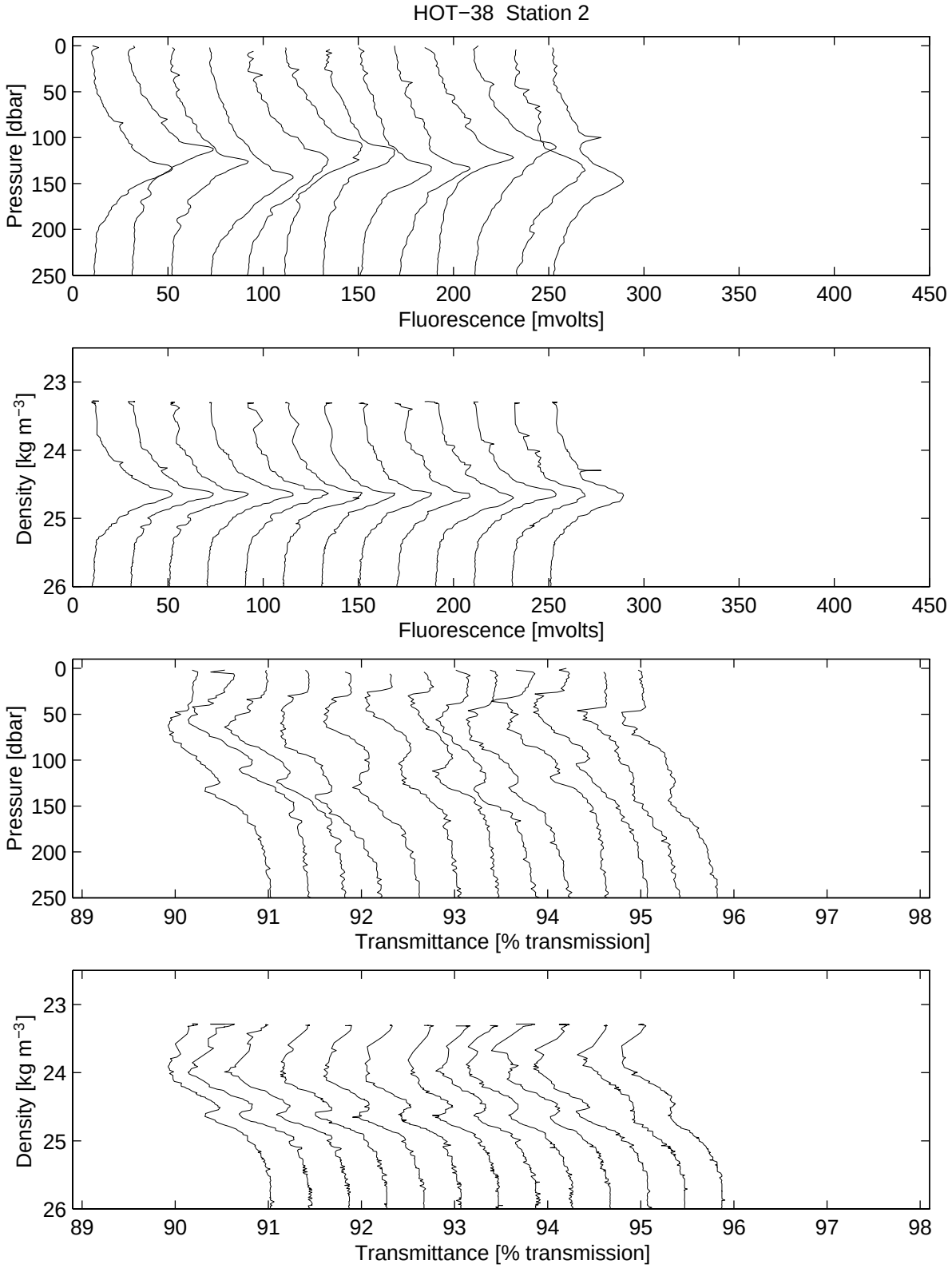
HOT−38 Station 2
Pressure [dbar]
Fluorescence [mvolts]
Density [kg m−3]
Fluorescence [mvolts]
Pressure [dbar]
Transmittance [% transmission]
Density [kg m−3]
Transmittance [% transmission]

Figure 6.3.6

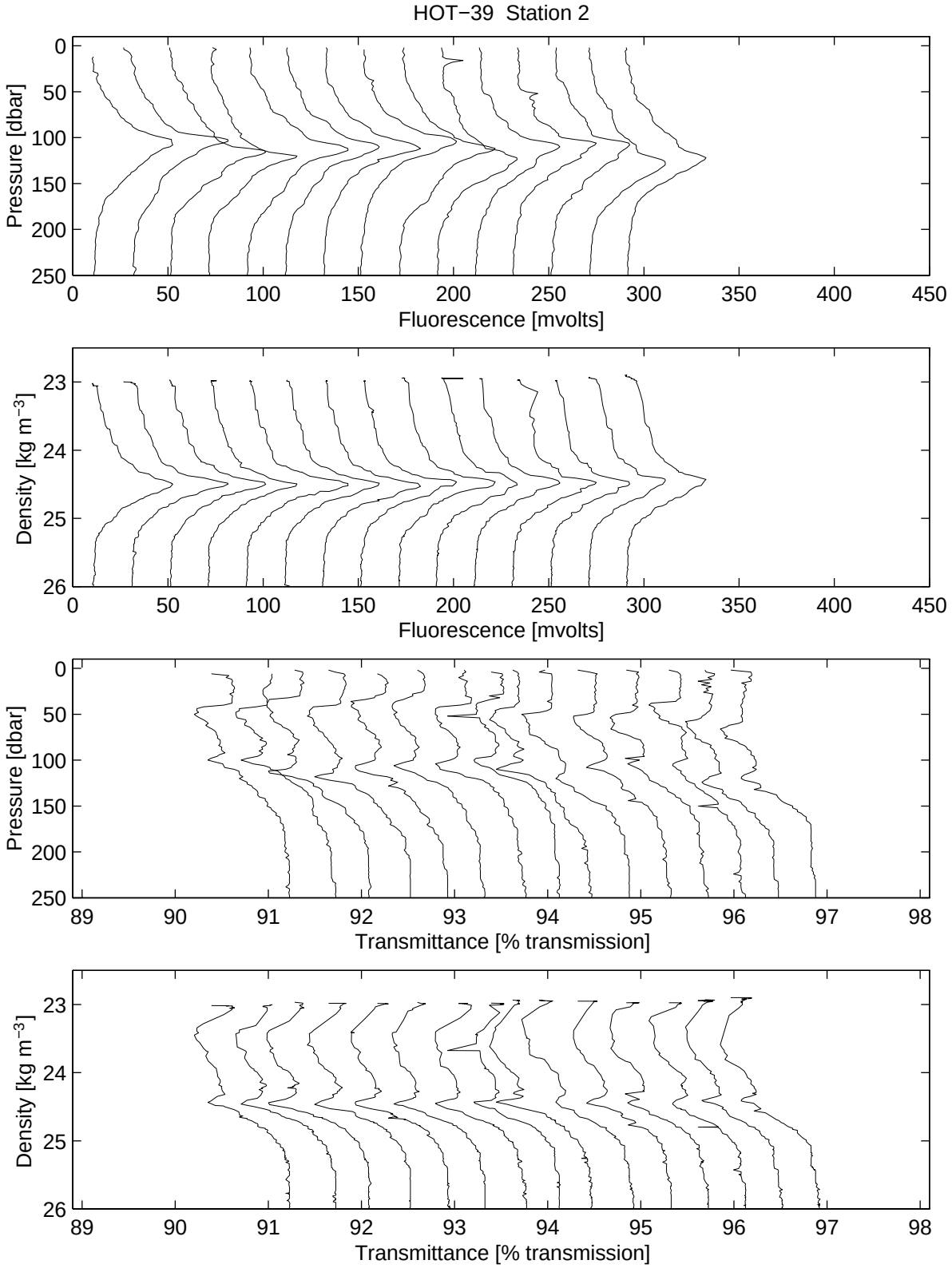
HOT−39 Station 2
Pressure [dbar]
Fluorescence [mvolts]
Density [kg m−3]
Fluorescence [mvolts]
Pressure [dbar]
Transmittance [% transmission]
Density [kg m−3]
Transmittance [% transmission]

Figure 6.3.7

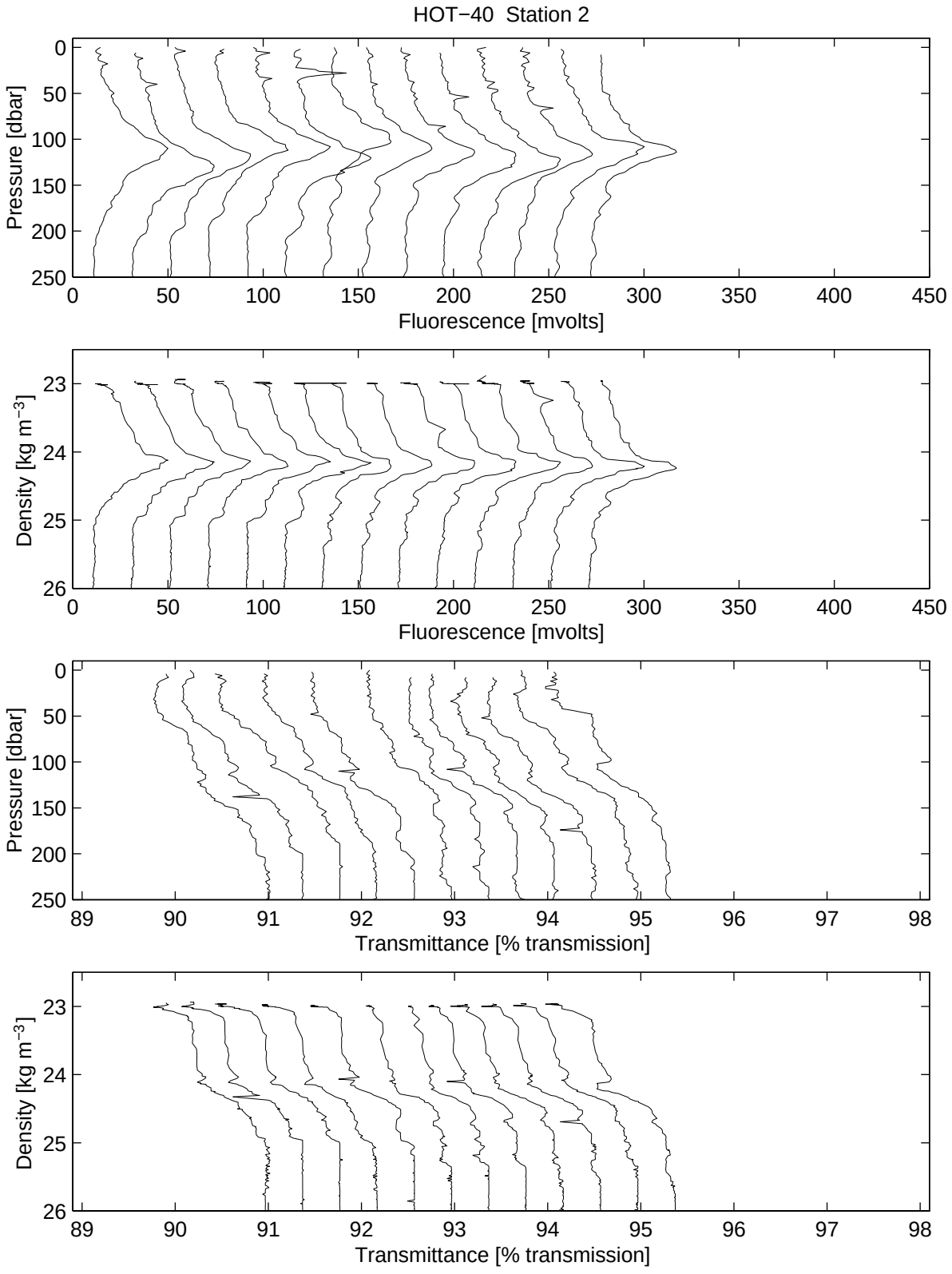
HOT−40 Station 2
Pressure [dbar]
Fluorescence [mvolts]
Density [kg m−3]
Fluorescence [mvolts]
Pressure [dbar]
Transmittance [% transmission]
Density [kg m−3]
Transmittance [% transmission]

Figure 6.3.8

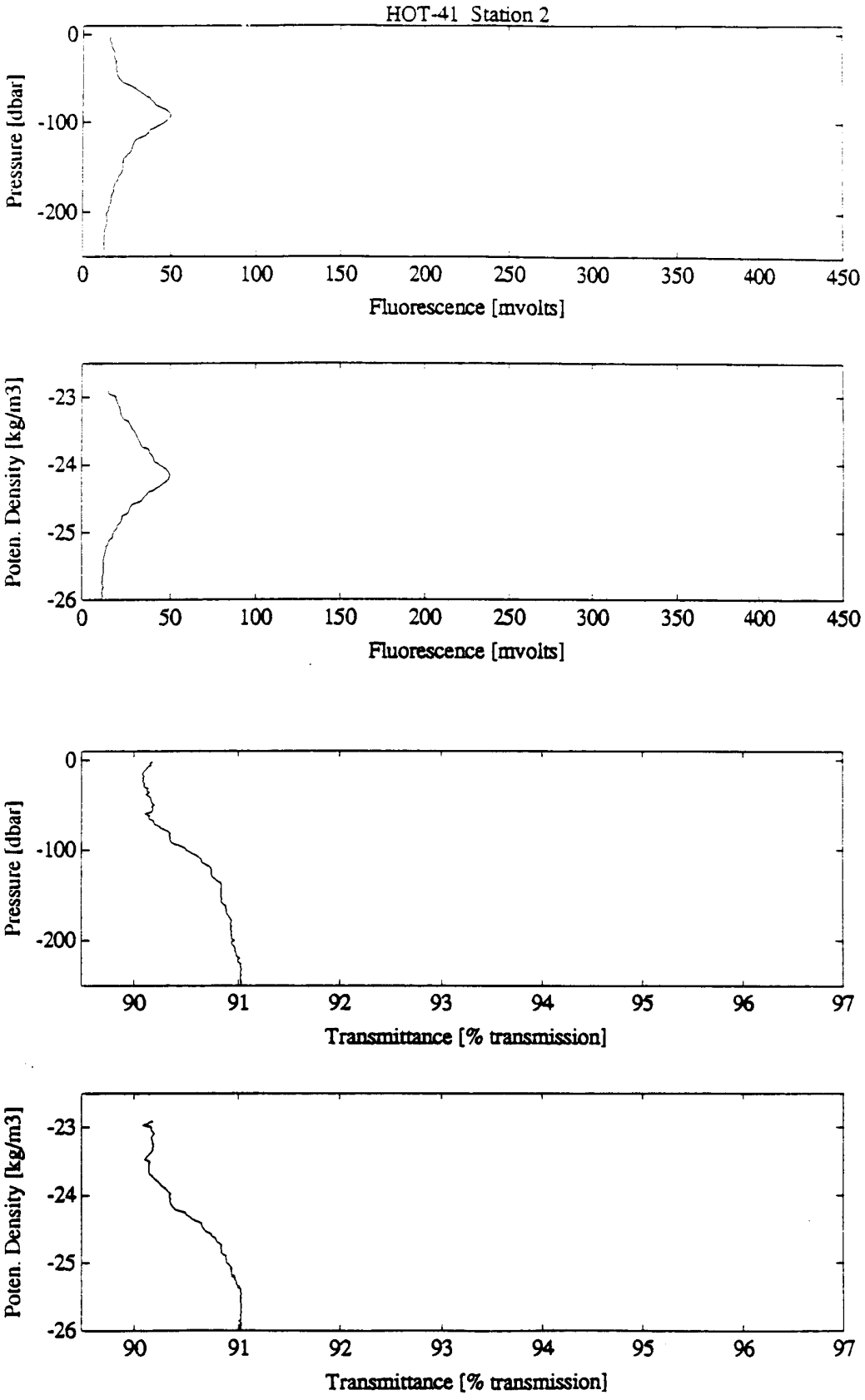

Figure 6.3.9

Figure 6.3.9

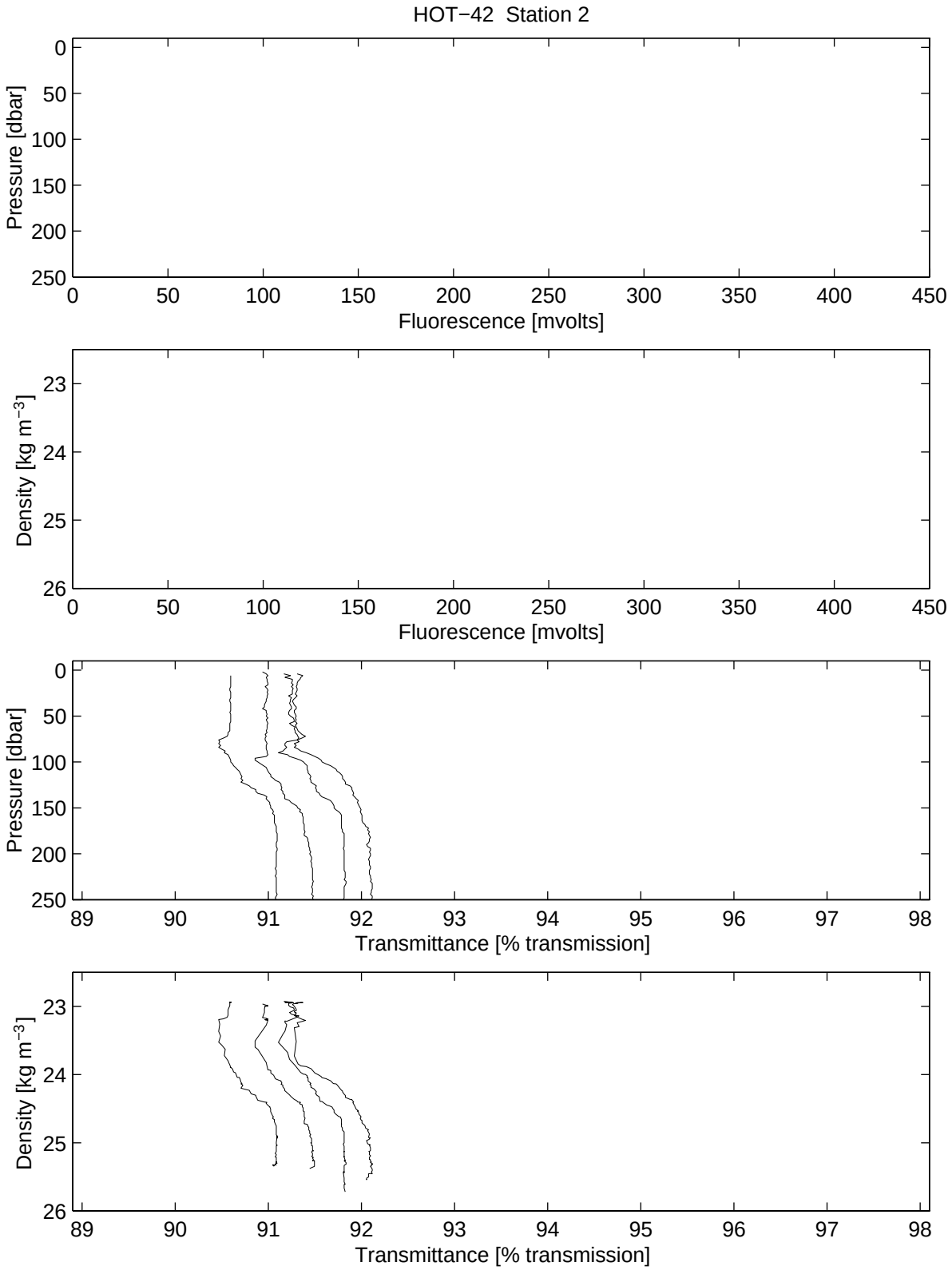
HOT−42 Station 2
Pressure [dbar]
Fluorescence [mvolts]
Density [kg m−3]
Fluorescence [mvolts]
Pressure [dbar]
Transmittance [% transmission]
Density [kg m−3]
Transmittance [% transmission]

Figure 6.3.10

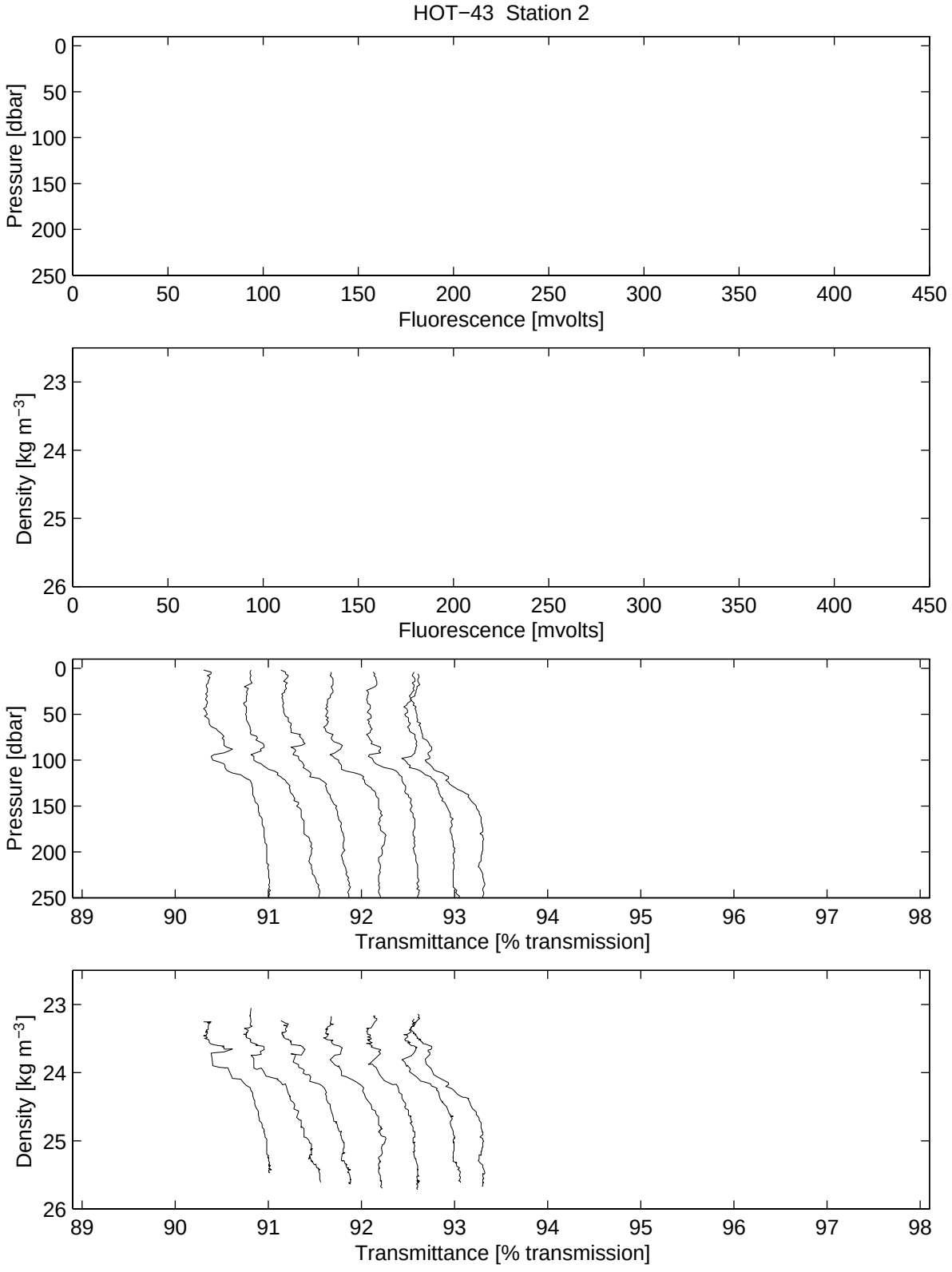
HOT−43 Station 2
Pressure [dbar]
Fluorescence [mvolts]
Density [kg m−3]
Fluorescence [mvolts]
Pressure [dbar]
Transmittance [% transmission]
Density [kg m−3]
Transmittance [% transmission]

Figure 6.3.11

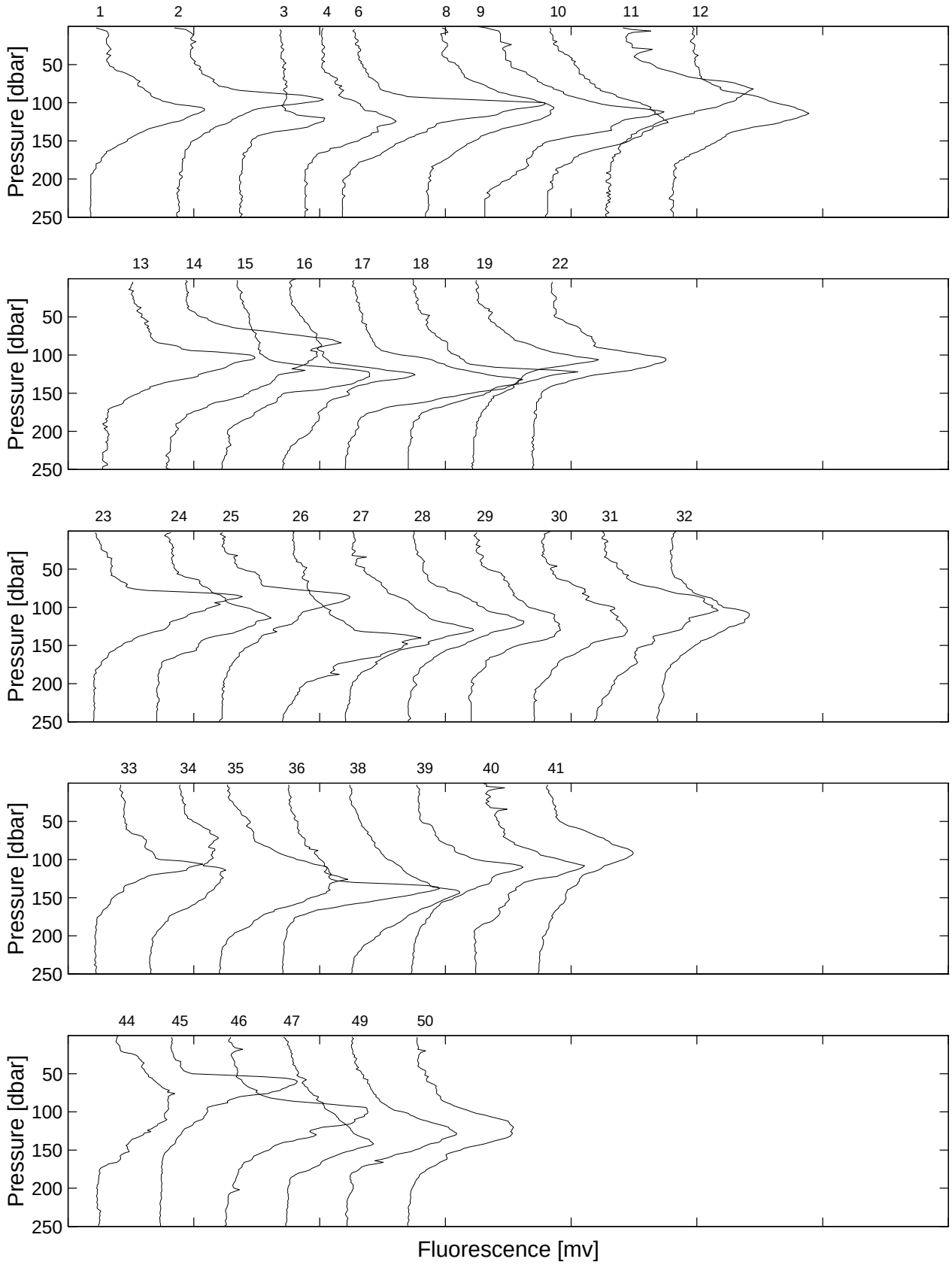
1 2 3 4 6 8 9 10 11 12
13 14 15 16 17 18 19 22
23 24 25 26 27 28 29 30 31 32
33 34 35 36 38 39 40 41
44 45 46 47 49 50
Pressure [dbar]
50
100
150
200
250
Fluorescence [mv]

Figure 6.3.12

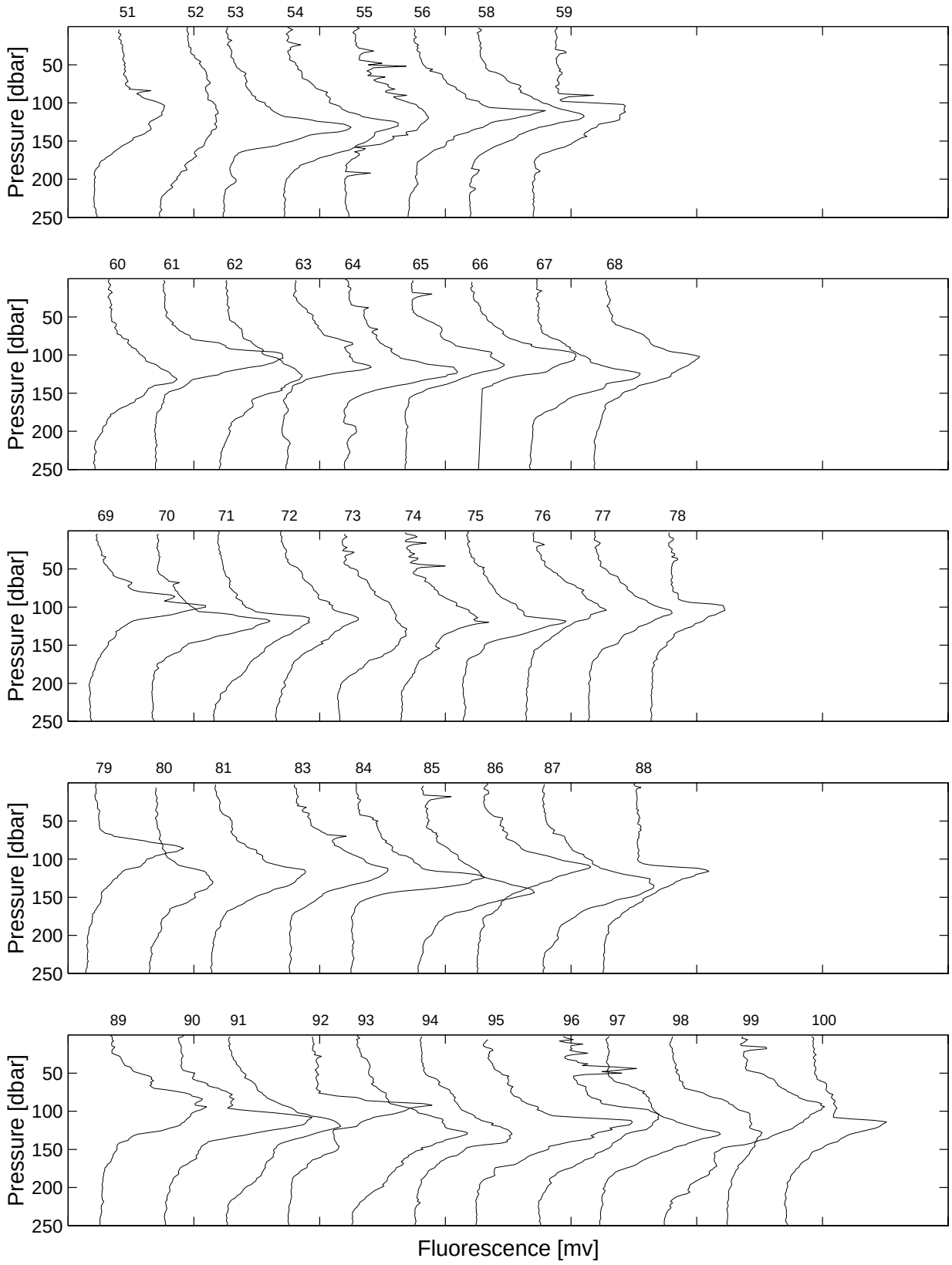

Figure 6.2.12 (Continued)

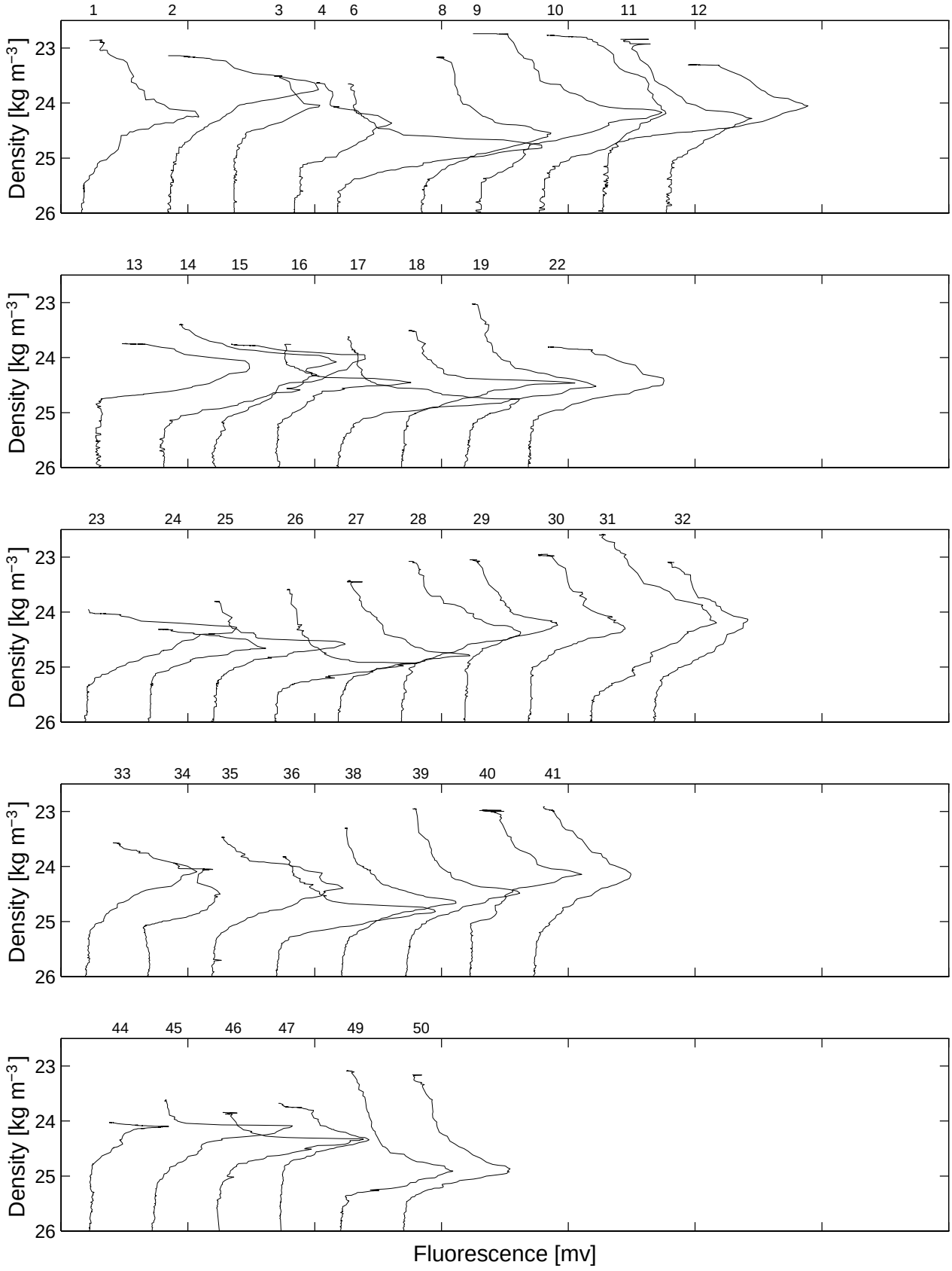
1 2 3 4 6 8 9 10 11 12
13 14 15 16 17 18 19 22
23 24 25 26 27 28 29 30 31 32
33 34 35 36 38 39 40 41
44 45 46 47 49 50
Density [kg m⁻³]
23
24
25
26
Fluorescence [mv]

Figure 6.3.13

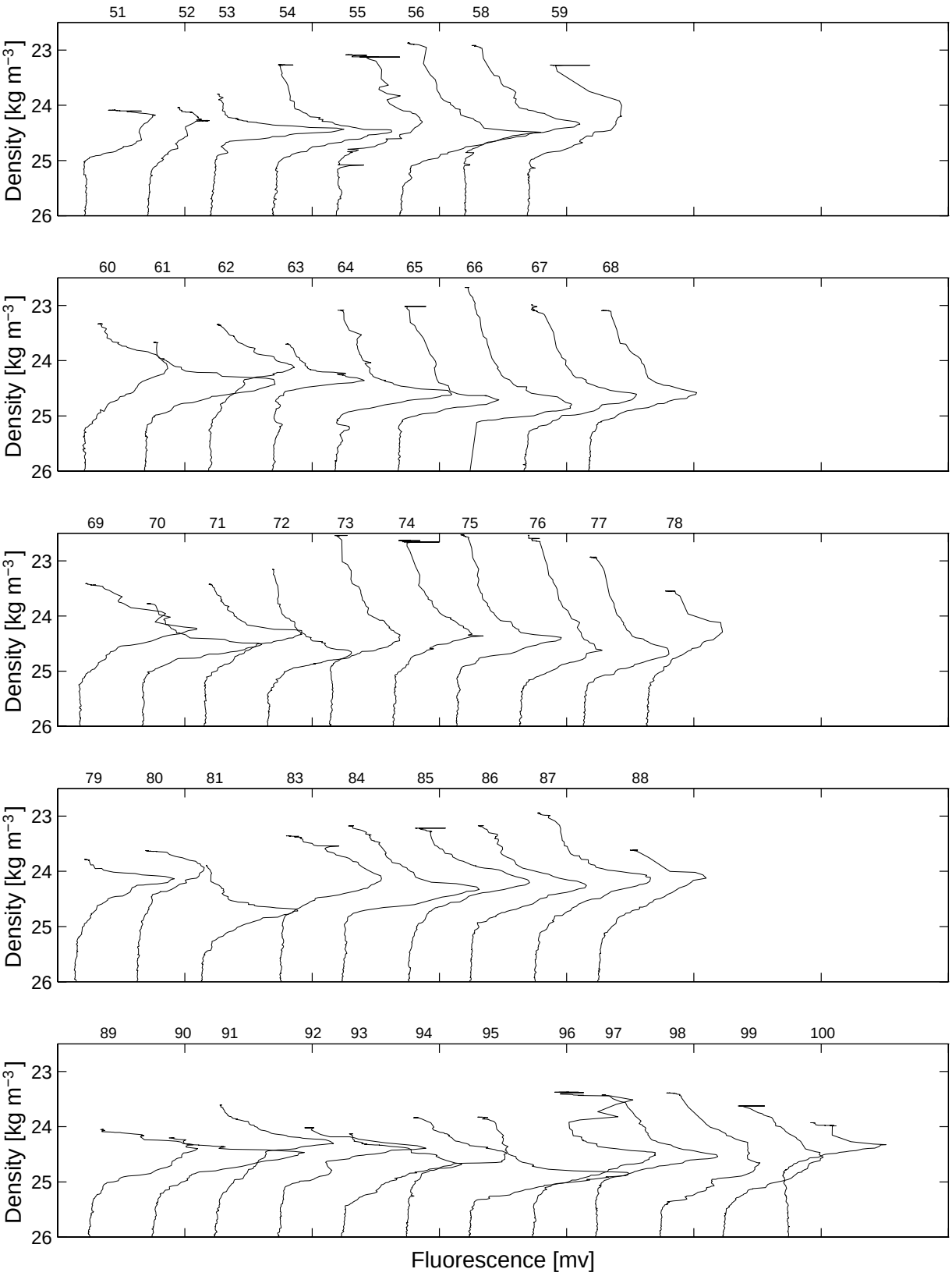

Figure 6.3.13 (Continued)

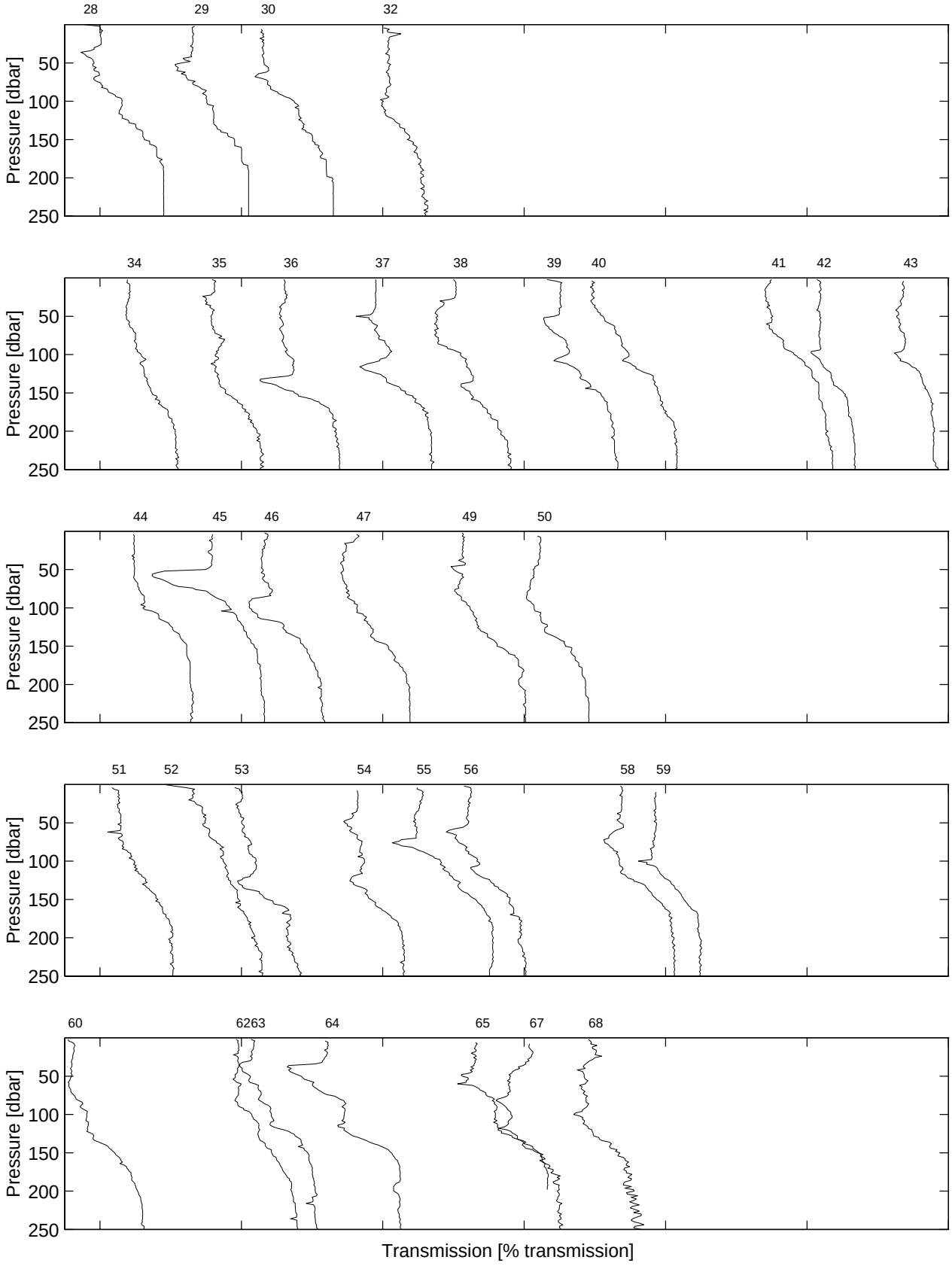
28
29
30
32
34
35
36
37
38
39
40
41
42
43
44
45
46
47
49
50
51
52
53
54
55
56
58
59
60
6263
64
65
67
68
Pressure [dbar]
50
100
150
200
250
Transmission [% transmission]

Figure 6.3.14

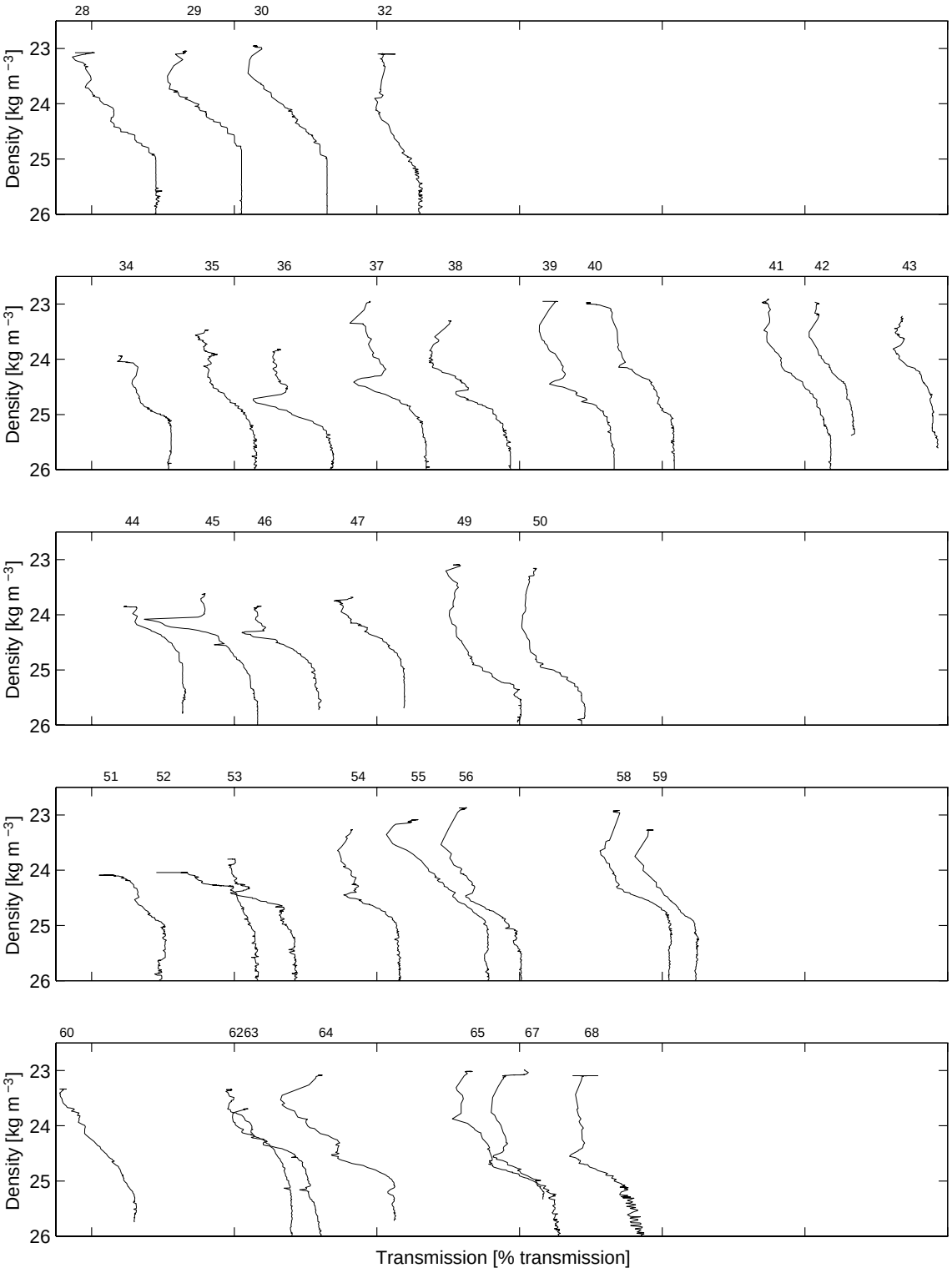

Figure 6.3.14 (Continued)

6.4. Biogeochemistry

Figure 6.4.1: Contoured time-series of DIC in the upper 1000 dbar at Station ALOHA normalized to 35 ppt salinity.

Figure 6.4.2: Contoured time-series of titration alkalinity in the upper 1000 dbar at Station ALOHA normalized to 35 ppt salinity.

Figure 6.4.3: Mean titration alkalinity and DIC in surface waters (0-50 dbars) at Station ALOHA. Upper Panel: Titration alkalinity plotted versus time for all HOT cruises. Error bars represent standard deviation of pooled samples collected between 0 and 50 dbar. Lower panel: As in upper panel except for DIC.

Figure 6.4.4: Soluble reactive phosphorus measured by the MAGIC procedure in the upper 250 dbar at Station ALOHA in 1992.

Figure 6.4.5: Nitrate plus nitrite measured by the nitrogen oxides analyzer in the upper 250 dbar at Station ALOHA in 1992.

Figure 6.4.6: Contoured time-series of chlorophyll *a* in the upper 200 dbar for all HOT cruises.

Figure 6.4.7: Particulate carbon at Station ALOHA on all HOT cruises. Upper panel: Mean particulate carbon concentration in the upper 50 dbar. Error bar represents the standard deviation of pooled samples collected between 0 and 50 dbar. Lower panel: As in upper panel but for 50 to 100 dbar.

Figure 6.4.8: As in Figure 6.4.7:except for particulate nitrogen.

Figure 6.4.9: As in Figure 6.4.7:except for particulate phosphorus.

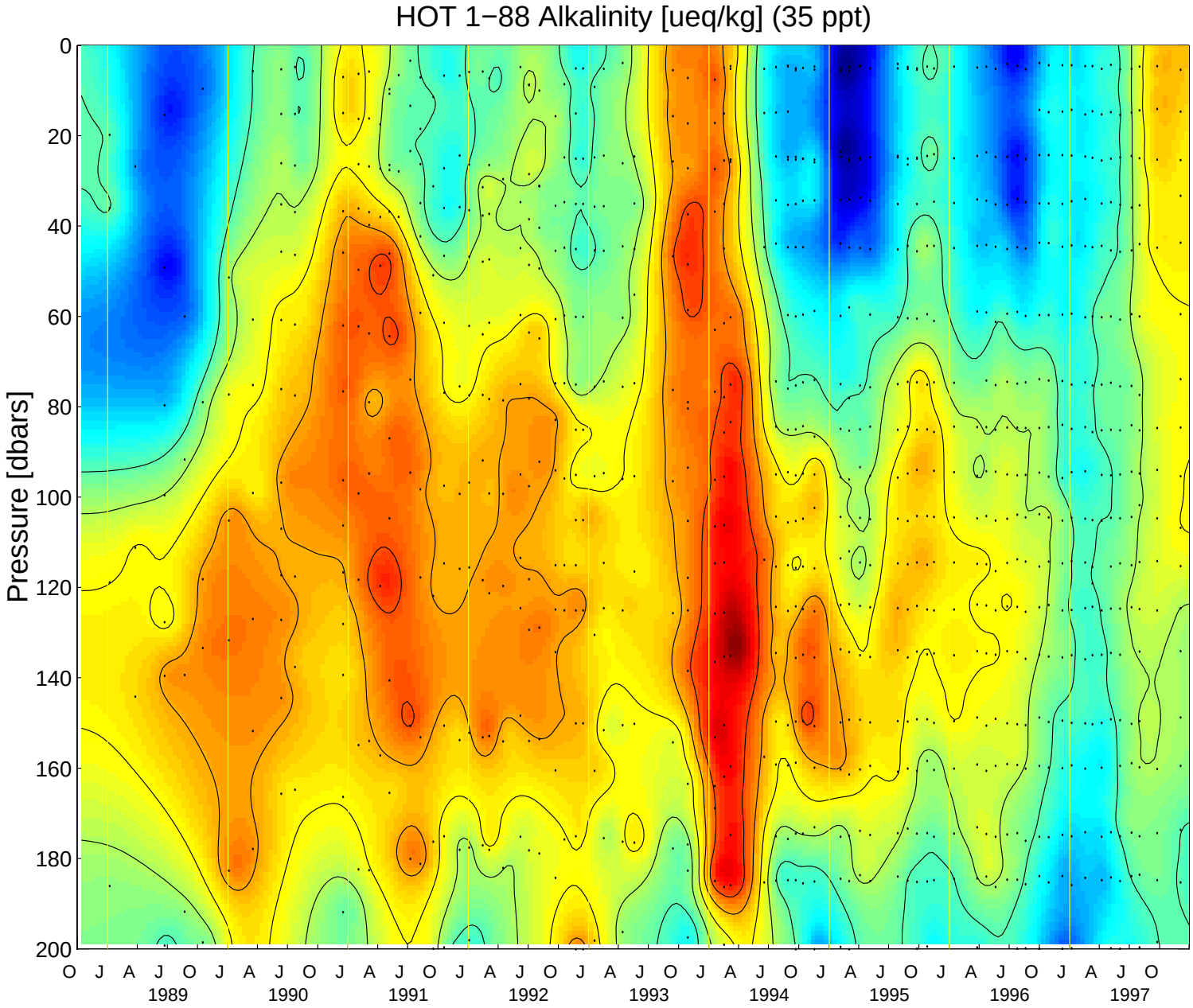
HOT 1−88 Alkalinity [ueq/kg] (35 ppt)
Pressure [dbars]
0
20
40
60
80
100
120
140
160
180
200
O J A J O J A J O J A J O J A J O J A J O J A J O J A J O J A J O J A J O J A J O J A J O
1989
1990
1991
1992
1993
1994
1995
1996
1997

Figure 6.4.1

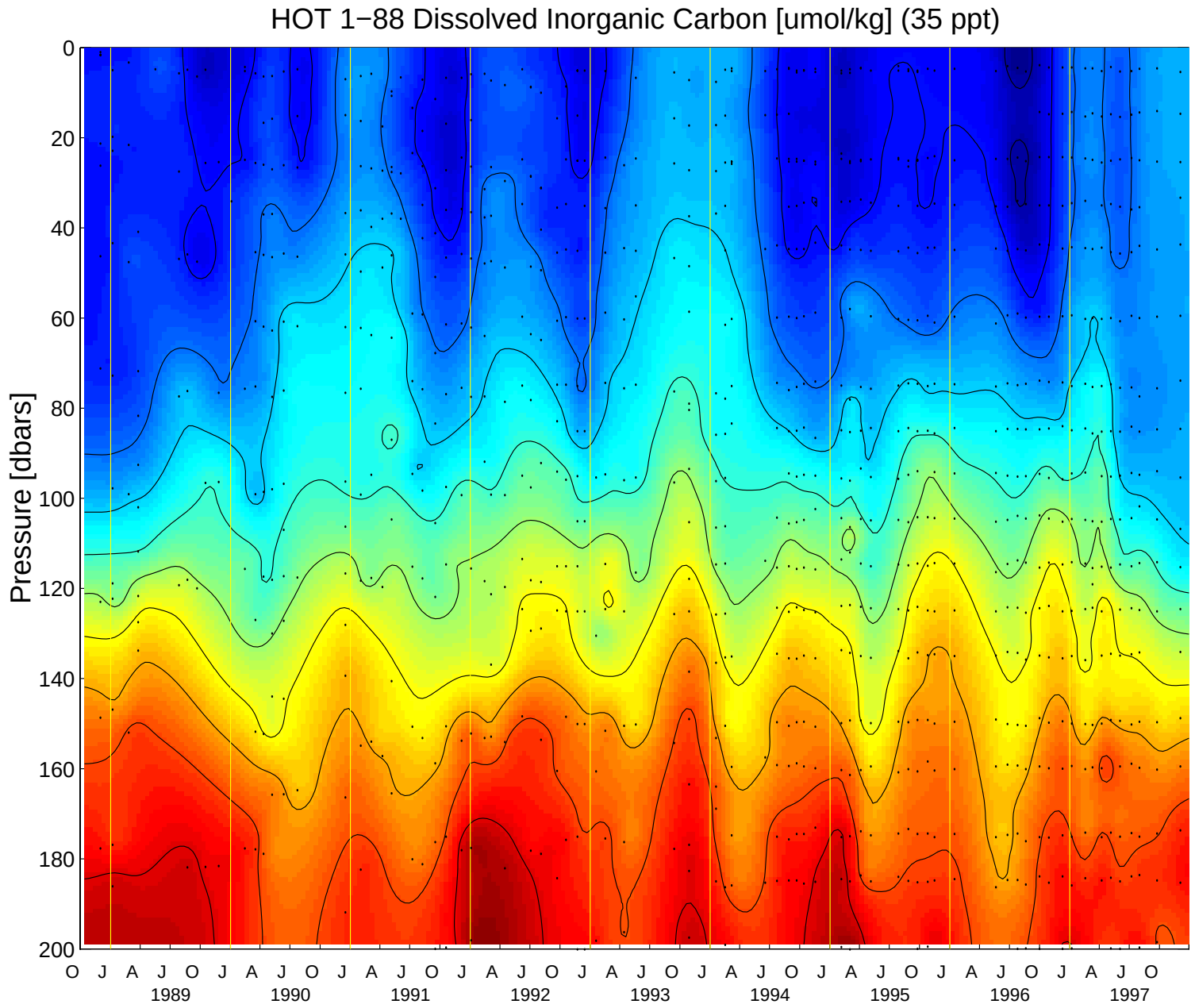
HOT 1−88 Dissolved Inorganic Carbon [umol/kg] (35 ppt)
Pressure [dbars]
0
20
40
60
80
100
120
140
160
180
200
O J A J O J A J O J A J O J A J O J A J O J A J O J A J O J A J O J A J O J A J O J A J O
1989
1990
1991
1992
1993
1994
1995
1996
1997

Figure 6.4.2

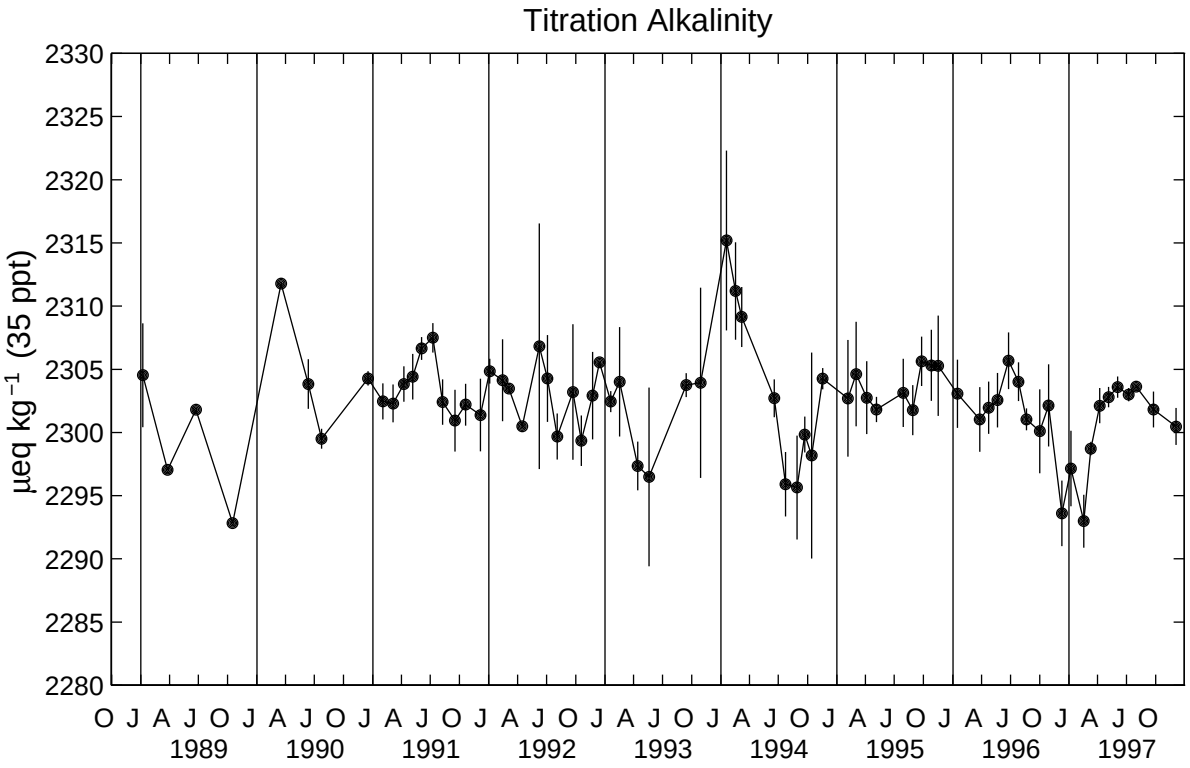
Titration Alkalinity
µeq kg⁻¹ (35 ppt)
2330
2325
2320
2315
2310
2305
2300
2295
2290
2285
2280
O J A J O J A J O J A J O J A J O J A J O J A J O J A J O J A J O J A J O J A J O
1989
1990
1991
1992
1993
1994
1995
1996
1997

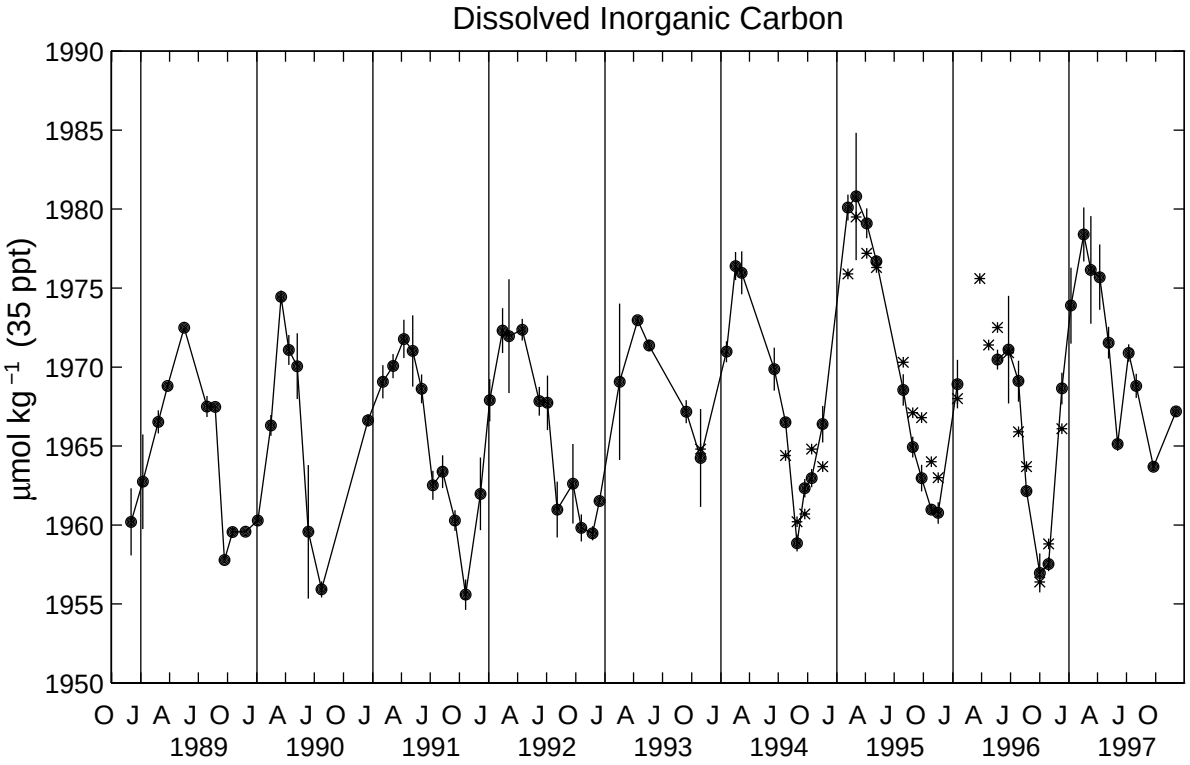
Dissolved Inorganic Carbon
µmol kg⁻¹ (35 ppt)
1990
1985
1980
1975
1970
1965
1960
1955
1950
O J A J O J A J O J A J O J A J O J A J O J A J O J A J O J A J O J A J O J A J O
1989
1990
1991
1992
1993
1994
1995
1996
1997

Figure 6.4.3

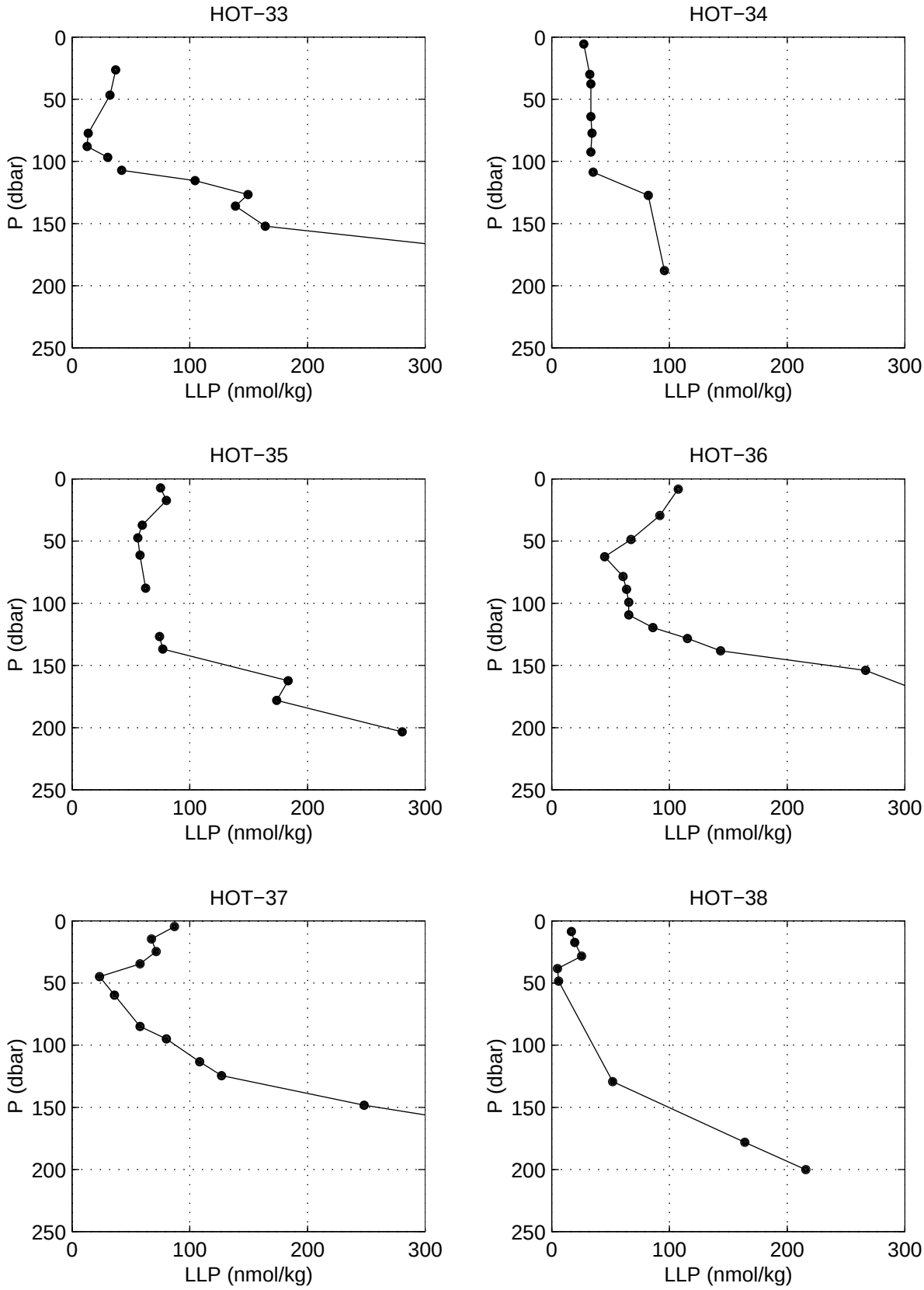
HOT−33
HOT−34
HOT−35
HOT−36
HOT−37
HOT−38
P (dbar)
LLP (nmol/kg)
0
50
100
150
200
250
0
100
200
300

Figure 6.4.4

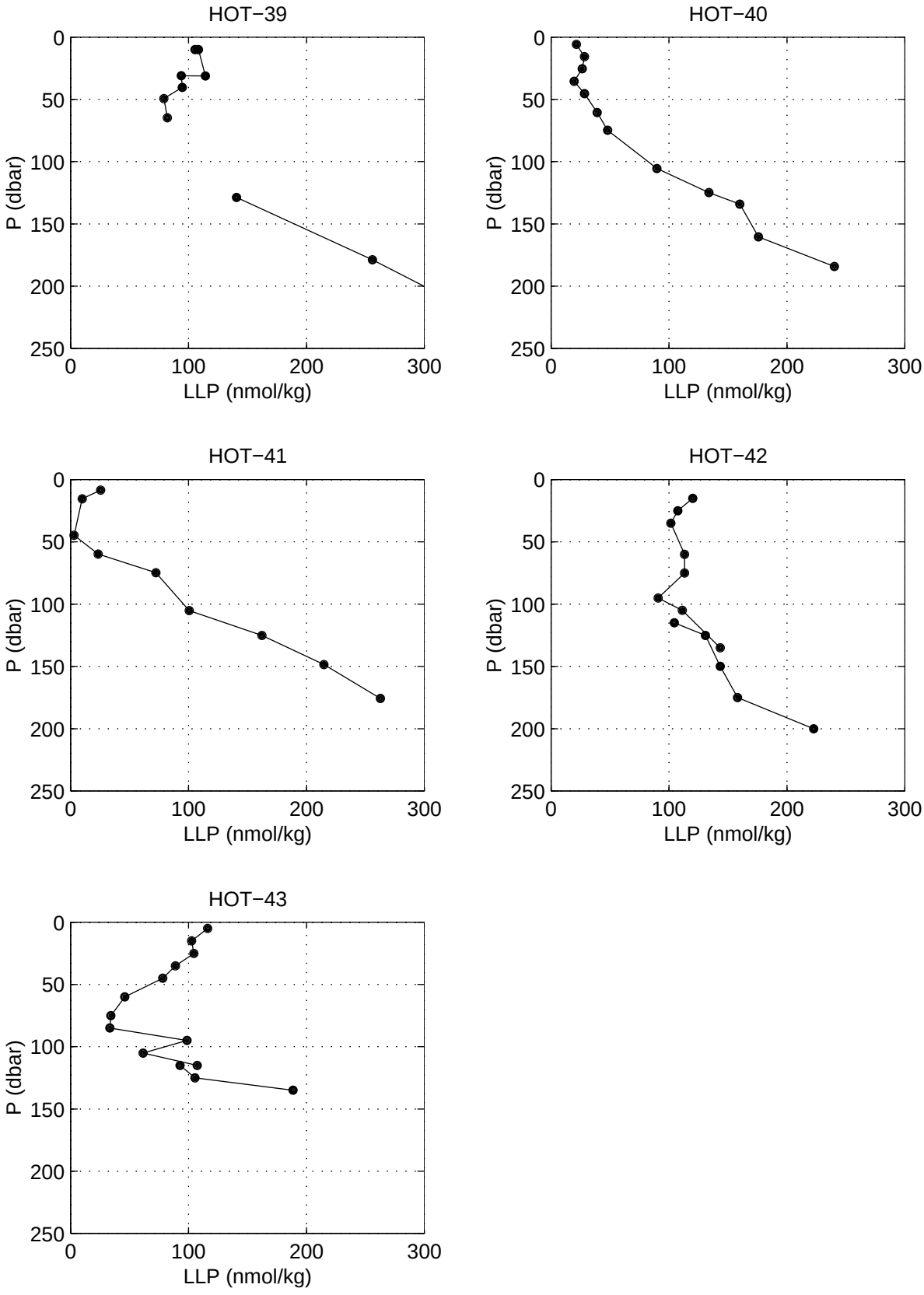

Figure 6.4.4 (continued)

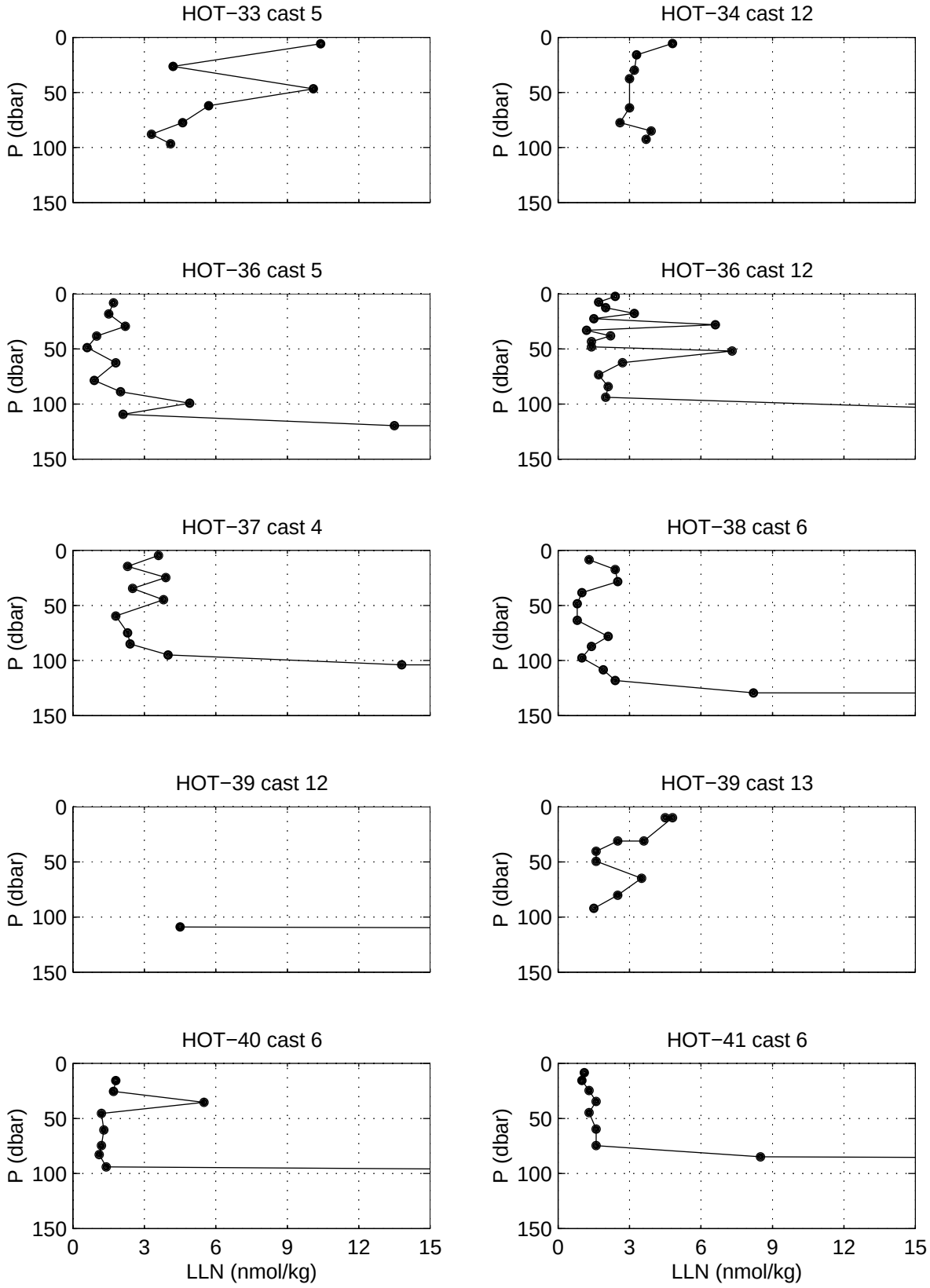
HOT−33 cast 5
HOT−34 cast 12
HOT−36 cast 5
HOT−36 cast 12
HOT−37 cast 4
HOT−38 cast 6
HOT−39 cast 12
HOT−39 cast 13
HOT−40 cast 6
HOT−41 cast 6
P (dbar)
0
50
100
150
0
3
6
9
12
15
LLN (nmol/kg)

Figure 6.4.5

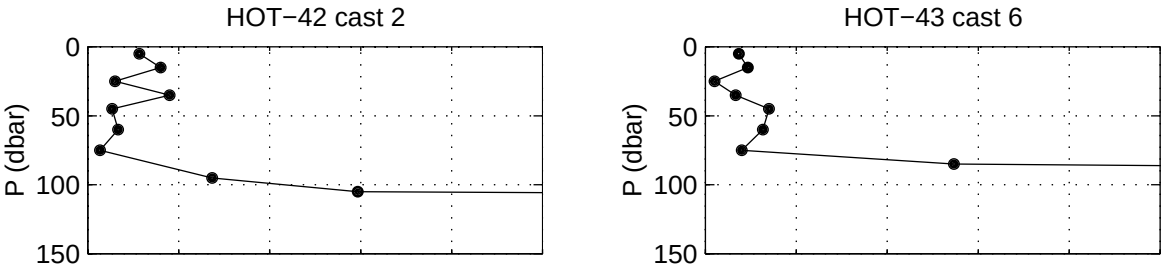

Figure 6.4.5 (continued)

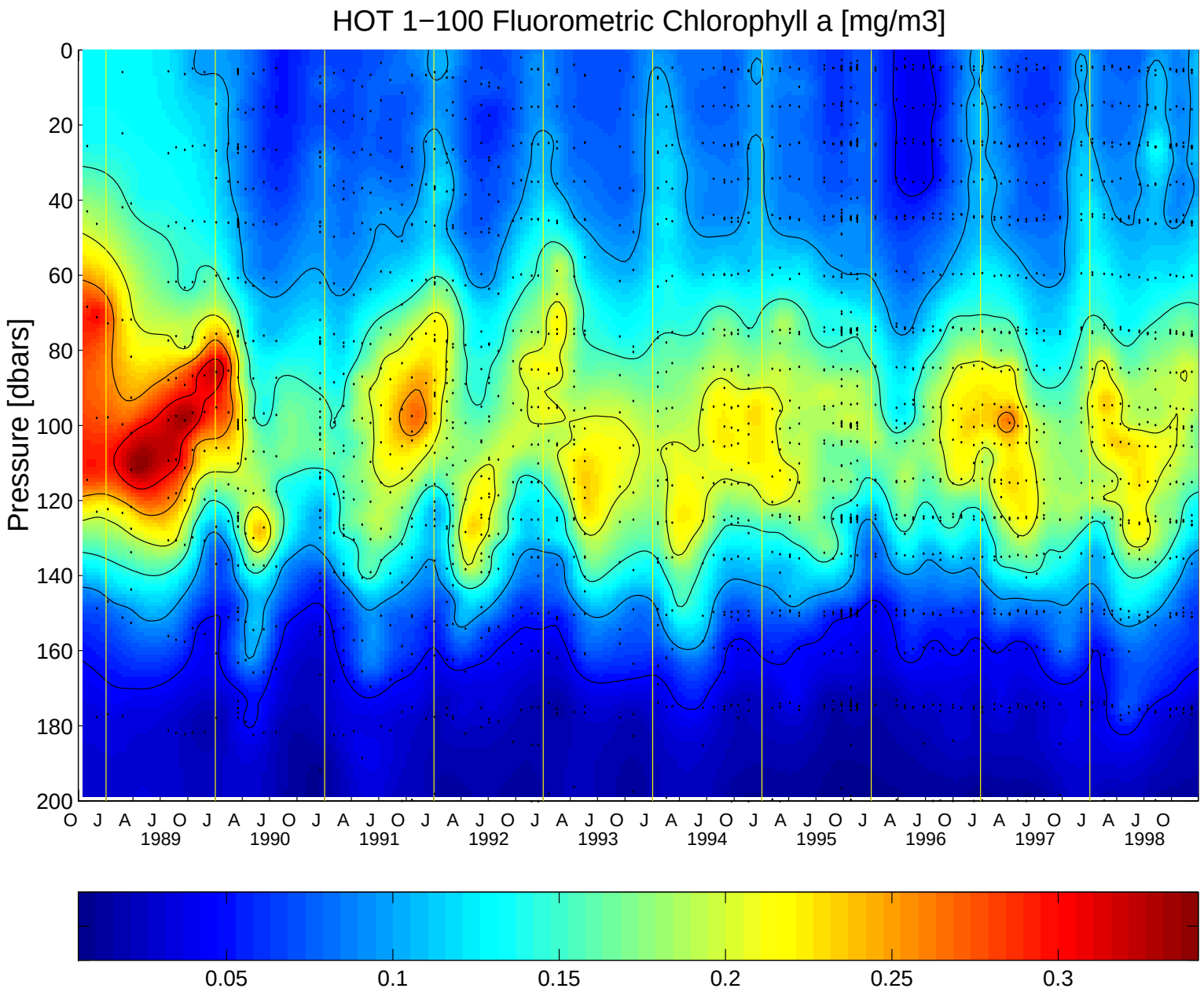
HOT 1−100 Fluorometric Chlorophyll a [mg/m3]
Pressure [dbars]
0
20
40
60
80
100
120
140
160
180
200
O J A J O J A J O J A J O J A J O J A J O J A J O J A J O J A J O J A J O J A J O J A J O J A J O
1989
1990
1991
1992
1993
1994
1995
1996
1997
1998
0.05
0.1
0.15
0.2
0.25
0.3

Figure 6.4.6

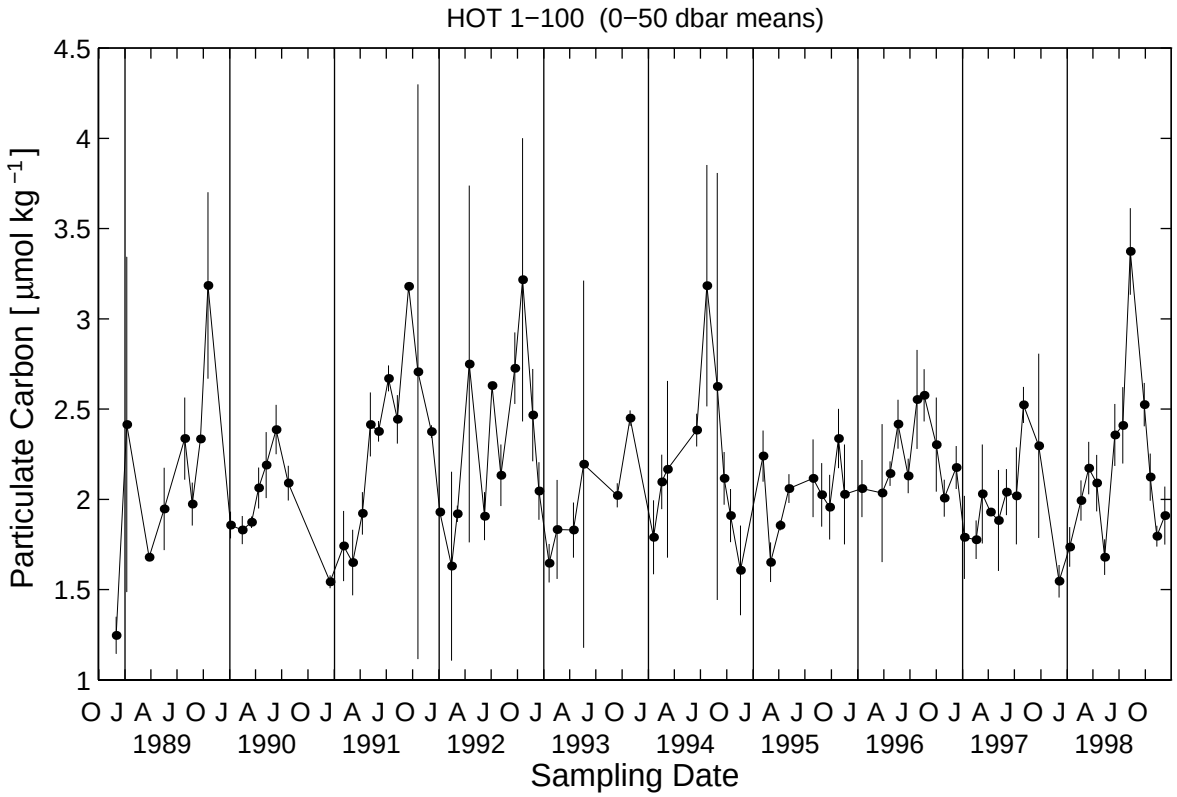
HOT 1−100 (0−50 dbar means)
Particulate Carbon [µmol kg −1]
4.5
4
3.5
3
2.5
2
1.5
1
O J A J O J A J O J A J O J A J O J A J O J A J O J A J O J A J O J A J O J A J O J A J O J A J O
1989 1990 1991 1992 1993 1994 1995 1996 1997 1998
Sampling Date

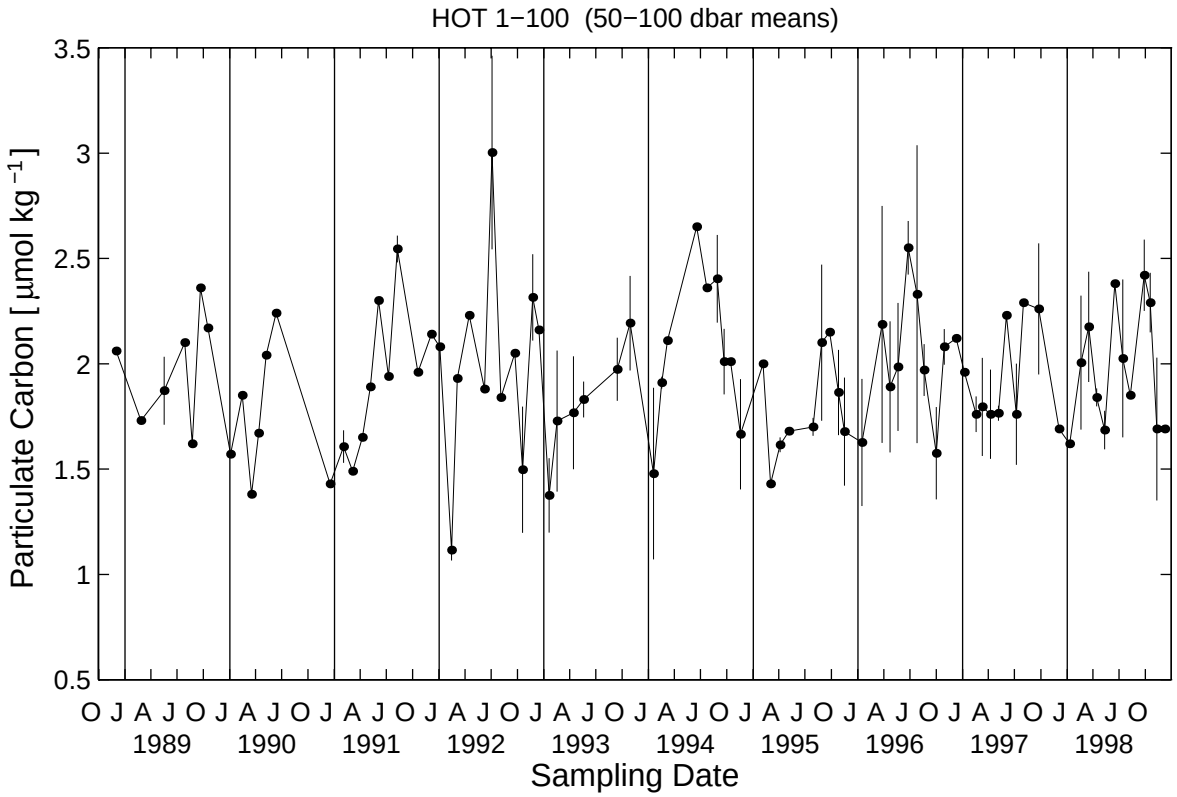
HOT 1−100 (50−100 dbar means)
Particulate Carbon [µmol kg −1]
3.5
3
2.5
2
1.5
1
0.5
O J A J O J A J O J A J O J A J O J A J O J A J O J A J O J A J O J A J O J A J O J A J O J A J O
1989 1990 1991 1992 1993 1994 1995 1996 1997 1998
Sampling Date

Figure 6.4.7

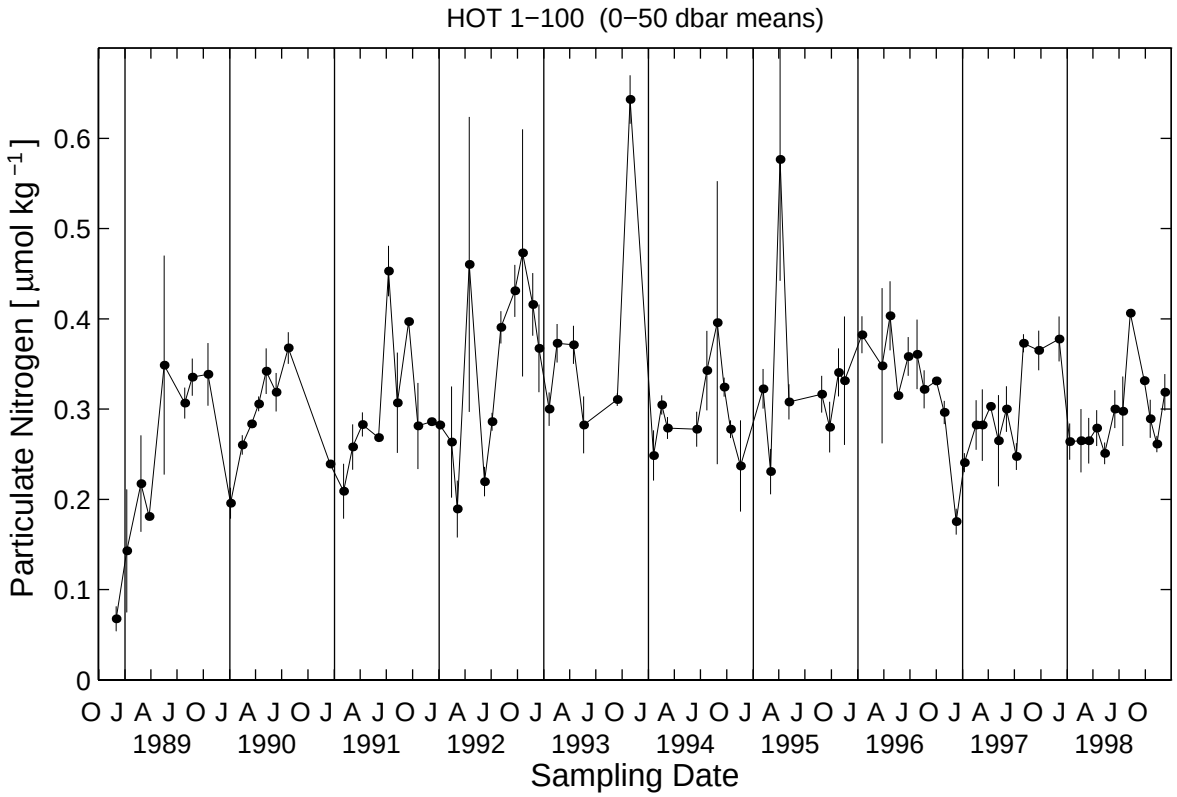
HOT 1−100 (0−50 dbar means)
Particulate Nitrogen [µmol kg⁻¹]
0
0.1
0.2
0.3
0.4
0.5
0.6
O J A J O J A J O J A J O J A J O J A J O J A J O J A J O J A J O J A J O J A J O J A J O J A J O
1989
1990
1991
1992
1993
1994
1995
1996
1997
1998
Sampling Date

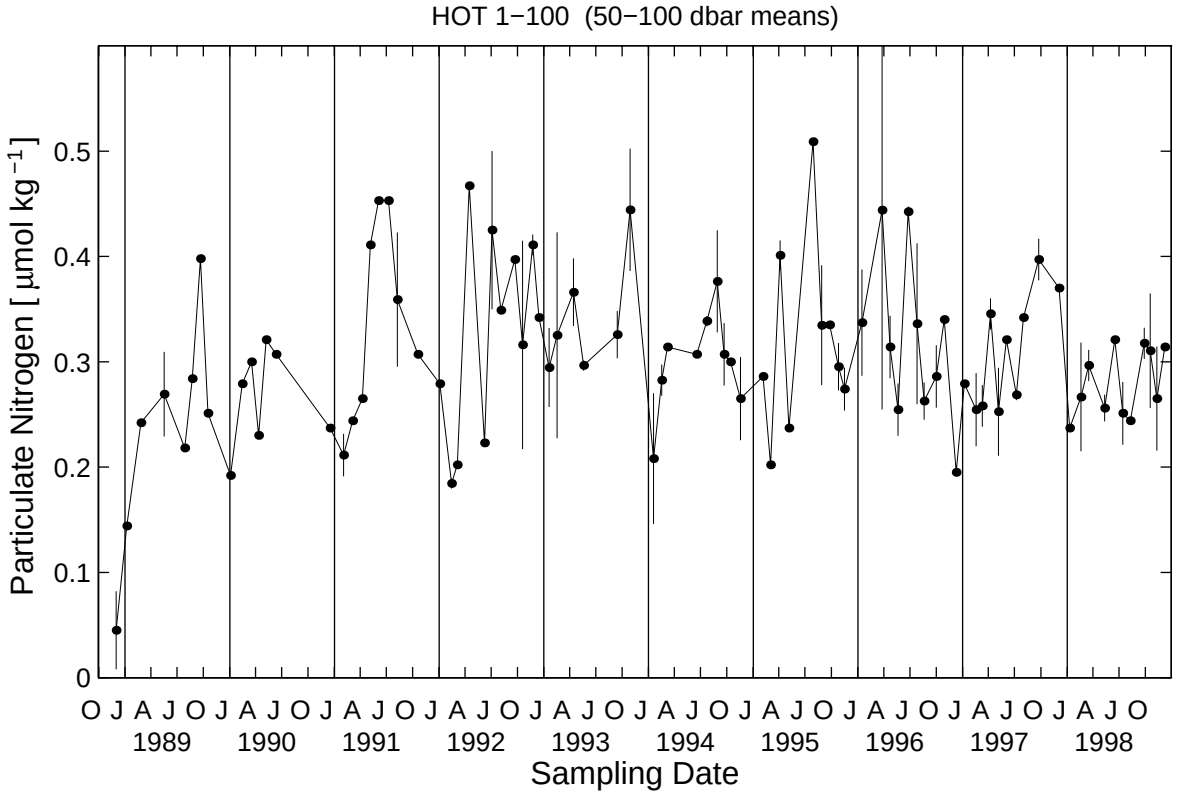
HOT 1−100 (50−100 dbar means)
Particulate Nitrogen [µmol kg⁻¹]
0
0.1
0.2
0.3
0.4
0.5
O J A J O J A J O J A J O J A J O J A J O J A J O J A J O J A J O J A J O J A J O J A J O J A J O
1989
1990
1991
1992
1993
1994
1995
1996
1997
1998
Sampling Date

Figure 6.4.8

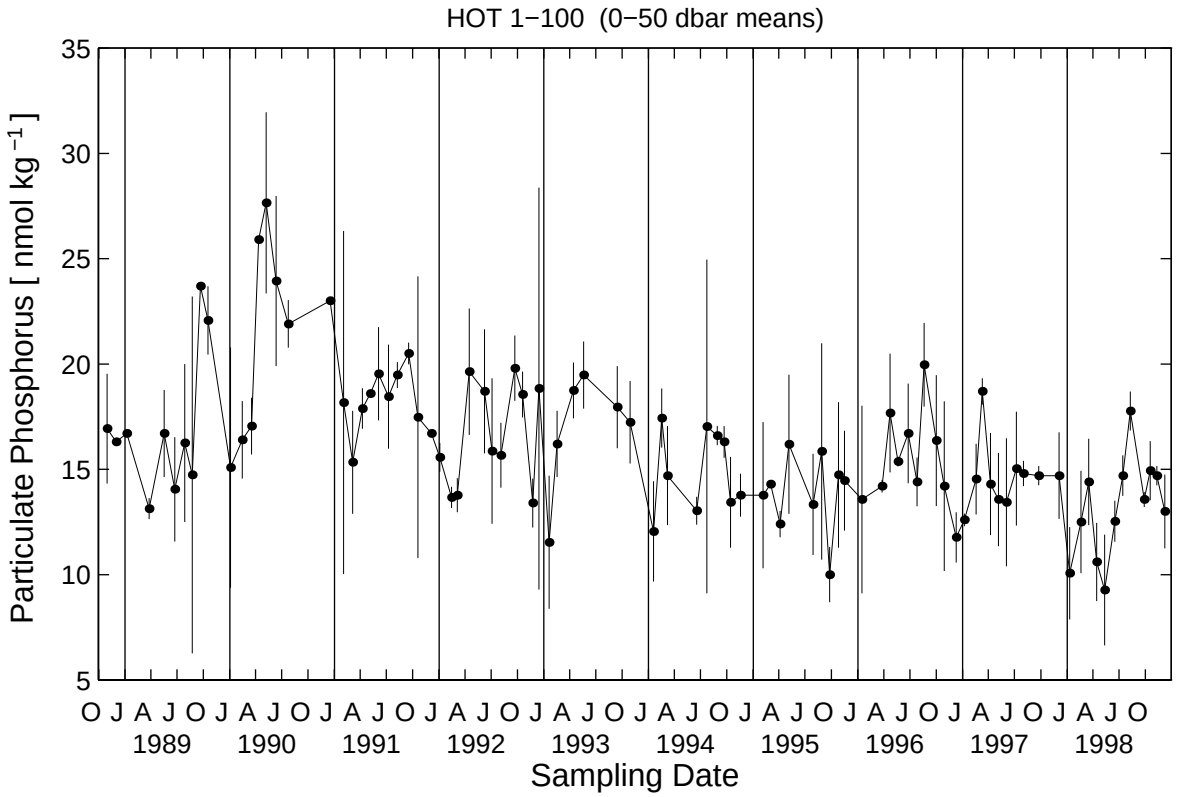
HOT 1−100 (0−50 dbar means)
Particulate Phosphorus [nmol kg⁻¹]
35
30
25
20
15
10
5
O J A J O J A J O J A J O J A J O J A J O J A J O J A J O J A J O J A J O J A J O
1989
1990
1991
1992
1993
1994
1995
1996
1997
1998
Sampling Date

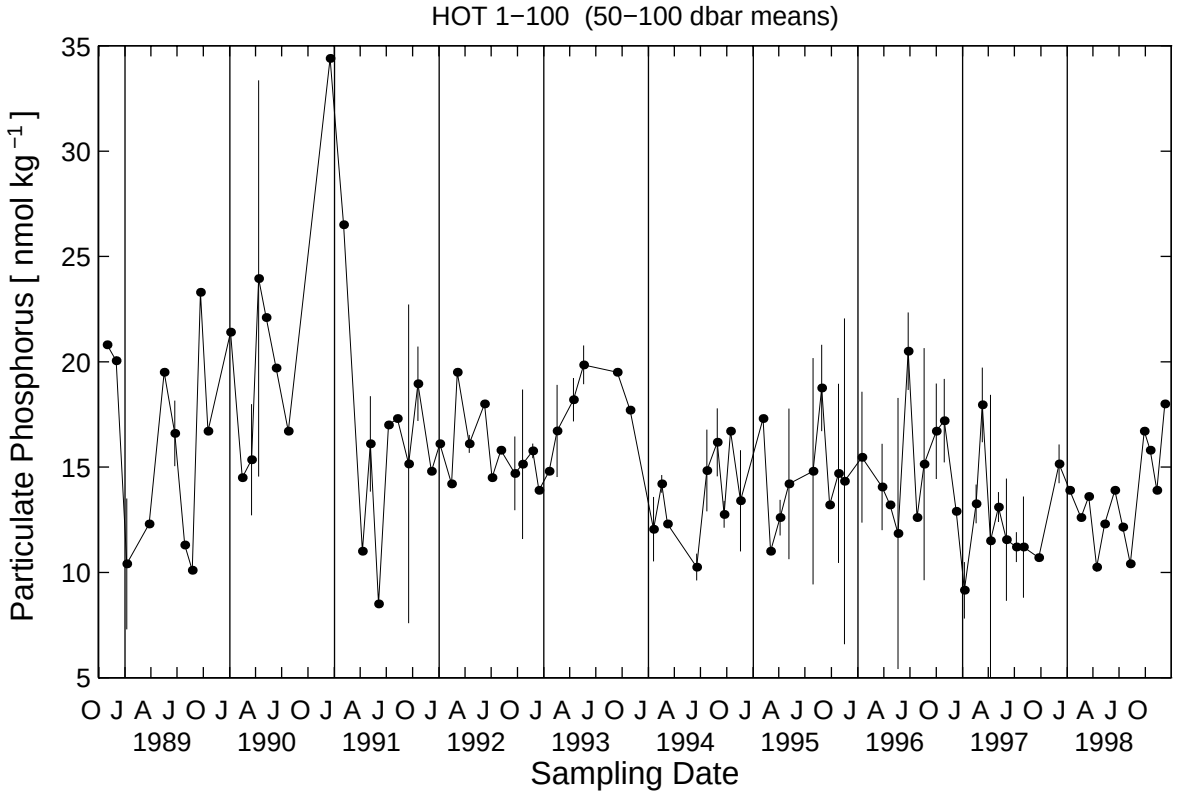
HOT 1−100 (50−100 dbar means)
Particulate Phosphorus [nmol kg⁻¹]
35
30
25
20
15
10
5
O J A J O J A J O J A J O J A J O J A J O J A J O J A J O J A J O J A J O J A J O
1989
1990
1991
1992
1993
1994
1995
1996
1997
1998
Sampling Date

Figure 6.4.9

6.5. Primary Production and Particle Flux

Figure 6.5.1: Integrated (0-200 m) primary production rates measured on all HOT cruises. Data for both *in situ* and on-deck incubations are presented. On HOT-15 (March 1990) primary production was measured on three consecutive days.

Figure 6.5.2: Carbon flux at 150 m measured on all HOT cruises from 1988 through 1992. Error bars represent the standard deviation of replicate determinations.

Figure 6.5.3: Same as Figure 6.5.2 but for nitrogen.

Figure 6.5.4: Same as Figure 6.5.2 but for phosphorus.

Figure 6.5.5: Same as Figure 6.5.2 but for total mass.

Figure 6.5.6: Contour plot of carbon flux for all cruises from 1988 through 1992.

Figure 6.5.7: Same as Figure 6.5.6 but for nitrogen.

Figure 6.5.8: Same as Figure 6.5.6 but for phosphorus.

Figure 6.5.9: Same as Figure 6.5.6 but for total mass.

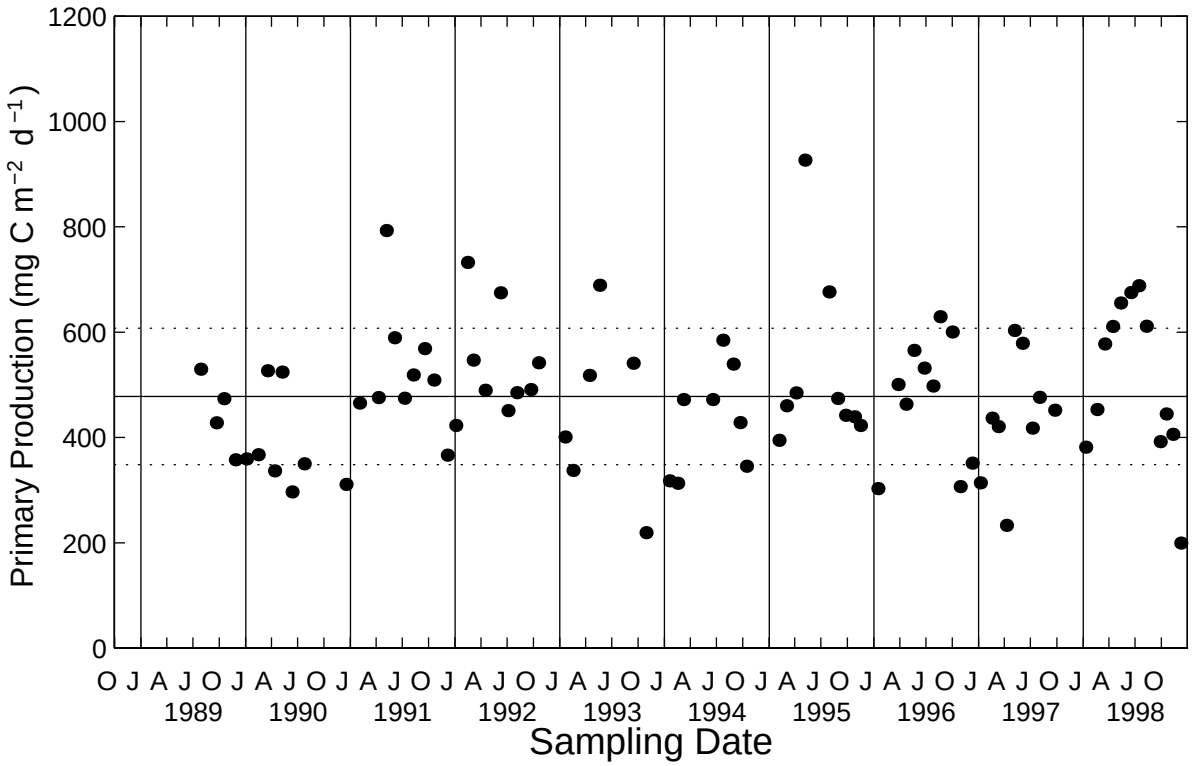
Primary Production (mg C m^{-2} d^{-1})
0
200
400
600
800
1000
1200
O J A J O J A J O J A J O J A J O J A J O J A J O J A J O J A J O J A J O J A J O J A J O J A J O J A J O J A J O J A J O J A J O J A J O
1989
1990
1991
1992
1993
1994
1995
1996
1997
1998
Sampling Date

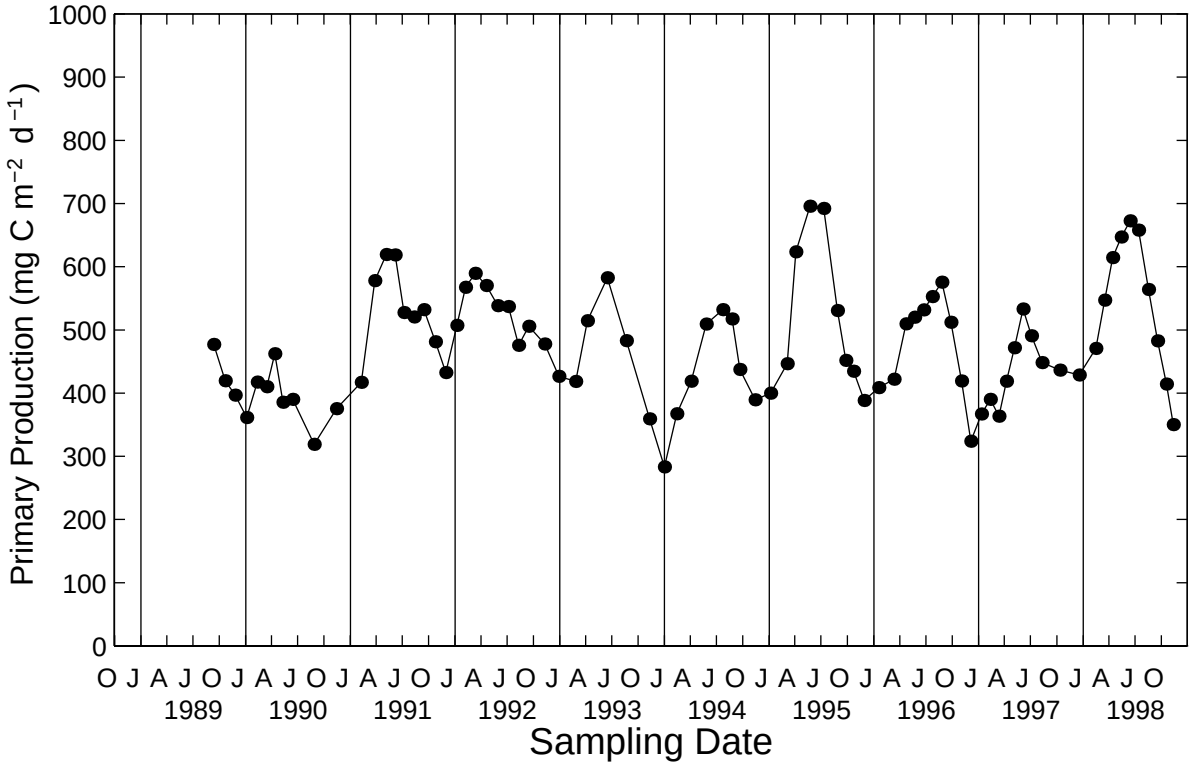
Primary Production (mg C m^{-2} d^{-1})
0
100
200
300
400
500
600
700
800
900
1000
O J A J O J A J O J A J O J A J O J A J O J A J O J A J O J A J O J A J O J A J O J A J O J A J O J A J O J A J O J A J O J A J O J A J O
1989
1990
1991
1992
1993
1994
1995
1996
1997
1998
Sampling Date

Figure 6.5.1

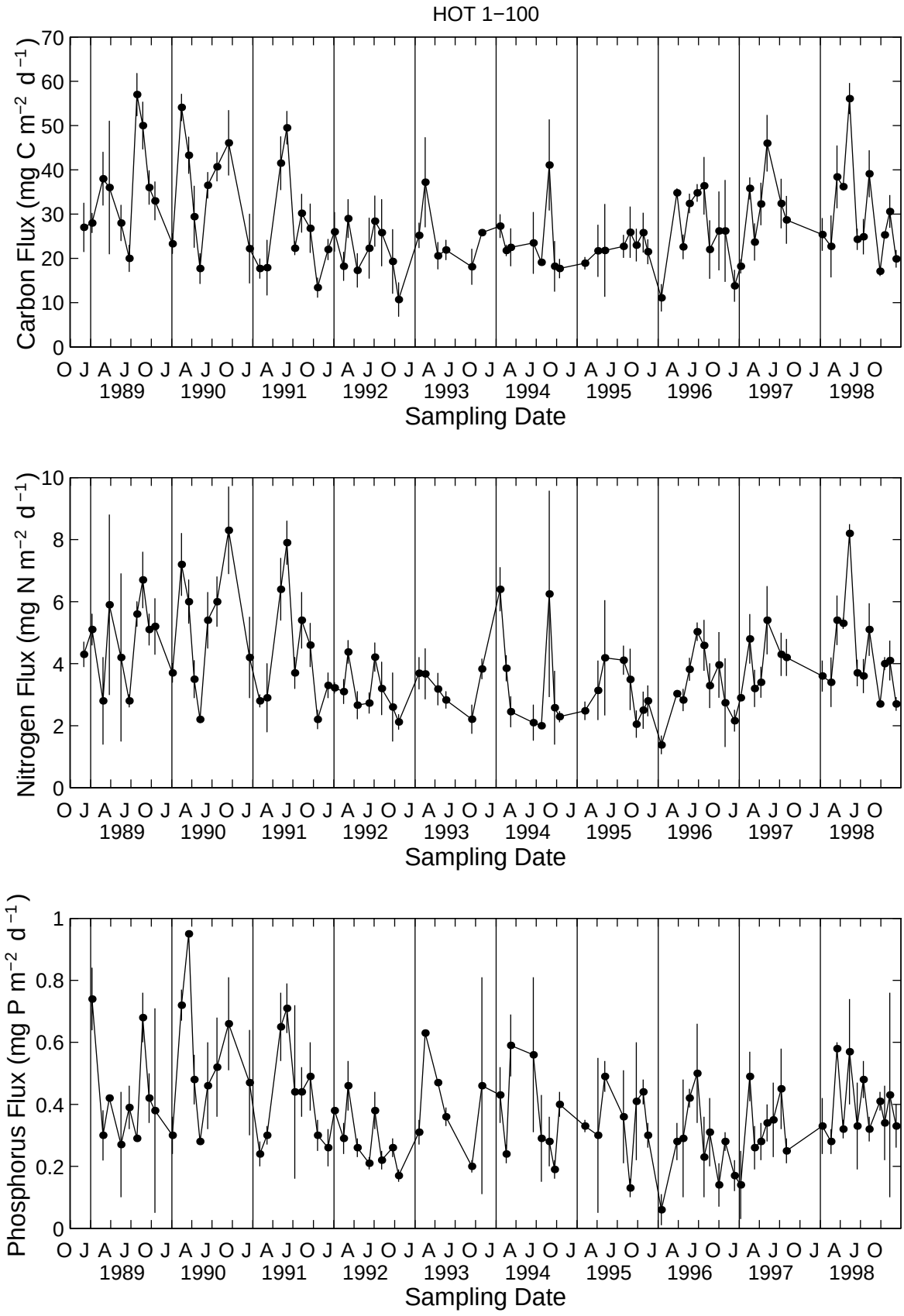

Figure 6.5.2 (upper panel), 6.5.3 (middle panel), 6.5.4(lower panel)

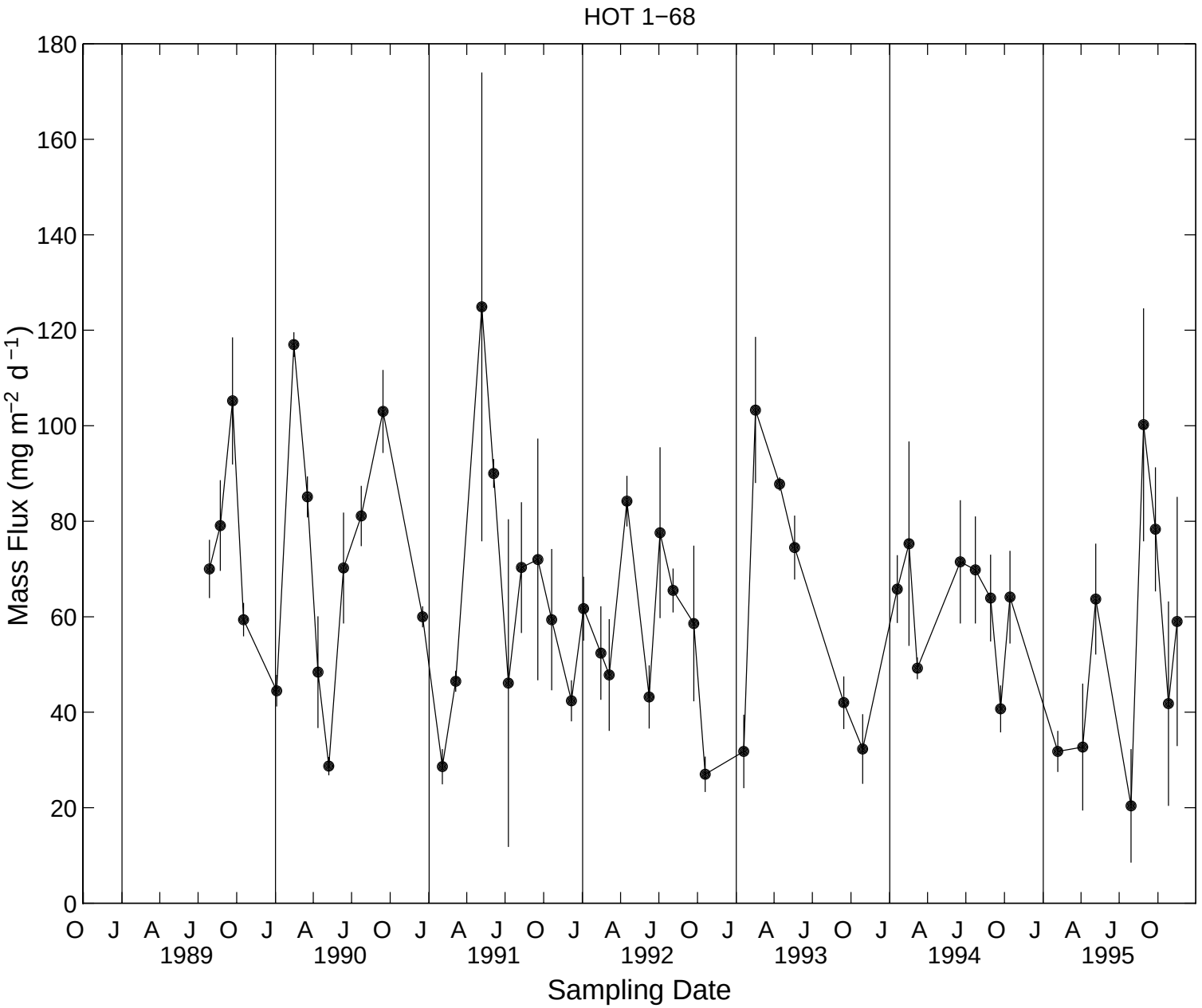
HOT 1−68
Mass Flux (mg m^{-2} d^{-1})
0
20
40
60
80
100
120
140
160
180
O J A J O J A J O J A J O J A J O J A J O J A J O J A J O
1989
1990
1991
1992
1993
1994
1995
Sampling Date

Figure 6.5.5

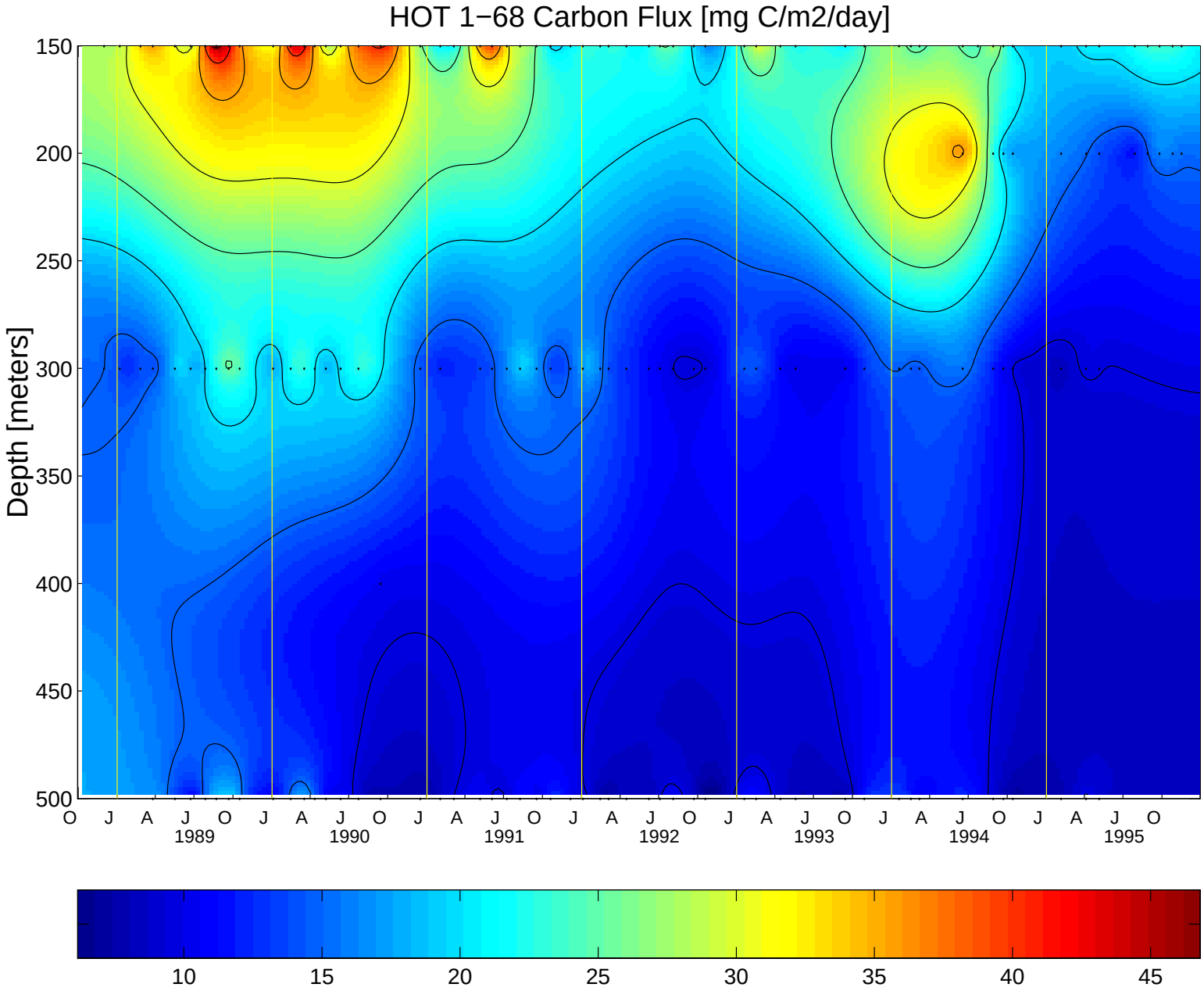
HOT 1−68 Carbon Flux [mg C/m2/day]
Depth [meters]
150
200
250
300
350
400
450
500
O J A J O J A J O J A J O J A J O J A J O J A J O J A J O
1989
1990
1991
1992
1993
1994
1995
10
15
20
25
30
35
40
45

Figure 6.5.6

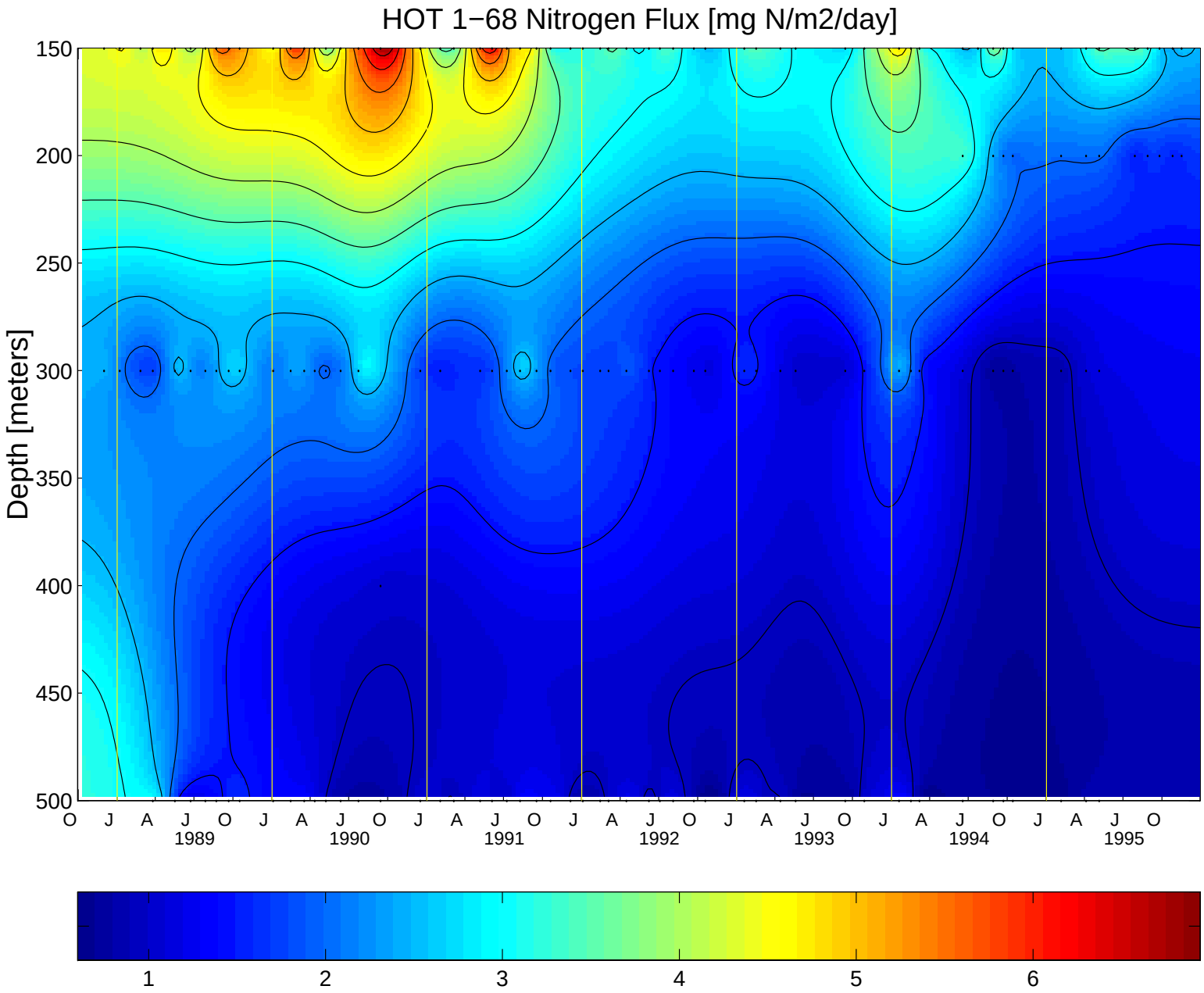
HOT 1−68 Nitrogen Flux [mg N/m2/day]
Depth [meters]
150
200
250
300
350
400
450
500
O J A J O J A J O J A J O J A J O J A J O J A J O J A J O
1989
1990
1991
1992
1993
1994
1995
1
2
3
4
5
6

Figure 6.5.7

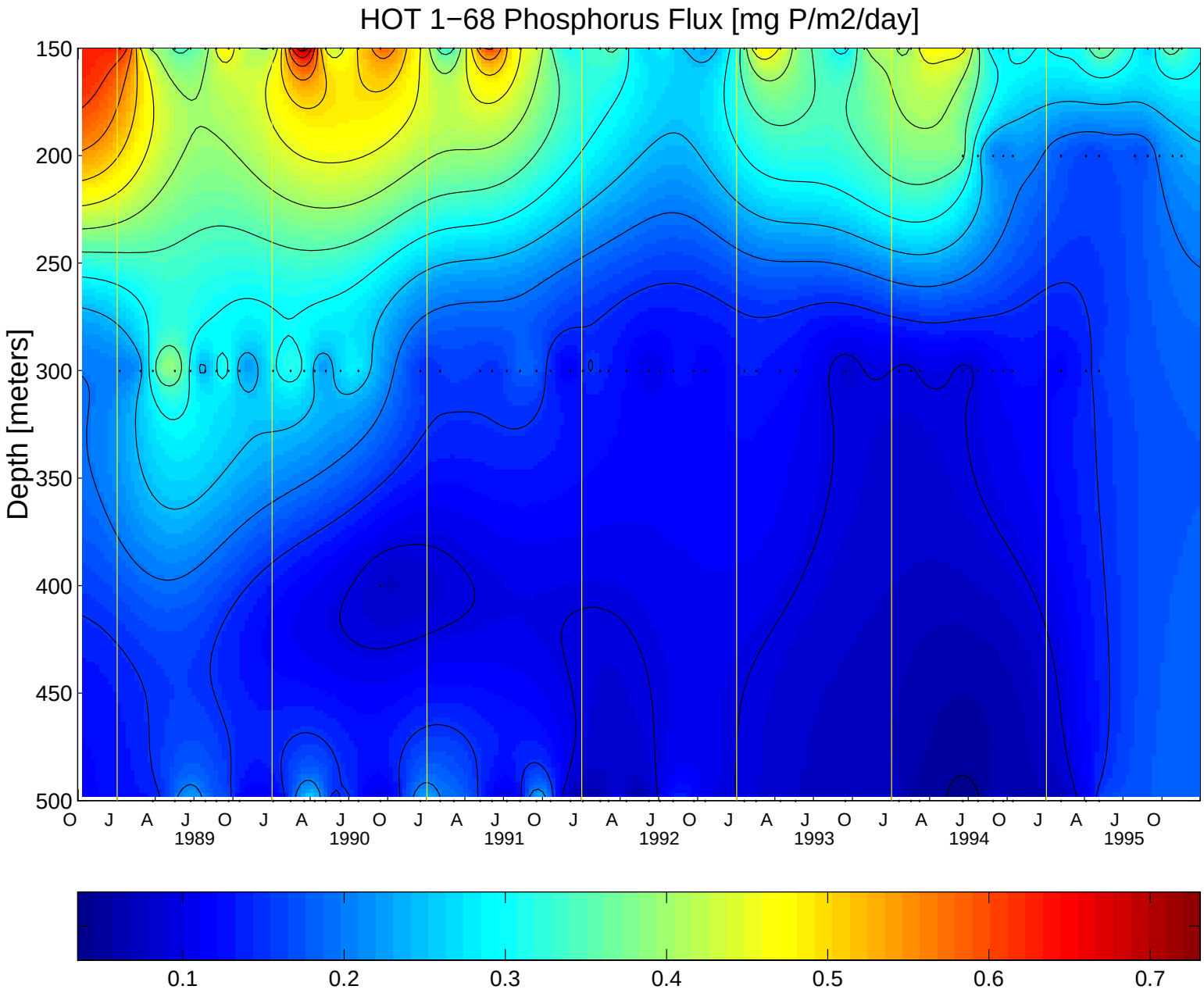
HOT 1−68 Phosphorus Flux [mg P/m2/day]
Depth [meters]
150
200
250
300
350
400
450
500
O J A J O J A J O J A J O J A J O J A J O J A J O J A J O
1989
1990
1991
1992
1993
1994
1995
0.1
0.2
0.3
0.4
0.5
0.6
0.7

Figure 6.5.8

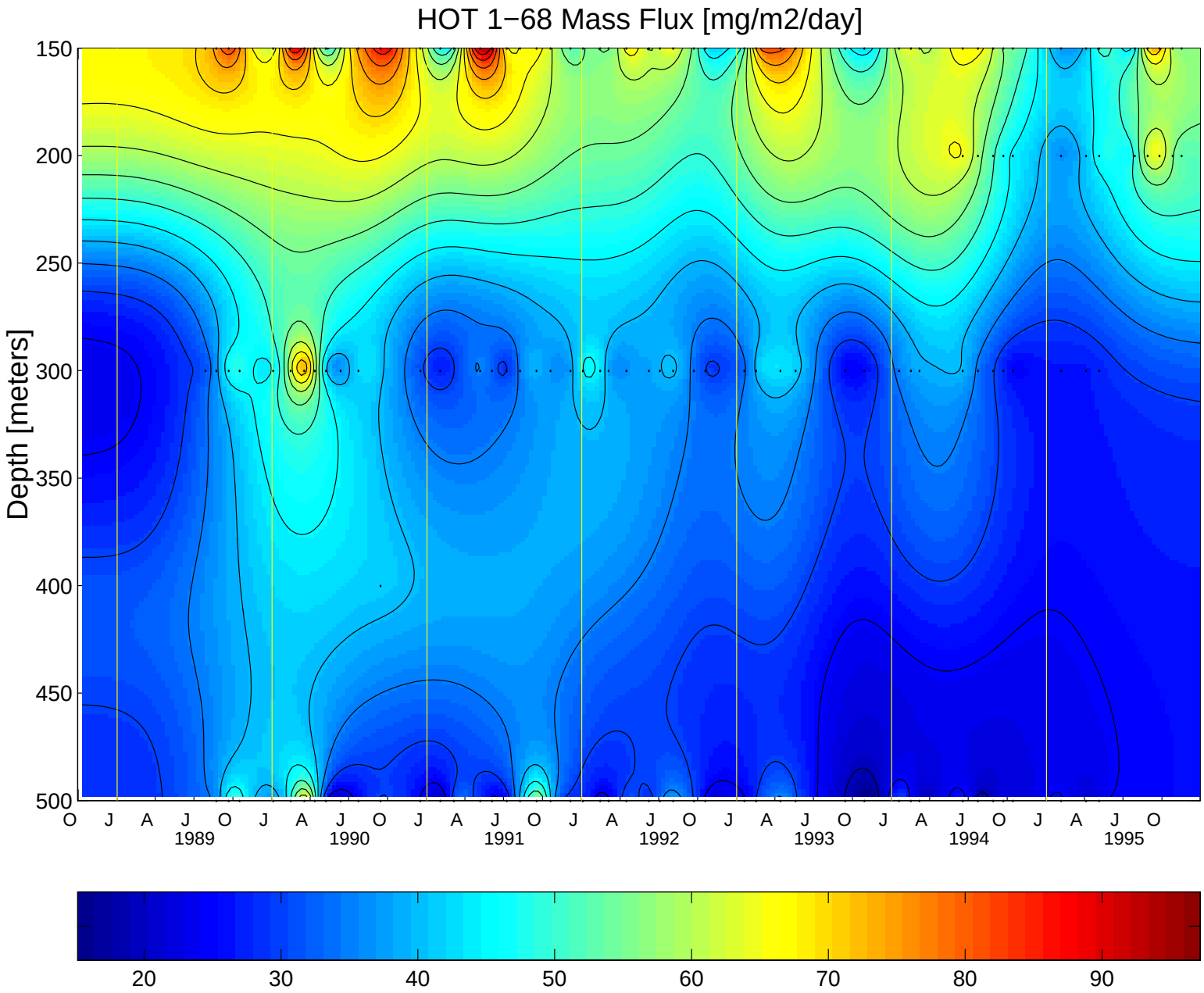
HOT 1−68 Mass Flux [mg/m2/day]
Depth [meters]
150
200
250
300
350
400
450
500
O J A J O J A J O J A J O J A J O J A J O J A J O J A J O
1989
1990
1991
1992
1993
1994
1995
20
30
40
50
60
70
80
90

Figure 6.5.9

6.6. ADCP Measurements

For each cruise with shipboard ADCP, the following figures (6.6.1-9) are provided:

Figures 6.6.1-9: Reference layer velocity (upper panels) and ship's longitude and latitude (lower panels) as functions of time. Time is given in days from the beginning of the year. For example, noon on 1 January is 0.5 decimal days. The reference layer velocity is shown averaged between fixes (steppy curves), and smoothed, as used in the final velocity estimates (smooth curves). Plus signs near the bottom of the reference layer velocity plots indicate ADCP data gaps. The ship's position is shown by asterisks at fixes and by a continuous curve (actually closely-spaced dots) as determined by fixes together with the ADCP data.

Figures 6.6.10a-18a: Velocity fields at Station ALOHA during HOT 33-41. The top panel shows hourly averages at 20-m depth intervals while the ship was at Station ALOHA. The orientation of each stick gives the direction of the current: up is northward, to the right is eastward. The bottom panel shows the results of a least-squares fit of the hourly averages to a mean, trend, semidiurnal and diurnal tides and an inertial cycle. In the first column, the arrow shows the mean current, and the headless stick shows the sum of the mean plus the trend at the end of the station. For each harmonic, the current ellipse is shown in the first column. The orientation of the stick in the second column shows the direction of that harmonic component of the current at the beginning of the station, and the arrowhead at the end of the stick shows the direction of rotation of the current vector around the ellipse.

Figures 6.6.10b-18b: Velocity field on the transits to and from the Station ALOHA. Velocity is shown as a function of latitude, averaged in 10-minute time intervals. Because HOT-37 was conducted in two segments, ADCP data are available for both legs on this cruise.

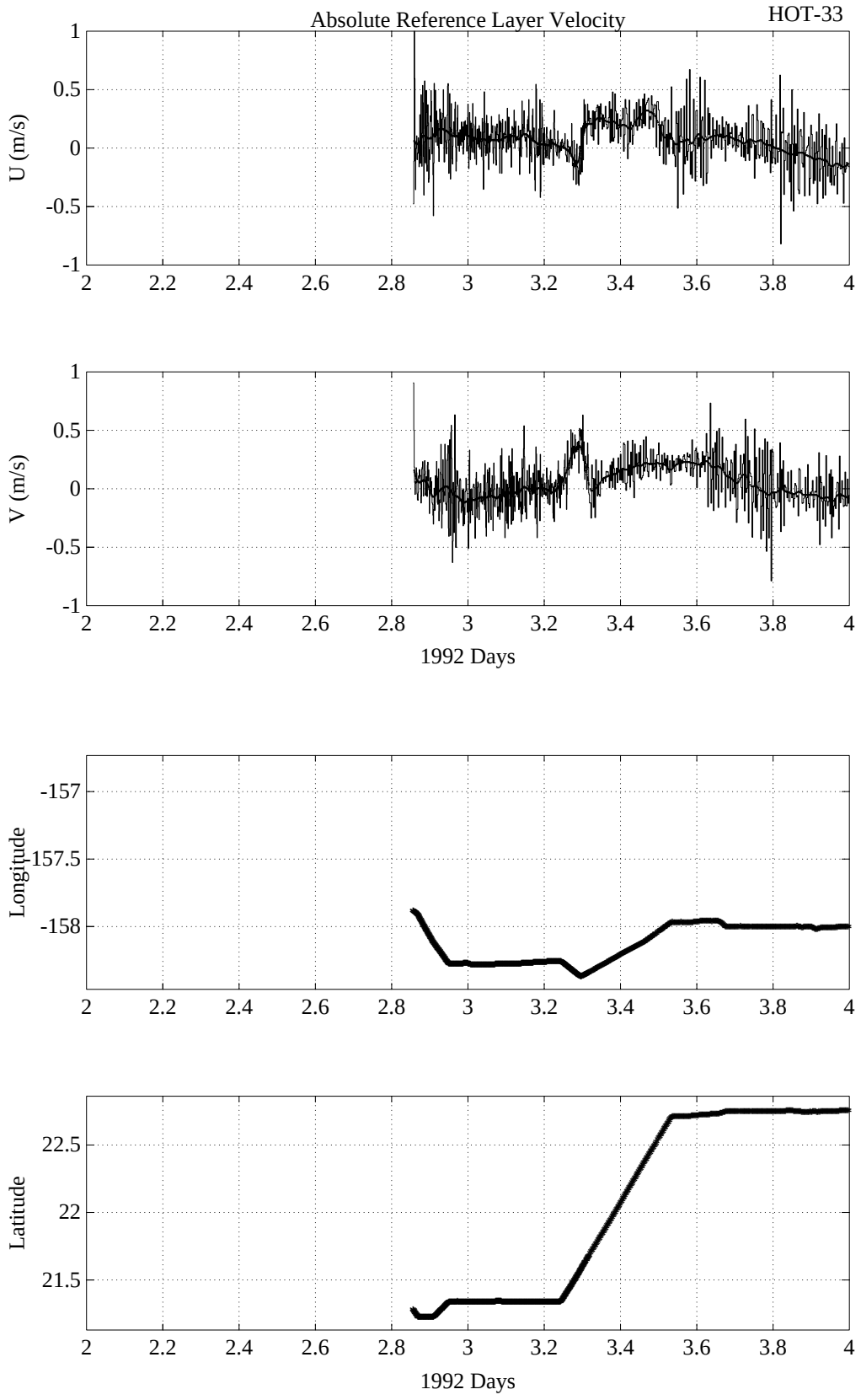
Absolute Reference Layer Velocity
HOT-33
U (m/s)
V (m/s)
Longitude
Latitude
1992 Days
1992 Days

Figure 6.6.1

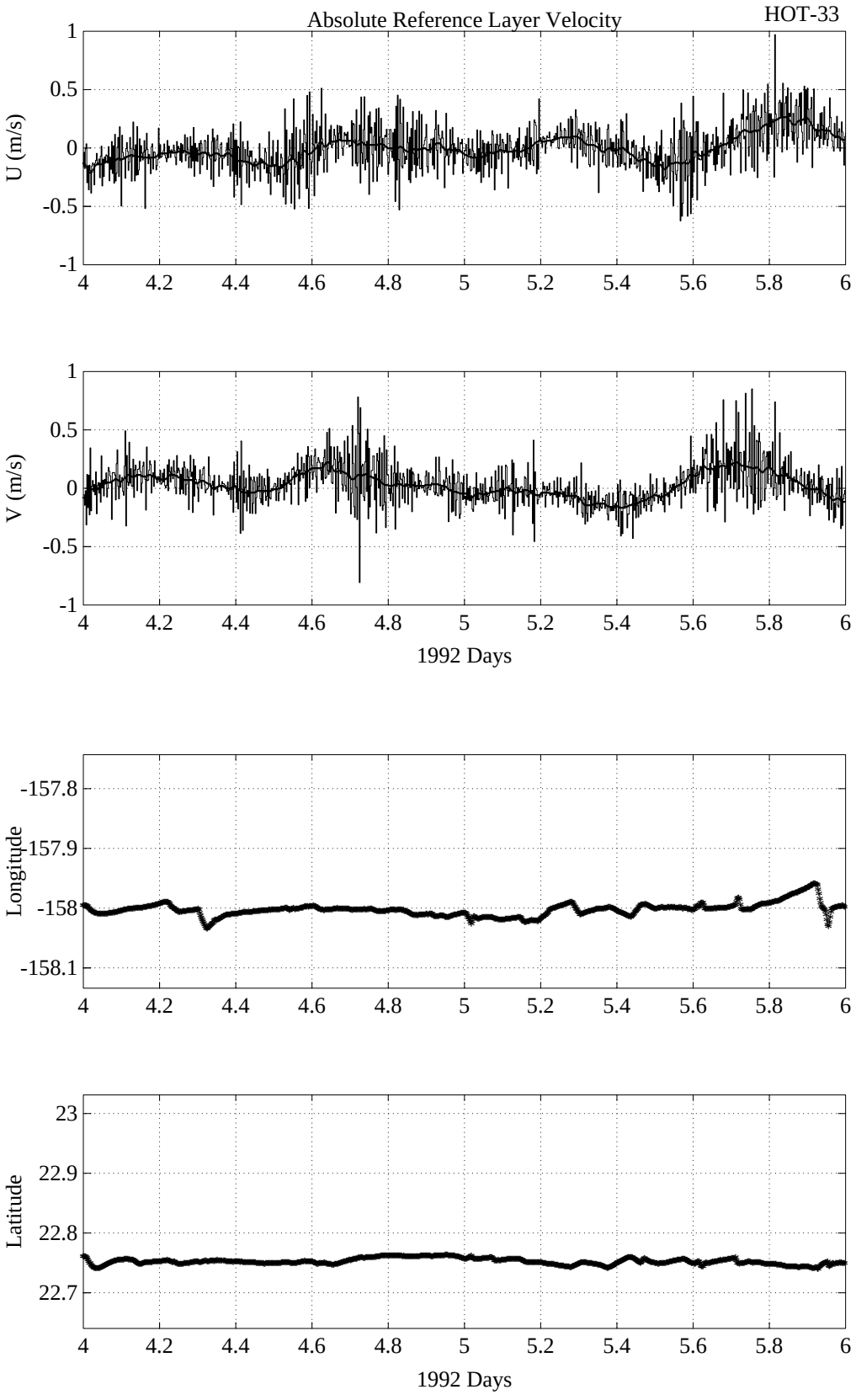

Figure 6.6.1 (continued)

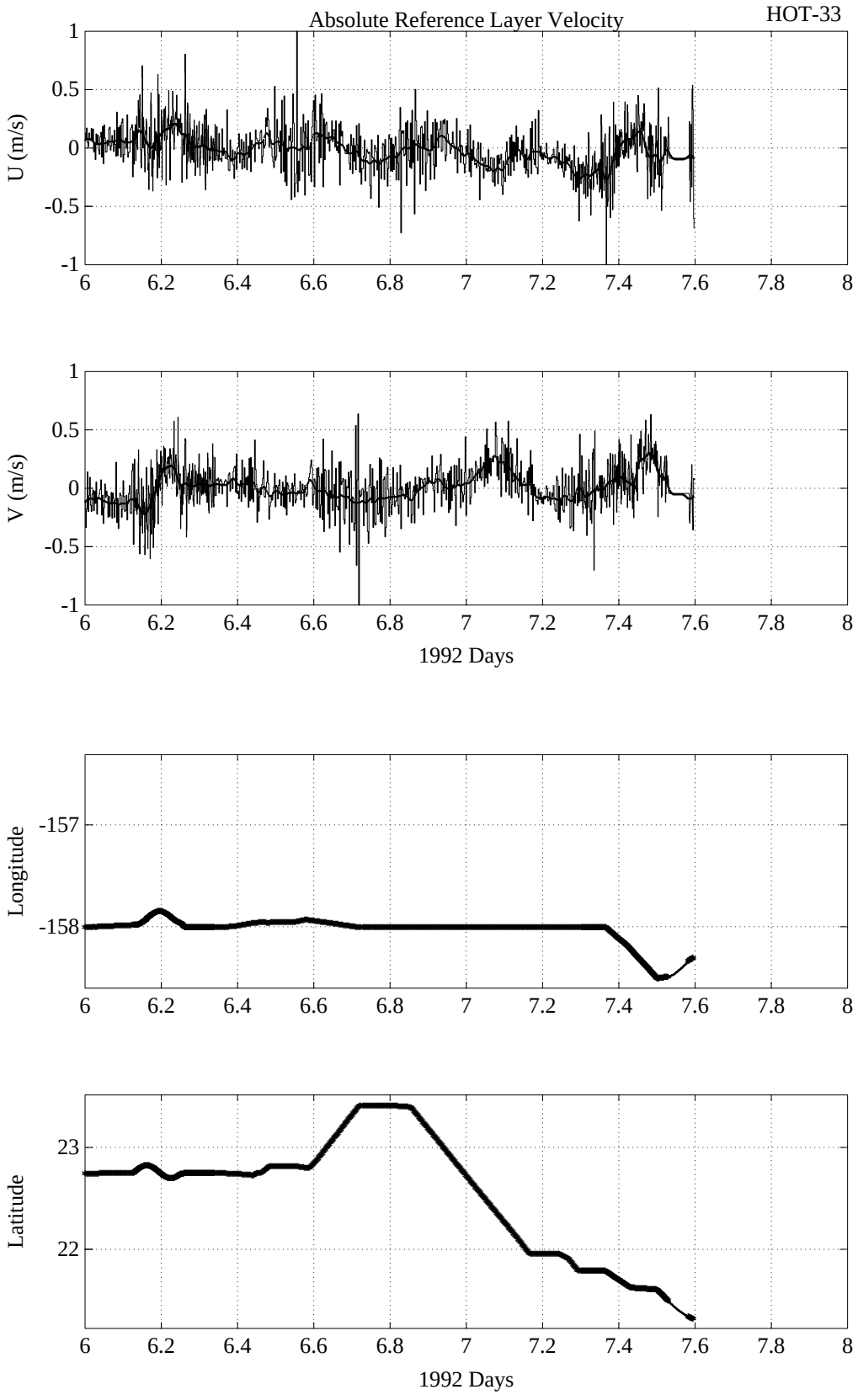

Figure 6.6.1 (continued)

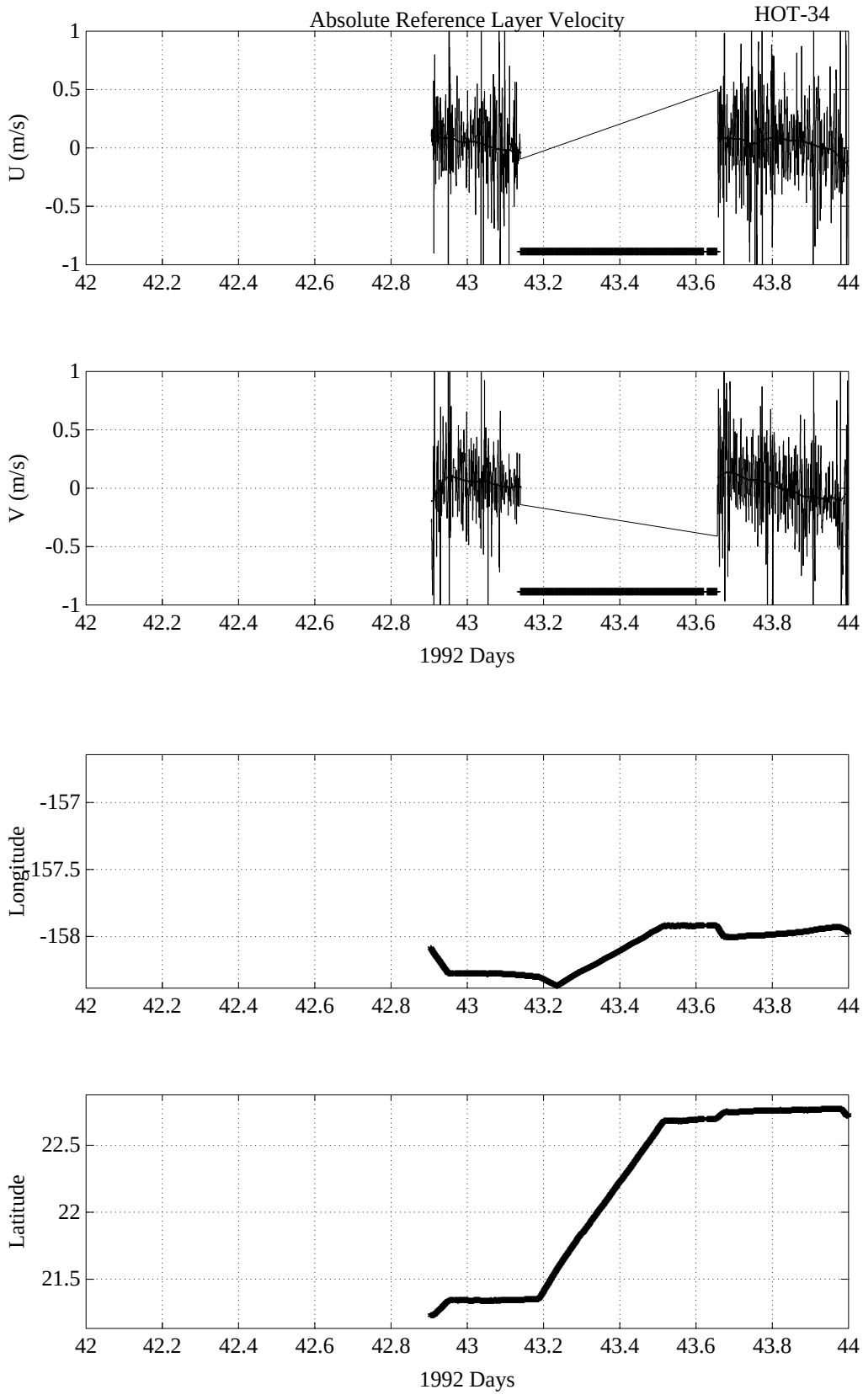
Absolute Reference Layer Velocity
HOT-34
U (m/s)
V (m/s)
1
0.5
0
-0.5
-1
42
42.2
42.4
42.6
42.8
43
43.2
43.4
43.6
43.8
44
1992 Days
Longitude
-157
-157.5
-158
Latitude
22.5
22
21.5

Figure 6.6.2

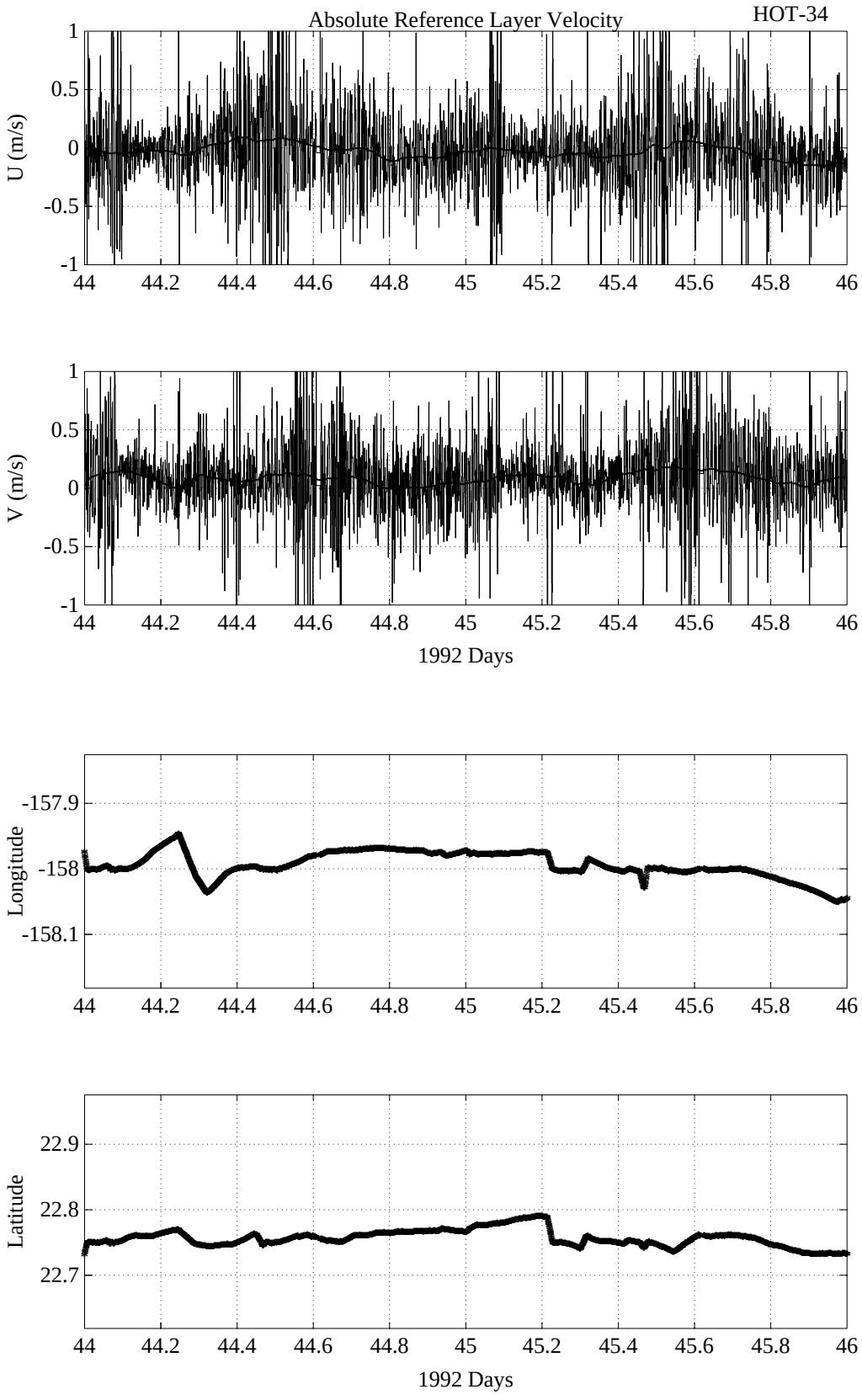

Figure 6.6.2 (continued)

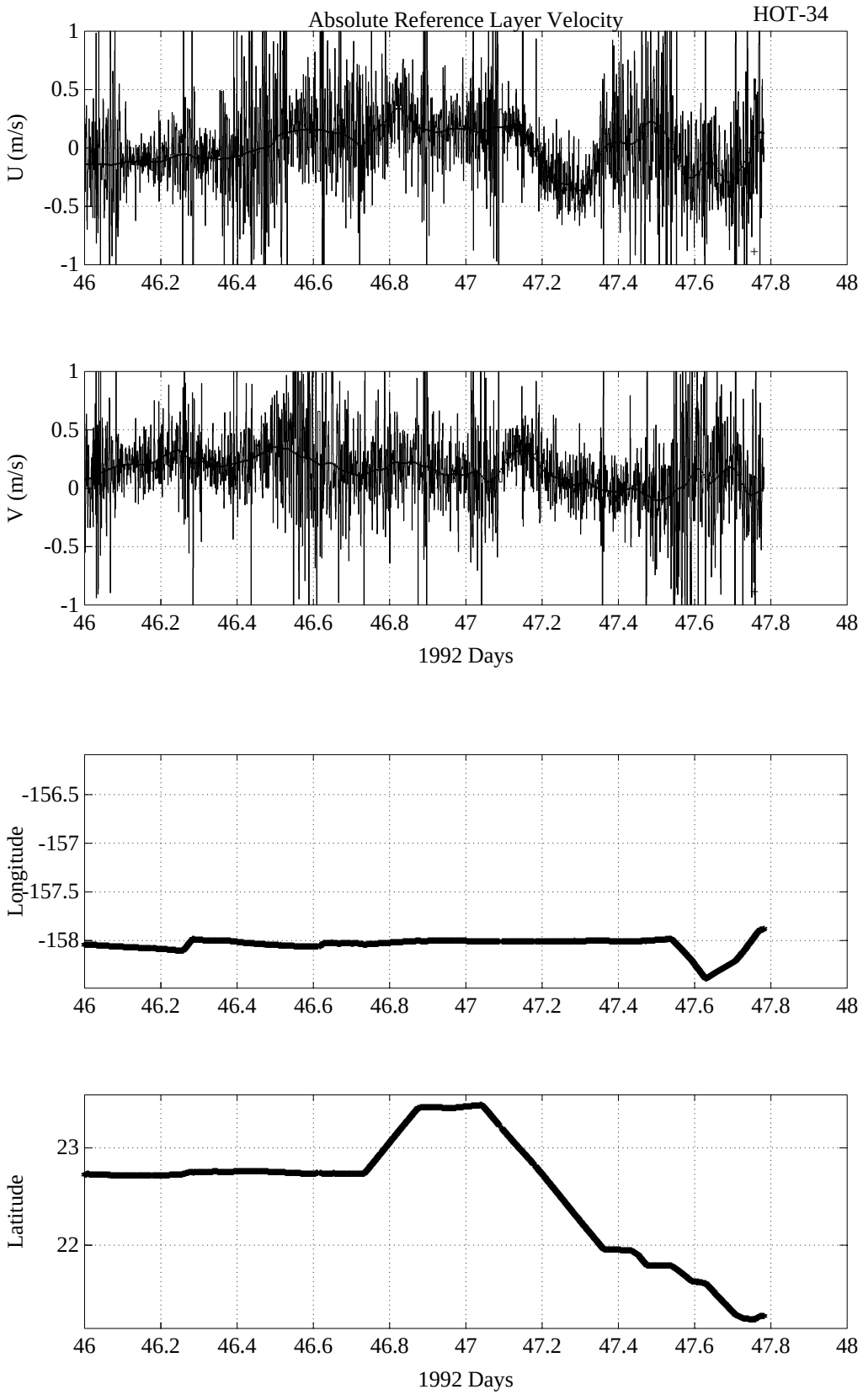

Figure 6.6.2 (continued)

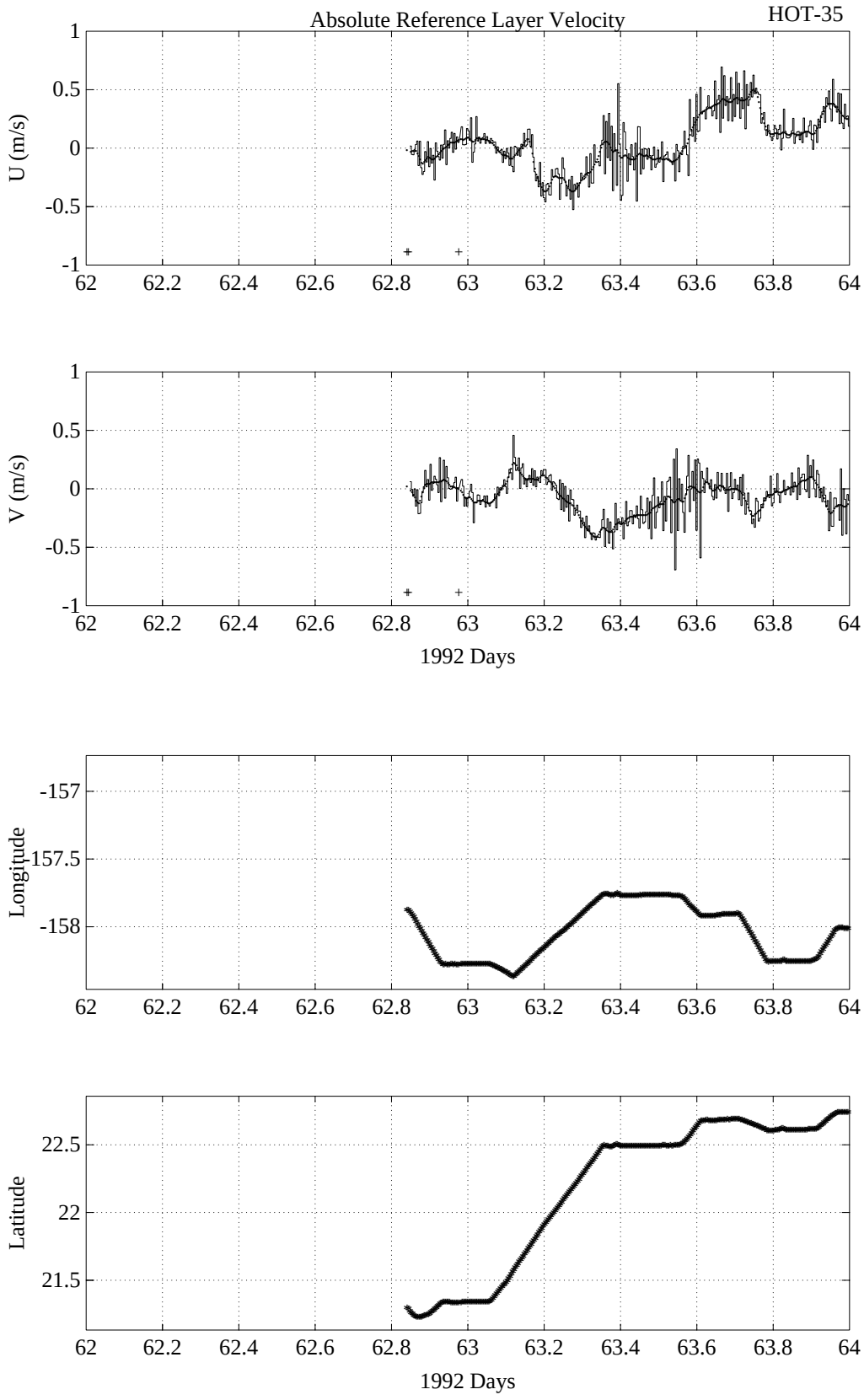
Absolute Reference Layer Velocity
HOT-35
U (m/s)
V (m/s)
Longitude
Latitude
1992 Days
1992 Days

Figure 6.6.3

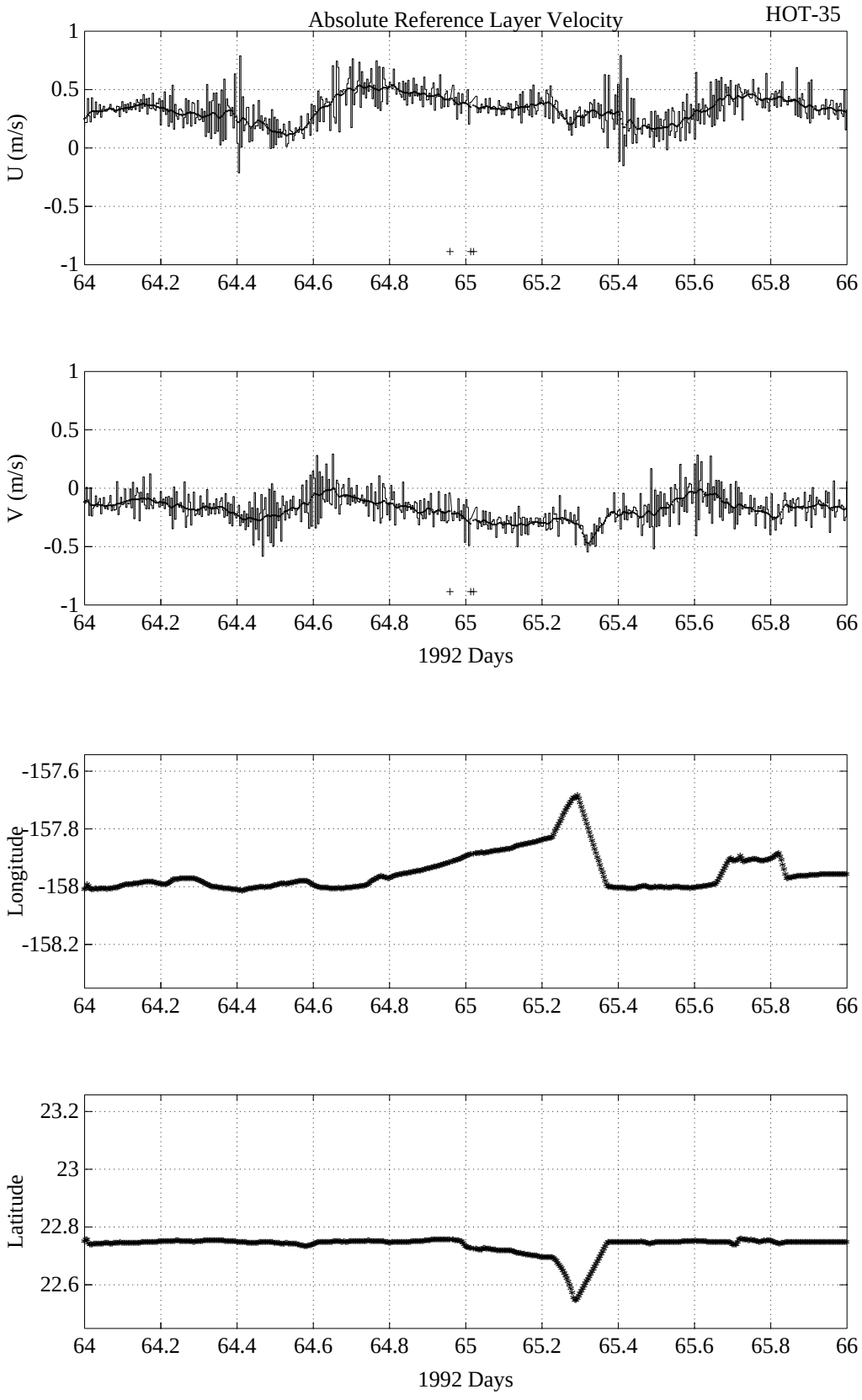

Figure 6.6.3 (continued)

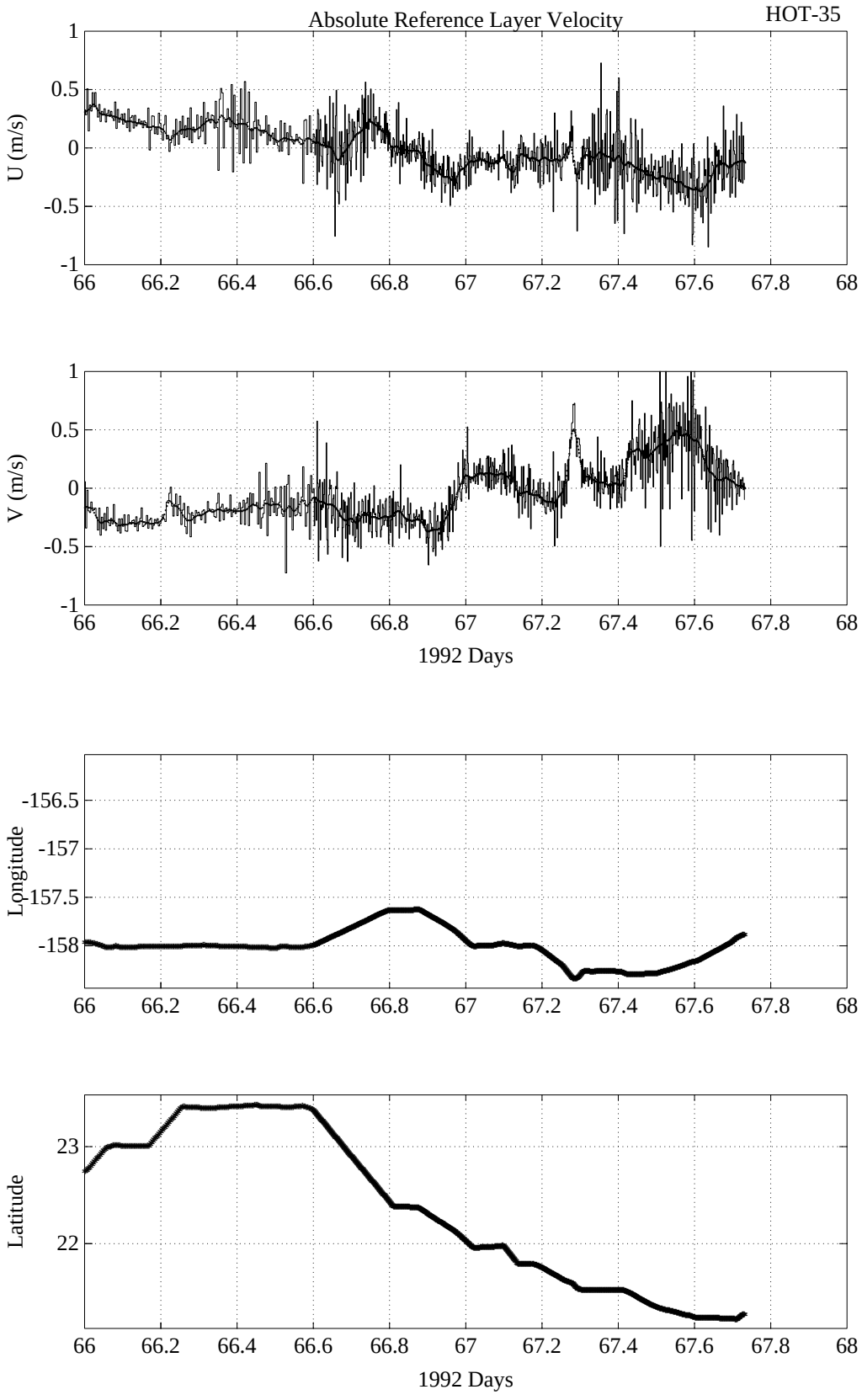

Figure 6.6.3 (continued)

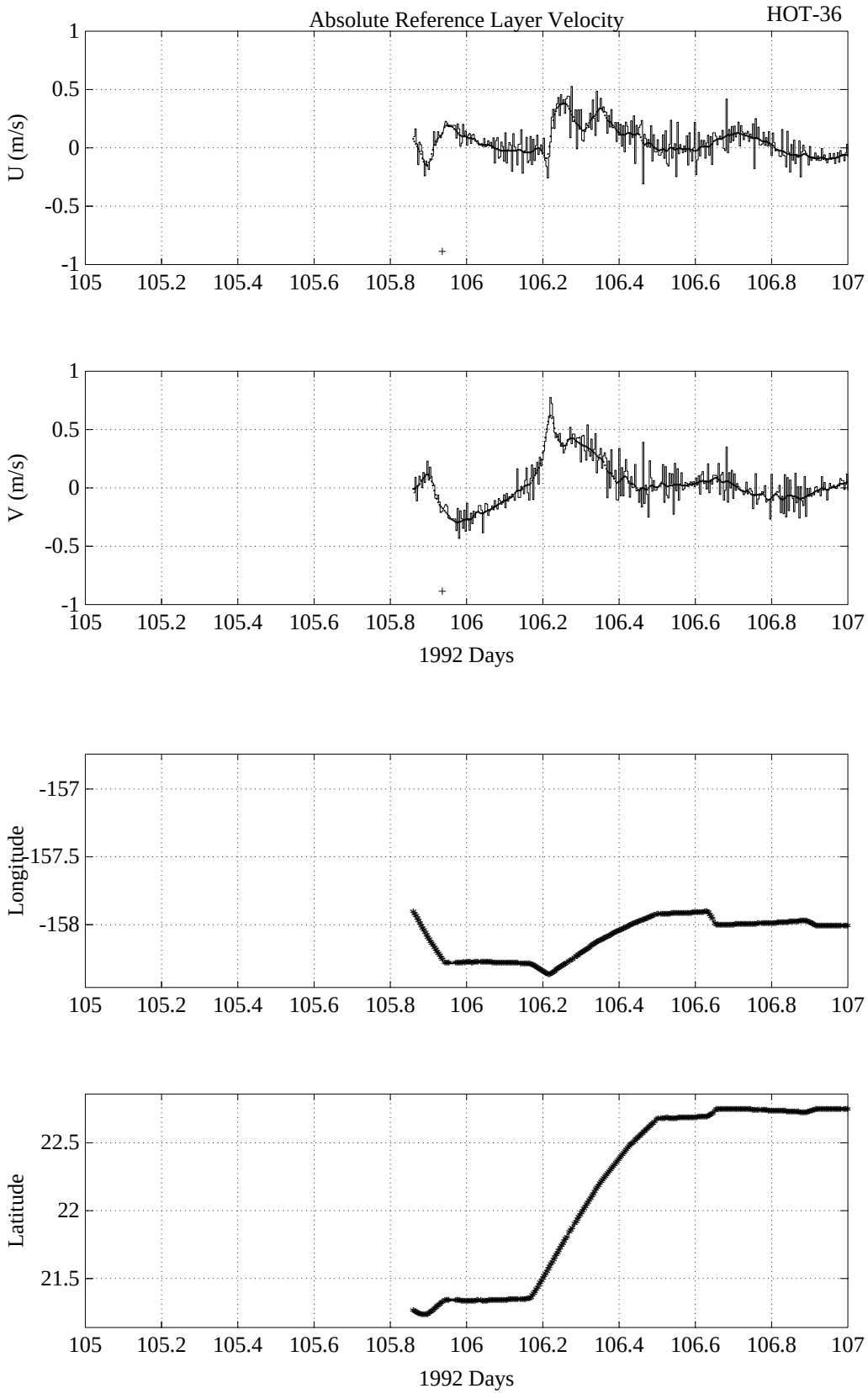
Absolute Reference Layer Velocity
HOT-36
U (m/s)
V (m/s)
Longitude
Latitude
1992 Days
1992 Days

Figure 6.6.4

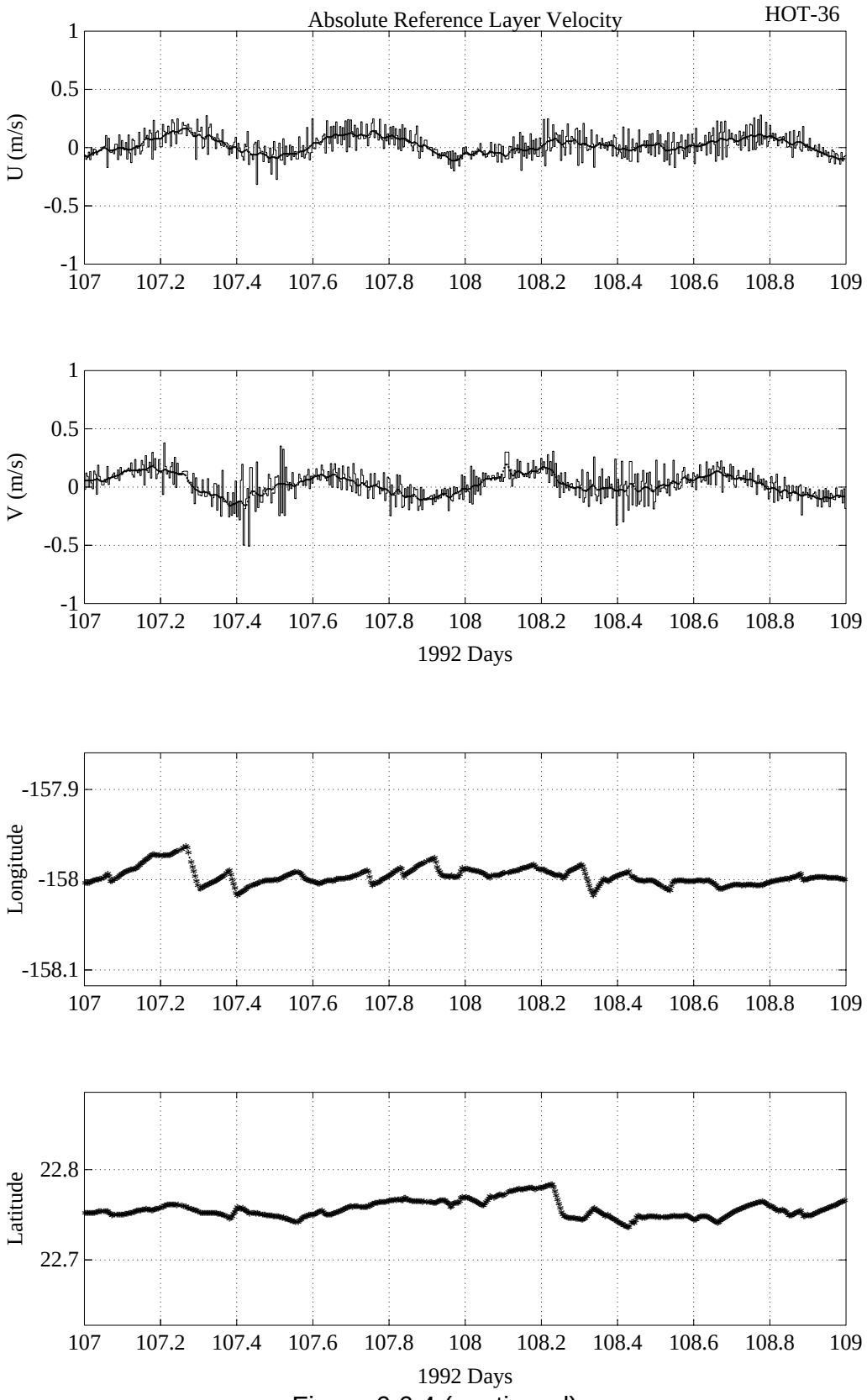

Figure 6.6.4 (continued)

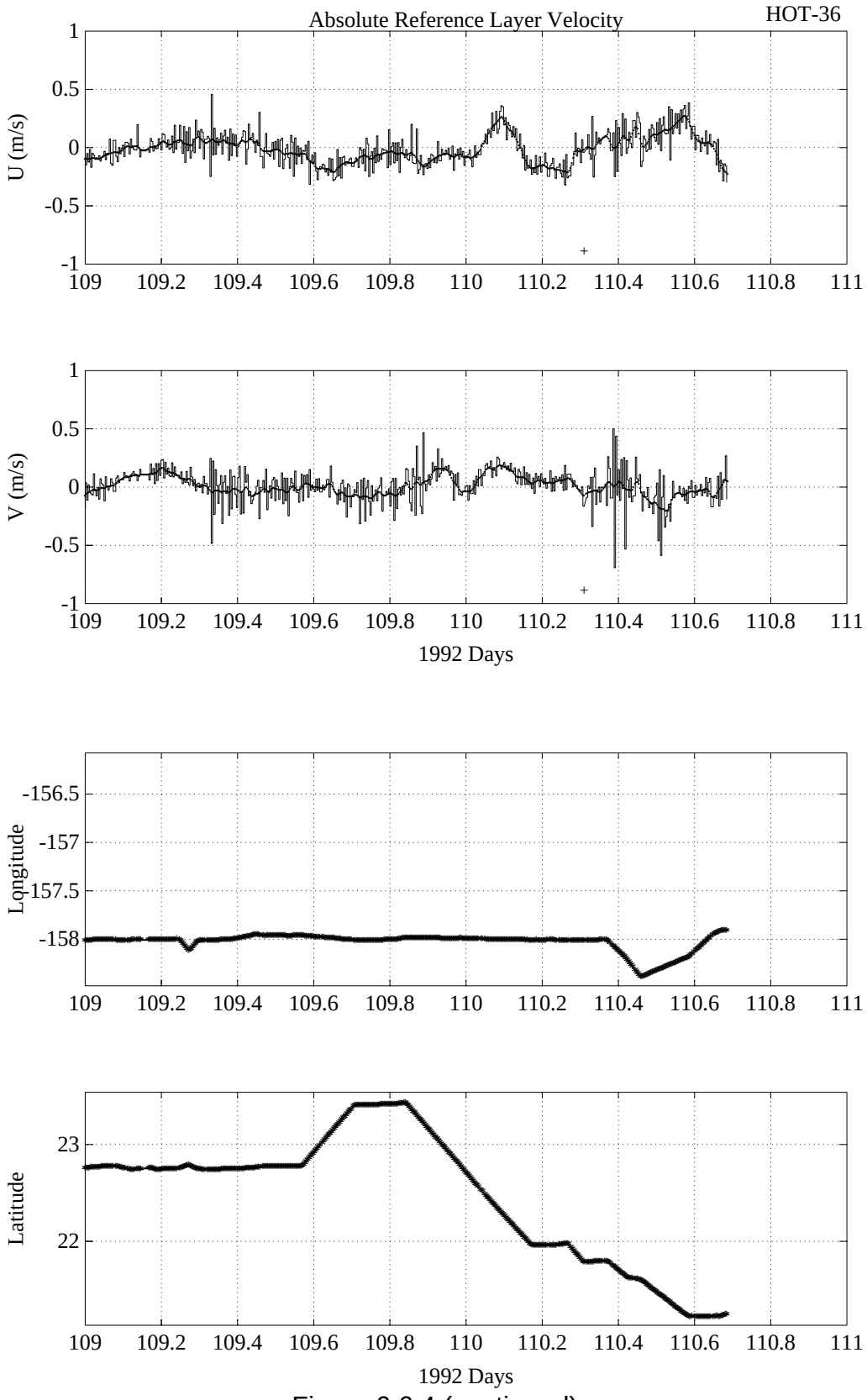

Figure 6.6.4 (continued)

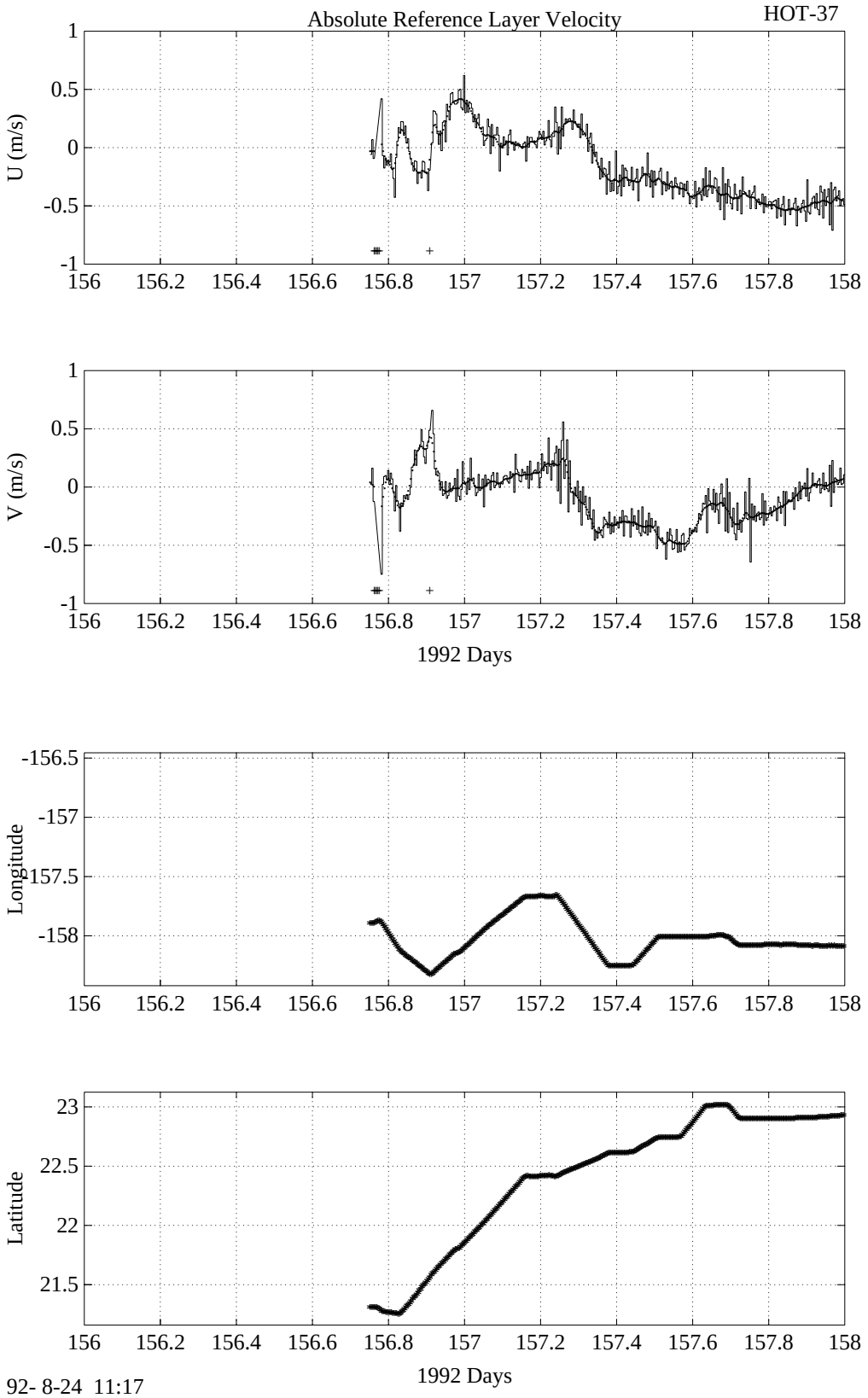
Absolute Reference Layer Velocity
HOT-37
U (m/s)
V (m/s)
Longitude
Latitude
1992 Days
92- 8-24 11:17

Figure 6.6.5

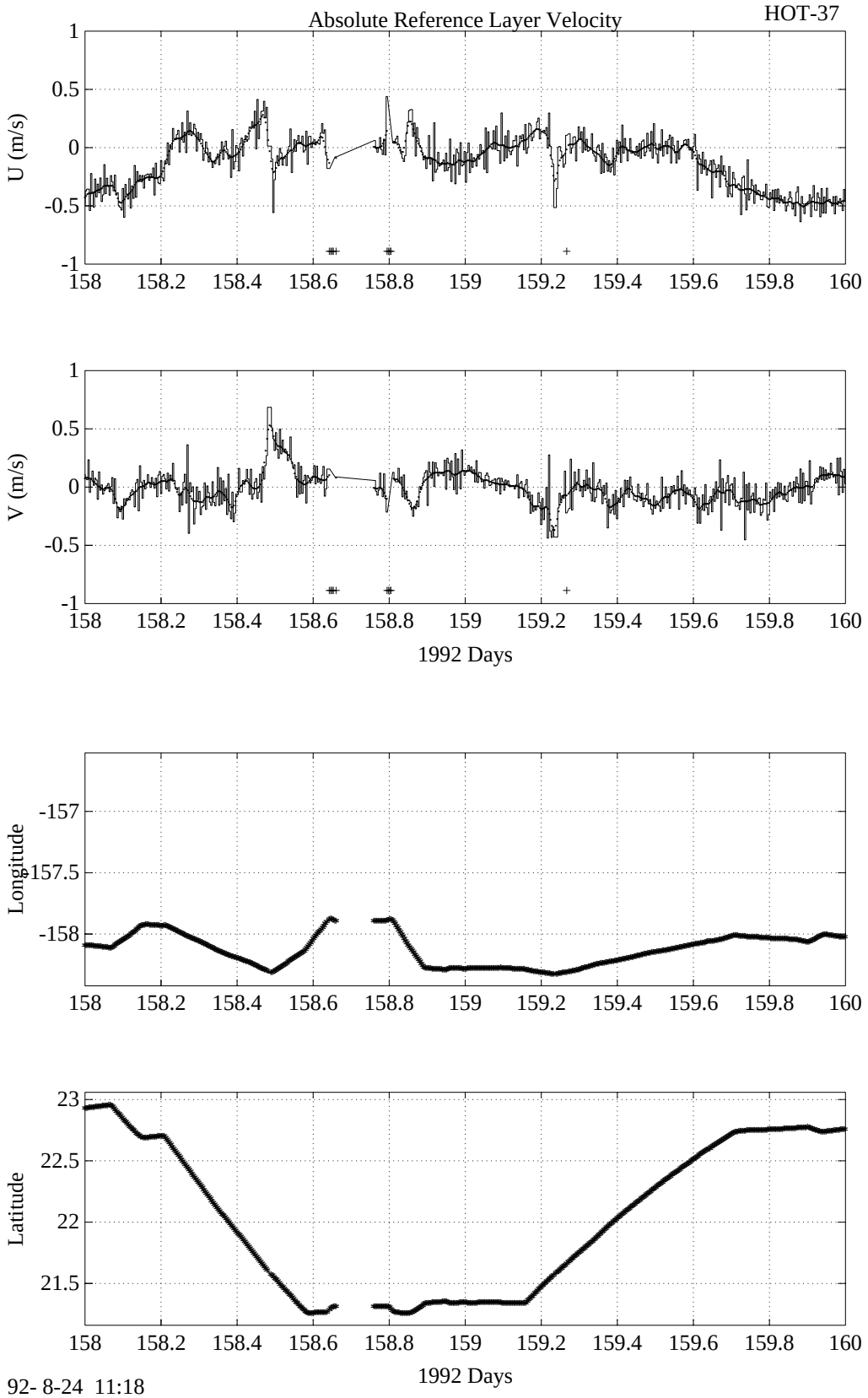

Figure 6.6.5 (continued)

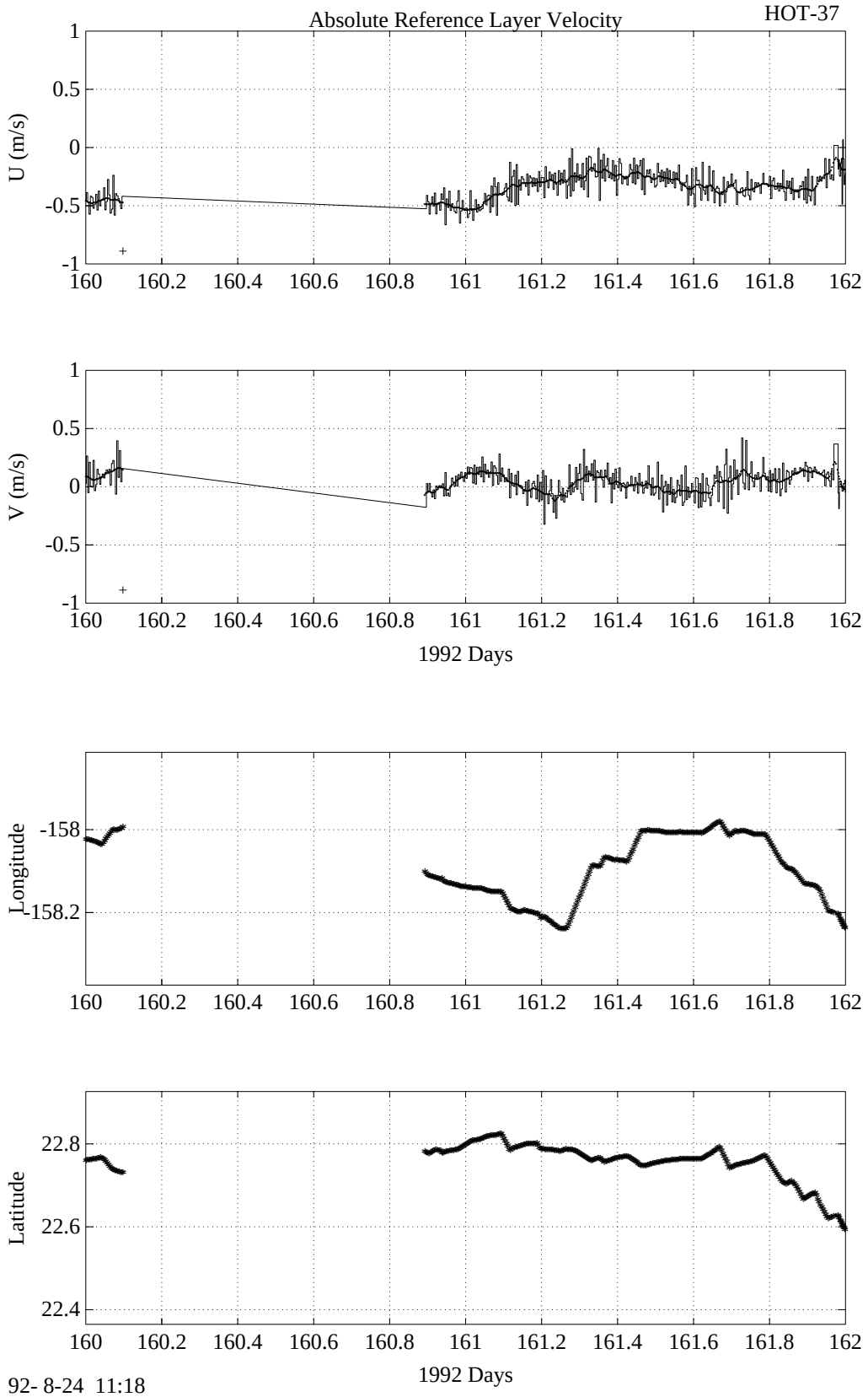

Figure 6.6.5 (continued)

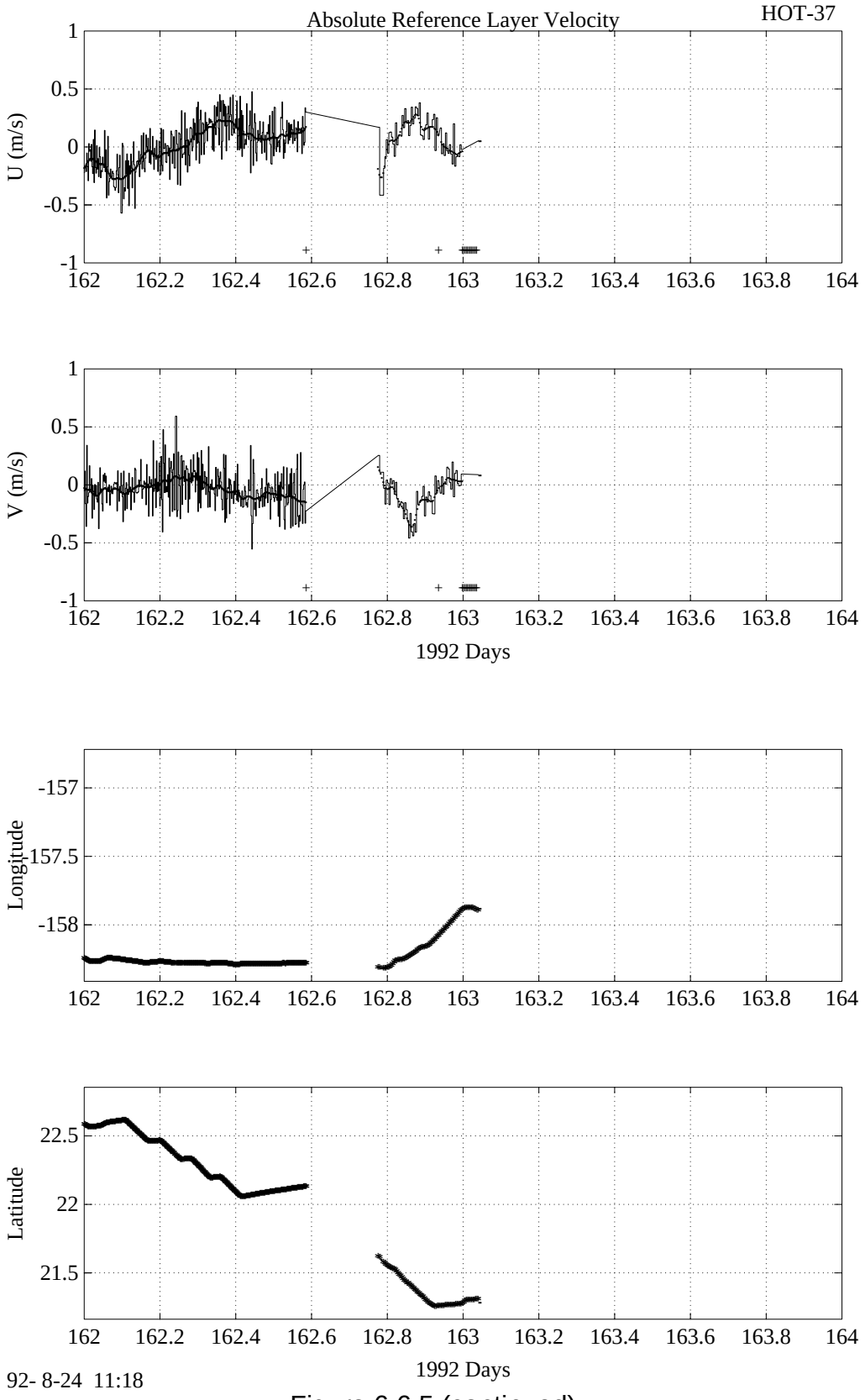

Figure 6.6.5 (continued)

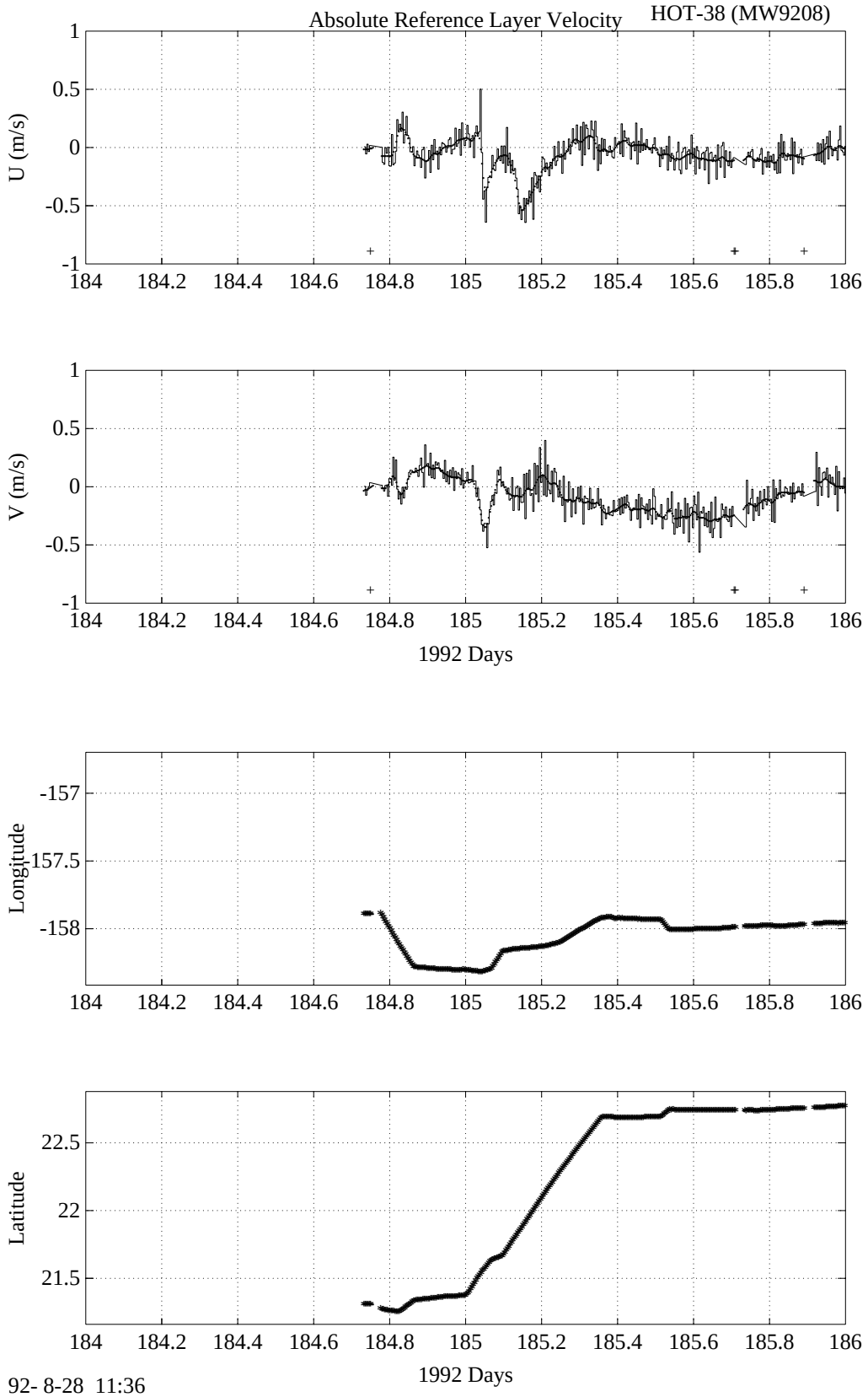
Absolute Reference Layer Velocity
HOT-38 (MW9208)
U (m/s)
V (m/s)
Longitude
Latitude
1992 Days
1992 Days
92- 8-28 11:36

Figure 6.6.6

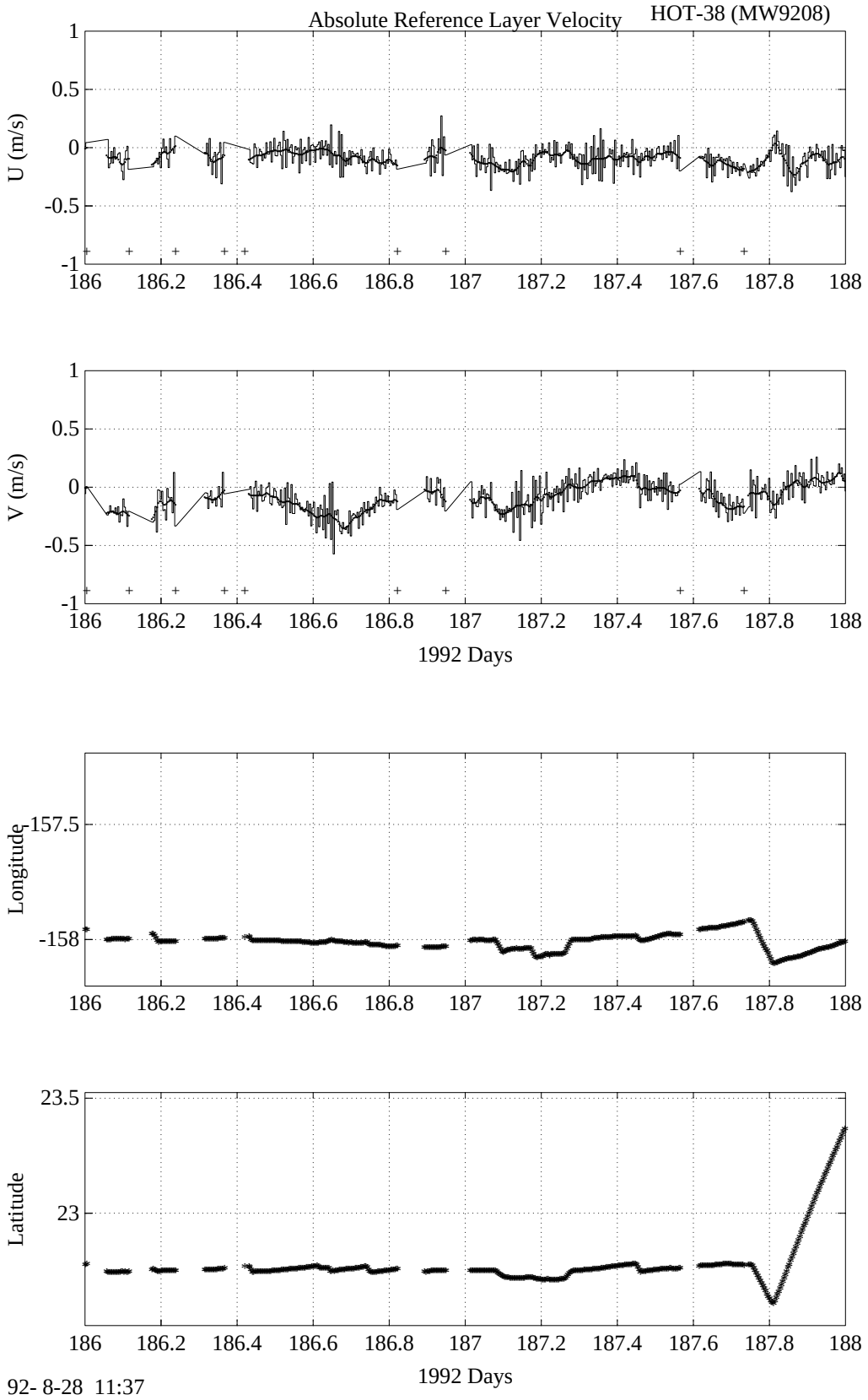

Figure 6.6.6 (continued)

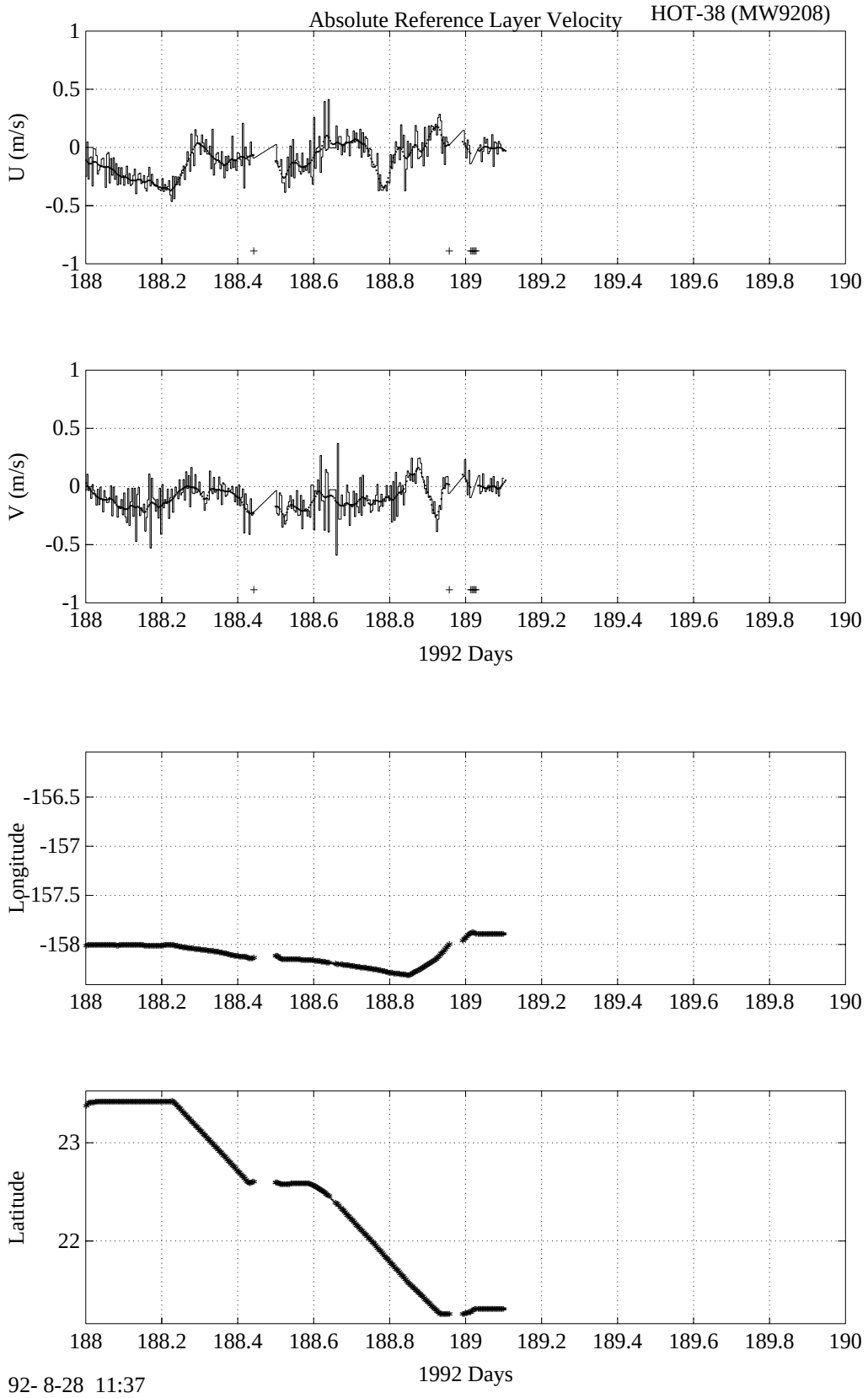

Figure 6.6.6 (continued)

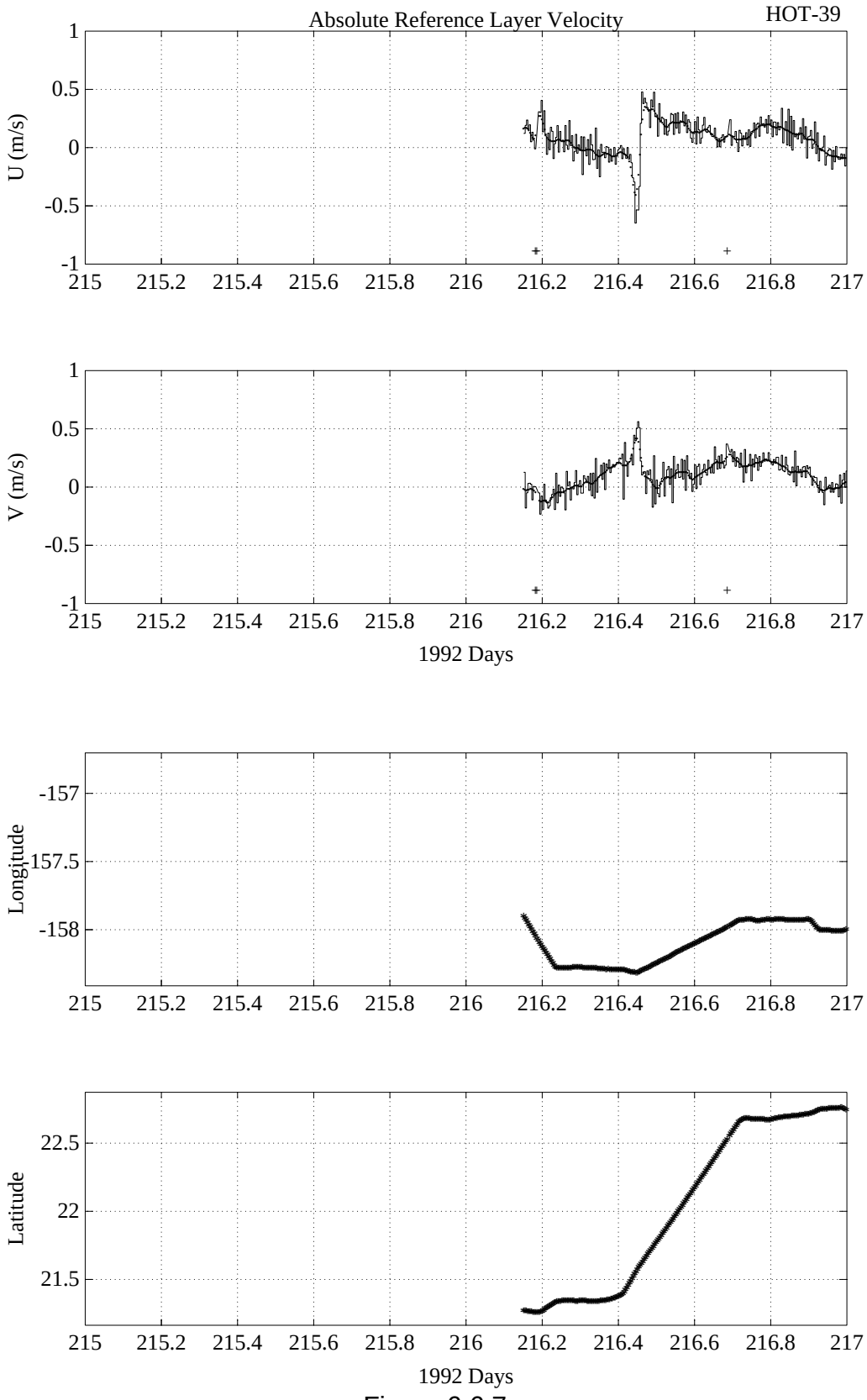
Absolute Reference Layer Velocity
HOT-39
U (m/s)
V (m/s)
Longitude
Latitude
1992 Days
1992 Days

Figure 6.6.7

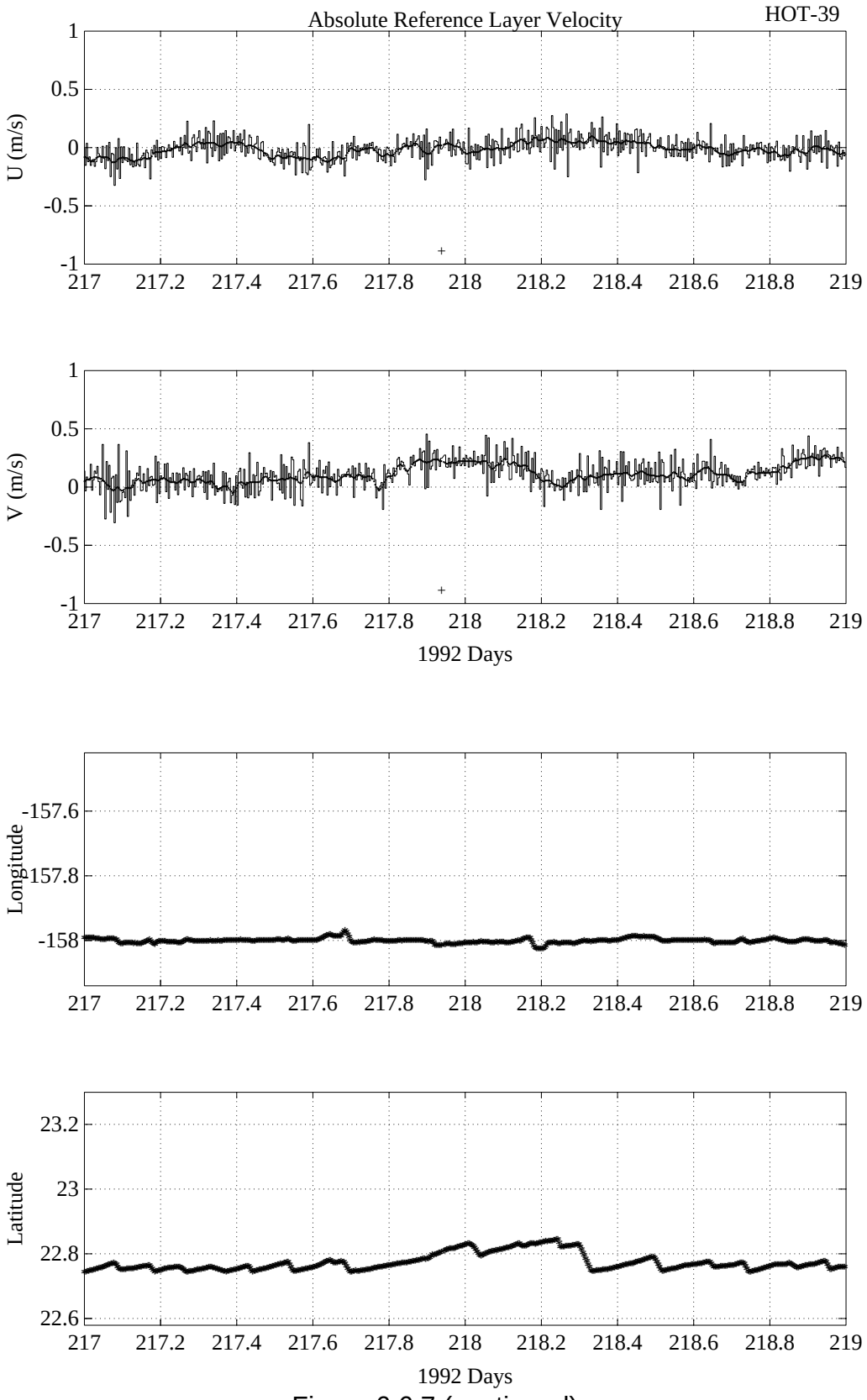

Figure 6.6.7 (continued)

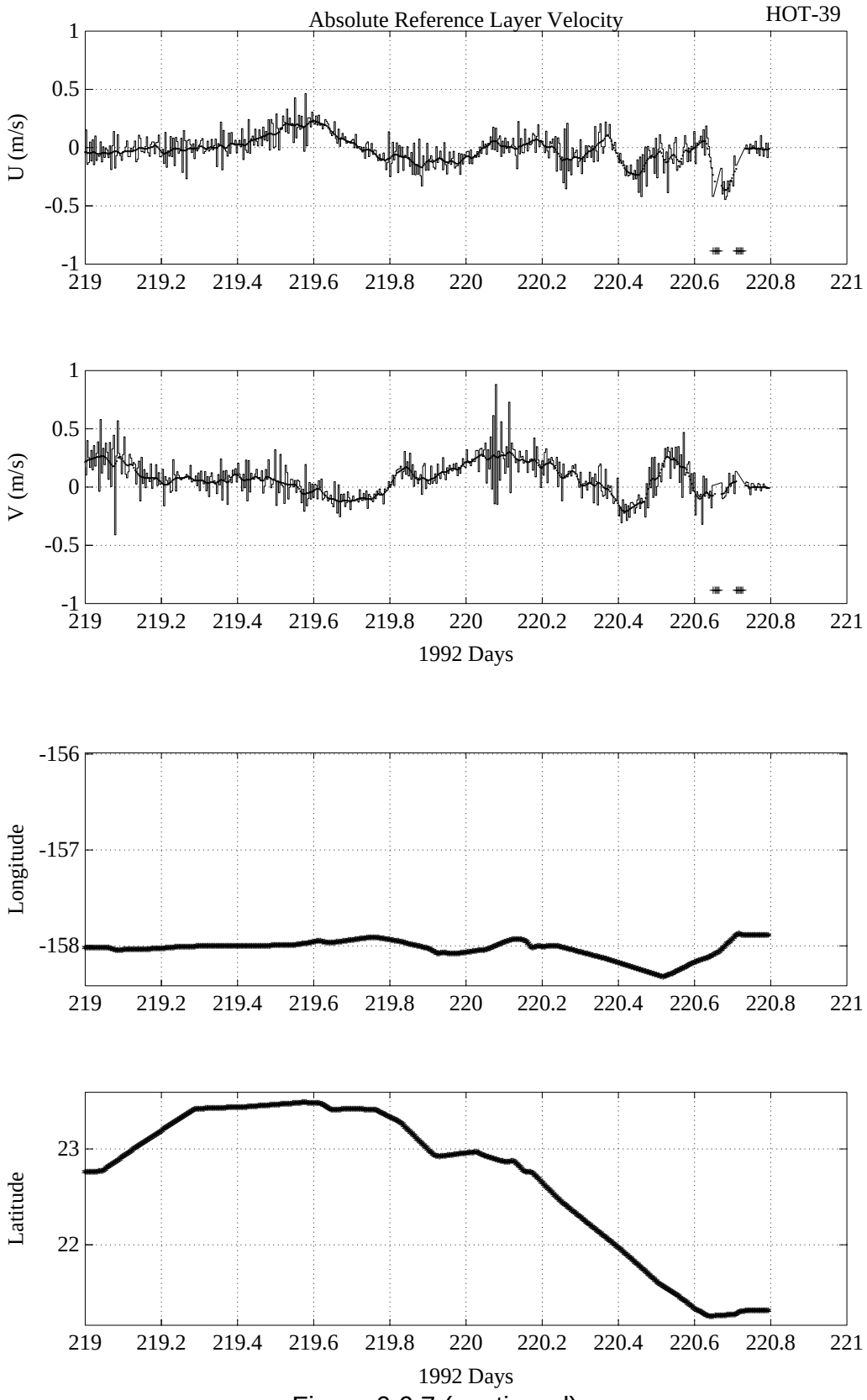

Figure 6.6.7 (continued)

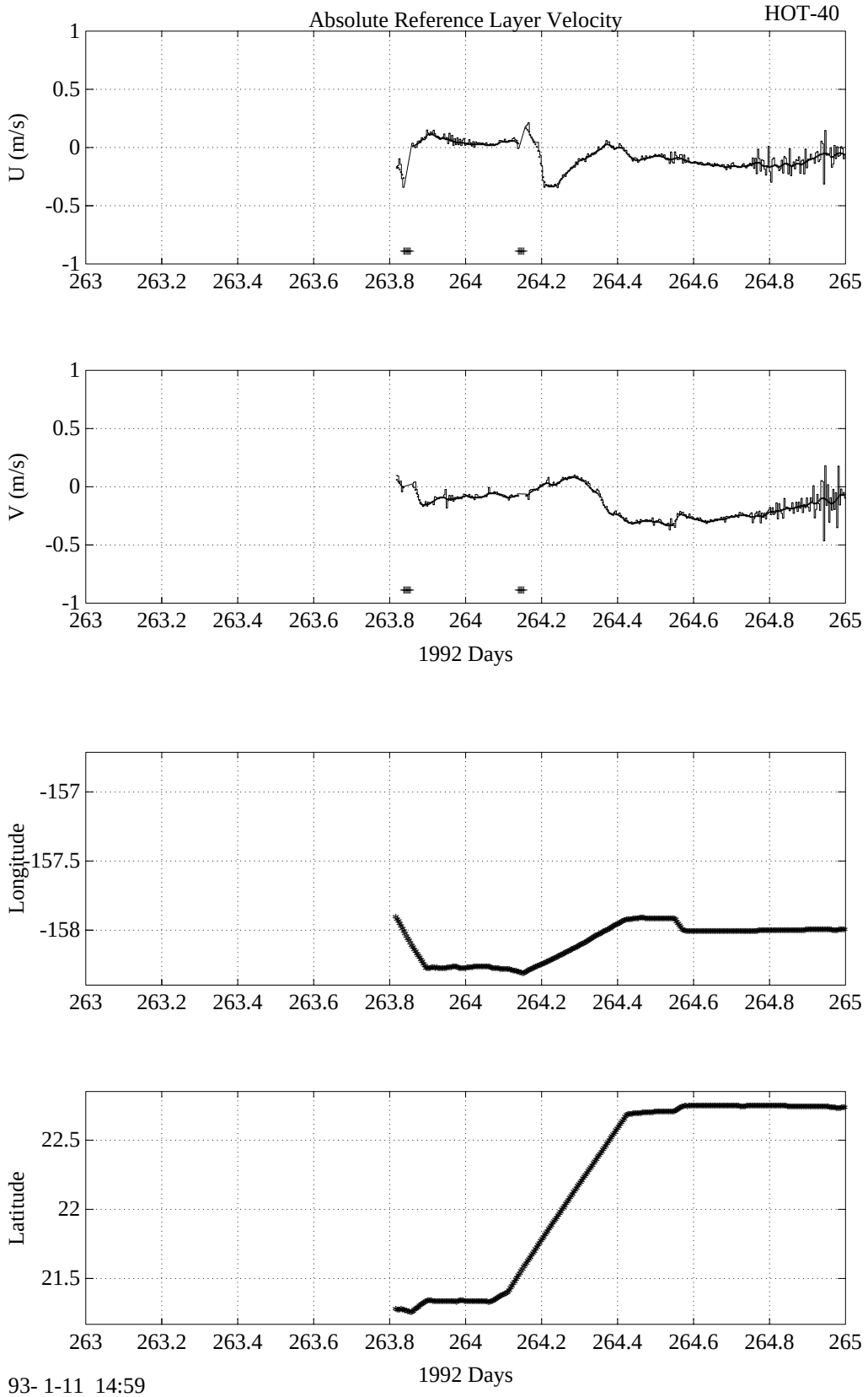
Absolute Reference Layer Velocity
HOT-40
U (m/s)
V (m/s)
Longitude
Latitude
1992 Days
1992 Days
93- 1-11 14:59

Figure 6.6.8

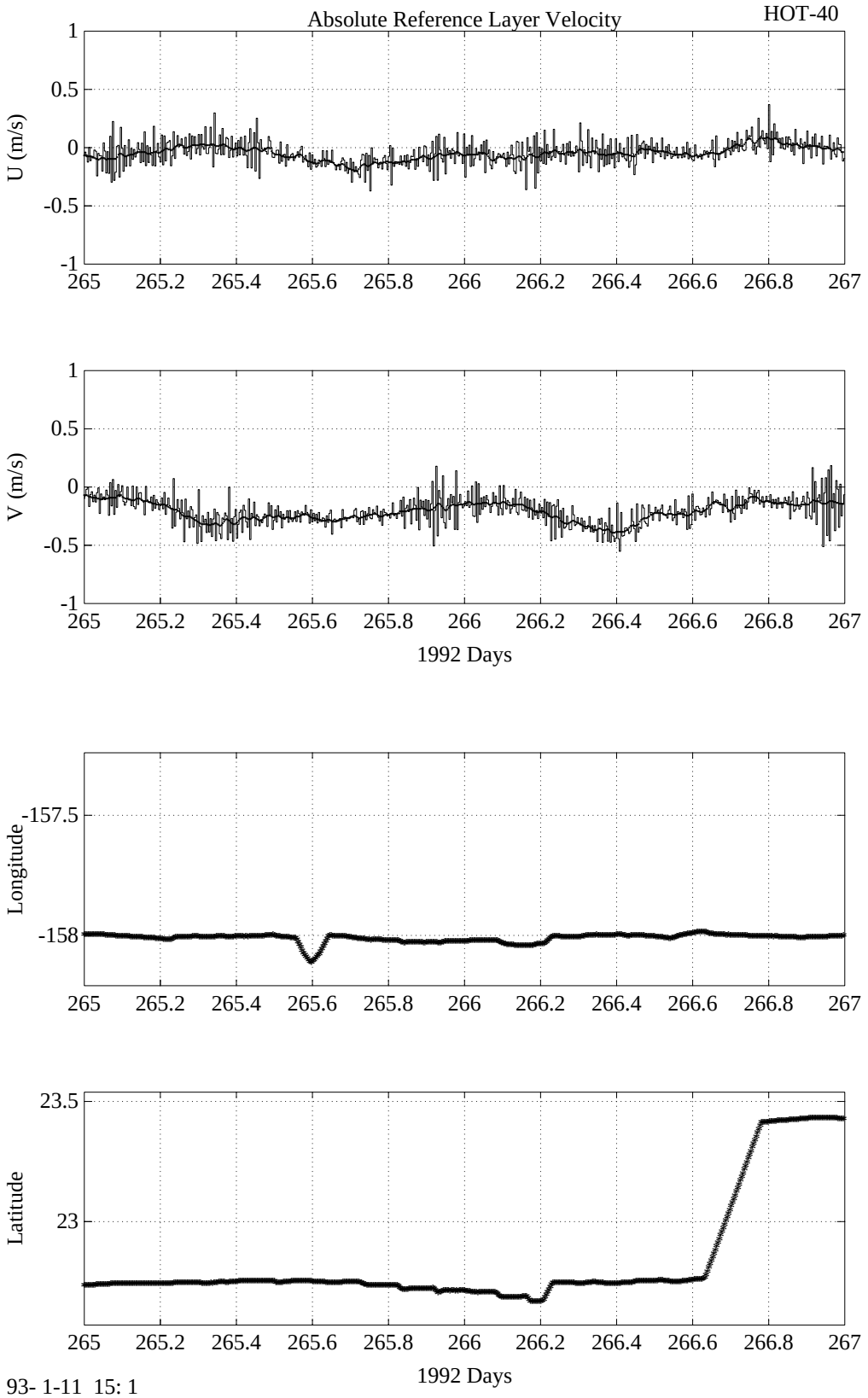

Figure 6.6.8 (continued)

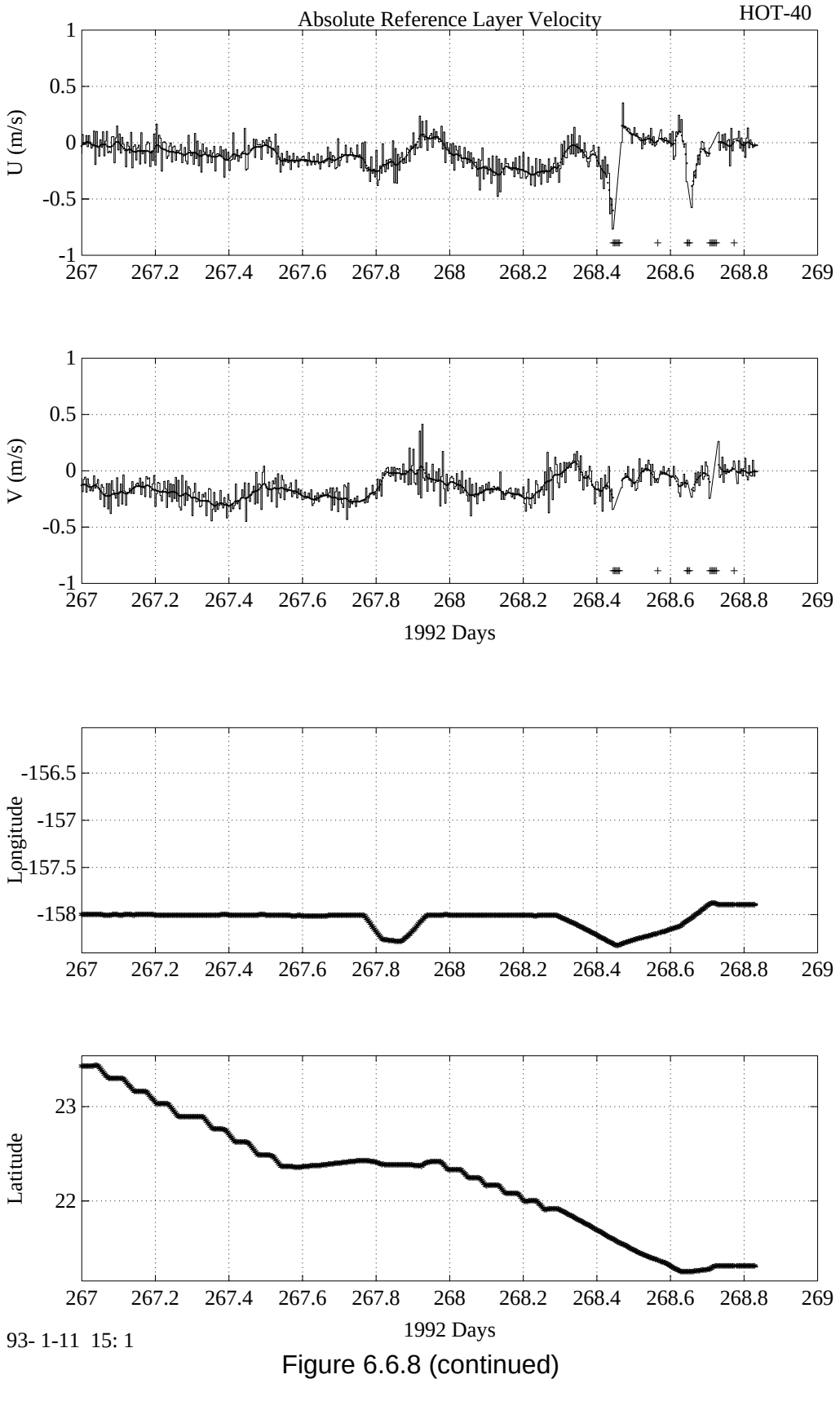

Figure 6.6.8 (continued)

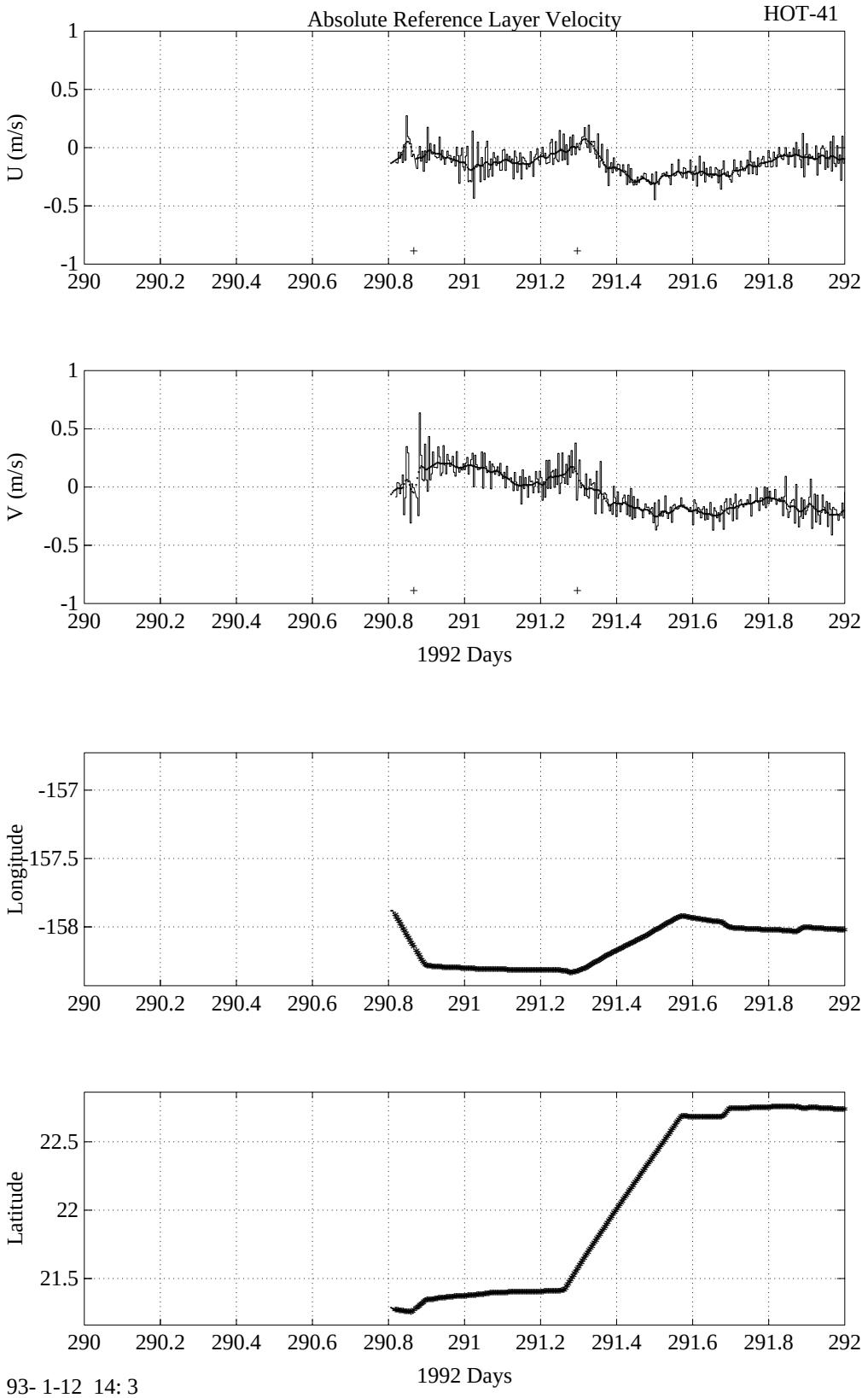
Absolute Reference Layer Velocity
HOT-41
U (m/s)
V (m/s)
Longitude
Latitude
1992 Days
1992 Days
93- 1-12 14: 3

Figure 6.6.9

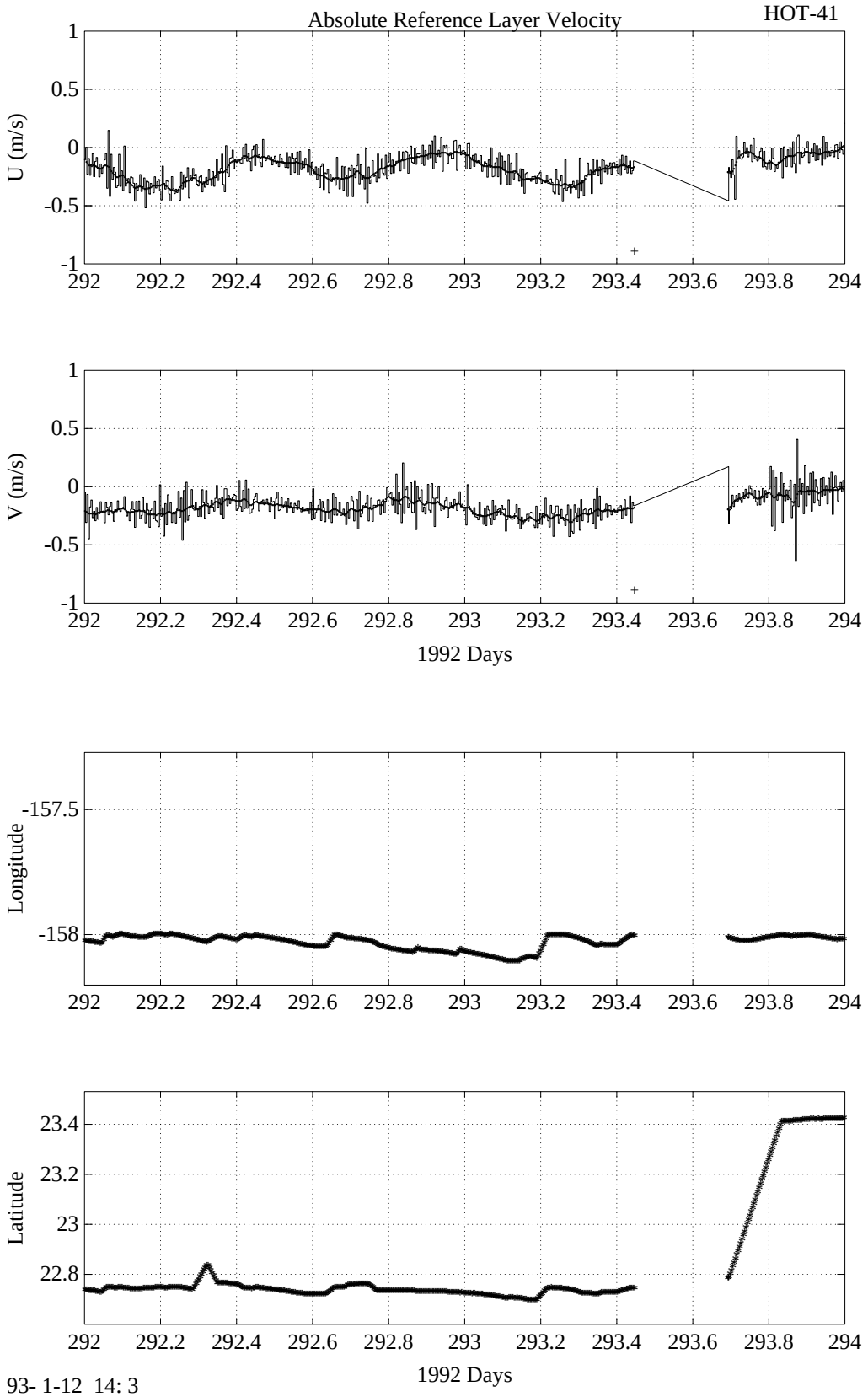

Figure 6.6.9 (continued)

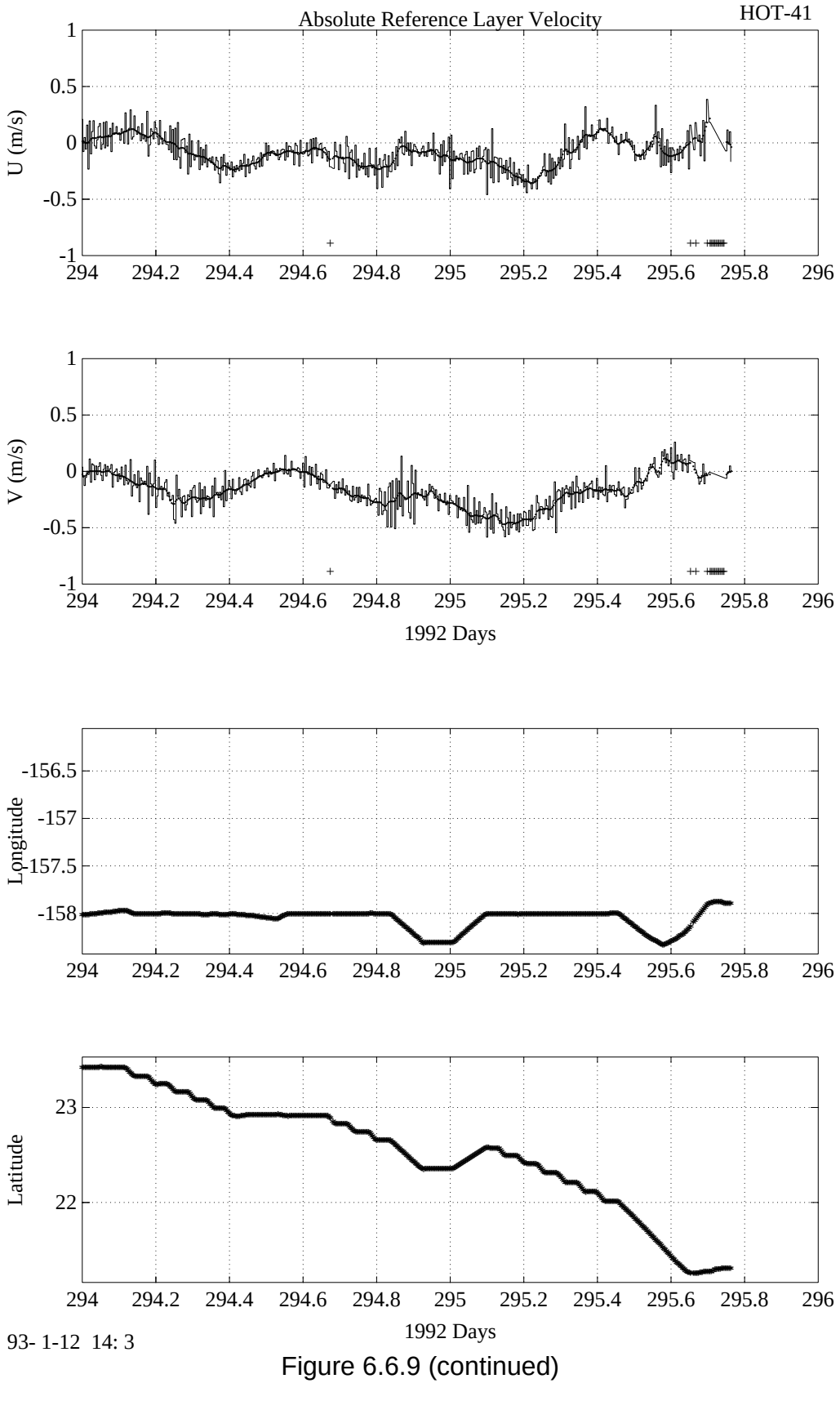

Figure 6.6.9 (continued)

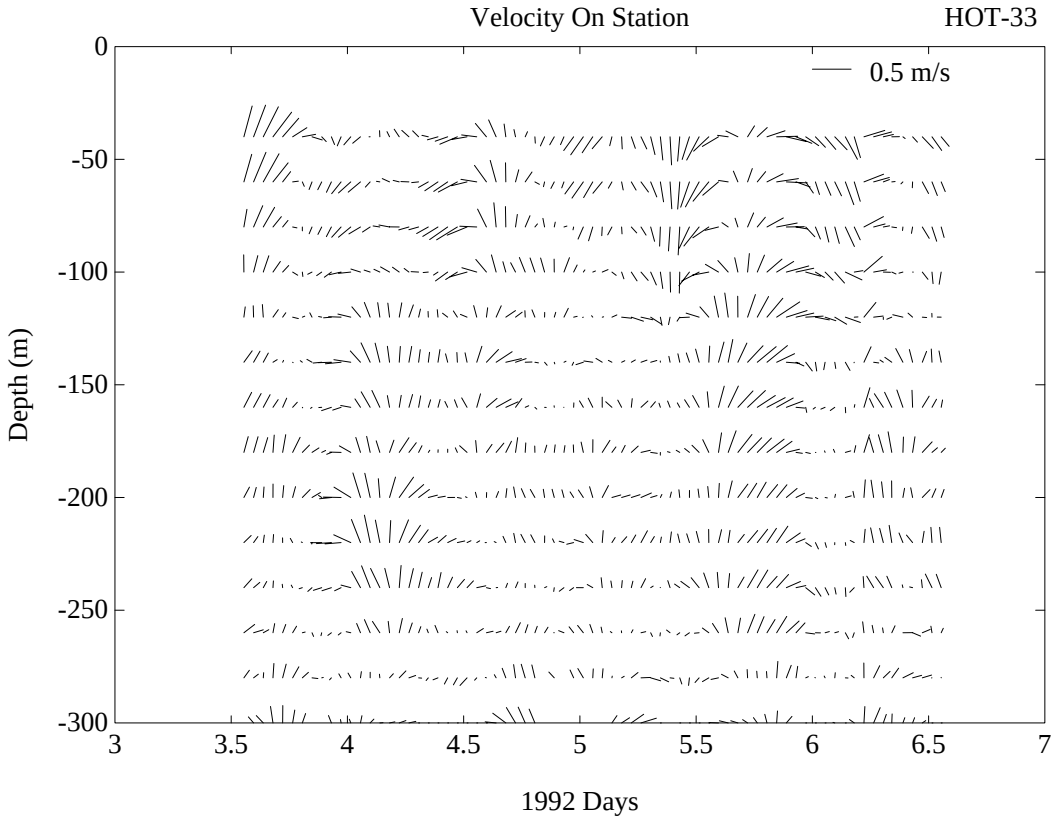

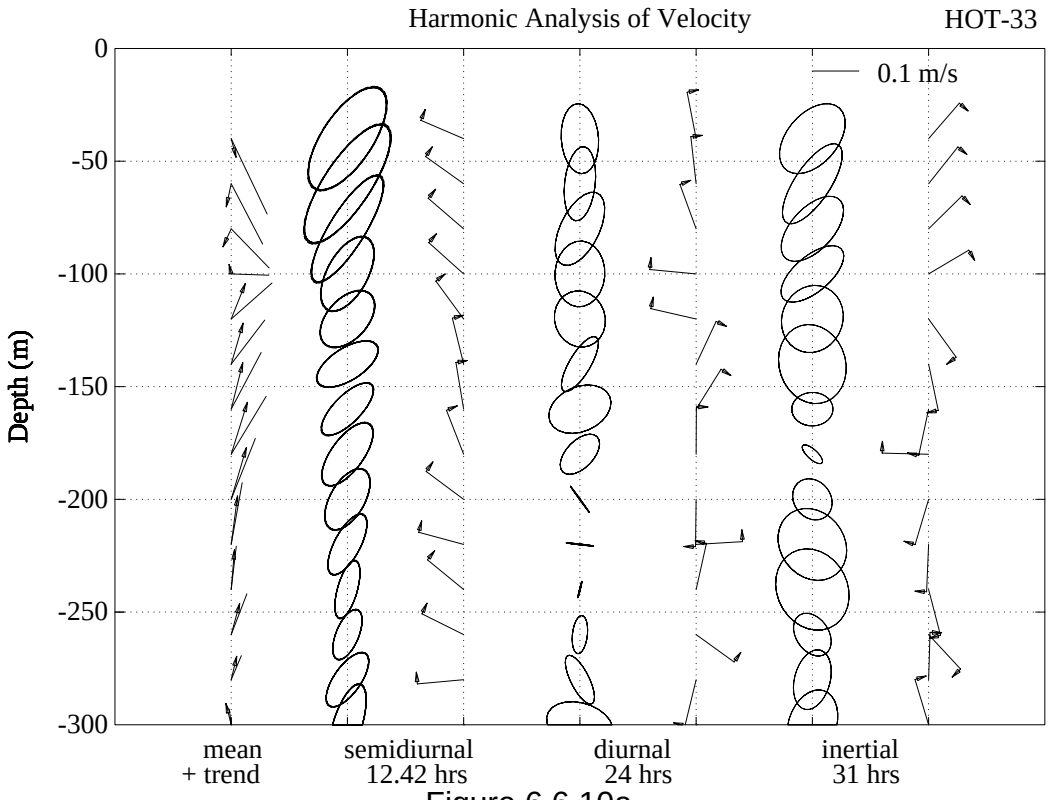

Figure 6.6.10a

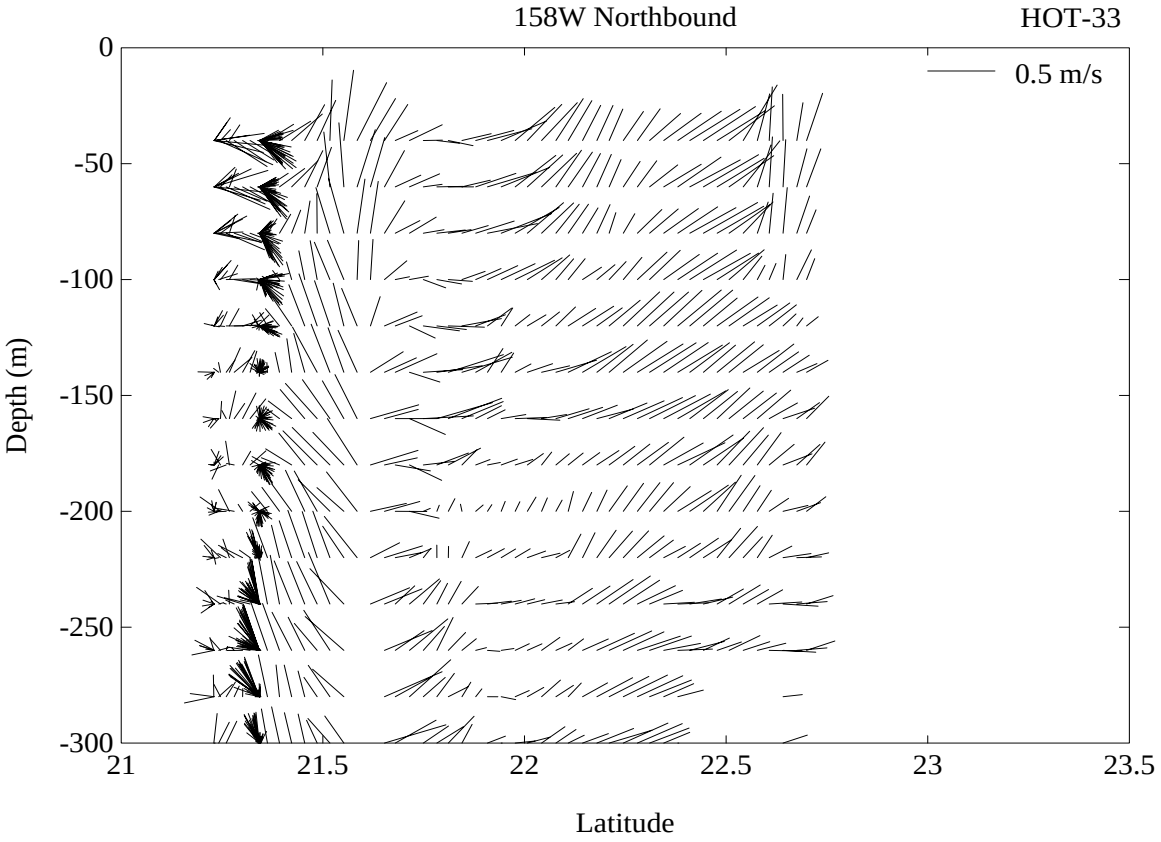

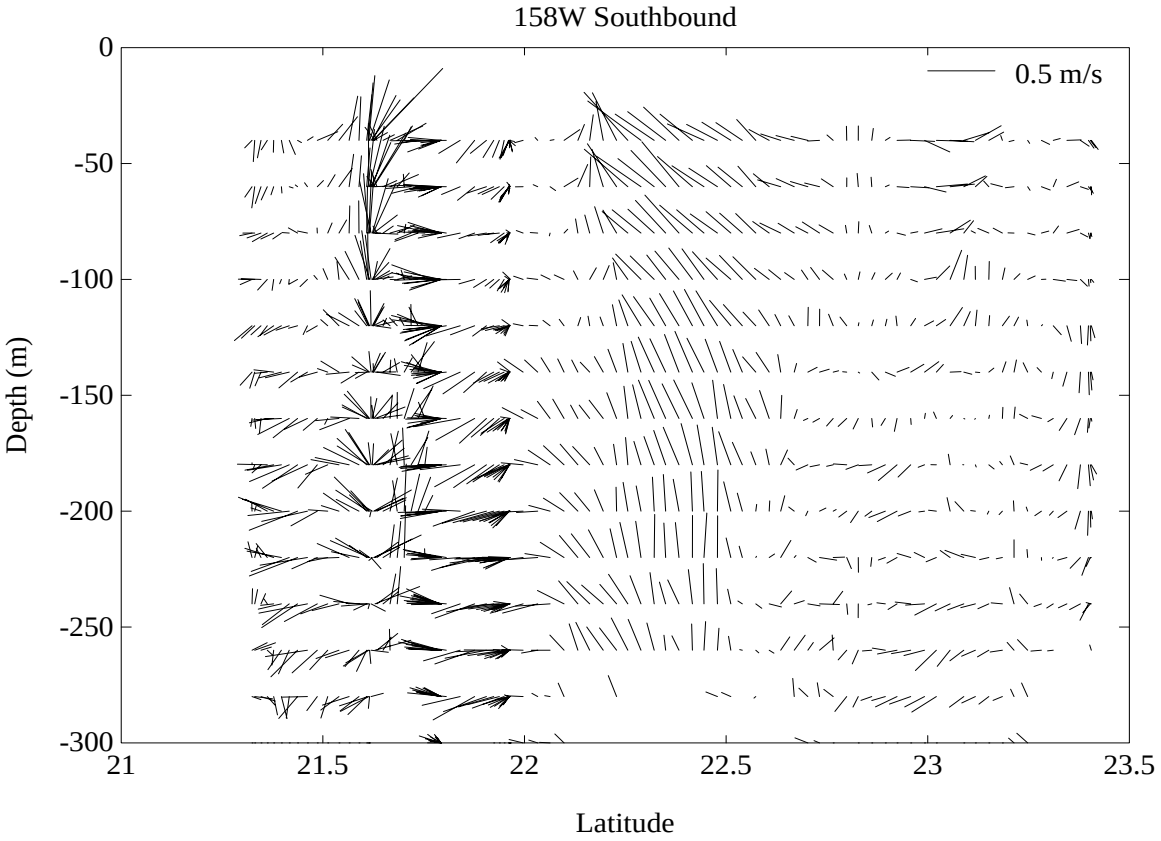

Figure 6.6.10b

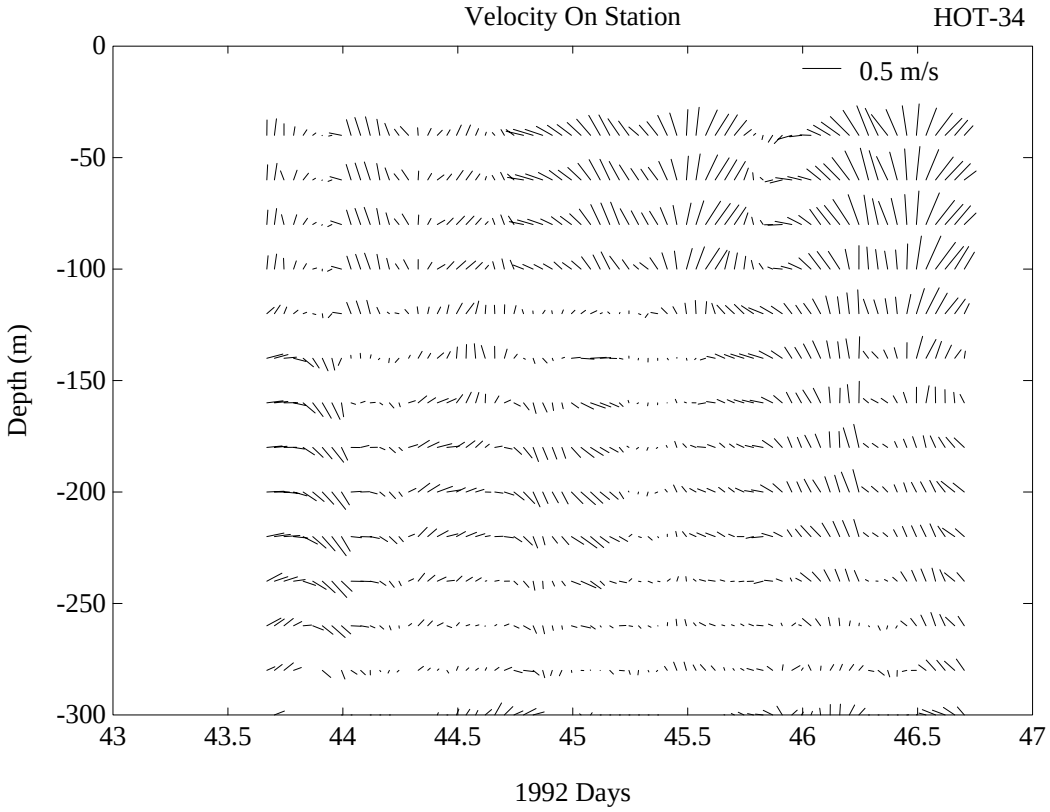

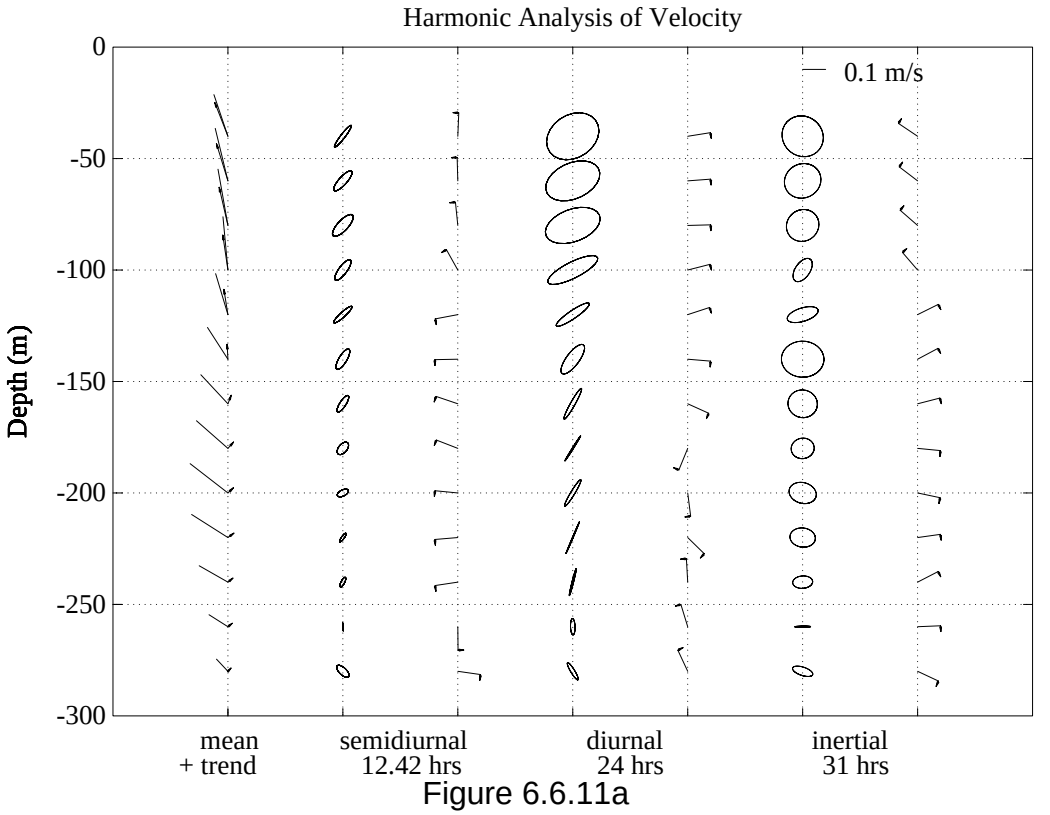

Figure 6.6.11a

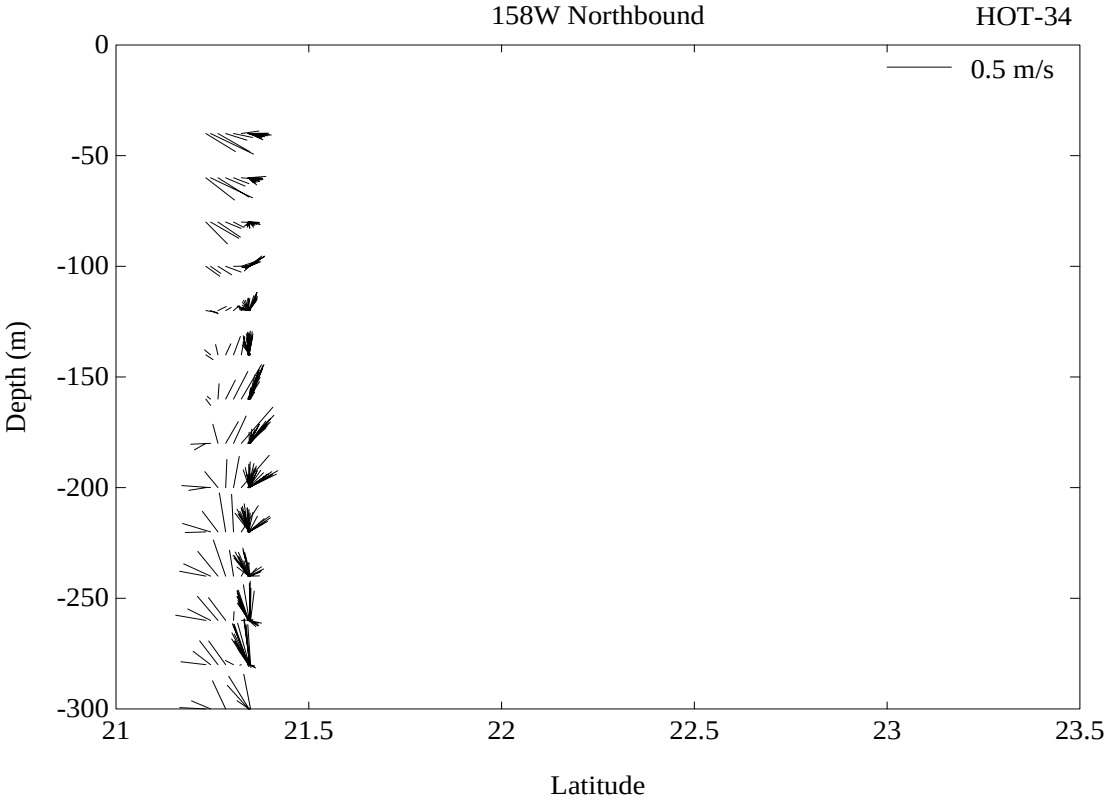

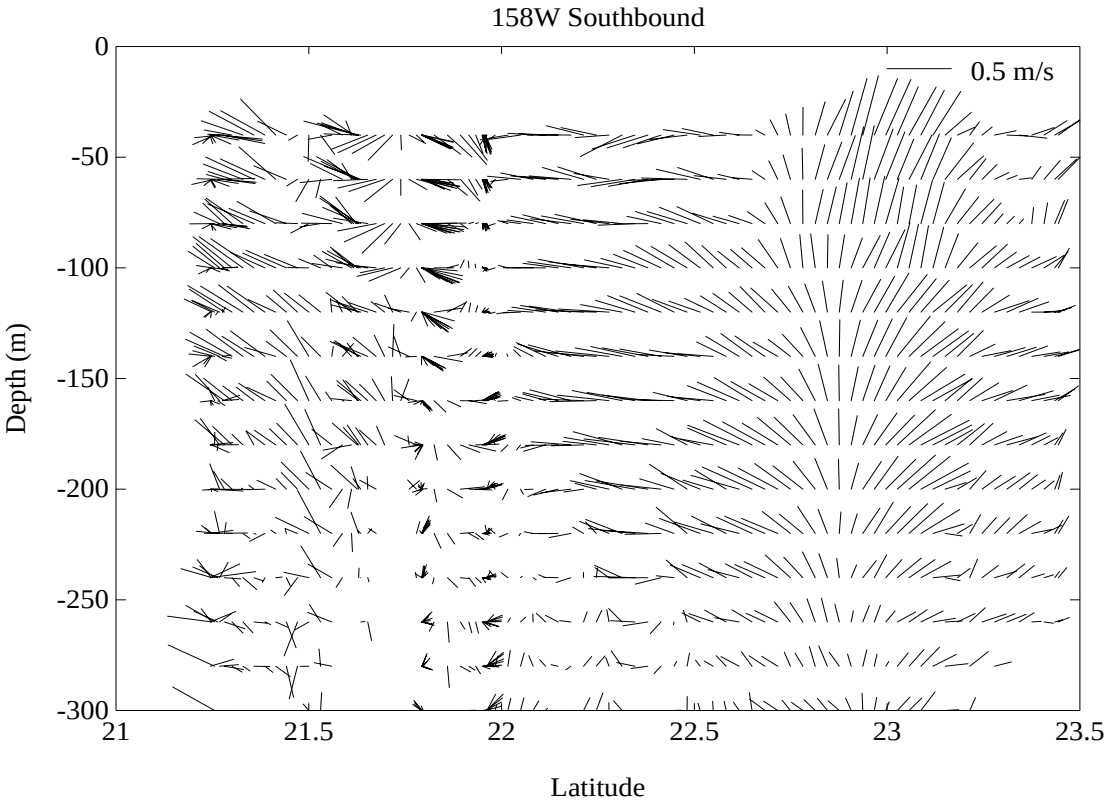

Figure 6.6.11b

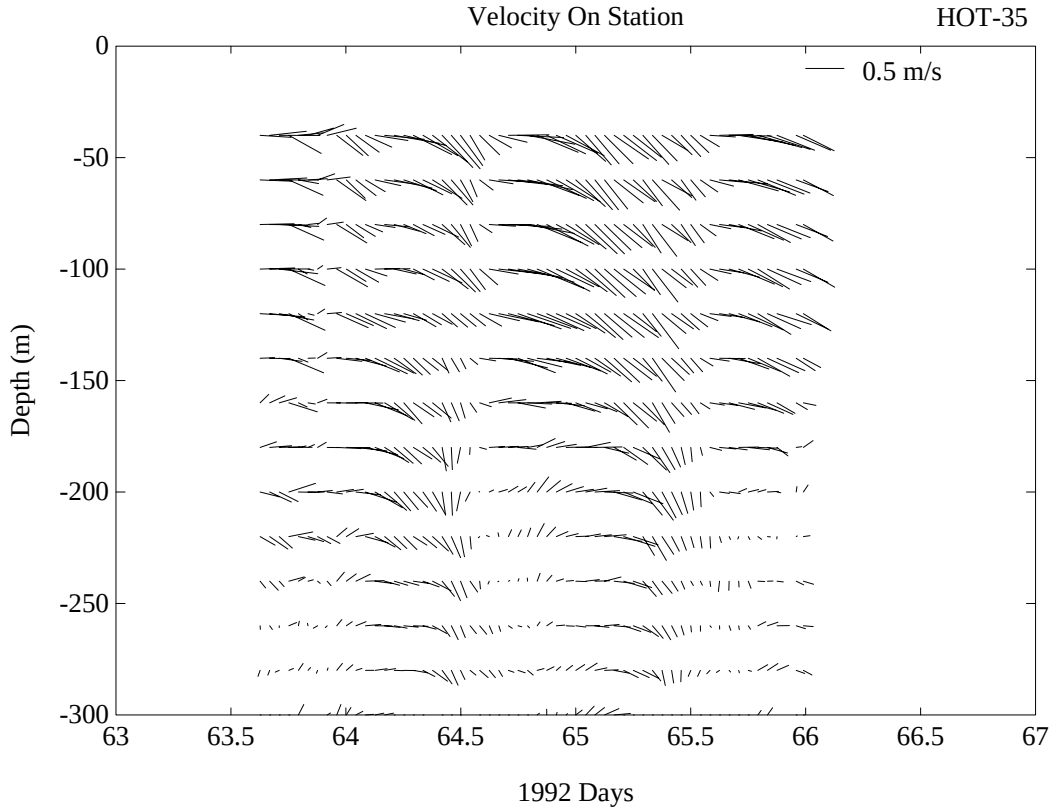

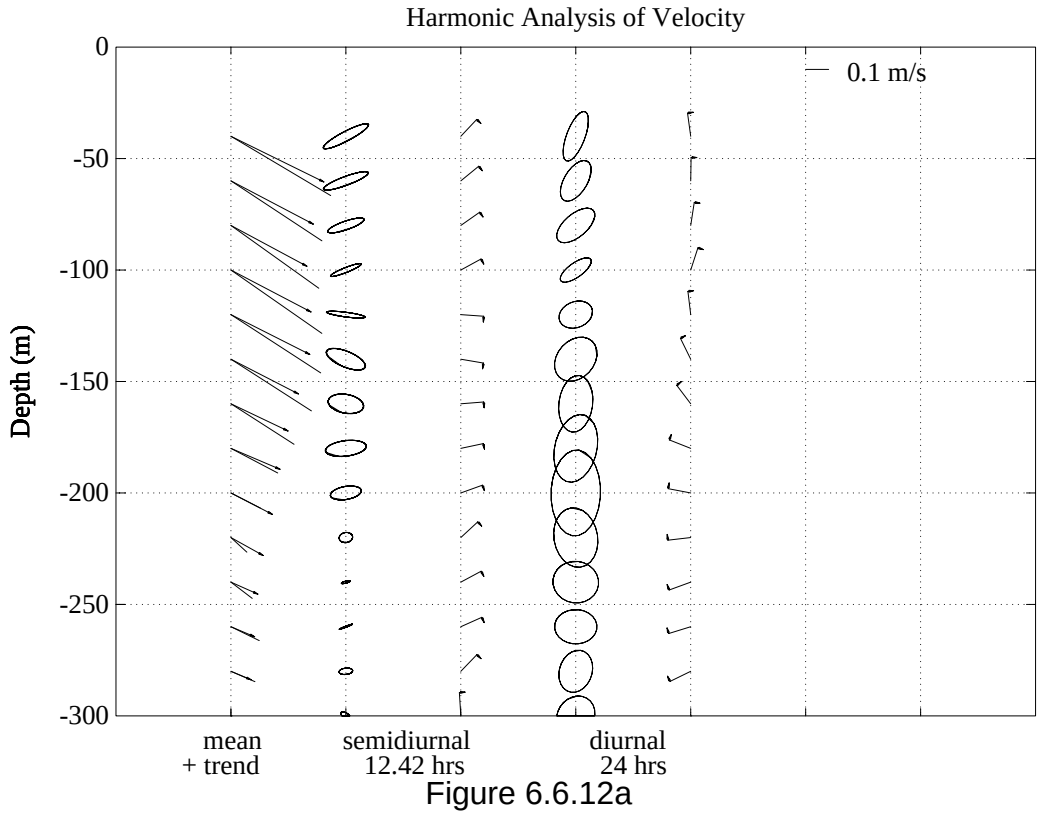

Figure 6.6.12a

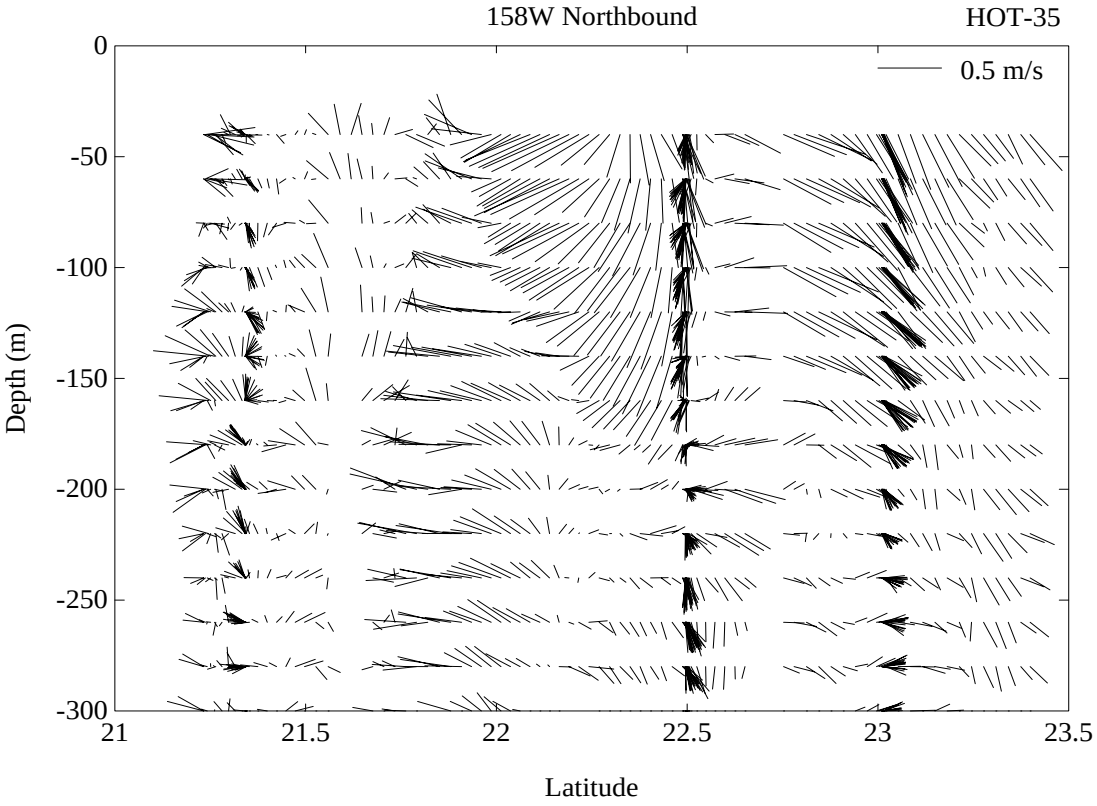

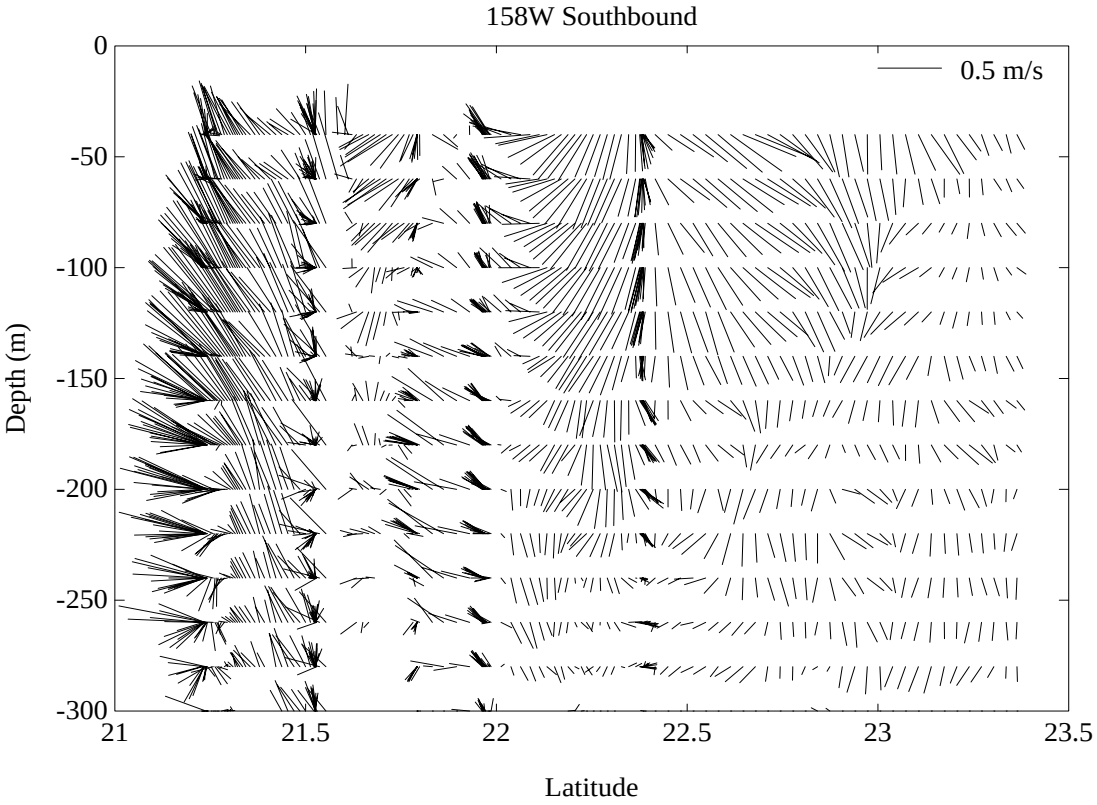

Figure 6.6.12b

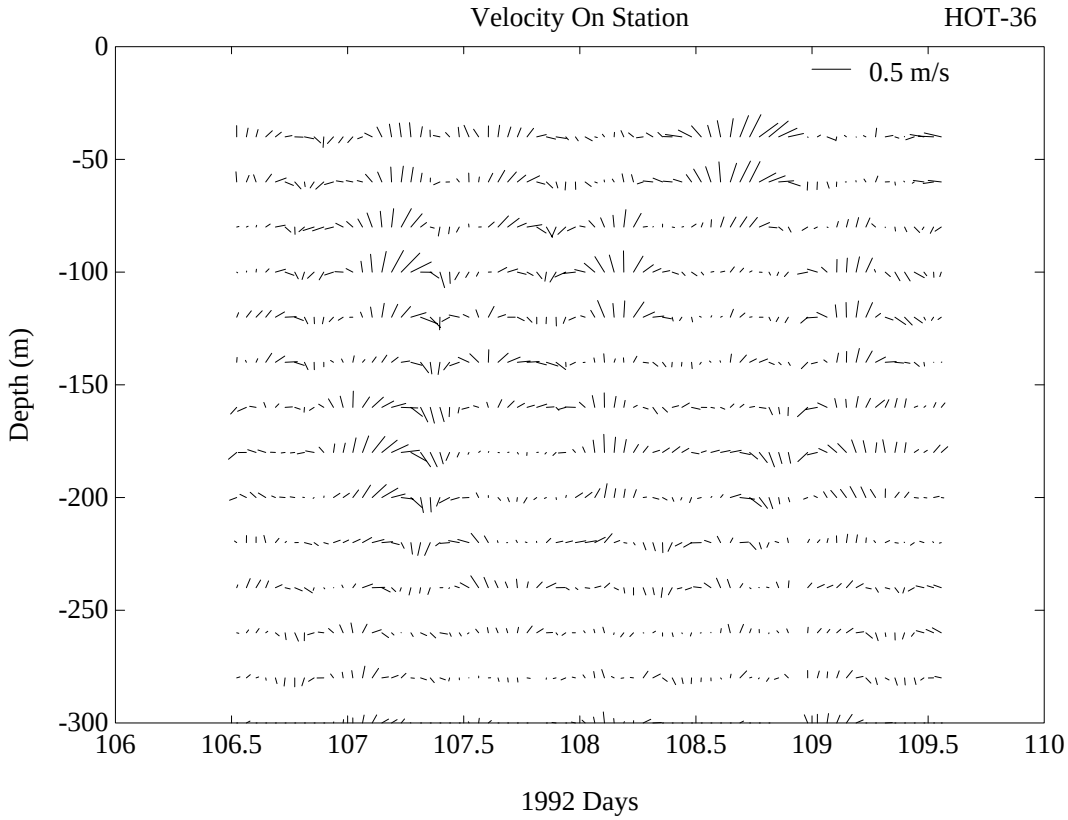

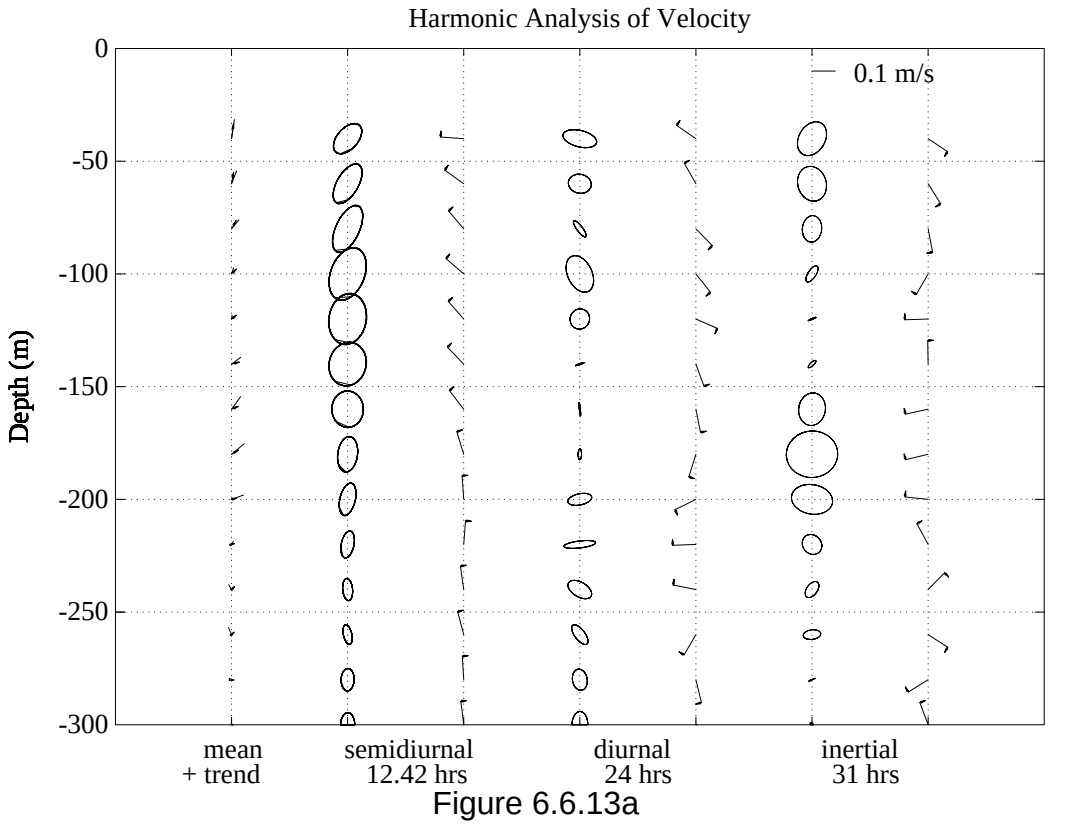

Figure 6.6.13a

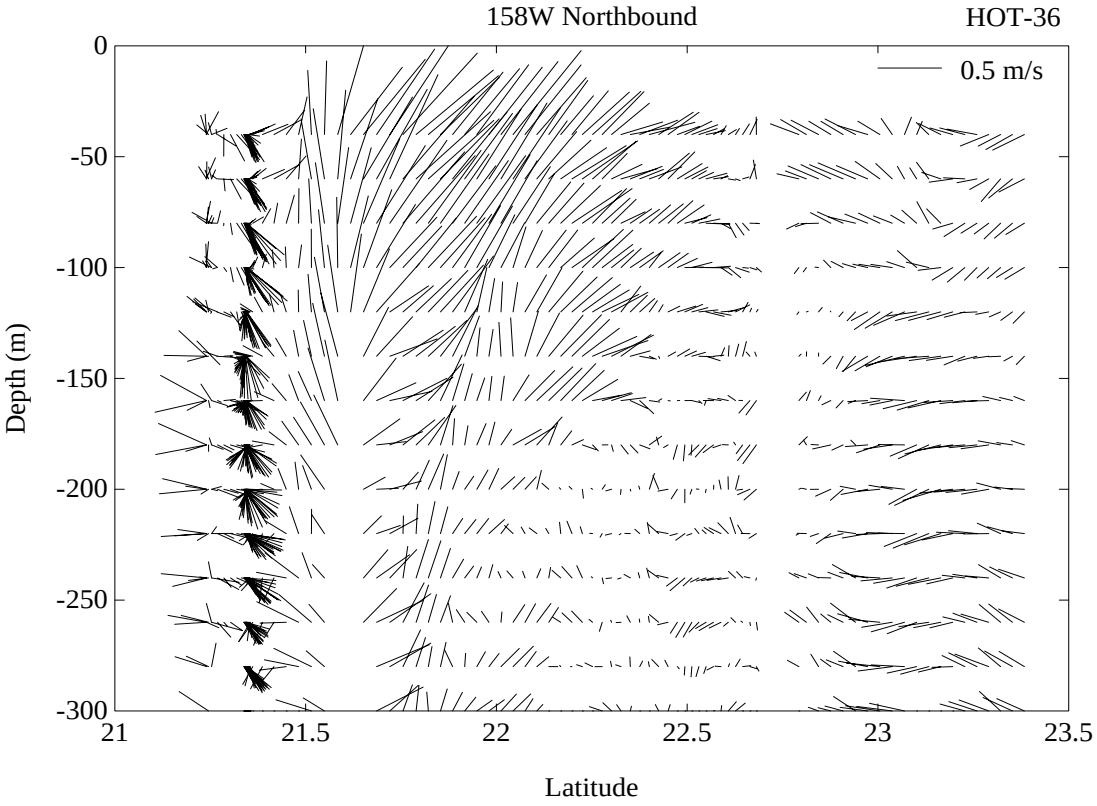

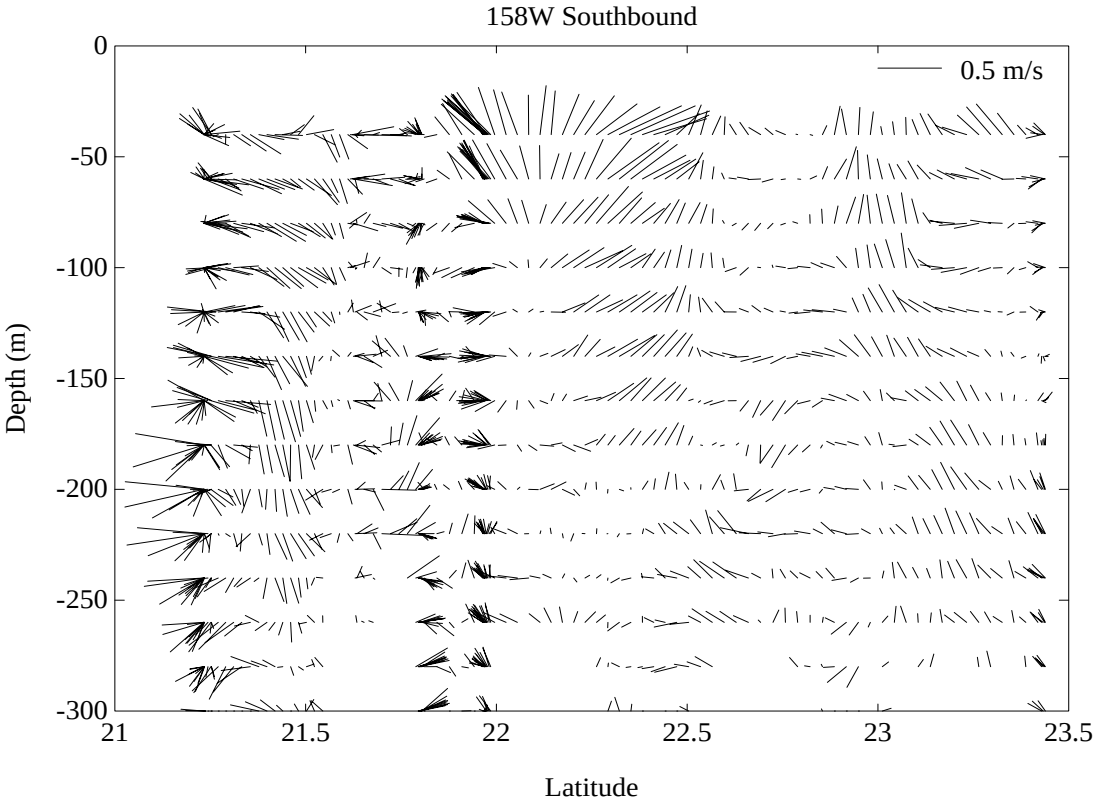

Figure 6.6.13b

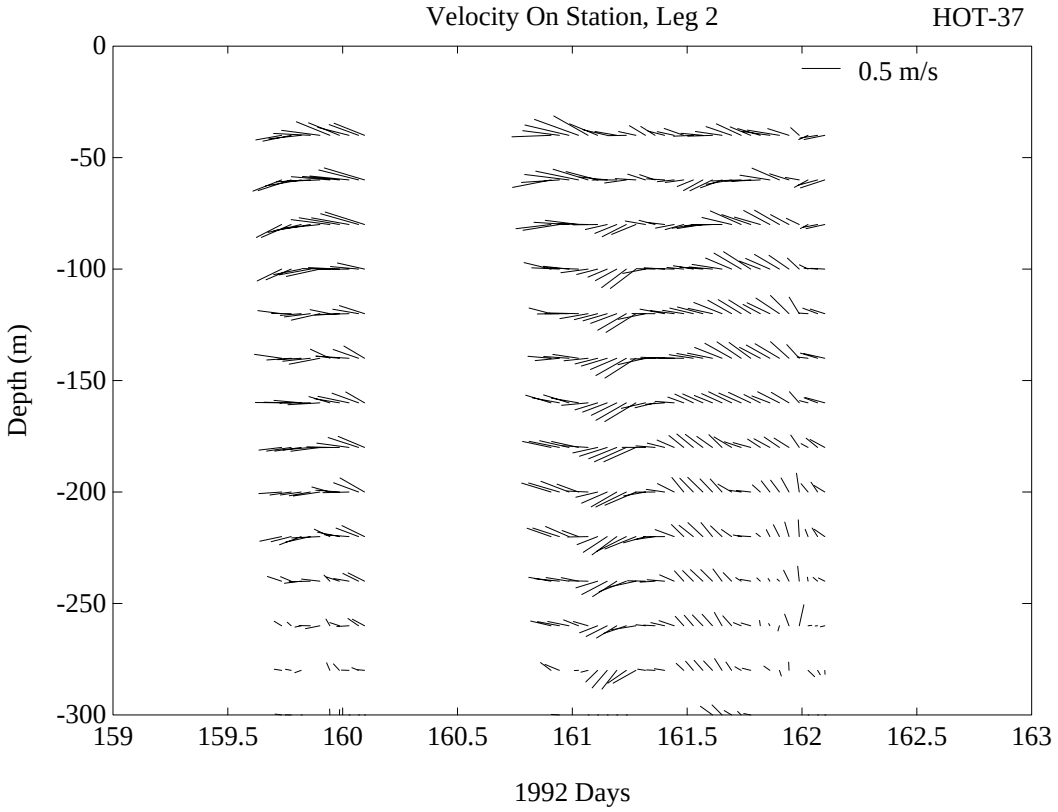

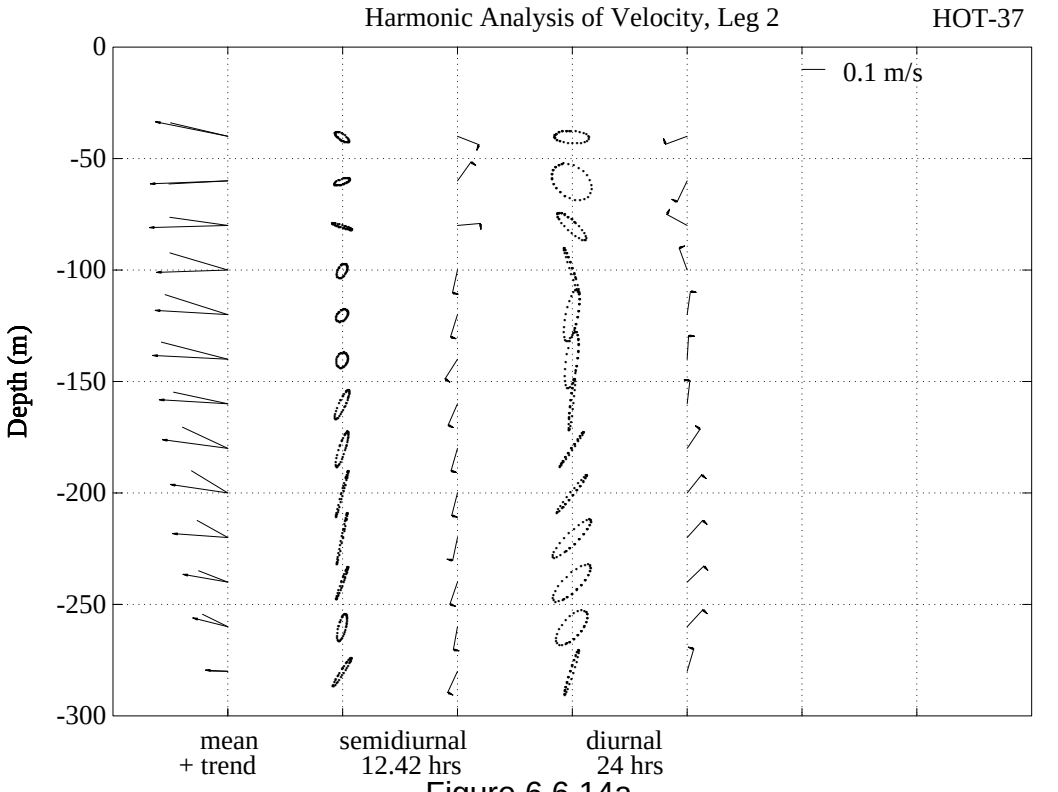

Figure 6.6.14a

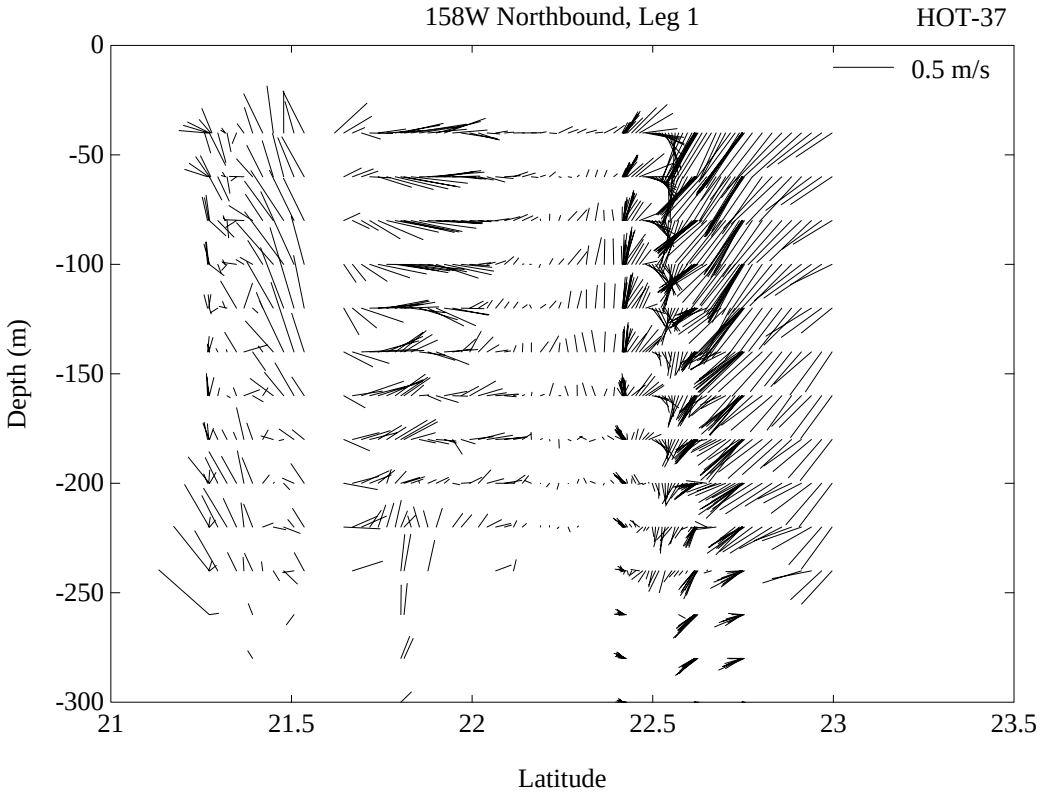

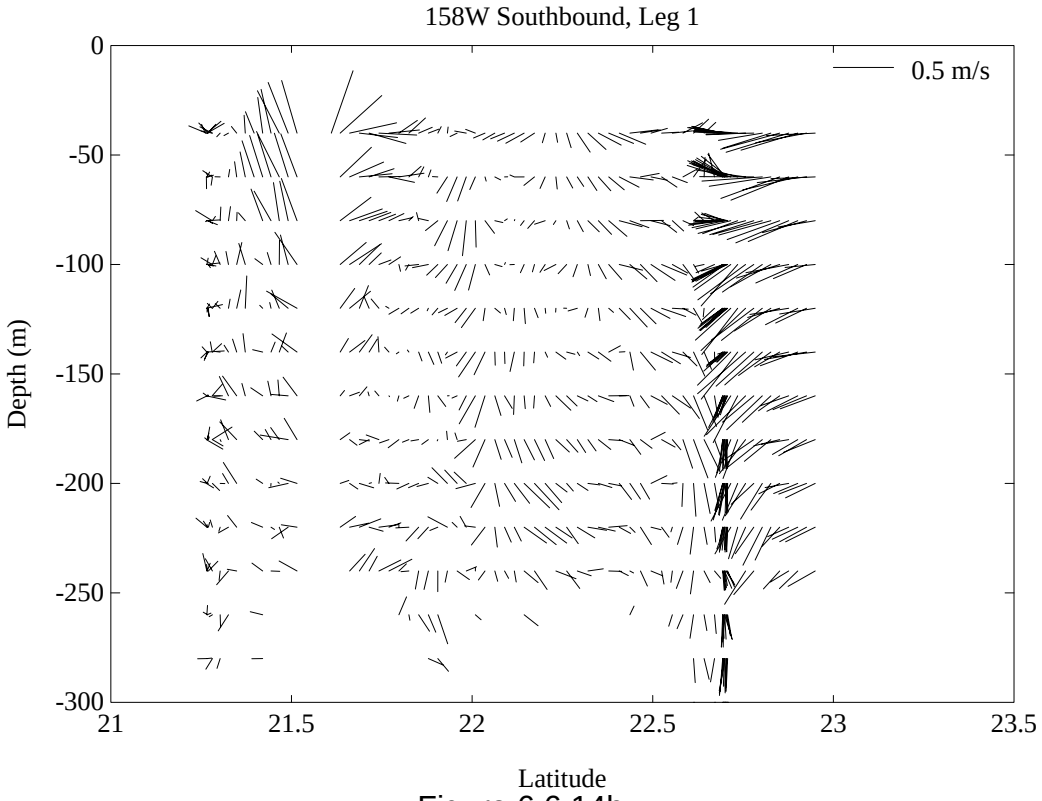

Figure 6.6.14b

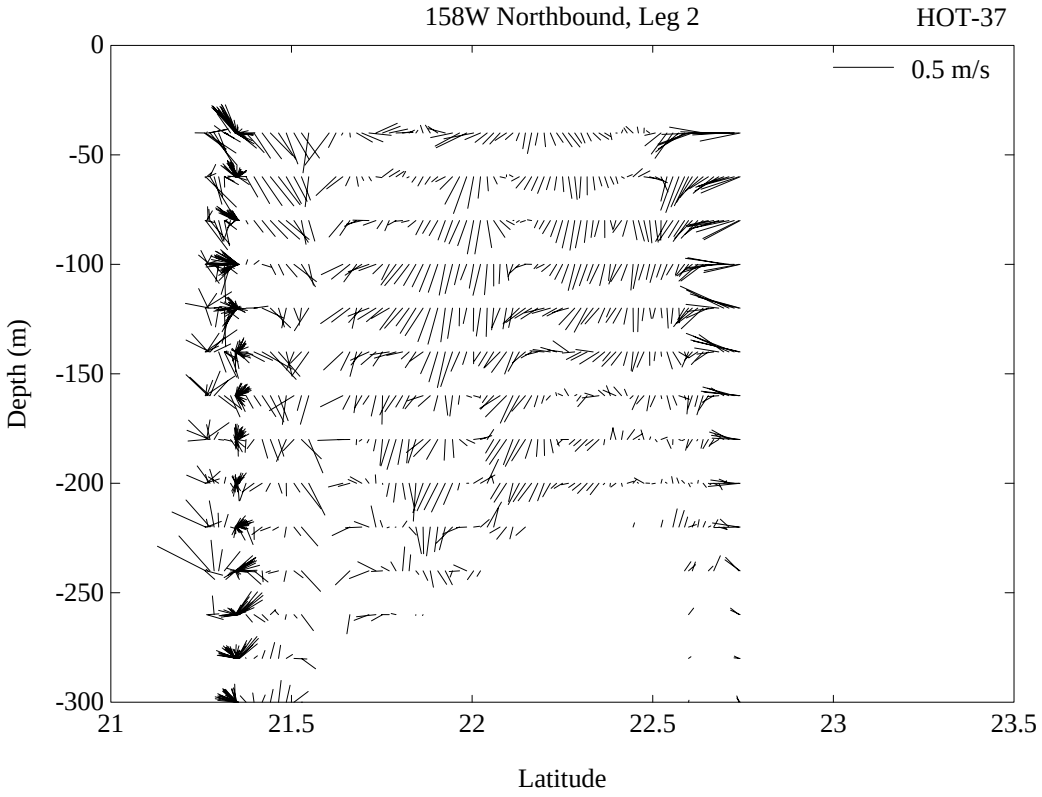

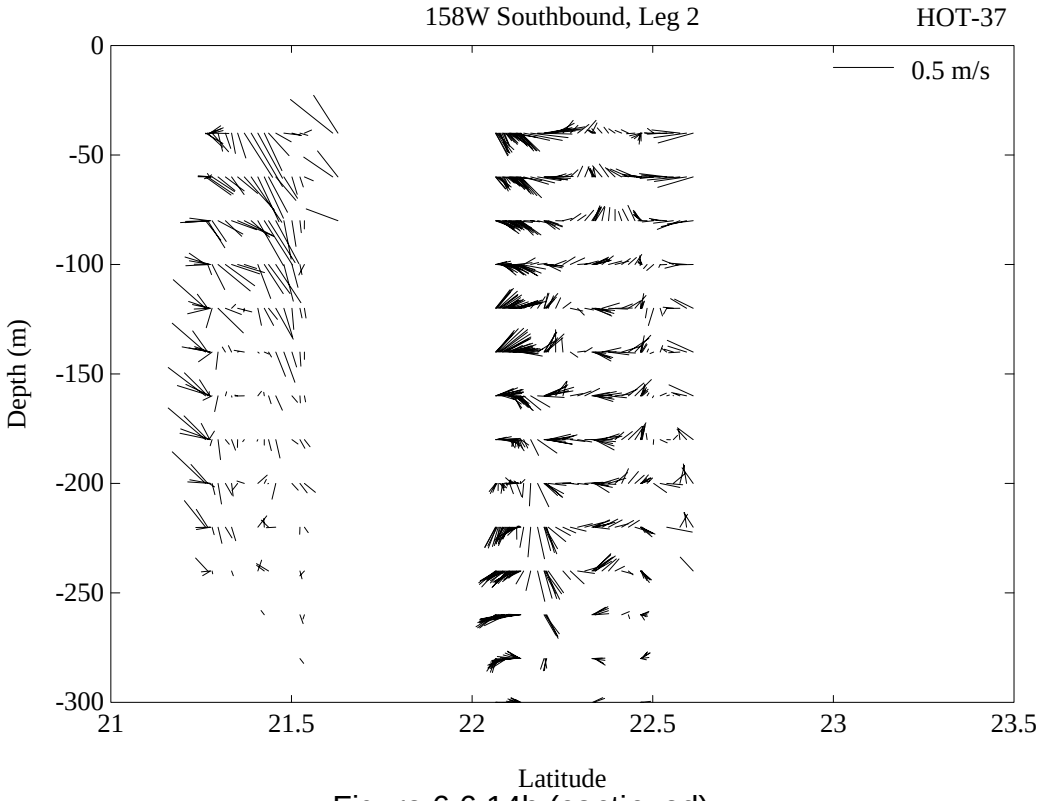

Figure 6.6.14b (continued)

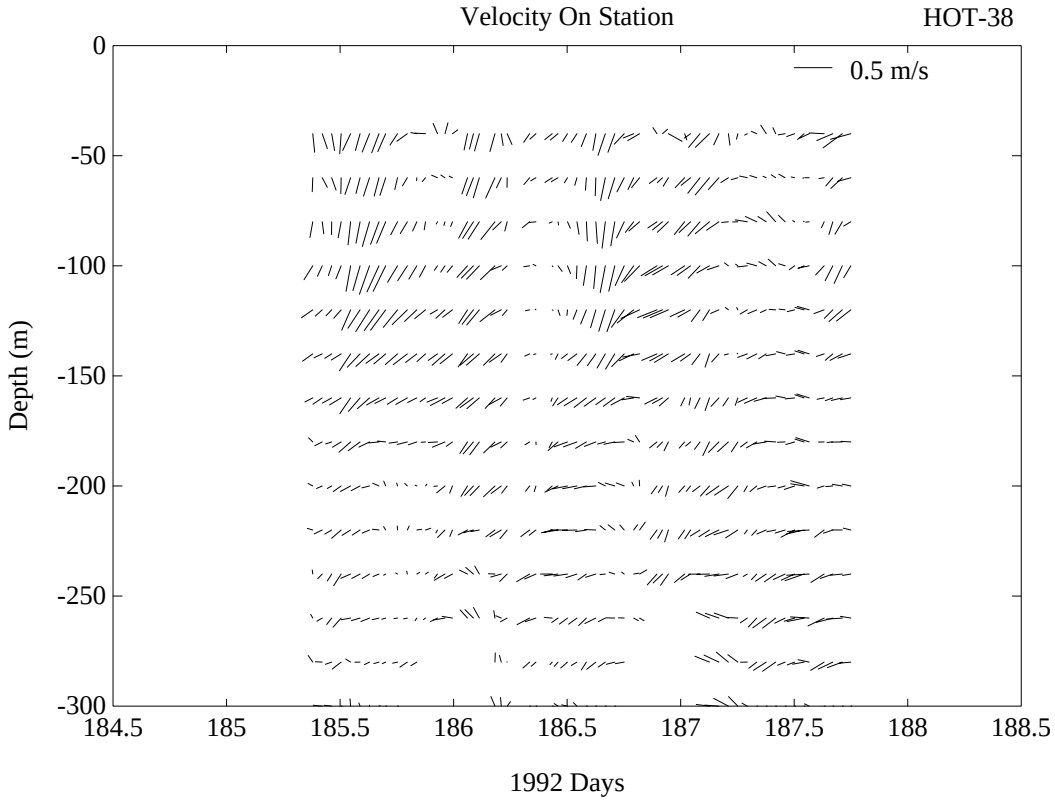

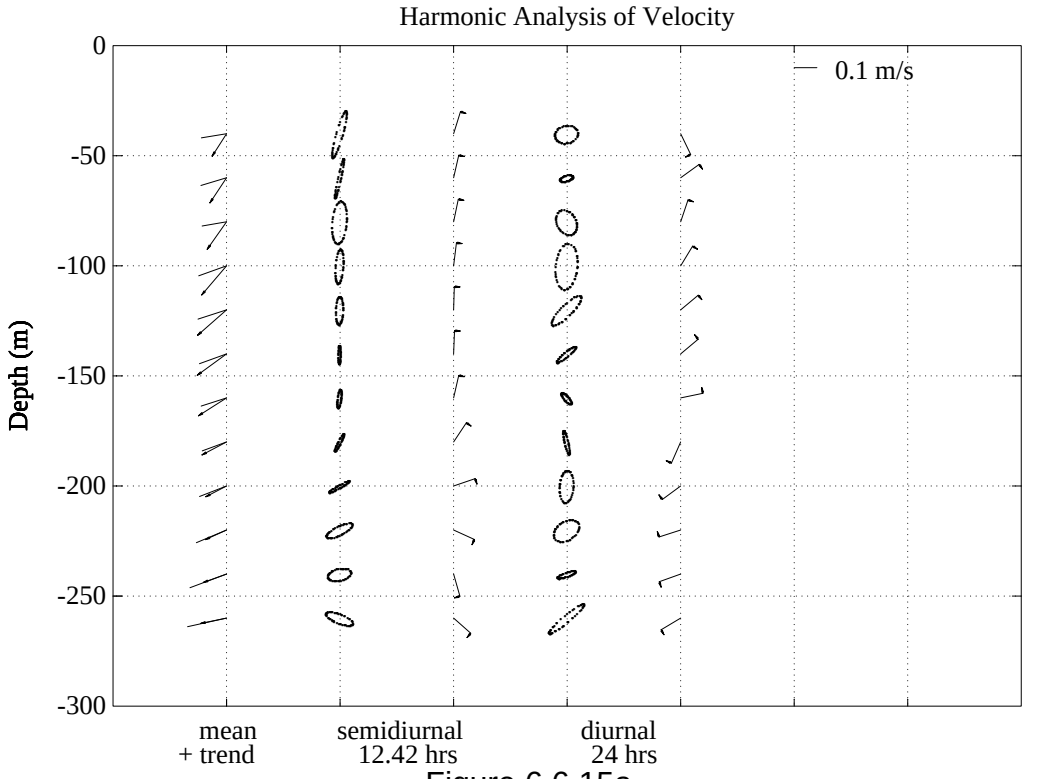

Figure 6.6.15a

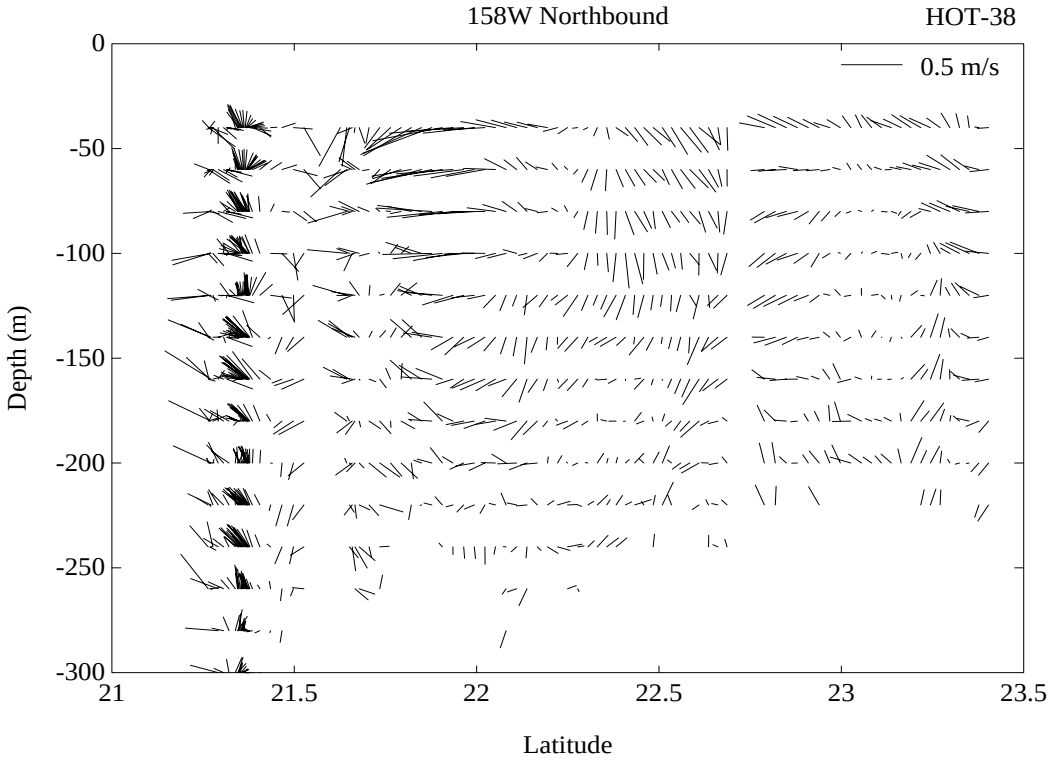

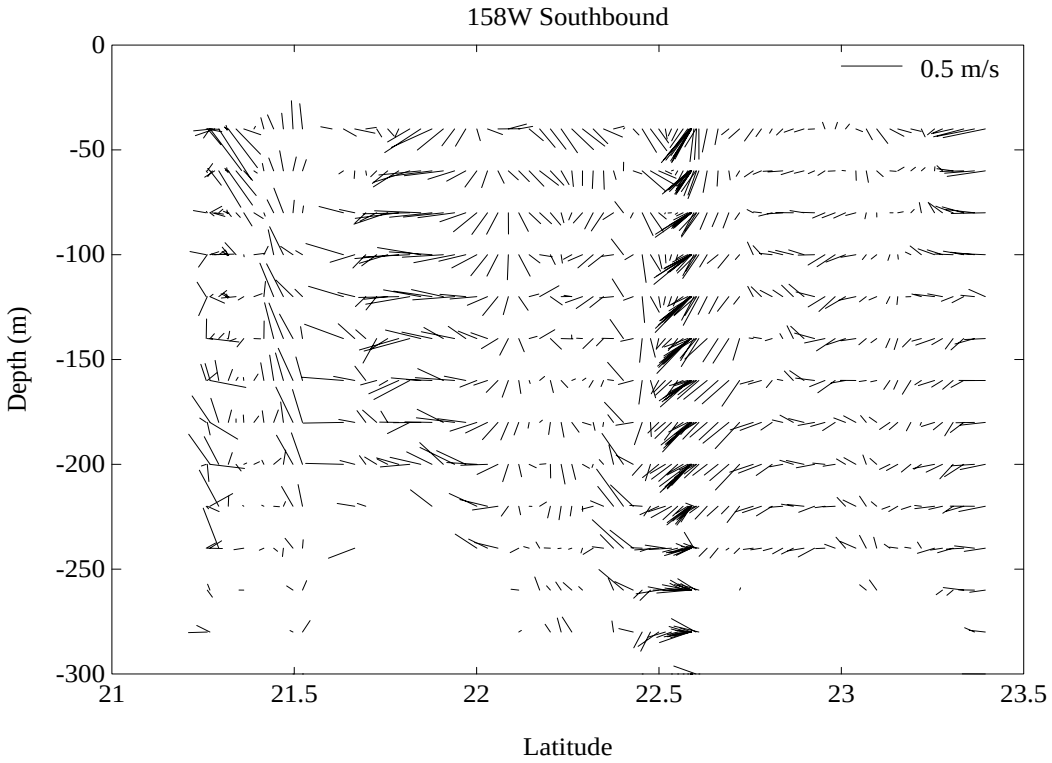

Figure 6.6.15b

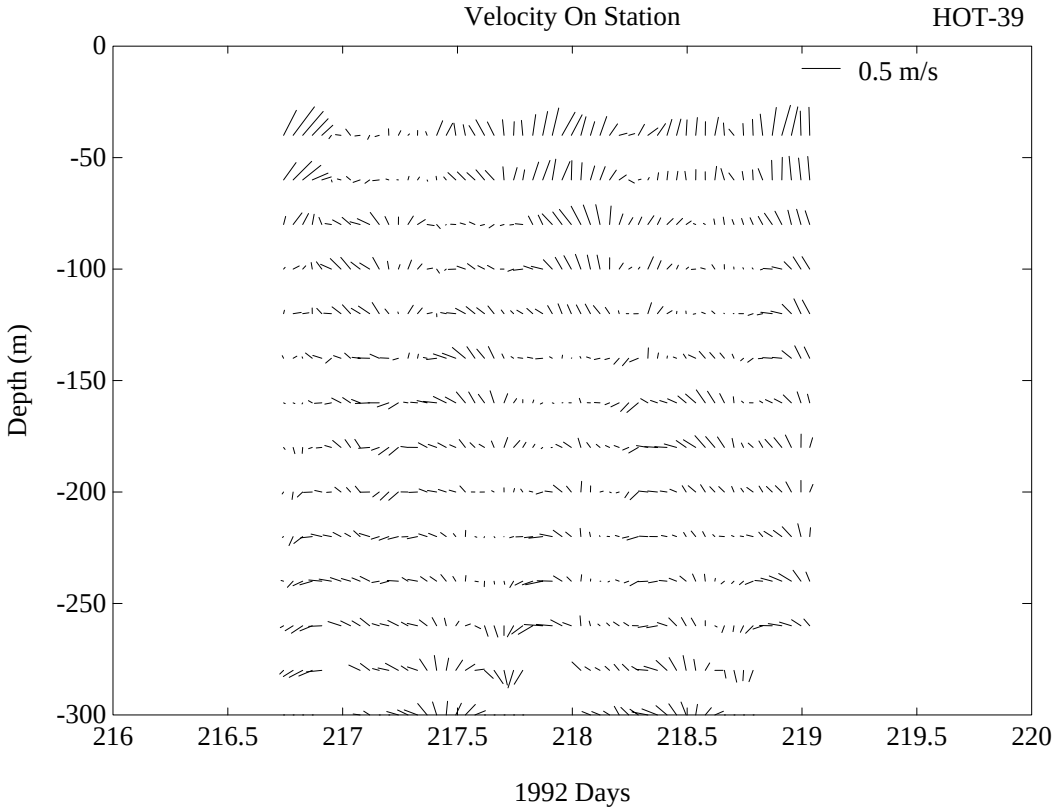

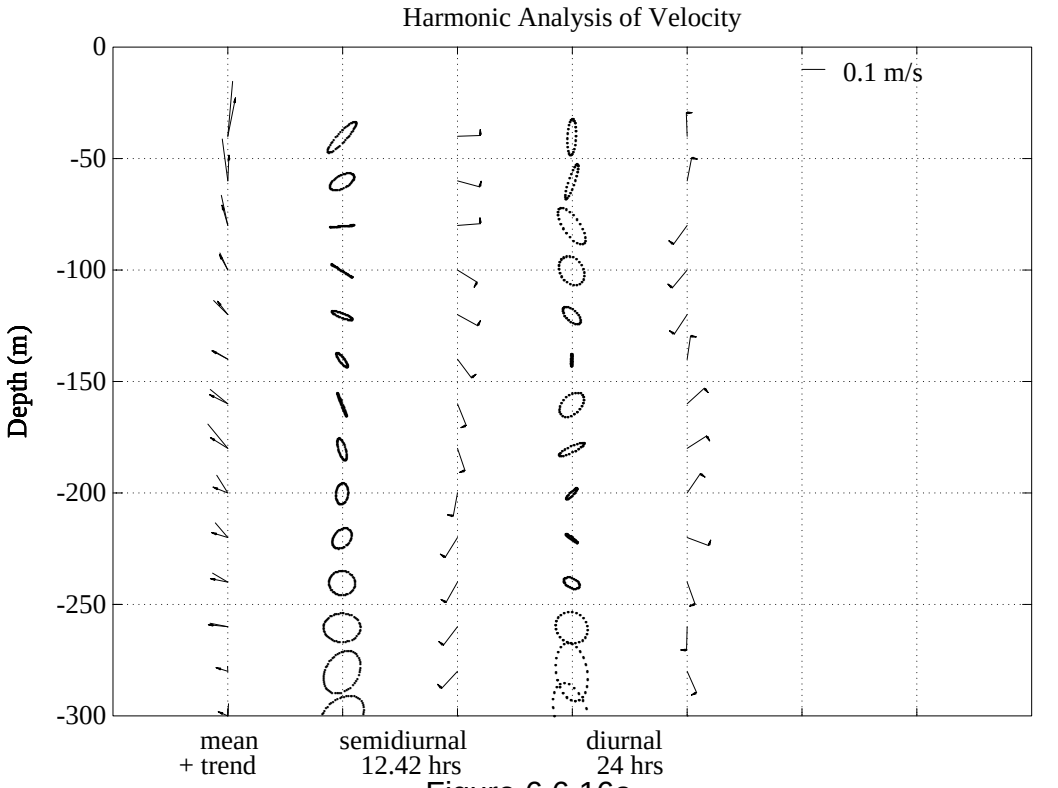

Figure 6.6.16a

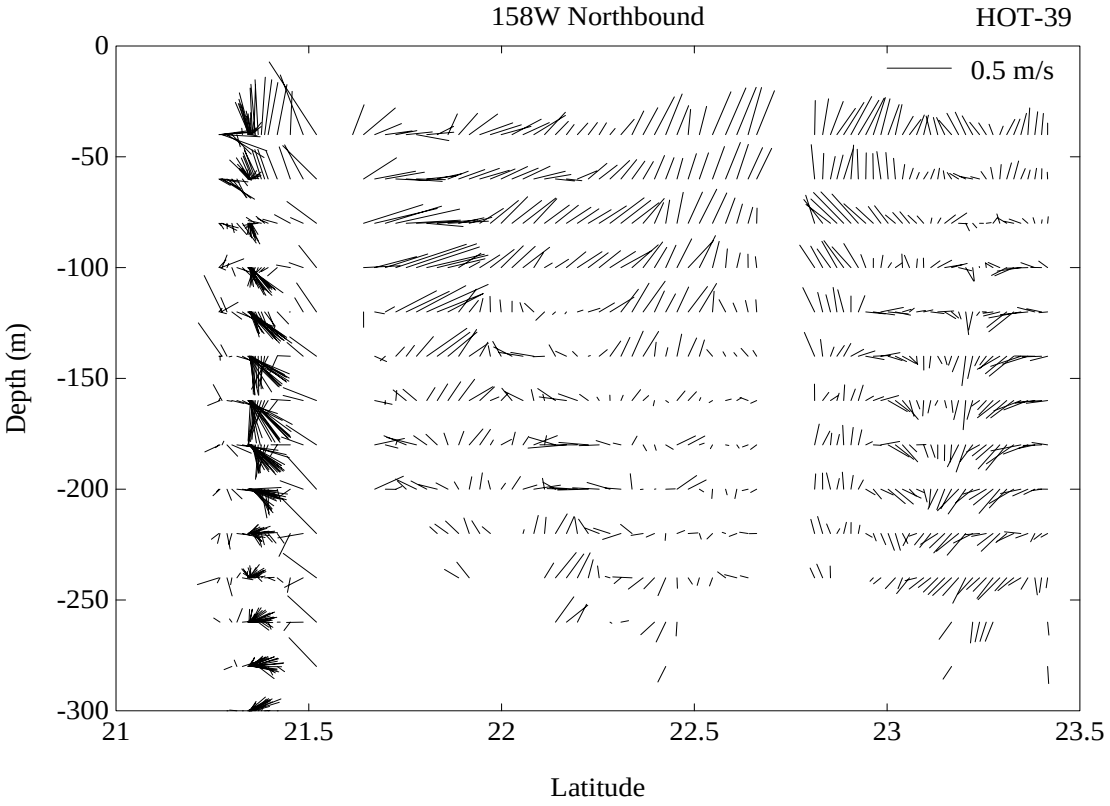

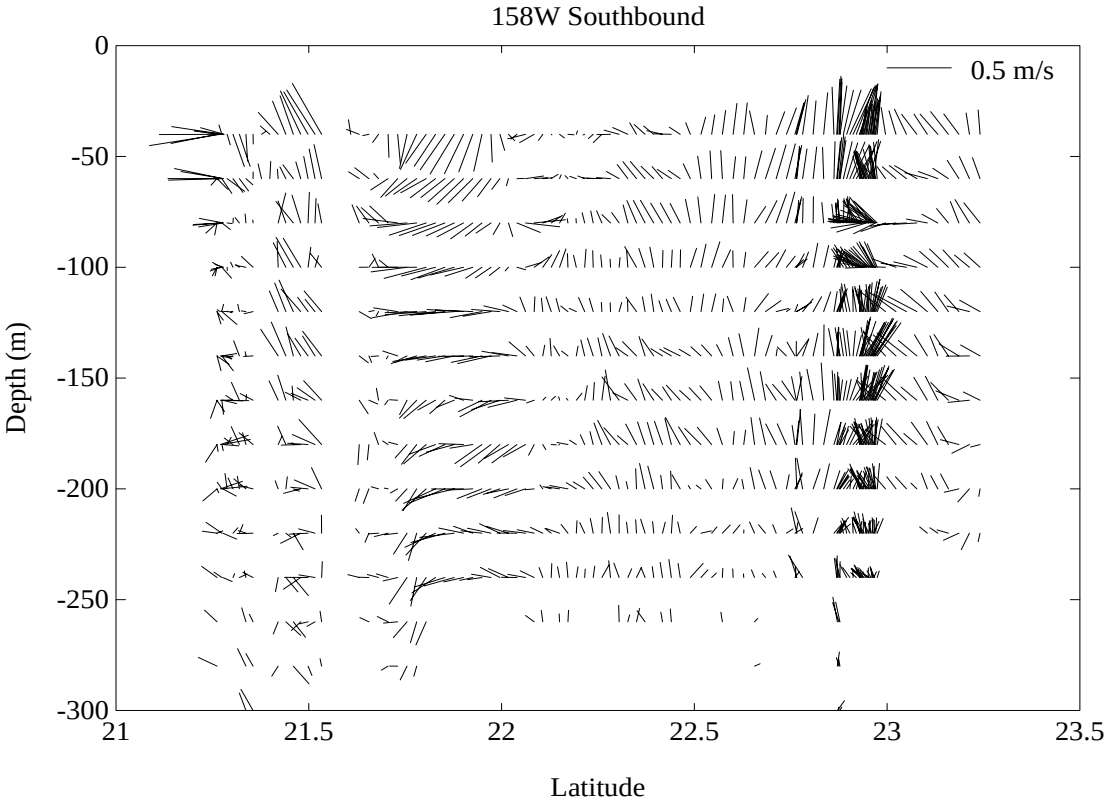

Figure 6.6.16b

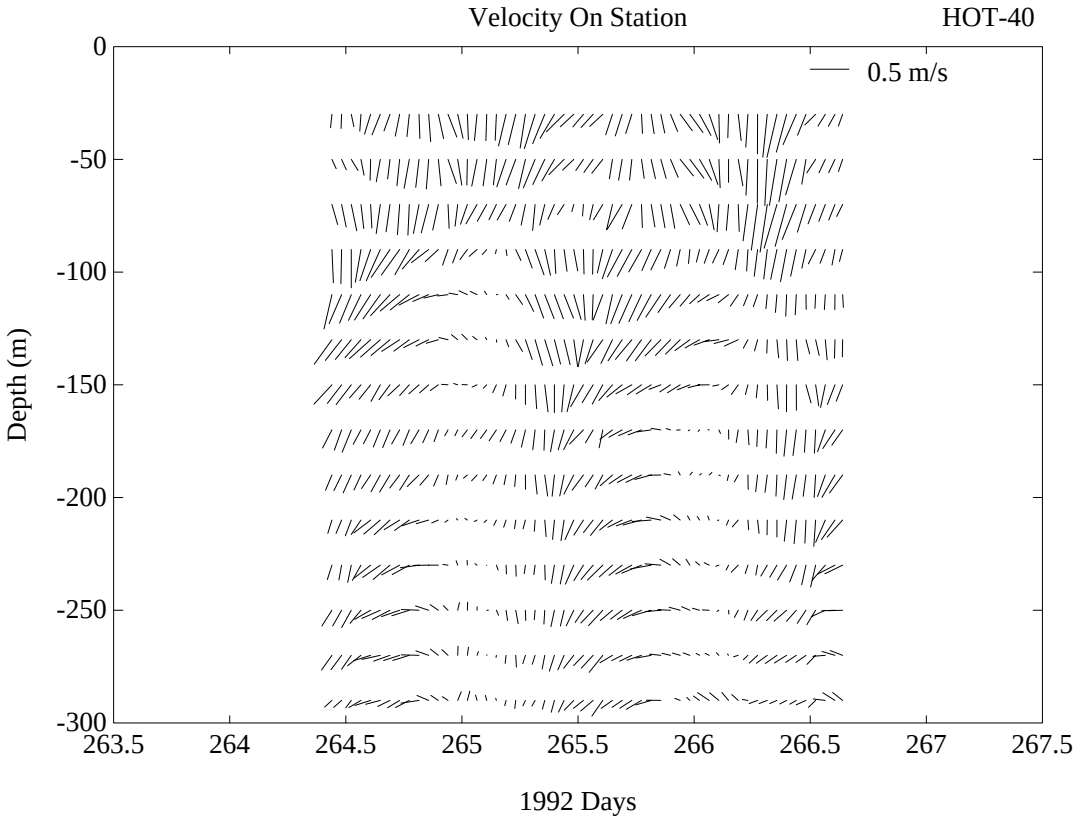

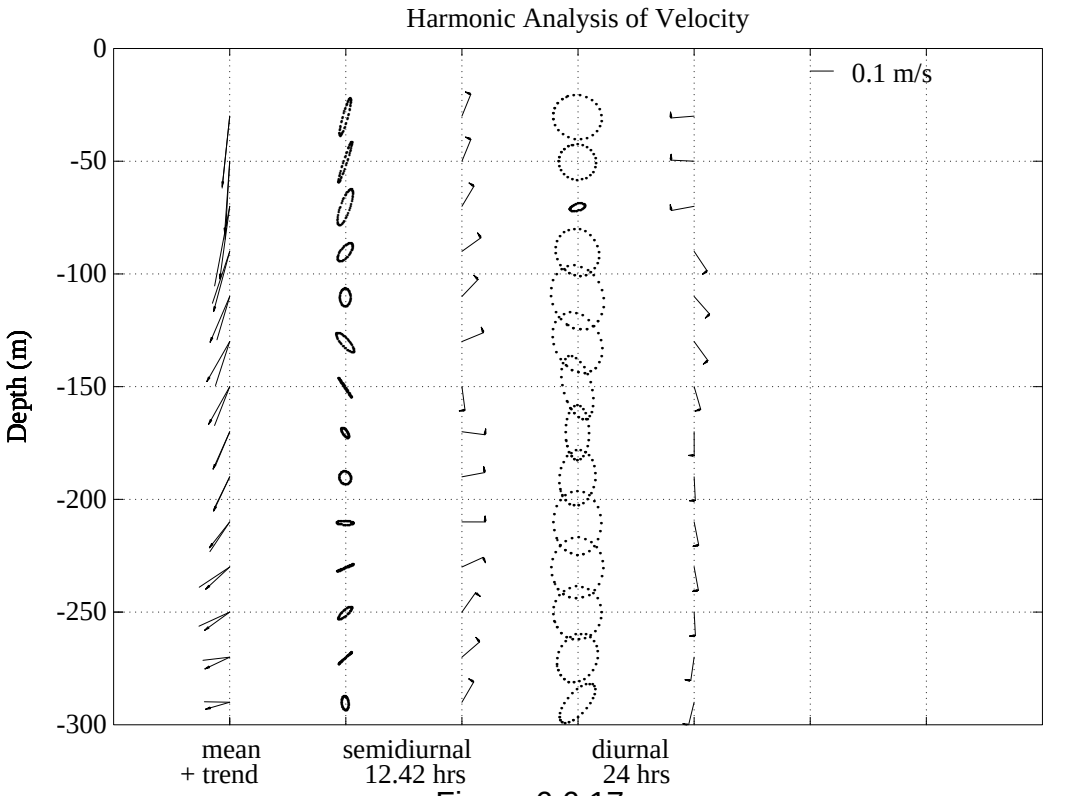

Figure 6.6.17a

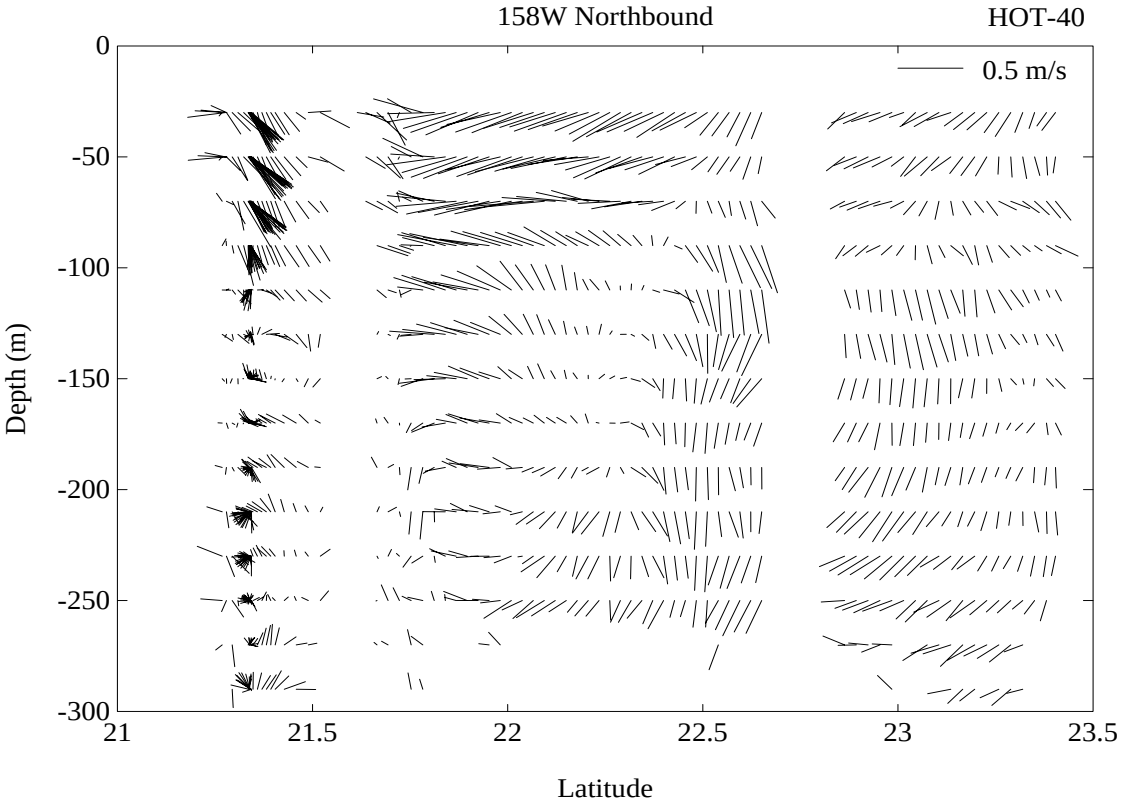

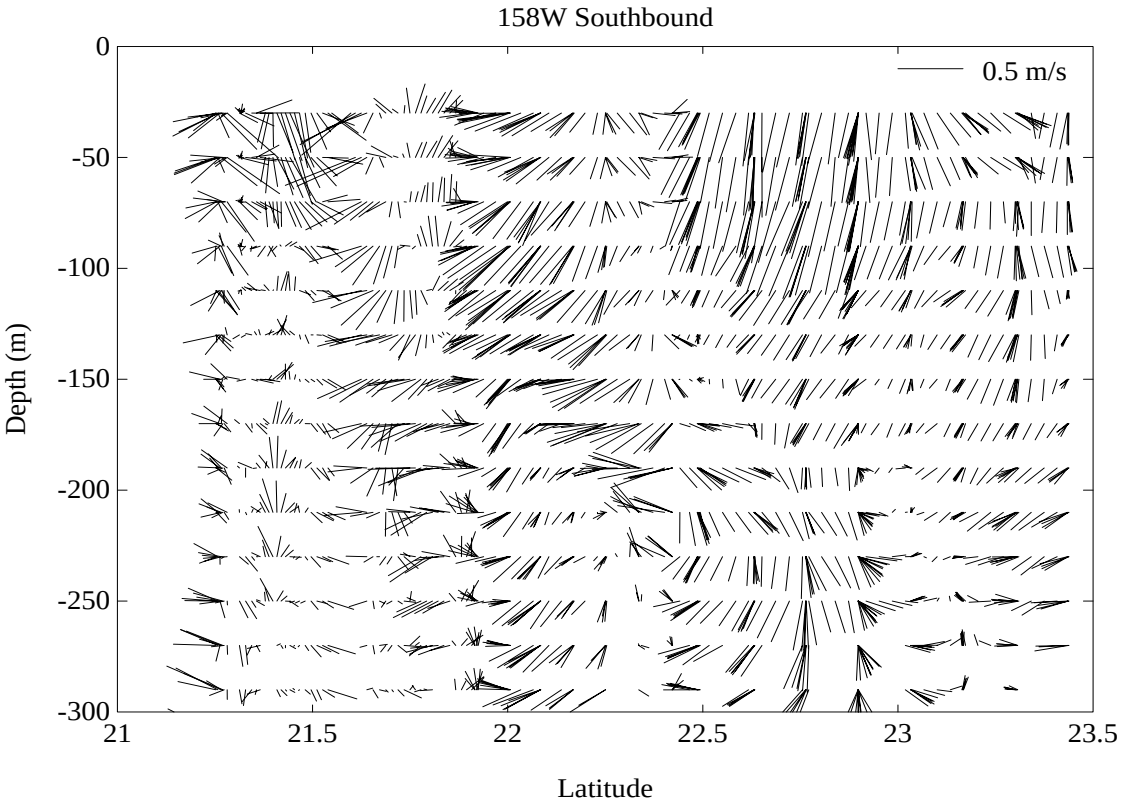

Figure 6.6.17b

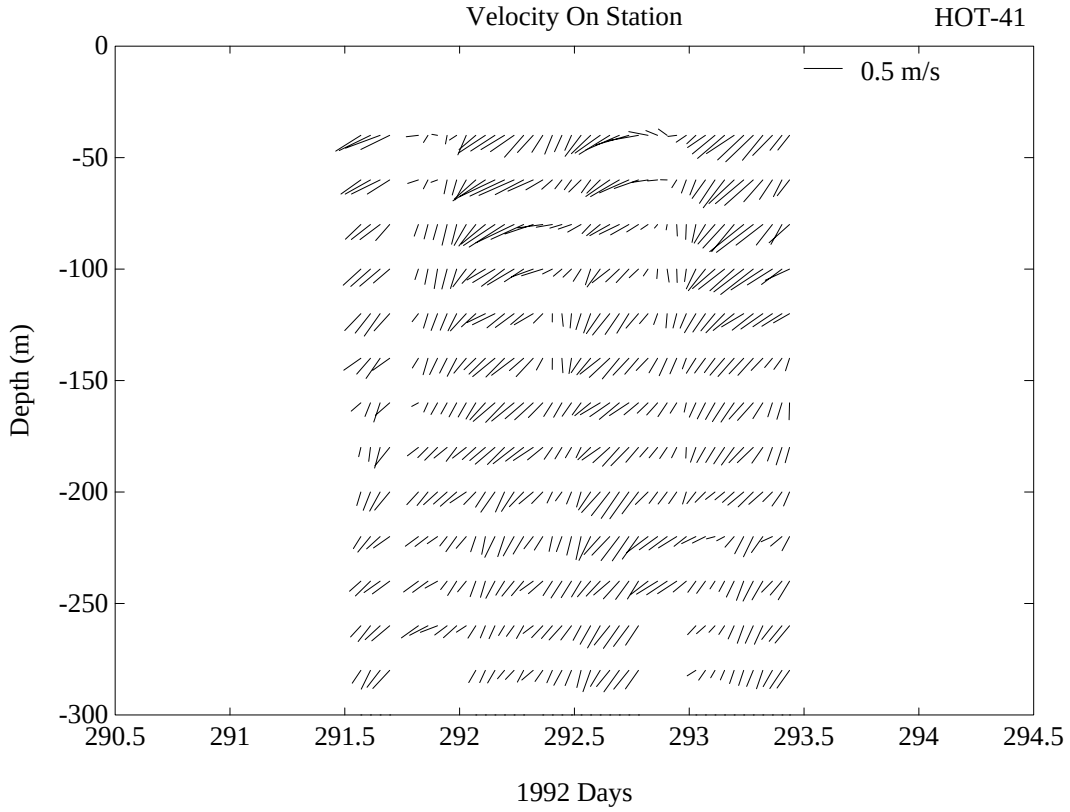

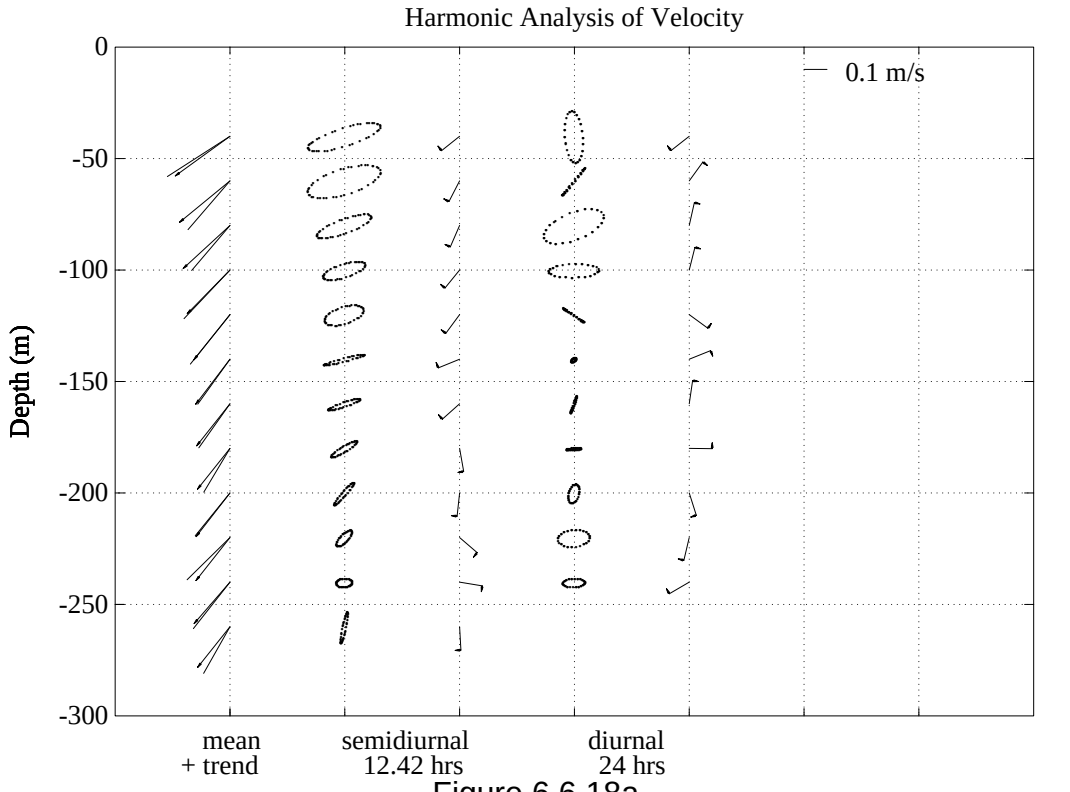

Figure 6.6.18a

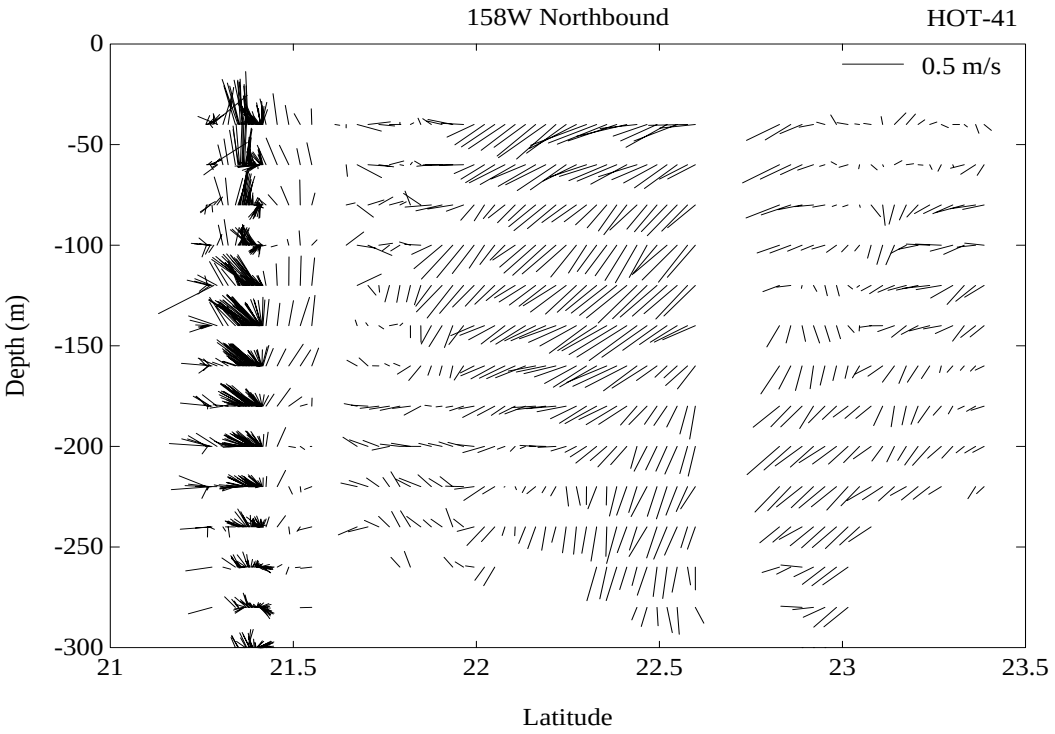

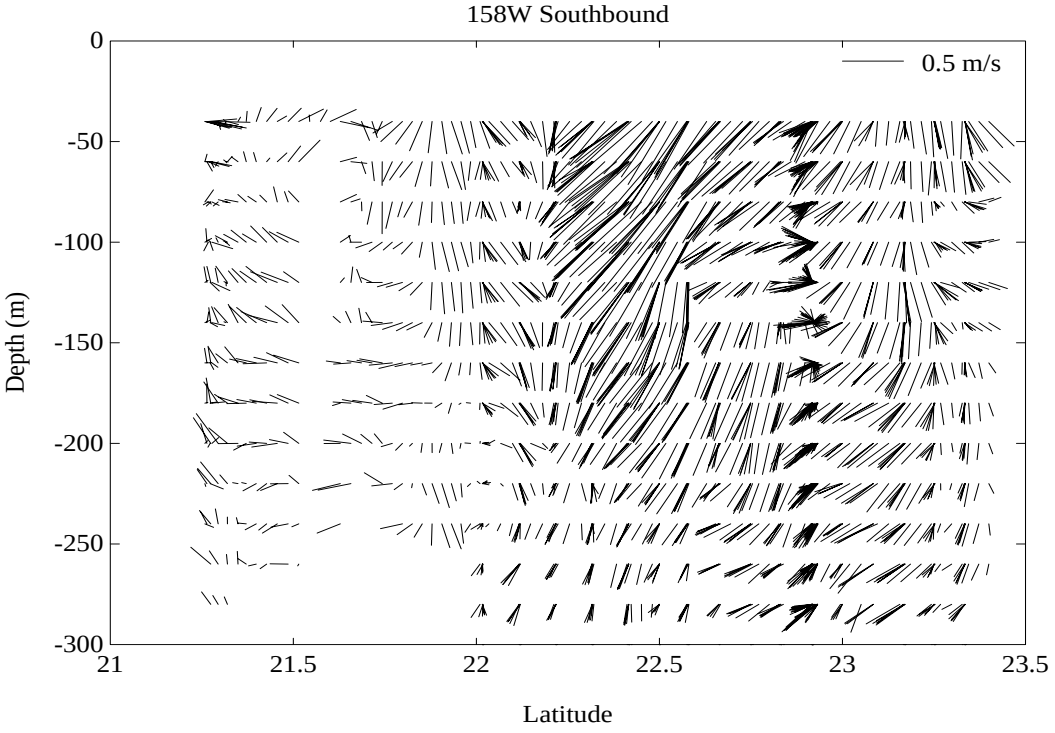

Figure 6.6.18b

6.7. Meteorology

Figure 6.7.1: Upper panel: Atmospheric pressure measured while at Station ALOHA during 1992. Open circles represent individual measurements. Lower panel: Sea surface temperature measured while at Station ALOHA during 1992.

Figure 6.7.2: Upper panel: Dry bulb temperature measured while on station during 1992. Lower panel: Wet bulb air temperature measure while as Station ALOHA during 1992.

Figure 6.7.3: Upper panel: Dry air temperature measured at Station ALOHA during 1992. Dry-wet air temperature measured at Station ALOHA during 1992.

Figure 6.7.4: True winds measured at Station ALOHA on HOT-33 and at NDBC Buoy 51001 during HOT-33. Upper panel: True winds measured at Station ALOHA. Lower panel: True winds collected by NDBC Buoy 51001.

Figure 6.7.5: As in Figure 6.7.4, except for HOT-34.

Figure 6.7.6: As in Figure 6.7.4, except for HOT-35.

Figure 6.7.7: As in Figure 6.7.4, except for HOT-36.

Figure 6.7.8: As in Figure 6.7.4, except for HOT-37.

Figure 6.7.9: As in Figure 6.7.4, except for HOT-38.

Figure 6.7.10: As in Figure 6.7.4, except for HOT-39.

Figure 6.7.11: As in Figure 6.7.4, except for HOT-40.

Figure 6.7.12: As in Figure 6.7.4, except for HOT-41.

Figure 6.7.13: Air temperature measured at Station ALOHA and NDBC buoy 51001. Upper panel: Air temperature measured at both the buoy and at Station ALOHA plotted against Julian day from 1 January 1990. Lower panel: Scatter plot of these data.

Figure 6.7.14: Sea surface temperature at Station ALOHA and the NDBC buoy. Upper and lower panels as described in Figure 6.7.13.

Figure 6.7.15: Atmospheric pressure at Station ALOHA and the NDBC buoy. Upper and lower panels as described in Figure 6.7.13.

Figure 6.7.16: Wind speed at Station ALOHA and the NDBC buoy. Upper and lower panels as described in Figure 6.7.13.

Figure 6.7.17: Wind direction at Station ALOHA and the NDBC buoy. Upper and lower panels as described in Figure 6.7.13.

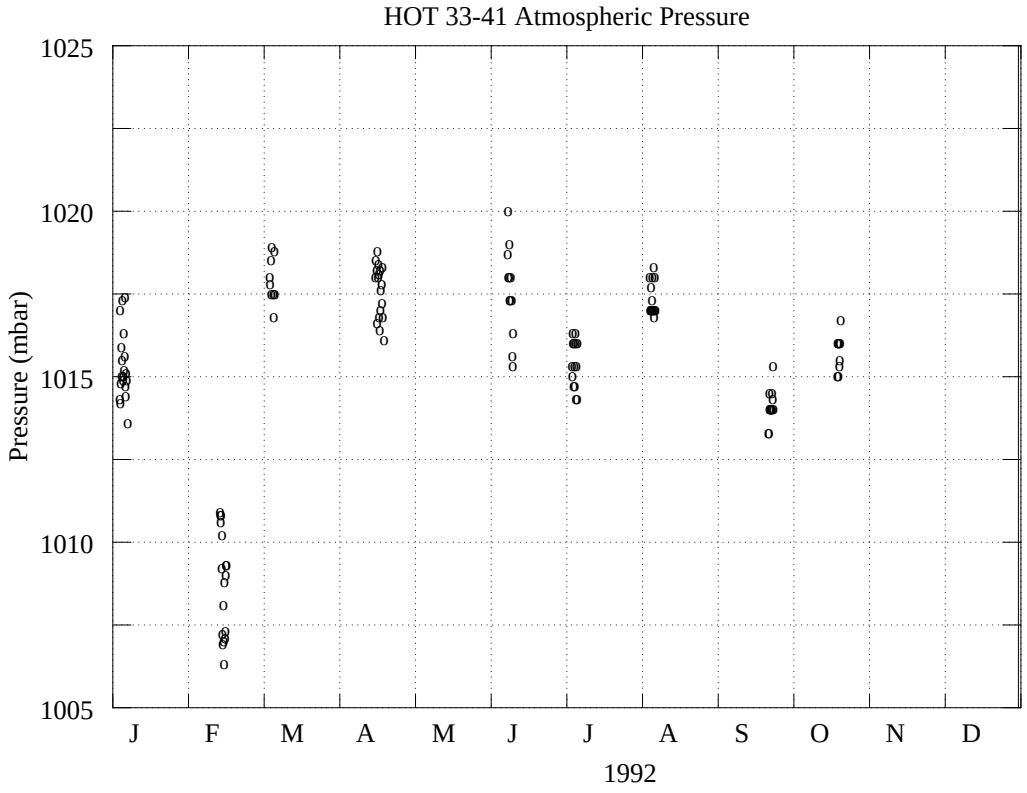
HOT 33-41 Atmospheric Pressure
Pressure (mbar)
1025
1020
1015
1010
1005
J
F
M
A
M
J
J
A
S
O
N
D
1992

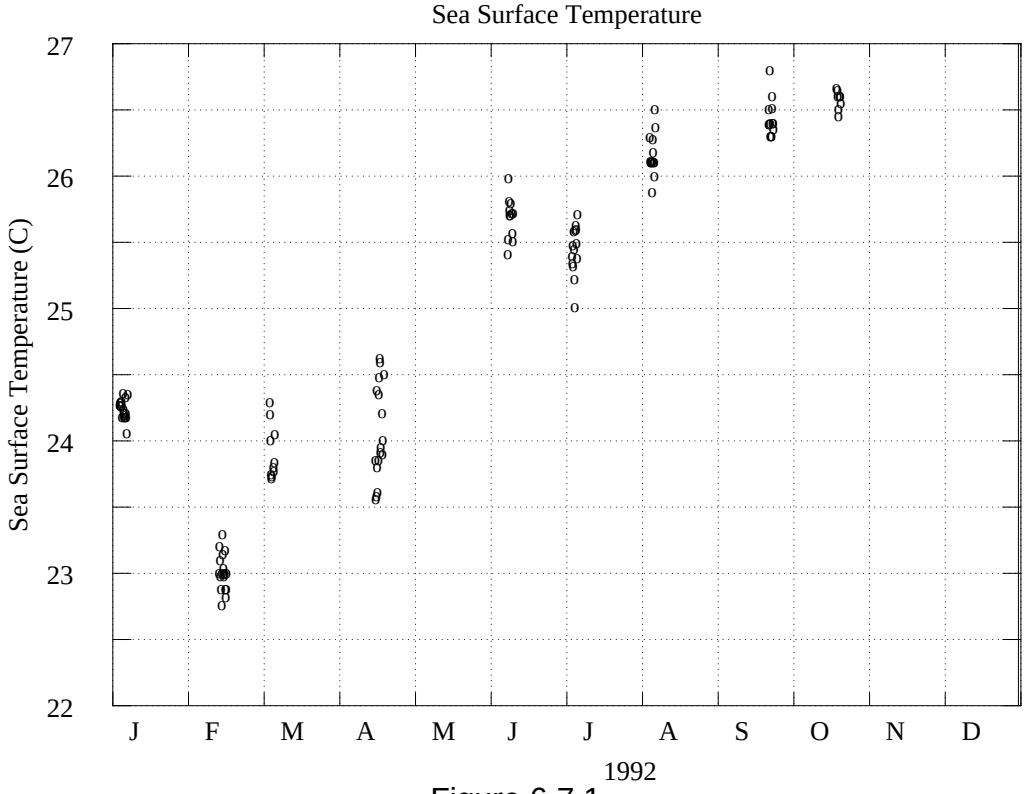
Sea Surface Temperature
Sea Surface Temperature (C)
27
26
25
24
23
22
J
F
M
A
M
J
J
A
S
O
N
D
1992

Figure 6.7.1

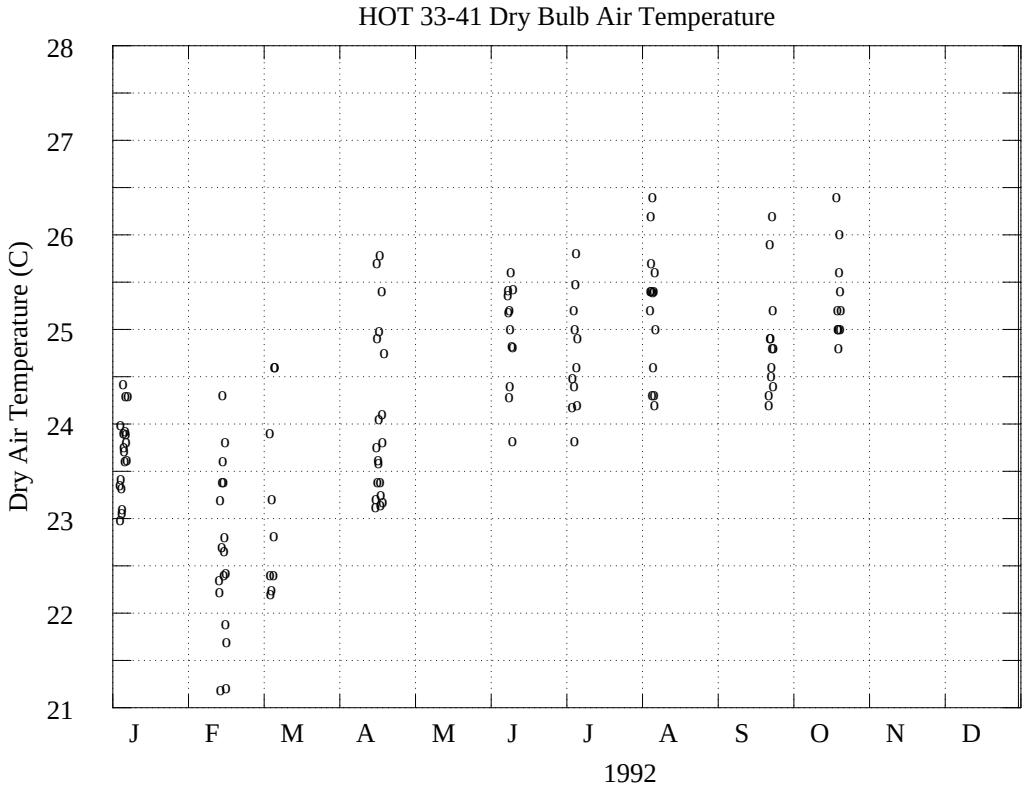
HOT 33-41 Dry Bulb Air Temperature
Dry Air Temperature (C)
28
27
26
25
24
23
22
21
J
F
M
A
M
J
J
A
S
O
N
D
1992

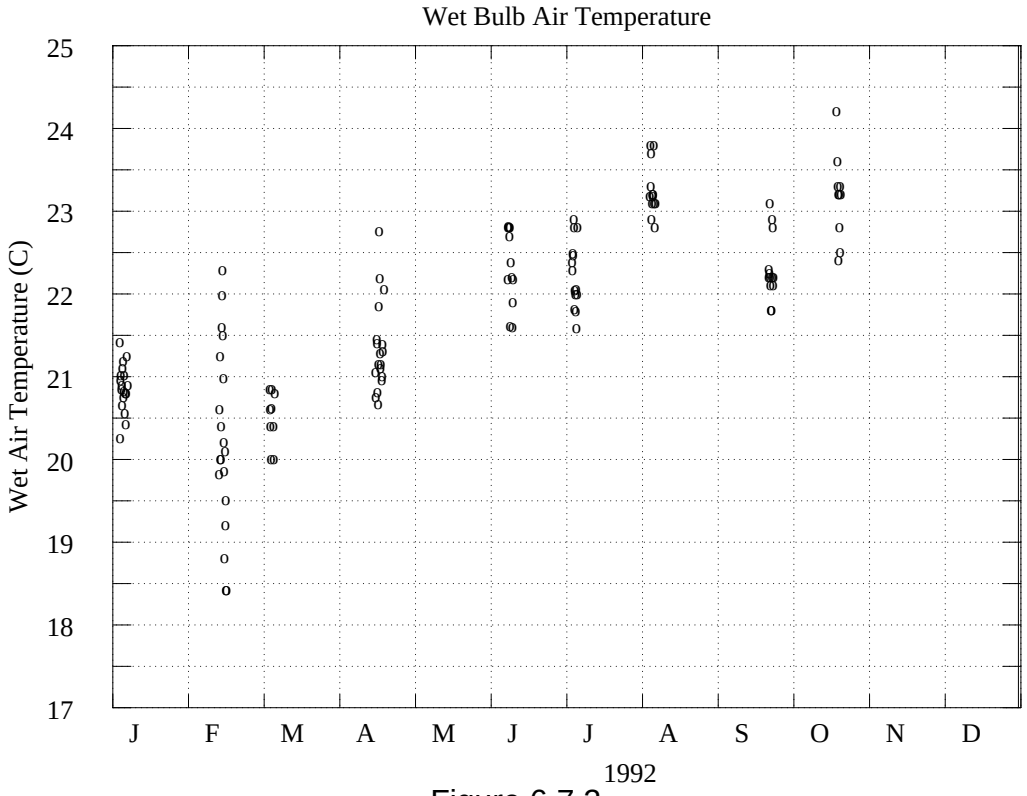
Wet Bulb Air Temperature
Wet Air Temperature (C)
25
24
23
22
21
20
19
18
17
J
F
M
A
M
J
J
A
S
O
N
D
1992

Figure 6.7.2

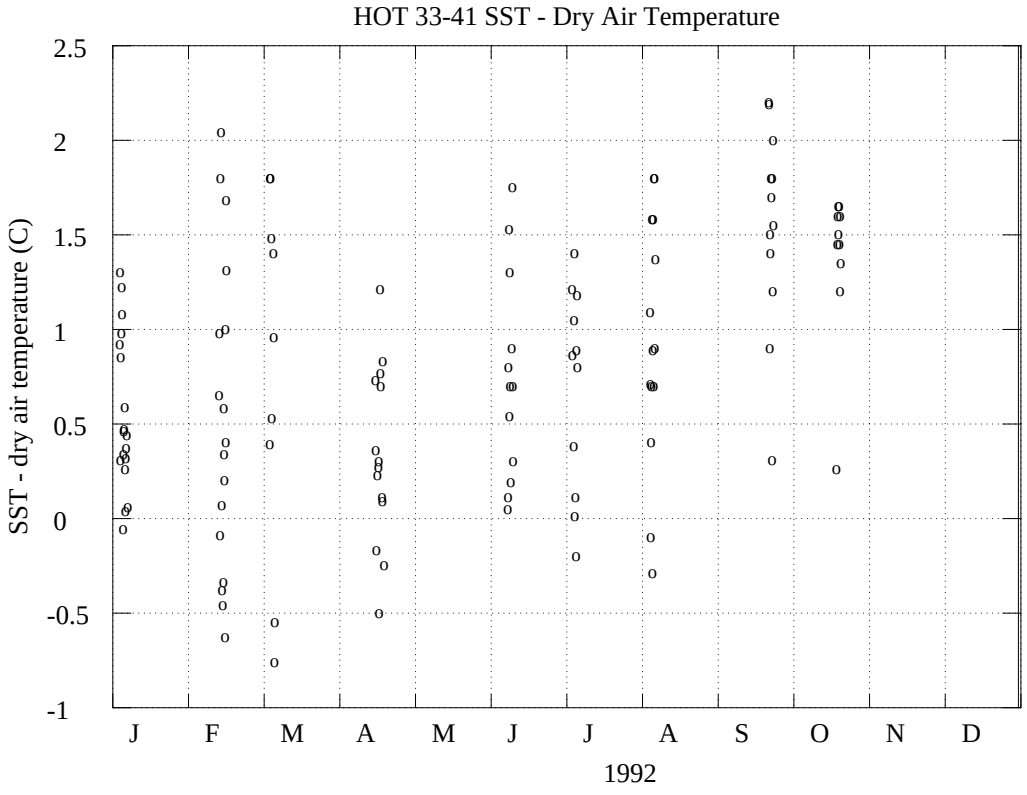
HOT 33-41 SST - Dry Air Temperature
SST - dry air temperature (C)
2.5
2
1.5
1
0.5
0
-0.5
-1
J
F
M
A
M
J
J
A
S
O
N
D
1992

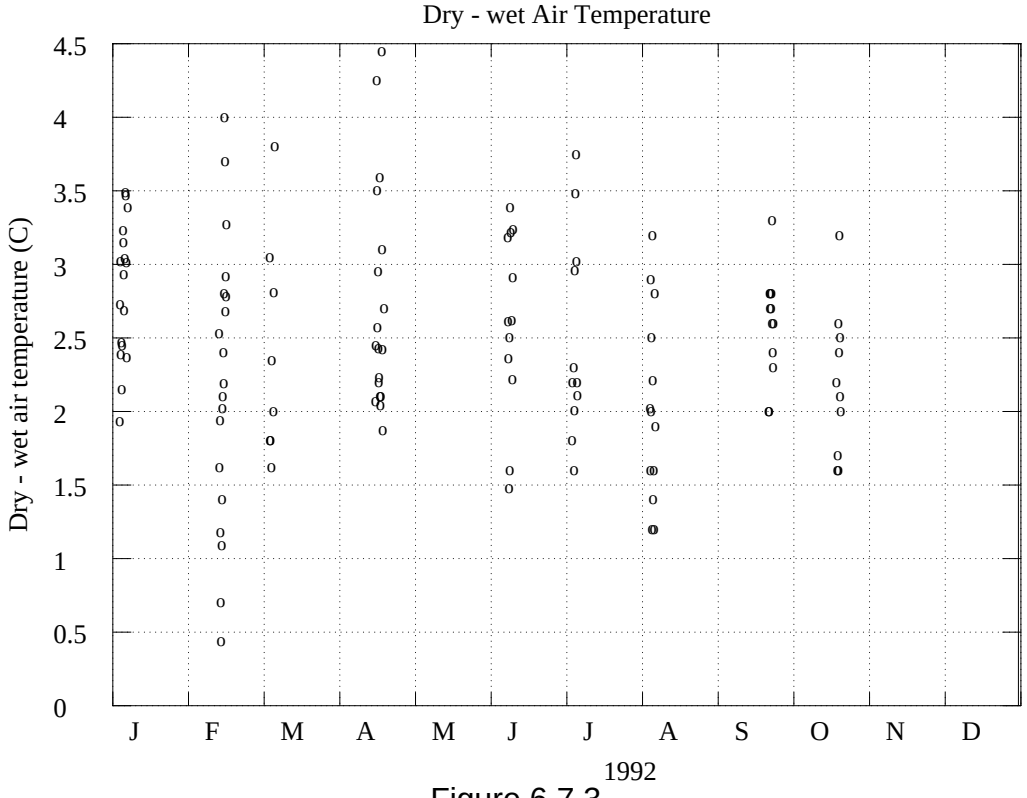
Dry - wet Air Temperature
Dry - wet air temperature (C)
4.5
4
3.5
3
2.5
2
1.5
1
0.5
0
J
F
M
A
M
J
J
A
S
O
N
D
1992

Figure 6.7.3

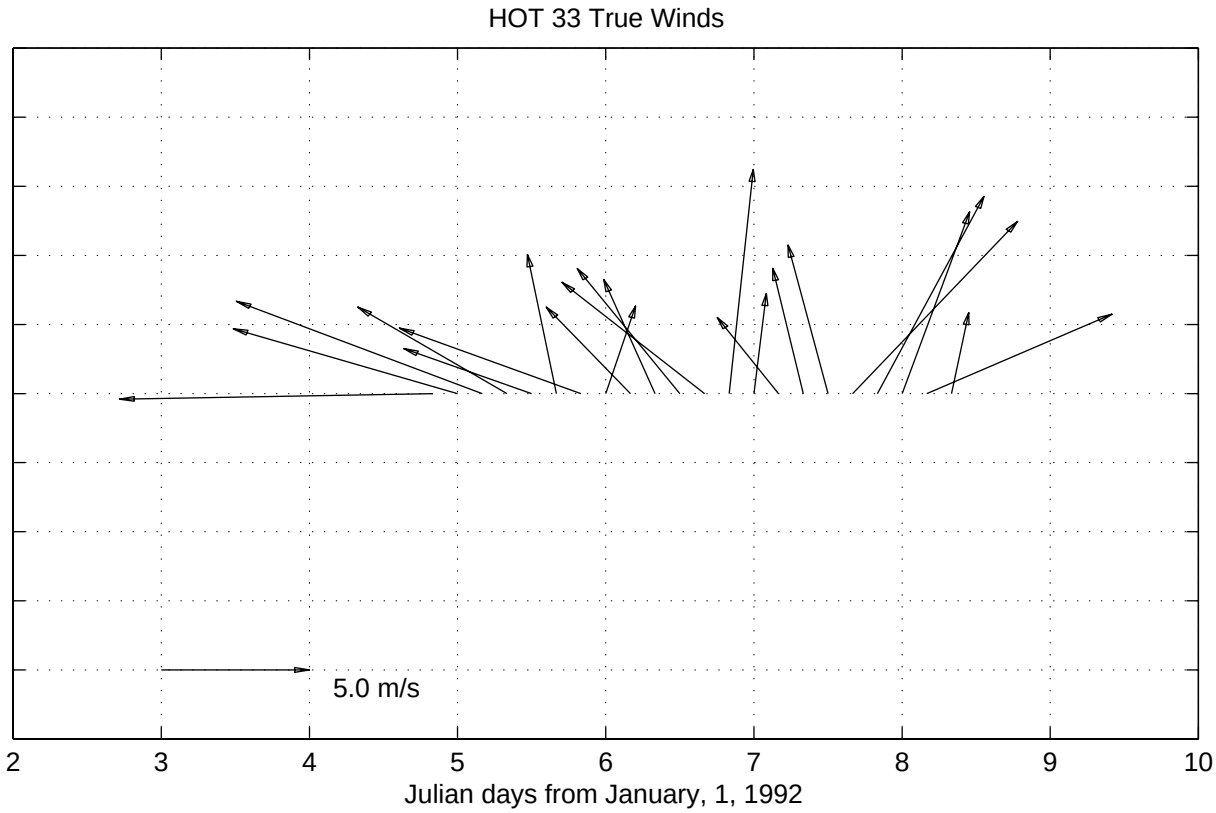
HOT 33 True Winds
5.0 m/s
2
3
4
5
6
7
8
9
10
Julian days from January, 1, 1992

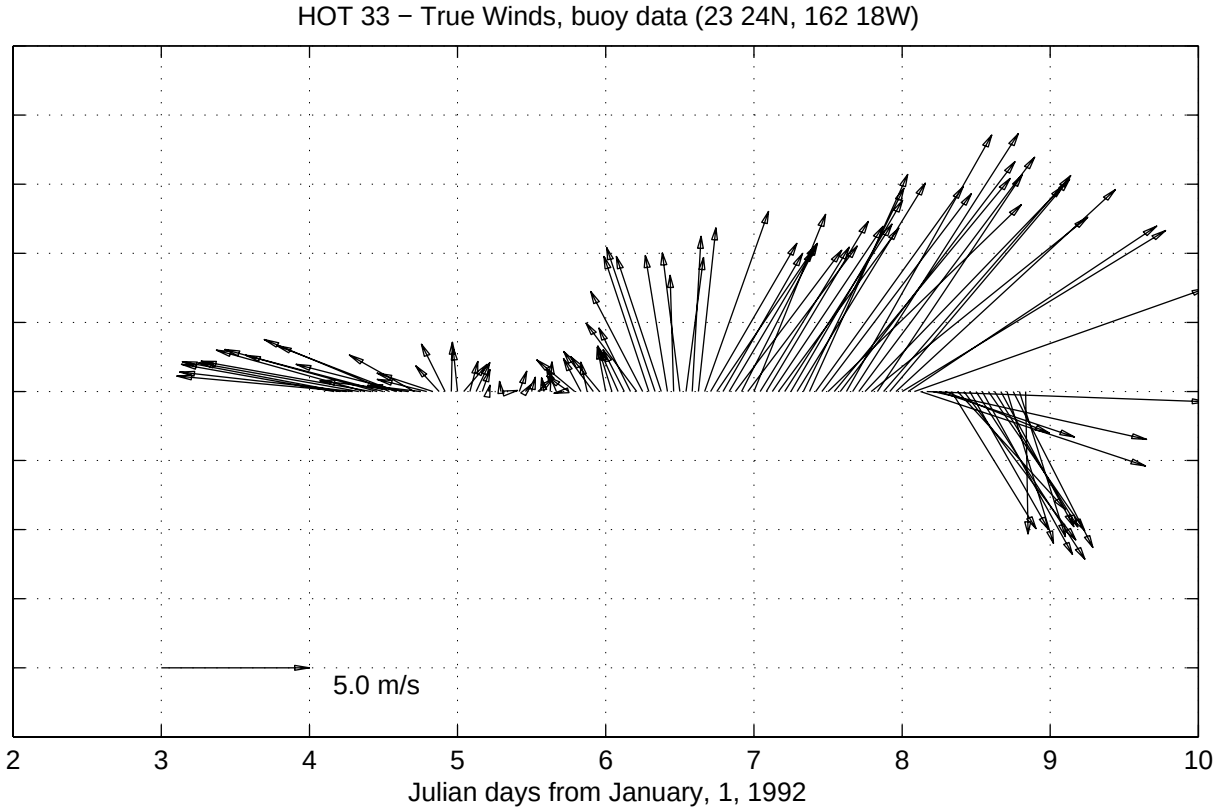
HOT 33 − True Winds, buoy data (23 24N, 162 18W)
5.0 m/s
2
3
4
5
6
7
8
9
10
Julian days from January, 1, 1992

Figure 6.7.4

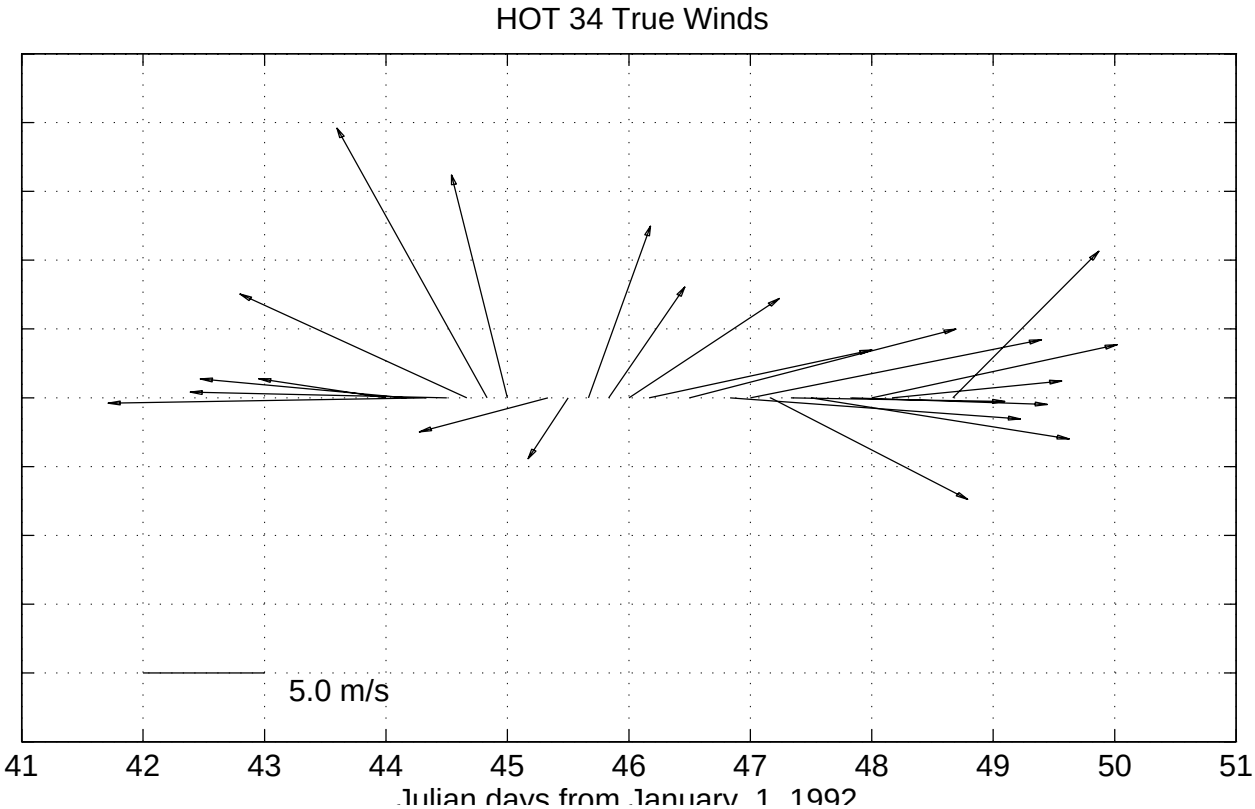
HOT 34 True Winds
5.0 m/s
41
42
43
44
45
46
47
48
49
50
51
Julian days from January, 1, 1992

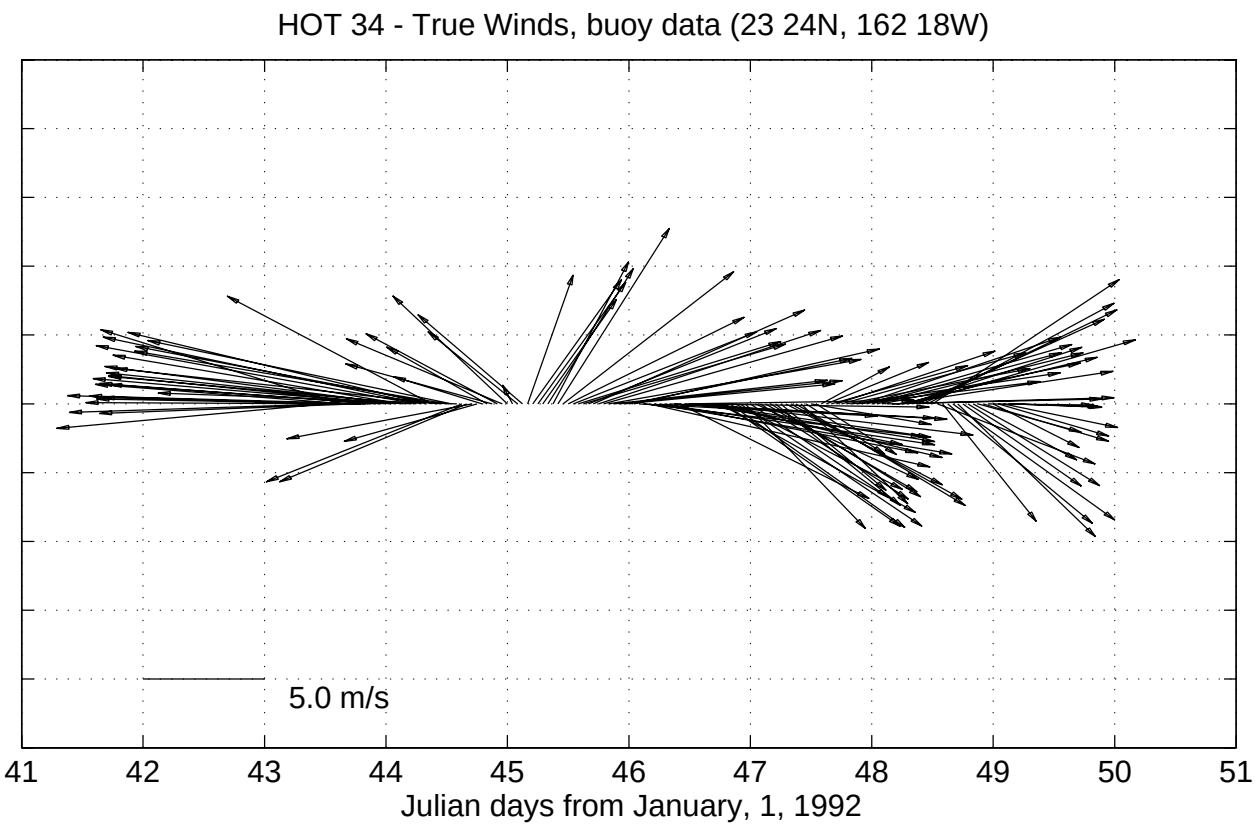
HOT 34 - True Winds, buoy data (23 24N, 162 18W)
5.0 m/s
41
42
43
44
45
46
47
48
49
50
51
Julian days from January, 1, 1992

Figure 6.7.5

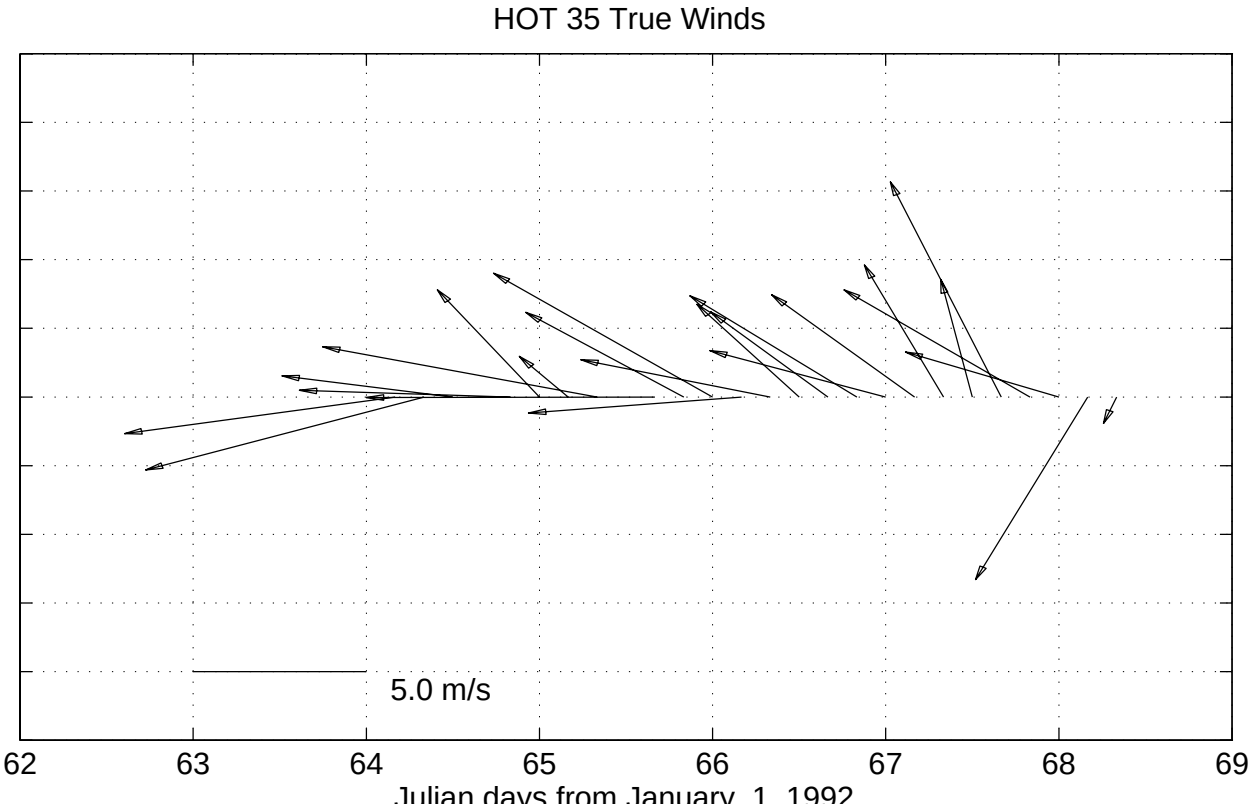

HOT 35 - True Winds, buoy data (23 24N, 162 18W)

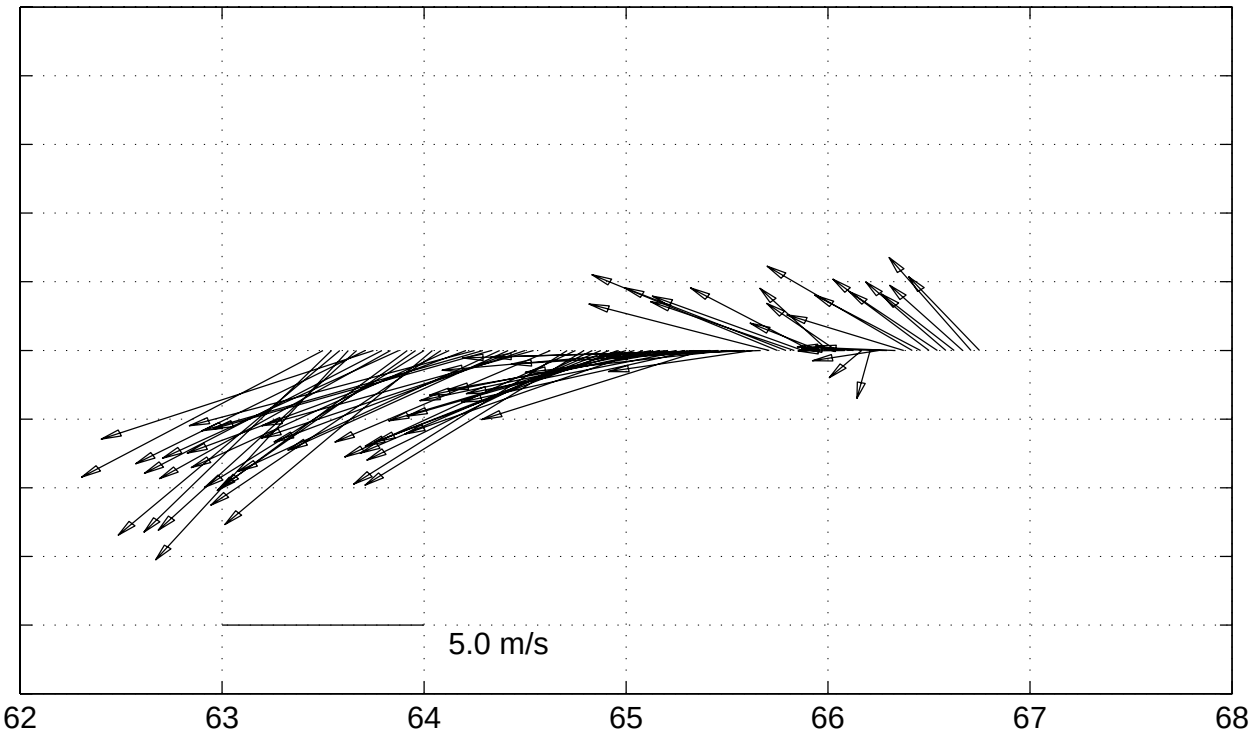

Figure 6.7.6

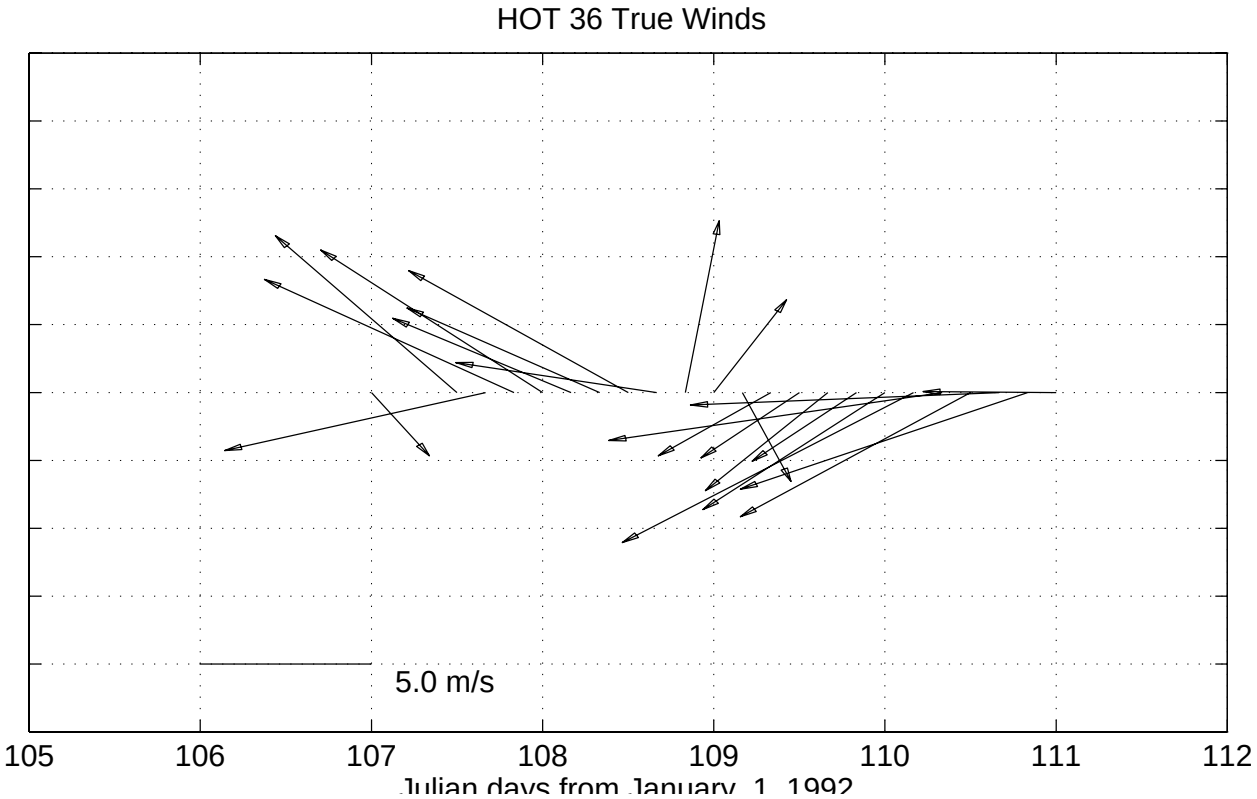
HOT 36 True Winds
5.0 m/s
105
106
107
108
109
110
111
112
Julian days from January, 1, 1992

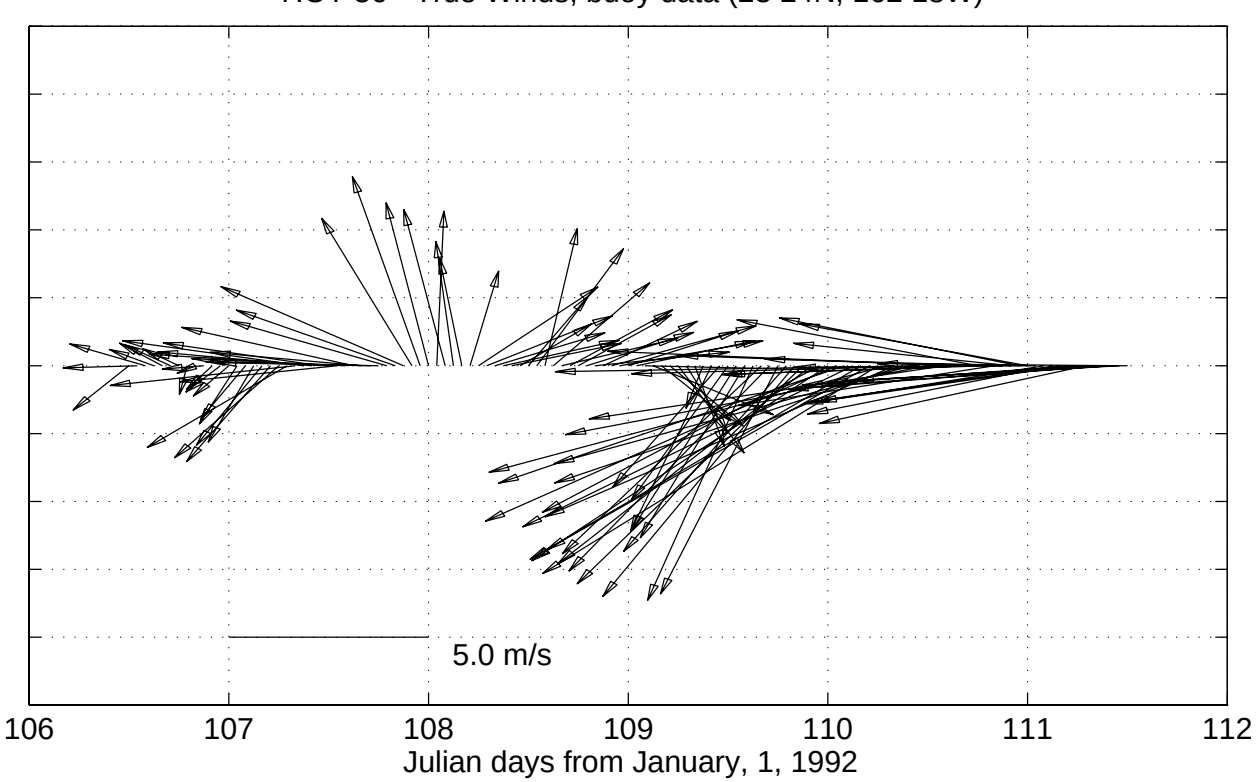
HOT 36 - True Winds, buoy data (23 24N, 162 18W)
5.0 m/s
106
107
108
109
110
111
112
Julian days from January, 1, 1992

Figure 6.7.7

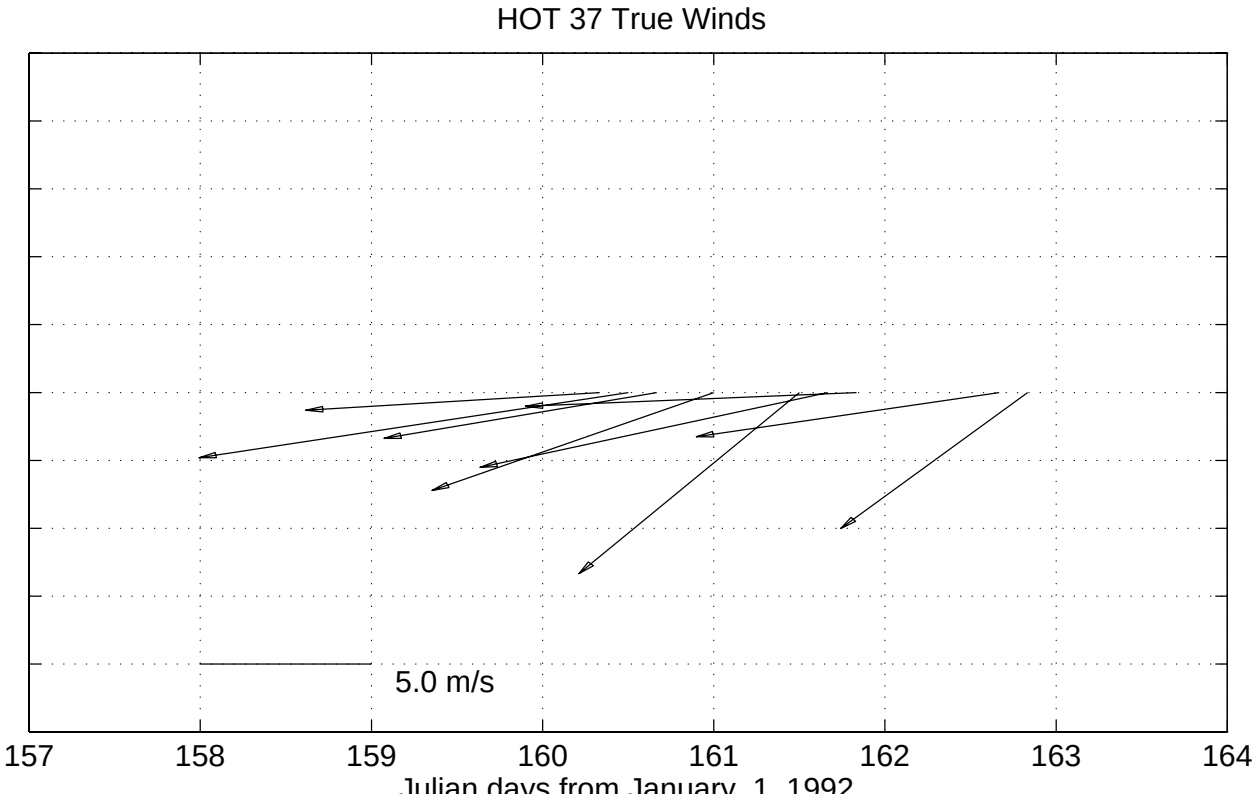
HOT 37 True Winds
5.0 m/s
157
158
159
160
161
162
163
164
Julian days from January, 1, 1992

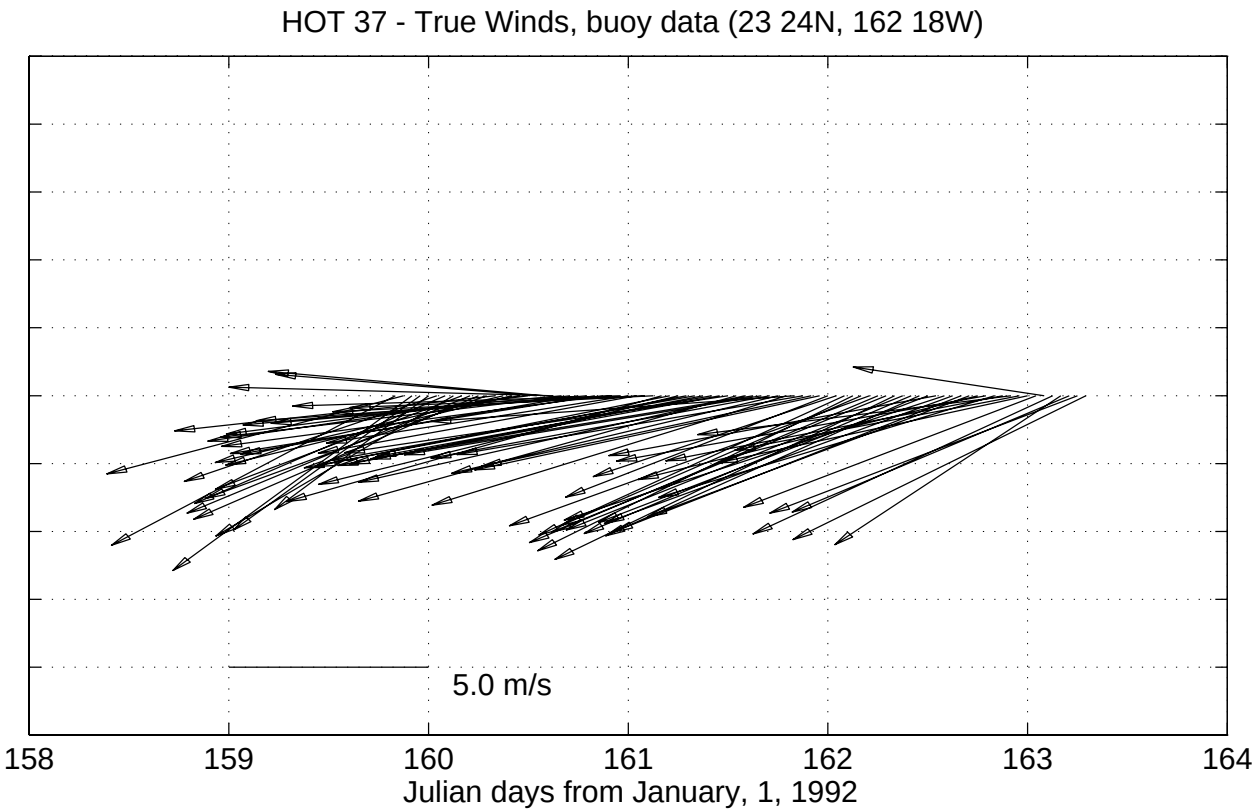
HOT 37 - True Winds, buoy data (23 24N, 162 18W)
5.0 m/s
158
159
160
161
162
163
164
Julian days from January, 1, 1992

Figure 6.7.8

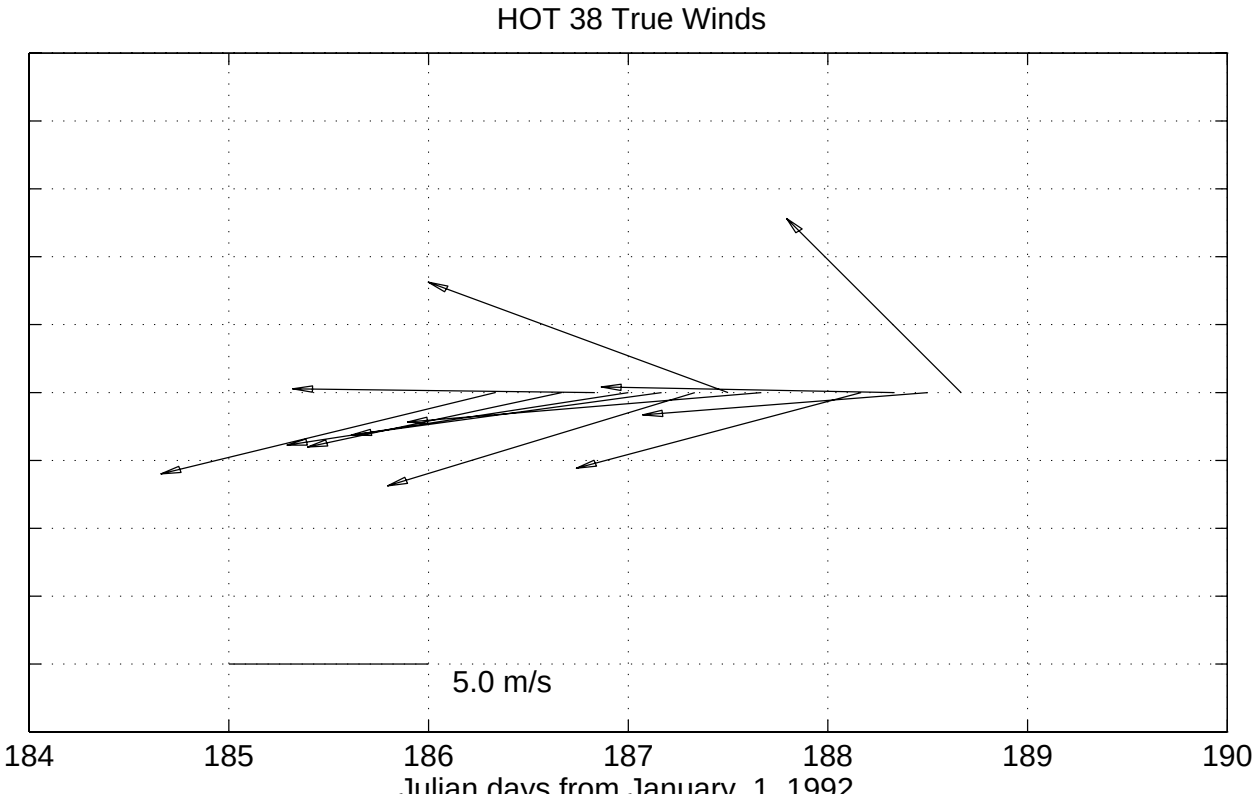
HOT 38 True Winds
5.0 m/s
184
185
186
187
188
189
190
Julian days from January, 1, 1992

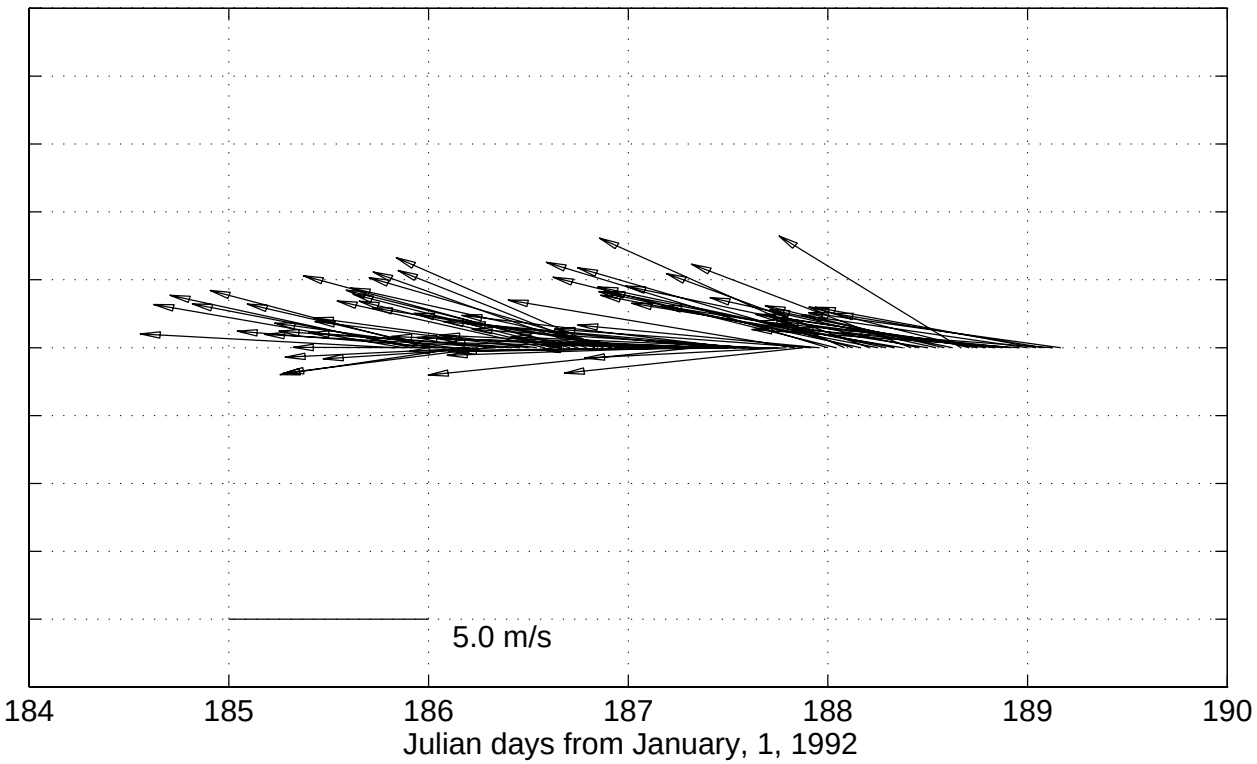
HOT 38 - True Winds, buoy data (23 24N, 162 18W)
5.0 m/s
184
185
186
187
188
189
190
Julian days from January, 1, 1992

Figure 6.7.9

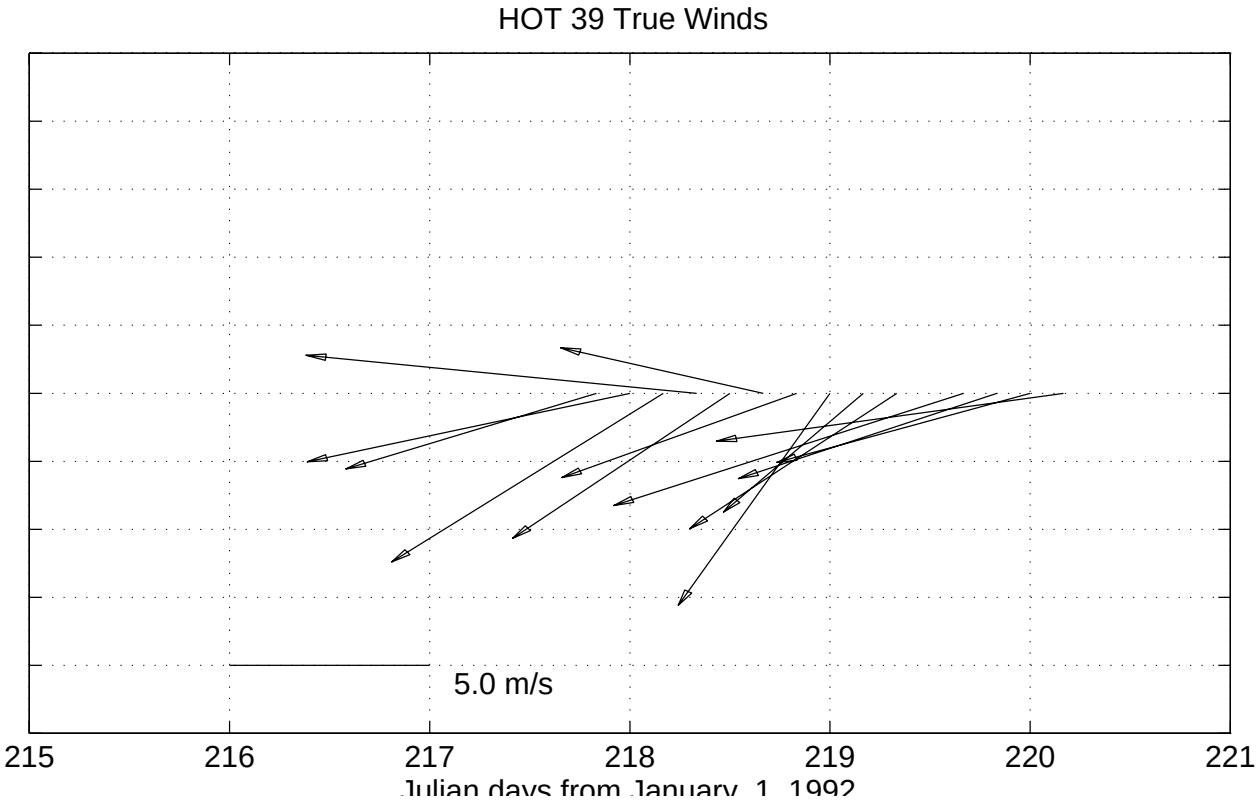
HOT 39 True Winds
5.0 m/s
215
216
217
218
219
220
221
Julian days from January, 1, 1992

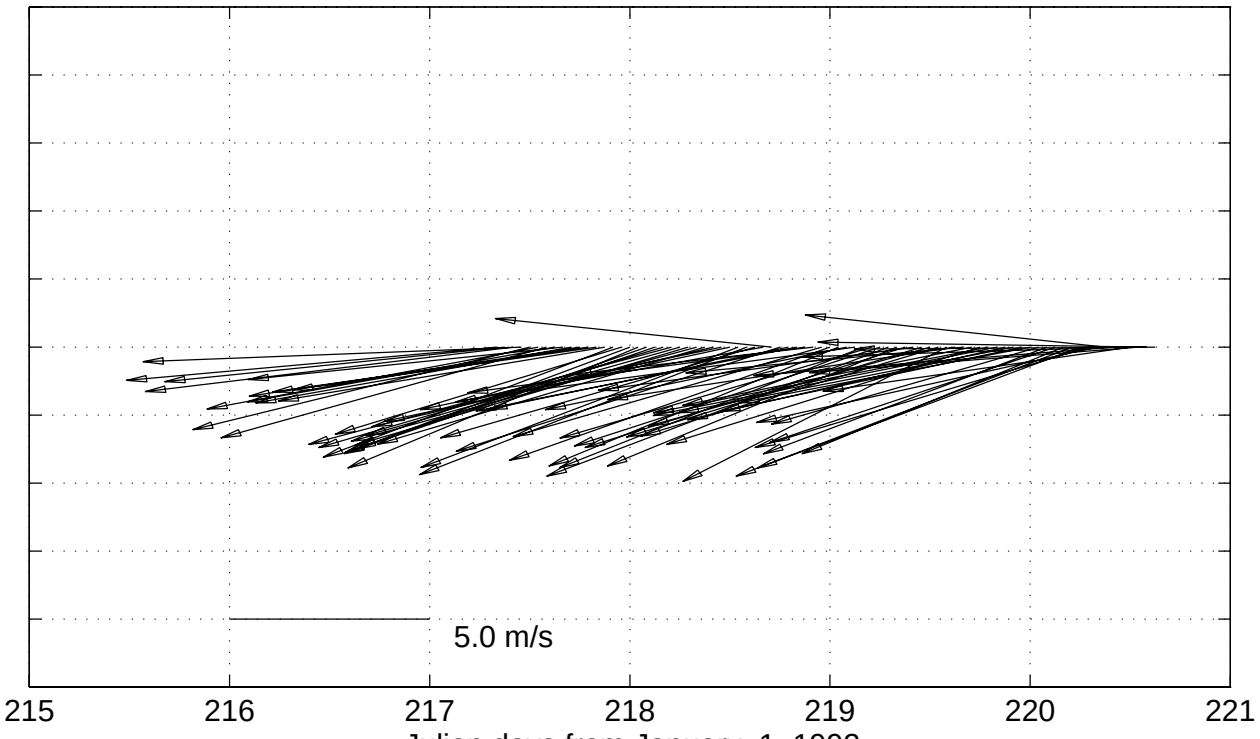
HOT 39 - True Winds, buoy data (23 24N, 162 18W)
5.0 m/s
215
216
217
218
219
220
221
Julian days from January, 1, 1992

Figure 6.7.10

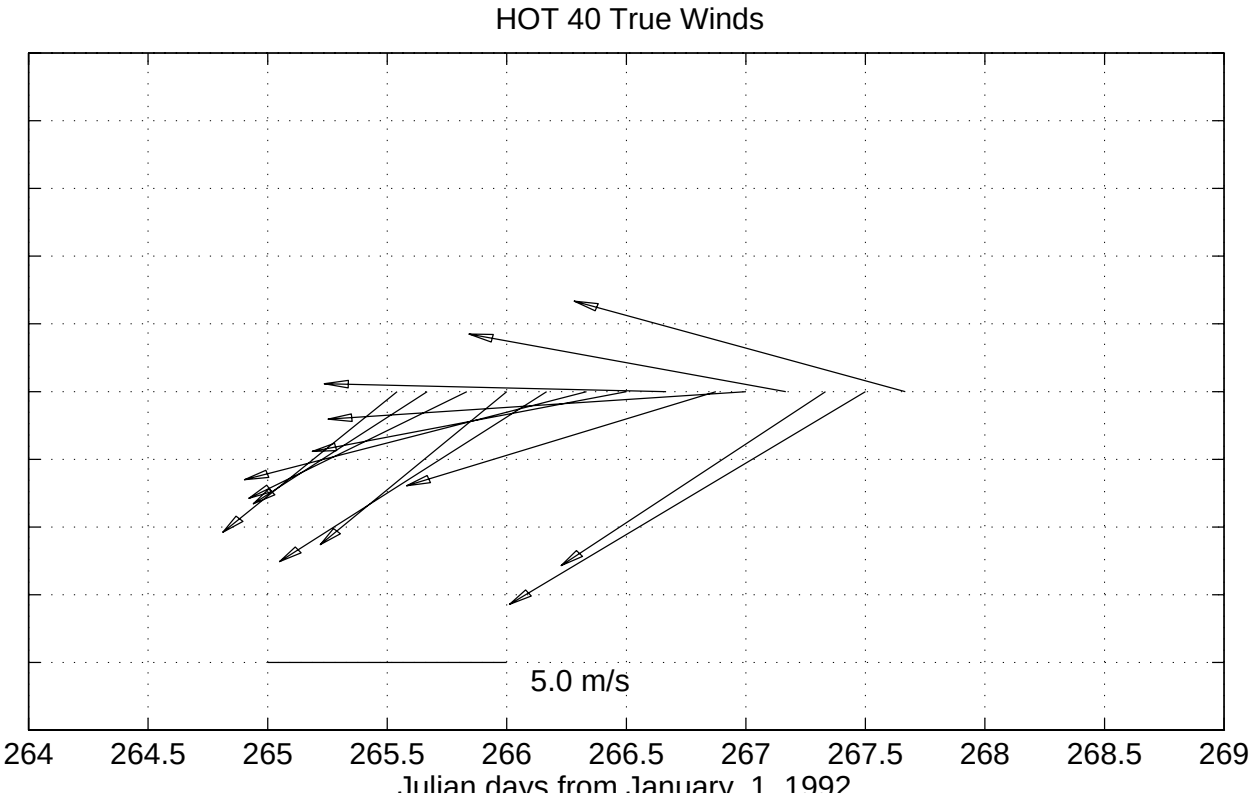
HOT 40 True Winds
5.0 m/s
264
264.5
265
265.5
266
266.5
267
267.5
268
268.5
269
Julian days from January, 1, 1992

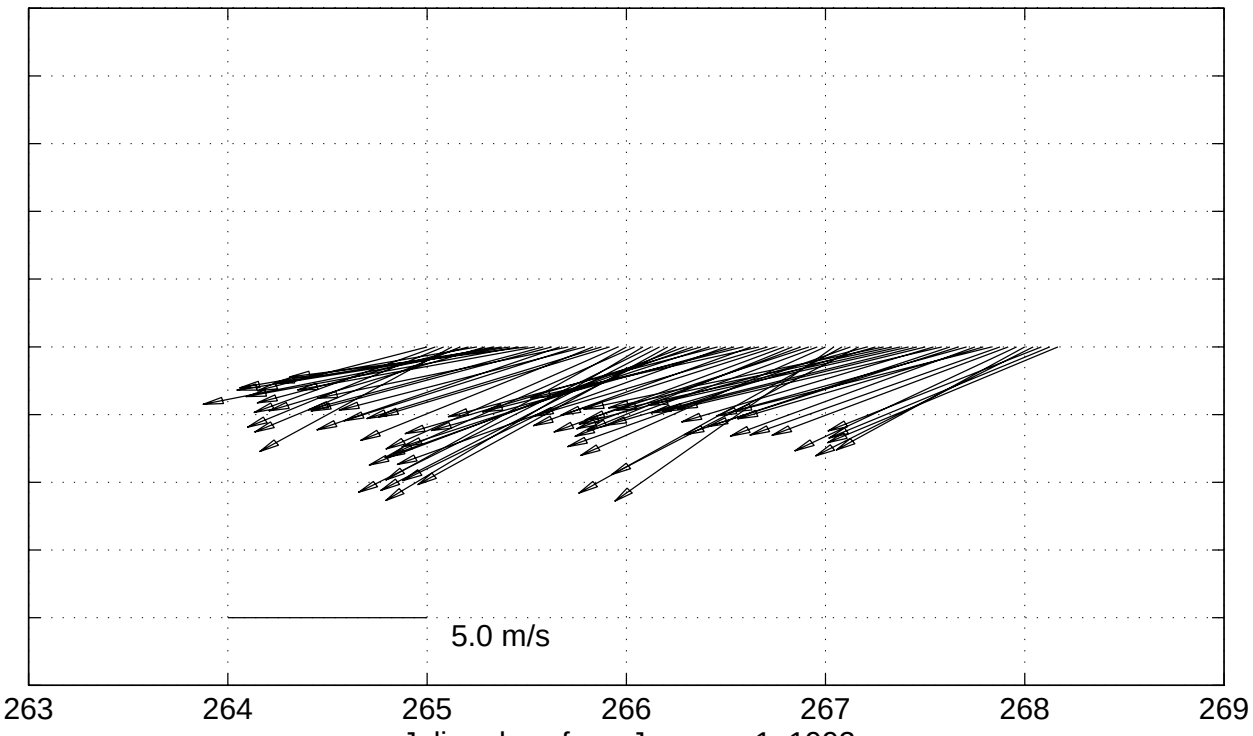
HOT 40 - True Winds, buoy data (23 24N, 162 18W)
5.0 m/s
263
264
265
266
267
268
269
Julian days from January, 1, 1992

Figure 6.7.11

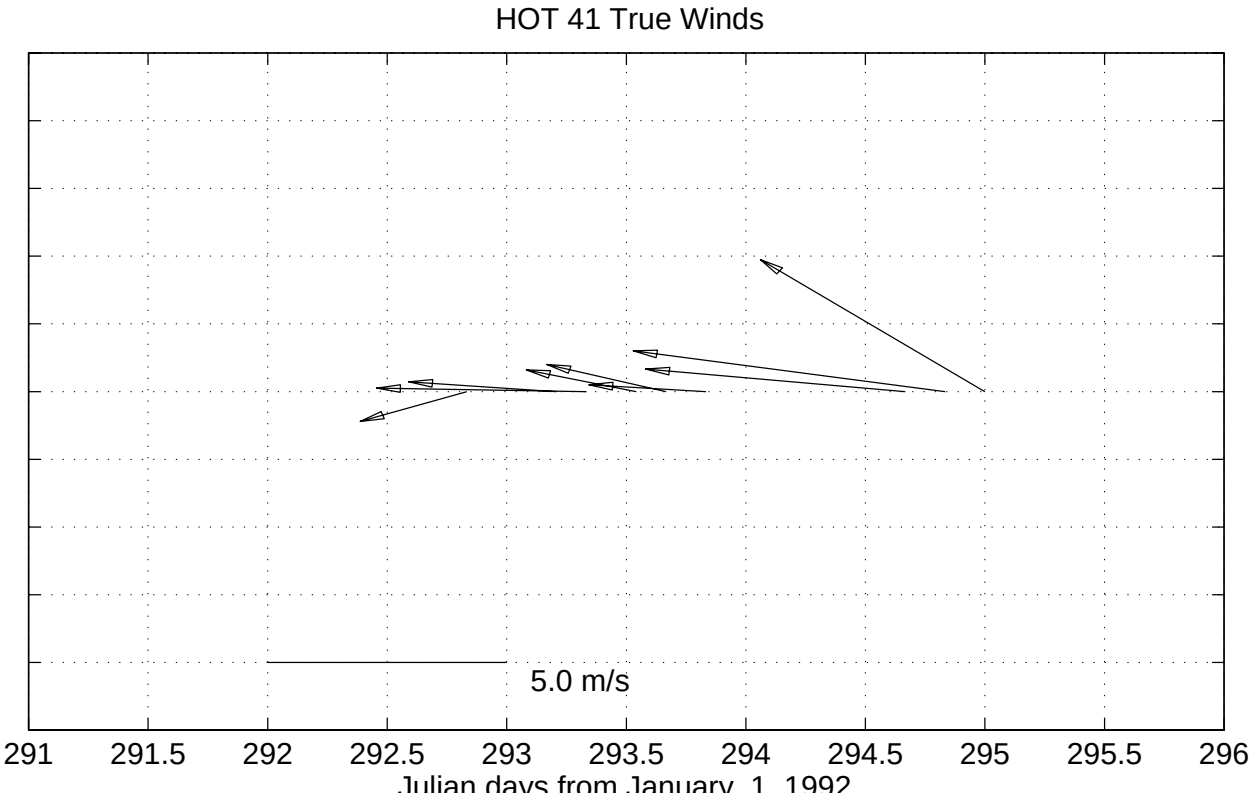
HOT 41 True Winds
5.0 m/s
291
291.5
292
292.5
293
293.5
294
294.5
295
295.5
296
Julian days from January, 1, 1992

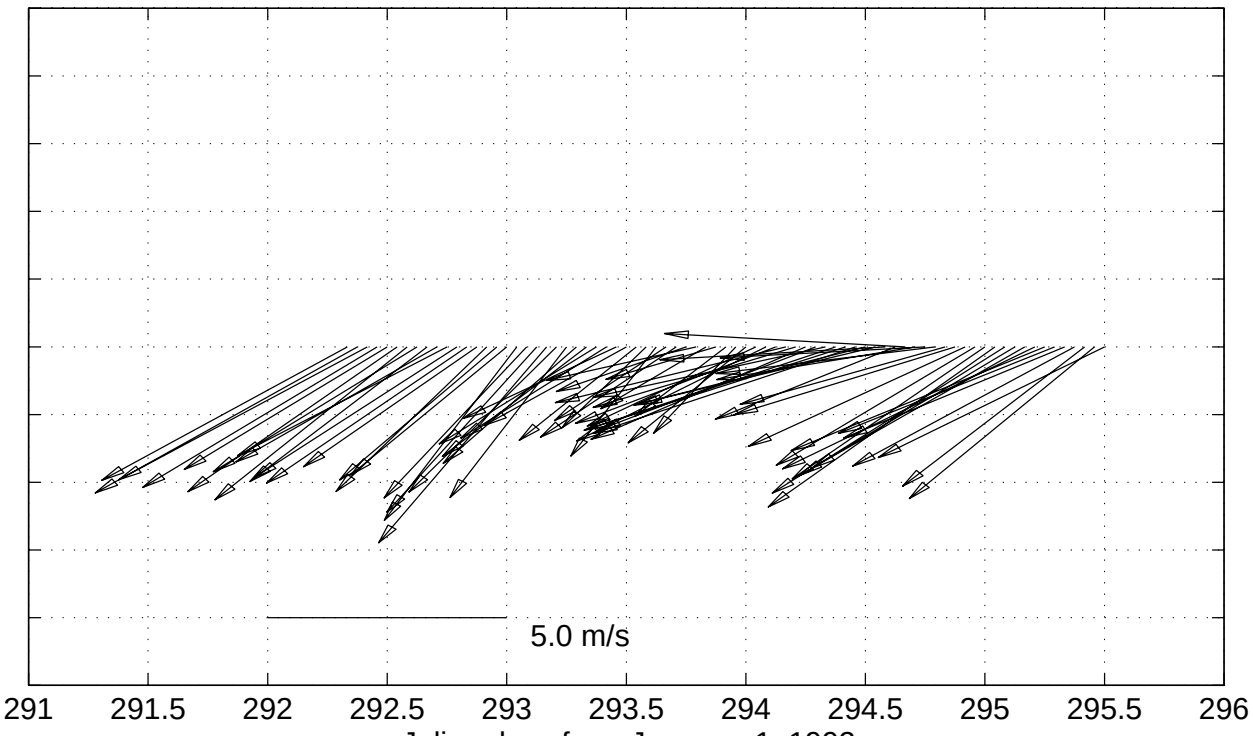
HOT 41 - True Winds, buoy data (23 24N, 162 18W)
5.0 m/s
291
291.5
292
292.5
293
293.5
294
294.5
295
295.5
296
Julian days from January, 1, 1992

Figure 6.7.12

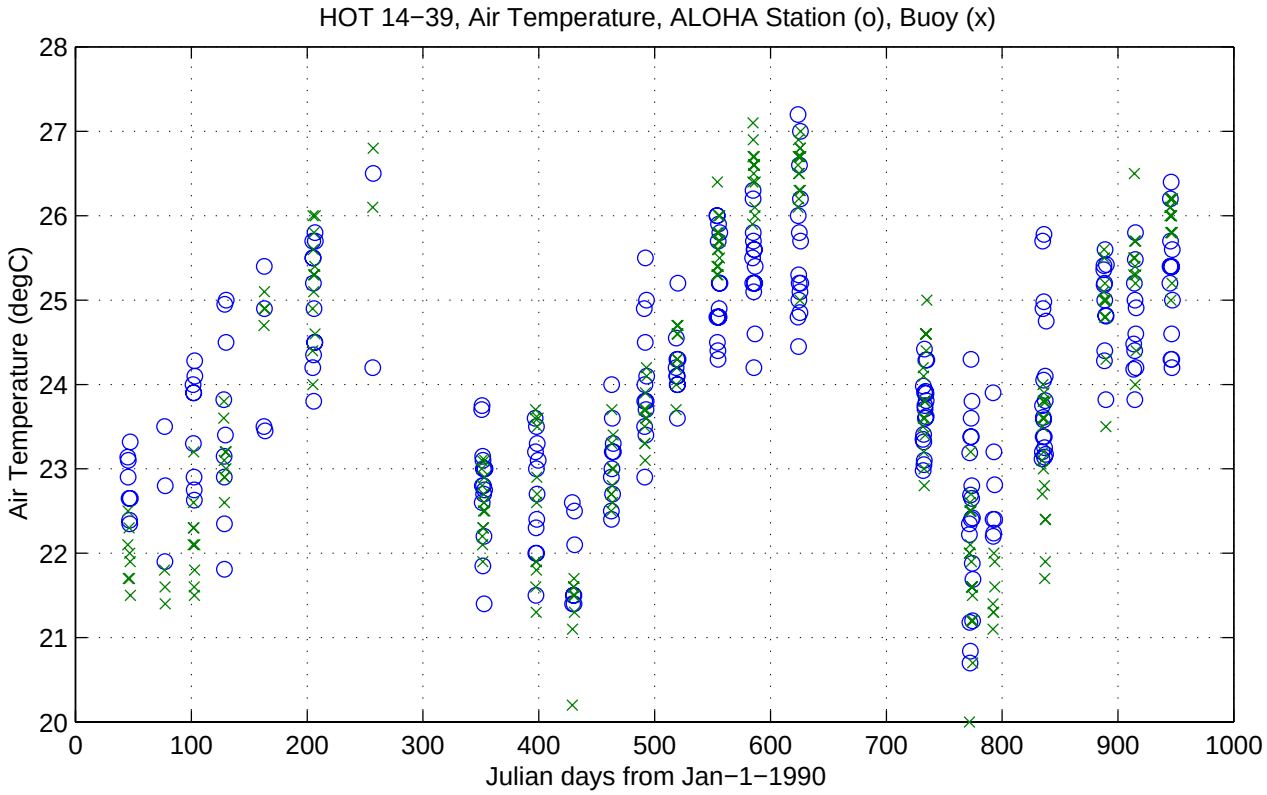
HOT 14−39, Air Temperature, ALOHA Station (o), Buoy (x)
Air Temperature (degC)
Julian days from Jan−1−1990
20
21
22
23
24
25
26
27
28
0
100
200
300
400
500
600
700
800
900
1000

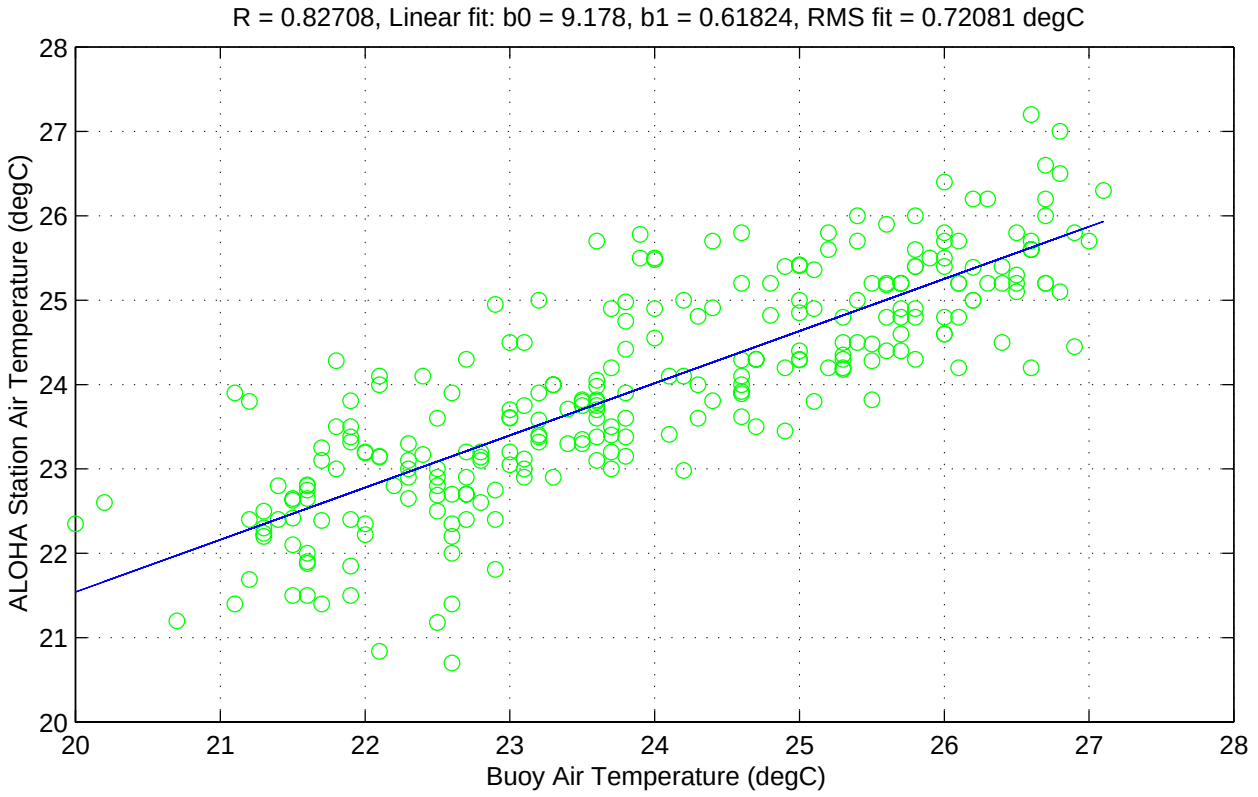
R = 0.82708, Linear fit: b0 = 9.178, b1 = 0.61824, RMS fit = 0.72081 degC
ALOHA Station Air Temperature (degC)
Buoy Air Temperature (degC)
20
21
22
23
24
25
26
27
28

Figure 6.7.13

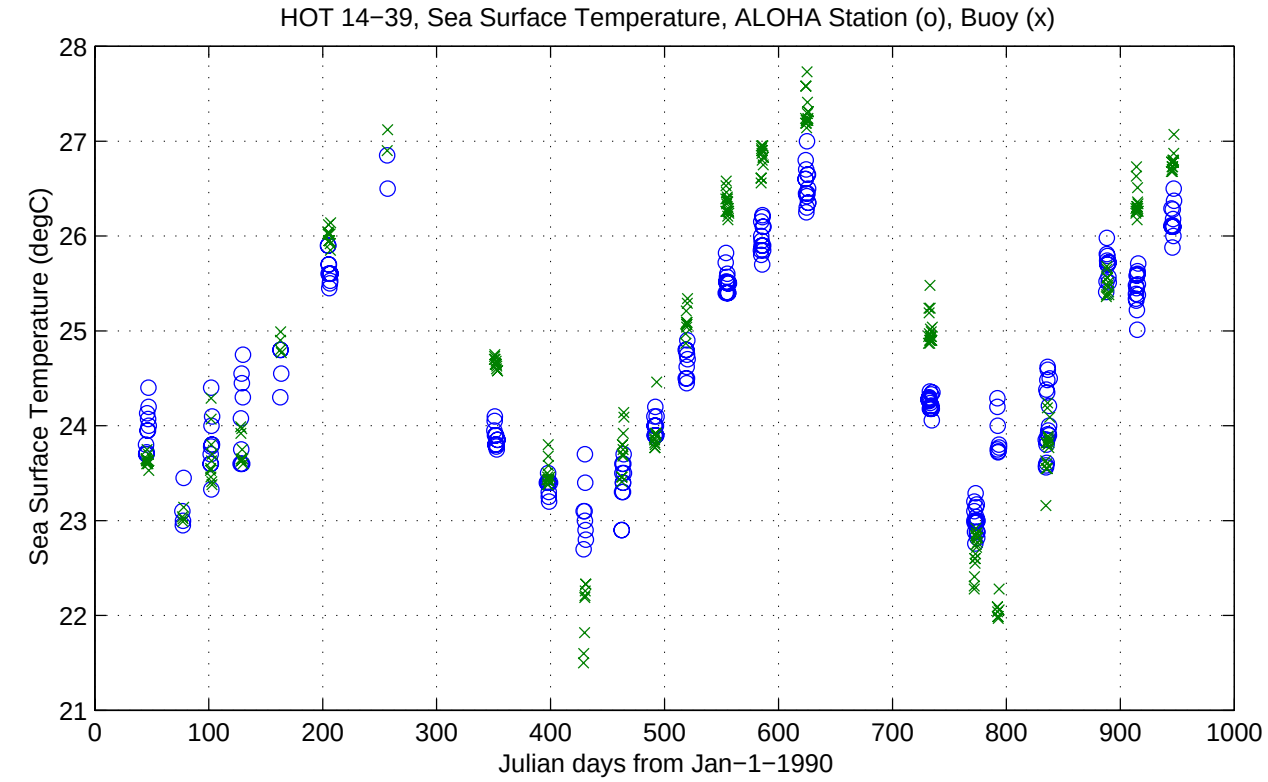
HOT 14−39, Sea Surface Temperature, ALOHA Station (o), Buoy (x)
Sea Surface Temperature (degC)
Julian days from Jan−1−1990
28
27
26
25
24
23
22
21
0
100
200
300
400
500
600
700
800
900
1000

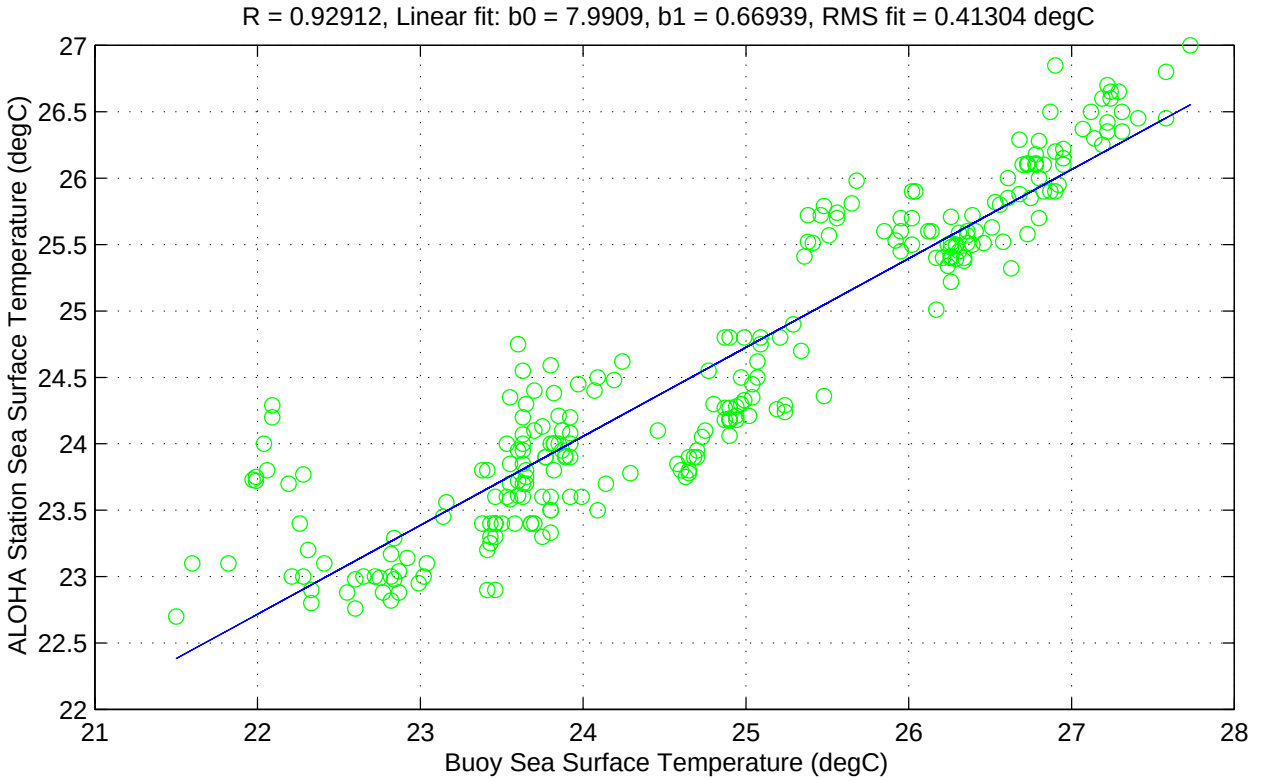
R = 0.92912, Linear fit: b0 = 7.9909, b1 = 0.66939, RMS fit = 0.41304 degC
ALOHA Station Sea Surface Temperature (degC)
Buoy Sea Surface Temperature (degC)
27
26.5
26
25.5
25
24.5
24
23.5
23
22.5
22
21
22
23
24
25
26
27
28

Figure 6.7.14

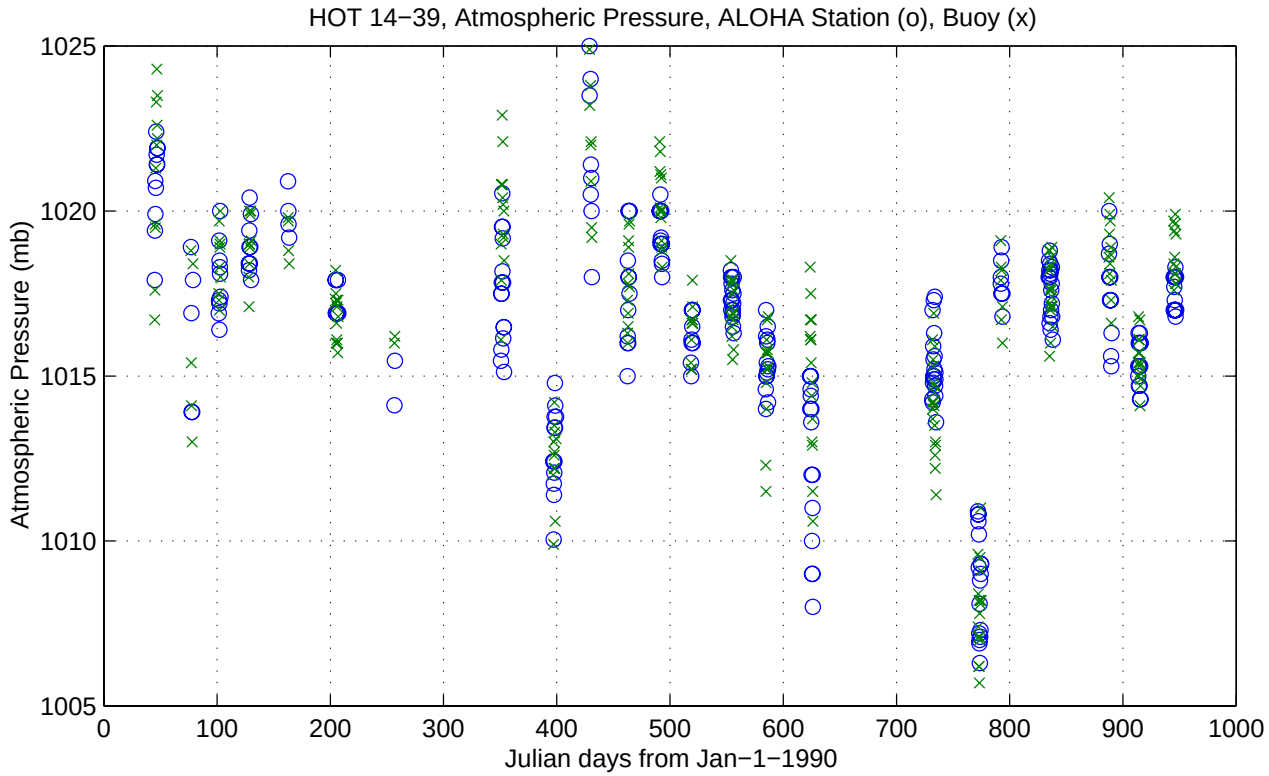
HOT 14−39, Atmospheric Pressure, ALOHA Station (o), Buoy (x)
Atmospheric Pressure (mb)
Julian days from Jan−1−1990
1025
1020
1015
1010
1005
0
100
200
300
400
500
600
700
800
900
1000

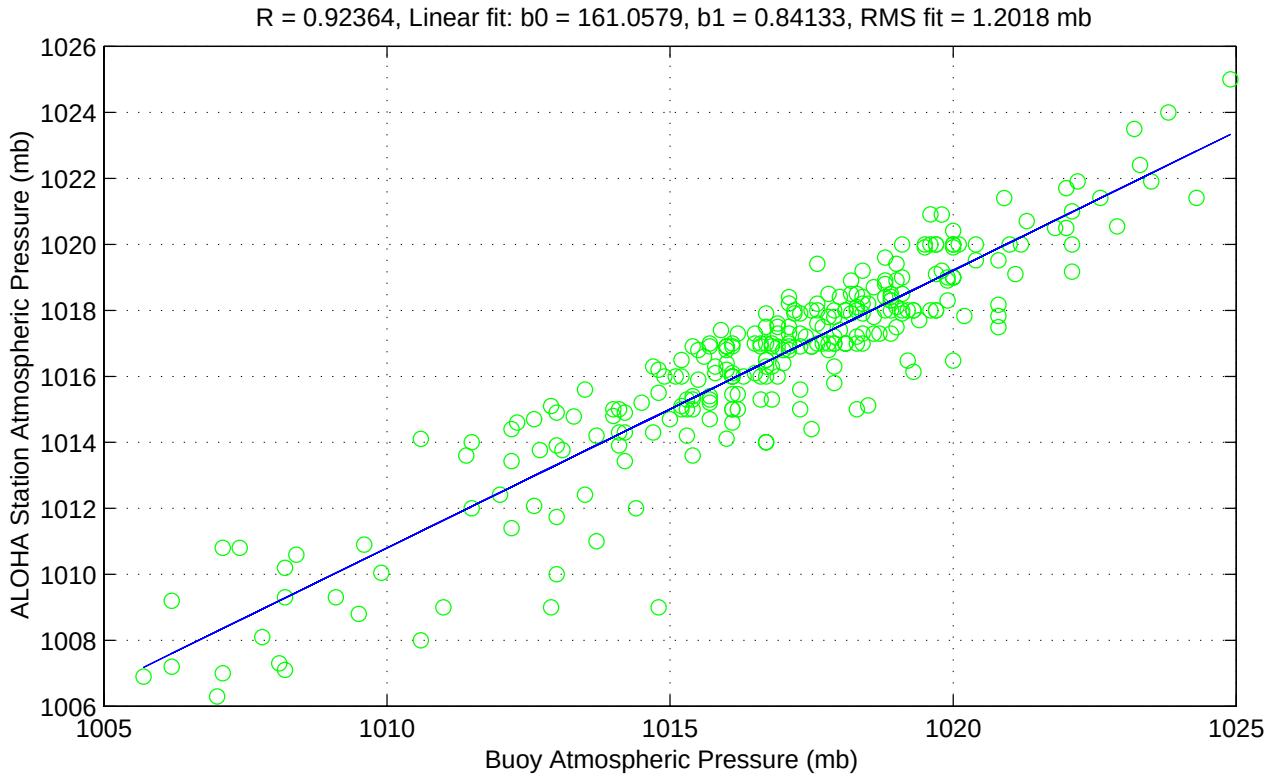
R = 0.92364, Linear fit: b0 = 161.0579, b1 = 0.84133, RMS fit = 1.2018 mb
ALOHA Station Atmospheric Pressure (mb)
Buoy Atmospheric Pressure (mb)
1026
1024
1022
1020
1018
1016
1014
1012
1010
1008
1006
1005
1010
1015
1020
1025

Figure 6.7.15

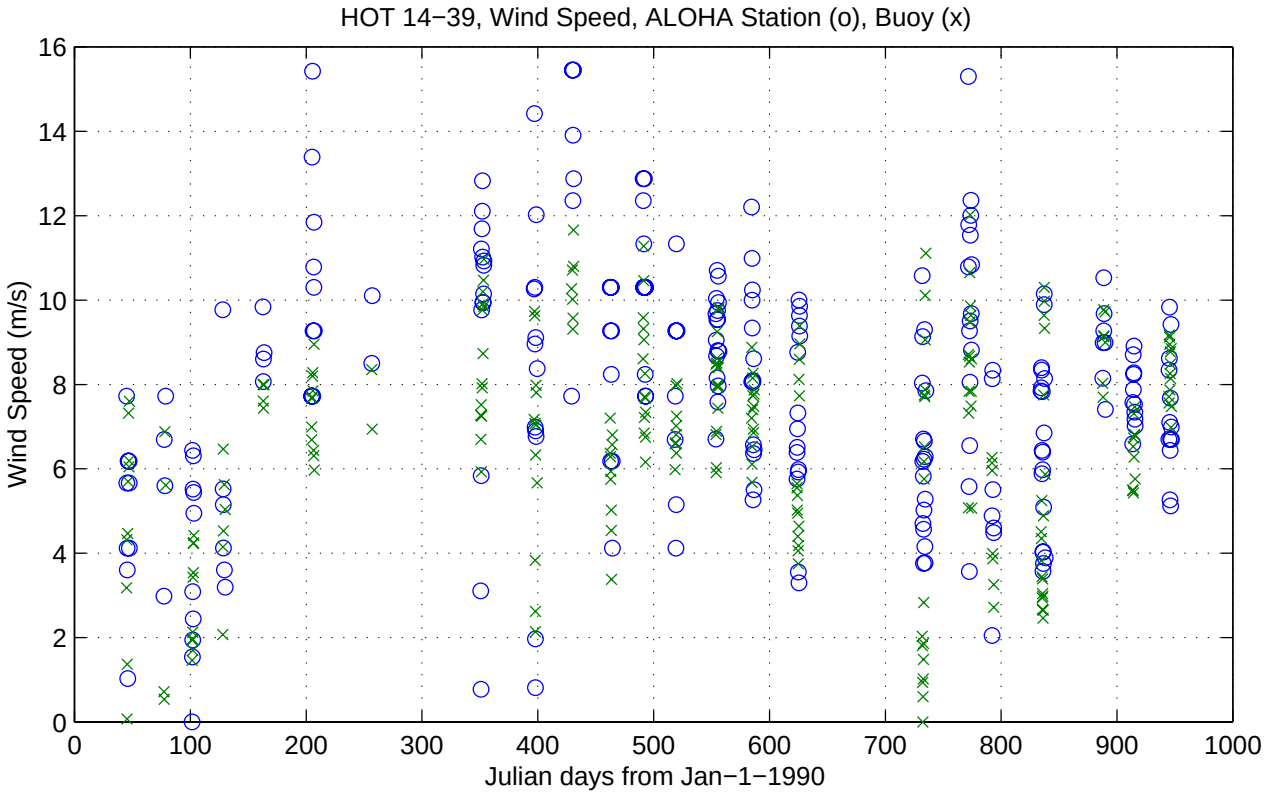
HOT 14−39, Wind Speed, ALOHA Station (o), Buoy (x)
Wind Speed (m/s)
Julian days from Jan−1−1990
0
2
4
6
8
10
12
14
16
0
100
200
300
400
500
600
700
800
900
1000

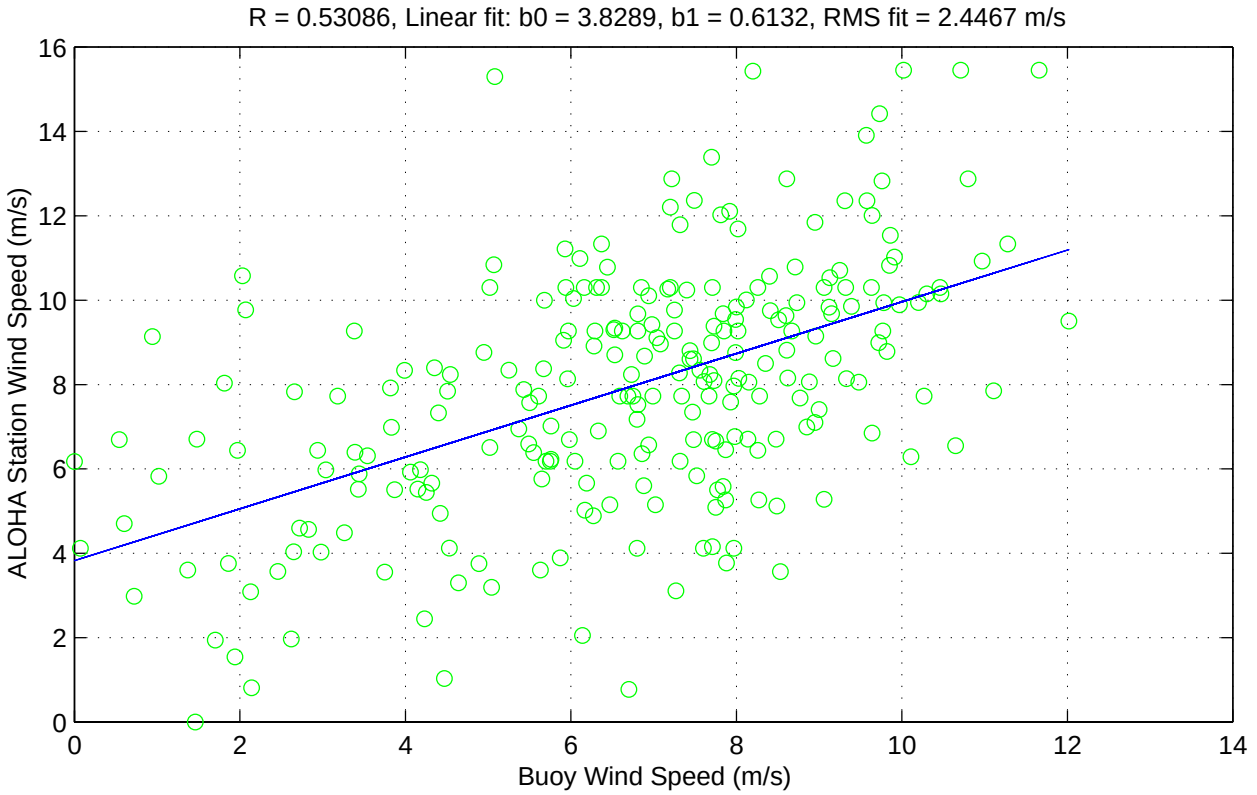
R = 0.53086, Linear fit: b0 = 3.8289, b1 = 0.6132, RMS fit = 2.4467 m/s
ALOHA Station Wind Speed (m/s)
Buoy Wind Speed (m/s)
0
2
4
6
8
10
12
14
16

Figure 6.7.16

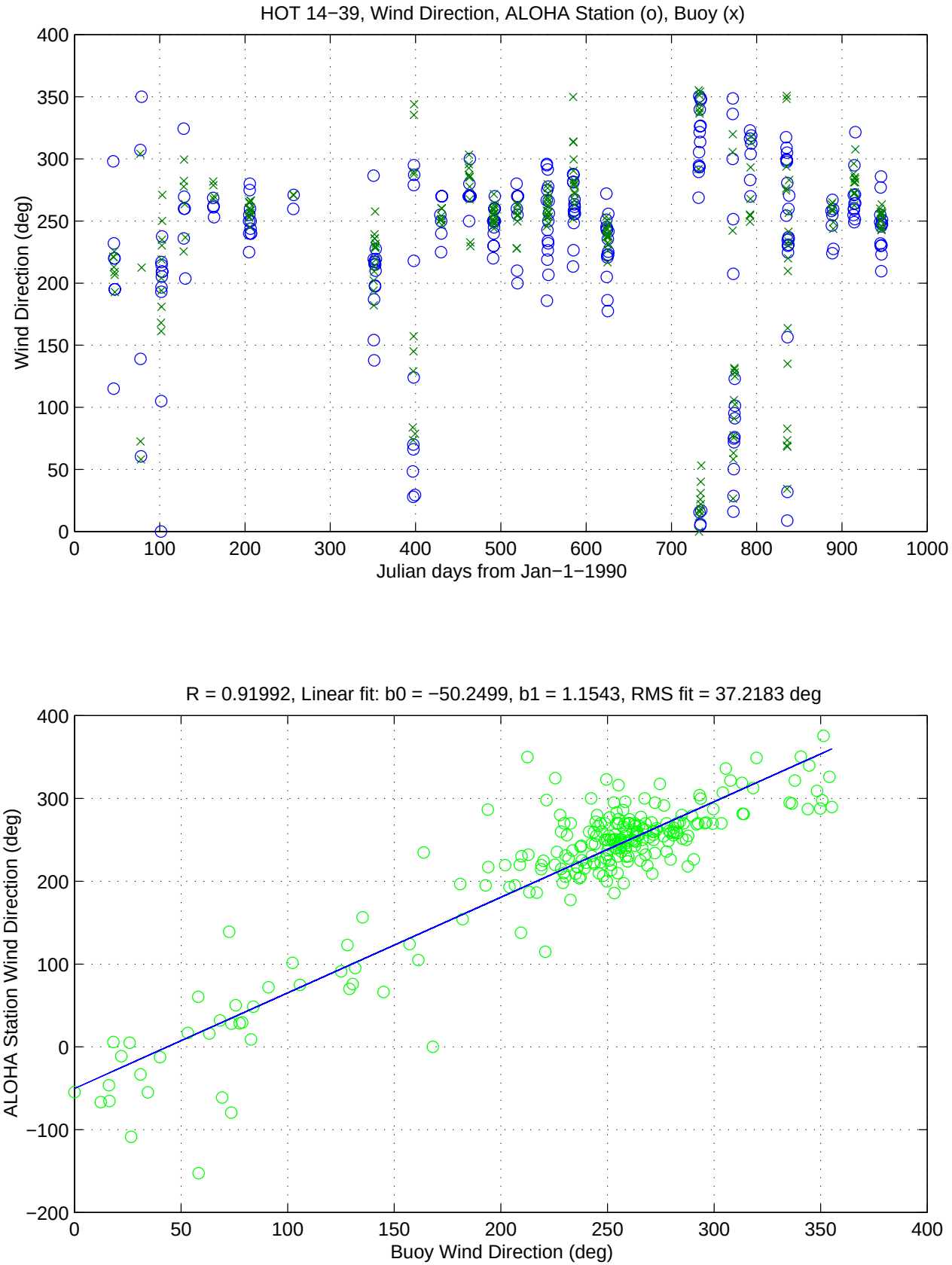
HOT 14−39, Wind Direction, ALOHA Station (o), Buoy (x)
Wind Direction (deg)
Julian days from Jan−1−1990
R = 0.91992, Linear fit: b0 = −50.2499, b1 = 1.1543, RMS fit = 37.2183 deg
ALOHA Station Wind Direction (deg)
Buoy Wind Direction (deg)

Figure 6.7.17

6.8. CTD Station Locations and Sediment Trap Drift Tracks

Figure 6.8.1: (Right panel) CTD station locations on HOT-33. CTD stations represented by open circles relative to Station ALOHA. Solid lines connect casts taken in sequence and numbers show location of first and last casts. Dashed line shows area nominally defined as Station ALOHA. (Left panel) Drift track for the sediment trap array during the 72-hour deployment period.

Figure 6.8.2: As in Figure 6.8.1, except for HOT-34.

Figure 6.8.3: As in Figure 6.8.1, except for HOT-35.

Figure 6.8.4: As in Figure 6.8.1, except for HOT-36.

Figure 6.8.5: As in Figure 6.8.1, except for HOT-37.

Figure 6.8.6: As in Figure 6.8.1, except for HOT-38.

Figure 6.8.7: As in Figure 6.8.1, except for HOT-39.

Figure 6.8.8: As in Figure 6.8.1, except for HOT-40.

Figure 6.8.9: As in Figure 6.8.1, except for HOT-41.

Figure 6.8.10: Other CTD locations on HOT-31 and HOT-32. (Not mentioned in Data Report 3). Station 3 is located 40 miles north of Station ALOHA, Station 4 is 10 miles offshore of the 400 m isobath north of Kahuku Point, and Station 5 is at the 400 m isobath off Kahuku.

Figure 6.8.11: Other CTD locations on HOT-33 and HOT-34.

Figure 6.8.12: Other CTD locations on HOT-35 and HOT-36.

Figure 6.8.13: Other CTD locations on HOT-37 and HOT-38.

Figure 6.8.14: Other CTD locations on HOT-39 and HOT-40.

Figure 6.8.15: Other CTD locations on HOT-41.

HOT−33

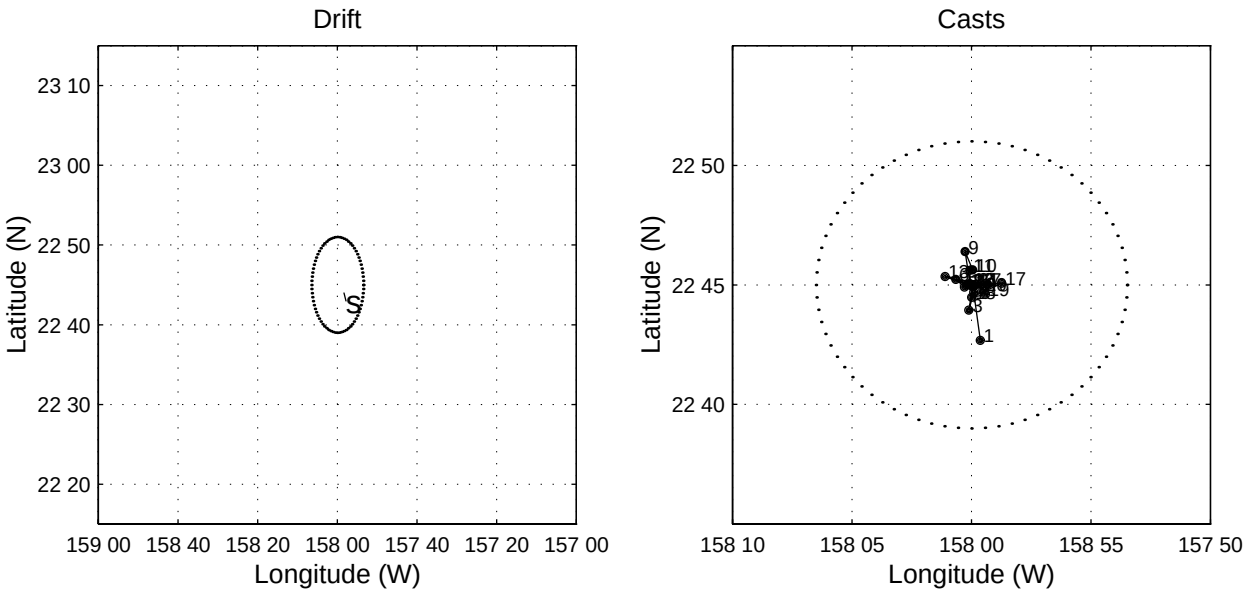

HOT−34

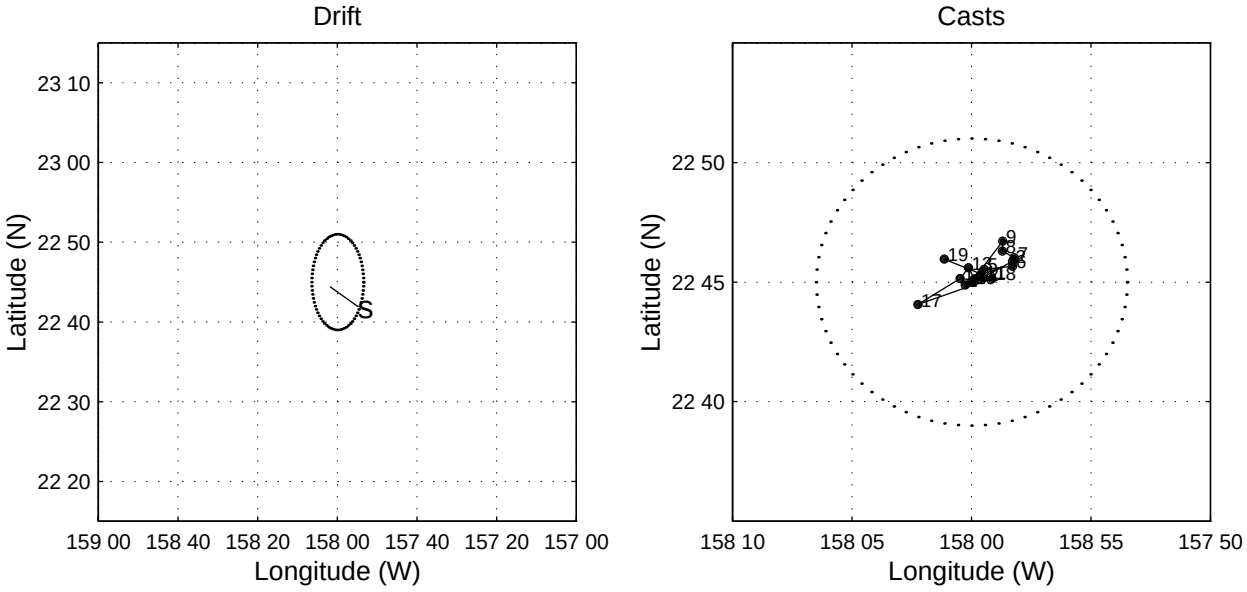

Figure 6.8.1-2

HOT−35

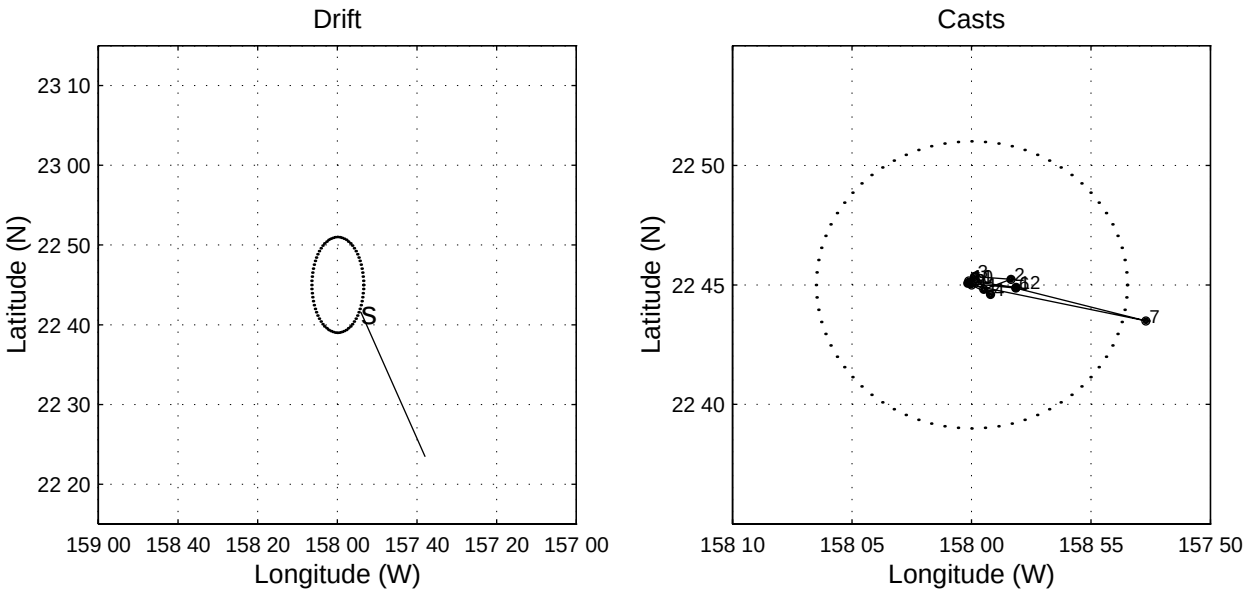

HOT−36

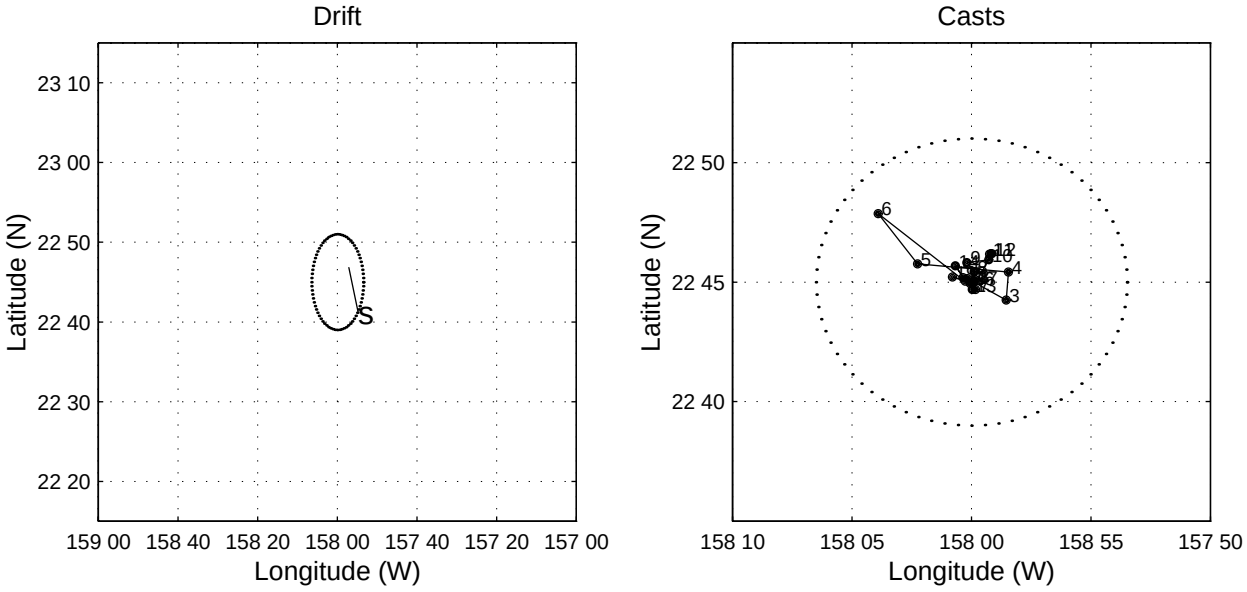

Figure 6.8.3-4

HOT−37

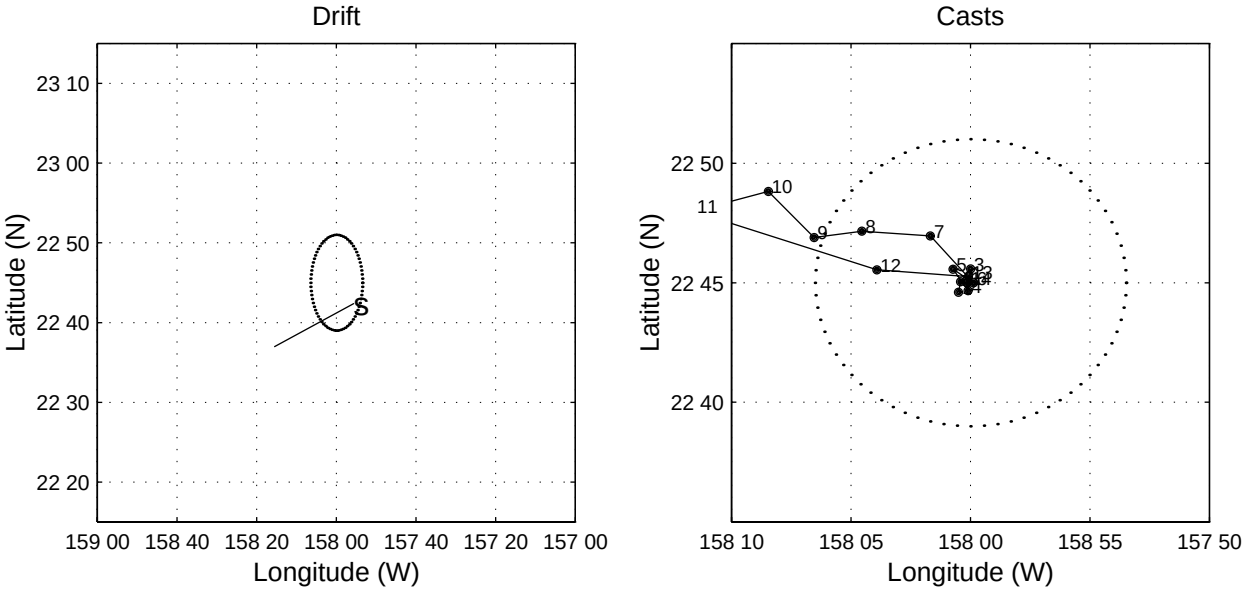

HOT−38

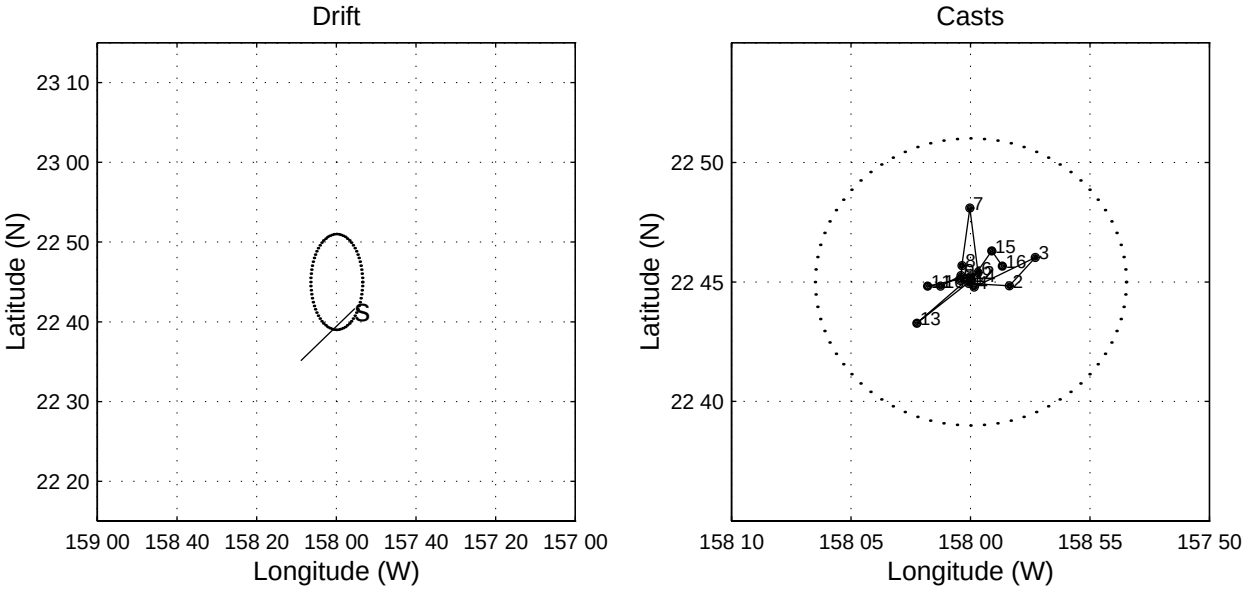

Figure 6.8.5-6

HOT−39

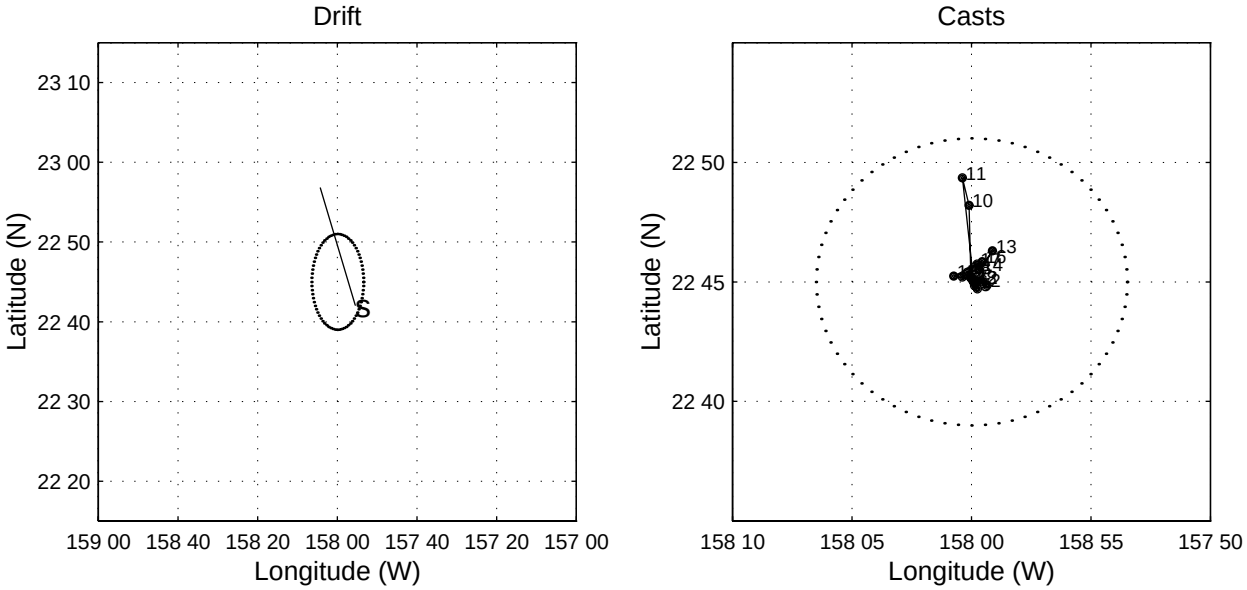

HOT−40

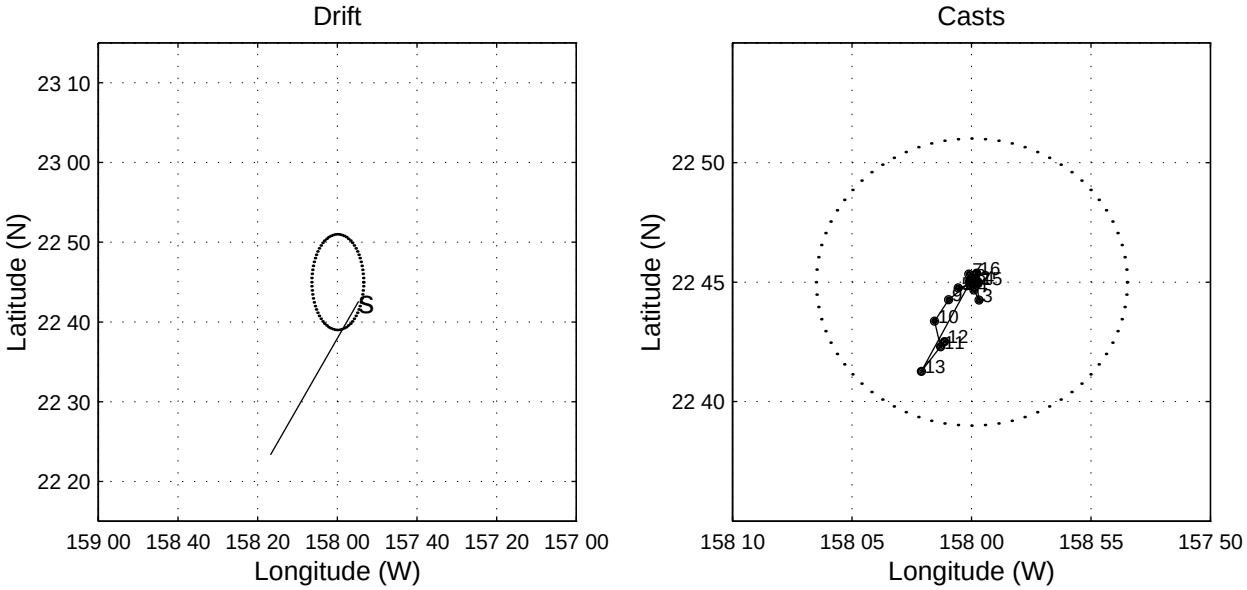

Figure 6.8.7-8

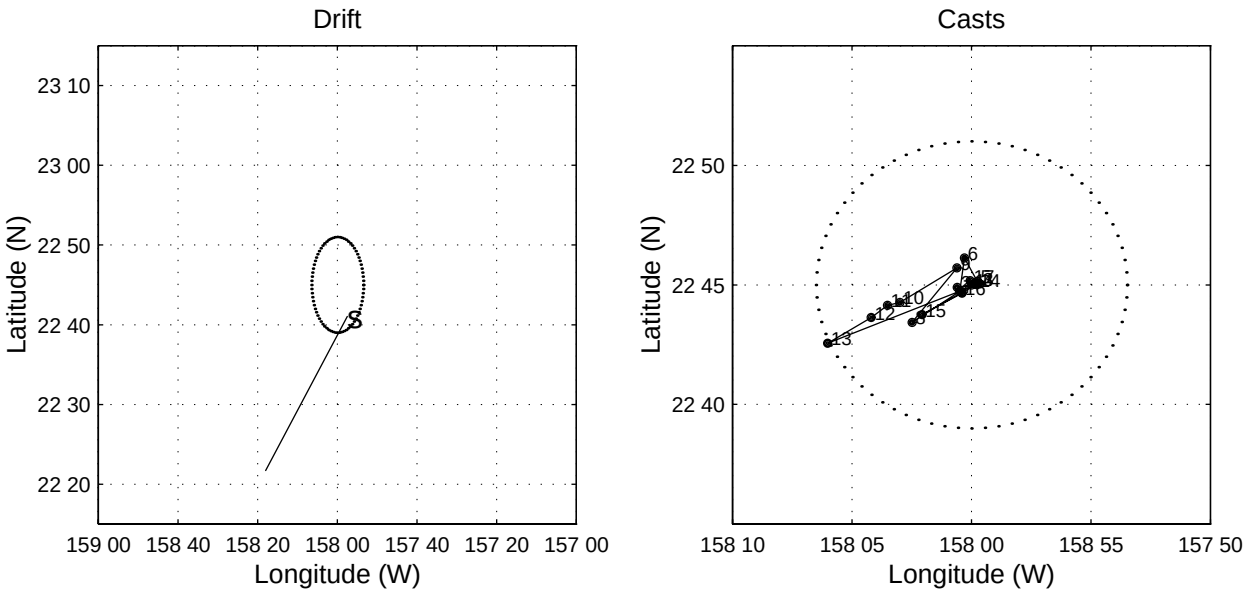
Drift
Casts
Latitude (N)
Longitude (W)
23 10
23 00
22 50
22 40
22 30
22 20
159 00
158 40
158 20
158 00
157 40
157 20
157 00
22 45
22 40
158 10
158 05
158 55
157 50

Figure 6.8.9

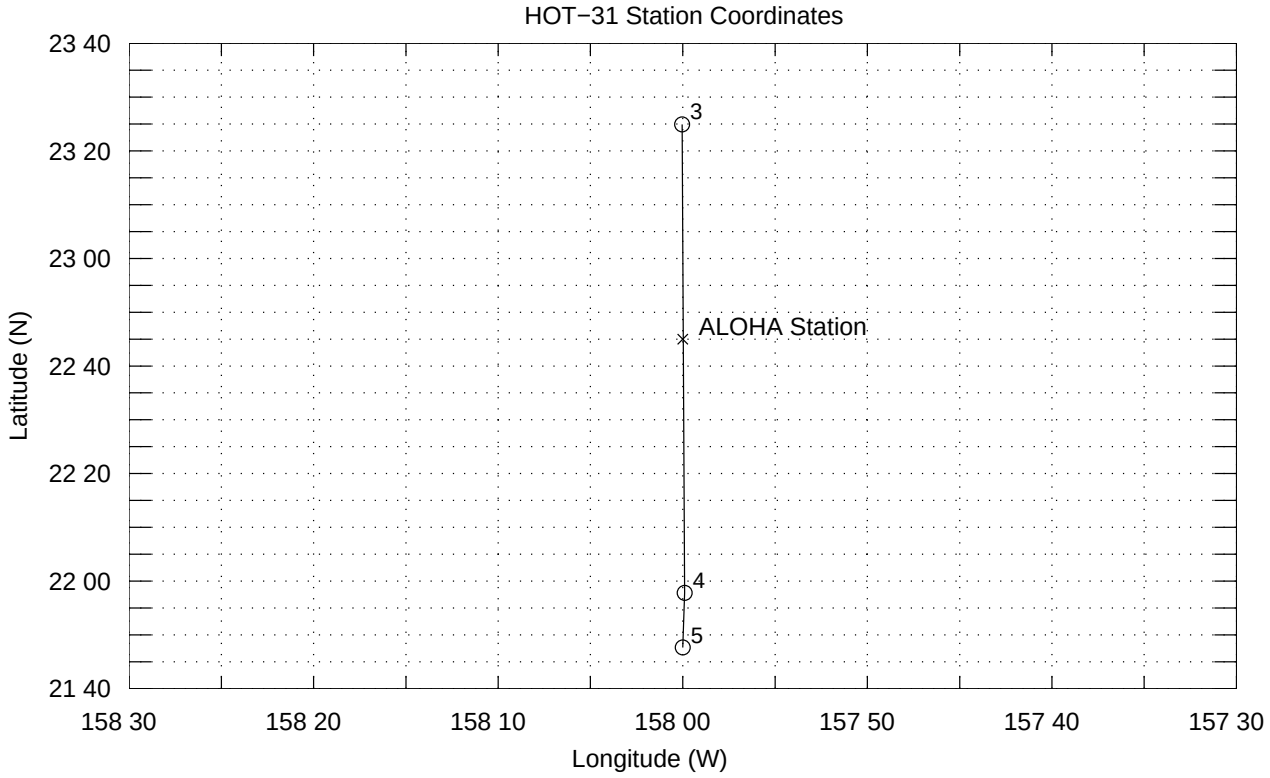
HOT−31 Station Coordinates
23 40
23 20
23 00
22 40
22 20
22 00
21 40
Latitude (N)
3
ALOHA Station
4
5
158 30
158 20
158 10
158 00
157 50
157 40
157 30
Longitude (W)

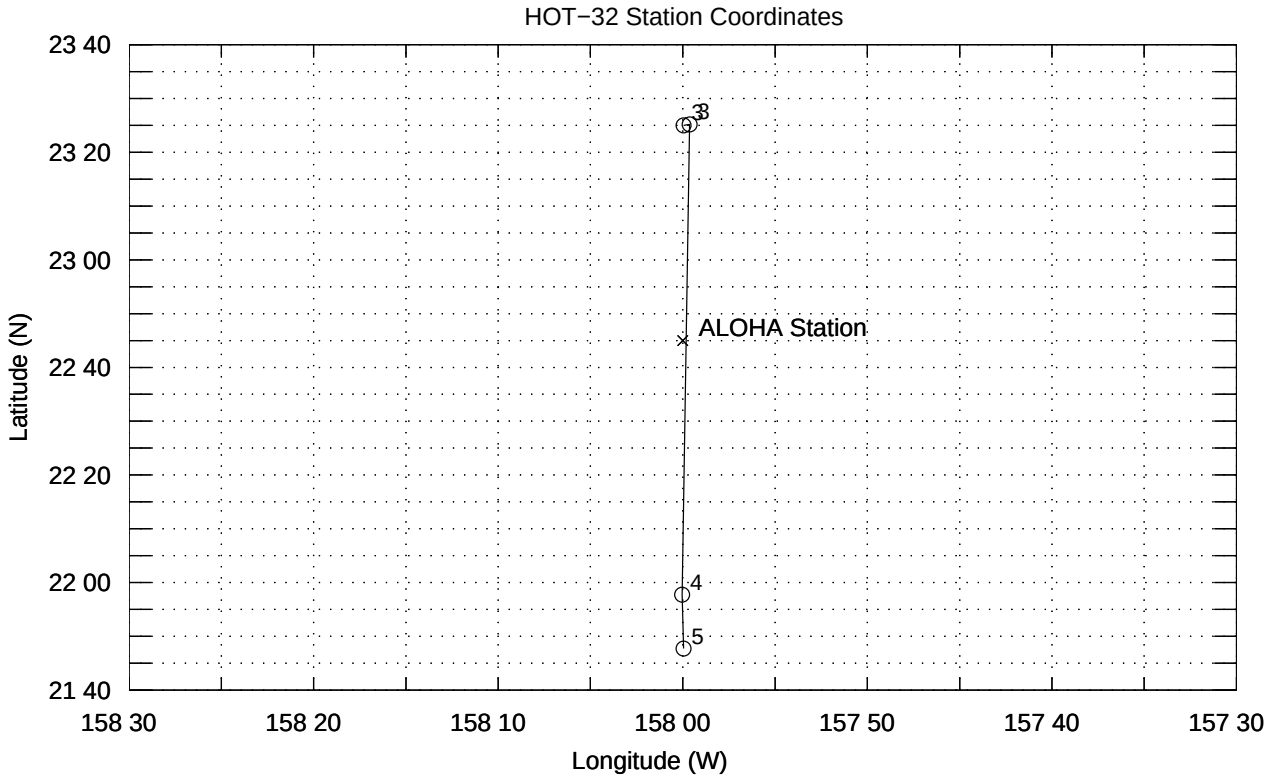
HOT−32 Station Coordinates
23 40
23 20
23 00
22 40
22 20
22 00
21 40
Latitude (N)
3
ALOHA Station
4
5
158 30
158 20
158 10
158 00
157 50
157 40
157 30
Longitude (W)

Figure 6.8.10

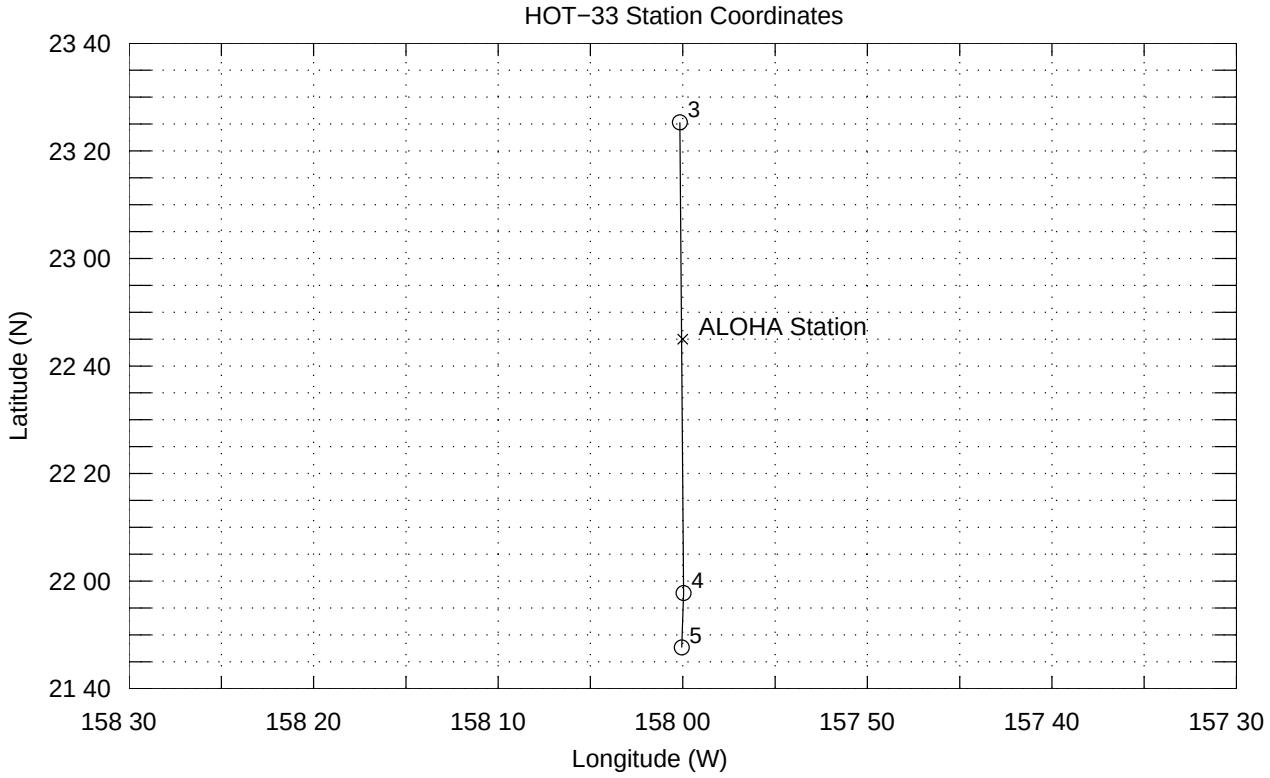
HOT−33 Station Coordinates
23 40
23 20
23 00
22 40
22 20
22 00
21 40
Latitude (N)
3
ALOHA Station
4
5
158 30
158 20
158 10
158 00
157 50
157 40
157 30
Longitude (W)

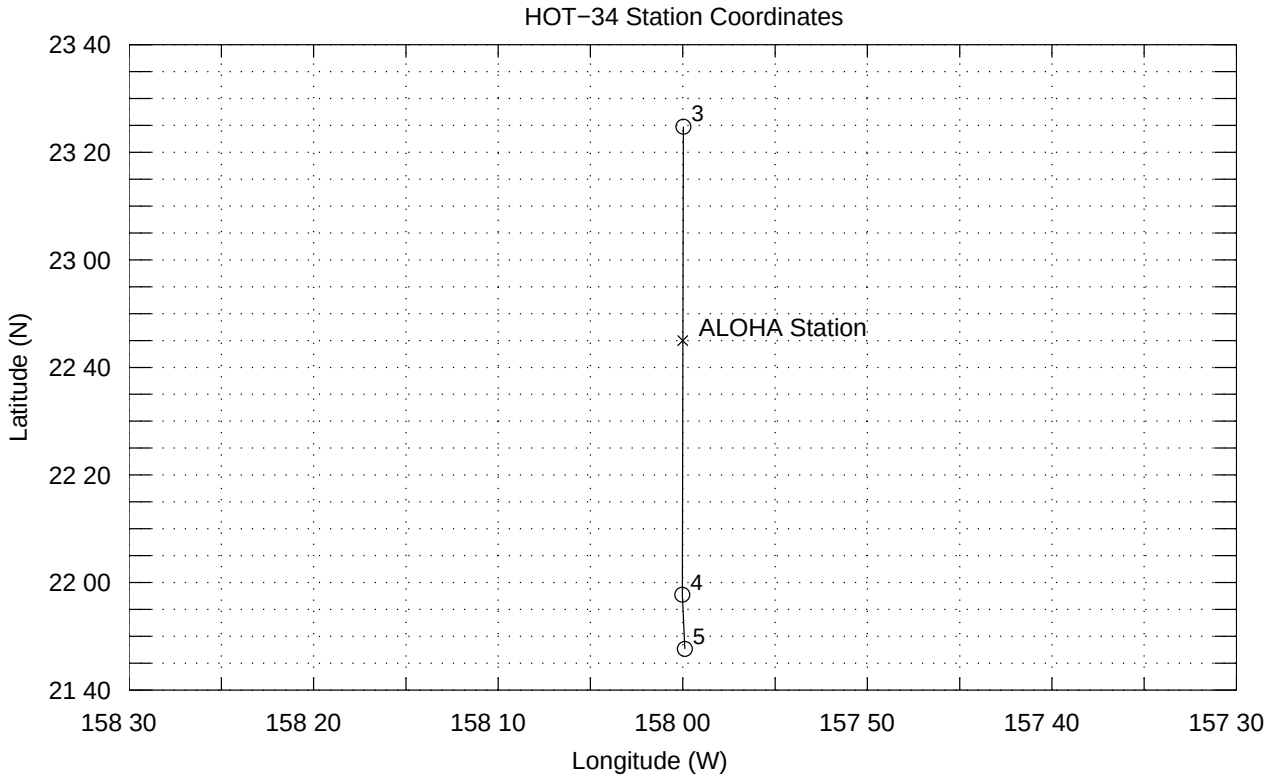
HOT−34 Station Coordinates
23 40
23 20
23 00
22 40
22 20
22 00
21 40
Latitude (N)
3
ALOHA Station
4
5
158 30
158 20
158 10
158 00
157 50
157 40
157 30
Longitude (W)

Figure 6.8.11

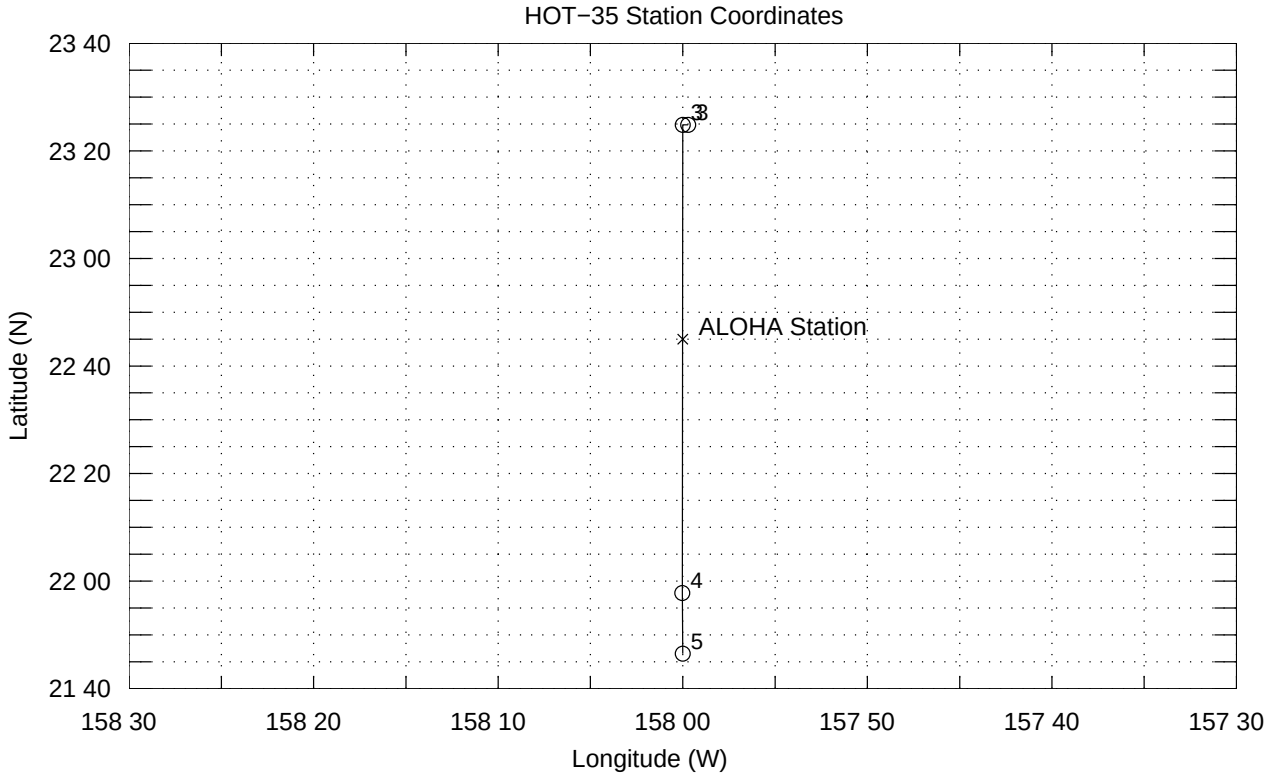
HOT−35 Station Coordinates
23 40
23 20
23 00
22 40
22 20
22 00
21 40
Latitude (N)
ALOHA Station
3
4
5
158 30
158 20
158 10
158 00
157 50
157 40
157 30
Longitude (W)

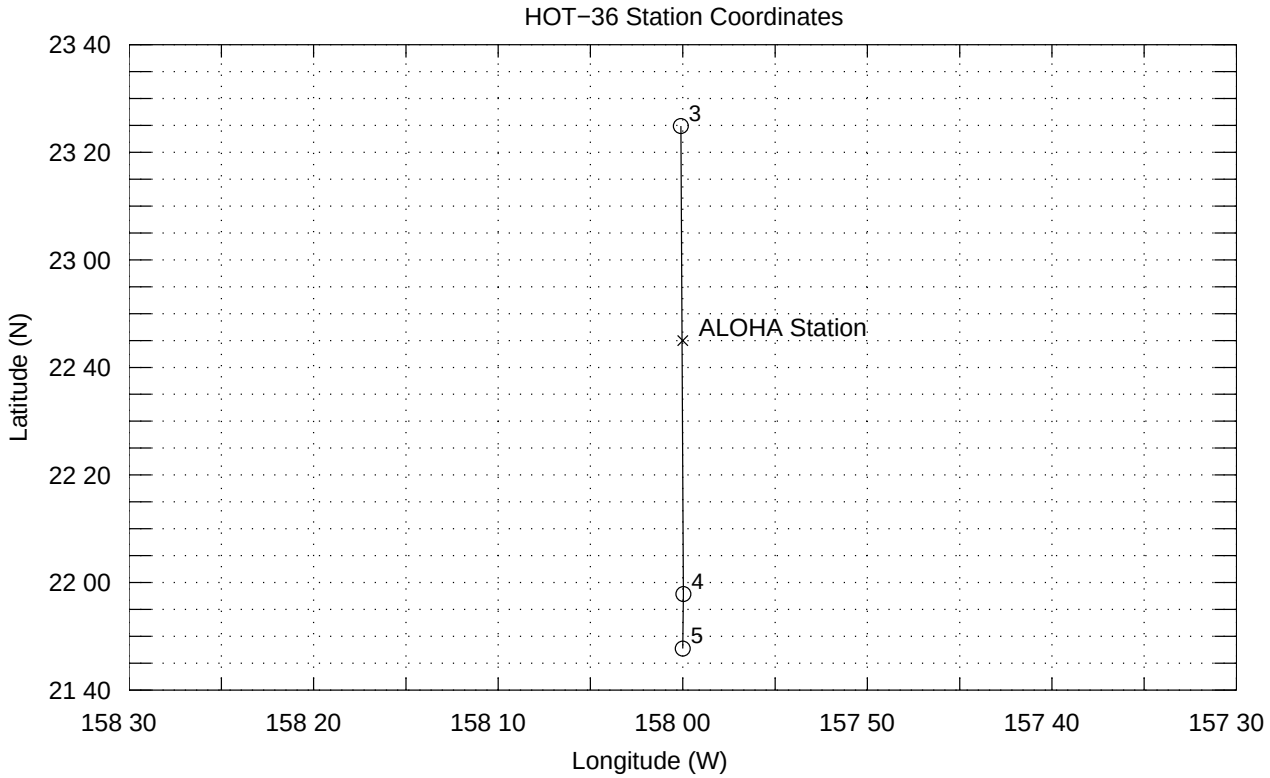
HOT−36 Station Coordinates
23 40
23 20
23 00
22 40
22 20
22 00
21 40
Latitude (N)
ALOHA Station
3
4
5
158 30
158 20
158 10
158 00
157 50
157 40
157 30
Longitude (W)

Figure 6.8.12

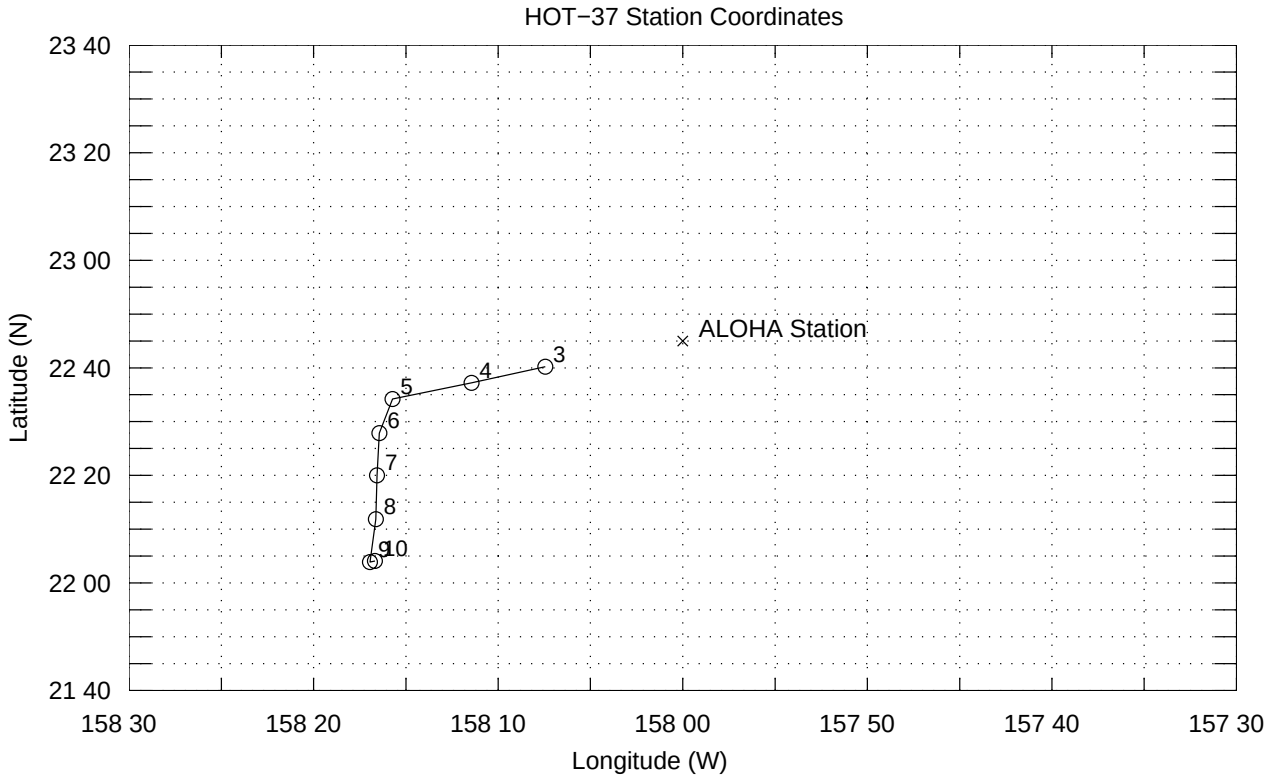
HOT−37 Station Coordinates
Latitude (N)
Longitude (W)
23 40
23 20
23 00
22 40
22 20
22 00
21 40
158 30
158 20
158 10
158 00
157 50
157 40
157 30
ALOHA Station
3
4
5
6
7
8
9
10

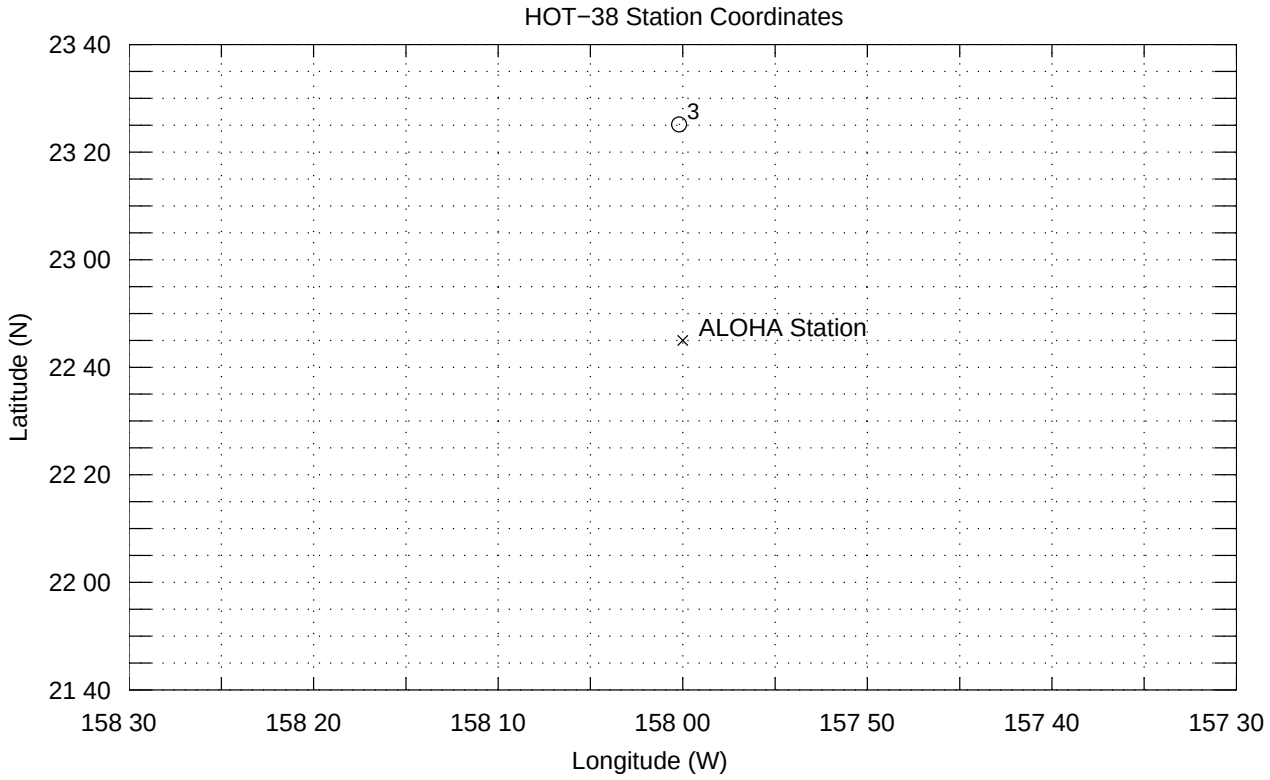
HOT−38 Station Coordinates
Latitude (N)
Longitude (W)
23 40
23 20
23 00
22 40
22 20
22 00
21 40
158 30
158 20
158 10
158 00
157 50
157 40
157 30
ALOHA Station
3

Figure 6.8.13

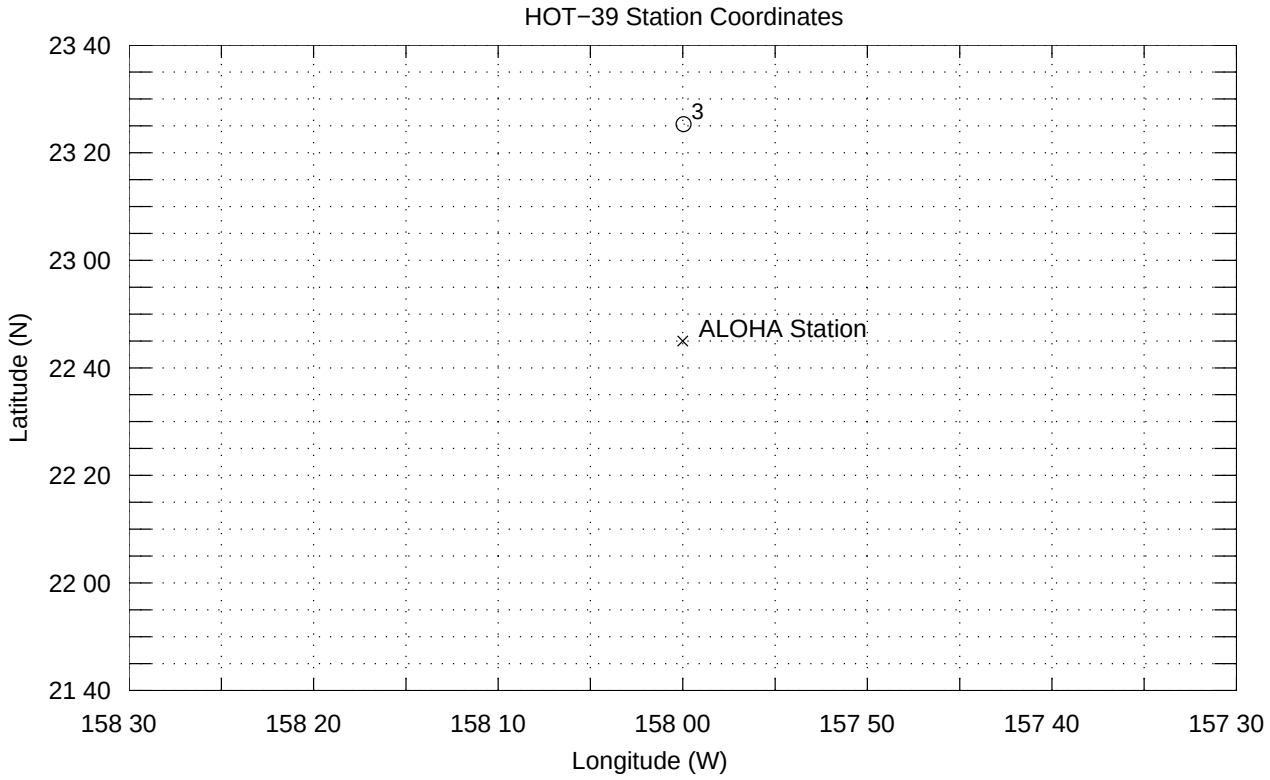
HOT−39 Station Coordinates
23 40
23 20
23 00
22 40
22 20
22 00
21 40
Latitude (N)
3
ALOHA Station
158 30
158 20
158 10
158 00
157 50
157 40
157 30
Longitude (W)

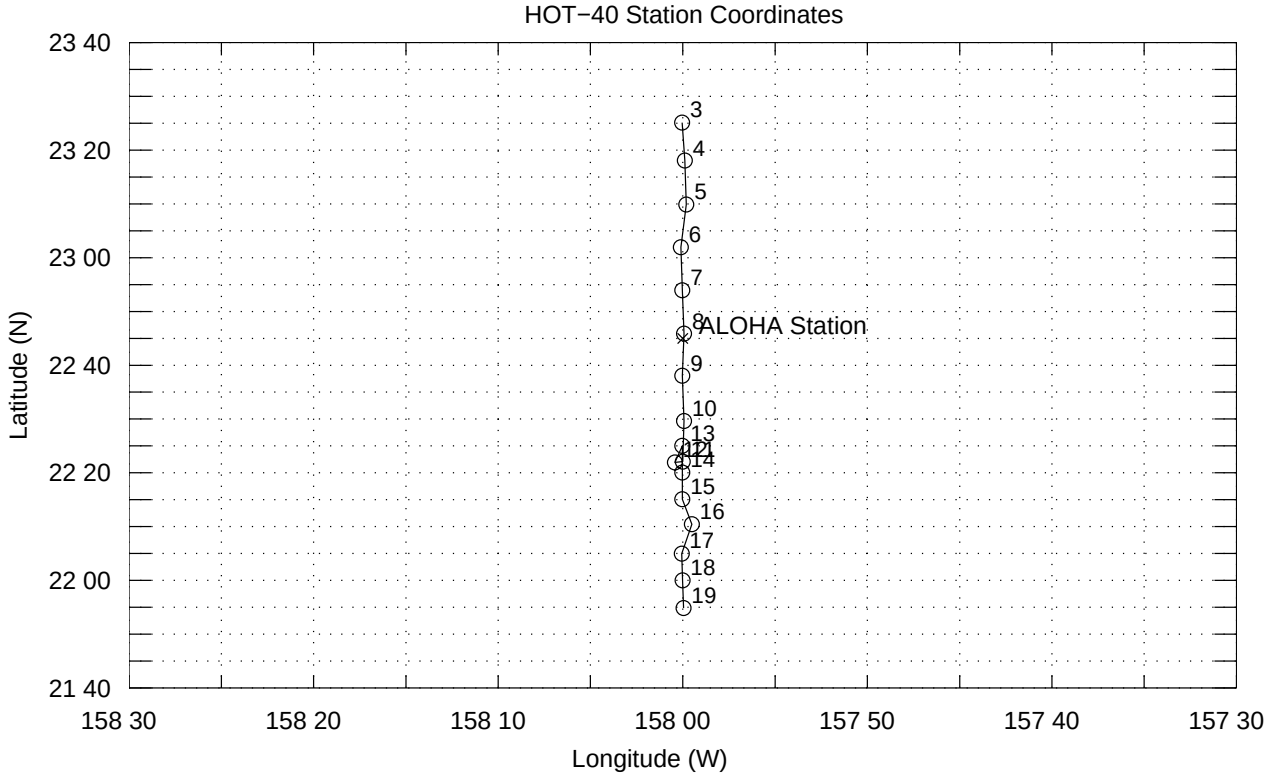
HOT−40 Station Coordinates
23 40
23 20
23 00
22 40
22 20
22 00
21 40
Latitude (N)
3
4
5
6
7
8
ALOHA Station
9
10
13
14
15
16
17
18
19
158 30
158 20
158 10
158 00
157 50
157 40
157 30
Longitude (W)

Figure 6.8.14

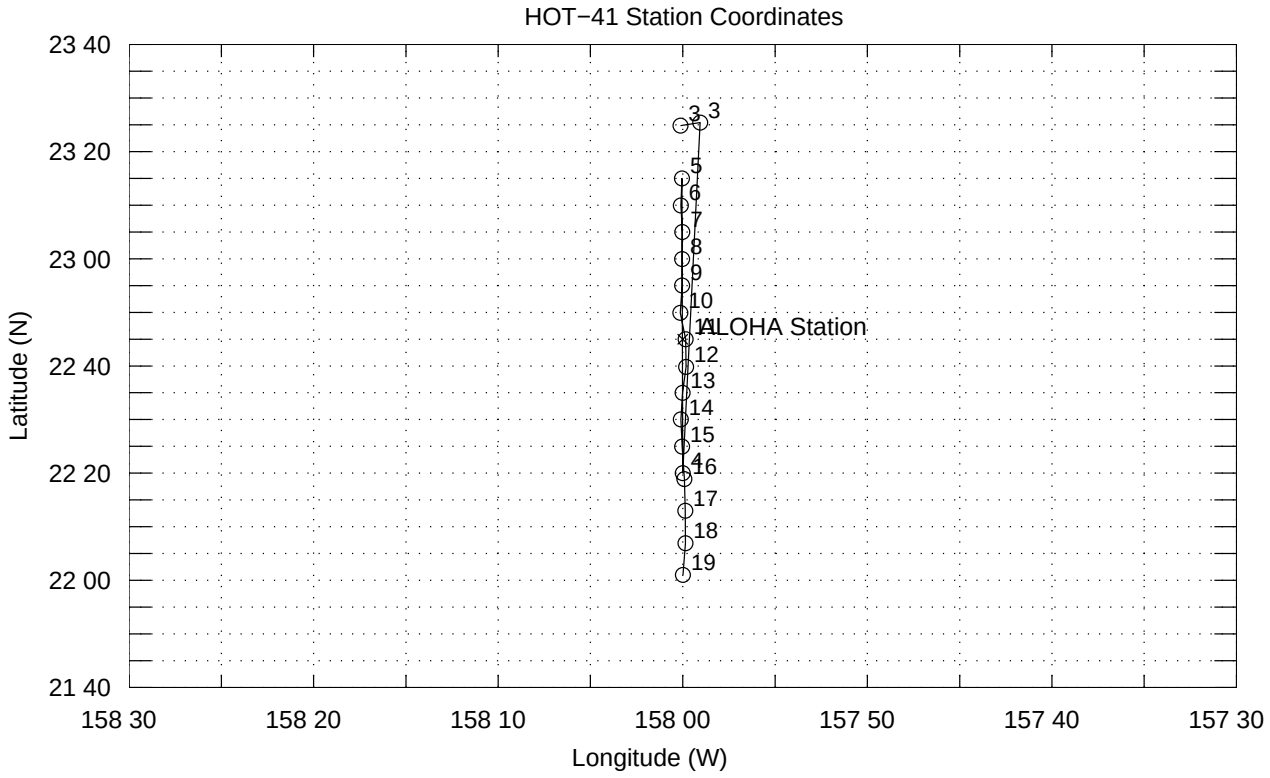
HOT−41 Station Coordinates
23 40
23 20
23 00
22 40
22 20
22 00
21 40
Latitude (N)
158 30
158 20
158 10
158 00
157 50
157 40
157 30
Longitude (W)
3
3
5
6
7
8
9
10
11
ALOHA Station
12
13
14
15
4
16
17
18
19

Figure 6.8.15

7. Hawaii Ocean Time-series Publications

Invited Presentations and Published Abstracts

1988 Karl, D. NSF-sponsored symposium on Dissertations in Chemical Oceanography, "Research opportunities in Hawaiian waters", Honolulu, Hawaii, November 1988.

1988 Karl, D. NSF/GOFS-sponsored workshop on sediment traps, "Determination of total C, N, P flux" and "Screens: A potential solution to the problem of swimmers", Gulf Coast Research Laboratory, Mississippi, November 1988.

1989 Winn, C. D., S. Chiswell, D. M. Karl and R. Lukas. Long time-series research in the Central Pacific Ocean. The Oceanography Society 1st Annual Meeting, Monterey, California.

1990 Chiswell, S. M. and R. Lukas. The Hawaii Ocean Time-series (HOT). EOS, *Transactions of the American Geophysical Union* 71, 1397.

1990 Karl, D. "JGOFS time-series programs," San Francisco, California, December 1990.

1990 Karl, D., R. Letelier, D. Bird, D. Hebel, C. Sabine and C. Winn. An Oscillatoria bloom in the oligotrophic North Pacific Ocean near the GOFS Station ALOHA. *EOS, Transactions of the American Geophysical Union* 71, 177-178.

1990 Winn, C. D., D. Hebel, R. Letelier, D. Bird and D. Karl. Variability in biogeochemical fluxes in the oligotrophic central Pacific: Results of the Hawaii Ocean Time-Series Program. *EOS, Transactions of the American Geophysical Union* 71, 190.

1991 Karl, D. "The Hawaii Ocean Time-series program: Carbon production and particle flux", The Oceanography Society 2nd Annual Meeting, St. Petersburg, Florida, March 1991.

1991 Karl, D. NATO symposium on Biology and Ecology of Diazotrophic Marine Organisms, "*Trichodesmium* blooms and new nitrogen in the North Pacific gyre", Bamberg, Germany, May 1991.

1991 Letelier, R., D. Karl, R. Bidigare, J. Christian, J. Dore, D. Hebel and C. Winn. Temporal variability of phytoplankton pigments at the U.S.-JGOFS Station ALOHA (22°45'N, 158°W). *EOS, Transactions of the American Geophysical Union* 72, 74.

1991 Winn, C., C. Sabine, D. Hebel, F. Mackenzie and D. M. Karl. Inorganic carbon system dynamics in the central Pacific Ocean: Results of the Hawaii Ocean Time-series program. *EOS, Transactions of the American Geophysical Union* 72, 70.

1992 Anbar, A. D. Rhenium in seawater: Confirmation of generally conservative behavior. *EOS, Transactions of the American Geophysical Union* 73, 278.

1992 Bidigare, R. R., L. Campbell, M. Ondrusek, R. Letelier and D. Vaulot. Characterization of picophytoplankton at Station ALOHA (22°45'N, 158°W) using HPLC, flow cytometry and immunofluorescence techniques. PACON 1992 Meeting, 1-5 June 1992.

1992 Karl, D. NSF-sponsored GLOBEC scientific steering committee meeting, "Hawaii Ocean Time-series (HOT) program: A GLOBEC 'Blue Water' initiative", Honolulu, Hawaii, March 1992.

1992 Karl, D. IGBP International Symposium on Global Change, "Oceanic ecosystem variability: Initial results from the JGOFS Hawaii Ocean Time-series (HOT) experiment", Tokyo, Japan, March 1992.

1992 Karl, D. Conoco HOT Topics Seminar Series, "The U.S.-JGOFS Hawaii Ocean Time-Series (HOT) Program: Biogeochemical Vignettes from the Oligotrophic North Pacific Ocean" and "Temporal Variability in Bioelement Flux at Station ALOHA (22°45'N, 158°W)", Woods Hole, Massachusetts, May 1992.

1992 Karl, D., C. Winn, D. Hebel, R. Letelier, J. Dore and J. Christian. The U.S.-JGOFS Hawaii Ocean Time-Series (HOT) program. American Society for Limnology and Oceanography Aquatic Sciences Meeting, Santa Fe, NM, February 1992.

1992 Campbell, L., R. R. Bidigare, R. Letelier, M. Ondrusek, S. Hall, B. Tsai and C. Winn. Phytoplankton population structure at the Hawaii Ocean Time-series station. American Society for Limnology and Oceanography Aquatic Sciences Meeting, Santa Fe, NM, February 1992.

1992 Lukas, R. Water mass variability observed in the Hawaii Ocean Time Series. *EOS, Transactions of the American Geophysical Union* 72, 70.

1992 Schudlich, R. and S. R. Emerson. Modelling dissolved gases in the subtropical upper ocean: JGOFS/WOCE Hawaiian Ocean Time-series. *EOS, Transactions of the American Geophysical Union* 73, 287.

1992 Tupas, L. M., B. N. Popp and D. M. Karl. Dissolved organic carbon in oligotrophic waters: Experiments on sample preservation, storage and analysis. *EOS, Transactions of the American Geophysical Union* 73, 287.

1992 Winn, C. D., D. Hebel, R. Letelier, J. Christian, J. Dore, R. Lukas and D. M. Karl. Long time-series measurements in the central North Pacific: Results of the Hawaii Ocean Time-series program. PACON conference, Kona, Hawaii, June 1992.

1993 Emerson, S., P. Quay, C. Stump, D. Wilber, and R. Schudlich. Oxygen cycles and productivity in the oligotrophic subtropical Pacific Ocean. Third Scientific Meeting of the Oceanography Society, Seattle, Washington.

Newsletters

1991 Lukas, R. and S. Chiswell. Submesoscale water mass variations in the salinity minimum of the North Pacific. *WOCE Notes*, 3(1), 6-8.

1992 Chiswell, S. Inverted echo sounders at the WOCE deep-water station. WOCE Notes, 4(4), 1-6.

1992 Firing, E. and P. Hacker. ADCP results from WHP P16/P17. WOCE Notes, 4(3), 6- 12.

plus a periodic column entitled "HOT Stuff", written by D. Karl, which appears in the U.S. JGOFS Program newsletter

Invited Book Chapters and Refereed Publications

1990 Giovannoni, S. J., E. F. DeLong, T. M. Schmidt and N. R. Pace. Tangential flow filtration and preliminary phylogenetic analysis of marine picoplankton. *Applied and Environmental Microbiology*, 56, 2572-2575.

1990 Collins, D. J., W. J. Rhea and A. van Tran. Bio-optical profile data report: HOT-3. National Aeronautics and Space Administration JPL Publ. #90-36.

1990 Firing, E. and R. L. Gordon. Deep ocean acoustic Doppler current profiling. In: G. F. Appell and T. B. Curtin (eds.), *Proceedings of the Fourth IEEE Working Conference on Current Measurements,* pp. 192-201. IEEE, New York.

1991 Karl, D. M., W. G. Harrison, J. Dore et al. Chapter 3. Major bioelements workshop report. In: D. C. Hurd and D. W. Spencer (eds.), *Marine Particles: Analysis and Characterization*, pp. 33-42. American Geophysical Union, Geophysical Monograph 63.

1991 Karl, D. M., J. E. Dore, D. V. Hebel and C. Winn. Procedures for particulate carbon, nitrogen, phosphorus and total mass analyses used in the US-JGOFS Hawaii Ocean Time-Series Program. In: D. Spencer and D. Hurd (eds.), *Marine Particles: Analysis and Characterization*, pp. 71-77. American Geophysical Union, Geophysical Monograph 63.

1991 Karl, D. M. and C. D. Winn. A sea of change: Monitoring the oceans' carbon cycle. *Environmental Science & Technology* 25, 1976-1981.

1991 Sabine, C. L. and F. T. Mackenzie. Oceanic sinks for anthropogenic CO_2. International *Journal of Energy, Environment, Economics* 1, 119-127.

1991 Schmidt, T. M., E. F. DeLong and N. R. Pace. Analysis of a marine picoplankton community by 16S rRNA gene cloning and sequencing. *Journal of Bacteriology*, 173, 4371-4378.

1991 Chiswell, S. M. Dynamic response of CTD pressure sensors to temperature. *Journal of Atmospheric and Oceanic Technology*, 8, 659-668.

1992 Karl, D. M., R. Letelier, D. V. Hebel, D. F. Bird and C. D. Winn. *Trichodesmium* blooms and new nitrogen in the North Pacific gyre. In: E. J. Carpenter et al. (eds.), *Marine Pelagic Cyanobacteria: Trichodesmium and Other Diazotrophs*, pp. 219-237. Kluwer Academic Publishers, Netherlands.

1992 Karl, D. M. and G. Tien. MAGIC: A sensitive and precise method for measuring dissolved phosphorus in aquatic environments. *Limnology and Oceanography*, 37, 105-116.

1992 Chen, R. F. and J. L. Bada. The fluorescence of dissolved organic matter in seawater. *Marine Chemistry*, 37, 191-221.

1992 Quay, P.D., B. Tilbrook and C. S. Wong. Oceanic uptake of fossil fuel CO_2: Carbon-13 evidence. *Science*, 256, 74-78.

1992 Karl, D. M. The oceanic carbon cycle: Primary production and carbon flux in the oligotrophic North Pacific Ocean. *Proceedings of the IGBP Symposium on Global Change*, Tokyo, Japan, in press.

1992 Benner, R., J. D. Pakulski, M. McCarthy, J. I. Hedges and P. G. Hatcher. Bulk chemical characteristics of dissolved organic matter in the ocean. *Science*, 255, 1561-1564.

1993 Anbar, A. D., R. A. Creaser, D. A. Papanastassiou and G. J. Wasserburg. Rhenium in seawater: Confirmation of generally conservative behavior. *Geochimica et Cosmochimica Acta*, 56, 4099-4103.

1993 Karl, D. M., G. Tien, J. Dore and C. D. Winn. Total dissolved nitrogen and phosphorus concentrations at US-JGOFS Station ALOHA: Redfield reconciliation. *Marine Chemistry*, 41, 203-208.

1993 Selph, K. E., D. M. Karl, M. R. Landry. Quantification of Chemiluminescent DNA probes using liquid scintillation counting. *Analytical Biochemistry*, 210, 394-401.

1993 Karl, D. M. Total microbial biomass estimation derived from the measurement of particulate adenosine-5'-triphosphate. In: P. F. Kemp, B. F. Sherr, E. B. Sherr and J. J. Cole (eds.), *Handbook of Methods in Aquatic Microbial Ecology*, pp. 359-368. Lewis Publishers, Boca Raton.

1993 Hedges, J. I., B. A. Bergamaschi and R. Benner. Comparative analyses of DOC and DON in natural waters. *Marine Chemistry*, 41, 121-134.

1993 Mopper, K. and C. A. Schultz. Fluorescence as a possible tool for studying the nature and water column distribution of DOC components. *Marine Chemistry*, 41, 229-238.

1993 Coble, P. G., C. A. Schultz and K. Mopper. Fluorescence contouring analysis of DOC intercalibration experiment samples: a comparison of techniques. *Marine Chemistry*, 41, 173-178.

1993 Winn, C. D., R. Lukas, D. Hebel, C. Carrillo, R. Letelier and D. M. Karl. The Hawaii Ocean Time- series program: Resolving variability in the North Pacific. In: N. Saxena (ed.), *Recent advances in marine science and technology, 92, Proceedings of the Pacific Ocean Congress (PACON)*, pp. 139-150.

1993 Letelier, R. M., R. R. Bidigare, D. V. Hebel, C. D. Winn and D. M. Karl. Temporal variability of phytoplankton community structure at the US-JGOFS Time-series Station ALOHA (22°45'N, 158°00'W) based on pigment analyses. *Limnology and Oceanography*, 38, 1420-1437.

1993 Campbell, L. and D. Vaulot. Photosynthetic picoplankton community structure in the subtropical North Pacific Ocean near Hawaii (Station ALOHA). *Deep-Sea Research*, 40, 2043-2060.

1994 Baines, S. B., M. L. Pace and D. M. Karl. Why does the relationship between sinking flux and planktonic primary production differ between lakes and oceans? *Limnology and Oceanography*, in press.

1994 Tupas, L. M., B. N. Popp and D. M. Karl. Dissolved organic carbon in oligotrophic waters: Experiments on sample preservation, storage and analysis. *Marine Chemistry*, in press.

1994 Thomas, F. I. M. and M. J. Atkinson. Field calibration of a potentiostatic micro-hole oxygen sensor. *Journal of Oceanic and Atmospheric Research,* in press.

1994 Atkinson, M. J., F. Thomas, E. Terrill, K. Morita and C. Liu. A potentiostatic oxygen sensor for oceanic CTDs. *Deep-Sea Research*, in press.

1994 Atkinson, M. A., F. Thomas, R. Lukas and C. Winn. New calibration equations for amperometric membrane oxygen sensors. *Deep-Sea Research*, in press.

1994 Campbell, L., H. A. Nolla and D. Vaulot. The importance of phtosynthetic prokaryote biomass in the subtropical central North Pacific Ocean (Station ALOHA). *Limnology and Oceanography*, in press.

1994 Atkinson, M. J., F. Thomas and N. Larson. Effects of pressure on oxygen sensors: a new pressure term for calibration equations. *Journal of Oceanic and Atmospheric Research*, in press.

Theses and Dissertations

1992 Sabine, C. L. Geochemistry of particulate and dissolved inorganic carbon in the central North Pacific. Ph.D. Dissertation, May 1992.

1993 Kennan, S. Variability of the intermediate water north of Oahu. M.S. Thesis, December 1993.

Data Reports

1990 Karl, D. M., C. D. Winn, D. V. W. Hebel and R. Letelier. Hawaii Ocean Time-series Program Field and Laboratory Protocols, September 1990. School of Ocean and Earth Science and Technology, Univ. of Hawaii, Honolulu, HI, 72 pp.

1990 Chiswell, S., E. Firing, D. Karl, R. Lukas and C. Winn. Hawaii Ocean Time-series Program Data Report 1, 1988-1989. School of Ocean and Earth Science and Technology, Univ. of Hawaii, Honolulu, HI, 269 pp.

1991 Winn, C., S. Chiswell, E. Firing, D. Karl and R. Lukas. Hawaii Ocean Time-series Program Data Report 2, 1990. School of Ocean and Earth Science and Technology, Univ. of Hawaii, Honolulu, HI, 175 pp.

1993 Winn, C., R. Lukas, D. Karl, E. Firing. Hawaii Ocean Time-series Program Data Report 3, 1991. School of Ocean and Earth Science and Technology Report 3, University of Hawaii, 228 pp.

8. Data Availability and Distribution

Data collected by the HOT program are made available to the oceanographic community as soon after processing as possible. In order to provide easy access to our data, we have provided summaries of our CTD and water column chemistry data on the enclosed IBM PC 3.5" high-density floppy diskette. CTD data at NODC standard pressures for temperature, potential temperature, salinity, oxygen and potential density are provided in ASCII files; water column chemistry data are provided in Lotus 1-2-3™ files. The pressure and temperature reported for each water column sample are derived from CTD temperature and pressure readings at the time of bottle trip. Densities are calculated from calibrated CTD temperature, pressure and salinity values. These densities are used, where appropriate, to express chemical concentrations on a per kilogram basis. With the exception of the results of replicate analysis, all water column chemical data collected during 1992 are given in these data sets.

The data included in the Lotus 1-2-3™ files have been quality controlled and the flags associated with each value indicate our estimate of the quality of each value. The text file `readme.txt` gives a description of data formats and quality flags.

A more complete data set, containing data collected since year 1 of the HOT program, as well as 2 dbar averaged CTD data, are available from two sources. The first is through NODC in the normal manner. The second source is via the world-wide Internet system. The data reside in a data base on a workstation at the University of Hawaii, and may be accessed using anonymous ftp on Internet.

In order to maximize ease of access, the data are in ASCII files. File names are chosen so that they may be copied to DOS machines without ambiguity. (DOS users should be aware that Unix is case-sensitive, and Unix extensions may be longer than 3 characters.)

The data are in a subdirectory called /pub/hot. More information about the data base is given in several files called `Readme.*` at this level. The file `Readme.first` gives general information on the data base; we encourage users to read it first.

The following is an example of how to use ftp to obtain HOT data. The user's command are denoted by underlined text. The workstation's Internet address is hokulea.soest.hawaii.edu, or 128.171.154.47 (either address should work).

1. At the Prompt >, type ftp 128.171.154.47.

2. When asked for your login name, type anonymous.

3. When asked for a password, type your internet address.

4. To change to the HOT database, type cd /pub/hot.

   To view files type ls. A directory of files and subdirectories will appear.

5. To obtain further information about the database type get Readme.first. This will transfer an ASCII file to your system. Use any text editor to view it.

6. To exit type bye.